SOVIET PHYSICS

JETP

A translation of Zhurnal Éksperimental'noĭ i Teoreticheskoĭ Fiziki.

Vol. 13, No. 5, pp 871-1080 (Russ. orig. Vol. 40, No. 5, pp 1237-1535, May 1961) November, 1961

NEUTRON YIELD OF THE REACTION BETWEEN TRITONS AND FLUORINE AND ALUMINUM NUCLEI

A. K. VAL'TER, P. I. VATSET, L. Ya. KOLESNIKOV, S. G. TONAPETYAN, K. K. CHERNYAVSKII, and A. I. SHPETNYĬ

Physico-Technical Institute, Academy of Sciences, Ukrainian S.S.R.

Submitted to JETP editor July 22, 1960

J. Exptl. Theoret. Phys. (U.S.S.R.) **40**, 1237-1243 (May, 1961)

The neutron yields from the $F^{19}(t, n)$ and $Al^{27}(t, n)$ reactions were studied for triton energies up to 2.4 Mev. The dependence on triton energy of the differential cross section for neutron emission at an angle of 0° was derived. Resonance of the differential cross section for the $F^{19}(t, n)$ reaction was used to determine excited levels of the intermediate nucleus Ne^{22} (Table 1). The symmetrical neutron distribution around 90° in the c.m.s. at five triton energies indicates that up to 2.1 Mev the $F^{19}(t, n)$ reaction proceeds mainly via formation of an intermediate nucleus. The total cross section for the $F^{19}(t, n)$ reaction was determined for several energies (Table II).

1. INTRODUCTION

NUCLEAR physics has obtained much valuable information by investigating the reactions of light nuclei with bombarding protons and deuterons. Reactions with tritium can undoubtedly be just as fruitful. However, the difficulty of producing tritium and certain special conditions for working with it can account for the fact that relatively few investigations have been published[1-10] concerning reactions between tritons and light nuclei.

The nucleus investigated in the present work was F^{19}. Since the solid target consisted of AlF_3 the neutron yield from the reaction $Al^{27}(t, n)$ also had to be investigated.

Neutron-producing reactions between tritons and light nuclei are characterized by the positive reaction energy Q and the appreciable excitation energy of intermediate nuclei. The following reactions of tritons with fluorine and aluminum are possible:

$$F^{19} + H^3 \rightarrow Ne^{22} \rightarrow Ne^{21} + n, \qquad Q = 11.145 \text{ Mev}, \qquad (1)$$

$$F^{19} + H^3 \rightarrow Ne^{22} \rightarrow Ne^{20} + 2n, \qquad Q = 4.388 \text{ Mev}; \qquad (1a)$$

$$Al^{27} + H^3 \rightarrow Si^{30} \rightarrow Si^{29} + n, \qquad Q = 11.578 \text{ Mev}, \qquad (2)$$

$$Al^{27} + H^3 \rightarrow Si^{30} \rightarrow Si^{28} + 2n, \qquad Q = 3.104 \text{ Mev}. \qquad (2a)$$

The minimum excitation energies of the intermediate nuclei Ne^{22} and Si^{30} are 21.510 and 22.188 Mev, respectively.[11] The present work was intended to study the neutron yields from the $F^{19}(t, n)$ and $Al^{27}(t, n)$ reactions and the excited levels of the intermediate nuclei.

2. EXPERIMENTAL PROCEDURE

The targets were prepared by evaporating aluminum fluoride on platinum disks and were weighed on a microbalance. The weights of the AlF_3 targets were 0.179, 0.200, 0.211, and 0.280 mg/cm^2. For 1.4-Mev tritons these thicknesses corresponded to energy losses of 60, 67, 70, and 92 kev, respectively. The Al^{27} target was 0.67-mg/cm^2 alumi-

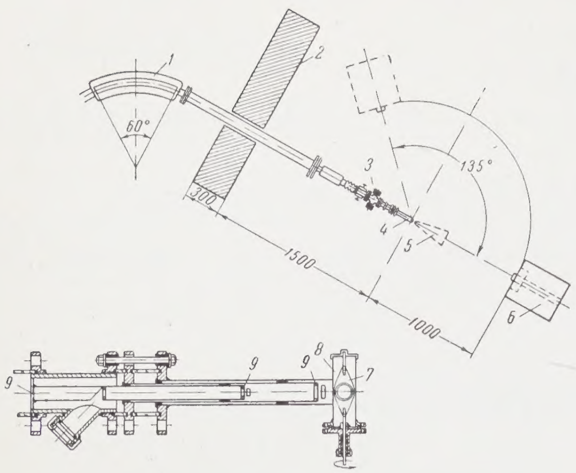

FIG. 1. Diagram of apparatus. 1 – magnetic analyzer, 2 – paraffin-borax shield, 3 – closure, 4 – target, 5 – 30-cm copper cone, 6 – neutron counter, 7 – target holder, 8 – T tube 0.2 mm thick, 9 – collimator diaphragms.

num foil in which 1.8-Mev tritons lost 170 kev. Target weights were checked by the relative neutron yield per unit weight.

Tritons were accelerated in the horizontal electrostatic generator at a pressure permitting energies up to 2.5 Mev. The generator voltage was stabilized by a corona triode. Stabilization was monitored by 60° ion-beam deflection in the magnetic analyzer. The generator voltage was measured from the current supplied to the magnetic analyzer. The voltage was calibrated from the thresholds of the T(p,n) and Li(p,n) reactions on ions of atomic and molecular hydrogen, with errors not above 0.5%.

Tritium diluted with helium in the ratio 1 : 12 was fed into the ion source through a bimetallic leak. The intensity ratio of the beams with masses 1 (H^+), 2 (HH^+, D^+), 3 (T^+), 4 (He^+), and 6 (TT^+) was 0.1 : 0.2 : 1 : 110 : 10. Since tritium and He^4 were admitted to the ion source, with hydrogen, deuterium, and He^3 comprising only a small amount of contamination, it was assumed that the beams with masses 3 and 6 were practically uncontaminated. The purity of these beams was confirmed by comparing the neutron yields in the Li(t,n) reaction using tritons with 0.5 Mev effective energy. In the neutron yield measurements the mean beam current for mass 3 was ~ 0.2 μa.

The number of tritons striking the target was determined by means of a sensitive current integrator giving 40.19 counts per microcoulomb.

The apparatus is represented schematically in Fig. 1. The target 4 was positioned in the beam path in a special holder 7. The beam was collimated by diaphragms 9 with 6 mm × 3 mm apertures. A light T tube 8 with 0.2-mm wall thickness was highly transparent to neutrons leaving the target in all directions. The target was rotated 180° by remote control employing selsyns. The triton beam could therefore be directed against either the front or back of the target.

The neutron flux was measured by a long proportional boron counter 6 rotated on a circle of one-meter radius around a vertical axis passing through the center of the target. The neutron counter was calibrated against a standard Ra + Be neutron source yielding 4.8×10^5 neutrons/sec, that was substituted for the target.* Counter efficiency was 1.008×10^4 neutrons/sr per count. The sensitivity of the neutron counter[12] was within ± 3% for neutrons from 25 kev to 5 Mev and dropped 11% for 14-Mev neutrons.

Background neutrons were taken into account in measurements of the neutron yield from the target. The diaphragms located before the magnetic analyzer 1 and the walls of the analyzer were strong sources of background neutrons generated in "spurious targets." In order to prevent direct entrance of these neutrons into the neutron counter a 30-cm shield 2 made of paraffin with an admixture of borax was set up at the exit of the triton beam from the magnetic analyzer. Under the given experimental conditions (Fig. 1) the neutron background consisted of a) neutrons generated in the "spurious targets" and collimator diaphragms, b) neutrons from the T(t,n) and C(t,n) reactions occurring in tritium impacted into the target by the beam, and in carbon deposited in small amounts on the target during bombardment by accelerated ions, and c) neutrons from all targets, scattered by the surroundings (floor, walls, ceiling etc.).

3. MEASUREMENTS

For the purpose of taking the background neutrons into account while measuring the neutron yield from the F^{19}(t,n) and Al^{27}(t,n) reactions, four measurements were obtained. In the first and second measurements the ion beam struck the face of the target without and with the presence of the cone 5; the third and fourth measurements were analogous for the back of the target. Each measurement corresponded to the same number of counts from the current integrator, the number depending on the neutron yield from the given target. From the four measurements obtained in this

---

*The background of neutrons scattered by the surrounding medium was 8% when the neutron counter was calibrated. For background measurements the counter was covered with a copper cone 30 cm high.

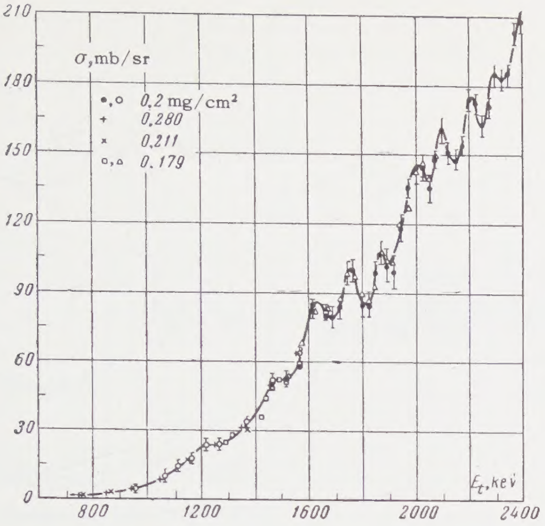

FIG. 2. Differential cross sections for neutron yield at 0° angle from triton reactions with aluminum fluoride targets of different thicknesses. E_t is triton energy.

manner the number of counts of the neutron counter induced by neutrons from the investigated reaction can be expressed by

$$N = N_1 - N_2 - N_3 + N_4 (t_2 + t_3 - t_1)/t_4, \qquad (3)$$

where t_1, t_2, t_3, t_4 are the respective times of the four measurements. Consideration of the measurement times is associated with the fact that the neutron background from the diaphragms and magnetic analyzer walls was essentially a function of time, since the current of the undivided beam did not vary with time, while the background of all other neutrons was a function of the triton beam intensity. The total neutron background was easily estimated by analyzing the four measurements with identical times.

With increasing triton acceleration the total background was observed to increase, reaching 30 — 40%. The difference between the third and fourth measurements, amounting to 6 — 10%, indicated the background due to neutrons from the T(t, n) and C(t, n) reactions. Because of the smallness of this quantity we neglected the neutron background from these reactions that was scattered by the surroundings. Periodic purification of the diaphragms in front of the magnetic analyzer reduced the total neutron background considerably.

4. RESULTS

The reaction of a triton with a fluorine or aluminum nucleus can produce a single neutron [Eqs. (1) and (2)] or two neutrons [Eqs. (1a) and (2a)]. Our technique did not distinguish between these reactions but determined only the total cross section σ(t, n) + σ(t, 2n). This total cross section will hereafter be understood when we refer to neutron yields.

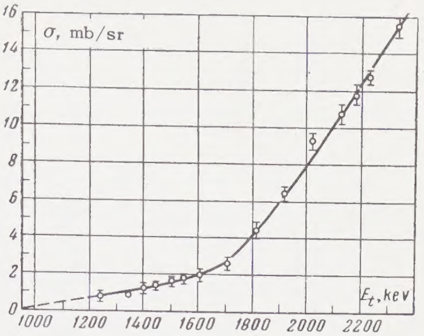

FIG. 3. Differential cross section for neutron yield from Al^{27}(t, n).

Figures 2 and 3 show the differential cross sections for neutron production at 0° in interactions of tritons with aluminum fluoride and aluminum, as a function of triton energy. From these data we obtained the differential cross section at 0° for F^{19}(t, n) vs triton energy, which is shown in Fig. 4.

From the resonances observed on the excitation curve of F^{19}(t, n) the excited levels of Ne^{22} above 22.510 Mev were determined; these are given in Table I. Only two levels, 22.7 and 23.1 Mev, were previously[9] discovered in this excitation region of Ne^{22} from the excitation function of F^{19}(t, α). The 23.1-Mev level agrees with 23.128 Mev within the limits of error.

The angular distribution of neutrons from the AlF_3 target gave the angular distribution for the reaction F^{19}(t, n) (Fig. 5).

Since the neutron yield from Al^{27}(t, n) comprises 6 — 8% of the yield from the AlF_3 target, a correction for neutrons from Al^{27}(t, n) introduced no appreciable error if the angular distributions of neutrons in the Al^{27}(t, n) and F^{19}(t, n) reactions were similar.

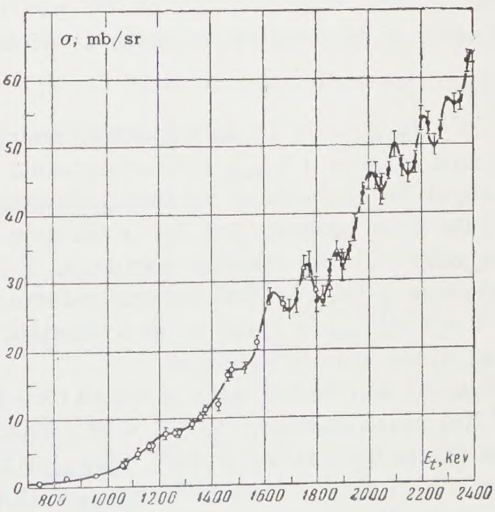

FIG. 4. Differential cross section for neutron yield at 0° angle from F^{19} (t, n) vs triton energy.

Table I. Levels of compound nucleus Ne^{22*}

No.	E_t, Mev	Energy level, Mev	Level width, kev
1	1.215	22.558±0.018	300
2	1.470	22.778±0.018	150
3	1.635	22.921±0.019	100
4	1.760	23.029±0.020	100
5	1.875	23.128±0.020	80
6	2.010	23.245±0.021	130
7	2.100	23.322±0.021	90
8	2.210	23.419±0.022	70
9	2.300	23.495±0.022	50

Table II. Total cross section for $F^{19}(t, n)$

E_t, Mev	σ_{tot}, mb
1.066	36.11±2.13
1.218	77.08±4.24
1.370	95,92±4.80
1.572	203,46±9.56
2.123	442,50±20.35

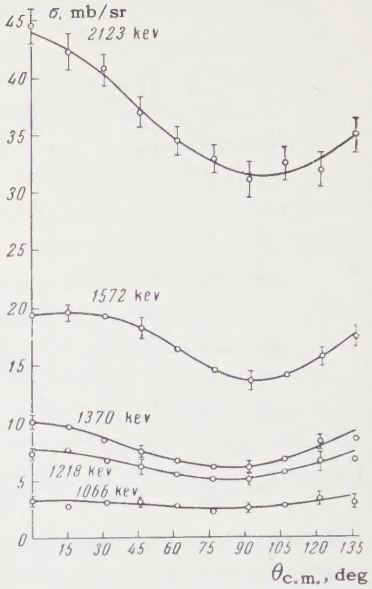

FIG. 5. Angular distributions of neutrons from $F^{19}(t, n)$ for different triton energies.

The angular distributions of neutrons are symmetrical around 90° in the c.m. system. This shows that the $F^{19}(t, n)$ reaction mainly involves the formation of a compound Ne^{22} nucleus. Table II shows the total cross sections for $F^{19}(t, n)$ calculated from the angular distributions assuming symmetry around 90°.

In calculating the absolute errors of the neutron yields we assumed ±3% error in determining the number of nuclei in AlF_3, ±1% for the number of Al nuclei, and ±1% for the number of tritons. The strength of the constant Ra + Be source was known to within ±3%.

Weisskopf's statistical formula[13] can be used to obtain a very rough estimate of the two-neutron contribution to the total cross section. We have

$$\sigma(t, 2n)/[\sigma(t, n) + \sigma(t, 2n)] \approx 1 - (1 + \varepsilon/T)\, e^{-\varepsilon/T}, \quad (4)$$

where $\epsilon = E_{max} - E_n$ is the maximum energy of the second neutron (E_{max} is the maximum excitation energy of the residual nucleus following ejection of the first neutron, and E_n is the neutron binding energy in the residual nucleus), T is the temperature of the residual nucleus determined from $T = \sqrt{4E_{max}/a}$, and a is a constant depending on the atomic weight A.

Heidmann and Bethe[14] give $a = 0.14\,(A - 12)$ Mev^{-1} for mass numbers $15 < A < 70$. Therefore for the excitation energy of Ne^{21} ($E_{max} = 13.15$ Mev, $a = 1.26\ Mev^{-1}$) and Si^{29} ($E_{max} = 13.6$ Mev, $a = 2.38\ Mev^{-1}$) the temperatures will be of the orders 6.5 and 4.8 Mev, respectively. With increasing excitation energy the ratio in Eq. (4) can increase approximately from 0.14 to 0.26 for $F^{19}(t, n)$, and from 0.14 to 0.3 for $Al^{27}(t, n)$.

On the other hand, using the experimental temperatures obtained by Gugelot and by Graves and Rosen[15] we obtain $T \approx 1.3$ Mev for Ne^{21} and $T \approx 1.2$ Mev for Si^{29}. In this case the ratio (4) can increase from 0.86 to 0.96 for $F^{19}(t, n)$, and from 0.73 to 0.93 for $Al^{27}(t, n)$.

The foregoing results show that reactions producing two neutrons make a considerable, if not the principal, contribution to the neutron yield from reactions of tritons with F^{19} and Al^{27}.

It must be emphasized, however, that we have obtained only very approximate cross section ratios.

In conclusion the authors wish to thank M. T. Dorofeev, and also the electrostatic generator group, for experimental assistance. The members of the group were V. I. Petran', I. G. Losev, Yu. K. Panteleev, V. M. Khurgin, N. S. Zlishchev, V. I. Krivoruchko, and G. E. Klitsenko.

---

[1] E. Almqvist, Can. J. Phys. **A28**, 433 (1950).

[2] R. W. Crews, Phys. Rev. **82**, 100 (1951).

[3] Pool, Kundu, Weiler, and Donaven, Phys. Rev. **82**, 305 (1951).

[4] Pepper, Allen, Almqvist, and Dewan, Phys. Rev. **85**, 155 (1952).

[5] Dewan, Pepper, Allen, and Almqvist, Phys. Rev. **86**, 416 (1952).

[6] Almqvist, Pepper, and Lorrain, Can. J. Phys. **32**, 621 (1954).

[7] Allen, Almqvist, Dewan, and Pepper, Phys. Rev. **96**, 684 (1954).

[8] N. Jarmie, Phys. Rev. **98**, 41 (1955).

[9] N. Jarmie, Phys. Rev. **104**, 1683 (1956).

[10] Ajzenberg-Selove, Jarmie, and Haddad, Bull. Am. Phys. Soc. **4**, 258 (1959).

[11] F. Ajzenberg-Selove and T. Lauritsen, Nuclear Phys. **11**, 1 (1959), p. 295; P. M. Endt and C. M. Braams, Revs. Modern Phys. **29**, 683 (1957).

[12] Vatset, Tonapetyan, and Dorofeev, Атомная энергия (Atomic Energy) **7**, 172 (1959).

[13] V. F. Weisskopf, Statistical Theory of Nuclear Reactions, Russ. Transl. IIL, 1952, p. 71; J. M. Blatt and V. F. Weisskopf, Theoretical Nuclear Physics (Wiley, New York, 1954), pp. 365-379.

[14] J. Heidmann and H. A. Bethe, Phys. Rev. **84**, 274 (1951).

[15] P. C. Gugelot, Phys. Rev. **81**, 51 (1951); E. R. Graves and L. Rosen, Phys. Rev. **89**, 343 (1953).

Translated by I. Emin
211

SOVIET PHYSICS JETP VOLUME 13, NUMBER 5 NOVEMBER, 1961

INTERACTION OF 14.1-Mev NEUTRONS WITH Be^9

S. A. MYACHKOVA and V. P. PERELYGIN

P. N. Lebedev Physics Institute, Academy of Sciences, U.S.S.R.

Submitted to JETP editor August 23, 1960

J. Exptl. Theoret. Phys. (U.S.S.R.) 40, 1244-1249 (May, 1961)

The interaction between 14.1-Mev neutrons and Be^9 was investigated by the nuclear emulsion method. Energy and angular distributions of neutrons and alpha particles produced in the (n, 2n) reaction were measured. The data obtained indicate that the reaction generally involves the formation of a 2.9-Mev excited state in the Be^8 nucleus (cross section 0.19 ± 0.06 b) and the 2.43 Mev excited level of the Be^9 nucleus. The cross section for excitation of the Be^9 (2.43 Mev) nucleus and for formation of the ground state in the Be^8 nucleus is 0.2 ± 0.1 b. Direct interactions also yield an appreciable contribution to the (n, 2n) reaction. The total cross section for the reaction is 0.54 ± 0.07 b.

INTRODUCTION

THE interaction of neutrons with Be^9 nuclei has been examined in a number of works,[1] but the mechanism of the reaction is at present still imperfectly known. There exist several possible methods of bringing about the (n, 2n) reaction on Be^9, involving both the formation of a compound nucleus and direct interactions.

1) Production of the compound nucleus Be^{10} and its decay according to the schemes

$$\text{a) } Be^{10} \to n + Be^{9*}, \qquad Be^{9*} \to n + Be^8 \to n + 2\alpha;$$

$$\text{b) } Be^{10} \to n + Be^{9*}, \qquad Be^{9*} \to \alpha + He^5 \to n + 2\alpha.$$

2) Formation of excited states of the Be^9 nucleus in the process of a direct interaction between neutrons and Be^9, and subsequent decay by scheme a) or b).

3) Breakup into three or four particles both with and without the formation of a compound nucleus:

$$Be^9 + n \to 2n + Be^8, \qquad Be^9 + n \to 2n + 2\alpha.$$

The interaction of neutrons with Be^9 has been most fully studied for the case of low-energy neutrons.[2] Experimental research with 14-Mev neutrons[3] has been devoted principally to determining the total cross section for the interaction between neutrons and Be^9. The formation of excited states of the Be^8 nucleus in the (n, 2n) reaction on Be^9 has only been examined in two works.[4,5] The results obtained in these works do not agree with one another. Thus, according to one of them,[4] the (n, 2n) reaction on Be^9 proceeds primarily with the formation of only one 2.9-Mev level of the Be^8 nucleus; results from the other work[5] indicate the significant role of ~5- and ~8-Mev levels in Be^8 formed during the (n, 2n) reaction on Be^9. The excitation of Be^8 levels has been investigated in many other reactions,[6] but this matter is not yet completely clarified.

In the present work an attempt has been made to evaluate the role of individual levels in the Be^8 nucleus which can be excited during the (n, 2n) reaction on Be^9. To get a more complete idea of the mechanism of the (n, 2n) reaction, the angular and energy distributions of alpha particles and neutrons produced in this reaction were investigated, for whatever the course of the (n, 2n) reaction on Be^9, the final reaction products are always alpha particles and neutrons.

EXPERIMENTAL METHODS AND RESULTS

The reaction $T(d, n)He^4$ served as the source of 14.1-Mev neutrons in all the experiments performed. The neutron flux on the radiator amounted to $\sim 1 \times 10^9$ neutrons/cm^2. In the first experiment NIKFI T-3 photoplates doped with metallic Be^9 powder were irradiated by neutrons. The beryllium powder was introduced between emulsion layers 100 μ thick. The amount of beryllium used is equivalent to uniform (by volume) doping with ~ 20 mg of beryllium compound solution per cm^3 of emulsion. The average grain diameter of the beryllium powder was 2 – 3 μ. The metallic powder was prepared by the spark discharge method.[7]

The irradiation was made parallel to the surface of the emulsion. In order to select events due to the (n, 2n) reaction on Be^9, all two-prong alpha stars with vertices located in the metallic beryl-

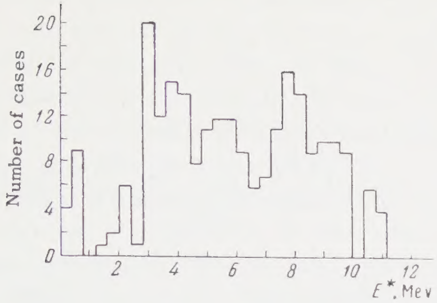

FIG. 1. Alpha-star distribution as dependent on excitation energy of Be^8 nucleus.

lium grains were chosen when scanning the developed plates. To estimate background events, an undoped layer of emulsion on these same plates was also scanned, choosing all two-prong alpha stars and also three-prong stars if one of the prongs was $\leq 3\ \mu$ in length. The background was evaluated under the assumption that it is possible to distinguish between background stars and true alpha stars arising in beryllium grains except when they are formed in the 1-μ emulsion layer directly adjoining the beryllium grains. The background constituted 5 — 7%.

About 250 cases could be related to the (n, 2n) reaction on Be^9. Among the alpha stars found, 22 cases of the reaction Be^9(n, α)He^6 were also discovered, which served as a control for the reliability of this experiment. When processing the alpha stars it was assumed that alpha stars corresponding to the (n, 2n) reaction on Be^9 were formed following the decay of excited Be^8 nuclei, and for each such star the energy of the corresponding Be^8 nuclear level was determined. The spectrum of excited states in the Be^9 nucleus constructed in such a manner with the background taken into account is presented in Fig. 1.

Two principal peaks stand out in the spectrum: the first peak corresponds to the 2.9-Mev excited level of the Be^8 nucleus, the second to the ~8-Mev level. When calculating the number of events related to decay from the 2.9-Mev level, we made use of data of reference 8 on the shape of the resonance line. The cross section for formation of the 2.9-Mev excited state in the Be^8 nucleus equals 0.19 ± 0.06 b. The cross section for alpha stars which could have been formed following the decay of a Be^8 nucleus in the ~8-Mev excited state is 0.14 ± 0.04 b. The data obtained are in good agreement with the results of Sakisaka.[5]

It is possible to distinguish on the spectrum another group of alpha stars, which corresponds to the ~5 Mev level of Be^8; the cross section for this group is 0.04 ± 0.02 b. However, as shown below, it is more probable that this group of alpha stars owes its origin to a process which occurs without the formation of the Be^8 nucleus.

In evaluating the cross sections presented above, corrections were made for the omission during scanning of alpha stars due to short-range alpha particles and for the loss of events lying in a plane perpendicular to the surface of the emulsion. The cross section for alpha stars corresponding to decay of a Be^8 nucleus in the ground state or of a Be^9 nucleus in the 2.43-Mev excited state (events which are energetically indistinguishable in this experiment) was not determined, since the correction for the omission of such events exceeds the number counted by several times. The large probability for omitting such alpha stars can be explained by the fact that the alpha particles forming them are of low energy. The cross section for the Be^9(n, α)He^6 reaction determined in this experiment is 11 ± 4 mb.

In the second experiment we examined the energy spectrum of alpha particles produced in the (n, 2n) reaction on Be^9 at various angles relative to the incident-neutron direction. A layer of metallic beryllium (~4 μ) deposited on a tantalum backing (a disc 5 cm in diameter) was used as the target. The incident neutron beam passed through a collimator constructed along the lines of Rosen's collimator.[9] NIKFI T-2 (100 μ) plates served as alpha-particle detectors. The irradiation was carried out in a vacuum chamber with continuous evacuation (0.1 mm mercury).

The experiment was set up in two geometries. In the first case a single-plate camera was used, which permitted the recording of alpha particles making an angle of 0° and small angles with respect to the direction of the incident neutron beam.

In the second experiment a multiplate camera was used, in which the photoplates were arranged in a circle around the targets at 20, 45, 65, 90, 105 and 120° to the incident neutron beam. The targets were placed in the center of the camera and turned with their coated surface towards the photoplates. To evaluate the background, an irradiation was made with an uncoated tantalum disk. The total number of alpha particles recorded in this experiment was ~2,500. Figure 2 presents energy spectra (to be more accurate, range distributions) for alpha particles emitted from the target at 0, 20, 65, 90 and 105° to the incoming neutron beam. The largest number of low-energy alpha particles is observed at the small angles. As the angle increases, the maximum is displaced toward the higher energy alpha particles. The total cross section for the (n, 2n) reaction on

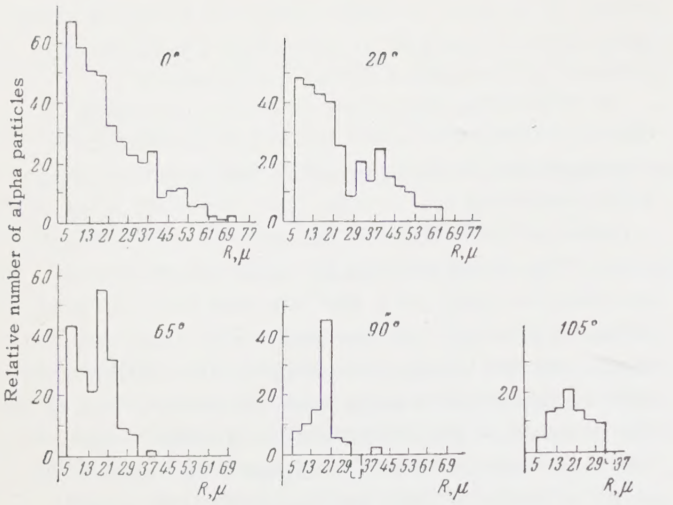

FIG. 2. Energy distribution of alpha particles (R is the range in microns).

Be^9, as calculated from the given angular distribution of alpha particles, is 0.48 ± 0.09 b [taking into account a correction for the loss of short-range (< 5 μ) alpha particles]. The cross section for the reaction $Be^9(n, t)Li^7$ was roughly estimated from this experiment and the experiment with alpha stars: the average was ~ 20 mb.

In the third experiment the energy and angular distributions of neutrons produced in the (n, 2n) reaction on Be^9 were investigated. Spectrum measurements were made for the scattering of collimated neutrons by a thin-walled glass sphere filled with metallic beryllium powder. Total weight of the powder was 125 g. Background was determined by measurements with an empty sphere. NIKFI Ya-2 (200 μ) photoplates served as neutron detectors. The irradiation was carried out in a special airtight box with controlled humidity. The plates were positioned around the beryllium sphere at 20, 40, 65, 90 and 120° to the incident neutron beam. About 5,000 tracks of recoil protons were recorded. The background amounted to ~ 40% of the effect. The data obtained were processed according to the method applied in Rosen's work.[10] The minimum energy at which recoil protons were recorded was 0.5 Mev.

The energy distributions of the neutrons emitted at angles of 40, 65, 90 and 120° are presented in Fig. 3. The angular distribution of neutrons with energies from 0.5 to 4 Mev and from 4 Mev to limiting energy values, which correspond to inelastic scattering of neutrons at the given angle, are presented in Fig. 4. The distribution of neutrons with energies greater than 4 Mev is strongly anisotropic. The total cross section for the reaction (n, 2n) on Be^9 was determined from the

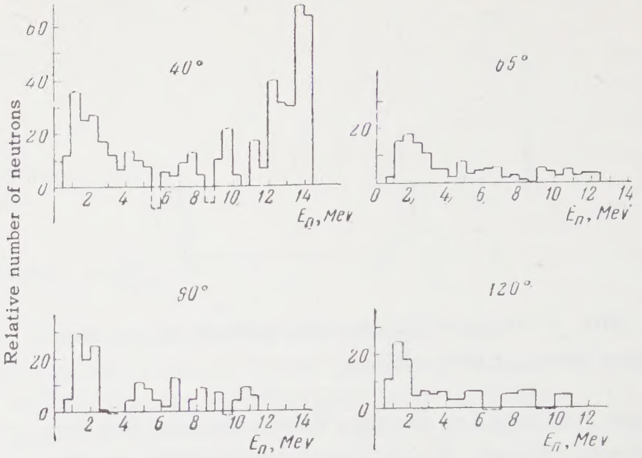

FIG. 3. Energy distribution of neutrons.

angular distribution of inelastically scattered neutrons to be σ = 0.6 ± 0.1 b. When calculating the cross section, the loss of tracks of recoil protons with energies below 0.5 Mev was taken into consideration, and a correction was also applied for multiple scattering of neutrons in the beryllium sphere.

DISCUSSION OF MEASUREMENT RESULTS

According to the results of our measurements with alpha particles and neutrons produced in the (n, 2n) reaction on Be^9, the total cross section for the reaction is 0.54 ± 0.07 b; this is in good agreement with the results of other authors.[3] Effective cross sections for the (n, 2n) reaction on Be^9 leading to the ground state in the Be^8 nucleus and the 2.43-Mev excited state in Be^9 can be estimated rather reliably. The stars formed in these cases consist of low-energy alpha particles; owing to the insufficient reliability in recording these events, their number was not determined in the experiment with alpha stars. The effective

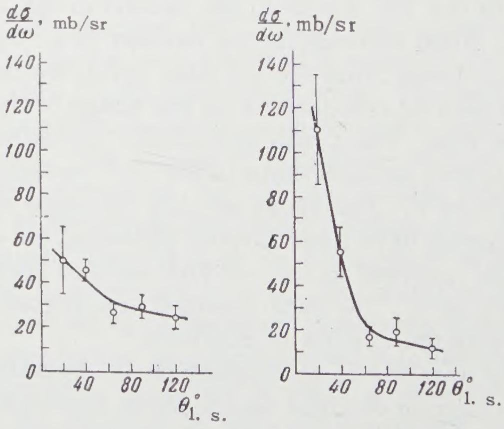

FIG. 4. Angular dependence of differential cross section for inelastic scattering of neutrons on Be^9.

cross section of interest to us can be computed, therefore, as the difference between the total effective cross section for the (n, 2n) reaction presented above and the effective cross section determined in the experiment with alpha stars. This difference amounts to 0.2 ± 0.1 b.

According to Anderson's data,[11] the cross section for the (n, n′) reaction on Be^9, leading to the formation of the 2.43-Mev excited state of the Be^9 nucleus, is 0.17 ± 0.03 b. Comparing these two values, we arrive at the conclusion that the formation of low-energy alpha stars occurs primarily upon the decay of the excited Be^9 nucleus from the 2.43-Mev level. In the experiment with alpha stars it was discovered that, along with stars due to decay of the Be^8 nucleus from the 2.9-Mev level, alpha stars are formed which may correspond to higher excited states of the Be^8 nucleus. The production of high-energy alpha particles in the (n, 2n) reaction on Be^9 is also confirmed by the shape of the alpha-particle energy spectrum, especially the spectrum of alpha particles emitted at large angles (for example 90°). From kinematic relations, alpha particles corresponding to the decay of highly excited nuclear states of Be^8 and Be^9 (decay of Be^9 into an alpha particle and a He^5 nucleus) become noticeable in the spectrum at large angles.

For reasons which we are about to state, it is most probable that the group of alpha stars associated with the ~ 5-Mev level of the Be^8 nucleus in reality owe their origin to a process which proceeds primarily without the formation of the Be^8 nucleus. This process may be explained either as the decay of a Be^9 nucleus into an alpha particle and a He^5 nucleus or as the four-particle decay of Be^{10}. At the same time, the group of alpha stars corresponding to the ~ 8 Mev level of the Be^8 nucleus is probably formed upon the decay of the Be^8 nucleus (possibly when the Be^8 nucleus decays from the broad, 11.7-Mev level with width $\Gamma = 6.7$ Mev[12]).

In reference 4, where beryllium was introduced into an emulsion in the form of a soluble compound, in order to reduce the background only those alpha stars were selected in which the alpha particles had equal ranges. Such a selection method favors the choice of cases corresponding to the decay of the Be^8 nucleus over other possible ways of forming two alpha particles. Here, it turned out that at energies up to ~ 7 Mev only alpha stars associated with the 2.9 Mev level of the Be^8 nucleus were observed; furthermore, the curve of the alpha star distribution falls off rather sharply on the high energy side. If we trace out a similar curve on our spectrum (Fig. 1), a considerable number of alpha stars remain in the ~ 5 Mev region beyond the curve; it is rather difficult to explain their origin as being due to the decay of the Be^8 nuclei in an excited state at 2.9 Mev. Moreover, applying an analogous selection process to our data, we discovered that only two groups of alpha stars, corresponding to the 2.9- and ~ 8-Mev excited states of the Be^8 nucleus, remain in the spectrum, which is also evidence for the above assertion. This conclusion is also confirmed by other works in which excited states of the Be^8 nucleus have been observed.[13] The shape of the spectra of alpha particles and neutrons is not inconsistent with these conclusions.

Therefore, the formation of a Be^8 nucleus in the 2.9-Mev excited state and the excitation of the 2.43-Mev level in the Be^9 nucleus seem to be basic channels for the (n, 2n) reaction on Be^9. It is possible that higher nuclear levels of Be^8 or Be^9 nuclei are also excited in the (n, 2n) reaction (the Be^9 levels of 6.8, 7.9 and 9.1 Mev; the 11.7-Mev level of Be^8). However, we cannot pursue in more detail the formation of excited states in the Be^8 and Be^9 nuclei. The scantiness of statistics does not allow us to distinguish with sufficient reliability groups of neutrons in the neutron spectra which could be due to transitions between various excited states of beryllium nuclei. Besides, the individual groups of neutrons will be extremely diffuse in energy because of the three-particle nature of the decay. A similar situation holds for the energy spectrum of alpha particles.

The absence of symmetry with respect to 90° in the angular distribution of neutrons with energies above 4 Mev (Fig. 4) indicates the marked contribution of direct processes to the Be^9(n, 2n) reaction for 14-Mev neutrons. Our experimental results are inadequate for a qualitative determination of the role, and even less the specific mechanism, of direct interactions in the investigated reaction.

The authors express gratitude to I. Ya. Barit and I. M. Frank for guidance and help in the work.

---

[1] E. Remy and K. Winter, Nuovo cimento **9**, 664 (1958). Winter, Torki, and Remy, Nuovo cimento **11**, 1 (1959). Vasil'ev, Komarov, and Popova, JETP **33**, 527 (1957), Soviet Phys. JETP **6**, 411 (1958).

[2] R. Wagner and P. Huber, Helv. Phys. Acta **31**, 89 (1958). G. J. Fischer, Phys. Rev. **108**, 99 (1957). Fowler, Hanna, and Owen, Phys. Rev. **98**, 249 (1955).

[3] L. Stewart and L. Rosen, Bull. Amer. Phys. Soc. **2**, 33 (1957). N. N. Flerov, Атомная энергия (Atomic Energy) **5**, 657 (1958). MacGregor, Ball, and Booth, Phys. Rev. **108**, 726 (1957). M. Sachs, Phys. Rev. **103**, 671 (1956).

[4] Cao Xuan Chuan, J. Phys. Radium **20**, 621 (1959).

[5] Masakatsu Sakisaka, J. Phys. Soc. Japan **14**, 554 (1959).

[6] V. Meyer and H. H. Staub, Helv. Phys. Acta **31**, 205 (1958).

[7] Perelygin, Myachkova, and Tolstov, Приборы и техника эксперимента (Instruments and Exptl. Techniques) (in press).

[8] B. J. Farmer and C. M. Class, Nucl. Phys. **15**, 626 (1960). T. A. Griffy and L. C. Biedenharn, Nucl. Phys. **15**, 636 (1960).

[9] Allred, Armstrong, and Rosen, Phys. Rev. **91**, 90 (1953).

[10] L. Rosen, Nucleonics **11**, **7**, 32; **11**, **8**, 38 (1953).

[11] Anderson, Gardner, McClure, Nakada, and Wong, Phys. Rev. **111**, 572 (1958). Bodansky, Eccles, and Halpern, Phys. Rev. **108**, 1019 (1957). E. M. Henley and P. D. Kunz, Phys. Rev. **118**, 248 (1960).

[12] F. Ajzenberg-Selove and T. Lauritsen, Nucl. Phys. **11**, 45 (1959).

[13] LaVier, Hanna, and Gelinas, Phys. Rev. **103**, 143 (1956). R. H. Spear, Austr. J. Phys. **11**, 502 (1958).

Translated by Mrs. J. D. Ullman
212

SOVIET PHYSICS JETP VOLUME 13, NUMBER 5 NOVEMBER, 1961

ANISOTROPY IN THE FISSION OF BISMUTH AND URANIUM IRRADIATED BY 660-Mev PROTONS

A. I. OBUKHOV and N. A. PERFILOV

Radium Institute, Academy of Sciences, U.S.S.R.

Submitted to JETP editor August 25, 1960

J. Exptl. Theoret. Phys. (U.S.S.R.) **40**, 1250-1252 (May, 1961)

The angular distribution of fission fragments from bismuth and uranium irradiated by 660-Mev protons was studied using nuclear emulsions. The perpendicular anisotropy coefficients were found to be 0.02 ± 0.06 and 0.04 ± 0.07 for bismuth and uranium respectively.

In the irradiation of nuclei by medium-energy particles, emission of fission fragments is observed predominantly at angles of 0 and 180° to the direction of the particles (longitudinal anisotropy).[1] This is due to the fact that the bombarding particle introduces an angular momentum perpendicular to the beam direction into the nucleus.[2-4] With increasing excitation energy of the fission, the angular distribution of the fragments tends to become isotropic.[4]

In the irradiation of uranium by 460-Mev protons[5] and 660-Mev protons,[6] and of tantalum by 450-Mev protons,[7] emission of fission fragments was observed predominantly at right angles to the beam (perpendicular anisotropy). A weak predominance of particle emission at 90° was observed for asymmetric fission in the irradiation of uranium and sodium by 155-Mev protons.[8] At the same time, a small longitudinal fission anisotropy was observed* in the irradiation of bismuth by 450-Mev protons.[9,7]

An explanation of the perpendicular anisotropy as being the result of a glancing collision of a fast bombarding particle with the nucleon of the nucleus has been proposed.[11] One of the particles taking part in the collision moves with a small velocity and at right angles, and is absorbed in the nucleus. The flux of such particles leads to an anisotropy longitudinal with respect to their direction and perpendicular with respect to the direction of the bombarding particles. However, according to such a mechanism, the perpendicular anisotropy could be expected only in fission with small excitation energies.[10]

In the present experiment, the fission anisotropy was studied using nuclear emulsions P-9 (ch) in the irradiation of bismuth by 660-Mev protons. For comparison, and in order to increase the accuracy of data obtained earlier,[6] the anisotropy of the fission of uranium induced by 660-Mev protons was studied with large statistics in the following three variants: for all fission events, for single fissions ($n_{\alpha p} = 0$), and for fissions with the emission of charged particles ($n_{\alpha p} \geq 1$). In order to check the method, the angular distribution of fission fragments in the irradiation of uranium with 14-Mev neutrons, i.e., in the energy range where the character of the anisotropy has been sufficiently well studied, was carried out.[1] The angles φ between the direction of the bombarding particle and the projection of the line passing through the end of the fission fragment ranges were measured. (This line coincides roughly with the direction of emission of fragments in the system of the nucleus undergoing fission.) The angular distribution in space, e.g., of a type $W(\theta) = 1 + C\sin^2\theta + D\sin^4\theta$, transforms in the projection into a distribution

$$\omega(\varphi) = 1 + c\sin^2\varphi + d\sin^4\varphi,$$
$$c = \tfrac{2}{3}\left(C + \tfrac{2}{5}D\right)/\left(1 + \tfrac{1}{3}C + \tfrac{3}{15}D\right),$$
$$d = \tfrac{8}{15}D/\left(1 + \tfrac{1}{3}C + \tfrac{3}{15}D\right). \qquad (1)$$

Using the method of least squares we found the anisotropy of the measured angular distribution of the projections of the emission directions of the fragments. From the anisotropy of the projections, we can transform to anisotropy in space using Eq. (1). The results obtained are shown in the table.

The excitation energy of nuclei at 660-Mev proton energy was found from the calculated relation between the longitudinal component of the momentum and the excitation energy.[7] The longitudinal component of the momentum of a nucleus was determined experimentally.[12] The value of the longitudinal anisotropy in the case of 14-Mev neutrons

---

*The recent report[10] of a systematic error in reference 9 makes the results given there uncertain.

	Number of fission events		Excitation energy, Mev	Type of angular distribution	Observed anisotropy
$U + n,\ E = 14$ Mev	Total:	3130	18.8	$1 + B\cos^4\theta$	$B = 0.46 \pm 0.11$
$Bi + p,\ E = 660$ Mev	Total:	5650	170 ± 25	$1 + C\sin^2\theta$	$C = 0.02 \pm 0.06$
$U + p,\ E = 660$ Mev	Total:	4441	140 ± 15	$1 + C\sin^2\theta$	$C = 0.04 \pm 0.07$
	$n_{\alpha p} = 0$	: 2083	85 ± 20		$C = 0.05 \pm 0.11$
	$n_{\alpha p} \geqslant 1$	: 2358	170 ± 25		$C = 0.01 \pm 0.10$

B = 0.46 ± 0.11 is in good agreement with the value W(0°)/W(90°) − 1 = 0.40 ± 0.14 found using an ionization chamber.[13]

In irradiation with 660-Mev protons, the perpendicular anisotropy is C = 0.02 ± 0.06 for bismuth and C = 0.04 ± 0.07 for uranium, i.e., the angular distribution of fission fragments is isotropic within the limits of experimental error. The results for uranium differ from the earlier data,[6] where a marked preponderance of emission of fragments at right angles was observed, i.e., W(90°)/W(0°) − 1 = 0.33 ± 0.19, increasing slightly with increasing excitation energy.

The reason for the discrepancy of the results, apart from statistical errors, may also be systematical errors due to the fact that in scanning a horizontal emulsion strip, the ends of the fragment tracks from fission events fall into the field of view, whereas the center of the event is outside the field of view, either above or below it. The probability of such an additional incidence increases with the angle between the emission of fission fragments and the direction of the strip. The detection of such events leads to a false perpendicular anisotropy (~ 0.12 for a field of view of 100 μm). In the present measurements, the emulsions were scanned in two mutually perpendicular directions to avoid possible systematical errors.

[1] I. Halpern, Ann. Rev. Nucl. Sci. **9**, 245 (1959).

[2] A. Bohr, First U. N. International Conference on the Peaceful Uses of Atomic Energy, 1955, Paper 911.

[3] V. M. Strutinskii, JETP **30**, 606 (1956), Soviet Phys. JETP **4**, 638 (1957); Атомная энергия (Atomic Energy) **2**, 508 (1957).

[4] I. Halpern and V. M. Strutinski, Second U. N. International Conference on the Peaceful Uses of Atomic Energy, 1958, Paper 1513.

[5] V. I. Ostroumov, Dokl. Akad. Nauk SSSR **103**, 409 (1955).

[6] Loshkin, Perfilov, and Shamov, JETP **29**, 292 (1955), Soviet Phys. JETP **2**, 116 (1956).

[7] N. T. Porile and N. Sugarman, Phys. Rev. **107**, 1410 (1957).

[8] J. W. Meadows, Phys. Rev. **110**, 1109 (1958).

[9] R. L. Wolke and J. R. Gutman, Phys. Rev. **107**, 850 (1957).

[10] M. V. Ramanian and N. Sugarman, Phys. Rev. **118**, 562 (1960).

[11] I. Halpern, Nucl. Phys. **11**, 522 (1959).

[12] A. I. Obukhov, JETP **35**, 1042 (1958), Soviet Phys. JETP **8**, 727 (1959).

[13] R. L. Henkel and J. E. Brolley, Phys. Rev. **103**, 1292 (1956).

Translated by H. Kasha
213

SOVIET PHYSICS JETP VOLUME 13, NUMBER 5 NOVEMBER, 1961

INELASTIC SCATTERING OF PROTONS BY Ne^{20} *NUCLEI*

P. V. SOROKIN, A. I. POPOV, V. E. STORIZHKO, and A. Ya. TARANOV

Physico-Technical Institute, Academy of Sciences, Ukrainian S.S.R.

Submitted to JETP editor November 5, 1960

J. Exptl. Theoret. Phys. (U.S.S.R.) **40**, 1253-1256 (May, 1961)

We have measured the absolute cross sections for the $Ne^{20}(p, p'\gamma)$ reaction and the angular distributions of p′ and γ corresponding to the first excited state of Ne^{20}, for resonance energies of 2.15 and 2.72 Mev. The partial widths and reduced widths for the 4.5- and 5.05-Mev levels of Na^{21} were determined. It is shown that the inelastic scattering of protons at 2.72 Mev is associated with a single level of the Na^{21} nucleus, having spin and parity $3/2^+$.

AMONG the resonances observed in the cross section for elastic scattering of protons by Ne^{20} nuclei, there is a resonance at $E_p = 2.72$ Mev corresponding to a level at 5.05 Mev in Na^{21}.[1,2] Attempts to determine the quantum numbers of this level by an analysis of experimental data on elastic scattering of protons by Ne^{20} proved to be unsuccessful.[1,2] The difficulty in the analysis is explained by the fact that this resonance is associated with closely spaced levels.

In the present work we have studied inelastic scattering of protons for $E_p = 2.72$ Mev for the purpose of obtaining additional information concerning the levels corresponding to this resonance. We have also studied the inelastic scattering $Ne^{20}(p, p'\gamma)$ at an energy of 2.15 Mev, corresponding to the 4.50 Mev level of Na^{21}, whose quantum numbers are reliably determined from data on elastic scattering.

METHOD OF MEASUREMENT

For the measurement of the angular distributions of the protons we used the chamber which has been described earlier.[3] The volume of the chamber was separated from the accelerator tube by a mica foil 0.5 μ thick. The chamber was filled with a normal isotopic mixture of neon (91% Ne^{20}) at a pressure of 8 mm Hg.

The scattered protons were recorded with a CsI(T1) crystal 0.1 mm thick and a FÉU-S photomultiplier. Pulses from the FÉU-S were analyzed by a 100-channel analyzer (AI-100). The energy resolution of the spectrometer was 6% for $E_p = 2$ Mev. In Fig. 1 we show the spectrum of protons scattered by Ne^{20} nuclei at an angle of 90° for the resonance energy $E_p = 2.72$ Mev.

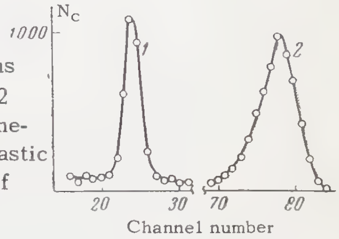

FIG. 1. Spectrum of protons scattered by Ne^{20} for $E_p = 2.72$ Mev. Peak 1 corresponds to inelastic scattering, peak 2 to elastic scattering (N_c is the number of pulses per channel).

In studying the γ rays from the $Ne^{20}(p, p'\gamma)$ reaction, the primary protons passed through a mica window 1 μ thick and entered a chamber 15 mm in diameter, filled with neon to a pressure of 10 mm Hg, which served as the target. The γ rays were recorded by a pair of FÉU-S photomultipliers with NaI(T1) crystals of dimensions 40 × 40 mm. One of them was held fixed, while the other rotated around the target. Pulses from the fixed photomultiplier entered a single-channel analyzer which gave the full absorption peak which corresponded to an energy $E_\gamma = 1.64$ Mev. This photomultiplier was used as a monitor.

The pulses from the movable photomultiplier were analyzed by an AI-100 100-channel pulse analyzer. The resolution of the γ spectrometer for the Cs^{137} γ rays was 9%. In Fig. 2 is shown part of the spectrum of the 1.64 Mev γ ray with the total absorption peak, taken for $E_p = 2.72$ Mev.

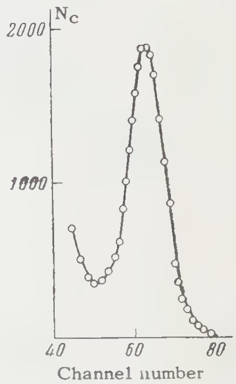

FIG. 2. Portion of the spectrum of γ rays around 1.64 Mev with total absorption peak, taken for $E_p = 2.72$ Mev.

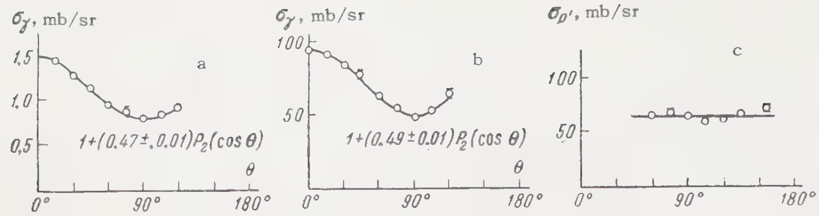

FIG. 3. Differential cross section for inelastic scattering of protons p′ and corresponding γ rays from the Ne^{20} (p,p′ γ) reaction: a – for E_r = 2.15 Mev; b – for E_r = 2.72 Mev.

For accelerating the protons we used the 4-Mev Van de Graaff accelerator of the Physico-Technical Institute of the Academy of Sciences of the Ukrainian S.S.R. The proton current at the target was ~ 1 μa.

RESULTS OF THE MEASUREMENTS

In Fig. 3 are shown the results of measurements of the cross section for inelastic scattering $Ne^{20}(p, p'\gamma)$ for protons p′ and γ rays as a function of the angle of scattering, at resonance energies E_r equal to 2.15 and 2.72 Mev. In the figure we show only the statistical errors which determine the precision of measurement of the angular distributions. The curves are drawn through the experimental points using the least squares method. Analytic expressions for the angular distributions are also shown in Fig. 3. The total cross sections are given in the table.

From data on elastic scattering it has been established[1,2] that the 4.50 Mev level of Na^{21}, corresponding to the resonance at 2.15 Mev, is formed by capture of a proton with orbital angular momentum $l = 2$; the spin and parity of this level is $3/2^+$. Using these data and assuming that the inelastically scattered proton emerges with orbital angular momentum $l' = 0$ and that the transition between the first excited 2^+ state and the ground 0^+ state of Ne^{20} is a pure E2-transition, we have calculated the angular distributions of the protons p′ and γ rays from the formulas given in the paper of Kraus et al.[4] From the table we see that the computed value of the coefficient A_2 in the angular distribution of the γ rays, $1 + A_2P_2(\cos\theta)$, is in good agreement with experiment. This agreement on the one hand is a check of the method, and on the other, what is more important, it shows the validity of the assumptions made in computing the angular distributions.

As one sees from the table, the angular distributions of the protons p′ (which are close to isotropic) and the γ rays for the resonance energy 2.72 Mev are in very good agreement with the computations if one assumes that there corresponds to this resonance a single level with spin and parity $3/2^+$. The result obtained does not agree with the data on elastic scattering, according to which this resonance cannot be explained by the presence of a single level.

In order to find other levels we carefully studied the shape of the resonance. Significant deviations from the shape corresponding to a single level were not found. We also measured the angular distributions of the γ rays for various energies of protons around the resonance. We still found the same results. All of this shows that only a single level is effective in the inelastic scattering at E_p = 2.72 Mev.

Using the expression for the area A under the resonance

$$A = 2\pi^2\lambda\!\!\!^-{}^2 (J + 1/2)\, \Gamma_p\Gamma_{p'} / \Gamma,$$

where $\lambda\!\!\!^-$ is the wave length of the impinging protons, J the spin of the intermediate state, Γ the total width of the level, Γ_p and $\Gamma_{p'}$ widths corresponding to elastic and inelastic scattering, we calculated the values of $\Gamma_p\Gamma_{p'}/\Gamma$. The results of these computations (cf. the table) do not depend on the target thickness or the sharpness of energy of the impinging protons.

Analysis of the γ ray spectrum shows that the cross section for radiative capture, $Ne^{20}(p, \gamma)Na^{21}$, for the resonances studied is very small. We can therefore assume that for the corresponding levels $\Gamma = \Gamma_p + \Gamma_{p'}$. From a comparison of the value Γ_p^2/Γ = 18 kev^2 and $\Gamma_p\Gamma_{p'}/\Gamma$ (cf. the table) for the 4.5-Mev level it follows that $\Gamma_{p'}/\Gamma_p$ = 0.005. This shows that for this level $\Gamma_p = \Gamma$ and $\Gamma_p\Gamma_{p'}/\Gamma = \Gamma_{p'}$ = 0.1 kev.

E_p, Mev	E_{exc}, Mev	Γ, Kev	σ_{res} mb	J^π	$\Gamma_p\Gamma_{p'}/\Gamma$, kev	$\gamma_{p'}^2$, kev	$\frac{\gamma_{p'}^2 \cdot 2mR^2}{3\hbar^2}$	A_2 for the γ ray	
								experiment	theory
2.15	4.50	17	13±3	$3/2^+$	0.10±0.03	50	0,02	0.47±0.03	0,5
2.72	5.05	36	800±100	$3/2^+$	10÷2	100	0,04	0,49±0.01	0,5

For the 5.05 Mev level the value $\Gamma_p \Gamma_{p'}/\Gamma = 10$ kev with a total width $\Gamma = 36$ kev can be obtained under the condition that $\Gamma_p = \Gamma_{p'}$. This means that in this case $\Gamma_{p'} = 18$ kev.

Using these values we calculated the reduced widths for inelastic scattering $\gamma^2_{p'} = \Gamma_{p'} A^2_{l'}/2\rho$. The barrier penetrability $A^2_{l'}/2\rho$ was determined from the graphs given in reference 5. The values of $\gamma^2_{p'}$ and their ratio to the quantity $3\hbar^2/2mR^2$ are given in the table.

The authors express their gratitude to A. K. Val'ter for his interest in the work and also to A. A. Tsygikalo and Yu. A. Kharchenko and the crew of the electrostatic generator.

[1] W. Haeberli, Phys. Rev. **99**, 640 (A), 1955.

[2] A. K. Val'ter et al., Izv. Akad. Nauk S.S.S.R. Ser. Fiz. **24**, 884, 1960.

[3] A. K. Val'ter et al., Izv. Akad. Nauk S.S.S.R. Ser. Fiz. **23**, 839, 1959; Columbia Tech. Transl, p. 833.

[4] A. A. Kraus, Jr. et al., Phys. Rev. **104**, 1667, 1956.

[5] Nuclear Reactions, ed. P. M. Endt and M. Demeur, **1**, Amsterdam 1959.

Translated by M. Hamermesh
214

SOVIET PHYSICS JETP VOLUME 13, NUMBER 5 NOVEMBER, 1961

NEUTRONS FROM THE C^{12} (t, n) *REACTION*

P. I. VATSET, L. Ya. KOLESNIKOV, and S. G. TONAPETYAN

Physico-Technical Institute, Academy of Sciences, Ukrainian S.S.R.

Submitted to JETP editor, November 25, 1960

J. Exptl. Theoret. Phys. (U.S.S.R.) **40**, 1257-1260 (May, 1961)

The neutron yield at an angle of 0° from the $C^{12}(t, n)$ reaction has been studied over a range of triton energies from 0.37 to 2.4 Mev. Seven resonances were observed corresponding to excited states of N^{15} with excitation energies of 15.887, 15.955, 16.066, 16.206 16.326, 16.430, 16.582, 16.67, and 16.77 Mev. For five values of the energy of the bombarding tritons we measured the angular distributions of the neutrons. It was established that the angular distributions for triton energies greater than 1 Mev are anisotropic, and that for energies above 1.5 Mev they are characterized by a marked predominance of neutrons in the backward direction. From the angular distributions we have determined the value of the total cross section of the reaction, which is equal to 4.8 ± 0.2 mb for $E_t = 0.652$ Mev and increases to 298.6 ± 19.7 mb for $E_t = 2.017$ Mev.

THE use of tritium in nuclear reactions as a bombarding particle is unquestionably of interest for nuclear spectrometry. In the interaction of tritons with nuclei one studies mainly reactions with yield of charged particles, whereas a study of the yield of neutrons has been comparatively slighted in the various papers.[1-6]

In the present paper we discuss the results of experiments on the yield of neutrons from the reaction

$$C^{12} + H^3 \rightarrow N^{15} \rightarrow N^{14} + n, \qquad Q = 4.007 \text{ Mev}. \qquad (1)$$

The minimum energy of excitation of the intermediate nucleus in reaction (1) is 14.848 Mev.[7] Measurement of the excitation function made it possible to obtain information concerning excited levels of the intermediate nucleus N^{15} with energies of excitation above this minimal energy. The study of the angular distributions of the outgoing neutrons for various triton energies made it possible to determine the total cross section for the $C^{12}(t, n)$ reaction for the corresponding triton energies.

The fact that in experimental practice one frequently observes a deposit of carbon on the target bombarded by accelerated ions makes the study of the reaction of tritons with carbon of technical interest.

Despite the high effective potential barrier for tritons on carbon, equal to 3.14 Mev, the yield of neutrons from the $C^{12}(t, n)$ reaction is sizable in the range of lower energies of impinging particles.

ARRANGEMENT OF THE EXPERIMENT AND RESULTS OF THE MEASUREMENTS

The arrangement of the experiment, the measurement technique, and the analysis of the background neutrons has been discussed in detail previously.[4,5]

In the studies we used targets of carbon which were deposited on a platinum disk 16 mm in diameter and 0.2 mm thick by using a smoky flame from a burner while burning purified benzene. To eliminate possible dirtying of the target, it was heated at a temperature somewhat lower than the ignition temperature of carbon. The target thickness was determined by weighing on a microbalance. The additional weight of the target was checked by the relative yield of neutrons per unit weight of target for a single triton energy.

In the experiments we used targets of thickness 0.14, 0.195, 0.22, and 0.24 mg/cm², in which the energy losses for tritions with an energy of 1.6 Mev were respectively 49, 66, 75, and 82 kev.

In Fig. 1 is shown the dependence on triton energy of the differential cross section for the yield of neutrons at an angle of 0°.

The differential cross section increases slowly from 0.22 ± 0.13 to 2.31 ± 0.24 mb/sr as the triton energy increases from 0.450 to 1.055 Mev, and then increases sharply, reaching a value of 56.4 ± 2.7 mb/sr for a triton energy of 2.371 Mev. The absolute errors of the cross section determination vary from 18 to 10% within the interval of triton

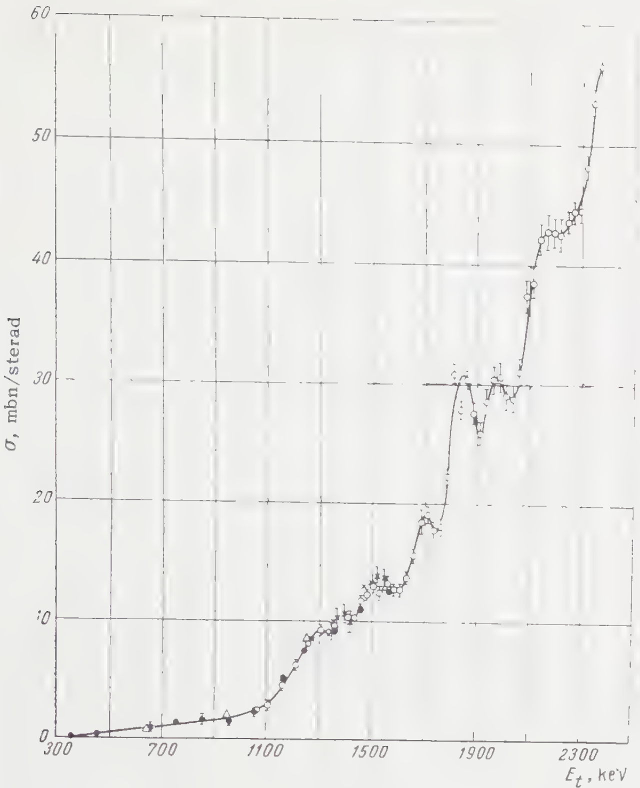

FIG. 1. Differential cross section for neutron yield at an angle of 0° from the reaction C^{12} (t,n) for target thicknesses: × – 0.14, • – 0.195, ○ – 0.22, Δ – 0.24 mg/cm^2.

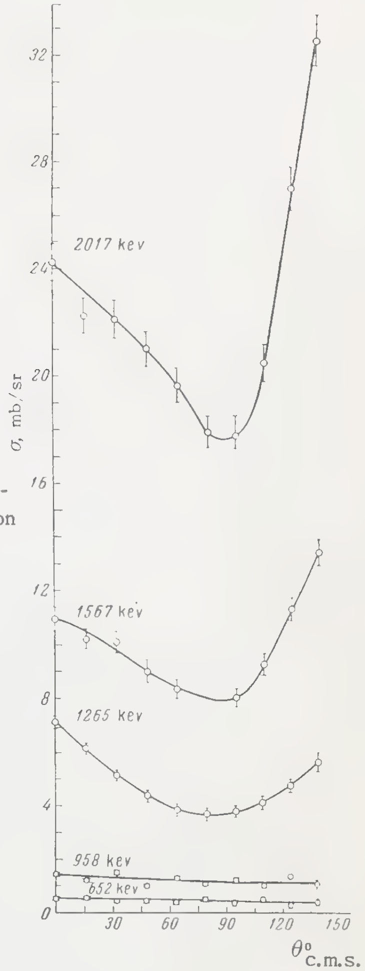

FIG. 2. Angular distributions in the C^{12} (t,n) reaction in the c. m. s.

energies from 0.650 to 1.1 Mev, and from 10 to 5% in the energy interval from 1.1 to 2.371 Mev.

In the determination of the absolute uncertainties, the error in determining the number of carbon nuclei was assumed to be ± 3%, the error in determining the number of tritons incident on the target ± 1%, the error in determining the strength of the standard Ra + Be source by which we calibrated the neutron detector was ± 3%, the error in determining the triton energies was ± 0.5%. No corrections were made for the yield of neutrons from the C^{13}(t, n) reaction.

On the excitation curve of the C^{12}(t, n) reaction we observe resonances for triton energies of 1.300, 1.385, 1.525, 1.700, 1.850, 1.980, and 2.170 Mev. In addition, the behavior of the experimental points indicates the presence of a resonance for a triton energy of 2.28 Mev, and finally the rise in the excitation function above 2.3 Mev gives a basis for assuming the existence of a resonance in the region of 2.4 Mev. To these resonances there correspond highly excited levels in N^{15}, whose energies are given in the table. In the same table, in the second column, we give the energy levels of N^{15} found by other authors (from the B^{11}(α, n) N^{14} reaction — the data of Haddad et al. given in reference 7, the N^{14}(n, α) B^{11} reaction — data from reference 8, C^{13}(d, p)C^{14},[9] and C^{13}(d, n) N^{14},[7,10] including the data from the latest paper of Ajzenberg and Lauritsen.[11]

There is no information in the literature concerning the energy level at 15.887 Mev. The level at 16.206 Mev has not previously been mentioned, but its presence is confirmed by the weak reso-

Energies of levels in N^{15} (Mev)

Data of the present work	Data from the literature	Data of the present work	Data from the literature
—	15.61 [7,11]	12.206±0.020	(16.24)[8]
15.887±0.018	—	16.326±0.021	16.38 [8,11]
—	15.92 [7,11]	16.430±0.022	16.47 [9] } 16.50[11]
15.955±0.019	15.93 [7,11]	16.582±0.023	16,59 [8]
—	15.99 [7,11]	16.67±0.03	16.67[8] } 16.69[11]
16.066±0.020	16.04[7],16.06[8],16,05[11]	16.77±0.05	16.72[10]

nance in the excitation function of the $N^{14}(n, \alpha)B^{11}$ reaction[8] for an α particle energy of ~ 5.8 Mev, which was not pointed out by the authors. The remaining levels, as one sees from the table, coincide within the limits of experimental error with those given in the literature. (For example, in the work of Gabbard et al.,[8] the error in the determination of the energy of the levels exceeds ± 70 kev.)

In Fig. 2 are shown angular distributions of the neutrons in the center of mass system from the $C^{12}(t, n)$ reaction, obtained for triton energies of 0.652, 0.958, 1.265, 1.567, and 2.017 Mev over an angular range from 0 to 135° with respect to the incident triton beam. For triton energies of 0.652 and 0.958 Mev the angular distributions are isotropic within the limits of error of the measurements. With increasing energy of the tritons the relative yield of neutrons at angles 0 and 135° increases.

A characteristic feature of the angular distribution is the increase in neutron yield in the backward direction with increasing triton energy. Thus for a triton energy of 1.265 Mev the angular distribution curve is almost symmetric around 90°. For an energy of 1.567 Mev the ratio of the differential cross section for neutrons at 135° to the cross section for neutrons at 0° becomes equal to 1.18, while for an energy of 2.017 Mev this ratio increases to a value of 1.28.

On the basis of the neutron angular distributions we obtain computed values for the total cross section for the yield of neutrons from the $C^{12}(t, n)$ reaction. For triton energies of 0.652, 0.958, 1.265, 1.567, and 2.017 Mev these cross sections are equal respectively to 4.9 ± 0.2, 14.6 ± 0.7, 59.6 ± 2.7, 129.5 ± 6.2, and 298.6 ± 19.7 mb.

---

[1] R. W. Crews, Phys. Rev. **82**, 100 (1951).

[2] Ajzenberg-Selove, Jarmie, and Haddad, Bull. Amer. Phys. Soc. **4**, 258 (1958).

[3] N. Jarmie, Phys. Rev. **98**, 41 (1955).

[4] A. K. Val'ter et al., JETP **40**, 1237 (1961), this issue, p. 971.

[5] A. K. Val'ter et al., Атомная энергия (Atomic Energy) in press.

[6] A. K. Val'ter et al., Ukr. J. Phys. (in press).

[7] F. Ajzenberg-Selove and T. Lauritsen, Nucl. Phys. **11**, 179 (1959).

[8] Gabbard, Bichel, and Bonner, Nucl. Phys. **14**, 277 (1959).

[9] F. P. G. Valckx, Ph. D. Thesis, University of Utrecht, 1956 (cf. also reference 7).

[10] J. B. Marion and G. Weber, Phys. Rev. **103**, 167 (1956). J. E. Richardson, Phys. Rev. **80**, 850 (1950).

[11] F. Ajzenberg-Selove and T. Lauritsen. Technical Report: Energy Levels of Light Nuclei, August, 1960.

Translated by M. Hamermesh
215

SOVIET PHYSICS JETP VOLUME 13, NUMBER 5 NOVEMBER, 1961

SPONTANEOUS FISSION OF Am^{241}

V. A. DRUIN, V. L. MIKHEEV, and N. K. SKOBELEV

Joint Institute for Nuclear Research

Submitted to JETP editor December 3, 1960

J. Exptl. Theoret. Phys. (U.S.S.R.) **40**, 1261-1262 (May, 1961)

A gas scintillation counter filled with xenon was used to measure the spontaneous-fission half-period of Am^{241}. A value of $(2.3 \pm 0.8) \times 10^{14}$ years was found, in contrast to the previously accepted value of 1.4×10^{13} years.

RESULTS of experiments for verifying the half-period of the spontaneous fission of Am^{241} were reported earlier.[1] However, the considerable background counting rate of the setup did not permit us to find the real value of the decay constant. Nevertheless, it followed from the experiment that the limit of the decay period as found by Segrè[2] was underestimated. In the meantime, we have continued our efforts to find and remove the sources of the background, and to check on the operation of the gas scintillation counter, in order to obtain a more exact value of the lifetime of Am^{241}.

The main sources of the background in our experiment may be induced fission of nuclei in the scintillation chamber, electromagnetic pickup in the electronic circuits, and instability of power supplies.

In the first series of experiments, a sample of U^{235} placed in the chamber for the calibration of the counter remained open during the experiments with Am^{241}. In spite of the fact that the counter was surrounded by cadmium and paraffin, it was impossible to exclude completely the possibility of the fission of U^{235} by thermal neutrons. In order to remove this sort of background, a magnetic shutter was placed into the chamber, which enabled us to close the U^{235} sample after carrying out check measurements. This arrangement achieved a marked decrease in the background.

The results of the measurements can be also distorted by electromagnetic pickup and instability of the power supplies. In particular, the pickup due to atmospheric discharges was dangerous, since the measurements were carried out during the summer. In order to remove this source of background, a "storm monitor" (a sensitive amplifier with an antenna at its input) was used. The pulses from the photomultipliers and from the storm monitor were simultaneously recorded on a pen recorder incorporated into the system.

After this refinement of the apparatus, the experiments on the spontaneous fission of Am^{241} were carried out. During the measurements, 12 pulses were recorded on the pen recorder. Two of these coincided with pulses from the storm monitor, and were therefore considered as background pulses.

In order to check the operation of the whole array, control experiments on the spontaneous fission of a sample of Pu^{240} were carried out in the presence of the working sample of Am^{241}. The counter characteristics had a good plateau, similar to the one in the previous experiment.[1] The result obtained for Pu^{240} is in agreement with the known data for the half-period of Pu^{240} within the limits of acceptable error.[3]

Thus, during 200 hours of measurement with a 60 μg Am^{241} sample, ten spontaneous-fission events were observed, which corresponds to a half-life of $(2.3 \pm 0.8) \times 10^{14}$ years.

The experiment was carried out under the supervision of Prof. G. N. Flerov.

---

[1] Mikheev, Skobelev, Druin, and Flerov, JETP **37**, 859 (1959), Soviet Phys. JETP **10**, 612 (1960).

[2] E. Segrè, Phys. Rev. **86**, 21 (1952).

[3] Chamberlain, Farwell, and Segrè, Phys. Rev. **94**, 156 (1954).

Translated by H. Kasha
216

SOVIET PHYSICS JETP VOLUME 13, NUMBER 5 NOVEMBER, 1961

PRODUCTION OF TRITIUM IN LEAD AND ALUMINUM BY HIGH-ENERGY PROTONS, DEUTERONS, AND ALPHA PARTICLES

V. V. KUZNETSOV

Joint Institute for Nuclear Research

Submitted to JETP editor December 3, 1960

J. Exptl. Theoret. Phys. (U.S.S.R.) **40**, 1263-1269 (May, 1961)

Experimental data are presented on the production of tritium in lead and aluminum by 70 — 390 Mev deuterons and 140 — 750 Mev α particles, and in zinc and cadmium by 750-Mev α particles. The tritium yields from aluminum and lead targets of different thicknesses bombarded with 660-Mev protons are given.

EXPERIMENTAL PROCEDURE

TRITIUM production by high-energy protons has been investigated by many authors,[1-9] but relatively few investigations of tritium production by deuterons and α particles have been published.[5,10] In the present work tritium production in metals by high-energy deuterons and α particles is studied.

As in earlier work,[7] the targets were made of aluminum and lead with the dimensions (1.5 — 2) × 6 × (15 — 30) mm, and were bombarded by 70 — 390 Mev deuterons and 140 — 750 Mev α particles in the internal beam of the synchrocyclotron of the Joint Institute for Nuclear Research.

Three to six target samples were fastened simultaneously to a heavy aluminum holder. Heat was removed from the target through the holder, which was clamped tightly to the synchrocyclotron probe. When lead targets were bombarded the deuteron beam was reduced to one-half or one-third of the maximum, 2×10^{12} deuterons/sec. The intensity of the α-particle beam was $(4 - 5) \times 10^{10}$ particles/sec. The beam direction was parallel to the 6-mm side of the target. Different bombarding energies were associated with the positioning of the targets in orbits of different radii within the vacuum chamber of the synchrocyclotron. Deuteron bombardment lasted from 2 to 5 min, while α particle bombardment lasted from 5 to 20 min.

The amount of tritium in a bombarded target was determined by separating the tritium component from the target using the vacuum system represented in Fig. 1. This system consists of a quartz tube 1 for melting the targets, a palladium filter 4 with an electric heater, where a hydrogen-tritium mixture was separated from the other gaseous reaction products, a mercury pump 5 producing the required pressure drop when the active hydrogen-tritium mixture was admitted, and a Geiger counter shielded (9) by 35 mm of steel and 35 mm of lead. The system was also equipped with glass reservoirs for hydrogen, pure helium, and alcohol (10), and with an extra vessel 11 for dilution of the highly active mixture.

The targets were melted in the 200-cm³ quartz tube in a hydrogen atmosphere at 40 — 100 mm Hg. Each melted target was kept in the hydrogen atmosphere at 850 — 950° C for 40 — 100 min, resulting in

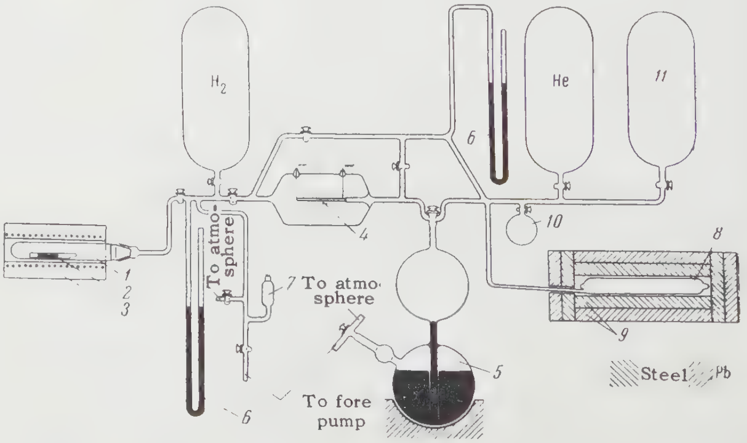

FIG. 1. Diagram of vacuum system: 1 – quartz tube, 2 – target, 3 – furnace, 4 – palladium filter, 5 – vacuum pump, 6 – mercury manometer, 7 – VK-1 vacuum tube, 8 – MS-9 counter, 9 – shield, 10 – ethyl alcohol container, 11 – additional vessel.

Target material	Energy of bombarding deuterons, Mev	N_T/N_{Na}	σ_T	No. of runs	Target material	Energy of bombarding α particles, Mev	N_T/N_{Na}	σ_T	No. of runs
Al	70	0.57±0.10	12.5±3.1	6	Al	140	1.48±0.16	44.7±9.1	8
Pb	70	1,85±0,44	40,8±12.5	6	Pb	140	3.27±0.41	98,1±21,2	13
Al	150	1.33±0.05	29.2±4.7	6	Al	300	2.10±0.12	52.5±9,2	6
Pb	150	3,60±0.13	79.2±12,8	6	Pb	300	3.76±0.74	94,0±25.4	8
Al	270	1.35±0.05	29,7±4.6*	6	Al	540	2.62±0.42	52,4±9,6*	6
Pb	270	3.78±0.22	83.6±14.6*	5	Pb	540	4.88±1,04	97.6±27,0*	10
Al	390	1.73±0.06	38.1±6.0*	9	Al	750	2.71±0.17	48.8±8.6*	6
Pb	390	3,97±0.91	87.3±15.9*	12	Zn	750	4,40±0.45	79.2±16.0*	2
					Cd	750	4.80±1.30	86.4±27.2*	2
					Pb	750	10.82±0.75	194.8±35.4*	14

*Cross sections σ_T for tritium production were obtained by using extrapolations of data on Na^{24} production in aluminum[11,12] by high-energy deuterons and α particles.

the removal of ~ 90% of the tritium; this was checked by remelting under the same conditions. The vacuum system made available for measurement 4 to 63% of the hydrogen-tritium mixture produced by melting of the targets. This mixture produced a pressure of 1 to 25 mm Hg in the counter.

Beta particles from tritium decay were registered by a cylindrical ~ 200 cm^3 counter with a copper cathode. The counter contained, in addition to the hydrogen-tritium mixture, a working mixture of ethyl alcohol at 15 mm and helium at 95 – 100 mm. The counter was operated in the Geiger region, in most instances with the following characteristics: 100 – 150 v plateau, plateau slope not greater than 10% at 100 v, and intrinsic background 130 – 200 pulses/min. Under higher hydrogen pressure (> 15 mm) the counter characteristics were adversely affected: ~ 50 – 80 v plateau, and 15 – 20% slope at 100 v. The measured tritium activity amounted to 500 to 10 000 pulses/min. The efficiency of β-particle registration from tritium decay is estimated at about 90%.

The deuteron and α particle intensities were monitored by aluminum foils, as described in reference 7. The dependences of the yields from the reactions $Al^{27}(d, \alpha p)Na^{24}$ and $Al^{27}(\alpha, \alpha 2pn)Na^{24}$ on bombarding energy were taken from the literature.[11,12] The cross sections for Na^{24} production in aluminum by deuterons above 200 Mev and α particles above 400 Mev were determined by extrapolating the Na^{24} yields to higher energies. The cross section for Na^{24} production in aluminum by 270-Mev and 390-Mev deuterons is estimated at ~ 22 mb. ~ 20 mb and ~ 18 mb are obtained for 540-Mev and 750-Mev α particles, respectively.

Beta particles from Na^{24} decay were registered by a counter with a quartz end window (< 5 mg/cm^2). The detecting equipment registered ~ 18% of the entire activity of a sample.

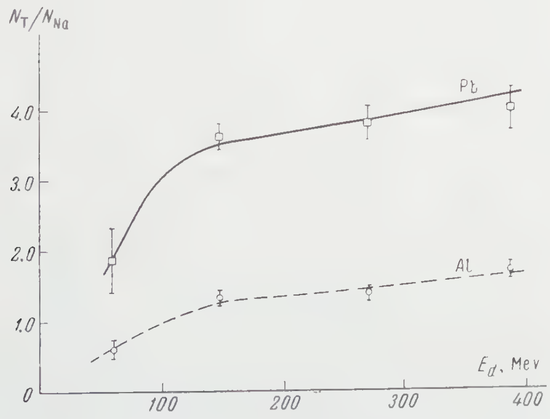

FIG. 2. Relative yields of tritium from aluminum and lead vs deuteron energy.

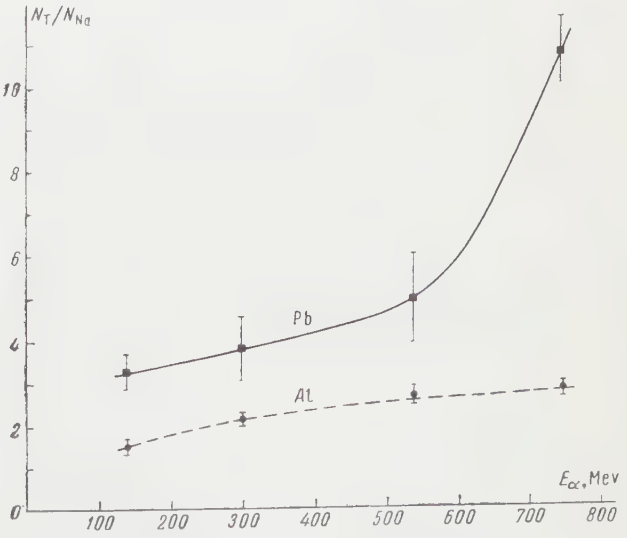

FIG. 3. Relative yields of tritium from aluminum and lead vs α-particle energy.

EXPERIMENTAL RESULTS

The table gives the relative yields N_T/N_{Na} and the cross sections σ_T for tritium production* in aluminum and lead bombarded with 70 — 390 Mev deuterons and 140 — 750 Mev α particles. The relative yields of tritium from zinc and cadmium bombarded by 750-Mev α particles are also given. The relative yields are the averages of at least five independent measurements, except for zinc and cadmium, in which cases only two measurements were averaged. Determination of the cross sections σ_T took into account the systematic experimental errors and the errors in determining the cross section for Na^{24} production in aluminum.

The probable experimental error was estimated by constructing a histogram of the departures of relative tritium yields from the average in all runs. The error, which was the half-width of the near-Gaussian distribution, was under 15%.

Figures 2 and 3 show the relative yields of tritium from aluminum and lead vs deuteron and α-particle energies. The relative yields from aluminum do not increase much with the bombarding energy. In the case of lead the increase is much more pronounced for both deuterons and α particles.

Figure 4 shows the dependence of tritium production by 750-Mev α particles on atomic number. The yield increases with the atomic number just as in the case of bombardment by 450-Mev and 660-Mev protons.[7] With 750-Mev α particles the tritium yield from lead is about four times greater than that from aluminum; corresponding values of A differ by a factor of about 8.

As a basis for deciding on target thicknesses the tritium yields were determined from 60 — 1500μ lead targets and 500 — 2000μ aluminum targets bombarded by an internal 660-Mev proton beam. Three 6 mm × 20 mm targets were fastened to the aluminum holder at one time. The beam path was parallel to the 6-mm side of the targets. Lead targets were covered with 2-mm aluminum. In this way the number of protons passing through the lead targets was reduced to less than one-tenth of the maximum intensity (5×10^{12} protons/sec), and the proton flux was more uniformly distributed throughout the target thickness.

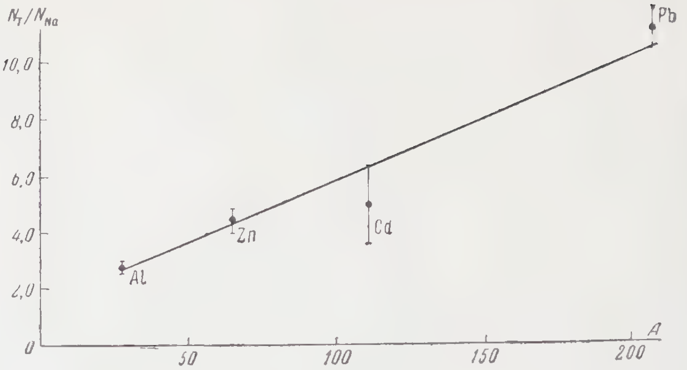

FIG. 4. Relative yield or tritium produced by 750-Mev α-particles vs atomic weight of target.

Figure 5 shows the experimental tritium yields from aluminum and lead targets of different thicknesses. The tritium yield is practically constant for lead thicknesses greater than 800μ and aluminum thicknesses greater than 500μ. For lead thicknesses less than 800μ the tritium yield is observed to decrease.

The triton energy spectrum can be determined indirectly from the given experimental setup with a lead target. For this purpose calculated curves of tritium yields from lead targets of different thicknesses are plotted in the figure. The method of calculation is similar to that described in reference 13 for the emission of lithium fragments from lead foils of different thicknesses bombarded with protons. In the present work it was assumed that the experimentally observed tritium was formed only by evaporation and that the angular distribution of the tritons is isotropic. The triton energy spectrum was obtained from the formula

$$P(E) = (E - V)\,\tau^{-2} e^{-(E-V)/\tau},$$

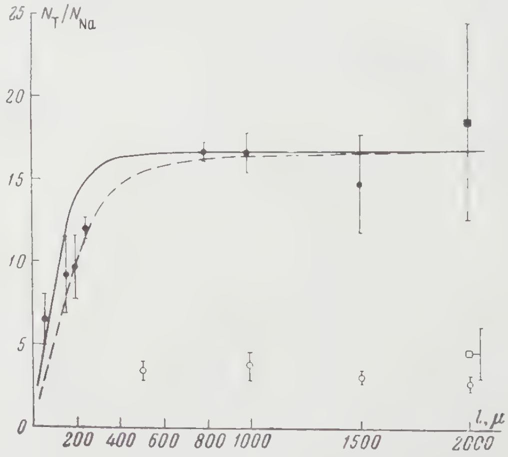

FIG. 5. Tritium yields from different thicknesses l of aluminum (open circles) and lead (filled circles) targets. The small squares represent data from reference 7. The solid curve was calculated from evaporation theory for τ = 3.5 Mev and V = 7 Mev, and the dashed curve for τ = 5 Mev and V = 7 Mev.

---

*The cross section for tritium production was determined from the formula $\sigma_T = \sigma_{Na} N_T/N_{Na}$, obtaining N from $N = N_0 e^{\lambda t_2}/(1 - e^{\lambda t_1})$, where t_1 is the duration of target bombardment, t_2 is the length of time from the determination of bombardment to the start of activity measurement, N_0 is the activity per gram-atom of the target material at the time t_2, and λ is the decay constant.

in Heisenberg's evaporation theory.[14] The parameters τ and V, representing the temperature of the nucleus and the Coulomb barrier, respectively, were selected to satisfy the experimental results.

The two curves shown in Fig. 5 were calculated with two sets of parameters: $\tau = 3.5$ Mev, $V = 7$ Mev and $\tau = 5$ Mev, $V = 7$ Mev. The second set is in better agreement with experiment.

The mean temperature $\tau = 5$ Mev is higher than that predicted by the existing evaporation theory ($\tau_{\text{evap}} \approx 3$ Mev). This indicates that evaporation is not the only mechanism for tritium production by high-energy protons. Wade et al.[5] observed some anisotropy of triton emission favoring the forward direction in proton, deuteron, and α-particle bombardments. Lefort et al.[8] observed ~10% fast tritons unaccounted for by the existing evaporation theory, in addition to the bulk of the tritons, which are associated with evaporation. The experimental tritium yields from lead targets of different thicknesses show that the triton kinetic energy does not generally exceed 30 — 40 Mev. Our experimental arrangement permits an additional contribution from cascade neutrons and neutrons of "evaporation" origin from both the target and screening aluminum. The additional triton yield from interactions of evaporation and cascade neutrons with the aluminum screening of the targets was investigated separately. A stack of 14 identical 400-μ aluminum foils was irradiated with 400-Mev deuterons for 10 min in the internal synchrocyclotron beam. Foil activity decreased progressively with depth in the stack. This experiment was intended to determine the systematic increase of N_T/N_{Na} from the first to the last foil. The failure to observe this increase indicates that less than 10% of the tritium results from interactions of cascade and evaporation neutrons with the aluminum.

DISCUSSION OF RESULTS

Figures 2 and 3 and the table show that the tritium yield from aluminum is not observed to increase strongly with the bombarding energy. However, the yield from lead increases appreciably with deuteron energy, and even more strongly as α-particle energy is increased from 540 to 750 Mev. In the latter case the effect apparently results from a considerable increase of the excitation energy due to nuclear capture of pions created in nucleon-nucleon collisions.

The mean excitation energies were calculated for the bombardment of both aluminum and lead by deuterons and α particles, using both the present data and the results given in reference 7. The formulas of Hagedorn and Macke were used,[14] showing direct dependence of tritium production probability on nuclear excitation energy. The combined data indicate that 70-Mev deuterons and 140-Mev α particles striking a target nucleus contribute almost all their energy to nuclear excitation. Hence the mean excitation energy of aluminum and lead bombarded by 390-Mev deuterons is estimated at ~65 Mev and ~110 Mev, respectively; for 750-Mev α particles the mean values are ~150 Mev and ~180 Mev, respectively.

An analysis of the tritium production cross sections in reference 7 at bombarding energies < 200 Mev shows highest probability for α particles, followed by deuterons and protons, in that order. A deuteron or α particle impinging on a target nucleus must evidently be treated as two or four independent particles, respectively, which participate independently in cascade development within the nucleus; this leads to large energy transfer to the target nucleus and thus to a high probability of tritium production. It must not be forgotten, however, that in deuteron and α-particle bombardments a possible contribution to triton production comes from neutron pickup by deuterons and proton stripping from α particles in nuclear force fields.[5,15]

In conclusion the author wishes to thank M. Ya. Kuznetsova, V. N. Mekhedov, and V. A. Khalkin for their interest and several critical comments.

---

[1] Currie, Libby, and Wolfgang, Phys. Rev. **101**, 1557 (1956).

[2] E. L. Fireman and F. S. Rowland, Phys. Rev. **97**, 780 (1955).

[3] E. L. Fireman, Phys. Rev. **97**, 1303 (1955).

[4] E. L. Fireman and J. Zähringer, Phys. Rev. **107**, 1695 (1957).

[5] Wade, Gonzalez-Vidal, Glass, and Seaborg, Phys. Rev. **107**, 1311 (1957).

[6] K. Goebel, CERN 58-2 (1958).

[7] V. V. Kuznetsov and V. N. Mekhedov, JETP **35**, 587 (1958), Soviet Phys. JETP **8**, 406 (1959).

[8] Lefort, Simonoff, Tarrago, and Bibron, J. phys. radium **20**, 959 (1959).

[9] L. A. Currie, Phys. Rev. **114**, 878 (1959).

[10] J. L. Yntema, Phys. Rev. Letters **4**, 297 (1960).

[11] Batzel, Crane, and O'Kelley, Phys. Rev. **91**, 939 (1953).

[12] M. Lindner and R. N. Osborne, Phys. Rev. **91**, 342 (1953).

[13] Wang, Kuznetsov, Kuznetsova, Mekhedov, and Khalkin, JETP **39**, 527 (1960), Soviet Phys. JETP **12**, 370 (1961).

[14] W. Heisenberg, editor, Kosmische Strahlung (Springer Verlag, Berlin), 1953.

[15] J. B. Mead and B. L. Cohen, Phys. Rev. Letters **5**, 105 (1960).

Translated by I. Emin
217

SOVIET PHYSICS JETP VOLUME 13, NUMBER 5 NOVEMBER, 1961

DEVIATIONS OF THE CROSS SECTIONS FOR SLOW NEUTRON REACTIONS ON LIGHT NUCLEI FROM THE 1/v LAW

A. A. BERGMAN and F. L. SHAPIRO

P. N. Lebedev Physics Institute, Academy of Sciences, U.S.S.R.

Submitted to JETP editor December 8, 1960

J. Exptl. Theoret. Phys. (U.S.S.R.) **40**, 1270-1281 (May, 1961)

The energy dependence of the cross section ratio for the reactions $Li^6(n, \alpha)$, $B^{10}(n, \alpha)$, and $He^3(n, p)$ are measured at neutron energies $E < 30$ kev. The correction found for the 1/v law, expressed as a constant term of the reaction cross section, is -0.03 ± 0.01 b, -0.40 ± 0.03 b, and -1.1 ± 0.2 b for Li^6, B^{10}, and He^3, respectively. Available data on the $Li^7(p, n)$ reaction indicate that the correction of the Be^7 cross section is -61 ± 7 b. The results, which are in good agreement with theoretical predictions, show that thermal neutrons are captured by He^3 into a state with 0^+ spin and parity, and also confirm the hypothesis that thermal-neutron capture by B^{10} and Be^7 proceeds through $\frac{7}{2}^+$ and 2^- states, respectively.

INTRODUCTION

THE detailed investigation of (n, α) and (n, p) reactions on light nuclei is important for the theory of nuclear reactions, the determination of the level schemes of light nuclei, and the technique of measuring neutron flux.

According to the general theory, the cross sections for reactions with neutrons having low energy E can be represented by

$$\sigma_r = \mathrm{const} \cdot E^{-1/2} + \Delta\sigma + \beta' E^{1/2} + \ldots .$$

The first term of this expansion is the familiar 1/v law, while the following terms represent departures from this law.

It can be shown[1] that the negative constant term $\Delta\sigma$ is determined only by the cross section for thermal neutron absorption and by the spin of the reaction channel (nuclear state). The term can therefore be determined without making assumptions regarding parameters and resonance interference. Close resonances produce departures from the 1/v law that are proportional in first approximation to the ratio E/E_r (E_r is the resonance energy), as a result of which the cross section contains a term proportional to $E^{1/2}$.

At sufficiently low neutron energies the constant term is the principal correction to the 1/v law. This term can be measured if it is sufficiently large (when the cross section for thermal neutron absorption is large) and β' is sufficiently small (in the case of light nuclei, i.e., for low level densities). These conditions are fulfilled in the (n, p) reaction on He^3 and Be^7, and in the (n, α) reaction on Li^6 and B^{10}. Measurement of $\Delta\sigma$ can be regarded as a method of determining the spin of the channel for these reactions.

In earlier work[2,3] we measured the energy dependence of the cross section ratios for $Li^6(n, \alpha)$, $He^3(n, p)$, and $B^{10}(n, \alpha)$, at neutron energies $E < 30$ kev. In the present work the ratio for $Li^6(n, \alpha)$ and $B^{10}(n, \alpha)$ was measured with considerably greater accuracy. The ratio for $Li^6(n, \alpha)$ and $He^3(n, p)$ was also somewhat improved.

We used the data on cross section ratios to determine the constant terms in the cross sections. The available data on $Be^7(n, p)$ and $Li^7(p, n)$ will be used in the same way.

The data also lead to certain conclusions concerning the energy dependence of the individual reactions and the resonances responsible for the thermal cross sections of these reactions. These questions have been discussed in our earlier papers[2,3] and will be touched on here only in connection with new data in the literature.

The cross section ratios were measured by means of a neutron spectrometer based on slowing-down times in lead. Since the technique was not explained in references 2 and 3, it will be described here.

EXPERIMENTAL TECHNIQUE

Measurements are obtained with a slowing-down-time-in-lead neutron spectrometer as follows.* A burst of fast neutrons lasting 0.5 μsec is generated within a large lead cube weighing ~ 110 tons at the beginning of each 1600-μsec cycle. At the time t after the burst neutrons are slowed down to the average energy

---

*For more details see reference 4.

$$\bar{E} = 186/(t + 0.5)^2 \text{ kev}, \qquad (1)$$

where t is the slowing-down time in microseconds.

For large slowing-down times ($t \geq 14$ μsec) the energy spectrum of the slowed neutrons is very nearly Gaussian with ~ 14% rms spread around the mean.[2,4] For shorter slowing-down times the neutron spectrum is broader; thus for t = 4 μsec the rms spread is ~ 30% and for t = 2.5 μsec it is ~ 35%.[14]

As a result of leakage from the lead cube and capture in lead, neutron density decreases with slowing-down time as

$$\rho(t) = \text{const}\cdot(t + 0.5)^{-\alpha}e^{-t/T}, \qquad (2)$$

with $\alpha = 0.35$ and T = 890 μsec for the given lead cube.

Several measuring channels in the lead cube at different distances from the target contain detectors registering reactions induced by slowed-down neutrons. For a sufficiently thin-walled detector (with respect to neutron absorption) the counting rate is

$$\begin{aligned} J(t) &= \text{const}\cdot\int n(E, t)\, v\sigma(E)\, \eta(E)\, dE \\ &= \text{const}\cdot\rho(t)\, v(\bar{E})\, \sigma(\bar{E})\, \eta(\bar{E})\, K(\bar{E}), \qquad (3) \end{aligned}$$

where n(E, t)dE is the neutron density from E to E + dE at slowing-down time t, v is the neutron velocity, σ(E) is the reaction cross section, η is the registration efficiency of the nuclear reaction in the detector. For neutron energies much smaller than the reaction energy η is practically independent of energy. K is a correcting factor taking into account the fact that the mean value $\overline{v\sigma(E)\eta(E)}$ is not generally equal to $v(\bar{E})\sigma(\bar{E})\eta(\bar{E})$.

The broader the neutron energy spectrum n(E, t), and the more the cross section departs from the 1/v law, the greater the difference between K and unity. Calculations show that K(E) is practically unity for the investigated reactions when $\bar{E} < 30$ kev. Therefore the counting-rate ratio of two detectors at the same point in the cube is proportional, except for a small correction, to the ratio of the reaction cross sections for energy equal to the mean neutron energy $\bar{E}(t)$. By measuring the counting-rate ratio of the two detectors as a function of the slowing-down time, we obtain the energy dependence of the cross section ratio.

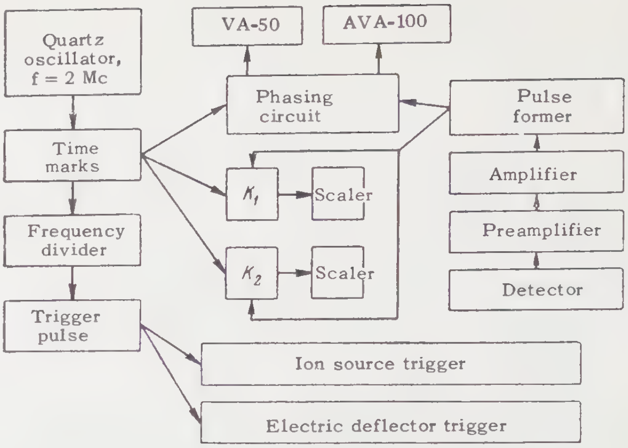

FIG. 1. Block diagram of circuit for slowing-down-time-in-lead neutron spectrometer. VA-50 and AVA-100 are 50-channel and 100-channel time analyzer; K_1 and K_2 are single-channel time analyzers.

APPARATUS

The neutron spectrometer (Fig. 1) was controlled by a quartz oscillator with frequency f = 2 Mc, the sinusoidal oscillations of which were transformed into synchronizing time marks and trigger pulses. Trigger pulses went to the time analyzers (see below), and through the delay lines also actuated the pulse circuits of the ion source and of the electric cutoff (deflector) for the ion beam.

Detector pulses were fed to the remote preamplifier and to the broad-band amplifier, discriminator, and time analyzers. The upper transmission limit of the entire amplifying circuit was 5 Mc.

In the present work we used a 50-channel time analyzer VA-50 with 0.5-μsec channels, two single-channel time analyzers, and a 100-channel time analyzer AVA-100 with channel widths varying from 1 to 80 μsec.

The 50-channel analyzer was equipped with a phasing circuit which phased shaped pulses in accordance with the synchronizing time markings, shifting them to the middle of each channel. This resulted in rigidly identical analyzer channel widths with no gaps between channels. The 100-channel analyzer was similarly equipped. The dead time determined by the pulse-phasing circuit was 2.5 μsec. In addition, counting losses of the analyzer channels were determined from the dead time of the electromechanical registers ($\tau_{\text{mech}} = 0.01$ sec) that recorded pulses from the individual channels.

The single-channel time analyzers, each of which fed two parallel scalers with 0.5-μsec re-

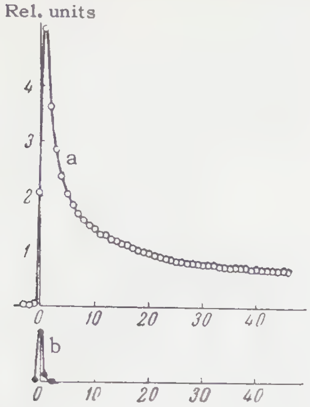

FIG. 2. a – counting rate (in relative units) of boron counter in channel of lead block vs slowing-down time; b – the same dependence for a high threshold of pulse-height discrimination. This curve represents the shape of the fast-neutron burst. Serial numbers of the analyzer channels (each 0.5 μsec wide) are plotted on the horizontal axis.

solving time, were adjusted and synchronized with respect to the pulse registration interval and the time from the start of the cycle to that interval.

The operating cycle of the spectrometer was 1600 μsec (625 bursts per sec). This provided for sufficiently small density of slowed neutrons remaining after each cycle.

The first two channels of the VA-50 analyzer registered only reactions induced by neutrons of the preceding cycle. The time stability of the spectrometer components was thus monitored from the position of the neutron burst (Fig. 2). The VA-50 analyzer covered neutron energies above 400 ev, while the AVA-100 analyzer covered lower energies.

The measuring interval of the two single-channel time analyzers K_1 and K_2 was 200 μsec, located 100 and 1400 μsec, respectively, from the start of the cycle. The high counting rate of K_1 represented ~ 8-ev neutrons, with very little departure from 1/v. Therefore the cross section ratio given by K_1 provides a good reference point for measurements.

Analyzer K_2 was operated at the end of the cycle, where the intensity was about one-ninth of that for K_1. This permitted convenient monitoring of the background, since even a small background increases appreciably the ratio of K_2 to K_1 counts.

The correct functioning of each analyzer and its dead time were checked regularly both electronically and by means of constant sources.

DETECTORS

In the present work the ratio between the cross sections for $Li^6(n, \alpha)$ and $B^{10}(n, \alpha)$ was measured by two identical proportional counters (Fig. 3) with 25-mm cathode diameter and 1.3-mm wire diameter,* which were filled with argon at 230 mm, CO_2 at 12 mm, and air at 7 mm Hg. One counter contained a 0.22-mg/cm^2 layer of natural boron, while the other contained a 1.13-mg/cm^2 layer of Li^6F. These homogeneous thin layers were vacuum deposited on aluminum foils. The principal requirement was short pulse delay.

For the purpose of measuring retardation the detectors were inserted into a channel of the lead cube close to the target, where there was a large flux of 14-Mev primary neutrons. Pulses from slow neutrons (i.e., after long slowing-down times) were cut off by raising the height-discrimination threshold. The time analyzer then traced the shape of the neutron burst (Fig. 2).

The burst registered by the detectors was compared with that registered by a fission ionization chamber containing layers of natural uranium.† The electrode gap in this chamber was 3 mm, and its gas filling was 95% argon and 5% CO_2, with operation at $\mathscr{E}/p \sim 7$ v/cm-mm Hg. The large pulses from the fission chamber permitted us to use the initial leading-edge segment for registration. We can therefore assume that the registration lag of the center of gravity of the neutron burst in the fission chamber does not exceed 0.03 μsec. In all instances the detectors were less than 0.07 μsec behind the fission chamber.

Measurements with different cutoff thresholds indicated that there were practically no additional time shifts of electronic origin between the compared detectors.

MEASUREMENTS

If the cross section ratios are to be measured with accuracy better than 1%, in addition to obtaining sufficient data it is necessary to take all steps that will reduce both random and systematic errors. Measurements were performed in the following order.

1) Gas multiplication in the compared counters was such as to produce equal mean pulses. The detectors were connected alternately to a single electronic channel.

---

*This diameter permitted a higher counter operating voltage for the purpose of producing higher electron mobility. The gas amplification factor was about 10.

†The fission of U^{238} is induced only by 1-Mev neutrons, i.e., by primary neutrons and those undergoing inelastic scattering on lead nuclei, which does not introduce any perceptible retardation. A small admixture of U^{235} was insignificant for the present measurements.

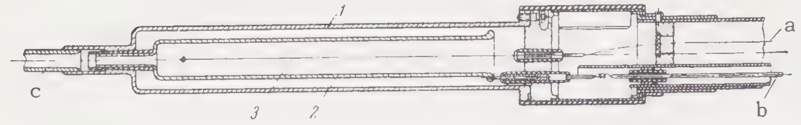

FIG. 3. Diagram of counters used to register $B^{10}(n, \alpha)$ and $Li^6(n, \alpha)$ reactions. 1 – thin steel shell; 2 – cathode (with interior lining of aluminum foil bearing deposited layer); 3 – 1.3-mm counter wire; a – lead to preamplifier; b – high-voltage lead; c – tube to stopcock.

2) The counting rates were such that counting losses did not exceed 1.5% and were as close to equality as possible in the two counters.

3) The two counters were used alternately for periods of 40 to 60 min during a total measuring time of a few days. The detectors were placed in exactly the same position in the lead block.

4) The fission chamber measured systematically the position of the neutron burst in the multichannel analyzers.

5) Backgrounds were measured systematically by omitting the electric cutoff pulse, i.e., when the ion beam did not impinge on the zirconium-tritium target.

RESULTS

Figure 2 shows the counting rate of the boron detector as a function of slowing-down time, as obtained in one of the 10 runs. The slowing-down time was measured from the center of gravity of the neutron burst, as determined by the fission chamber and corrected for lag of the boron detector after the fission chamber. We also used measurements in the course of which the neutron bursts did not drift in the VA-50 analyzer and the background was very small and stable. Less than 20% of the measurements were rejected.

For each run, after introducing corrections for the background and counting loss, the counting-rate ratio of the two detectors was determined (Fig. 4). For each time channel the mean ratio for the different runs was calculated, with normalization to the ratio obtained with K_1. The rms spread of the normalized ratios around the mean value was close to the statistical spread.

The mean ratio of the counts from analyzers K_2 and K_1, corrected for the background, was smaller by 1.85 ± 0.35% for the Li^6F layer than for the boron counter. This difference was incomparably larger than could be expected from departures from the 1/v law. The cause of the discrepancy lay in different degrees of neutron absorption by the layers and by the incompletely identical counters. The observed absorption effect was several times greater than absorption in a single transit. This was confirmed by special measurements with interchangeable absorbers, which showed that the observed absorption was proportional to the neutron slowing-down time. Therefore the correction for absorption during short slowing-down times (in channels of the VA-50 analyzer) was negligibly small.

After introducing the corrections listed in the table, including those for absorption, and using Eq. (1) to convert from slowing-down time to energy, the curves in Figs. 5 and 6 were obtained, showing the energy dependence of the cross section ratio for $Li^6(n, \alpha)$ and $B^{10}(n, \alpha)$ and for $Li^6(n, \alpha)$ and $He^3(n, p)$.

The solid curves in Figs. 5 and 6 are parabolas plotted by least squares. The parameters of these parabolas are discussed below; the errors shown include the rms random errors and an estimate of possible systematic errors.

The experimental results represented in Figs. 5 and 6 do not include a correction for the depend-

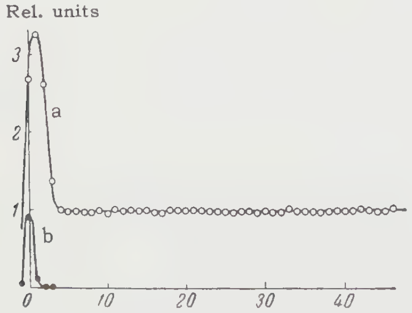

FIG. 4. a – counting-rate ratio of boron and lithium counters vs slowing-down time; b – shape of fast-neutron burst measured by uranium fission chamber. Serial numbers of the 0.5-μsec analyzer channels are plotted on the horizontal axis.

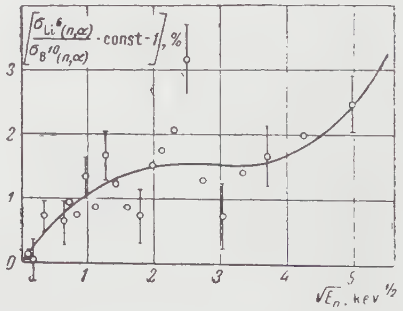

FIG. 5. Departure of cross section ratio for $Li^6(n, \alpha)$ and $B^{10}(n, \alpha)$ from its value in the thermal region vs square root of neutron energy. The solid curve represents Eq. (7), plotted through the experimental points by least squares.

Corrections of the cross section ratios for $Li^6(n, \alpha)$ and $B^{10}(n, \alpha)$, and for $Li^6(n, \alpha)$ and $He^3(n, p)$*

	$\sigma_{Li^6}/\sigma_{B^{10}}$			$\sigma_{Li^6}/\sigma_{He^3}$		
$\sqrt{E_n}$, kev$^{1/2}$	4.98	3.33	0.09 (analyzer K_1)	5.26	2.73	0.09 (analyzer K_1)
Correction for neutrons from D–D reaction**, %	—0.15±0.10	0	0	—1.25±0.2	—0.35±0.05	0
Correction for counting loss, %	0.98±0.25	—0.09±0.02	0	0,55±0.1	0	0
Correction for background (except D–D neutron background), %	0	0	0.08	0	0	0.06
Correction for absorption, %	0	0	0.23±0.04	0	0	none
Correction for neutron dispersion, %	—0.46	0	0	—0.13	0	0
Correction for instrumental time resolution, %	—0.26	0	0	—0.4±0.2	0	0
Total	0.11±0.35	—0.09±0.02	0.31±0.04	—1.2±0,4	—0.35±0,05	0.06

*The correction for neutrons of the preceding cycle was negligibly small.

**Neutrons from the D – D reaction appeared when the ion beam was deflected by the electric cutoff and struck the wall of the target tube.

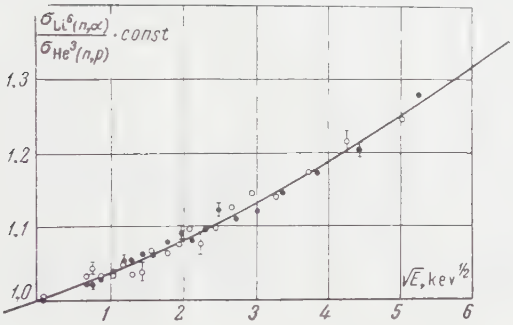

FIG. 6. Cross section ratio for $Li^6(n, \alpha)$ and $He^3(n, p)$ vs square root of neutron energy. The curve is normalized to unity for $E_n = 0$. ○ – first (preliminary) run; ● – second run; solid curve – parabola (12) plotted by least squares from the second run.

ence of registration efficiency on neutron energy. This correction is proportional to neutron energy, affecting only one (β) of the parabola parameters and was therefore introduced directly into the values of this parameter (see footnote on page 897 and the footnote under this column.

DISCUSSION OF RESULTS

1. As has been shown in reference 1, the cross section for a reaction induced by S neutrons (with orbital moment $l = 0$) can be represented by*

$$\sigma_r = \frac{(\sigma_r E^{1/2})_0 E^{-1/2}}{1 + \alpha E^{1/2} + \beta E + \gamma E^2 + \ldots}$$

$$= (\sigma_r E^{1/2})_0 (E^{-1/2} - \alpha + \beta^* E^{1/2} + \ldots), \tag{4}$$

where

$$\alpha = \frac{m}{\pi \hbar^2}\left(\frac{A}{A+1}\right)^2 (\sigma_r E^{1/2})_0 [x_-^2 / g_- + (1 - x_-)^2 / (1 - g_-)], \tag{5}$$

m is the neutron mass, A is the mass number of the target nucleus, $(\sigma_r E^{1/2})_0$ is the value of $\sigma_r E^{1/2}$ for $E \rightarrow 0$ (i.e., practically for thermal neutrons), $g_- = I/(2I + 1)$ is the statistical weight of the reaction channel with spin $J = I - 1/2$ (I is the target-nucleus spin), and x_- is the relative contribution of this state to the cross section for thermal neutrons.

Equation (4) is applicable to low neutron energies, when the terms beginning with γE^2 are small compared with 1 and βE. The constant term in the cross section, which was discussed above, is related to α by

$$\Delta\sigma = -\alpha (\sigma_r E^{1/2})_0. \tag{6}$$

The measured cross section ratio for Li^6 and B^{10} (Fig. 5) is well represented by

$$\sigma_{Li}/\sigma_B = \text{const } [1 + (\alpha_B - \alpha_{Li}) E^{1/2} + \beta_{Li/B} E + \gamma_{Li/B} E^2] \tag{7}$$

with the following constant coefficients:

$$\alpha_B - \alpha_{Li} = (1.43 \pm 0.20) \cdot 10^{-2} \text{ kev}$$
$$\beta_{Li/B} = -(0.37 \pm 0.09) \cdot 10^{-2} \text{ kev} \quad *$$
$$\gamma_{Li/B} = (0,73 \pm 0,27) \cdot 10^{-4} \text{ kev}$$

Equation (7) follows directly from (4) when we neglect all terms of higher order than E^2 as well as

---

*Neutron capture with $l \geq 1$ contributes to higher terms of the expansion, beginning with $\beta^* E^{1/2}$.

*After corrections for the variation of registration efficiency with neutron energy, we have $\beta_{Li/B} = -(0.35 \pm 0.09)$.

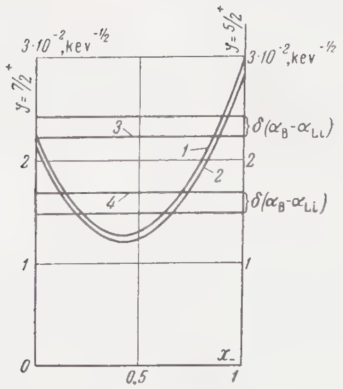

FIG. 7. Dependence of the coefficient α_B on the ratio of contributions by states with spin and parity $\frac{5}{2}^+$ and $\frac{7}{2}^+$. The two curves correspond to two values of the thermal cross section for $B^{10}(n, \alpha)$: $1 - \sigma = 4000$ b; $2 - \sigma = 3800$ b. The straight lines represent experimental values of α_B for the two limits of α_{Li}: $3 - \alpha_{Li} = 0.80 \times 10^{-2}$ kev$^{-1/2}$; $4 - \alpha_{Li} = 0.26 \times 10^{-2}$ kev$^{-1/2}$. $\delta(\alpha_B - \alpha_{Li})$ is the experimental error of α.

the $E^{3/2}$ term, which must be very small since it is absent rigorously from the denominator in (4) and because σ_{Li}/σ_B is close to a constant.

Using the cross sections for thermal neutron absorption,[5,6] we find that for Li^6 ($I = 1^+$), depending on our hypothesis regarding the ratio of the contributions from the states with spins $\frac{1}{2}$ and $\frac{3}{2}$ to the thermal cross section, the variation of α is given by

$$0{,}26 \cdot 10^{-2} \leqslant \alpha_{Li} \leqslant 0.80 \cdot 10^{-2}\ \text{kev}^{-1/2}. \qquad (8)$$

Combining this result with the measured value of $\alpha_B - \alpha_{Li}$, we obtain

$$1.69 \pm 0{,}20 \leqslant \alpha_B \cdot 10^2 \leqslant 2{,}23 \pm 0.20. \qquad (9)$$

In Fig. 7 these limits are compared with the values of α_B calculated for different ratios of the contributions from the channels with spins $\frac{5}{2}$ and $\frac{7}{2}$. The spin and parity of the B^{10} ground state is 3^+.*

The experimental results appear to be in agreement with each of the two hypotheses:

a) Neutrons are captured principally into the state $J = \frac{5}{2}^+$ with an appreciable number going to the state $J = \frac{7}{2}^+$, or

b) Neutrons are captured into the state $J = \frac{7}{2}^+$ with none or very few going into the state $J = \frac{5}{2}^+$.

Recent measurements of the γ-ray spectrum resulting from thermal-neutron capture in B^{10},[8] show that capture proceeds predominantly through the spin $\frac{7}{2}$ channel. The second of the two given possibilities is thus realized.

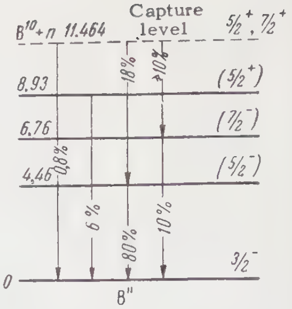

FIG. 8. Scheme of γ-ray transitions in B^{11} (produced by $B^{10} + n$ capture). Transition probabilities in radiative capture are shown.[8]

2. The measurements given in reference 8 (represented in Fig. 8) make it possible to estimate the contribution x_- of the $\frac{5}{2}^+$ state to the capture of thermal neutrons by B^{10}, which in turn permits the calculation of α_B, so that α_{Li} can be determined from the experimental values of $\alpha_B - \alpha_{Li}$.

Capture into the state $J = \frac{5}{2}^+$ should lead to E1 transitions to the B^{11} ground state with the emission of 11.43-Mev quanta. The number of these transitions from the $\frac{5}{2}^+$ state per capture is, in any event, smaller than the total yield of 11.43-Mev quanta, i.e.,

$$x_-\,\Gamma_\gamma / \Gamma < 8 \cdot 10^{-3} \sigma_\gamma\,\sigma,$$

where σ is the total absorption cross section, σ_γ is the cross section for radiative capture, and Γ_γ and Γ are the partial and total widths of the compound nucleus in the state $J = \frac{5}{2}^+$.

Similarly, for the transition from the $\frac{7}{2}^+$ capture state to the 4.46-Mev level of B^{11} ($E_{\gamma'} = 6.98$ Mev) we have

$$(1 - x_-)\,\Gamma_{\gamma'}/\Gamma' \approx \Gamma_{\gamma'}/\Gamma' = 0{,}18\,\sigma_\gamma/\sigma.$$

Assuming that this is an electric dipole transition, we take $\Gamma_{\gamma'}/\Gamma_\gamma = (E_{\gamma'}/E_\gamma)^3$. Assuming, furthermore, $\Gamma = \Gamma'$, we obtain $x_- < 1\%$.*

Substituting in (5), with a certain amount of margin, $x_- = 3 \pm 3\%$, we obtain

$$\alpha_B = (2.06 \pm 0.14) \cdot 10^{-2}\ \text{kev}^{-1/2}. \qquad (10)$$

Using the measured value of $\alpha_B - \alpha_{Li}$, we thus arrive at

$$\alpha_{Li} = (0.63 \pm 0.24) \cdot 10^{-2}\ \text{kev}^{-1/2}. \qquad (11)$$

Figure 9 shows that the value of α_{Li} agrees better with the hypothesis that thermal-neutron capture by Li^6 proceeds predominantly through the state $J = I - \frac{1}{2} = \frac{1}{2}$. However, the calculation is insufficiently accurate to furnish a decisive result.

---

*The literature gives two values of the thermal cross section for $B^{10}(n, \alpha)$: ~3800 b[5,7] and ~4000 b.[6] We assume $\sigma = 3900 \pm 100$ b.

*If $E_\gamma = 6.98$ Mev does not represent an E1 transition, the estimated value of x_- will be still smaller.

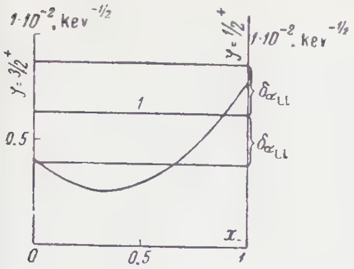

FIG. 9. Dependence of the coefficient α_{Li} on the ratio of contributions from the states with spin and parity $3/2^+$ and $1/2^+$. The straight line 1 is the experimental value of α_{Li}. $\delta(\alpha_{Li})$ is the experimental error in α_{Li}.

According to (6), (10), and (11) the constant terms in the cross sections for boron and lithium are

$$\Delta\sigma_{B^{10}} = -0.40 \pm 0.03 \quad \text{b}, \qquad \Delta\sigma_{Li} = -0.03 \pm 0.01 \ \text{b}.$$

The $B^{10}(n, \alpha)$ reaction is known to have two branches, with Li^7 formed in its ground and excited states, respectively. For thermal neutrons the yield ratio of the two branches is 6.2%.[9] The value of α_B given above pertains to the energy dependence of the total cross section. By measuring the energy dependence of the branching ratio we could determine α for the branch in which ground-state Li^7 is produced and determine the relative contributions of the $5/2^+$ and $7/2^+$ channels for this branch.

3. The coefficients β and γ in (4), which gives the energy dependence of the reaction cross section, are principally determined by the compound-nucleus states excited by S neutrons.[1,2]* The coefficients are large if the levels responsible for the thermal cross section are close to the neutron binding energy; otherwise they are small. $\beta > 0$ and $\beta < 0$ for levels lying below and above the binding energy, respectively. Li^7 has no levels close to the binding energy,† so that β_{Li} and γ_{Li} must be small. Since in (7) $\beta_{Li/B} \approx \beta_B - \beta_{Li}$ and $\gamma_{Li/B} \approx \gamma_B - \gamma_{Li}$, our measured values of $\beta_{Li/B}$ and $\gamma_{Li/B}$ are close to β_B and γ_B, respectively. The sign and magnitude of β and the magnitude of γ indicate that the thermal cross section of B^{10} is determined mainly by the level or levels located hundreds of kev above the neutron binding energy in B^{11}. This agrees with the hypothesis that the 11.46-Mev and 11.68-Mev levels of B^{11} are responsible for the thermal cross section.[11]

4. In earlier work[3] we measured the energy dependence of the cross section ratio for $Li^6(n, \alpha)$ and $He^3(n, p)$, which is well represented by

$$\sigma_{Li} / \sigma_{He} = \text{const} \cdot [1 + (\alpha_{He} - \alpha_{Li}) E^{1/2} + \beta_{Li/He} E] \qquad (12)$$

with the constants

$$\alpha_{He} - \alpha_{Li} \quad (3.54 \pm 0.5)\ 10^{-2}\ \text{kev}^{-1/2},$$
$$\beta_{Li/He} = (2.87 \pm 1.3)\ 10^{-3}\ \text{kev}^{-1}.^*$$

Making use of (11), we now obtain

$$\alpha_{He} = (4.17 \pm 0.55) \cdot 10^{-2}\,\text{kev}^{-1/2}.$$
$$\Delta\sigma_{He} = -1.1 \pm 0.2 \ \text{b}.$$

α_{He} is close to the largest possible value, (4.65 ± 0.25) × 10^{-2} $\text{kev}^{-1/2}$, which is obtained if the He^3 cross section in the thermal region[5] is determined completely by the 0^+ reaction channel. This differs markedly from the value (1.65 ± 0.09) × 10^{-2} $\text{kev}^{-1/2}$ corresponding to the 1^+ channel, which makes the contribution $x_- = 6 \pm 6\%$.

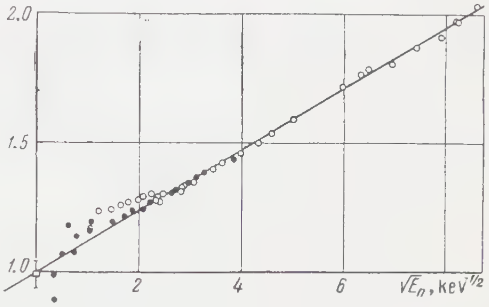

FIG. 10. The plot of $(\sigma E^{1/2})^{-1/2} = f(E^{1/2})$ for the $Be^7(n, p)$ reaction. ○ – from measurements of $Li^7(p, n)$ with a 9.3-mg/cm² LiF target;[13] ● – the same with a 6.5-mg/cm² target. □ – data in reference 9.

We note that this conclusion, although based on measurements of the cross section ratio for $Li^6(n, \alpha)$ and $He^3(n, p)$, is not actually associated with any hypotheses regarding the energy dependence of the cross section for the first of these reactions. Only the experimental value (11) of α_{Li} is used, or, if convenient, the equivalent theoretical inequality (8).

We must therefore reject the argument of Bame and Cubitt,[12] who obtained a considerable departure from the 1/v law in measurements of the $Li^6(n, \alpha)$ cross section, which, combined with the value of σ_{Li}/σ_{He} in reference 3 indicates that the 1/v law is valid for He^3. The large value of α_{He} inevitably leads to a considerable departure from 1/v for the $He^3(n, p)$ reaction. At the same time, the low accuracy (10 – 15%) of Bame and Cubitt's measurements throws doubt on the reliability of their conclusions. In addition, reference 14 contains data indicating that the cross section for $B^{10}(n, \alpha)$ obeys the 1/v law within about 5% up to E ~ 100 kev. Since, according to the present

---

*Including the near-threshold state discussed by Baz'.[10]

†The nearest level excited by S neutrons is 830 kev below the neutron binding energy in Li^7.[8]

*After introducing corrections for the variation of registration efficiency with neutron energy, we obtain

$$\beta_{Li/He} = (3.2 \pm 1.4) \cdot 10^{-3}\ \text{kev}^{-1}.$$

work, the cross sections for $Li^6(n, \alpha)$ and $B^{10}(n, \alpha)$ vary in an identical manner (within 2%) for $E \leq 25$ kev, it follows that for the first of these reactions the departure from $1/v$ should not exceed 7%. A conclusive determination of the energy dependence of the $Li^6(n, \alpha)$ cross section requires that the measured cross section ratio be supplemented by a precision measurement of the energy dependence of one of the (n, α) or (n, p) reactions. We are preparing to obtain these measurements.

5. The $Be^7(n, p)$ reaction should exhibit an especially large departure from $1/v$, since Be^7 is characterized by a very large thermal-neutron absorption cross section $\sigma_r = 51\,000 \pm 6000$ b.* The energy dependence of the cross section for this reaction can be obtained by measuring the cross section for the reverse reaction[13] $Li^7(p, n)$ and using the reciprocity theorem. An analysis of these data in accordance with (4) shows that within error limits α and β satisfy

$$\beta = (\alpha/2)^2. \qquad (13)$$

Equation (13) is easily confirmed[1] under the following conditions: a) Re f = 0 or $(\mathrm{Re}\, f)^2 \ll (\mathrm{Im}\, f)^2$, where f is the logarithmic derivative of the neutron wave function on the nuclear surface, b) Im f = const, and c) $x_- = 0$ or $x_- = 1$, or $x_- = g_- = 0.375$. In this case (4) has the very simple form

$$\sigma_r E^{1/2} = (\sigma_r E^{1/2})_0 \Big/ \left(1 + \frac{1}{2}\alpha E^{1/2}\right)^2. \qquad (14)$$

Figure 10 shows that the experimental results[13,15] agree well with (14) when

$$\alpha = 0.24 \pm 0.01\ \text{kev}^{-1/2}. \qquad (15)$$

This corresponds to two possible values of the relative contribution to the thermal cross section by the state with $J = I = \frac{1}{2} = 1$, which are $x_- = 0 \pm 0.07$ and 0.75 ± 0.07. We must reject the second value, which would result in a large departure from (14).† Thus thermal neutron capture by Be^7 proceeds practically entirely through the 2^- channel. This conclusion also follows from an analysis based on resonance theory,[13] according to which the cross section for $Be^7(n, p)$ at low neutron energies is determined by a very broad 2^- level, close to the neutron binding energy in Be^8. Baz'[10] regards this level as a special near-threshold state.

The constant term in the cross section of Be^7 is $\Delta\sigma_{Be} = -61 \pm 7$ b. If neutron capture through the state with $J = 1^-$ is entirely absent, it follows from (15) that the thermal cross section of Be^7 is $51\,000 \pm 2100$ b.

The authors thank A. N. Volkov and A. M. Klabukov, who perfected and adjusted the electronic equipment of the spectrometer for slowing-down time measurements.

---

*This value was obtained by averaging Hanna's data[15] for the total absorption cross section (48 000 ± 9000 b) and for the (n, p) cross section (53 000 ± 8000 b).

†We reject the unlikely possibility that (13) results from an accidental coincidence of independent parameters, rather than from the fulfillment of conditions a), b), and c).

[1] F. L. Shapiro, JETP **34**, 1648 (1958), Soviet Phys. JETP **7**, 1132 (1958).

[2] Bergman, Isakov, Popov, and Shapiro, JETP **33**, 9 (1957), Soviet Phys. JETP **6**, 6 (1958).

[3] Bergman, Isakov, Popov, and Shapiro, Ядерные реакции при низких и средних энергиях (Nuclear Reactions at Low and Intermediate Energies) Trans. All-Union Conference, 1957, Acad. Sci. Press, 1958, p. 17; Proc. International Conference on Neutron Interactions, Columbia Univ., N.Y., 1957, p. 191.

[4] Bergman, Isakov, Popov, and Shapiro, ibid., p. 140; Bergman, Isakov, Murin, Shapiro, Shtranikh, and Kazarnovskii, Trans. of the Geneva Conference **4**, 166, 1955.

[5] D. J. Hughes and R. B. Schwartz, Neutron Cross Sections, BNL-325, 2nd ed., 1958.

[6] Hughes, Maqurno, and Brussel, Supplement 1 to BNL-325, 1960.

[7] Safford, Taylor, Rustad, and Havens, Bull. Am. Phys. Soc. **5**, 288 (1960).

[8] G. A. Bartholomew and P. J. Campion, Can. J. Phys. **35**, 1347 (1957); F. Ajzenberg-Selove and T. Lauritsen, Nuclear Phys. **11**, 1 (1959).

[9] G. C. Hanna, Phys. Rev. **80**, 530 (1950).

[10] A. I. Baz', Advances in Physics (Supplement of Phil. Mag.) **8**, 349 (1959).

[11] H. Bichsel and T. W. Bonner, Phys. Rev. **108**, 1025 (1957).

[12] S. J. Bame and R. L. Cubitt, Phys. Rev. **114**, 1580 (1959).

[13] R. L. Macklin and J. H. Gibbons, Phys. Rev. **109**, 105 (1958).

[14] Bilpuch, Weston, and Newson, Ann. Phys. **10**, 456 (1960).

[15] R. C. Hanna, Phil. Mag. **46**, 381 (1955).

Translated by I. Emin
218

SOVIET PHYSICS JETP VOLUME 13, NUMBER 5 NOVEMBER, 1961

INVESTIGATION OF REORIENTATION OF THE GUANIDINIUM ION IN THE FERROELECTRIC $C(NH_2)_3 \cdot Al(SO_4)_2 \cdot 6H_2O$ *BY THE NUCLEAR MAGNETIC RESONANCE METHOD*

A. G. LUNDIN, G. M. MIKHAĬLOV, and S. P. HABUDA

Physics Institute, Siberian Division Academy of Sciences; The Siberian Technological Institute

Submitted to JETP editor December 14, 1960

J. Exptl. Theoret. Phys. (U.S.S.R.) **40**, 1282-1287 (May, 1961)

Reorientation of the $[C(NH_2)_3]^+$ ion has been detected in the ferroelectric $C(NH_2)_3 \cdot Al(SO_4)_2 \cdot 6H_2O$ at temperatures above 130° K by means of nuclear magnetic resonance. The temperature dependence of the second moment of the absorption line of a polycrystalline sample has been examined between 90 and 400° K. The height of the potential barrier for the reorientation of the $C(NH_2)_3$ group has been estimated and some conclusions are drawn regarding the reorientation mechanism.

IT has been remarked in the literature[1,2] that the properties of the ferroelectric guanidine aluminum sulfate hexahydrate (GASH) are determined to a marked degree by the peculiarities of the guanidinium ion $[C(NH_2)_3]^+$. On the basis of the structural investigation of Geller and Booth[3] it has been noted that in the GASH structure this ion is but weakly bound to its surroundings and that this could lead to its mobility.

In the present paper the question of the mobility of the guanidinium ion is investigated by means of the nuclear magnetic resonance (NMR) of its protons. The apparatus used for these studies has been described earlier.[4] Temperature measurements were carried out in a special dewar similar to that described by Gutowsky et al.[5] For the experiments a monocrystal of GASH was used, cut into the shape of a cube oriented along the principal axes, with dimensions $8 \times 8 \times 8$ mm (the $\bar{3}$ axis of the GASH crystal was taken as the z axis, and the y axis was taken perpendicular to the prism face). For studying polycrystalline samples a powdered GASH was compressed under a pressure of 100 kg/cm² into a cylindrical tablet of diameter 10 mm and height 12 mm.

The spectra were recorded in a magnetic field $H_0 = 3000$ oe with a time constant of 1 – 2 sec and field scanning rates of 0.08 and 0.04 oe/sec. Field modulation amplitude was 0.8 oe. In order to avoid saturation in the monocrystal at low temperatures the rf oscillator was adjusted to the lowest possible power level at which stability could be maintained. With polycrystalline samples saturation was observed in the same temperature range at significantly higher power levels.

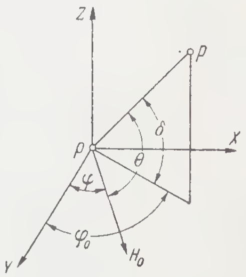

FIG. 1. Definition of angles for different orientations of the vector pp in the magnetic field.

It is well known that systems containing relatively isolated pairs of nuclei, for example pairs of protons in molecules of water of crystallization, give an NMR spectrum in the form of a doublet with a component separation equal to[6]

$$\Delta H = 3\mu r^{-3}(3\cos^2\theta - 1) = 3\mu r^{-3}[3\cos^2(\varphi - \varphi_0)\cos^2\delta - 1]. \quad (1)$$

Here μ is the magnetic moment of the nucleus (proton), r is the distance between the protons, θ is the angle between the direction of the proton-proton (pp) vector and the direction of the external magnetic field H_0, φ is the angle between H_0 and one of the crystal axes that lie in the plane of rotation of the crystal (or the magnetic field relative to the crystal[4]), φ_0 is the angle between this axis and the projection of the vector pp on the plane of rotation, and δ is the angle between the vector pp and the plane of rotation (Fig. 1). By measuring H_0 for different values of φ, one can determine r, φ_0, and δ.

In the elementary cell of GASH there are three formula units $C(NH_2)_3 \cdot Al(SO_4)_2 \cdot 6H_2O$,[3] i.e., 18 molecules of H_2O; however, in conformity with the symmetry of the crystal, these pertain to three coplanar, but not collinear, pp vectors.[7,8]

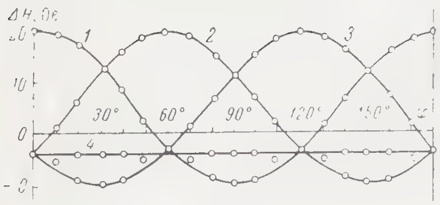

FIG. 2. Angular dependence of the doublet splittings in the spectra of a monocrystal of GASH at room temperature.

Thus the proton resonance spectrum of GASH should be composed of a sum of the spectra of the water protons and the protons of the $C(NH_2)_3$ group.

In Fig. 2 is shown the room temperature dependence of the doublet splitting of the proton resonance spectra of a GASH monocrystal on the orientation of the magnetic field rotating about the z axis, which is perpendicular to the basal plane. Curves 1, 2, 3 pertain to the values $r = 1.63 \pm 0.015$ A, $\delta = 0$, and φ_0 equal respectively to 0, 60, and 120°. (The angles are measured from the y axis of the GASH monocrystal.) This gives three pp vectors lying in the basal plane at an angle of 60° with one another. Curve 4 corresponds to a pp vector that is situated perpendicular to the plane of the base with $r = 2.18 \pm 0.015$ A, $\varphi_0 = 0$, and $\delta = 90°$. Just the same orientational dependence for the fourth vector is obtained if it is located in the basal plane and rotates in this plane at a sufficiently high rate, since[9] in this case one also obtains a doublet with a splitting between components:

$$\Delta H = \frac{3\mu}{2r^3}\,[3\cos^2(\varphi - \varphi_0)\cos^2\delta - 1]. \qquad (2)$$

Here the symbols mean the same as in Eq. (1), but now the angles φ_0 and δ describe not the direction of the vector pp, but the direction of the axis of its reorientation. In this case curve 4 corresponds to $r = 1.73 \pm 0.02$ A, $\varphi_0 = 0$, and $\delta = 90°$.

The intensities of the spectral components were determined by the areas under the resonance peaks. It turned out that the intensity of the peak corresponding to curve 4 of Fig. 2 amounted to $\frac{1}{3}$ of the total intensity of the spectrum. Considering that the z axis, perpendicular to the basal plane, is a threefold axis and that the number of water protons amounts to $\frac{2}{3}$ of the total number of protons in the GASH crystal, we come to the conclusion that curves 1, 2, and 3, which account for $\frac{2}{3}$ of the intensity of the spectrum, correspond to different vectors pp of the waters of crystallization, and curve 4 corresponds to the $C(NH_2)_3$ group. Thus the investigation of the angular dependence of the spectra at room temperature leads to the conclusion that the vectors pp of the waters of crystallization lie in the basal plane at angles of 60° with one another and have a proton separation of $r = 1.63 \pm 0.015$ A, and the vectors pp of the group $C(NH_2)_3$ are distributed perpendicular to the basal plane with $r = 2.18 \pm 0.015$ A, or rotate in the basal plane, in which case $r = 1.73 \pm 0.02$ A. Analogous conclusions have been obtained also by Spence and Muller.[7]

In reference 8, indirect evidence was presented that rendered unlikely the supposition that the vec-

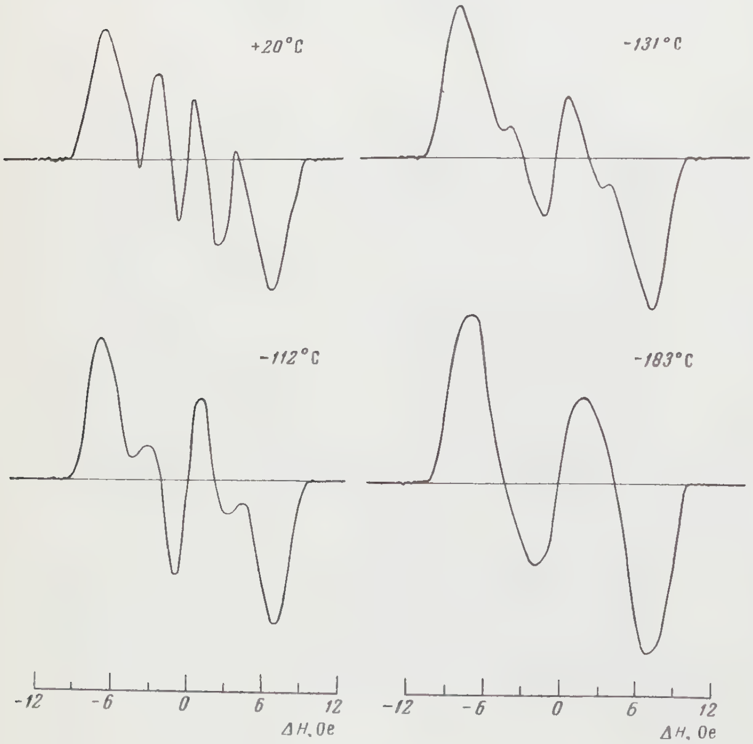

FIG. 3. Derivative proton resonance spectra of a monocrystal of GASH at different temperatures.

tors pp of the guanidinium group were perpendicular to the basal plane. On the other hand, preliminary low-temperature investigations of polycrystalline GASH by NMR were reported by McCall.[10] A broadening of the spectrum was observed, which could indicate a cessation of any kind of internal motion leading at room temperature to a decrease in the line width. It was assumed that this motion was associated with the guanidinium ion. However, direct demonstration of the presence of mobility of the guanidinium ion at room temperature was not given. We obtained a direct demonstration of the presence of reorientation of this ion in the basal plane by a study of the temperature dependence of the proton resonance spectrum of GASH.

The temperature dependence of the form of the spectrum was first studied in monocrystalline samples of GASH. An orientation of $\varphi = 30°$ was chosen (see Fig. 2), for which the spectrum consists of two doublets: An outer one, which in reality is an unresolved dual doublet belonging to H_2O, and an inner one belonging to the guanidinium ion. The derivative NMR spectrum for this orientation at room temperature is shown in Fig. 3.

The form of the spectrum does not change when the temperature is reduced to −100° C. Below this temperature the intensity of the outer doublet begins to increase at the expense of the inner one, and by −145° C the inner doublet has completely disappeared. Moreover, the spectrum hardly changes as the temperature is lowered down to −183° C.

An investigation of the angular dependence of the spectra of a monocrystal of GASH at −183° C showed that at this temperature the doublet corresponding to curve 4 in Fig. 2 is absent, whereas the intensity of the doublets corresponding to the curves 1, 2, and 3 in Fig. 2 has increased by $\frac{1}{3}$, in comparison with the intensity of the same doublets at room temperature.

This means that at temperatures below −145° C the vectors pp of the NH_2 group of the guanidinium ion are situated at angles of 60° with one another and this "triangle" of the vectors pp is oriented in just the same way as the triangle of the vectors pp of the waters of crystallization. No splitting of the lines caused by an inequality of the proton separation in H_2O and NH_2 was ever observed.

Thus, at temperatures above −145° C, the guanidinium ion $[C(NH_2)_3]^+$, existing as a planar group in agreement with the structure investigations of Geller and Booth,[3] reorients itself around the z axis, which is perpendicular to the basal plane of GASH, and this leads to a change in the shape and width of the NMR spectrum.

One can describe the effect of the reorientation on the NMR line width in terms of the "correlation time" of the motion τ_c introduced by Bloembergen, Purcell, and Pound,[11] which is a measure of the time interval during which a molecule (or a group of atoms within a molecule that contains the nuclei under study) completes a transition from one state of motion to another (for rotational motion τ_c is equal to the time necessary to rotate about an angle of one radian).

Such transitions can be transitions between vibrational states in the same potential well, transitions between vibrational states from one well to another by means of the quantum mechanical tunnel effect, or transitions to levels lying above a potential barrier. In this case the molecule rotates (reorients itself) in conformity with classical theory as long as it does not return to some vibrational level of one of the wells.

Since the amplitude of the vibrational motions is not large, they give only a small contribution to the change in line width.[12] Hence they can be left out of consideration. Nor shall we consider the possibility of reorientation by means of the tunnel effect, since from the calculations of Das[13] it follows that this can be neglected in comparison to the classical reorientation for rotating groups containing nuclei that are heavier than protons.

The probability of rotation of a molecule through an angle $2\pi/N$, where N is the multiplicity of the periodic potential barrier V_0, according to Das,[13] in the classical rotation case is*

$$W = (N/2\pi)\ (2V_0/J)^{1/2} \exp\,(-V_0/kT). \tag{3}$$

Here J is the moment of inertia of the reorienting group, k is the Boltzmann constant, and T is the absolute temperature. From this it is easy to calculate the time necessary for rotation through an angle $2\pi/N$, which is inversely proportional to W, and the correlation time τ_c necessary to make a rotation through one radian.

Instead of τ_c it is more convenient to use an expression for the correlation frequency of reorientation ν_c, related to the correlation time by the equation $2\pi\nu_c\tau_c = 1$. For this we find

$$\nu_c = (1/2\pi)\ (2V_0/J)^{1/2} \exp\,(-V_0/kT). \tag{4}$$

The correlation frequency of reorientation, on the other hand, can be determined from experimental data by the dependence of the second moment of the NMR line of a polycrystalline sample on the basis of an expression assumed by Gutowsky and Pake:[14]

---

*In Das[13] this expression is erroneously written in a form that differs from Eq. (3) by the factor ½.

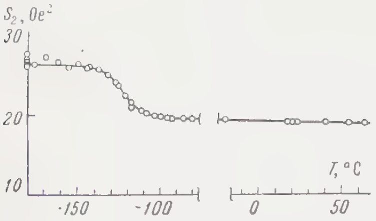

FIG. 4. Temperature dependence of the second moment of the NMR line of polycrystalline GASH.

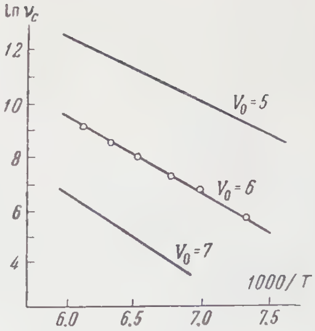

FIG. 5. Temperature dependence of the correlation frequency of reorientation of the guanidinium ion. Points – experimental data; curves – results of calculation with different values of V_0.

$$\ln \nu_c = \ln \frac{\gamma S_2^{1/2}}{2\pi} - \ln \tan\left(\frac{\pi}{2}\, \frac{S_2 - V_2}{U_2 - V_2}\right), \tag{5}$$

where S_2 is the second moment of the absorption line[9] at a given temperature, V_2 and U_2 are the second moments at higher and lower temperatures, and γ is the gyromagnetic ratio. A comparison of (5) and (4) makes it possible to determine the height of the potential barrier V_0 for classical reorientation.

Equation (5) is derived for the case in which the second moment is completely caused by groups reorienting themselves above a certain temperature. It is not possible to use it for a calculation of the correlation frequency from experimental data on the dependence of the second moment of the NMR line of polycrystalline GASH since the second moment in this case consists of two parts:

$$S_2 = \tfrac{2}{3} S_2(H_2O) + \tfrac{1}{3} S_2(NH_2), \tag{6}$$

where $S_2(H_2O)$ is the second moment arising from protons of "motionless" molecules of H_2O, and $S_2(NH_2)$ is the second moment caused by protons of the $[C(NH_2)_3]^+$ ions. The coëfficients in the right member of Eq. (6) are proportional to the relative numbers of protons occurring in water molecules and guanidinium ions in a crystal of GASH.

In order to make use of Eq. (5), it is necessary to eliminate from S_2 the constant component $S_2(H_2O)$ belonging to water molecules. From Eq. (6) we obtain

$$S_2(NH_2) = 3S_2 - 2S_2(H_2O), \tag{6'}$$

and substituting into (5),

$$\ln \nu_c = \ln \frac{\gamma\,(3S_2 - 2S_2(H_2O))^{1/2}}{2\pi} - \ln \tan\left(\frac{\pi}{2}\, \frac{S_2 - V_2}{U_2 - V_2}\right). \tag{5'}$$

Figure 4 shows the experimental temperature dependence of the second moment for powdered GASH. The value of $S_2(H_2O)$ can be calculated using the data presented above on the inter-proton distance in the water molecules and the data on the distribution of the other protons in GASH[8] with the aid of the formula of Van Vleck.[15]

Calculation of $S_2(H_2O)$ gives for GASH the value 21.5 oe^2, of which the intra-molecular part, arising from the interaction between the pair of protons in H_2O amounts to 19.5 oe^2, and the intermolecular part, caused by the interaction with protons from other water molecules and $C(NH_2)_3$ groups, amounts to 2 oe^2. The same magnitude for the intermolecular part is also obtained from the experimental data on the width of the resolved peaks.

It should be noted that if we also calculate $S_2(NH_2)$ in the same manner (using Van Vleck's formula and knowing the structure of the guanidinium ion), then the theoretical value of the second moment of a polycrystalline sample of GASH, calculated from Eq. (6), turns out to be lower than the experimentally observed magnitude of the second moment of GASH by approximately 10% both before and after the rotational transition. However, this discrepancy, the source of which is not clear, practically makes no difference in the magnitude of the height of the potential barrier as calculated below.

In Fig. 5 are presented the experimental values of the correlation frequency at various temperatures, based on Eq. (5′). Also indicated is the theoretical temperature dependence calculated from Eq. (4) for $V_0 = 5$, 6, and 7 kcal/mole. The moment of inertia of the guanidinium ion was calculated on the basis of the known structure of this ion[3] and the data of the present paper on the inter-proton distance in the NH_2 groups and is $J = 167.88 \times 10^{-40}$ g-cm^2.

The excellent agreement between the experimental data and the values calculated from Eq. (4) with $V_0 = 6$ kcal/mole attests to the correctness of the model assuming classical reorientation of the guanidinium ion in the GASH structure.

The existence of reorientation of the guanidinium ion at temperatures above −145° C is important for the explanation of the ferroelectrical properties of GASH. In particular, it is possible that the strong increase in polarization time of GASH at low temperatures[16] is associated with the decrease in mobility of the $C(NH_2)_3$ group.

The authors express their thanks to N. D. Sokolov and K. S. Aleksandrov for discussions of the work and for useful suggestions.

---

[1] Holden, Mertz, Remeika, and Matthias, Phys. Rev. **101**, 962 (1956).

[2] N. S. Rez and L. A. Varfolomeeva, Рост кристаллов (Growth of Crystals) **2**, Gostekhizdat, 1959, p. 126.

[3] S. Geller and D. P. Booth, Z. Krist. **111**, 117 (1959).

[4] A. G. Lundin and G. M. Mikhaĭlov, Приборы и техника эксперимента No. **2**, 92 (1960), Instruments and Exptl. Techniques, No. **2**, 272 (1960).

[5] Gutowsky, Meyer, and McClure, Rev. Sci. Instr. **24**, 644 (1953).

[6] G. E. Pake, J. Chem. Phys. **16**, 327 (1948).

[7] R. D. Spence and J. Muller, J. Chem. Phys. **26**, 706 (1957).

[8] Aleksandrov, Lundin, and Mikhaĭlov, Кристаллография **5**, 84 (1960), Soviet Phys.-Crystallography **5**, 77 (1960).

[9] E. R. Andrew, Nuclear Magnetic Resonance, Cambridge University Press, 1955.

[10] D. W. McCall, J. Chem. Phys. **26**, 706 (1957).

[11] Bloembergen, Purcell, and Pound, Phys. Rev. **73**, 679 (1948).

[12] E. R. Andrew, J. Chem. Phys. **18**, 607 (1950).

[13] T. P. Das, J. Chem. Phys. **27**, 763 (1957).

[14] H. S. Gutowsky and G. E. Pake, J. Chem. Phys. **18**, 162 (1950).

[15] J. H. Van Vleck, Phys. Rev. **74**, 1168 (1948).

[16] A. G. Chynoweth, Phys. Rev. **102**, 1021 (1956).

Translated by L. M. Matarrese
219

SOVIET PHYSICS JETP VOLUME 13, NUMBER 5 NOVEMBER, 1961

NUCLEAR RESONANCE OF Sn^{119} *IN METALLIC TIN*

Yu. S. KARIMOV and I. F. SHCHEGOLEV

Institute for Physics Problems, Academy of Sciences, U.S.S.R.

Submitted to JETP editor December 16, 1960

J. Exptl. Theoret. Phys. (U.S.S.R.) **40**, 1289-1292 (May, 1961)

The dependence of the second moment of the absorption line of Sn^{119} on the external magnetic field was measured between 900 and 5800 oe in metallic tin. A value of $\delta = 1.0 \times 10^{-3}$ was obtained for the Knight-shift anisotropy. The indirect exchange coupling constant between neighboring nuclei was found to be $A = 2.5$ kc/sec.

NUCLEAR magnetic resonance in metallic tin was first observed by McGarvey and Gutowsky.[1] They reported that the width of the resonant absorption line was several times greater than what was expected from the dipole-dipole interaction between the nuclei. Later, Bloembergen and Rowland,[2] during an NMR (nuclear magnetic resonance) investigation of tin at high fields, discovered that the line was also strongly asymmetric. They presumed that the anomalous line width and asymmetry could be attributed to anisotropy in the Knight shift of metallic tin.

In fact, finely dispersed samples are always used in NMR experiments on metals, and if the shift is anisotropic an additional source of line broadening exists, associated with the different orientations of the individual crystallites with respect to the external magnetic field. Since the Knight shift is proportional to the external field, its contribution to the line width will increase with increasing field, becoming particularly large in strong fields.

In the present work we investigated the anomalous line width in metallic tin more thoroughly. In order to distinguish between contributions from different causes to the absorption line width, the dependence of the second moment of the absorption line of Sn^{119} on the external field was studied.

An NMR spectrometer described previously[3] was used for the measurements. It is to be noted that in all experiments the instability of the magnetic field and its inhomogeneity over the sample volume, taken together, did not exceed 2×10^{-4} and thus did not contribute to the line width.

All experiments were conducted at the temperature of liquid helium. This yielded a higher signal-to-noise ratio and permitted experiments in small fields.

Measurements were made on two samples, which were prepared by mixing finely powdered metal in vacuum grease and differed in particle size. For one of the samples the powder was obtained by filing tin with a barrette file and contained particles $10-30\mu$ in size. This is much greater than the skin depth in tin, which is $2-3\mu$ at liquid-helium temperature in the frequency range used.[4] The powdered tin for the other sample was obtained by reducing $SnSO_4$ with fine zinc dust in a 1.5% aqueous solution of gelatin and contained particles $2-3\mu$ in size, i.e., of the same order as the skin depth.

As is known, NMR investigation of metals is complicated by the circumstance that the finite depth of penetration of the rf field into the sample causes the resonant absorption to be determined not only by the imaginary part χ'' of the complex nuclear susceptibility $\chi = \chi' - i\chi''$, but also by its real part χ'. This occurs because the value of χ' determines the skin depth: with an increase in χ' the skin depth decreases, and the absorption, other things being equal, decreases. A careful analysis of this problem was made by Chapman, Rodes, and Seymour.[5] In their paper it is shown that the absorption of energy due to nuclear resonance in a finely dispersed metallic sample is determined by the quantity $a\chi' + b\chi''$, where the value of a/b depends on the ratio of the dimension of the particle to the skin depth and approaches unity as the particle size is increased.

It has been observed, however, that the effect of χ' on the absorption line shape is in fact always less than can be expected from this relation.[5,6] Nor did we observe distortion of the absorption lines in our two samples, and their locations and second moments coincided within experi mental error.

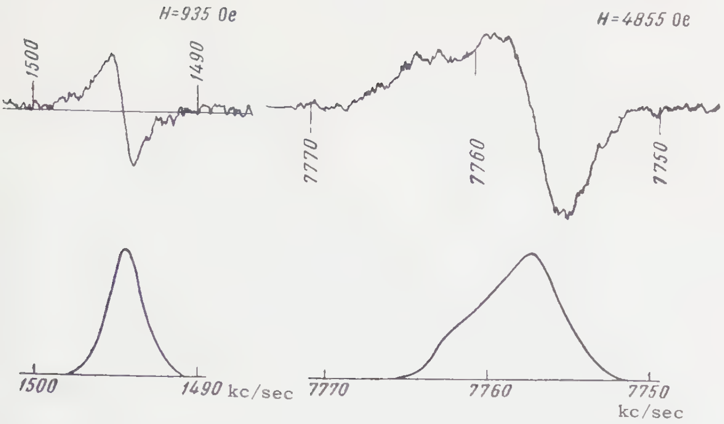

FIG. 1. Upper, derivative traces of Sn^{119} absorption lines; lower, integrated line shapes.

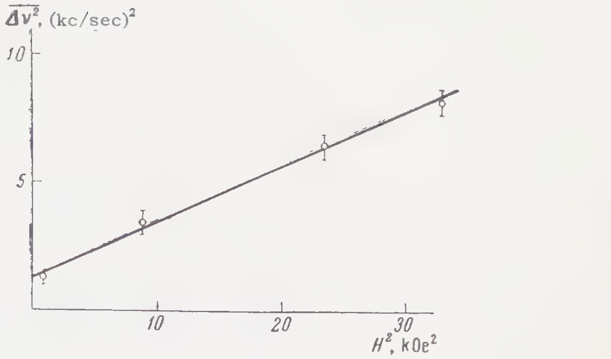

FIG. 2. Dependence of the second moment of the Sn^{119} absorption line on the square of the external magnetic field.

We should like to indicate at this point that there exists at least one effect which will lessen the effect of the real part of the susceptibility on the absorption line shape. Namely, an increase in χ' leads to an increase in the inductance of the resonant circuit in which the sample is located, with the result that the resonant resistance of the circuit increases and with it the amplitude of the rf voltage across the circuit. It is easy to show that when account is taken of this effect the magnitude of the resonance absorption signal is determined by the expression

$$(Q + a/b)\chi'' + (Qa/b - 1)\chi',$$

where Q is the figure of merit of the circuit. Since the Q of a circuit containing much metal is not large, the second term can become significantly less than the first even when the ratio a/b is not very small.

As an illustration, we present in Fig. 1 derivative traces of the absorption lines of Sn^{119} in metallic tin in two different magnetic fields H. It is seen that a marked widening of the line is observed with an increase in field, and asymmetry appears. In Fig. 2 is shown the dependence of the second moment $\overline{\Delta\nu^2}$ on the square of the external field.* This dependence can be expressed in the form

$$\overline{\Delta\nu^2} = kH^2 + \overline{\Delta\nu_0^2}.$$

As already mentioned, the Knight shift is proportional to the external field. Hence the part of the second moment caused by the anisotropy of the Knight shift will be proportional to the square of the field. For tetragonal white tin we can write[7]

$$\overline{\Delta\nu^2_{\text{anis}}} = (1/45\pi^2)\gamma^2\delta^2H^2,$$

where the anisotropy of the Knight shift is

$$\delta = (\nu_{\parallel} - \nu_{\perp})/\nu_0,$$

where γ is the nuclear gyromagnetic ratio, ν_0 the resonant frequency of Sn^{119} in a nonmetallic sample, $\nu_{\parallel}$ and $\nu_{\perp}$ are the resonant frequencies of Sn^{119} in the metal when the field is directed respectively along the tetragonal axis and perpendicular to it.

If one considers that the sole reason for the dependence of the second moment on field is the Knight anisotropy, it is necessary to assume

$$k = (1/45\ \pi^2)\gamma^2\delta^2.$$

From the data presented in Fig. 2 it can then be determined that

$$\delta = (1.0 \pm 0.1)\cdot 10^{-3}.$$

The error indicated here is the scatter of δ in the different experiments.

A value 1.2 ± 0.2 (kc/sec)^2 was obtained for $\overline{\Delta\nu_0^2}$. At the same time, for a sample with natural isotopic composition the second moment caused by dipole-dipole interaction is given by Van Vleck's formula as $\overline{\Delta\nu^2_{\text{dip}}} = 0.15$ (kc/sec)^2, i.e., one-eighth as large.

We can attempt to explain this discrepancy by using the Ruderman and Kittel hypothesis of indirect exchange interaction, between the nuclei in the metal which arises from the conduction electrons. Because of the presence of two different isotopes (Sn^{117} and Sn^{119}), this interaction makes the following contribution to the second moment of the isotope under investigation

$$\overline{\Delta\nu^2_{\text{exch}}} = [I(I+1)/3]\, f \sum_j A_{ij}^2,$$

where I is the spin, f is the concentration of the other isotope (in our case, Sn^{117}), and A_{ij} is the indirect exchange interaction constant between nucleus i and nucleus j. Assuming $A_{ij} \sim 1/R_{ij}^3$, where R_{ij} is the distance between nucleus i and nucleus j, and summing in $\overline{\Delta\nu^2_{\text{ex}}}$ over the 22 nearest neighbors, we can obtain from our experimental data $A = 2.5$ kc/sec for the exchange interaction constant between nearest neighbors. This is found to be in qualitative agreement with those values for A which can be derived from Ruderman and Kittel's formula by using reasonable values for the parameters entering into this formula.

---

*The second moment was calculated relative to the center of gravity of the line.

In conclusion, we express our deep gratitude fo Academician P. L. Kapitza for his interest in the work, to A. S. Borovik-Romanov for a discussion of the results, and N. N. Mikhaĭlov for assitance in preparing the samples.

---

[1] B. R. McGarvey and H. S. Gutowsky, J. Chem. Phys. **21**, 2114 (1953).

[2] N. Bloembergen and T. J. Rowland, Acta Met. **1**, 731 (1953).

[3] Yu. S. Karimov and I. F. Shchegolev, JETP **40**, 3 (1961), Soviet Phys. JETP **13**, 1 (1961).

[4] A. L. Schawlow and G. E. Devlin, Phys. Rev. **113**, 120 (1959).

[5] Chapman, Rodes, and Seymour, Proc. Phys. Soc. (London) **B70**, 345 (1957).

[6] A. G. Redfield, Phys. Rev. **101**, 67 (1956).

[7] N. Bloembergen and T. J. Rowland, Phys. Rev. **97**, 1679 (1955).

[8] M. A. Ruderman and C. Kittel, Phys. Rev. **96**, 99 (1954).

Translated by L. M. Matarrese
220

SOVIET PHYSICS JETP VOLUME 13, NUMBER 5 NOVEMBER, 1961

RELAXATION ABSORPTION OF ELECTROMAGNETIC ENERGY IN THE ANTI-FERROMAGNETIC SUBSTANCE $CoCl_2$

R. T. MINA

Institute for Physics Problems, Academy of Sciences, U.S.S.R.

Submitted to JETP editor December 21, 1960

J. Exptl. Theoret. Phys. (U.S.S.R.) **40**, 1293-1295 (May, 1961)

The absorption of electromagnetic energy in a single crystal of the antiferromagnet $CoCl_2$, which has a Curie point at 25°K, was investigated at a frequency of 37 300 Mc/sec in magnetic fields up to 6 koe.

THE antiferromagnet $CoCl_2$ has a rhombohedral lattice. Thorough neutron diffraction investigations[1] have shown that the magnetic moments of the Co^{++} ions of each sublattice are located in alternate planes, which are perpendicular to the three-fold axis C_3. The weak anisotropy of the molecular field in each of these planes leads to the formation of antiferromagnetic domains. However, in external fields greater than 1.5 koe directed perpendicular to the C_3 axis the antiferromagnet consists of a single domain.

The monocrystals studied in the present work were grown in vacuum from a melt of preliminarily dehydrated salt. The samples obtained were transparent, homogeneous, and bluish in color. Orientation and quality of the different specimens were controlled by x rays.

The energy absorbed in the sample was determined from the power transmitted through a resonator in which the sample was placed. The transmitted power was registered on a peak-reading voltmeter, whose reading was inversely proportional to the square of the power absorbed by the sample. To prevent changes in the natural frequency of the resonator from affecting the results of the measurements, the generator frequency was modulated with a period of 0.03 sec within limits exceeding the range of resonator frequency change.

The results obtained for two orientations of the samples are presented in Figs. 1, 2, and 3.

From Figs. 1 and 2 it is seen that at a certain temperature and corresponding value of constant magnetic field H the absorbed power is at a maximum. Common to both cases is the disappearance of a non-monotonic temperature dependence of the absorbed power in fields greater than 5.5 koe.

As can be seen from Fig. 3, the power absorbed by the antiferromagnet in the paramagnetic state

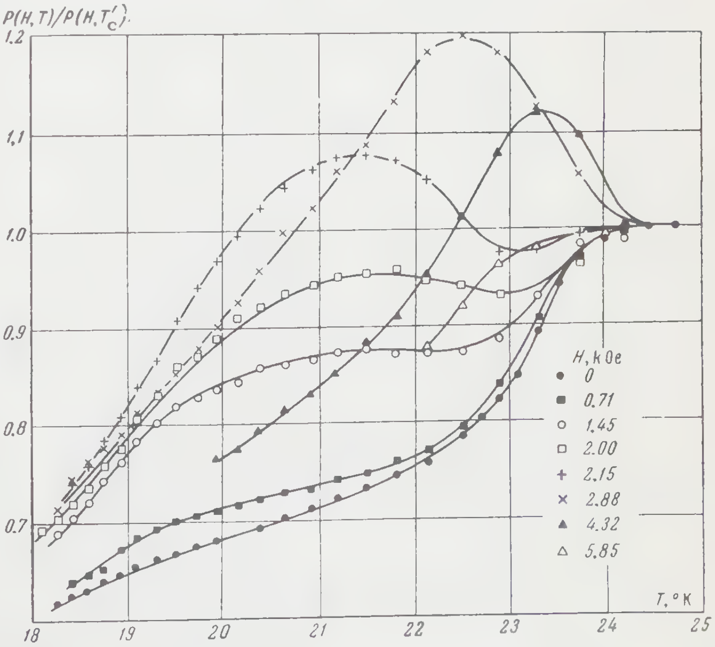

FIG. 1. Ratio of the power absorbed by a monocrystal of $CoCl_2$ at temperature T to that absorbed at $T'_C = 26°K$, $P(H, T)/P(H, T'_C)$, for various values of the constant field H. The C_3 axis of the crystal, the alternating field H′, and the constant field H are mutually perpendicular.

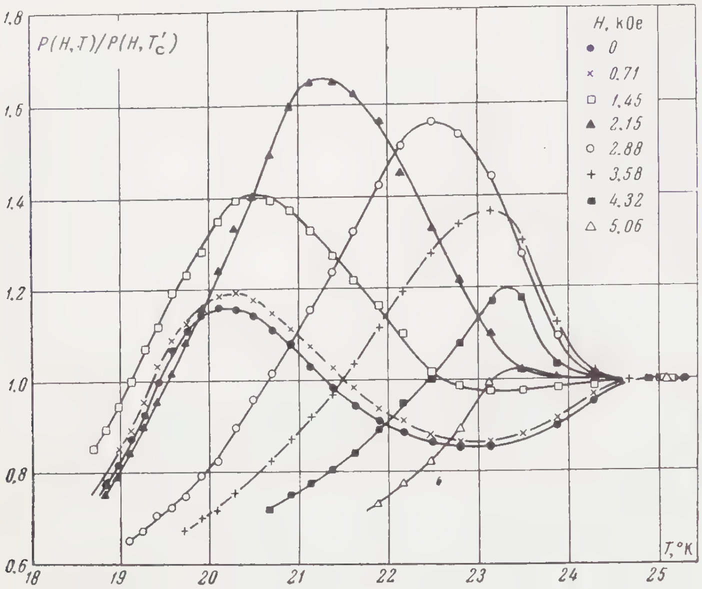

FIG. 2. Ratio of the power absorbed by a monocrystal of $CoCl_2$ at temperature T to that absorbed at $T'_C = 26°K$, $P(H, T)/P(H, T'_C)$, for various values of the constant field H. The crystal axis was parallel to the alternating field H′ and perpendicular to the constant field H.

decreases with an increase in the constant field. A similar phenomenon has also been observed[2] in paramagnetic salts. In the latter case it is associated with the existence of spin-spin and spin-lattice relaxation in the paramagnet.[3]

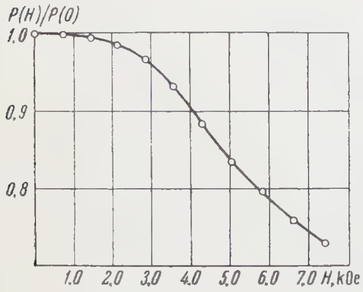

FIG. 3. Ratio of powers P(H)/P(0) absorbed by a monocrystal of $CoCl_2$ at a given field H and at H = 0 at 25.5°K. The orientation of the crystal with respect to the alternating and constant fields is the same as that of Fig. 2.

No temperature dependence of power absorbed by the sample was observed above the Curie point in the interval 25 — 40° K. However, further increase in temperature up to 80° K results in a decrease of absorption in the monocrystal.

The data presented above suggests a relaxation mechanism for the observed absorption. The relaxation processes that establish equilibrium in the spin system of the antiferromagnet can be characterized by a certain time τ. Since τ increases as the temperature of the antiferromagnet is decreased,[4,5] and the relaxation absorption of electromagnetic energy of frequency ω has the form

$$P(\omega,\tau) \sim \omega\tau/[1 + (\omega\tau)^2],$$

the magnitude of P goes through a maximum as $\omega\tau \sim 1$. Unfortunately, the dependence of P on the magnitude of the constant field has not been studied theoretically.

Experiments were also carried out with the antiferromagnet $CoBr_2$, which has a Curie point at 18° K and a structure analogous to that of $CoCl_2$. The data obtained with a sample of $CoBr_2$ with the same orientation as that of Fig. 2 were completely similar to those obtained for $CoCl_2$.

The author is deeply grateful to Academician P. L. Kapitza and Corresponding-Member A. I. Shal'nikov for their interest in the work, to M. S. Khaĭkin, under whose leadership the work was completed, to A. S. Borovik-Romanov for many discussions of the results, and to N. N. Mikhaĭlov for his assistance in growing the single crystals.

---

[1] Wilkinson, Cable, Wollan, and Koehler, Phys. Rev. **113**, 497 (1959).

[2] A. I. Kurushin, Izv. Akad. Nauk SSSR, Ser. Fiz. **20**, 1232 (1956), Columbia Tech. Transl. p. 1122.

[3] I. G. Shaposhnikov, Dissertation, Perm State University, 1959.

[4] G. I. Urushadze, JETP **39**, 680 (1960), Soviet Phys. JETP **12**, 476 (1961).

[5] Kaganov, Tsukernik, and Chunis, Физика металлов и металловедение (Phys. of Metals and Metallography) **10**, 797 (1960).

Translated by L. M. Matarrese
221

SOVIET PHYSICS JETP VOLUME 13, NUMBER 5 NOVEMBER, 1961

SPONTANEOUS FISSION PERIODS OF Np^{237}, Pu^{238}, AND Pu^{242}

V. A. DRUIN, V. P. PERELYGIN, and G. I. KHLEBNIKOV

Joint Institute for Nuclear Research

Submitted to JETP editor December 26, 1960

J. Exptl. Theoret. Phys. (U.S.S.R.) **40**, 1296-1298 (May, 1961)

An attempt has been made to determine the true spontaneous-fission half-period of Np^{237} by employing nuclear photographic emulsions. Prior to development, the photographic plates were treated with potassium ferrocyanide to remove the background α-particle tracks. The reliability of this method was checked by measuring the spontaneous-fission half-periods of Pu^{238} and Pu^{242}, which were independently determined using a proportional counter. The results obtained for plutonium by the various methods are identical and agree with other available data. Only three fragment tracks were detected in the Np^{237} photographic measurements. Thus, only a lower limit of 10^{18} years can be established for the half-period, as compared with the usually accepted value of 4×10^{16} years.

1. In the experiments of Segrè and his collaborators, the half-periods for spontaneous fission were already determined in 1945 — 1946 for a large number of both even and odd nuclei.[1] However, not all the data were obtained with the same accuracy. A check of the decay half-periods of Th^{232} (reference 2) and Am^{241} (reference 3) showed that their true values are higher by one to three orders of magnitude. The purpose of the present experiment was to achieve a higher accuracy in the measurement of the half-periods for the spontaneous fission of the odd-even isotope Np^{237} and the even-even isotopes Pu^{238} and Pu^{242}.

2. The investigated elements were coated electrolytically on a platinum support. The amount of the substance and the layer thickness were determined by counting the rate of α particles using a special arrangement with known geometry.[4] The uniformity of the samples was checked by counting α rays over separate parts of the layer. In addition, radiography of certain samples was carried out.

Seven samples were prepared, three of Np^{237} of ~ 20 mg each (density ~ 1 mg/cm^2), two of pure Pu^{238} (0.27 and 0.35 μg), and two consisting of a mixture of the isotopes Pu^{238} (14%) and Pu^{242} (86%), and containing 0.37 and 0.30 μg of Pu^{238} respectively. The isotope content of the mixture in the latter case was determined using a large magnetic α spectrometer.[5] In all calculations, the value of the partial half-periods of α decay for Pu^{238} was assumed to equal 86.4 years.[6]

3. The measurement of the spontaneous-fission half-period of the plutonium isotopes was carried out by two methods. In the first series of experiments, a cylindrical proportional counter 100 mm in diameter, 250 mm long, and filled with methane at 80 mm Hg was used for counting the fragments. The integral pulse spectrum was analyzed. The counting characteristics of the array had a sufficiently good plateau. The mean counting rate of the fragments was equal to 0.92 particles per hour for pure Pu^{238}, and to 7 particles per hour for the mixture of $Pu^{242} + Pu^{238}$. The statistical accuracy was not less than 5%, and the total error was not greater than 10%. As a result of the measurements, the following values for the half periods were obtained: 5.2×10^{10} years for Pu^{238}, and 6.7×10^{10} years for Pu^{242}.

In a second series of experiments, the method of oxidizing the latent image in nuclear emulsions was used in order to discriminate fission fragments against the background of a large number of α particles.[7] The work was carried out using an NIKFI (Research Institute of the Motion Picture Industry) P-8 emulsion 100μ thick. $K_3Fe(CN)_6$ was used for the oxidation. By means of special tests, it was established that the maximum acceptable $K_3Fe(CN)_6$ concentration amounts to $1:8 \times 10^3$. In our experiment, the concentration was not higher than $1:2 \times 10^4$. Such a concentration ensures good detection of fission fragments, and is sufficient to remove the background up to 10^{11} α particles per cm^2.

The plates were irradiated by samples of Pu^{238} and Pu^{242} for ten to one hundred hours. After the exposure, the emulsions were subjected to the action of the oxidizer (at 15° C for 30 min), were then washed with distilled water (15° C for 30 min), and then developed in diluted D-19 developer (1:3) (at 19° C for 30 min).

As has been shown by experiments, the effect studied could be imitated by tracks of α particles which appeared due to the decay of radioactive nuclei during the process of washing out the oxidizer and of the development. Special measures were therefore taken to prevent the introduction of impurities into the emulsion during the exposure. On the scanned plates, the density of tracks of spontaneous fission amounted to 800 per cm^2 for Pu^{242} and 200 per cm^2 for Pu^{238}. It has been established that the fragment tracks are detected in the angle interval 20 — 70°, i.e., the detection efficiency amounts to $(66 \pm 5)\%$.

The measured half-periods for the spontaneous fission of Pu^{238} and Pu^{242} were found to be $(5.0 \pm 0.6) \times 10^{10}$ years and $(6.5 \pm 0.7) \times 10^{10}$ years respectively.

The fact that the results obtained by us using various methods are identical, and are also in good agreement with data already known, permits us to conclude that the method of using nuclear emulsions may be successfully applied for measuring the half-period for the spontaneous fission of Np^{237}. The difficulty consists of the fact that long exposures (several days) are necessary to obtain a marked effect. In such a case, there is a danger of the fading of the latent image when the emulsion is kept for a long time at normal room temperature and humidity. However, control experiments on the fission of U^{235} induced by thermal neutrons showed that the fading could not lead to a considerable decrease in the detection efficiency of spontaneous-fission fragments of Np^{237}.

45 cm^2 of the emulsion were scanned altogether, and two-thirds of the area was scanned consecutively by two observers to avoid bias. Instead of an expected 100 events, only three tracks were found. The observed effect is too small to enable us to speak about an exact value of the decay constant of Np^{237}. It only determines the lower limit of the spontaneous-fission half-period of Np^{237}, for which a value of 10^{18} years is indicated. The difference between our results and those of Segre shows that the fission probability of Np^{237} is evidently considerably less than has been believed.

The authors would like to thank Prof. G. N. Flerov, who supervised the work, and also A. M. Semchinova for help in work with the emulsions.

---

[1] E. Segrè, Phys. Rev. **86**, 21 (1952).

[2] Klochkov, Skobkin, Terent'ev, and Flerov, Doklady Akad. Nauk SSSR **118**, 69 (1957), Soviet Phys.-Doklady **3**, 79 (1958).

[3] Mikheev, Skobelev, Druin, and Flerov, JETP **37**, 859 (1959), Soviet Phys. JETP **10**, 612 (1960).

[4] V. A. Karnaukhov and V. L. Mikheev, Приборы и техника эксперимента (Instruments and Exptl. Techniques) No. 6, 60 (1960).

[5] S. A. Baranov and A. G. Zelenkov, ibid., No. 5, 3 (1959).

[6] Strominger, Hollander, and Seaborg, Revs. Modern Phys. **30**, 823 and 824 (1958).

[7] Semchinova, Donets, and Perelygin, Paper presented at the 3rd International Conference on Nuclear Photography, Moscow, 1960.

Translated by H. Kasha
222

SOVIET PHYSICS JETP VOLUME 13, NUMBER 5 NOVEMBER, 1961

VISCOSITY AND HYSTERESIS PROPERTIES AT LOW TEMPERATURES OF MANGANESE IRON FERRITES CONTAINING COBALT ADMIXTURES

K. M. BOL'SHOVA and T. A. ELKINA

Moscow State University

Submitted to JETP editor December 29, 1960

J. Exptl. Theoret. Phys. (U.S.S.R.) **40**, 1299-1301 (May, 1961)

The magnetic viscosity, magnetostriction, and hysteresis properties of a polycrystalline ferrite of composition $Mn_{1.75}Co_{0.05}Fe_{1.2}O_4$ were studied in the low temperature region. An extremely high viscosity was found in the temperature region from −100 to −150° C in static fields up to 250 oersteds. The remagnetization time was measured and found to be of the order of tens of minutes to hours. It was demonstrated that in this temperature region Perminvar and rectangular loops are formed in oscillatory fields. The character of the variation in the form of the loop in increasing oscillatory fields is compared with the magnetic viscosity found in static fields.

IN the present work, a study has been carried out, in the low-temperature region, of the magnetic viscosity, magnetostriction and hysteresis properties of a polycrystalline sample of manganese-iron ferrite containing a small admixture of cobalt ($Mn_{1.75}Co_{0.05}Fe_{1.2}O_4$).

Magnetization measurements on this ferrite in the low temperature region showed that in weak and moderate magnetic fields (from 4 to 250 oersteds) it possesses a very high magnetic viscosity. The intensity of magnetization of the sample continues to rise after it has been held in a constant field for 17 hours, while when the field is reversed the sample remains magnetized in the former direction of the field for a period which in a number of cases exceeded 1 hour (in one experiment the remagnetization time reached 174 minutes). The existence of such a high magnetic viscosity (for remagnetization of a substance) is nowhere indicated in the literature.

The experiments were carried out at various temperatures and in various magnetic fields. The viscosity is most pronounced over the temperature interval from −100 to −150° C, in fields not exceeding 250 oersteds.

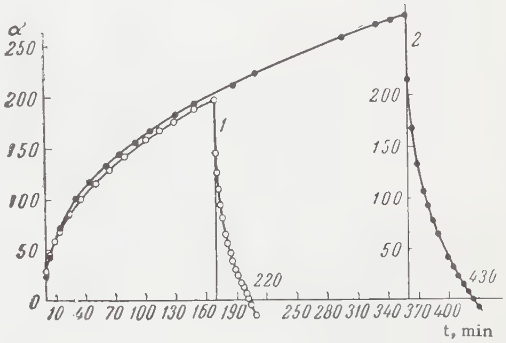

FIG. 1. Magnetization and remagnetization curves for the ferrite $Mn_{1.75}Co_{0.05}Fe_{1.2}O_4$ as a function of time in an 18.8-oe field, at a temperature of −125°C: curve 1 – field direction reversed after 2 hr 50 min; curve 2 – experiment repeated, field direction reversed after 6 hr (α – galvanometer deflection, proportional to intensity of magnetization).

As an example of the data obtained, Fig. 1 presents curves showing the variation of intensity of magnetization with time at −125° C, in a field of 18.8 oersteds. Magnetization and remagnetization curves are given for the sample held in the field for different periods of time. In a given experiment the sample was demagnetized at room temperature; the measurement temperature was then established, the sample was held at this temperature for at least an hour (in order to establish a uniform temperature throughout the whole volume of the sample), and only then was the magnetic field applied. The same experiment was also carried out under other conditions: the sample was

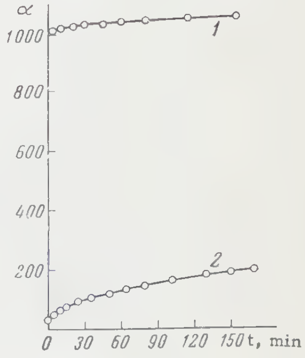

FIG. 2. Magnetization curves for the ferrite $Mn_{1.75}Co_{0.05}Fe_{1.2}O_4$ as a function of time in an 18.8-oe field, at a temperature of −125°C; curve 1 – sample demagnetized at −125°C; curve 2 – sample demagnetized at room temperature.

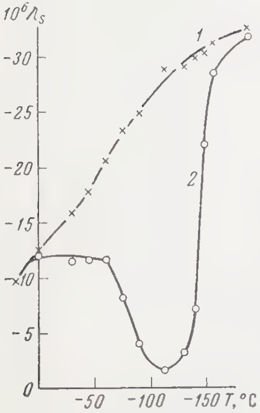

FIG. 3. Temperature dependence of the saturation magnetostriction λ_s for $Mn_{1.75}Co_{0.05}Fe_{1.2}O_4$: curve 1 – sample demagnetized each time at room temperature; curve 2 – sample demagnetized at the temperature of the measurement.

demagnetized, not at room temperature, but at the temperature of the measurement. This change in the conditions of demagnetization exerted a strong effect upon the viscous properties of the sample: the viscosity was markedly reduced, although it did not vanish entirely, while the intensity of magnetization of the sample showed a substantial increase (Fig. 2).

The saturation magnetostriction in the same ferrite was measured in a 2500 oersted field with the aid of cemented-on pick-ups. The influence of the viscosity was manifested in the fact that the value for the magnetostriction proved strongly dependent upon the way in which the sample was demagnetized. In Fig. 3. are presented curves showing the temperature dependence of the magnetostriction for demagnetization of the sample at room temperature (curve 1) and at the temperature of the measurement (curve 2).

In the same temperature region, hysteresis loops were observed for the ferrite sample under study in an alternating field (50 cps) by oscillographic means. It was found that Perminvar and rectangular loops are produced in the same range of weak and moderate fields for which viscosity is evident. If a sample demagnetized at room temperature is placed in an increasing alternating field, then for fields up to a few tens of oersteds an inclined line is seen on the oscilloscope screen — no loop is present. As the field is further increased, the line changes visibly, first into a Perminvar, then a normal, and finally, into a rectangular loop. If the sample is demagnetized at the measurement temperature, the Perminvar and normal loops are not formed at all, and, as the field is increased, the "line" obtained in a weaker-field region changes discontinuously into a rectangular loop having an extremely high rectangularity factor (about 0.97).

The experimental data thus obtained show that the character of the change in form of the hysteresis loop in alternating fields is closely associated with the magnetic viscosity which appears in this material in static fields. Where the remagnetization times are extremely long (of the order of several tens of minutes when the sample is held in the field for approximately 6 hours), the loop in an alternating field has the form of a line. At some specific value of the field (at a temperature of − 125° C this field is 43 oersteds) the remagnetization time falls very sharply (becoming less than 1 minute), and in this same field the line is transformed after a short time into a Perminvar loop.

In fields for which the loops become rectangular after a brief time in the field, the viscosity is even less pronounced.

The results obtained may be explained on the assumption that the ferrite which we have investigated undergoes a magnetic "annealing"; i.e., a uniaxial anisotropy arises in each of its domains under the influence of the magnetic field, with the axis of easy magnetization directed along the magnetization vector of the given domain. The development of uniaxial anisotropy in the ferrite under study is evidently the result of an electron diffusion process which is governed by the magnetic field.[1]

It is most natural to assume that an exchange of electrons takes place between the Mn^{2+} ions and manganese ions of higher valency (in manganese-iron ferrites containing excess manganese, in addition to Mn^{2+} ions, manganese ions of higher valency are always present). The role of the cobalt ions in this process is as yet insufficiently clear.

More detailed information on the ferrite described, and on other manganese-iron ferrites containing excess manganese (with and without cobalt), will be published in the future.

In conclusion, we consider it an agreeable duty to express our gratitude to Professor K. P. Belov for his attention to the present work.

---

[1] A. Kienlin, Zs. Angew. Phys. **10**, 12 (1958).

Translated by S. D. Elliott
223

SOVIET PHYSICS JETP VOLUME 13, NUMBER 5 NOVEMBER, 1961

PRODUCTION OF $Y^0(\Lambda, \Sigma^0)$ *AND* K^0 *PARTICLES ON LIGHT NUCLEI BY 2.8-Bev/c PIONS*

Ya. Ya. SHALAMOV, V. A. SHEBANOV, and A. F. GRASHIN

Institute of Theoretical and Experimental Physics, Academy of Sciences, U.S.S.R.

Submitted to JETP editor December 29, 1960

J. Exptl. Theoret. Phys. (U.S.S.R.) 40, 1302-1312 (May, 1961)

The production of $Y^0(\Lambda, \Sigma^0)$ hyperons and K^0 mesons by 2.8-Bev/c π^- mesons on light nuclei was studied in a freon $(C_2F_5Cl_3)$ bubble chamber. The Y^0 and K^0 production cross sections are $(2.5 \pm 0.5)\%$ and $(7 \pm 1)\%$ respectively of the total cross section for inelastic processes. The cross sections for these processes, as well as the angular and momentum distributions of the particles produced, were determined from 143 $Y^0 + K^0$ and $K^0 + \overline{K}^0$ production events. The ratio of the cross section is $\sigma(K^0\overline{K}^0)/\sigma(Y^0K^0) = 0.65 \pm 0.15$ and their sum is $\sigma(K^0\overline{K}^0) + \sigma(Y^0K^0) = (3.2 \pm 0.8)\%$ of the total cross section for inelastic processes. 80 — 90% of the $Y^0 + K^0$ production events are accompanied by a π-meson production, but in 70 — 80% of the $K^0 + \overline{K}^0$ production events, no π meson is emitted.

A characteristic feature is that, in the $K^0 + \overline{K}^0$ production, the K^0 mesons carry off practically all of the available energy, whereas a soft hyperon spectrum is observed in $Y^0 + K^0$ production events.

The cross section for the reactions $\pi^- + \pi^+ \rightarrow K^0 + \overline{K}^0$ ($\sigma \sim 2$ mb) and $\pi^- + K^{0,+} \rightarrow \pi^{-,0} + K^0$ ($\sigma \gtrsim 10$ mb) can be estimated for final kinetic energies of the particles in the c.m.s. ≤ 0.5 Bev by assuming that, in the reaction under consideration, the pole diagrams make a large contribution, at least for small transferred momenta.

DETAILED experimental data have become available on the production of strange particles in π^-p collisions near the threshold in the 0.9 — 1.3 Bev energy range.[1,2] The production of $Y^0(\Lambda, \Sigma^0)$ hyperons and K^0 mesons in collisions of π mesons with nuclei has been studied at 1.5 and 1.9 Bev.[3-5]

Kuznetsov et al.[6] measured the ratio of the cross sections $\sigma(K^0\overline{K}^0)/[\sigma(\Lambda K^0)] + \sigma(\Sigma^0K^0)] = 0.51 \pm 0.19$ for the xenon nucleus at 2.8-Bev/c π^--meson momentum. The production of strange particles in π^-p collisions has been studied at 6.8 Bev/c.[7]

In the present experiment, the production of $Y^0(\Lambda, \Sigma^0)$ hyperons and K^0 mesons on carbon, fluorine, and chlorine nuclei by π^- mesons with 2.8-Bev/c momentum was studied. The experiment was carried out by means of a 17-liter freon bubble chamber[8] using the external π^--meson beam of the proton synchrotron at the High-Energy Laboratory of the Joint Institute for Nuclear Research.

EXPERIMENTAL METHOD

In the experiments with the 2.8-Bev/c π^--meson beam (momentum spread $\Delta p/p = 10\%$), about 60 000 stereoscopic photographs were obtained using the freon $(C_2F_5Cl_3)$ bubble chamber without magnetic field.[8] All photographs were scanned by two independent observers. In the scanning, those interactions of π^- mesons with nuclei that were accompanied by V decays correlated with the point of interaction were selected. These correspond to the decays $\Lambda \rightarrow p + \pi^-$ or $K^0 \rightarrow \pi^+ + \pi^-$. About 2000 such events were found. Out of these, 149 were accompanied by double V decays. After the analysis of these events, six were considered as background events because of the noncoplanarity of one of the V decays with the point of interaction. The remaining 143 events were identified as associated particle production $Y^0(\Lambda, \Sigma^0) + K^0$ or $K^0 + \overline{K}^0$. These events were then analyzed in detail, as well as that part of the data which enables us to obtain information on the total production cross section of Y^0 and K^0 particles on nuclei. It should be noted that we did not differentiate experimentally between the events of Λ and Σ^0 production, but the total yield for the $Y^0(\Lambda, \Sigma^0)$ hyperons was found.

The spatial analysis of the photographs was carried out with a stereo-projector, by means of which the coplanarity was checked, and the angles of emission and the particle ranges were measured. The decay particles were identified by a kinematic analysis of the angles between the direction of motion of the V particles and of their decay products, by range and ionization measurements, and from the multiple scattering of particles in the working liquid of the chamber. Out of 101 detected events of associated production of Y^0 and K^0 particles, 41 Λ hyperons were identified from the angles of emission of the particles and their ranges (mainly from the proton ranges), 42 Λ hyperons were identified from the angles and the ionization J of protons at $J \geq 2J_{\min}$, 13 Λ hyperons from the angles and ionization at $J \sim 1.5 \times J_{\min}$, and 5 Λ hyperons from the energy and momentum conservation laws.

The momenta of the Λ and K^0 particles were determined from calculated kinematic relations between the angles of emission of the decay products, using the tables of Leipuner.[9] The accuracy of the momentum measurements was determined by the measurement accuracy for the emission angles of the decay products of Λ and K^0 particles, and amounted to about 10% on the average. In order to find the absolute yield of Y^0 and K^0 particles, the total number of interactions of π^- mesons in the working volume of the chamber was counted, and a correction was applied to the number of detected Λ and K^0 particles. In the correction, the following factors were taken into account: the fractions of Λ and K^0 particles decaying into neutral particles, the fraction of long-lived K^0 mesons, the geometrical coefficients α_1 and α_2, and the fractions of Λ and K^0 decay events that were not detected in the chamber either because of the short range of the decay products or because of relatively small emission angles. (In the latter case, the decays might be imitated by high-energy electron-positron pairs.)

The geometrical coefficient α_1 is determined by the detection probability of Λ and K^0 particles in the effective volume, and is given by the equation $\alpha_1^{-1} = 1 - \exp(-L/L_0)$, where L is the "potential" range of Λ and K^0 particles and L_0 is the decay mean free path. The mean value $\bar{\alpha}_1$ was found to be equal to 1.16 for Λ particles and 1.20 for K^0 particles.

The coefficient α_2 is related to the decreased detection efficiency of V decays in the plane perpendicular to the plane photographed. It is determined experimentally and is, on the average, equal to 1.15 ± 0.08 both for Λ and K^0 particles.

The resulting values of the correction factors used to multiply the number of Λ and of K^0 particles detected in the chamber are 2.70 and 4.20 respectively.

EXPERIMENTAL RESULTS

1. Cross Section for the Production of the Particle Pairs $Y^0 + K^0$ and $K^0 + \bar{K}^0$, and Total Cross Section for the Production of Y^0 and K^0 Particles

The associated production processes $Y^0 + K^0$ and $K^0 + \bar{K}^0$ on nuclei were studied in the following reactions:

$$\begin{aligned} &\text{a) } \pi^- + A \to \Lambda + K^0 + m\pi + A', \\ &\text{b) } \pi^- + A \to \Sigma^0 + K^0 + m\pi + A'; \end{aligned} \quad (1)$$

$$\pi^- + A \to K^0 + \bar{K}^0 + n\pi + A'. \quad (2)$$

The measurements did not differentiate between reactions (1a) and (1b), and therefore the total cross section σ_1 for the associated production Y + K^0 and $\Sigma^0 + K^0$ was measured.

Out of 143 events of the associated production $Y^0 + K^0$ and $K^0 + \bar{K}^0$, 101 (5) events were considered as $Y^0 + K^0$, and 42 (4) as $K^0 + \bar{K}^0$. (The figures in the parentheses refer to the number of doubtful cases, in which no clear choice between $Y^0 + K^0$ and $K^0 + \bar{K}^0$ could be made.) The ratio of the cross sections for reactions (2) and (1) calculated from these events is $\sigma_2/\sigma_1 = 0.65 \pm 0.15$; the undetermined cases have been taken into account in calculating the error. The value obtained is in agreement, within the limits of experimental error, with the value for the xenon nucleus 0.51 ± 0.19 given by Kuznetsov et al.[6] for the same π^--meson energy. The total cross section $\sigma_1 + \sigma_2$ amounts to (3.2 ± 0.8)% of the total cross section for inelastic interactions of π^- mesons with fluorine nuclei. In calculating the results, it was assumed that the cross section per nucleus varies little between the lightest nucleus (C) and the heaviest one (Cl) of the mixture.

A rough estimate of the cross section for the production of the $K^0 + \bar{K}^0$ and $Y^0 + K^0$ pairs per nucleon gives $\sigma'(K^0\bar{K}^0) \approx \sigma'(Y^0K^0) \approx 0.5$ mb. The large value of the cross section for the production of $K^0 + \bar{K}^0$ pairs at 2.65-Bev π^--meson energy indicates a fast increase in this cross section with increasing energy of the π^- mesons above 1.5 Bev. (No production of $K^0\bar{K}^0$ pairs is observed at 1.5 Bev.[3])

The total cross section for the production of Y^0 and K^0 particles was obtained by a triple scanning of about 3000 pictures. A total of 8015 interactions of π^- mesons with nuclei, 73 events of Y^0-particle production, and 143 events of K^0-particle production were detected in these pictures. The total yield of $Y^0(\Lambda,\Sigma^0)$ hyperons amounted to $(2.5 \pm 0.5)\%$ and the yield of K^0 mesons to $(7 \pm 1)\%$, relative to the total cross section for inelastic interactions of π^- mesons with nuclei. From a comparison of these results with the data for carbon at 1.5-Bev π^--meson energy,[3] i.e., (1.7 ± 0.4) and $(1.4 \pm 0.5)\%$ for Y^0 and K^0 particles respectively, it is clear that the yield of Y^0 hyperons is greater by a factor of 1.5, and that of K^0 mesons by a factor of five.

In order to determine the value of m and n in reactions (1) and (2), an analysis of the stars correlated with a given pair of strange particles was carried out. The most reliabile result is given by the analysis according to the number of γ rays accompanying the production of strange particles. For the Y^0-hyperon production, this number, as determined from 30 conversion events $\gamma \rightarrow e^+ + e^-$ for the $Y^0 + K^0$ process and from 85 events for the $Y^0 + K^{+,0}$ process was found to equal $n_\gamma(Y^0K^0) = 1.0 \pm 0.15$. For the $K^0 + \overline{K}^0$ production, the value found from three events is $n_\gamma(K^0\overline{K}^0) = 0.22 \pm 0.15$. The number of π^0 mesons is therefore equal to $n_{\pi^0}(Y^0K^0) \leq 0.5 \pm 0.07$ and $n_{\pi^0}(K^0\overline{K}^0) = 0.11 \pm 0.07$. The inequality sign in the first case is due to the possible detection of electron-positron pairs produced as a result of the conversion of γ rays from the $\Sigma^0 \rightarrow \Lambda + \gamma$ decays. The number of charged mesons in stars was determined from the number of particles having a relativistic ionization. The total mean number of π mesons in the reactions (1) and (2) is equal to $m = 1.2 \pm 0.15$ and $n = 0.6 \pm 0.15$.

2. Angular and Momentum Distribution

The angular and momentum distributions for Λ and K^0 particles are shown in Fig. 1. The angular distributions of Λ and K^0 particles in the laboratory system (l.s.) are strongly peaked forward: 80 — 90% of the particles are within a cone with $\cos\theta \geq 0.8$. The momentum spectrum of Λ particles was studied at $p_\Lambda \geq 300$ Mev/c and the spectra of K^0 mesons at $p_{K^0} \geq 100$ Mev/c. The spectrum of Λ particles has a maximum at 600 Mev/c and decreases rapidly at higher momenta. The spectra of K^0 mesons in both reactions have a maximum for $p_{K^0} \approx 1$ Bev/c and continue up to 2.5 Bev/c. An estimate of possible distortions of the momentum spectra caused by a difference in the correction factors for different momentum values was carried out. The difference, however, was not greater than 10 — 15%, and it was therefore neglected. The possibility of determining the momentum of Σ^0 particles by measuring the momenta of Λ particles in the $\Sigma^0 \rightarrow \Lambda + \gamma$ decay was analyzed. The distortion of the Σ^0 spectrum caused by this decay is negligible, and, in our case, amounts to 4 — 7% depending on the Σ^0 momentum. Therefore, the momentum spectrum of the Λ hyperons is henceforth considered as a total spectrum of the $Y^0(\Lambda,\Sigma^0)$ hyperons.

An interesting result was obtained in considering the total kinetic energy carried away by the two K^0 mesons in $K^0 + \overline{K}^0$ production events. In Fig. 2, each $K^0 + \overline{K}^0$ production event is denoted by a rectangle with a number showing the number of prongs in the star. In the figure, the arrow denotes the available energy corresponding to the energy of the π^--meson beam, and limits determined by its energy half-width are shown. The mean energy in the spectrum is $\overline{T} = 1.30$ Bev. The mean energy of the $K^0 + \overline{K}^0$ production events is greater than this value because of inelastic interactions of K^0 mesons in nuclei. If we consider the distribution of the energy carried away by K^0 mesons in prong-

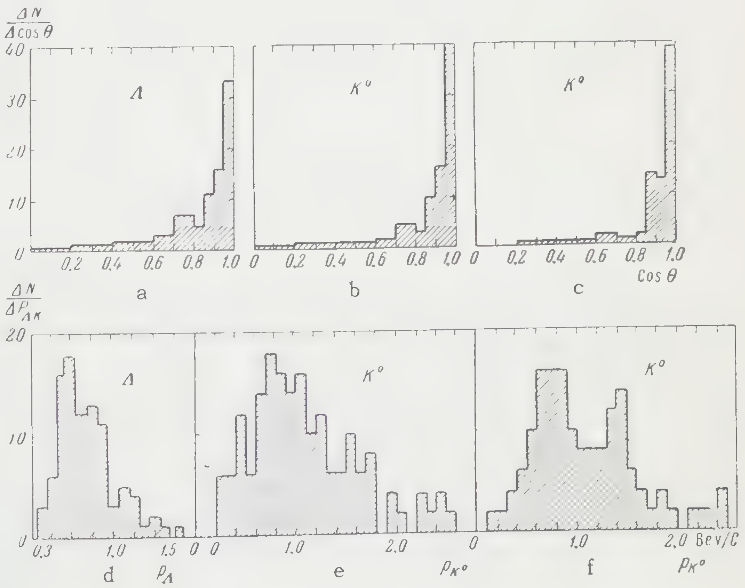

FIG. 1. Angular and momentum distributions for Λ and K° particles in the l.s. a, b, d, e – for reactions (1); c, f – for reactions (2).

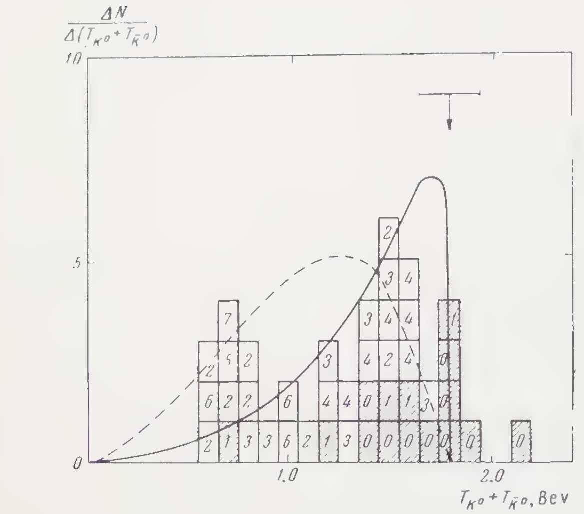

FIG. 2. Distribution of the total kinetic energy T carried away by K^0 and $\bar{K}^0$ mesons in the l.s. The dotted and solid lines represent the theoretical curves for the phase volume and for the polar diagrams of Fig. 4 respectively.

less and one-prong stars (the shaded rectangles in Fig. 2), for which we can assume a relatively small energy loss by K^0 mesons as a result of the inelastic collisions, then the mean value of the energy carried away by the two K^0 mesons is found to be 1.60 Bev. Thus, the characteristic feature of the associated production of $K^0 + \bar{K}^0$ is the large value of the energy carried away by the K mesons, close to the limiting value. The total uncertainty in the energy of two K^0 mesons carried away in a $K^0 + \bar{K}^0$ associated production event, in addition to the uncertainty in the energy of the π^--meson beams, is determined only by the accuracy of the K^0-meson energy measurement and by the Fermi width of the momenta of nucleons taking part in the production of $K^0 + \bar{K}^0$, and, in our case, amounts to ±0.25 Bev. This means, in particular, that if the energy carried away by the K^0 mesons in a $K^0 + \bar{K}^0$ event is equal to the limiting value, then all events will have a distribution with an energy width of 0.5 Bev.

3. Mean Number of π Mesons Accompanying the Elementary Act of Production of $Y^0 + K^0$ and $K^0 + \bar{K}^0$

In the determination of the cross sections and of the features of particle production from data obtained on light nuclei, a considerable uncertainty is introduced by the contributions of the nucleus. Nevertheless, it is possible to study a number of features of the elementary processes for a given π^--meson energy. In order to estimate the influence of the nucleus, calculations based on the optical model were carried out, using a simplified one-dimensional model. Calculations carried out for the fluorine nucleus (the average nucleus of the freon mixture) show that 1) about 70% of Λ hyperons produced in the nucleus do not interact with nuclear matter, and 2) 15 — 20% of K^0 and 30 — 40% of $\bar{K}^0$ mesons undergo inelastic interactions in the nucleus. The following values were used in the calculations: mean free path of π^- meson in nuclear matter $\lambda_\pi = 4 \times 10^{-13}$ cm, cross section $\sigma(\Lambda + N) \approx 30 -$ 40 mb, cross sections $\sigma(K^0 + N)$ and $\sigma(\bar{K}^0 + N)$ for the mean K^0-particle momentum of 1.1 Bev/c are 17 and 40 mb respectively, similarly as for $K^+ + N$ and $K^- + N$ events, according to the data of Crawford et al.[10]

Taking into account the fraction of inelastic interactions of K^0 and $\bar{K}^0$ mesons in nuclei calculated according to the optical model, and knowing the average number of π mesons produced as a result of inelastic collisions, we can estimate the number of secondary mesons in reactions (1) and (2), m_1 and n_1. The average number of π mesons produced per inelastic interaction of K^0 and $\bar{K}^0$ mesons in a nucleus was determined from preliminary experimental data obtained in an experiment using the same bubble chamber (altogether 20 events of such interactions were observed), and amounts to 1.0 ± 0.25. Hence, we obtain the estimate $m_1 = 0.2$, $n_1 = 0.5 - 0.6$ and, consequently, the total number of π mesons produced in an associated production event $Y^0 + K^0$ and $K^0 + \bar{K}^0$ is, on the average, equal to $m' = 1 \pm 0.2$ and $n' = 0.0$ $\pm$ 0.3 respectively.

The results obtained show that the production of Y^0 hyperons in π^-N collisions of 2.8-Bev/c π^- mesons is, in 80 — 90% of the events, accompanied by the production of a π meson, while the production of a $K^0 + \bar{K}^0$ pair is, in 70 — 80% of the cases, not accompanied by an emission of a π meson. Thus, the production of the $K^0\bar{K}^0$ and Y^0K^0 pairs on nucleons in a nucleus evidently occurs mainly in the following elementary reactions:

$$\pi^- + p \rightarrow K^0 + \bar{K}^0 + n; \qquad (1')$$

$$\text{a) } \pi^- + p \rightarrow \begin{matrix} \Lambda^0 + K^0 + \pi^0 \\ \Sigma^0 + K^0 + \pi^0 \end{matrix}, \qquad (2')$$

$$\text{b) } \pi^- + n \rightarrow \begin{matrix} \Lambda + K^0 + \pi^- \\ \Sigma^0 + K^0 + \pi^- \end{matrix}.$$

Additional information on the elementary reactions on nucleons in a nucleus were obtained by analyzing the prongless stars accompanying the $Y^0 + K^0$ and $K^0 + \bar{K}^0$ production events. For the first case, 20 (out of 101) such events were found, and in 8 of these electron-positron pairs were de-

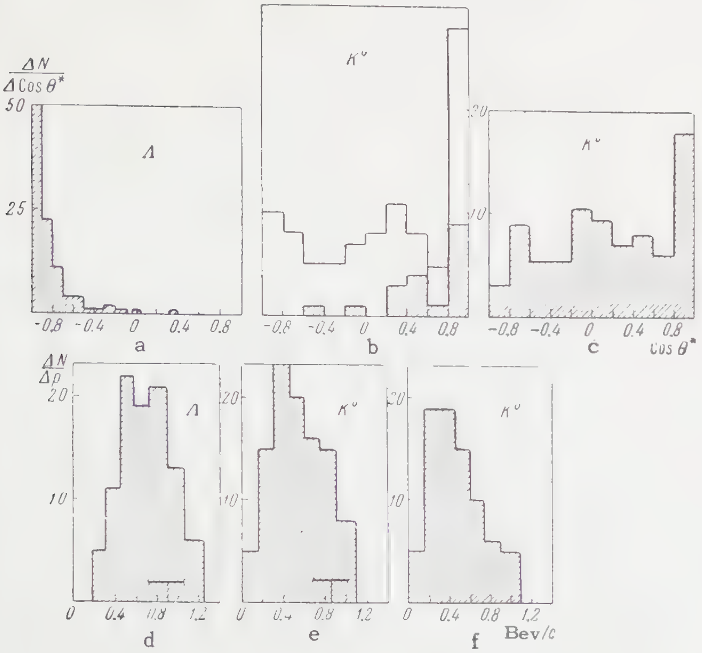

FIG. 3. Angular and momentum distributions of Y^0 and K^0 particles in the pion-nucleon c.m.s.: a, b, d, e – for cases of associated production of $Y^0 + K^0$, and c, f – for $K^0 + \overline{K}^0$ pairs. In the spectra d and e the limiting values of momenta obtained taking the Fermi motion of nucleons in the nucleus into account are indicated.

tected originating in the photon conversion correlated with the prongless star. (In one case, there were two such pairs present.) If we assume that in all of these 20 events a reaction of the type (2′)a occurred, then we should observe 8 – 10 π^0 mesons in the chamber, which was actually the case in the experiment. Unfortunately, it is impossible to estimate the relative contribution of the reaction involving the Σ^0 hyperon from the data. For the second case ($K^0 + \overline{K}^0$ pairs), 10 prongless stars (out of 42) that were not accompanied by electron-positron pairs, according to reaction (1′), were observed. If, in the production of $K^0 + \overline{K}^0$, one π^0 meson was present, we would detect 4 – 5 events in which prongless stars are accompanied by electron-positron pairs.

4. Angular and Momentum Distributions of Y^0 and K^0 Particles in the Pion-Nucleon C.M.S.

Under the assumption that the production of $Y^0 + K^0$ and $K^0 + \overline{K}^0$ pairs occurs in π-N collisions, and neglecting secondary interactions of Y^0 and K^0 particles in nuclei, we have obtained the angular and momentum distributions of Y^0 and K^0 particles in the c.m.s. (see Fig. 3). In this system, all Y^0 particles propagate into the backward hemisphere, with a very large fraction of the particles (> 80%) being contained in a cone

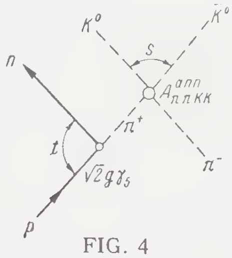

FIG. 4

with $\cos\theta^* \leq -0.8$. The angular distribution of K^0 particles produced together with the Y^0 particles is peaked forward. This is especially noticeable for prongless stars, whose distribution is shown shaded in the figure. The forward direction of the total momentum of the two K^0 mesons is characteristic for the production process $K^0 + \overline{K}^0$ (the forward-backward relation is equal to 3.3 ± 0.8). In all prongless stars, the total momentum of the two K^0 mesons is directed forwards only.

ESTIMATES OF THE ππKK FOUR-BRANCH VERTEX FROM OBSERVED EXPERIMENTAL DATA

The experimental data obtained shows that, in reactions (1′) and (2′), the final baryons have a relatively small energy in the l.s., which corresponds to small transferred momentum

$$-t = 2m_N(\omega - m) - (m - m_N)^2,$$

where ω and m are the total energy in the l.s. and the baryon mass respectively, and m_N is the nucleon mass.

From general theoretical considerations,[11–13] we can expect that, for a small momentum transfer, the main contribution to the reactions (1′) and (2′) is due to single-meson pole diagrams, shown in Figs. 4 and 5. For the same reason, a comparison of theoretical predictions for the momentum spectrum with experimental data in the range of small t should enable us to find the annihilation cross section

$$\pi^- + \pi^+ \rightarrow K^0 + \overline{K}^0 \tag{3}$$

and the scattering cross section

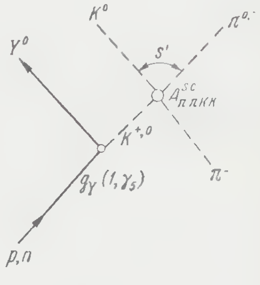

FIG. 5

$$\pi^- + K^{0,+} \to \pi^{-,0} + K^0 \tag{4}$$

from the data on reactions (1′) and (2′) respectively. However, the data on the baryon spectra is very poor, and does not permit us to use the extrapolation method of Chew and Low.[11] Instead, it is possible to compare the integral cross sections in a certain part of the spectrum corresponding to a small momentum transfer, which is equivalent to the consideration of the sum of partial cross sections with large orbital momenta.[12,13]

As will be seen in the following discussion, it is necessary to consider a relatively large part of the spectrum in which diagrams without poles should, in general, make the same contribution as pole diagrams. Although it is difficult at present to obtain any reliable estimate of the validity of the approximation made, we can assume that the values obtained for the cross sections for the reactions (3) and (4) are correct at least to within one order of magnitude.

For the process (1′), the polar approximation gives the laboratory neutron spectrum in the form

$$d\sigma = 2g^2\frac{|t|}{(t-\mu^2)^2}\int\limits_{4\mu_k^2}^{s_m(\omega)} \sqrt{(s-4\mu^2)s}\,\sigma^{\text{ann}}_{\pi^-\pi^+}(s)\,ds\,\frac{d\omega}{8\pi m p_0^2},$$

where

$$\sigma^{\text{ann}}_{\pi^-\pi^+}(s) = \frac{4}{s}\sqrt{\frac{s-4\mu_k^2}{s-4\mu^2}}\int|A^{\text{ann}}_{\pi\pi KK}/16\pi|^2\,d\Omega_{\text{ann}}, \tag{5}$$

$$s_m(\omega) - 2p_0\sqrt{\omega^2-m^2} - 2(\omega-m)(m+\omega_0)+\mu^2,$$

$$t = -2m(\omega - m),$$

where μ and μ_k are the masses of the π and K mesons, p_0 and ω_0 are the momentum and energy of the incident π meson in the l.s., $g^2 = 14.5$, $\sigma^{\text{ann}}_{\pi\pi}(s)$ is the cross section for the process (3) as a function of the square of the energy s in the c.m.s. for the same process, and s_m is the maximum possible value of s for a given energy ω of the recoil neutron.

We shall assume that the square of the invariant matrix element $A^{\text{ann}}_{\pi\pi KK}$ ($\pi\pi$KK is the four-branch vertex in the annihilation channel) averaged over the angles does not produce an additional dependence on s, i.e., we shall assume that $\int|A^{\text{ann}}_{\pi\pi KK}|\,d\Omega_{\text{ann}} = \text{const}$. In this case, in addition to the factor $t/(t-\mu^2)^2$ from the vertex NNπ, the laboratory spectrum is determined only by the invariant phase volume of the final particles

$$\int\Phi(\omega)\,d\omega = \int\frac{dp}{\omega}\frac{dp_1}{\omega}\frac{dp_2}{\omega}\,\delta(\Sigma p). \tag{6}*$$

If the masses of all particles are different, then

$$\Phi(\omega) = \frac{2\pi^2}{p_0}\left\{\sqrt{[s_m-(\mu_1+\mu_2)^2]\,[s_m-(\mu_1-\mu_2)^2]}\right.$$
$$-2(\mu_1^2+\mu_2^2)\operatorname{Arth}\sqrt{\frac{s_m-(\mu_1+\mu_2)^2}{s_m-(\mu_1-\mu_2)^2}}$$
$$\left.+2(\mu_1^2-\mu_2^2)\operatorname{Arth}\left(\frac{\mu_1-\mu_2}{\mu_1+\mu_2}\sqrt{\frac{s_m-(\mu_1+\mu_2)^2}{s_m-(\mu_1-\mu_2)^2}}\right)\right\} \tag{6′}$$

where $s_m = 2p_0\sqrt{\omega^2-m^2} + m^2 + m_0^2 + \mu_0^2 + 2m_0\omega_0 - 2\omega(m_0+\omega_0)$, p_0 and ω_0 are the momentum and energy of the incident particle in the l.s., m_0 is the mass of the target, ω and m are the energy and mass of the particle under consideration in the l.s., and μ_1 and μ_2 are the masses of the two other final particles.*

The theoretical distributions of the kinetic energy of two K^0 mesons in the l.s., $T = \omega_0 - m_N - \omega - 2\mu_k$, are shown in Fig. 2 [the dotted line represents the normalized curve of the phase space (6′)]. If we consider the experimental spectrum obtained from prongless and one-prong stars (where the distortions from the interaction of K^0 mesons in the nucleus are at a minimum), then we can conclude that there is a qualitative agreement between the theoretical curve and the experiment.†

In such a case, the comparison of integral cross sections over different parts of the spectrum leads roughly to the same values of the $\pi\pi$KK four-branch vertex. Because of this, we shall integrate the theoretical spectrum over the interval $\Delta T = 0 - 0.5$ Bev ($|t| \le m_N^2$), and shall compare it with the total experimentally measured cross section equal to 0.5 mb. This gives the following result for the $\pi\pi$KK four-branch vertex in the annihilation channel

$$\int|A^{\text{ann}}_{\pi\pi KK}/16\pi|\,d\Omega_{\text{ann}}/4\pi \approx \tfrac{1}{4}, \quad \sigma^{\text{ann}}_{\pi\pi} \approx 2\text{ mb} \tag{7}$$

---

*Arth = $\tanh^{-1}$.

*It should be noted that formula (6′) is applicable for the region of the spectrum $\omega_- \le \omega \le \omega_+$, where

$$2E^2\omega_\pm = (m_0+\omega_0)(E^2+m^2-(\mu_1+\mu_2)^2)$$
$$\pm p_0\sqrt{[E^2-(m+\mu_1+\mu_2)^2][E^2-(m-\mu_1-\mu_2)^2]},$$
$$E^2 = m_0^2 + \mu_0^2 + 2m_0\omega_0.$$

For some values of the particle mass, values $m \le \omega < \omega_-$ are permissible, i.e., not all kinematically possible energy values are realized in the region under consideration. For $m \le \omega < \omega_-$, we should, in such a case, substract from (6′) a similar term, substituting

$$s_m \to -2p_0\sqrt{\omega^2-m^2} + m_0^2 + m^2 + \mu_0^2 + 2m_0\omega_0 - 2\omega(m_0+\omega_0).$$

†Thus, e.g., the mean values of the energy $\overline{T}$ according to the theoretical and experimental spectrum for prongless and one-prong stars are equal to 1.45 and 1.60 Bev respectively. $\overline{T}$ taken from the phase curve equals 1.15 Bev.

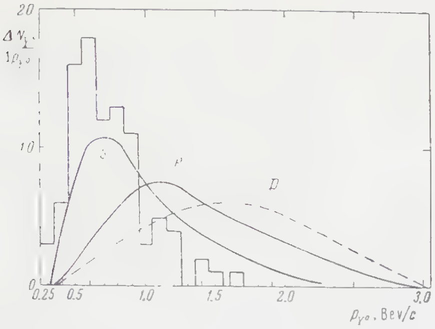

FIG. 6. Momentum spectrum in the l.s. of hyperons for: S – scalar, P – pseudoscalar; Φ – phase volume curve.

and corresponds to the region in which the square of the energy s varies in the range $4\mu_k^2 \leq s \leq 2.5 \times m_N^2$ (the kinetic energy of K^0 and $\bar{K}^0$ mesons in their c.m.s. $T_{c.m.s.} \lesssim 0.5$ Bev). It is evident that we can disregard the assumption $\int | A^{ann}_{\pi^-\pi^+} | \times d\Omega_{ann} = \text{const.}$, in which case the estimate obtained will signify some value averaged over the energy interval in the annihilation channel $T_{c.m.s.} \lesssim 0.5$ Bev.

We can consider the process of hyperon production (2′) in a similar way. In this case, the polar contribution (Fig. 5) is given by the cross section for the process (4)

$$\sigma^{sc}_{\pi K}(s') = (4/s') \int | A^{sc}_{\pi\pi KK} / 16\pi | \, d\Omega_{sc}, \qquad (8)$$

equal to half the sum of the cross section for the elastic scattering and charge exchange (s′ is the square of the total energy in the c.m.s. for the same process). For simplicity, we shall again assume that $\int | A^2 | d\Omega_{sc} = \text{const.}$ and, depending on the parities in the polar diagrams of the vertices NYK, we shall consider three possible variants: 1) NΛK and NΣK are scalar, 2) NΛK and NΣK are pseudoscalar, and 3) NΛK and NΣK have different parities.

Figure 6 shows the momentum spectra of hyperons in the l.s. for variants 1 and 2, and also the spectrum corresponding to the curve of the phase space (6′). The curve for variant 3 has a form intermediate between that of 1 and 2 varying with the ratio of the constant g^2_Σ / g^2_Λ. For the scalar variant, the theoretical spectrum is in agreement with the experimental one. The variants 2 and 3 give harder spectra. This shows that, for a pseudoscalar interaction, the nonpolar diagram should contribute more at least for $p \gtrsim m_N$ ($|t| \gtrsim m^2$), since, without this contribution, it is impossible to explain the fast decrease of the spectrum in the range $p \gtrsim 0.7$ Bev. For the same reason, we shall compare the integral cross sections over the range $p \leq 0.7$ Bev, which encompasses about half of the hyperons (~ 0.25 mb).

This leads to the following values of the ππKK four-branch vertex in the scattering channel for the different variants:

$$\begin{aligned} &1) \quad \int | A^{sc}_{\pi\pi KK} / 16\pi |^2 \, d\Omega_{sc} / 4\pi \approx 1.7 / [g^2_\Lambda(S) + g^2_\Sigma(S)], \\ &2) \quad \int | A^{sc}_{\pi\pi KK} / 16\pi |^2 \, d\Omega_{sc} / 4\pi \approx 30 / [g^2_\Lambda(P) + g^2_\Sigma(P)], \\ &3) \quad \int | A^{sc}_{\pi\pi KK} / 16\pi |^2 \, d\Omega_{sc} / 4\pi \approx 1.7 / [g^2(S) + g^2(P)/17] \end{aligned} \qquad (9)$$

and corresponds to the range of variation of the square of the energy $(\mu_K + \mu)^2 \leq s' \leq 1.5 \, m_N^2$ (kinetic energy in the c.m.s. $T'_{c.m.s.} \lesssim 0.5$ Bev).

For variants 1 and 2, only the top limits of the interaction constants are at present established:[14]

$$g^2_\Lambda(S) = g^2_\Sigma(S) < 0.6, \qquad g^2_\Lambda(P) = g^2_\Sigma(P) < 10,$$

which leads to the cross section averaged over the interval $T'_{c.m.s.} \lesssim 0.5$ Bev

$$\bar{\sigma}^{sc}_{\pi\pi} \gtrsim 30 \text{ mb} \ \text{(variants 1 and 2)}. \qquad (10)$$

For the variant 3, even softer top limits are obtained, which leads to a cross section

$$\bar{\sigma}^{sc}_{\pi\pi} \gtrsim 10 \text{ mb} \ \text{(variant 3)}. \qquad (11)$$

The results (10) and (11) are in agreement with the estimate of the cross section of πK scattering for $T'_{c.m.s.} \approx 0$ obtained earlier in an analogous manner.[16] If, however, the constants of the NYK interaction are several times less than the limiting values used by us, then the amplitudes (9) would lead to rather high values for the cross section for πK scattering.

In conclusion, we shall briefly discuss the possible contributions from nonpolar diagrams neglected in the above approximation. The pole spectra for the reaction (1′) (see Fig. 2) and for the scalar variant of reaction (2′) (see Fig. 6) are in agreement with experimental data, and yet differ significantly from the phase curve (6′) because of an additional dependence of the polar amplitude on the transferred momentum t. Similarly, there is no reason to assume large contributions from nonpolar amplitudes, since otherwise the nonpolar amplitudes should, in the physical range, have the same dependence on t as the polar amplitudes. It is interesting to note that an analogous situation also occurs in a number of other experiments at high energies reported at the 10th Conference on High-Energy Particle Physics, Rochester, 1960. However, it should be mentioned that the range $t \approx -m_N^2/2$ corresponding to the mean part of experimentally measured baryon spectra is far from the poles $t = \mu^2$ for (1′) and $t = \mu_k^2$ for (2′), so that the polar amplitudes are in this case already not large and do not depend strongly on t.

In contrast to the cases studied, it is necessary to assume a contribution from nonpolar diagrams for pseudoscalar variants of reaction (2′) in order that the sum of polar and nonpolar contributions should have a sufficiently strong variation for $t \gtrsim -m_N^2$ and give a decreasing experimental spectrum in the interval $-m_N^2/2 \gtrsim t > -m_N^2$. To this end, it turns out to be necessary to introduce two constant amplitudes independent of t (nonpolar amplitudes for two possible spin invariants γ_5 and $\gamma_5\hat{p}_0$). We can assume that nonpolar amplitudes are not much greater than the polar ones. In such a case, the values obtained for the cross section of πK scattering may vary by several times.

In conclusion, we express our gratitude to Academician A. I. Alikhanov for helpful advice, to Academician V. I. Veksler who made it possible to carry out the experiments, to I. Ya. Pomeranchuk for discussion of the results, and to Yu. S. Krestnikov, V. P. Rumyantseva, N. S. Khropov, and Yu. I. Makarov for help in the experiment.

---

[1] Eisler, Plano, Prodell, Samios, Schwart, and Steinberger, Nuovo cimento **10**, 468 (1958).

[2] Proceedings of the 1958 Annual International Conference on High-Energy Physics at CERN, edited by B. Ferretti, Geneva, CERN Scientific Information Service, 1958, p. 147.

[3] Bowen, Hardy, Reynolds, Sun, Tagliari, Werbrouck, and Moore, Phys. Rev. **119**, 2130 (1960).

[4] Slaughter, Harth, and Block, Phys. Rev. **109**, 2111 (1958).

[5] Blumenfeld, Chinowsky, and Lederman, Nuovo cimento **13**, 296 (1958).

[6] Kuznetsov, Ivanovskaya, Prokesh, and Chuvilo, Proceedings of the 1960 Annual International Conference on High-Energy Physics at Rochester, University of Rochester, 1960, p. 382.

[7] Wang, Wang, Veksler, Vrana, Ding, Ivanov, Kladnitskaya, Kuznetsov, Nguen, Nikitin, Solov'ev, and Ch'eng, JETP **40**, 464 (1961), Soviet Phys. JETP **13**, 323 (1961).

[8] Blinov, Lomanov, Meshkovskii, Shalamov, and Shebanov, Приборы и техника эксперимента (Instruments and Exptl. Techniques) No. 1, 35 (1958).

[9] L. B. Leipuner, Some Relativistic Two Body Kinematics Tables, Brookhaven National Laboratory, 1958.

[10] Crawford Jr., Cresti, Cood, Solmitz, Stevenson, and Ticho, Phys. Rev. Lett. **2**, 174 (1959); W. L. Alvarez, Proc. High-Energy Physics Conf., Kiev, 1959.

[11] G. F. Chew and F. E. Low, Phys. Rev. **113**, 1640 (1959).

[12] L. B. Okun' and I. Ya. Pomeranchuk, JETP **36**, 300 (1959), Soviet Phys. JETP **9**, 207 (1959).

[13] V. B. Berestetskii and I. Ya. Pomeranchuk, JETP **39**, 1078 (1960), Soviet Phys. JETP **12**, 752 (1960).

[14] Kycia, Kerth, and Baender, Phys. Rev. **118**, 553 (1960).

[15] Ya. I. Granovskii and V. N. Starikov, JETP **40**, 537 (1961), Soviet Phys. JETP **13**, 375 (1961).

[16] G. Kosta and L. Tenaglia, Nuovo cimento **18**, 368 (1960).

Translated by H. Kasha
224

SOVIET PHYSICS JETP VOLUME 13, NUMBER 5 NOVEMBER, 1961

PION INTERACTION IN THE FERMI STATISTICAL THEORY

V. S. BARASHENKOV

Joint Institute for Nuclear Research

Submitted to JETP editor July 9, 1960

J. Exptl. Theoret. Phys. (U.S.S.R.) **40**, 1313-1315 (May, 1961)

On the assumption of a resonance π-π interaction the energy spectra are calculated for the π mesons and nucleons produced in inelastic N-N collisions at energy E = 9 Bev. The results of the calculations are compared with experiment.

RECENTLY there have been frequent discussions in the literature of the effect of a possible resonance π-π interaction on calculations made with the statistical theory of the multiple production of particles.[1-8] In several papers it was shown[3,6,7] that for the case of π-N and N-N collisions inclusion of this interaction within the framework of the Fermi theory makes the agreement between the calculated and experimental multiplicity distributions of the stars poorer. On the other hand, Rus'kin[2] and Lebedev and Petrun'kin[5] have been able by including the resonance π-π interaction to get better agreement with experiment in the case of the theoretical momentum distributions of the particles produced in π-p collisions at energies E = 1.0 Bev and E = 1.4 Bev. Statistical calculations must be viewed with caution, however, at energies of the order of 1 Bev, at which there is still very small production of secondary particles. In fact, a more exact analysis[5] has shown that inclusion of the resonance π-π interaction does not explain the experiments as well as Rus'kin[2] believed it did; agreement with experiment can also be obtained without including the π-π interaction, if one carries out all of the statistical calculations in a more correct way.

Since the influence of the resonance interaction of the π mesons increases with increasing energy, we have calculated the momentum spectra of the secondary π mesons and protons for p-p collisions at E = 9 Bev. The results of the calculations are shown in Figs. 1 and 2. In these calculations it was assumed that the spin and isotopic spin of the π-meson isobar are equal to unity, and that its mass μ^* is four times the mass of the π meson. All of the other assumptions and the method of calculation are the same as in reference 3. The experimental data shown in Figs. 1 and 2 are taken from references 9 and 10. The totals of the experimental data for protons are shown in Fig. 2.*

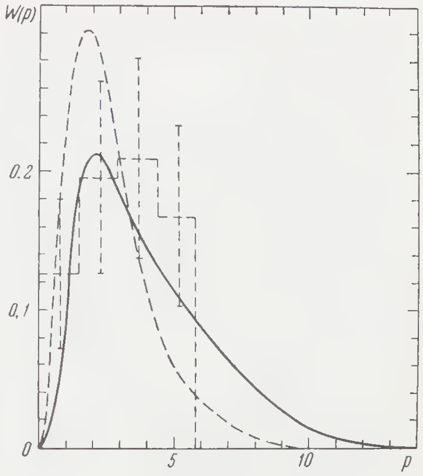

FIG. 1. Momentum distributions of π mesons in the center-of-mass system. The solid curve is that calculated without inclusion of the π-π interaction; the dashed curve is obtained with this interaction included. The dashed histogram shows the experimental data. Values of the momentum p are shown in units μc, where μ is the mass of the π meson.

As can be seen, in both cases the momentum distributions in the theory without the π-π interaction and in the theory with this interaction are nearly the same; but in agreement with the previous papers[3,6] inclusion of the resonance interaction between the π mesons does not on the whole improve the agreement between theory and experiment (cf. reference 11).

---

*In references 9 and 10, 28 π-meson tracks and 106 proton tracks were analyzed. Figures 1 and 2 show the mean statistical errors. In this connection the total number of protons was taken as 164, since in reference 10 there were 40 protons added owing to various corrections.

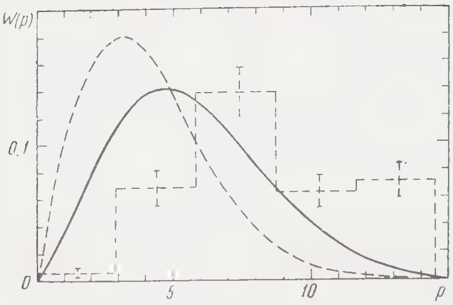

FIG. 2. Momentum distributions of protons in the c. m. s. The notations are the same as in Fig. 1.

Mean Momenta $\bar{p}$ (in Bev/c) of Particles in the c. m. s.

Type of Calculation	π mesons	Protons
Without π-π interaction	0.57	0.79
With π-π interaction included	0.42	0.71
Experimental values*	0.4±0.1	1.1±0.3

*The mean dispersion stated is $\bar{p} = [\sum_n N_n(p_n - \bar{p})^2/\sum_m N_m]^{1/2}$.

This can also be seen from the data in the table, which shows the theoretical and experimental values of the mean momenta of the particles in the center-of-mass system (c. m. s.). In the theory with the π-π interaction included the mean number of particles produced in one act is approximately 20 percent larger than the experimental value.

On the other hand, it has been shown by Eberle and by Zastavenko[1] that without inclusion of the π-π interaction it is hard to explain the experimental data on annihilation. Later this result was confirmed by more exact calculations.[4,7,8]

Thus within the framework of the Fermi statistical theory there are difficulties with a consistent treatment of the resonance π-π interaction.

The question arises again about the resonance interaction of π mesons in a theory which takes peripheral collisions into account (cf. e.g., references 11 and 12). The difference between the multiplicities and momentum spectra of the particles produced in central and peripheral collisions, and the as yet unknown cross sections with which these two types of collisions occur in the experiment, allow us at present to include the π-π interaction without contradiction with experiment. More detailed experimental data and numerical computations are needed, however, to give final conclusions on these questions.

---

[1] E. Eberle, Nuovo cimento **8**, 610 (1958). L. G. Zastavenko, Theoretical Physics Report, Joint Institute for Nuclear Research, 1958.

[2] V. I. Rus'kin, JETP **36**, 164 (1959), Soviet Phys. JETP **9**, 113 (1959); JETP **37**, 105 (1950), Soviet Phys. JETP **10**, 74 (1960).

[3] V. S. Barashenkov and V. M. Mal'tsev, JETP **37**, 884 (1959), Soviet Phys. JETP **10**, 630 (1960).

[4] F. Cerulus, Nuovo cimento **14**, 827 (1959).

[5] A. I. Lebedev and V. A. Petrun'kin, JETP **38**, 1337 (1960), Soviet Phys. JETP **11**, 962 (1960).

[6] R. Hagedorn, Nuovo cimento **15**, 246 (1960).

[7] V. S. Barashenkov, Report at Second All-Union Conference on Field Theory and Elementary Particles, Uzhgorod, 1960; Fortschr. der Physik **9**, 29 (1961).

[8] V. M. Maksimenko, JETP **38**, 652 (1960), Soviet Phys. JETP **11**, 469 (1960).

[9] Bogachev, Bunyatov, Merekov, Sidorov, and Yarba, JETP **38**, 1346 (1960), Soviet Phys. JETP **11**, 968 (1960).

[10] Wang, Vishki, Gramenitskii, Grishin, Dalkhazhav, Lebedev, Nomofilov, Podgoretskii, and Strel'tsov, JETP **39**, 957 (1960), Soviet Phys. JETP **12**, 663 (1961).

[11] Barashenkov, Wang, and Mal'tsev, JETP **38**, 650 (1960), Soviet Phys. JETP **11**, 467 (1960).

[12] Barashenkov, Maltsev, and Mihul, Nuclear Phys. **13**, 583 (1959). V. S. Barashenkov, Nuclear Phys. **15**, 486 (1960).

Translated by W. H. Furry
225

SOVIET PHYSICS JETP VOLUME 13, NUMBER 5 NOVEMBER, 1961

A KINETIC EXAMINATION OF SOME EQUILIBRIUM PLASMA CONFIGURATIONS

A. I. MOROZOV and L. S. SOLOV'EV

Submitted to JETP editor August 3, 1960

J. Exptl. Theoret. Phys. (U.S.S.R.) **40**, 1316-1324 (May, 1961)

Certain one-dimensional plasma configurations with effective dimensions of the order of the Larmor radius are analyzed.

INTRODUCTION

THERE are many plasma systems of practical interest whose properties cannot be described within the framework of magnetohydrodynamics. Typical examples are systems with acute-angle geometries and adiabatic traps with ion injection (Ogra, Astron). Problems involved in systems of this kind were first considered by Ferraro[1] in connection with the interaction of solar corpuscular streams with the magnetic field of the earth. Later, kinetic analyses of certain particular equilibrium configurations were carried out by a number of authors.[2-5] In the present work we develop a general approach to the problem and consider several concrete systems.

As is well known, magnetohydrodynamics applies when the Larmor radii of both electrons and ions are small compared with the scale of the field inhomogeneities. We, however, shall be interested in systems with dimensions of the order of the effective Larmor radius for electrons or ions. Here we can consider two limiting cases: in one there is a transition region of the order of the Larmor radius between the plasma (with no magnetic field) and the magnetic field; in the other, the entire region occupied by the plasma is characterized by dimensions of the order of the Larmor radius (Ogra, Astron).

In the present work we limit ourselves to one-dimensional problems (all quantities depend on one coordinate only).

1. GENERAL RELATIONS

We first consider the case in which all quantities depend only on the single Cartesian coordinate x. If collisions are neglected, the equilibrium plasma configuration is described by the Vlasov equations:

$$v_x \frac{\partial f_e}{\partial x} - \frac{e}{m}\left(\mathbf{E} + \frac{1}{c}\,[\mathbf{vH}]\right)\frac{\partial f_e}{\partial \mathbf{v}} = 0, \tag{1a*}$$

$$v_x \frac{\partial f_i}{\partial x} + \frac{e}{M}\left(\mathbf{E} + \frac{1}{c}\,[\mathbf{vH}]\right)\frac{\partial f_i}{\partial \mathbf{v}} = 0;$$

$$\operatorname{div}\mathbf{E} = 4\pi e\int (f_i - f_e)\,d\mathbf{v}, \qquad \operatorname{rot}\mathbf{H} = \frac{4\pi e}{c}\int \mathbf{v}\,(f_i - f_e)\,d\mathbf{v},$$

$$\mathbf{E} = -\nabla\Phi, \qquad \mathbf{H} = \operatorname{rot}\mathbf{A}. \tag{1b*}$$

When the magnetic field does not have a longitudinal component H_x, the equations for the characteristics of (1a)

$$m v_x d\mathbf{v}/dx = -e\,(\mathbf{E} + c^{-1}\,[\mathbf{vH}]),$$

$$M v_x\,d\mathbf{v}/dx = e\,(\mathbf{E} + c^{-1}[\mathbf{vH}]) \tag{2}$$

have the six integrals

$$v_x^2 + v_y^2 + v_z^2 - 2e\Phi/m = C_{0e}^2, \qquad v_y - eA_y/mc = C_{ye},$$

$$v_z - eA_z/mc = C_{ze}, \qquad v_x^2 + v_y^2 + v_z^2 + 2e\Phi/M = C_{0i}^2,$$

$$v_y + eA_y/Mc = C_{yi}, \qquad v_z + eA_z/Mc = C_{zi}. \tag{3}$$

However, if $H_x \neq 0$, the system in (2) has only four integrals. We shall limit ourselves to the case in which $H_x = 0$.

Knowing the complete set of integrals (3) we can write the general solution of the system (1a):

$$f_e = f_e\,(v^2 - 2e\Phi/m,\ v_y - eA_y/mc,\ v_z - eA_z/mc),$$

$$f_i = f_i\,(v^2 + 2e\Phi/M,\ v_y + eA_y/Mc,\ v_z + eA_z/Mc). \tag{4}$$

Substituting Eq. (4) in Eq. (1b) we have

$$\frac{d^2\Phi}{dx^2} = -4\pi e\int (f_i(\mathbf{v}, \mathbf{A}, \Phi) - f_e(\mathbf{v}, \mathbf{A}, \Phi))\,d\mathbf{v},$$

$$\frac{d^2\mathbf{A}}{dx^2} = -\frac{4\pi e}{c}\int \mathbf{v}\,(f_i(\mathbf{v}, \mathbf{A}, \Phi) - f_e(\mathbf{v}, \mathbf{A}, \Phi))\,d\mathbf{v}. \tag{5}$$

If f_i and f_e are given as functions of C_0^2, C_y, and C_z, then (5) determines the dependence of Φ and **A** on x. This system of equation has one first integral, which expresses the conservation of momentum:

$$\frac{H^2 - E^2}{8\pi} = \int v_x^2\,(Mf_i + mf_e)\,d\mathbf{v}. \tag{6}$$

The functions $f_{i,e}(C_0^2, C_y, C_z)$ are arbitrary functions of their arguments. In actual calculation they must be chosen on the basis of various physical considerations, for example, stability considerations. In what follows we limit ourselves to configurations which may be called "single-Larmor" systems. In such systems, in which, for example, all the ions cross some plane $x = x_0$, the electrons may also have this property (two-component systems) or may be characterized by a Boltzmann distribution (single-component systems). A unique feature of such systems is the fact that assigning the distribution function for the "non-Boltzmann" particles in one plane $x = x_0$ is sufficient to determine the distribution of particles over the entire space. This situation is typical of a system in which injection is used.

---

*$[\mathbf{vH}] = \mathbf{v} \times \mathbf{H}$.

*rot = curl.

Assuming that the potentials Φ and $\mathbf{A}$ vanish at $x = x_0$, we have

$$C_0^2 = v_0^2, \qquad C_y = v_{0y}, \qquad C_z = v_{0z}. \tag{7}$$

Whence we obtain the condition

$$C_0^2 \geqslant C_y^2 + C_z^2. \tag{8}$$

This condition determines the region of integration over $d\mathbf{v}$ in the right-hand side of the equations in (5). Substituting the expressions for C_0^2, C_y, and C_z from Eq. (3) in Eq. (8), we obtain the following condition on the region of integration over velocity:

$$v_x^2 + 2e\Phi/M \geqslant e^2A^2/M^2c^2 + 2e\mathbf{vA}/Mc \tag{9*}$$

for the ions; a similar procedure holds for the electrons.

If the system has axial symmetry, all quantities depend only on r, and in this case $H_r = 0$; hence the equations for the characteristics of the system (1a) have a complete set of integrals

$$\begin{aligned} &v^2 - 2e\Phi/m = C_{0e}^2, \qquad r\,(v_\varphi - eA_\varphi/mc) = C_{\varphi e}, \\ &v_z - eA_z/mc = C_{ze}, \qquad v^2 + 2e\Phi/M = C_{0i}^2, \\ &r\,(v_\varphi + eA_\varphi/Mc) = C_{\varphi i}, \qquad v_z + eA_z/Mc = C_{zi}, \end{aligned} \tag{10}$$

while (5) is replaced by

$$\begin{aligned} &\frac{1}{r}\frac{d}{dr}r\frac{d\Phi}{dr} = -4\pi e\int (f_i - f_e)\,d\mathbf{v}, \\ &\frac{d}{dr}\frac{1}{r}\frac{d}{dr}rA_\varphi = -\frac{4\pi e}{c}\int v_\varphi\,(f_i - f_e)\,d\mathbf{v}, \\ &\frac{1}{r}\frac{d}{dr}r\frac{dA_z}{dr} = -\frac{4\pi e}{c}\int v_z\,(f_i - f_e)\,d\mathbf{v}. \end{aligned} \tag{11}$$

The solution of (5) and (11) can be simplified considerably if the plasma is assumed to be neutral. In this case, from the fact that $n_i = n_e$ we obtain a relation between Φ and $\mathbf{A}$ and it is sufficient to consider the equation for $\mathbf{A}$ only.

2. PLANE ONE-COMPONENT SYSTEMS

As we have noted above, by one-component systems we mean systems in which the current is due to only one kind of particle; the second serves simply for charge compensation and is characterized by a Boltzmann distribution $n = n_0 \exp(-Ze\Phi/T)$. We shall see below that in general the mean energy of the "Boltzmann" particles must be much smaller than the energy of the "current-carrying" particles if the effect of the electric field on the motion of the latter is to be neglected.

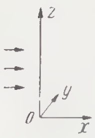

FIG. 1

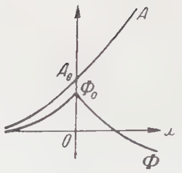

FIG. 2

A. Consider a monoenergetic ion beam normally incident on a magnetic field. Suppose that at $x = -\infty$ all the ions have the came velocity v_0, which is in the x direction (Fig. 1), while there are no magnetic or electric fields ($\Phi = 0$, $\mathbf{A} = 0$). At $x = +\infty$ the magnetic field is uniform along the axis and given by H_0, while the electric field, and the ion and electron densities all vanish.

Substituting in Eq. (5) the ion distribution function

$$f_i = 2v_0n_0\delta(v^2 + 2e\Phi/M - v_0^2)\,\delta(v_y + eA/Mc)\,\delta(v_z), \tag{12}$$

we obtain equations for the potentials

$$\begin{aligned} &\frac{d^2A}{dx^2} = \frac{4\pi e n_0}{c}\frac{eA}{Mc}\left[1 - \frac{2e\Phi}{Mv_{0i}^2} - \left(\frac{eA}{Mc}\right)^2\frac{1}{v_{0i}^2}\right]^{-1/2}, \\ &\frac{d^2\Phi}{dx^2} = -4\pi e n_0\left\{\left[1 - \frac{2e\Phi}{Mv_{0i}^2} - \left(\frac{eA}{Mc}\right)^2\frac{1}{v_{0i}^2}\right]^{-1/2} - e^{e\Phi/T}\right\}. \end{aligned} \tag{13}$$

Here, n_0 is the particle number density at $x = -\infty$. $A \equiv A_y$, $A_z \equiv 0$, and T is the electron temperature in energy units.

Suppose that at the point $x = 0$ the quantity in the radical in Eq. (13) vanishes. This is then the turning point for the ions. Consequently, the system in (13) applies for $x < 0$; at $x > 0$,

$$d^2\Phi/dx^2 = 4\pi e n_0 e^{e\Phi/T}, \qquad d^2A/dx^2 = 0. \tag{14}$$

From Eqs. (13) and (14) and the boundary conditions we see that the qualitative behavior of the potentials A and Φ is that shown in Fig. 2.

In the region $x > 0$ Eq. (14) can be integrated with the boundary conditions given above, and we have

$$A = A_0 + H_0x, \qquad x = D_e\,(e^{-e\Phi/2T} - e^{-e\Phi_0/2T}). \tag{15}$$

Here, A_0 and Φ_0 are the values of the potentials at $x = 0$ while $D_e = \sqrt{T/4\pi e^2 n}$ is the electron Debye radius. Thus, the effective thickness of electron sheath protruding into the region $x > 0$

---

*$\mathbf{v}A = \mathbf{v}\cdot\mathbf{A}$.

is of the order of the Debye radius, as is to be expected.

In the region x < 0 the fields are described by (13); it is convenient to write these equations in the dimensionless form

$$\frac{d^2a}{d\xi^2} = \frac{a}{\sqrt{1-\alpha\psi-a^2}},$$

$$\frac{d^2\psi}{d\xi^2} = -\frac{Mc^2}{T}\left(\frac{1}{\sqrt{1-\alpha\psi-a^2}} - e^{\psi}\right) \qquad (16)$$

Here,

$$\psi = e\Phi/T, \qquad a = eA/Mcv_{0i}, \qquad \xi = x/D_{ic},$$

$$\alpha = 2T/Mv_{0i}^2; \qquad D_{ic} = c/\omega_{0i}, \qquad \omega_{0i}^2 = 4\pi e^2 n_0/M.$$

If $Mc^2/T \gg 1$, that is, if the electron energy is much less than the ion energy, the plasma can be considered neutral everywhere except in the region of the ion turning point, whose width must be of the order of the electron Debye radius. From the neutrality condition we obtain an equation which relates ψ and A:

$$e^{\psi} = 1/\sqrt{1-\alpha\psi-a^2}. \qquad (17)$$

If $\alpha \ll 1$, as we have assumed at the beginning, the equations for the potentials assume the form

$$d^2a/d\xi^2 = a/\sqrt{1-a^2}, \qquad (18a)$$

$$\psi = -\tfrac{1}{2}\ln(1-a^2). \qquad (18b)$$

Equation (18a) has the integral

$$\tfrac{1}{2}(da/d\xi)^2 = \text{const} - \sqrt{1-a^2}. \qquad (19)$$

For the boundary conditions $a|_{x\to-\infty} \to 0$, $\dot{a}|_{x\to-\infty} \to 0$ the constant of integration is found to be unity. Integrating Eq. (19) again with this condition, we have

$$\xi = \ln\left|\operatorname{tg}\frac{\chi}{4} \Big/ \operatorname{tg}\frac{\pi}{8}\right| + 2\left(\cos\frac{\chi}{2} - \cos\frac{\pi}{4}\right), \qquad \sin\chi = a. \qquad (20)^*$$

A similar relation has been obtained earlier by Ferraro[1] but in contrast with his work, in which a two-component plasma is considered, in our case the transition sheath is of the order of the ion Larmor radius rather than the electron Larmor radius.

B. We next consider the plasma system shown in Fig. 3, which might be called a single-Larmor sheath. As before, we assume that all ions have the same velocity and that this velocity is along the x axis at x = 0. We assume that the electrons, which compensate the charge, are cold.

This plasma system is described by (18) but the integral (19) now assumes the form

$$\dot{a}^2 = h_1^2 + 2\left(1 - \sqrt{1-a^2}\right). \qquad (21)$$

Here,

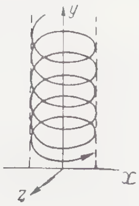

FIG. 3

$$h_1 = H_1 eD_{ic}/Mcv_{0i},$$

while H_1 is the strength of the magnetic field at x = 0.

Integrating Eq. (21) we obtain the variation of the field:

$$\xi = -4k^{-2}[E(k) - E(k, \pi/2 - \chi)] + 2(1 + 2/k^2)[K(k) - F(k, \pi/2 - \chi)], \qquad (22)$$

where $k^2 = 4/(4+h_1^2)$, $a = \sin\chi$ and $E(k)$, $E(k,\varphi)$, $K(k)$ and $F(k,\varphi)$ are elliptic integrals. The case k = 1 has been considered above. The case $k \to 0$, corresponding to $h_1 \to \infty$, can be easily computed by expanding (21) in powers of h_1^{-1}:

$$h = h_1 + h_1^{-1}\left(1 - \sqrt{1 - h_1^2\xi^2}\right). \qquad (23)$$

C. We now consider the boundary between the plasma and the field in the case in which the ions at $x = -\infty$ are characterized by a Maxwellian distribution in the presence of cold electrons that compensate the space charge (Fig. 1). The ion distribution function is assumed to be*

$$f = n_0(\pi c_T^2)^{-3/2}\exp\{-v^2/c_T^2\}. \qquad (24)$$

Here, n_0 is the particle number density at $x \to -\infty$ while c_T is the thermal velocity. Substituting Eq. (24) in Eq. (5) and introducing the dimensionless variables

$$a = eA/Mcc_T, \qquad \eta_x = v_x/c_T,$$

$$\eta_y = v_y/c_T, \qquad \xi^2 = x^2 4e^2 n_0/Mc_T^2,$$

after integration over v_z we obtain

$$\frac{d^2a}{d\xi^2} = \iint_G \eta_y \exp\{-(\eta_x^2 + \eta_y^2)\}\, d\eta_x\, d\eta_y. \qquad (25)$$

The region of integration G is determined by (9) which, in our case, assumes the dimensionless form (cf. Fig. 4)

$$\eta_x^2 \geqslant a^2 + 2\eta_y a. \qquad (26)$$

Integrating the right-hand side of Eq. (25) over η_y we have

$$\ddot{a} = \frac{a}{2}\int_0^\infty \exp\{-a^2(1+\xi^2)^2/4\}\, d\xi. \qquad (27)$$

---

*tg = tan.

*In assuming that the electrons are cold, as a first approximation we assume that the electric field vanishes completely.

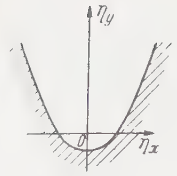

FIG. 4

Whence, using the boundary condition a = 0, $\dot{a} = 0$ at x → − ∞, we have

$$\dot{a}^2 = \frac{\pi}{2} - 2\int_0^\infty \frac{\exp\{-a^2(1+\xi^2)^2/4\}}{(1+\xi^2)^2} d\xi. \tag{28}$$

Integrating once again, we find the explicit functional dependence a = a (ξ):

$$a(\xi) = \sqrt{\frac{2}{\pi}} \int_0^a dx \left[1 - \frac{4}{\pi}\int_0^\infty \exp\{-x^2(1+\xi^2)^2/4\} \right. \\ \left. \times d\xi/(1+\xi^2)^2\right]^{-1/2}. \tag{29}$$

The expression in the right-hand side of Eq. (29) is a universal function for a. In choosing the constant of integration in Eq. (29) we take account of the fact that at small values of a the field increases with coordinate according to a power relation and the point at which the field appears is taken to be the origin. Calculating Eq. (29) for small values of ξ, we have

$$a \approx 0.0028\,\xi^4, \tag{30}$$

whereas for large values of ξ

$$a \approx \xi\sqrt{\pi/2}. \tag{31}$$

A curve of Eq. (29) is shown in Fig. 5.

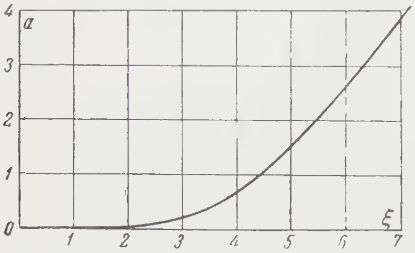

FIG. 5

3. MOTION IN AN AXIALLY SYMMETRIC FIELD

A. Suppose that a plasma cylinder is formed by monochromatic ions ($v = v_0$) and cold electrons characterized by a Maxwellian distribution ($T_e \ll Mv_i^2/2$). Suppose further that $H_\varphi = H_r = 0$, $H_z \neq 0$ and that all quantities depend only on r. If, in addition, we assume that $v_{iz} = 0$, the ion trajectories in this system will be of the form shown in Fig. 6a or Fig. 6b, depending on whether the Larmor radius is greater than or less than the radius of the cylinder.

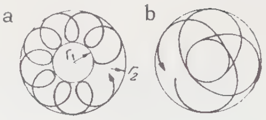

FIG. 6

For the assumptions made above Eq. (11) becomes

$$\frac{d}{dr}\left(\frac{1}{r}\frac{d}{dr} rA_\varphi\right) = -\frac{4\pi Q}{cr}\left(\frac{P}{Mr} - \frac{eA_\varphi}{Mc}\right)\left[v_0^2 - \left(\frac{P}{Mr} \right.\right. \\ \left.\left. - \frac{eA_\varphi}{Mc}\right)^2\right]^{-1/2} \tag{32}$$

Here, Q is the radial particle flux while P is the generalized momentum:

$$Q = enrv_r = \text{const}, \qquad P = r(Mv_\varphi + eA_\varphi/c) = \text{const}. \tag{33}$$

Introducing the dimensionless quantities

$$a = eA_\varphi/Mcv_0, \qquad p = P/Mv_0, \tag{34}$$

we obtain the following equation for a

$$\frac{d}{dr}\left(\frac{1}{r}\frac{dra}{dr}\right) = -\frac{4\pi eQ}{Mc^2 v_0}\frac{p/r - a}{r\sqrt{1-(p/r-a)^2}}. \tag{35}$$

The magnetic field inside the cylindrical tube with inner radius r_1 and outer radius r_2 is determined by Eq. (35), where r_1 and r_2 are roots of the expression in the radical in Eq. (35). The field outside r_2 and inside r_1 is uniform. For a known value of a, the constant Q can be expressed in terms of the number of particles over the cross section of the cylinder N:

$$N = \int_{r_1}^{r_2} n2\pi r dr.$$

Using Eq. (33) we have

$$N = \frac{2\pi Q}{cv_0}\int_{r_1}^{r_2}\frac{dr}{\sqrt{1-(p/r-a)^2}}. \tag{36}$$

If the ion current is small, Eq. (35) can be solved by successive approximations. In the zeroth approximation the field is uniform and $A_\varphi = H_0 r/2$. In this case the quantity Q is given approximately by

$$Q = e^2 H_0 N / 2\pi^2 Mc. \tag{37}$$

Substituting the zeroth approximation for A_φ in the right-hand side of Eq. (35) and integrating, taking account of Eq. (37) we obtain an expression for the magnetic field H:

$$H = H_0\left\{1 - \frac{2e^2N}{\pi Mc^2}\arccos\frac{r_1 r_2/r + r}{r_1 + r_2}\right\}, \\ r_1 \leqslant r \leqslant r_2. \tag{38}$$

For the case shown in Fig. 6a we must take $r_1 > 0$ in Eq. (38) whereas for the case shown in

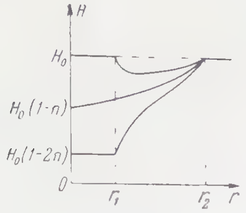

FIG. 7

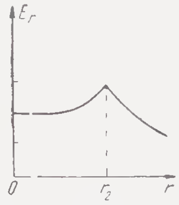

FIG. 8

Fig. 6b, in place of r_1 we must substitute $-r_1$. When $r_{1,2} \to \infty$ Eq. (38) becomes Eq. (23). Curves of the function in (38) for $r_1 > 0$, $r_1 < 0$ and $r_1 = 0$ are shown in Fig. 7. Attention is merited by the peculiar variation of the function $H(r, r_1, r_2)$ as r_1 goes through zero.

A similar result has been obtained by Tonks[5] by numerical integration of Eq. (35). This author has considered both dilute and dense plasmas. Later, Tonks[6] generalized these results to the case in which there is a spread of the momentum P.

Equation (38) shows that the small parameter used above in the method of successive approximations is the so-called "linear proton" $\Pi = e^2N/Mc^2$. It is not difficult to obtain terms in the expansion proportional to Π^2 and higher in Eq. (38).

We now consider the motion of particles in the cylindrical column. The equation of motion is

$$d\varphi/dr = v_\varphi / rv_r.$$

On the other hand, the field equation $(dH/dr = 4\pi j_\varphi/c)$ can be put in the following form [using (33)]:

$$dH/dr = -(4\pi\ Q/c)\ (v_\varphi / rv_r).$$

It follows that

$$H = -(4\pi Q/c)\ \varphi + \text{const.} \tag{39}$$

Taking account of Eq. (39) and the curves, we see that when $r_1 > 0$ (Fig. 6a), in the first approximation particles do not go around the axis of the system, whereas when $r_1 < 0$ (Fig. 6b) they do.

B. If the plasma is very dilute and the magnetic field is very strong, the preceding calculations can be applied to a cloud of fast particles in the absence of compensating electrons. In accordance with Eq. (33), the density distribution is related to the vector potential by the expression

$$n = \frac{Q}{ev_0}\ \frac{1}{r}\left[1-\left(\frac{p}{r}-a\right)^2\right]^{1/2} \tag{40}$$

Assuming as the zeroth approximation that the magnetic field is uniform, $a = \alpha r$, we write the equation div **E** $= 4\pi en$ in the form

$$\frac{1}{r}\ \frac{d}{dr} rE_r \quad \frac{4\pi Q}{rv_0}\left[1-\left(\frac{p}{r}-a\right)^2\right]^{-1/2}. \tag{41}$$

Integrating, and substituting the values of Q and p and α in terms of r_1 and r_2, we obtain the final formula for the electric field distribution inside the annular region:

$$E_r = \frac{2eN}{\pi r}\ \arccos \frac{r_1^2 + r_2^2 - 2r^2}{r_2^2 - r_1^2} \tag{42}$$

The field inside the ring $r < r_1$ vanishes while the field outside the cylinder is $E_r = 2eN/r$. In the case $r_1 = 0$ the electric field distribution is given by the expression

$$E_r = \frac{4eN}{\pi r_2}\ \frac{\arcsin (r / r_2)}{r\quad r_2} \tag{43}$$

and is shown in Fig. 8.

4. TWO-COMPONENT SYSTEMS

As an example of a two-component system we consider normal incidence of monochromatic fluxes of ions and electrons on a magnetic field. In general, the ion and electron velocities will be different at infinity, being designated by v_{0i} and v_{0e} respectively.* After substitution of the distribution functions

$$\begin{aligned} f_i &= 2v_{0i}n_0\delta\ (v^2 + 2e\Phi/M - v_{0i}^2)\ \delta(v_y + eA / Mc)\ \delta(v_z), \\ f_e &= 2v_{0e}n_0\delta\ (v^2 - 2e\Phi/m - v_{0e}^2)\ \delta(v_y - eA/mc)\ \delta(v_z) \end{aligned} \tag{44}$$

Equation (5) assumes the following form in the region of common motion:

$$\begin{aligned} d^2\psi / d\xi^2 &= (c^2 / v_{0e}^2)\left[(1+\psi-a^2)^{-1/2} - (1-\theta\psi-\mu\theta a^2)^{-1/2}\right], \\ d^2a/d\xi^2 &= a\left[(1+\psi-a^2)^{-1/2} + \sqrt{\mu\theta}\,(1-\theta\psi-\mu\theta a^2)^{-1/2}\right]. \end{aligned} \tag{45}$$

Here

$$eA/mv_{0e}c = a, \qquad 2e\Phi/mv_{0e}^2 = \psi, \qquad \xi^2 = x^2 4\pi e^2 n_0 / mc^2,$$
$$\mu = m / M, \qquad \theta = mv_{0e}^2 / Mv_{0i}^2.$$

The ions and electrons have turning points at

$$1 + \psi - a^2 = 0, \qquad 1 - \theta\psi - \mu\theta a^2 = 0. \tag{46}$$

If $\mu\theta < 1$, the electrons come to rest first, while if $\mu\theta > 1$, the ions come to rest first.

If the plasma is nonrelativistic, then $c^2/v_{0e}^2 \gg 1$ and in solving (47) we may assume neutrality,† that is to say, $n_i = n_e$. Then the first equation in (45) gives a relation between ψ and a:

---

*The case $v_{0i} = v_{0e}$ has been considered by Ferraro.[1]

†In general, this procedure is valid only for pressures of approximately $H^2/8\pi$; it may not hold if the pressures are much smaller than $H^2/8\pi$.

$$\psi = (1 - \mu\theta)\, a^2/(1 + \theta). \tag{47}$$

Substituting this value of ψ in the second equation of (45) we have

$$d^2 a_1 / d\xi_1^2 \quad a_1 / \sqrt{1 - a_1^2}, \tag{48}$$

where

$$a_1 = a\, [(1 + \mu)\theta/(1 + \theta)]^{1/2}, \qquad \xi_1 = \xi\, [1 + \sqrt{\mu\theta}]^{1/2}. \tag{49}$$

Equation (48) is identical with Eq. (18). In particular, this leads to the result that the thickness of the transition sheath is

$$\delta \sim (mc / 4\pi e^2 n_0)\, [1 + \sqrt{\mu\theta}]^{1/2}.$$

The quantity δ is of the order of electron Larmor radius in the field H_0 computed for the mean energy of the ions and electrons.

Similar conclusions can be obtained for a sheath of the type considered in Sec. 2C. Here, when neutrality obtains the thickness of the sheath is of the order of the electron Larmor radius. With a Maxwellian distribution the boundary between the plasma and the field, as before, will be of the order of the electron Larmor radius, but the actual pattern of the transition sheath cannot be expressed in simple analytic form.

---

[1] V. C. A. Ferraro, J. Geophys. Research **57**, 15 (1952).

[2] O. B. Firsov, Физика плазмы и проблема управляемых термоядерных реакций (Plasma Physics and the Problem of a Controlled Thermonuclear Reaction), Acad. Sci. Press, U.S.S.R., Vol. 3, p. 327.

[3] B. A. Trubnikov, ibid., Vol. 4, p. 309.

[4] R. Z. Sagdeev, ibid., Vol. 3, p. 346.

[5] L. Tonks, Report to the Second All-Union Conference on Gaseous Electronics, Moscow, 1958.

[6] L. Tonks, Phys. Rev. **118**, 2 (1960).

Translated by H. Lashinsky
226

SOVIET PHYSICS JETP VOLUME 13, NUMBER 5 NOVEMBER, 1961

CERTAIN PROBLEMS IN RELATIVISTIC GAS DYNAMICS OF CHARGED PARTICLES

V. N. TSYTOVICH

P. N. Lebedev Physics Institute, Academy of Sciences, U.S.S.R.

Submitted to JETP editor August 23, 1960

J. Exptl. Theoret. Phys. (U.S.S.R.) **40**, 1325-1332 (May, 1961)

A number of general problems in relativistic gas dynamics of charged particles in external fields and self-consistent fields are considered. An analog is found for potential motion, and the theorem for conservation of magnetic flux along a fluid contour is generalized. The one-dimensional problem of relativistic breakup of a charged layer in external fields is solved.

1. INTRODUCTION

THE relativistic motion of a conducting gas is characterized by a number of features, which can lead to effects that are qualitatively different from those found for nonrelativistic motion. For example, Veksler[1] has shown that when an ionized gas mass collides with a concentration of magnetic force lines the ions transfer an appreciable part of their energy to the electrons; the electrons then become relativistic, even if the initial gas velocities are nonrelativistic. At relativistic gas velocities this limiting-current effect becomes still more important. It leads to a situation such that even for negligibly small collision frequencies ν_{eff} between the electrons and ions (i.e., high conductivity), in the reference system attached to a given gas element $\mathbf{E} + \mathbf{v} \times \mathbf{H}$ does not vanish and is determined by the inertia force which, in the ultra-relativistic limit, can be large because of the relativistic mass increase. The magnetic field flux through the fluid contour is therefore not conserved and the "freezing" of the magnetic lines of force is disturbed.

Thus, one of the peculiarities of relativistic motion of a conducting gas mass is that the magnetic lines of force may not be frozen. As a result, the description of this motion by equations which contain the two vectors $\mathbf{v}$ and $\mathbf{H}$, the hydrodynamic velocity and the magnetic field (relativistic magnetogasdynamics), is no longer possible. The remark pertains especially to transient processes in which the inertia force in the accompanying reference system may be large.

In order to investigate the relativistic motion of a conducting gas it is convenient to consider relativistic two-component gas dynamics in electromagnetic fields. By virtue of what has been indicated above, interest attaches in the relativistic case only to the situation in which the friction of one component against the other is negligibly small compared with the effect of the interaction with the self-consistent field. For this reason, we can consider the equations separately for each of the components in the electromagnetic fields, including in the latter external fields and the fields produced by all the gas components.

The relativistic gas dynamics of a neutral gas have been considered by Khalatnikov.[2] In Sec. 1 of the present work we extend the corresponding results of Khalatnikov to include self-consistent fields and external electromagnetic fields. In spite of the fact that the magnetic lines of force may not be frozen for relativistic motion of an electron-ion plasma, it is found that in those cases for which the ion current is small it is possible to extend the theorem of conservation of magnetic flux along a fluid contour.

In problems which are of interest in accelerator technology, for example the case of a charged electron gas, either the inertia term in the equations of motion is considerably greater than the term that contains the pressure derivatives, or else the external fields have an important effect on the motion. In both cases the characteristic dimensions and the time intervals, which determine the possibility of applying the hydrodynamic analysis, are, to a large extent, determined by the initial and boundary conditions, and by the variations in the external field.

In the present work we consider one-dimensional relativistic breakup of a charged gas layer in vacuum when the inertia term is the principal one. We also consider relativistic collisions between a charged layer and constant external fields. The electric fields produced by breakup of a quasineutral plasma layer in a vacuum are also analyzed.

2. SOME GENERAL PROBLEMS

By virtue of the above considerations, the equation of relativistic motion for a gas of charged particles in an electromagnetic field can be written in the form of an equation for each component s:[3]

$$\partial T^{(s)}_{\mu\nu}/\partial x_\nu = F_{\mu\nu} j^{(s)}_\nu, \qquad T^{(s)}_{\mu\nu} = w^{(s)} u^{(s)}_\mu u^{(s)}_\nu + p^{(s)} \delta_{\mu\nu},$$
$$n^{(s)}_{\text{lab}} = n^{(s)}/\sqrt{1 - v^{(s)2}}, \tag{1}$$

where $u^{(s)}_\mu$ is the 4-velocity of the gas, $p^{(s)}$ is the pressure of the gas, $w^{(s)} = \epsilon^{(s)} + p^{(s)}$ is the heat function per unit proper volume, $\epsilon^{(s)}$ is the internal energy per unit proper volume, $j^{(s)}_\mu = e^{(s)} n^{(s)} u^{(s)}_\mu$ is the current produced by particles of a given type, $n^{(s)}$ is the proper density of particles of this type, $v^{(s)}$ is the three-dimensional velocity (the velocity of light is equal to unity). In addition, each component obeys a continuity equation

$$\frac{\partial}{\partial x_\nu} n^{(s)} u^{(s)}_\nu = 0.$$

We determine the motion and the fields, by using in addition to Eq. (1) the Maxwell equations

$$\partial F_{\mu\nu}/\partial x_\nu = 4\pi\Big(j^{(0)}_\mu + \sum_s j^{(s)}_\mu \Big), \tag{2}$$

where $j^{(0)}_\mu$ is the current that produces the external fields. Multiplying (1) scalarly by $u^{(s)}_\mu$ and taking account of the equations of continuity, the condition $u^{(s)}_\mu F_{\mu\nu} j^{(s)}_\nu = 0$, and $u^{(s)}_\mu u^{(s)}_\mu = -1$, we find by virtue of the thermodynamic law that entropy is conserved along the phase trajectories.

If at any instant of time (or on some hypersurface of the 4-dimensional manifold x_μ) the entropy is the same at all points, then the motion is isentropic. In what follows we confine ourselves to isentropic motion so that Eq. (1) can be written in simple form ($W^{(s)} = w^{(s)}/n^{(s)}$)

$$u^{(s)}_\mu \frac{\partial}{\partial x_\mu} W^{(s)} u_\nu = -\frac{\partial W^{(s)}}{\partial x_\nu} + eF_{\nu\mu} u^{(s)}_\mu. \tag{3}$$

We find an analog for the condition for potential motion for a gas of charged particles in an electromagnetic field. As shown by Khalatnikov,[2] the relativistic analog of this condition for a neutral gas is $Wu_\mu = \partial\varphi/\partial x_\mu$. It is simple to generalize this result to the case in which electromagnetic fields are present. Introducing the 4-potential of the electrodynamic field A_μ, we see that Eq. (3) has a solution of the following form:

$$W^{(s)} u^{(s)}_\mu = -eA_\mu + \partial\varphi^{(s)}/\partial x_\mu, \tag{4}$$

which is the required generalization. The fourth relation in (4) is an analog of the Bernoulli equation.

We show further that (4) is always satisfied for the one-dimensional nonstationary case. For one-dimensional motion all quantities depend on x_1 and x_4, and Eq. (3) can be written in the form

$$u_4^2 \frac{\partial W^{(s)}}{\partial x_1} + u_4 \frac{\partial}{\partial x_4} W^{(s)} u_1 + W^{(s)} u_1 \frac{\partial u_1}{\partial x_1} = eu_4 \left(\frac{\partial A_4}{\partial x_1} - \frac{\partial A_1}{\partial x_4} \right) \tag{5}$$

Since $u_4 \neq 0$, it follows from Eq. (5) that

$$\frac{\partial}{\partial x_1} (W^{(s)} u_4 + eA_4) = \frac{\partial}{\partial x_4} (W^{(s)} u_1 + eA_1), \tag{6}$$

and this proves that the motion is potential.

We now consider the case of one-dimensional motion in the presence of a current perpendicular to the direction of motion. We assume that the charged fluid being considered is an electron fluid with charge partially or completely compensated by the ion component, whose contribution to the current density can be neglected. As before, we assume that all quantities depend only on x_1 and x_4 but $u_3 \neq 0$ and $A_3 \neq 0$. Then, the projection of Eq. (3) on the x_3 axis gives $x_0 = -ix_4$, $u_1^{(e)} = v^{(e)}\gamma^{(e)}$, $\gamma^{(e)} = (1 - v^{(e)2} - v_3^{(e)2})^{-1/2}$

$$\frac{\partial}{\partial x_0} W^{(e)} v_3^{(e)} \gamma^{(e)} + v \frac{\partial}{\partial x_1} W^{(e)} v_3^{(e)} \gamma^{(e)} = e(E_3 + v^{(e)} H_2). \tag{7}$$

It follows from Eq. (7) that the inertia force, which may be large at relativistic velocities, disturbs the freezing even if the electrical conductivity is infinite, $E_3 \neq -vH_2$. Instead of finding the relation between H_2 and E_3, which follows from Eq. (7), it is convenient to find the condition imposed on the potential. We write Eq. (7) in the form

$$\left(u_1 \frac{\partial}{\partial x_1} + u_4 \frac{\partial}{\partial x_4} \right) (W^{(e)} u_3^{(e)} + eA_3) = \frac{d}{ds} (W^{(e)} u_3^{(e)} + eA_3) = 0. \tag{8}$$

Hence it follows that the quantity $p_3 = W^{(e)} u_3^{(e)} + eA_3$ is conserved along the trajectory. This result is valid not only for one-dimensional motion. To satisfy Eq. (8) it is sufficient that all quantities be independent of x_3 (cyclical coordinate).

If the inertia term $W^{(e)} u_3^{(e)}$ can be neglected the conservation relation (8) reduces to the conservation of flux through the fluid contour ($A_3 \sim \Phi$). If p_3 is the same for all points at the initial time, then it remains so at all subsequent times. It can be shown that this one-dimensional nonstationary motion is always potential motion. The first equation in (3) can be written in the form

$$(1 + u_1^{(e)2}) \frac{\partial W^{(e)}}{\partial x_1} + u_4^{(e)} \frac{\partial}{\partial x_4} W^{(e)} u_1^{(e)} + W^{(e)} u_1^{(e)} \frac{\partial u_1^{(e)}}{\partial x_1}$$
$$= eu_4^{(e)} (\partial A_4/\partial x_1 - \partial A_1/\partial x_4) + eu_3^{(e)} \partial A_3/\partial x_1. \tag{9}$$

We use the identity $u_1^{(e)2} + u_3^{(e)2} + u_4^{(e)2} = -1$ and the relation

$$e\partial A_3/\partial x_1 = -u_3^{(e)} \partial W^{(e)}/\partial x_1 - W^{(e)} \partial u_3^{(e)}/\partial x_1,$$

which follows from the condition

$$W^{(e)} u_3^{(e)} + eA_3 = \text{const}.$$

Equation (9) is then reduced to the form

$$\frac{\partial}{\partial x_1}(W^{(e)}u_4^{(e)} + eA_4) = \frac{\partial}{\partial x_4}(W^{(e)}u_1^{(e)} + eA_1), \qquad (10)$$

which shows that the motion is potential.

Finally, we consider 3-dimensional motion and obtain a generalization of the Thomson theorem for the conservation of circulation of velocity. We use the notation $p_\mu^{(s)} = W^{(s)}u_\mu^{(s)} + eA_\mu$ and for the 4-curl of this quantity $p_{\mu\nu}^{(s)} = \partial p_\mu^{(s)}/\partial x_\nu - \partial p_\nu^{(s)}/\partial x_\mu$. We now find the substantive derivative of $p_{\mu\nu}^{(s)}$ with respect to proper time

$$\frac{d}{ds}\, p_{\mu\nu}^{(s)} = p_{\mu\alpha}^{(s)} \frac{\partial u_\alpha^{(s)}}{\partial x_\nu} - p_{\nu\alpha}^{(s)} \frac{\partial u_\alpha^{(s)}}{\partial x_\mu}. \qquad (11)$$

In deriving the last relation we have used Eq. (3), $u_\alpha^{(s)}\partial u_\alpha^{(s)}/\partial x_\nu = 0$, and the Maxwell equations

$$\partial F_{\nu\mu}/\partial x_\alpha + \partial F_{\alpha\nu}/\partial x_\mu + \partial F_{\mu\alpha}/\partial x_\nu = 0.$$

It is apparent that in the nonrelativistic limit $W \approx m$, $u_i \approx v_i$, $u^4 \approx i$, Eq. (11) leads in the absence of electromagnetic fields to a relation for the conservation of circulation of velocity along the fluid contour in differential form.

3. SOME ONE-DIMENSIONAL PROBLEMS

a) Relativistic breakup of a layer of charged particles in vacuum. The relativistic breakup of a layer of neutral gas in vacuum has been considered by Landau[4] and Khalatnikov[2] in connection with the hydrodynamic theory for the multiple production of particles. In the decay of a cluster of charged particles of the same sign the collective effect of the total electric field produced by the particles may have a decisive effect on its decay.

We consider the limiting case of a monatomic gas at nonrelativistic temperatures. By virtue of the proof given above, the one-dimensional motions are always potential,

$$Wu_1 = -eA_1 + \partial\varphi/dx_1, \qquad Wu_4 = -eA_4 + \partial\varphi/dx_4.$$

Making use of gauge invariance, we can write $\varphi = 0$ so that the field and the motion of the gas are described by the potentials A_1 and $A_0 \equiv -iA_4$ only. The electric field is expressed simply in terms of W and $u \equiv u_1$ ($u_4 = i\sqrt{1 + u^2}$):

$$eE = \frac{\partial}{\partial x_0} Wu + \frac{\partial}{\partial x_1} W\sqrt{1+u^2}. \qquad (12)$$

From the electric field equations we obtain the relation

$$\frac{\partial E}{\partial x_0} + \frac{u}{\sqrt{1+u^2}}\frac{\partial E}{\partial x_1} = 0. \qquad (13)$$

Rather than seek u as a function of x_1 and x_0, we seek x_1 as a function of x_0 and u: $x_1 = \psi(x_0, u)$.

Taking $d\psi/du \neq 0$ and $\chi \equiv (e/m)E(x_0, u)$, we transform Eqs. (12) and (13) to expressions in the variables x_0 and u:

$$\frac{\partial\chi}{\partial x_0} + \chi\frac{\partial\chi}{\partial u} = \frac{T_0}{m} G \frac{\partial\chi}{\partial u},$$

$$\frac{\partial\psi}{\partial x_0} + \chi\frac{\partial\psi}{\partial u} = \frac{u}{\sqrt{1+u^2}} + \frac{T_0}{m} G\frac{\partial\psi}{\partial u}; \qquad (14)$$

$$G = 5\left(\frac{n}{n_0}\right)^{2/3}\left[\frac{1}{2} + \frac{1}{3}\frac{u}{n}\left(\frac{\partial n}{\partial x_0} - \frac{\partial n}{\partial u}\frac{\partial\psi/\partial x_0}{\partial\psi/\partial u}\right)\right.$$

$$\left. + \frac{1}{3}\frac{\sqrt{1+u^2}}{n}\left(\frac{\partial\psi}{\partial u}\right)^{-1}\frac{\partial n}{\partial u}\right]. \qquad (15)$$

Here we use $W = m + \frac{5}{2}T_0(n/n_0)^{2/3}$, where T_0 and n_0 are the initial temperature and density of the gas, m is the rest energy and the remaining terms are all of first order in T_0/m.

The density n must be inserted in (14) in the form

$$n = \frac{1}{r_0\sqrt{1+u^2}}\frac{\partial\chi/\partial u}{\partial\psi/\partial u}, \qquad r_0 = 4\pi\frac{e^2}{m}. \qquad (16)$$

Since $T_0 \ll m$, the solution of (14) and (15) can be found in the form of an expansion in the parameter T_0/m; we keep only the first two terms:

$$\chi = \chi_0 + \chi_1 T_0/m, \qquad \psi = \psi_0 + \psi_1 T_0/m + \ldots \qquad (17)$$

The equations for the successive approximation are obtained easily from (15). The system for the zeroth approximation

$$\frac{\partial\chi_0}{\partial x_0} + \chi_0\frac{\partial\chi_0}{\partial u} = 0, \qquad \frac{\partial\psi_0}{\partial x_0} + \chi_0\frac{\partial\psi_0}{\partial u} = \frac{u}{\sqrt{1+u^2}}$$

is found to be linear (the linearity of the equations is trivial for the higher approximation). The system (18) can be solved successively since the boundry or initial conditions for χ_0 can be given independently of physical considerations and apart from the constant e/m, χ_0 coincides with the magnitude of the electric field. From the value of χ_0 we then find the solution for the second equation in (18).

We present the results of analysis of the breakup of a charged layer of thickness $2l$. We assume that at the initial time $x_0 = 0$ the gas density is zero everywhere except for the layer $-l < x_1 < l$, where it is constant and equal to the value n_0. We assume that at the initial time the electric field inside the layer is a linear function of x_1. With these assumptions we find

$$\psi = u/n_0 r_0 x_0 + (x_0/u)(\sqrt{u^2+1} - 1),$$
$$u = v\gamma = v/\sqrt{1 - v^2}, \qquad (19)$$

where v is the hydrodynamic velocity.

Taking $\psi = x_1$, we obtain an implicit expression for the velocity v as a function of x_1 and x_0. The solution in (19) applies when $|\psi| \leq l + (ln_0r_0)^{-1} \times (\sqrt{1 + l^2n_0^2r_0^2x_0^2} - 1)$. The equality sign corresponds to motion of the layer boundary. The boundary of the layer moves with uniform acceleration when $x_0 \ll 1/ln_0r_0$ and inertially when $x_0 \gg 1/ln_0r_0$.

It follows from Eq. (19) that in the nonrelativistic limit ($\gamma = 1 + \epsilon$, $\epsilon \ll 1$)

$$\varepsilon = n_0^2 r_0^2 x_0^2 x_1^2 / 2\,(1 + n_0 r_0 x_0^2 / 2)^2. \qquad (20)$$

The energy of the particles increases as the square of the distance from the center of the layer. At a fixed point it first increases with time and then decreases. This last situation is explained as follows: at a given point, for large values of x_0 slow particles start to arrive from the center (these may not have high energies in the weak self-consistent fields at the center) whereas the fast particles leave this point. The characteristic time interval for the growth of energy at a given point is $\sqrt{2/n_0r_0}$. If $x_0 \ll 1/ln_0r_0$ and $2n_0r_0l^2 \ll 1$ the maximum energy of the particles at the layer of the boundary $\epsilon_{\max} = \frac{1}{2} n_0^2 r_0^2 x_0^2 l_0^2 \ll 1$ is nonrelativistic. When $n_0r_0l^2 \gg 1$ and $l \gg x_0 \gg 1/ln_0r_0$ the energy becomes relativistic.

It is also easy to find the energy distribution in the ultrarelativistic case. The results are as follows: the energy increases linearly with increasing x_1. The distribution of particle density can be found from Eq. (16):

$$\frac{n}{n_0} = \left\{ \sqrt{1 + u^2} + n_0 r_0 x_0^2 \left[1 - \frac{(u^2 + 1)(\sqrt{1 + u^2} - 1)}{u^2 \sqrt{1 + u^2}} \right] \right\}^{-1} \qquad (21)$$

In order to determine the region of applicability of the results obtained above, using Eqs. (14) and (15) we find the next approximation in T_0/m. The criterion is $T_0/m \ll n_0r_0l^2$. The method described here has also been used to solve the problem of breakup in vacuum with other density distributions, in particular, a layered structure.

The other limiting case, in which temperature effects are basically responsible for the expansion of the layer while the interaction with the self-consistent field is treated by perturbation methods (high temperatures), is of interest only in considerations of multiple production of particles and will be considered in a separate paper.

b) Breakup of a neutral plasma layer in vacuum. The ions and electrons will be treated as two charged fluids which, at the initial time, have the same fixed density in a layer of thickness $2l$. The initial temperatures are assumed to be different. By virtue of the above, the motion of electron and ion fluids is potential motion:

$$W^{(e)} u_\mu^{(e)} = -eA_\mu + \partial\varphi^{(e)} / \partial x_\mu; \quad W^{(i)} u_\mu^{(i)} = eA_\mu + \partial\varphi^{(i)} / \partial x_\mu,$$

where the index e refers to electrons while the index i refers to ions. Carrying out a gauge transformation of the electromagnetic potentials $A_\mu = A'_\mu + \partial\chi/\partial x_\mu$, we can write $\chi = \varphi^{(e)}$ and $\varphi = \varphi^{(i)} + \varphi^{(e)}$. Then the motion of the electron fluid is described by the electromagnetic field potentials, while the potential φ characterizes the total motion of the two fluids:

$$W^{(e)} u_\mu^{(e)} = -eA_\mu, \qquad W^{(i)} u_\mu^{(i)} + W^{(e)} u_\mu^{(e)} = \partial\varphi / \partial x_\mu; \qquad (22)$$

$$eE = \frac{\partial}{\partial x_0} W^{(e)} u^{(e)} + \frac{\partial}{\partial x_1} W^{(e)} \sqrt{1 + u^{(e)2}}, \qquad u^{(e)} \equiv u_1^{(e)}. \qquad (23)$$

The electric fields produced in breakup tend to restore the disturbed neutrality of the plasma. We consider breakup while the disturbance of neutrality is still small. Here, as an approximation, we can assume the electron and ion velocities and densities to be the same. It then follows from Eq. (22) that

$$(\overline{W}^{(i)} + \overline{W}^{(e)})\, u_\mu = \partial\varphi / \partial x_\mu, \qquad \mu = 1, 4,$$

where $\overline{W}^{(i)}$ and $\overline{W}^{(e)}$ are the values of the heat functions at the same densities while u_μ is the common velocity. Substitution in the continuity equations (for the electrons and ions) leads to the standard solutions in which, however, we have in place of the heat functions $\overline{W}^{(i)} + \overline{W}^{(e)}$. This leads to a change in the rate of decay of the layer because we must substitute here in place of the velocity of sound

$$\frac{n}{\overline{W}^{(i)} + \overline{W}^{(e)}} \frac{d}{dn} (\overline{W}^{(i)} + \overline{W}^{(e)}) = c_{\text{acous}}^2.$$

At nonrelativistic temperatures

$$\overline{W}^{(i)} + \overline{W}^{(e)} = m^{(i)} + m^{(e)} + \tfrac{5}{2} (T^{(i)} + T^{(e)})\, (n/n_0)^{2/3}.$$

When $T^{(e)} \gg T^{(i)}$ we have $c_{\text{acous}}^2 = 5T^{(e)}/3m^{(i)}$. In other words, the initial stage of breakup is described by a rarefaction wave that moves over the layer with a velocity determined by the temperature of the electrons and the mass of the ions. In later stages, after collision of the rarefaction waves, we also have the usual pattern with $c_{\text{acous}}^2 = 5T^{(e)}/3m^{(i)}$.

It is easy to find, in the next approximation, the electric fields and the differences in electron and ion density and velocity. For a simple wave we have

$$\frac{\Delta n}{n} = \frac{m^{(i)}}{9\pi e^2 n_0 x_0^2} \left(1 - \frac{1}{5} \frac{x_1}{x_0} \frac{m^{(i)}}{T^{(e)}} \right)^3, \qquad (24)$$

$$\frac{\Delta v}{v} = \frac{m^{(i)}}{27\pi e^2 n_0 x_0^2} \left(1 + \frac{3}{5} \frac{x_1}{x_0} \frac{m^{(i)}}{T^{(e)}} \right) \left(1 - \frac{1}{5} \frac{x_1}{x_0} \frac{m^{(i)}}{T^{(e)}} \right)^{-2}. \qquad (25)$$

If we neglect the region in direct proximity to the edge of the flowing gas, $x \ll 5x_0T_4/m$, neutralization starts when $x_0^2 \gg 4m^{(i)}/9m^{(e)}r_0n_0$ where $r_0 = 4\pi e^2/m$. In the stage described by the general solution, the electric fields decay more rapidly.

c) *Motion of a charged layer into a region with constant electric field.* We assume that at the initial time $x_0 = 0$ there is a decaying layer of thickness $2l$ which is breaking up with an initial relativistic velocity $u_{in} \gg 1$ into a region occupied by a constant electric field along the x axis, $eE_{in}/m = \chi_{in}(x_1)$. Neglecting temperature effects and making use of gauge invariance, we have

$$\chi + \chi_{in} = \frac{\partial u}{\partial x_0} + \frac{\partial}{\partial x_1}\sqrt{1 + u^2}, \tag{26}$$

$$\frac{\partial \chi}{\partial x_0} + \frac{u}{\sqrt{1 + u^2}}\,\frac{\partial \chi}{\partial x_1} = 0. \tag{27}$$

As above, we introduce $x_1 = \psi(x_0, u)$ so that Eqs. (26) and (27) are transformed to

$$\frac{\partial \chi}{\partial x_0} + (\chi + \chi_0)\,\frac{\partial \chi}{\partial u} = 0, \qquad \frac{\partial \psi}{\partial x_0} + (\chi + \chi_0)\,\frac{\partial \psi}{\partial u} = \frac{u}{\sqrt{1 + u^2}}. \tag{28}$$

In the problem being considered the solution of this system can be obtained in parametric form (the parameter t varies within the following limits: $-l\sqrt{1 + u_{in}^2} < t < l\sqrt{1 + u_{in}^2}$)

$$x_0 = \int_t^{\psi}\Big[\sqrt{u_{in}^2 + 1} + \chi_{in}(t)\,(\psi'' - t) - \int_t^{\psi''}\chi_{in}(\psi')\,d\psi'\Big]$$
$$\times\Big\{\Big[\sqrt{u_{in}^2 + 1} + \chi_{in}(t)\,(\psi'' - t) + \int_t^{\psi''}\chi_{in}(\psi')\,d\psi'\Big]^2 - 1\Big\}^{-1/2} d\psi'', \tag{29}$$

$$\sqrt{1 + u^2} - \sqrt{1 + u_{in}^2} = \chi_{in}(t)\,(\psi - t) + \int_t^{\psi}\chi_{in}(\psi')\,d\psi', \tag{30}$$

where $\chi_{in}(t)$ is the initial distribution of the proper electric field inside the layer. For an initial density n_0 constant along the layer, we have $\chi_{in} = n_0 r_0 t$. For an external field which increases linearly the calculation of Eq. (29) leads to elliptic integrals.

d) *Motion of a charged layer into a region occupied by a constant magnetic field.* A magnetic field causes current to flow, i.e., produces a component u_3 in the velocity of the electron gas. We assume that at the initial time $u_3 = 0$ and that there is no magnetic field within the layer, $A_3 = 0$. Hence, by virtue of what has been shown above, $u_3 = -eA_3/m$ if temperature effects are neglected.

We consider the case in which the shielding of the external field by the produced current is small and we can take $u_3 \approx u_3^0 = -e/m\,A_3^0(x_1)$, where $A_3^0(x_1)$ is the potential of the external field. Finding $x_1 = \psi(x_0, u)$ we obtain

$$\frac{\partial \psi}{\partial x_0} + \left(\chi - \frac{u_3^0}{(1 + u^2 + u_3^{02})^{1/2}}\,\frac{eH_2^0}{m}\right)\frac{\partial \psi}{\partial u} = \frac{u}{(1 + u^2 + u_3^{02})^{1/2}}, \tag{31}$$

$$\frac{\partial \chi}{\partial x_0} + \left(\chi - \frac{u_3^0}{(1 + u^2 + u_3^{02})^{1/2}}\,\frac{eH_2^0}{m}\right)\frac{\partial \chi}{\partial u} = 0, \tag{32}$$

where $H_2^0 = -\partial A_3^0/\partial x_1$ is the external magnetic field and $\chi = eE/m$ is the proper electric field.

In the case in which a layer $2l$ moves at the initial time with relativistic velocity $u_{in} \gg 1$ into a region occupied by a magnetic field the solution of (31) and (32) is of the form

$$\sqrt{1 + u^2 + u_3^{02}(\psi)} - \sqrt{1 + u_{in}^2} = (\psi - t)\,\chi_n(t),$$

$$x_0 = \int_t^{\psi} d\psi'\Big[\sqrt{1 + u_{in}^2} + \chi_{in}(t)\,(\psi' - t)\Big]$$
$$\times\{[\sqrt{1 + u_{in}^2} + \chi_{in}(t)\,(\psi' - t)]^2 - u_3^{02}(\psi') - 1\}^{-1/2}, \tag{33}$$

$$-l\sqrt{1 + u_{in}^2} < t < l\sqrt{1 + u_{in}^2}. \tag{34}$$

For an external field which increases linearly with distance the calculation of Eq. (34) leads to elliptic integrals. When the magnetic field changes abruptly, the calculation can be carried out in closed form.

In conclusion I wish to take this opportunity to express my gratitude to V. I. Veksler, M. S. Rabinovich, A. A. Rukhadze for valuable discussions of the result of this work. I also wish to acknowledge a number of valuable comments by M. A. Leontovich.

---

[1] V. I. Veksler, Doklady Akad. Nauk SSSR **118**, 263 (1958), Soviet Phys.-Doklady **3**, 84 (1958).

[2] I. M. Khalatnikov, JETP **27**, 529 (1954).

[3] L. D. Landau and E. M. Lifshitz, Механика сплошных сред (Mechanics of Continuous Media) Gostekhizdat 1954.

[4] L. D. Landau, Izv. Akad. Nauk. SSSR, Ser. Fiz. **17**, 51 (1953).

Translated by H. Lashinsky
227

SOVIET PHYSICS JETP VOLUME 13, NUMBER 5 NOVEMBER, 1961

NUCLEON-NUCLEON INTERACTIONS AT $E \approx 10^{11}$ ev

I. M. DREMIN and D. S. CHERNAVSKII

P. N. Lebedev Physics Institute, Academy of Sciences, U.S.S.R.

Submitted to JETP editor September 21, 1960

J. Exptl. Theoret. Phys. (U.S.S.R.) **40**, 1333-1337 (May, 1961)

Peripheral nucleon-nucleon collisions at energies around 10^{11} ev are considered. As in reference 2, the pole approximation is used. The results are compared with experimental data.[3,6] The usual form[2] of the one-meson approximation is not valid for large values of "virtuality" k^2 and needs to be improved by taking into account the dependence on k^2 of the πN interaction cross section.

1. Some time ago it was proposed[1] that inelastic nucleon-nucleon interaction processes in the high-energy region be described by using diagram techniques in the pole approximation. It was found[2] that this approximation gives a satisfactory description of the experimental data at 9 Bev. At this energy, however, only those processes in which the "virtuality" of the intermediate pion (see Fig. 1) is relatively small, $k^2 \lesssim (7\mu)^2$, contribute significantly to the cross section; here k is the four-momentum of the intermediate pion and μ is the pion mass. Therefore, of course, the conclusion that the pole approximation is applicable is limited to just the region $0 < k^2 \leq (7\mu)^2$.* In order to resolve the question of the applicability of this approximation for $k^2 > (7\mu)^2$, it is necessary to consider higher-energy processes.

Experimental data on NN interactions at energies $E_l \sim 200$ Bev[3] show that the inelasticity coefficient is small in the majority of cases (this immediately indicates that peripheral collisions play an essential role). Moreover, these data show that there are two types of interaction which differ in nature, namely: 1) asymmetric interactions in which in the center-of-mass system (c.m.s.) the secondary pions emerge predominantly in the direction of one of the primary nucleons; 2) the symmetric case in which in the c.m.s. the secondary pions are nearly isotropic although the inelasticity coefficients of both nucleons are small.

In terms of diagrams, the first type of process can be interpreted as a special case of the diagram shown in Fig. 1, namely the case in which the nucleons are not equally excited. The diagram in Fig. 2 corresponds to the symmetric case. This is also a one-meson diagram.

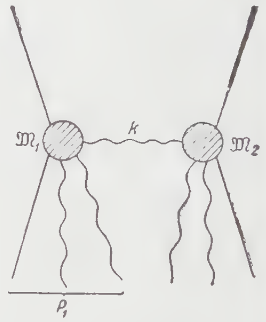

FIG. 1. General one-meson diagram for NN interaction. The numbers of pions emitted from the vertices can be different.

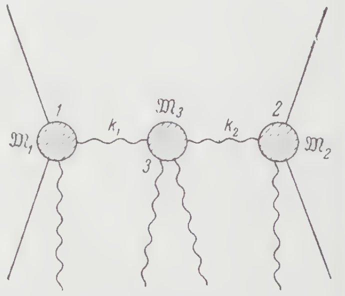

FIG. 2. One-meson diagram for NN interaction with intermediate $\pi\pi$ interaction.

It should be noted that such a division of processes and diagrams into different categories makes sense only for sufficiently high energies. In fact, the case in which three excited states are formed can be distinguished from that in which only two are formed only if their relative velocities $\bar{v}$ (more exactly, the quantities $\bar{\gamma} = (1-\bar{v}^2)^{-1/3}$) are sufficiently large: $\ln \bar{\gamma} \gtrsim \Sigma$, where Σ is the half-width of the angular distribution of secondary particles in their center-of-mass system:

$$dN/d\lambda = \exp(-\lambda^2/\Sigma), \qquad \lambda = \ln \operatorname{tg}(\vartheta/2).*$$

---

*It should be noted that even reference 2 points out that the πN interaction cross section, $\sigma_{\pi N}(k^2)$, might decrease with increasing k^2 for $k^2 \gtrsim (6\mu - 7\mu)^2$. Here, as in reference 2, $\hbar = c = 1$; $k^2 = \mathbf{k}^2 - k_0^2$.

*tg = tan.

The smallest value of Σ is 1 (which occurs for an isotropic distribution) and consequently a necessary condition for resolving the two cases is $\bar{\gamma} \gtrsim 2.7$.

For the diagram in Fig. 2, the best conditions for the resolution occur when the excited state at vertex 3 (with mass $\mathfrak{M}_3$) is at rest in the c.m.s. and the nucleons are equally excited (their masses are $\mathfrak{M}_1$ and $\mathfrak{M}_2$) and move in opposite directions. $\mathfrak{M}_3$ is of the order of magnitude $\mathfrak{M}_3 \sim 2\gamma_c\mu$ with $\gamma_c = (1 - v_c^2)^{-1/2}$ and v_c the velocity of the c.m.s. with respect to the laboratory system. The conservation laws give $\bar{\gamma}_{\max} = \gamma_c(\mathfrak{M}_3 - \mu)/\mathfrak{M}_{1,2}$. The minimum value for the mass of the excited nucleons is $\mathfrak{M}_{1,2} = 1.3\,m$, where m is the nucleon mass (this is the mass of the "usual" isobar which appears in the work of Tamm, Gol'fand, and Faĭnberg[4]). Then the condition $\bar{\gamma} \gtrsim 2.7$ leads to the inequality $\gamma_c > 4$. From this it follows that such a process can be observed at an energy $E_{\text{lab}} \sim 200$ Bev ($\gamma_c = 10$).

2. In order to compute the total cross section for peripheral one-meson collisions at the energy $E_{\text{lab}} = 200$ Bev, we used expression (5) of reference 1:*

$$\sigma_{NN}(E_0) = \frac{2}{(2\pi)^3 p_0 E_0^2} \int dz \int dy \int d(\cos\vartheta)$$

$$\times \frac{\sqrt{z^2 - m^2\mu^2}\,\sqrt{y^2 - m^2\mu^2}\,P_1}{[\mu^2 + \varkappa^2 + 2p_0P_1(1 - \cos\vartheta)]^2}\,\sigma_{\pi N}(z)\,\sigma_{\pi N}(y),$$

where

$$z = (\mathfrak{M}_1^2 - m^2 - \mu^2)/2, \qquad y = (\mathfrak{M}_2^2 - m^2 - \mu^2)/2, \quad (1)$$

E_0 and p_0 are the energy and momentum of the primary nucleon in the c.m.s. E_1 and P_1 are the energy and momentum of the isobar in the c.m.s.

$$\varkappa^2 = 2(E_0E_1 - p_0P_1) - \mathfrak{M}_1^2 - m^2,$$

$$\varkappa^2 + 2p_0P_1(1 - \cos\vartheta) = k^2,$$

ϑ is the angle between $\mathbf{p}_0$ and $\mathbf{P}_1$; $\sigma_{\pi N}(z)$ is the total πN interaction cross section at an energy (in the pion-nucleon c.m.s.) equal to $\mathfrak{M}_1$. The energy of the pion in the lab system is $\omega_{\text{lab}} = z/m$.

We note that the main contribution to the integral comes from $\sigma_{\pi N}(\omega_{\text{lab}})$ with $\omega_{\text{lab}} \sim 7 - 10$ Bev. On the basis of the data of Belyakov et al.[5] the magnitude of the cross section $\sigma_{\pi N}$ was taken to be constant and equal to 30 mb.

Integration of (1) over all values of y and z allowed by the conservation laws gave the result $\sigma_{NN} = 1400$ mb. The values of k^2 which contributed most were $k^2 \sim (50\mu - 100\mu)^2$. Such a large cross section is absurd and shows that the pole approximation is not valid for such large values of k^2. It should be emphasized that giving up any one of all the assumptions on which the pole method is based* (especially, giving up the equality $\sigma_{\pi N}(\mathfrak{M}, k^2) = \sigma_{\pi N}(\mathfrak{M}, k^2 = -\mu^2)$) can lead to the necessary decrease of the calculated cross section σ_{NN} by almost two orders of magnitude (see reference 2).

Thus, the result obtained above can be interpreted to mean that the cross section $\sigma_{\pi N}(\mathfrak{M}, k^2)$ is not a constant independent of k^2, but decreases strongly with increasing k^2. In order to find out the values of k^2 at which this occurs, expression (1) was integrated with the supplementary limitation that the integral was taken only over the region $k^2 \leq \delta^2$.†

We give the result of the integration for various values of δ:

δ/μ:	3	4	5	7	10	14	(no limit on k^3 ‡
σ_{NN}, mb:	8	16	28	80	190	420	1400

If δ is determined by the requirement that the calculated cross section not exceed the value obtained experimentally (for $E_{\text{lab}} \sim 10^{11}$ ev, $\sigma_{\exp} \approx 30$ mb[3,6]), then we find $\delta \sim 4\mu$, corresponding to a value of $\mathfrak{M}$ of about 4 Bev. Previously,[1] in studying the NN interaction at $E_{\text{lab}} = 9$ Bev, we concluded that the pole method is valid clear up to $k^2 \sim (7\mu)^2$ (equivalent to $\delta \gtrsim 7\mu$), which corresponds to $\mathfrak{M} \sim 2$ Bev. By comparing the results obtained here and in reference 1, one can conclude that the function $\sigma(\mathfrak{M}, k^2)$ is a complicated nonmultiplicative function of its variables such that the decrease of σ with increasing k^2 begins sooner for larger values of $\mathfrak{M}$.**

It should be mentioned that Berestetskii and Pomeranchuk[7] were the first to point out that the cross section σ_{NN} calculated in the pole approximation, with the assumption that $\sigma_{\pi N}$ is constant, increases without bound as the energy increases. However, in further investigating the problem they still in essence assumed that σ is muliplicative, $\sigma(\mathfrak{M}, k^2) = \sigma(\mathfrak{M})f(k^2)$. It seems to us that the example cited shows that it is unlikely that σ is

---

*In formula (2) of reference 1, P_1 was set equal to p_0, since there we considered the region in which k^2 is small. Here the exact expression is given.

*These assumptions are considered in more detail in reference 2.

†This is equivalent to approximating the function $\sigma(\mathfrak{M}, k^2)$ by the step function

$$\sigma(\mathfrak{M}, k^2) = \sigma(\mathfrak{M}, k^2 = -\mu^2) \text{ for } k^2 \leq \delta^2, \quad \sigma(\mathfrak{M}, k^2) = 0 \text{ for } k^2 > \delta^2.$$

‡The maximum value of k^2 is determined by the conservation laws.

**In the approximation used above, this means that δ decreases with increasing $\mathfrak{M}$.

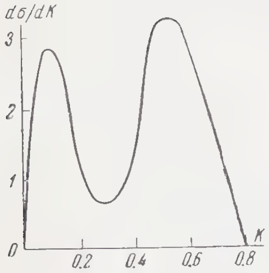

FIG. 3 Distribution of inelasticity coefficient K.

multiplicative, but rather that a more complicated dependence actually occurs.

In a comparison with the experimental data,[3,6] it is necessary to consider other features of the process besides the total cross section. However, this gives rise to some difficulties connected with the necessity of taking into account the dependence of $\sigma(\mathfrak{M}, k^2)$ on k^2. The step approximation to this function seems rather crude and, moreover, the choice of δ is not unique. Therefore, we limit our further considerations to those features which depend weakly on δ and on the form of $\sigma(\mathfrak{M}, k^2)$.

We have calculated the distribution of inelasticity coefficients K for these events. The results of the computation are shown in Fig. 3* (with $\delta = 4\mu$). The peak at $K = 0.0 - 0.2$ stands out. This peak comes from the cases in which an elastic πN interaction occurs at one of the vertices. At high energies, the elastic part of the πN interaction is basically diffractive and amounts to one-third of the total. Therefore, the fraction of such cases is about 33 per cent. In this case, the inelasticity coefficient of the nucleon at one of the vertices is $K_1 = \mathfrak{M}_2^2/E_0^2$, where $\mathfrak{M}_2$ is the "mass" of the excitation at the other vertex. In our case, $E_0 = 10$ Bev, $\mathfrak{M}_2 \sim 4$ Bev, $K \approx 0.16$. The other peak in the curve is due to the cases in which the πN interaction is inelastic. There the inelasticity coefficient is $K \gtrsim 0.5$.

These features of the distribution depend weakly on the assumed value of δ and are essentially due to the presence of diffractive πN interaction at high energies. These results are in qualitative agreement with the experimental data. It should be noted that according to this curve the charge-exchange probability should be small when the energy loss of the particle is small.

3. In order to obtain theoretical results for the so-called symmetric cases which have been observed experimentally,[3,6] the process represented in Fig. 2 was considered. An expression for the cross section for such a process can be obtained by a method analogous to that used in reference 1:

$$\sigma = \frac{32}{(2\pi)^8 E_0^2 I} \int \frac{d^4k_1\, d^4k_2}{(k_1^2+\mu^2)^2 (k_2^2+\mu^2)^2}\, \omega_1 E' I_1 \sigma_1 \cdot \omega_1 \omega_2 I_3 \sigma_3 \cdot \omega_2 E'' I_2 \sigma_2. \quad (2)$$

Here σ is the desired cross section, σ_i is the cross section for the process corresponding to vertex i ($i = 1, 2, 3$),* I_i are the corresponding particle current densities, k_1 and k_2 are the four-momenta of the virtual pions, and E' and E'' are the energies of the primary nucleons in the rest system of the excited nucleons.

It is convenient to use the following as independent variables:

$$z = \tfrac{1}{2}(\mathfrak{M}_1^2 - m^2 - \mu^2),\ y = \tfrac{1}{2}(\mathfrak{M}_2^2 - m^2 - \mu^2),$$

$$\mathfrak{M}_3, \quad E_1, \quad \vartheta_{1,2}, \quad \varphi_{1,2}.$$

Here $\mathfrak{M}_i$ is the mass of the excitation at vertex i, $E_{1,2}$ are the energies of the isobars formed at vertices 1 and 2, and $\vartheta_{1,2}$ and $\varphi_{1,2}$ are the polar and azimuthal angles at which the isobars are emitted in the c.m.s. Then

$$\begin{aligned} k_1^2 + \mu^2 &= \mu^2 + \varkappa_1^2 + 2p_0 P_1 (1 - \cos\vartheta_1), \\ k_2^2 + \mu^2 &= \mu^2 + \varkappa_2^2 + 2p_0 P_2 (1 + \cos\vartheta_2), \\ \varkappa_i^2 &= 2(E_0 E_i - p_0 P_i) - \mathfrak{M}_i^2 - m^2. \end{aligned} \quad (3)$$

The integration was carried out with the supplementary limitation $k_{1,2}^2 \le \delta^2$. In this process, the values of $\mathfrak{M}_{1,2}$ which contribute strongly are smaller than those in the process of Fig. 1 for the same value of E_0. Therefore, for this process we took the larger value of δ, $\delta = 7\mu$. We note that the integrand in (2) has sharp maxima at $\vartheta_1 = 0$, $\vartheta_2 = \pi$; this simplifies the integration.

On the basis of the expression (2), distributions of $\mathfrak{M}_1$, $\mathfrak{M}_2$, and $\mathfrak{M}_3$ were obtained.† It turned out that the distributions of $\mathfrak{M}_{1,2}$ were such that only values of $\mathfrak{M}_{1,2}$ near 1.3 m contribute significantly. The contribution of values of $\mathfrak{M}_{1,2}$ greater than 1.5 m was negligibly small. This is due to two circumstances: first, the integrand is a decreasing function of $\mathfrak{M}_{1,2}$ and second, $\sigma_{\pi N}(\mathfrak{M}_{1,2})$ has a strong maximum at $\mathfrak{M}_{1,2} = 1.3$ m and then falls rapidly.

The $\mathfrak{M}_3$ distribution is shown in Fig. 4; clearly values of $\mathfrak{M}_3$ between 2m and 4m are dominant. The maximum in the distribution occurs at $\mathfrak{M}_3 = 3$m; we note that its position is determined by the condition $\mathfrak{M}_3 = (2\mu/m) E_0$.

---

*In the report we sent to the High-energy Physics Conference (Rochester, 1960), results of analogous calculations with $\delta = 7\mu$ were given (see reference 8).

*We took the πN interaction cross sections (σ_1 and σ_2) from experiment. $\sigma_3 = \sigma_{\pi\pi}$ was taken to be constant.

†We do not give these calculations here because they are so long.

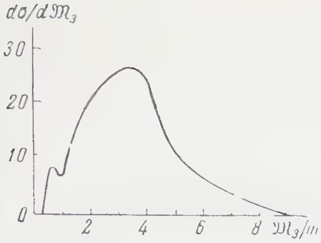

FIG. 4. Distribution of mass of excited $\pi\pi$ cloud ($\mathfrak{M}_3$).

The inelasticity coefficients can be estimated by using the $\mathfrak{M}_3$ distribution, the nucleon excitations $\mathfrak{M}_{1,2}$, and the conservation laws. According to this estimate, K varies between 0.2 and 0.4. All these quantities depend weakly on the choice of δ and agree qualitatively with the experimental data.[3,6]

The magnitude of the cross section for process (2), on the other hand, depends very strongly on the choice of δ; moreover, it involves the unknown quantity $\sigma_{\pi\pi}$. Therefore the estimate of the cross section can be off by orders of magnitude. For $\delta = 7\mu$, the calculation gives $\sigma_2 \approx 0.16\,\sigma_{\pi\pi}$. If $\sigma_{\pi\pi} \sim \sigma_{\text{geom}} \approx 60$ mb, then $\sigma_2 = 10$ mb; this is not in disagreement with experiment.[3,6]

It should be noted that all these results, as well as the experimental data,[3,6] are still preliminary and need to be more accurately determined. From the theoretical point of view, the main question is the best way of taking into account the dependence of the πN interaction on k^2.

In conclusion, the authors thank E. L. Feĭnberg, N. A. Dobrotin, and S. A. Slavatinskii for their constant interest in this work, for fruitful discussions, and for evaluations of the experimental data.

---

[1] I. M. Dremin and D. S. Chernavskii, JETP **38**, 229 (1960), Soviet Phys. JETP **11**, 167 (1960).

[2] Gramenitskii, Dremin, Maksimenko, and Chernavskii, JETP **40**, 1093 (1961), Soviet Phys. JETP **13**, 771 (1961).

[3] S. A. Slavatinskii, Report to the International Conference on Cosmic Rays, Moscow, 1959.

[4] Tamm, Gol'fand, and Faĭnberg, JETP **26**, 649 (1954).

[5] Belyakov, Wang, Glagolev, Dalkhazhav, Lebedev, Mel'nikova, Nikitin, Petrzhilka, Sviridov, Suk, and Tolstov, JETP **39**, 937 (1960), Soviet Phys. JETP **12**, 650 (1961).

[6] N. A. Dobrotin, Report to the International Conference on High-Energy Physics, Rochester, 1960.

[7] V. B. Berestetskii and I. Ya. Pomeranchuk, JETP **39**, 1078 (1960), Soviet Phys. JETP **12**, 752 (1961).

[8] I. M. Dremin and D. S. Chernavskii, Preprint, Phys. Inst. Acad. Sci., 1960.

Translated by M. Bolsterli
228

SOVIET PHYSICS JETP VOLUME 13, NUMBER 5 NOVEMBER, 1961

PHASE-SHIFT ANALYSIS OF pp-SCATTERING AT AN ENERGY OF 150 Mev

I. M. GEL'FAND, A. F. GRASHIN, and L. N. IVANOVA

Submitted to JETP editor October 6, 1960

J. Exptl. Theoret. Phys. (U.S.S.R.) **40**, 1338-1342 (May, 1961)

A nine-parameter phase-shift analysis (in which the single meson "tail" is taken into account) is applied to the experimental data on 150 Mev pp-scattering (the cross section, polarization, depolarization and rotation of polarization) by aid of a new numerical method (the "ravine" method). Two distinct solution regions are obtained, which are similar to those previously obtained for an energy of 95 Mev. The solution found by Stabler and Lomon[6] lies in one of these regions. The results are compared with the theoretical estimates for the peripheral phase shifts.

1. RESULTS OF ANALYSIS

A new numerical method (the "ravine" method) has been successfully used for the analysis of data on pp-scattering at an energy of 95 Mev. In contrast with the generally used "local" method, this new method makes it possible to find the possible values of the scattering phases with great accuracy.[1] In the same paper, analysis was similarly carried out of data on pp-scattering at 142 — 147 Mev; data on the cross section $\sigma(\theta)$ and polarization $P(\theta)$ for 17 angles of scattering[2*] together with data on the depolarization $D(\theta)$ for 5 angles[9] and on the rotation of the polarization $R(\theta)$ for 8 angles.[4]

As independently variable parameters, characteristic phases were selected with account of Coulomb interaction $\delta_0({}^1S_0)$, $\delta_2({}^1D_2)$, $\delta_1^0({}^3P_0)$, $\delta_1^1({}^3P_1)$, $\delta_1^2({}^3P_2)$, $\delta_3^3({}^3F_3)$, and the matrix elements

$$\xi_2 = \mathrm{Re}\,[S^2_{1,3}/2i], \qquad \eta_3^2 = \mathrm{Re}\,[(S_3^2 - e^{2i\Phi_3})/2i],$$

$$\eta_3^4 = \mathrm{Re}\,[(S_3^4 - e^{2i\Phi_3})/2i]$$

($S^J_{J-1,J+1}$, S^J_l is the scattering matrix with account of Coulomb interaction, Φ_3 is the Coulomb F phase). Here, just as in the analysis for 95 Mev,[1] it was assumed that

$$\mathrm{Im}\,[(S_3^4 - e^{2i\Phi_3})/2i] = 0,$$

and all higher matrix elements were taken into account in the single-meson approximation.

As a result of the analysis, two distinct solution regions were obtained, which lie within the limits shown in the table. The limits for region I are indicated by the criterion $\chi^2 \leq 2\overline{\chi^2}$ ($\overline{\chi^2} = 38$ is the mean mathematical expectation), while for region II, which has a larger value of χ^2, the limits are indicated by the criterion $\chi^2 \leq 3\overline{\chi^2}$.

The inclusion of data on $R(\theta)$ played an important role in obtaining the comparatively narrow separated regions. Analysis without these data leads to a much broader range of solutions such as the region obtained in analysis of the data on 95 Mev.[1] Data are also given in the table for two points from regions I and II: the points 1, 2 and 4, 5, respectively; The curves $D(\theta)$, $R(\theta)$ and $A(\theta)$ corresponding to these points are shown in Figs. 1 — 3. More recent, more accurate data,[5] containing additional measurements at angles of 12, 21, and 31°, are plotted in Fig. 1, along with the experimental points used by us in the analysis.[3] We have not plotted the curves for the cross section and polarization, since the different solutions practically coincide within the limits of experimental error.

Analysis was also carried out with data on depolarization obtained at Harwell (cited by Hwang et al.[3] and indicated by the dashes in Fig. 1). This change of data leads only to a certain shift in the regions and to an increase in the values of χ^2. Data for single points of regions I and II (3 and 6, respectively), which were obtained with the changed data, are given in the table. It is interesting to note that we did not succeed in obtaining solutions with larger negative values of the polarization at angles $\theta \approx 70°$.

As has already been pointed out earlier,[1] regions I and II are analogs of the corresponding regions I and II found for 95 Mev, while according

---

[*] The data of Palmieri et al.[12] for angles of 18.7, 22.8, 24.9, 46.5° and also $\theta \leq 8.3°$ and $\theta \geq 92°$ were not taken into consideration in determining the square deviation, for the results are very sensitive to possible inaccuracies in the angles, owing to the large, rapidly changing Coulomb contribution to the cross section at small angles (4.13, 6.2 and 8.34°), and the remaining data furnish practically no added information.

Limits of regions of solution and certain solutions

Phase shifts	Limits of region I	Points			Limits of region II	Points		
		1	2	3		4	5	6
χ^2	$\leqslant 2\,\overline{\chi^2}$	37	82	62	$\leqslant 3\,\overline{\chi^2}$	58	68	70
${}^1S_0$	11—23	16.9	15.9	16.2	—35——6	—8.8	—26.8	—14.5
${}^1D_2$	5—9	7.7	6.8	7.6	3—10	8.0	6.4	7.7
${}^3P_0$	1—11	7.6	5.0	11.8	—30——20	—23.8	—22.2	—25.1
${}^3P_1$	—20——15	—16.9	—18.2	—18.0	2.5—9.5	5.2	8.7	7.3
${}^3P_2$	14—17	16.0	16.3	15.2	14—20	18.4	15.6	17.5
ξ_2	—3.5——1	—1.9	—2.5	—2.9	—5.5——0.5	—4.6	—0.8	—4.0
$\eta^2{}_3$	—2.5—1.5	—1.4	1.7(T)	—0.9	—3.5—1	0.4	—0.3	—0.5
${}^3F_3$	—1—4	1.1	—1.1(T)	0.7	—2.5—2.5	—2.0	2.5	—1.9
$\eta^4{}_3$	—0.5—1.5	—0.08	0.9(T)	0.7	—1—1	—0.4	—0.06	—0.02

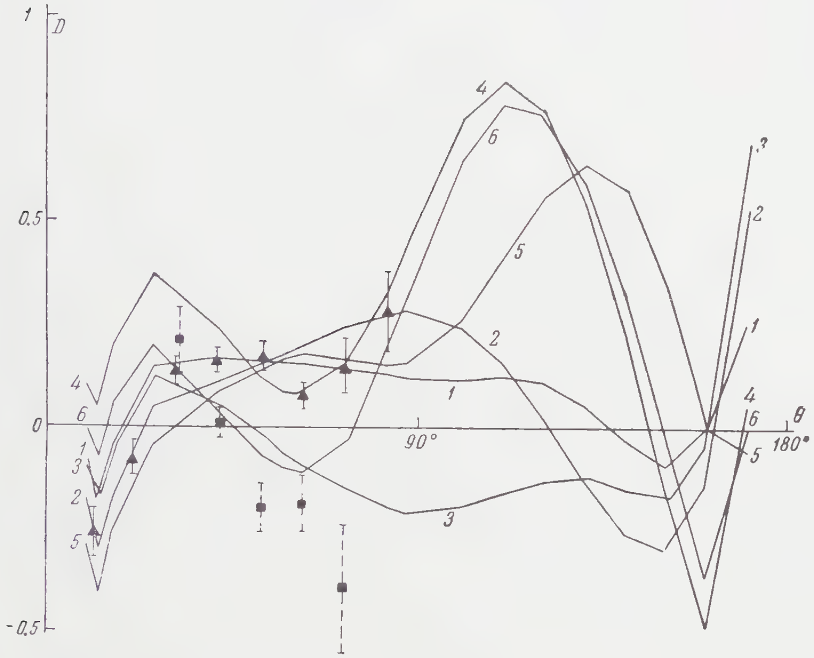

FIG. 1

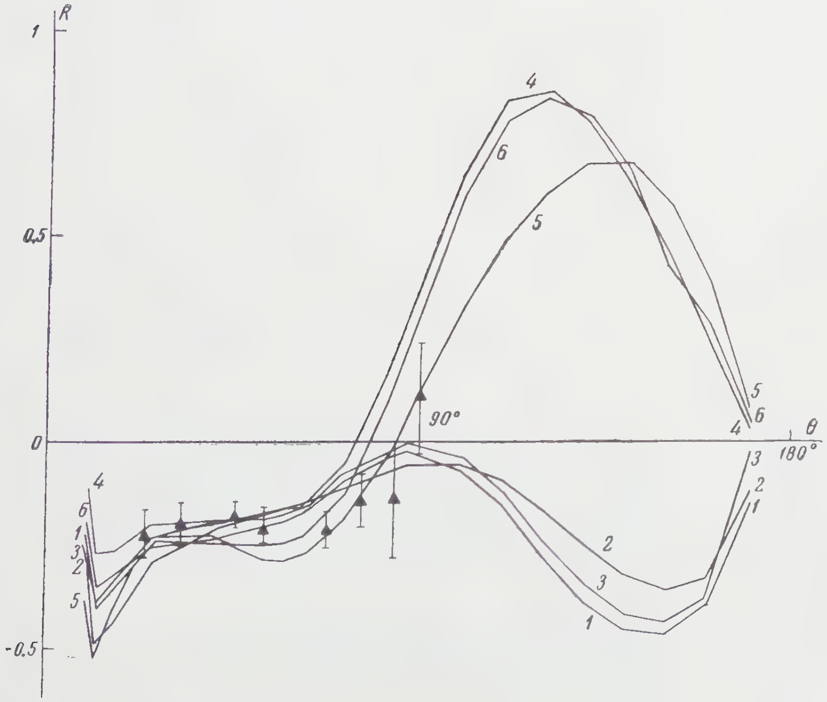

FIG. 2

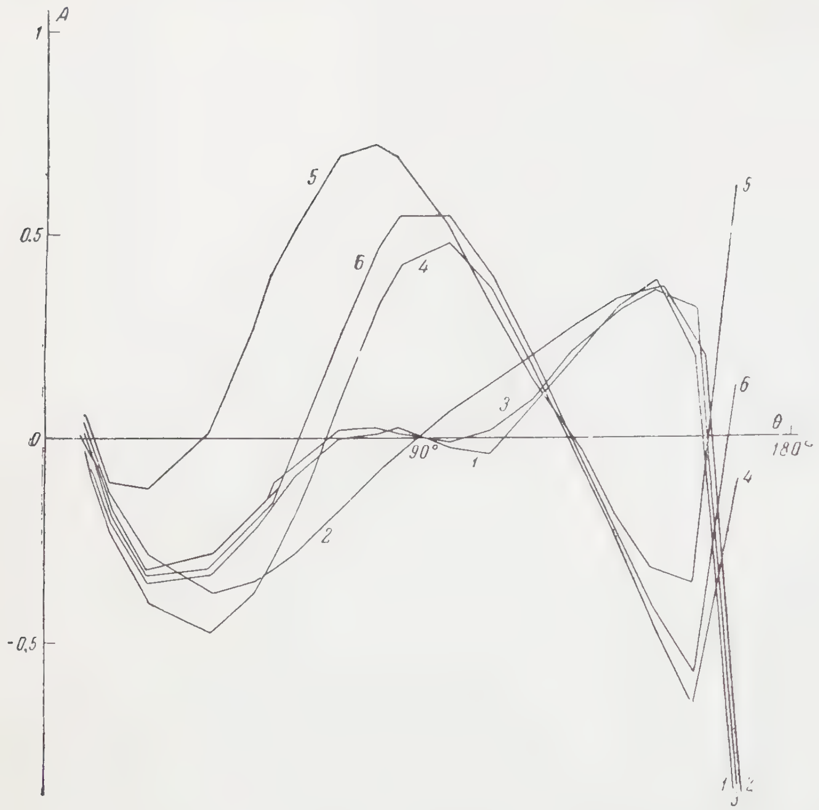

FIG. 3

to the values of the ^{1}S phase the region I is to be preferred. The solution found by Stabler Lomon[6] lies in the first region, but the tolerances for the possible values of the phase, which they derived, by means of the error matrix are far too low.

2. COMPARISON WITH THEORY

For energies of 150 Mev, the D and F phases and the mixing parameter can be regarded as "weakly peripheral," since the interaction in the corresponding states effectively takes place at distances $r_{\text{eff}} \approx 1.5/\mu$ (μ is the mass of the π meson). The single-meson approximation gives a value of $\delta_2 = 3.3°$ for the ^{1}D phase (δ_2 is the sum of the purely nuclear and pure Coulomb phases); the estimate $\Delta\delta_2 = 1°$ is obtained for the two-meson correction. The results of the analysis show that the two-meson phase shift obtained previously[7,8] gives the correct sign and order of magnitude for the correction to the single-meson phase shift. If the contribution from the next peripheral order of approximation (3-meson, and so forth) is unimportant, then the conclusion can be drawn that the 2-meson phase evidently exceeds the obtained estimate by several fold. Preliminary, more accurate theoretical estimates also agree with this conclusion; they show that a contribution to the D phase is obtained from a rather broad region of integration over the momentum transfer t beyond the closest singularity $t = 4\mu^2$. In this region, the compensation[7,8] in amplitudes, which is characteristic for the point $t = 4\mu^2$, is partially disrupted; therefore, the method used previously (removal of the amplitudes from under the integral at the point $t = 4\mu^2$) can lead to a somewhat lower result.

To explain the role of the F phase and the mixing parameter ξ_2, three additional variants of the analysis were carried out in which: 1) these phases were "fixed" in the single-meson approximation, like the higher phases, 2) the mixing parameter was varied in comparison with the previous variant,* 3) all phases, beginning with F, and ξ_2 were assumed to be equal to zero. In the first and second variants, it was not possible to obtain solutions with χ^2 less than 150. In the second variant, points were obtained for the first region with $\chi^2 \approx 2\overline{\chi^2}$, one of which (point 2) is shown in the table, while for the second region only points with $\chi^2 \approx 120$ were obtained.

The results of the analysis thus show that these phases are important for the analysis of the data at hand, while for the solution I the deviation from the single-meson approximation is important only in the mixing parameter, and amounts to 20 — 80 percent; for solution II, on the other hand, the corrections to the single-meson F phase and the possible single-meson values of the mixing parameter are important. If solution I is true, and the three-meson and higher peripheral contributions are unimportant for the tensor forces which make a contribution to the mixing parameter, then it follows that the two-meson approximation exceeds the estimate obtained earlier by a factor 10 – 50.[8] Such a conclusion requires more detailed investigation, since the authors do not see now any possibility for such a large increase in the previously obtained estimate. In this connection we note that for the mixing parameter we lack the compensation of the contributions of perturbation theory and the dispersion terms, which is characteristic of all the remaining phases in the region of integration over the transferred momentum $t \approx 4\mu^2$; in other cases, this compensation can serve as the source of a decrease in estimates in the use of the "peripheral" method (see references 7 and 8). For a clarification of this contradiction it is also desirable to improve the experimental data so as to obtain more accurate phase-shift analyses. In this case, data on D and R at angles of $\theta \gtrsim 90°$ are important for unambiguous choice of solution.

---

*In variants 1) and 2), the two-meson correction was taken into consideration for the $^3F_4$ state.[8]

The authors are grateful to I. Ya. Pomeranchuk and Ya. Smorodinskii for discussions and useful comments, and to S. L. Ginzburg for help in the calculations.

---

[1] Borovikov, Gel'fand, Grashin, and Pomeranchuk, JETP **40**, 1106 (1961), Soviet Phys. JETP **13**, 780 (1961).

[2] Palmieri, Cormack, Ramsey, and Wilson, Ann. Physik **5**, 299 (1958).

[3] Hwang, Ophel, Thorndike, Wilson, and Ramsey, Phys. Rev. Lett. **2**, 310 (1959).

[4] Bird, Edwards, Rose, Taylor, and Wood, Phys. Rev. Lett. **4**, 302 (1960).

[5] Hwang, Ophel, Thorndike, and Wilson, Phys. Rev. **119**, 352 (1960).

[6] R. C. Stabler and E. L. Lomon, Nuovo cimento **15**, 150 (1960).

[7] Galanin, Grashin, Ioffe, and Pomeranchuk, JETP **37**, 1663 (1959) and **38**, 475 (1960), Soviet Phys. JETP **10**, 1179 (1960) and **11**, 347 (1960); Nucl. Phys. **67**, 218 (1960).

Translated by R. T. Beyer
229

SOVIET PHYSICS JETP VOLUME 13, NUMBER 5 NOVEMBER, 1961

ON THE MOMENTUM DISTRIBUTION FUNCTION OF A FERMI-PARTICLE GAS IN THE HIGH-DENSITY LIMIT

I. O. KULIK

Physico-Technical Institute, Academy of Sciences, Ukrainian S.S.R.

Submitted to JETP editor October 28, 1960

J. Exptl. Theoret. Phys. (U.S.S.R.) **40**, 1343-1352 (May, 1961)

Field theoretical methods are used to study a fermion gas with Coulomb interactions at zero temperature. We renormalize the interaction lines and the free particle propagation lines so that we can take correlation and exchange effects of the interaction into account. We have evaluated in the high-density limit (Gell-Mann–Brueckner limit) the momentum distribution function of the particles at zero temperature. The applicability of the high-density approximation for describing the interaction between the electrons in a metal is discussed.

A timely problem of solid state theory is the study of the interaction between particles in systems with a large number of degrees of freedom. The use of quantum field-theoretical methods (see references 1 to 10 and others) based upon the introduction of Green's functions, i.e., particle propagation functions, has turned out to be very fruitful for solving this problem.

The present paper is devoted to a study of the effects of inter-particle interactions in a high-density electron gas. The first to pose a similar problem correctly were Gell-Mann and Brueckner[8] who evaluated the electron gas correlation energy as a power series in the reciprocal of the density. In the present paper we evaluate the momentum distribution function of the particles in the ground state (this turns out to be different from the Fermi distribution function) as a power series in the reciprocal of the electron gas density. We note that it turns out that there is an essential need to use a field-theoretical technique to evaluate the momentum distribution function of the particles, as the difference between the distribution function and the Fermi distribution function is itself a quantum effect.

We consider a system of interacting fermions with a Hamiltonian*

$$H = -\frac{\hbar}{2m}\sum_{\alpha}\int d\mathbf{x}\psi_{\alpha}^{+}(\mathbf{x})\,\Delta\psi_{\alpha}(\mathbf{x})$$
$$+\frac{1}{2}\sum_{\alpha,\,\beta}\int d\mathbf{x}d\mathbf{y}\psi_{\beta}^{+}(\mathbf{y})\,\psi_{\alpha}^{+}(\mathbf{x})\,v(|\mathbf{x}-\mathbf{y}|)\,\psi_{\alpha}(\mathbf{x})\,\psi_{\beta}(\mathbf{y}). \quad (1)$$

Here $\psi_{\alpha}(\mathbf{x})$ and $\psi_{\alpha}^{+}(\mathbf{x})$ are the field function operators in the Schrödinger representation ($\alpha = \pm 1/2$ is the spin index); $v(|\mathbf{x}|)$ is the Coulomb interaction potential:

$$v(\mathbf{x}) = \frac{1}{V}\sum_{\mathbf{q}\neq 0} v(q)\,e^{i\mathbf{q}\mathbf{x}}, \qquad v(q) = \frac{4\pi e^2}{q^2} \quad (2)$$

($\mathbf{q} \neq 0$ indicates that we consider a system of N electrons in a space filled with a compensating positive constant charge density). We note that although most equations in the following are valid for any $v(q)$ any actual calculations are performed for Coulomb forces.

To describe various properties of the interaction it is convenient to go over to a time-dependent form of the theory. We shall use the Matsubara field-theoretical technique[1,2] (at $T = 0$); to do this we introduce field functions $\psi_{\alpha}(x)$ in the "modified Heisenberg representation"

$$\psi_{\alpha}(x) = e^{Ht}\psi_{\alpha}(\mathbf{x})\,e^{-Ht}, \qquad x \equiv (\mathbf{x},\ t), \quad (3)$$

$$\partial\psi_{\alpha}/\partial t = [H,\ \psi_{\alpha}(x)]_{-} \quad (4)$$

[and similarly $\psi_{\alpha}^{+}(x)$].

The single-particle and two-particle electron Green's functions are defined by the usual equations

$$G_{\alpha\beta}(x;\ x') = \langle T(\psi_{\alpha}(x)\,\psi_{\beta}^{+}(x'))\rangle, \quad (5)$$

$$G_{\alpha\beta\gamma\delta}(x_1 x_2;\ x_1' x_2') = \langle T(\psi_{\alpha}(x_1)\,\psi_{\beta}(x_2)\,\psi_{\delta}^{+}(x_2')\,\psi_{\gamma}^{+}(x_1'))\rangle, \quad (6)$$

where $\langle\ldots\rangle$ indicates an average over the physical vacuum, i.e., over that state of the system of interacting particles with the lowest energy (ground state).

One can obtain in the usual way an equation for G by starting from the equations of motion (4):

---

*Here and henceforth we measure energies and frequencies in the same units; they are connected through the equation $\varepsilon = \omega$. Similarly, we put $\mathbf{p} = \mathbf{k}$ ($\mathbf{p}$ – momentum; $\mathbf{k}$ – wave vector).

$$\left(\frac{\partial}{\partial t} - \frac{\hbar}{2m}\Delta\right) G_{\alpha\beta}(x;\ x') - \sum_{\gamma}\int dy v(|\mathbf{x}-\mathbf{y}|)\, G_{\alpha\gamma\beta\gamma}(xy;\ x'y) = \delta^4(x-x')\,\delta_{\alpha\beta}. \tag{7}$$

When there are no periodic or external fields $G_{\alpha\beta}(x;\ x') = G(x - x')\,\delta_{\alpha\beta}$. To evaluate the Green's function explicitly we can use a formal expansion of Eq. (7) in a power series in v. In the zeroth approximation we get

$$G^{(0)}(x-x') = \begin{cases} -\dfrac{1}{V}\sum\limits_{\mathbf{k}} n^{(0)}(k)\exp\{i\mathbf{k}(\mathbf{x}-\mathbf{x}') - \varepsilon_k^0(t-t')\}, & t<t' \\ \dfrac{1}{V}\sum\limits_{\mathbf{k}} (1-n^{(0)}(k))\exp\{i\mathbf{k}(\mathbf{x}-\mathbf{x}') - \varepsilon_k^0(t-t')\}, & t>t' \end{cases} \tag{8}$$

where

$$n^{(0)}(k) = \begin{cases} 1, & k<k_F \\ 0, & k>k_F \end{cases}$$

is the Fermi distribution function at $T = 0$.

The contributions from the first and second approximations are given by the diagrams of Figs. 1 and 2. To obtain the corresponding contribution to G from a given diagram it is necessary to write for each full-drawn line $G^{(0)}(x - x')$ and for each dotted line $v(|\mathbf{x} - \mathbf{x}'|)$. The product obtained is then integrated over coordinate space at each vertex and over the time coordinates of the vertices with a different time coordinate* and multiplied by $(-1)^{n+l}2^l$, where n is the order of the diagram, i.e., the number of dotted interaction lines, and l the number of closed electron loops.† We note that diagrams of the type of Fig. 1b lead to a zero contribution as the momentum transferred along the dotted line is here zero while according to (2) $\mathbf{q} \neq 0$. We have omitted all such diagrams in Fig. 2.

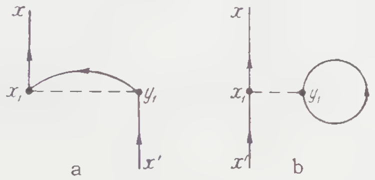

FIG. 1

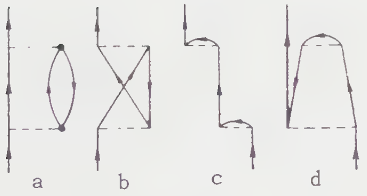

FIG. 2

As an example we shall write down the contribution from the diagram of Fig. 1a:

$$G_a^{(1)}(x-x') = -\int d^4x_1 dy_1 v(|\mathbf{x}_1-\mathbf{y}_1|)\, G^{(0)}(x-x_1) \times G^{(0)}(x_1-y_1)\, G^{(0)}(y_1-x'). \tag{9}$$

We consider the Fourier-representation of the Green's functions. If we write

$$G(x-x') = V^{-1}\sum_{\mathbf{k}} G_k(t-t')\exp\{i\mathbf{k}(\mathbf{x}-\mathbf{x}')\},$$

we get from (5) (dropping for the sake of simplicity the spin indices):

$$G_k(t) = \begin{cases} \langle a_k e^{-Ht} a_k^+\rangle e^{E_0 t}, & t>0, \\ -\langle a_k^+ e^{Ht} a_k\rangle e^{-E_0 t}, & t<0. \end{cases} \tag{10}$$

We now follow Galitskii and Migdal[4] and write the operators a_k and a_k^+ in the energy representation, and (10) is then transformed to

$$G_k(t) = \begin{cases} \sum\limits_s |(a_k)_{0s}|^2 \exp\{-(E_s-E_0)t\}, & t>0 \\ -\sum\limits_s |(a_k^+)_{0s}|^2 \exp\{(E_s-E_0)t\}, & t<0 \end{cases} \tag{11}$$

(the sum over s is over all excited states of the system).

In the first sum in (11) $E_s = E_s(N-1)$, in the second sum $E_s = E_s(N+1)$. We have $E_s(N-1) - E_0(N) = \epsilon_s - \mu + O(N^{-1})$; $E_s(N+1) - E_0(N) = \epsilon_s + \mu + O(N^{-1})$, where $\mu = \partial E_0/\partial N$ is the chemical potential and $\epsilon_s = E_s(N) - E_0(N)$ the excitation energy ($\epsilon_s > 0$). Hence,

$$G_k(t) = \begin{cases} e^{-\mu t}\sum\limits_s |(a_k)_{0s}|^2 e^{-\varepsilon_s t}, & t>0 \\ -e^{-\mu t}\sum\limits_s |(a_k^+)_{0s}|^2 e^{\varepsilon_s t}, & t<0. \end{cases} \tag{12}$$

$G_k(t)e^{\mu t}$ is thus a regular function as $t \to \pm\infty$ and can thus be expanded in a Fourier integral. We change thus to the expansion

$$G_k(t) = \frac{1}{2\pi i}\int_C G_k(\varepsilon)\, e^{-\varepsilon t} d\varepsilon, \tag{13}$$

where the integration contour C is a vertical straight line in the complex plane of the variable ϵ which cuts the real axis in the point $\epsilon = \mu$ (Fig. 3).

One can obtain from (12) Lehmann's expansion[11]

$$G_k(\varepsilon) = \int_{-\infty}^{\infty} \frac{\rho(k,\ E)}{E+\mu-\varepsilon}\, dE, \tag{14}$$

where $\rho(k, E)$ is a real positive function. $G_k(\epsilon)$

---

*The times corresponding to the end points of dotted lines are the same as we assume the interaction v to be instantaneous.

†Similar rules for assignments are, for instance, also used in reference 3 for the usual time-dependent Green's functions.

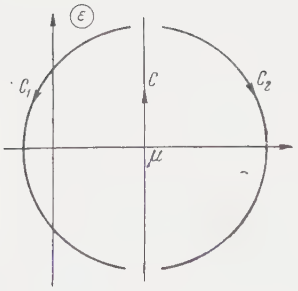

FIG. 3

is a regular function in the upper and lower half-plane of the complex variable ϵ but may have singularities (poles) on the real axis.*

It can be seen from Eq. (10) that once the single-particle Green's function G is known, one can evaluate the momentum distribution function of the particles:

$$n(k) = \langle a_k^+ a_k \rangle \tag{15}$$

using the relation

$$n(k) = -\lim_{t \to -0} G_k(t). \tag{16}$$

n(k) is equal to the quantum-mechanical average of the number of particles in a state with a well defined momentum k. When there is no interaction $n(k) = n^{(0)}(k)$ [see Eq. (8)] which corresponds to a filled Fermi-sphere (Fermi-filling). The effect of the interaction leads to a transition of electrons from the Fermi sphere and occupation of states with $k > k_F$; as a result there occur holes $(k < k_F)$ and particles $(k > k_F)$.

Migdal and Galitskii[4,7] considered the distribution function (15) and established some general properties of this function. In particular, they showed that the discontinuity in n(k) at $k = k_F$ remains whatever the interaction between the particles. This fact is confirmed in the present paper by a direct calculation of the momentum distribution function of the particles n(k) as a power series in the reciprocal of the density of the electron gas.

We turn to the calculation of n(k). We get in first approximation from (9) (see Fig. 1a)

$$G_k^{(1)}(t) = e^{-\mu t} \Sigma_k^{(1)} \frac{1}{2\pi} \int_{-\infty}^{\infty} \frac{e^{-i\nu t}}{(\varepsilon_k^0 - \mu - i\nu)^2} d\nu, \tag{17}$$

$$\Sigma_k^{(1)} = \frac{1}{V} \sum_q v(q)\, n^{(0)}(k+q). \tag{18}$$

Using (16) we get from this for the distribution function

$$n^{(1)}(k) = -\Sigma_k^{(1)} \frac{1}{2\pi} \int_{-\infty}^{\infty} \frac{d\nu}{(\varepsilon_k^0 - \mu - i\nu)^2} = \Sigma_k^{(1)} \delta(\varepsilon_k^0 - \mu). \tag{19}$$

The diagram of Fig. 1a leads thus everywhere except at $k = k_F$ to a zero value of n(k), while at $k = k_F$, n(k) turns out to be infinite. The same is true, as one can easily check, for the diagrams of Fig. 2c, d, Fig. 4 a–e, and so on.

However, if we sum all such diagrams (i.e., if we "renormalize") the infinities disappear. We renormalize the free particle propagation lines, by taking the sum of the infinite class of diagrams of the kind of Fig. 1a, Fig. 2c,d, Fig. 4 a–e, and so on. We shall call all such diagrams exchange diagrams.* We denote the corresponding renormalized propagation function by $S(x - x')$. In Fig. 5 we give the graphic equation for S where the thin line corresponds to $G^{(0)}$ and the thick line to S. One verifies easily that an expansion of S for small v leads to the exchange diagrams for S which were enumerated in the foregoing.

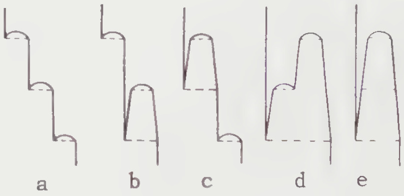

FIG. 4

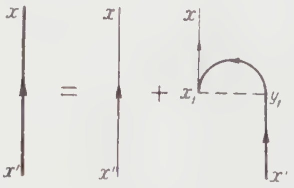

FIG. 5

The equation for S can also be obtained from (7) if we put

$$G_{\alpha\beta}(x; x') = S(x - x')\, \delta_{\alpha\beta},$$

$$G_{\alpha\beta\gamma\delta}(x_1 x_2; x_1' x_2') = S(x_1 - x_1')\, S(x_2 - x_2')\, \delta_{\alpha\gamma}\delta_{\beta\delta} - S(x_1 - x_2')\, S(x_2 - x_1')\, \delta_{\alpha\delta}\delta_{\beta\gamma}. \tag{20}$$

It has the form

---

*We note that the poles of the Fourier component of the time-dependent causal Green's function $G_k^c(\varepsilon)$ (in the usual Heisenberg representation) lie either above or below the real axis, which corresponds to the presence of damping of the corresponding quasi-particles. Similar problems have been considered by a number of authors.[3,5,6] In the present paper we aim mainly at studying the momentum distribution function of the particles for which the technique used here is relatively more convenient.

*We call exchange diagrams those diagrams which are obtained by iterations from diagrams of lower order by successively adding to one of the propagation lines the simplest diagram of Fig. 1a.

$$\left(\frac{\partial}{\partial t} - \frac{\hbar}{2m}\Delta\right) S(x - x')$$
$$+ \int dy\, v(|\mathbf{x} - \mathbf{y}|)\, S(x - y)\, S(y - x') = \delta^4(x - x'). \quad (21)$$

Using the Fourier representation we write (21) in the form

$$(\varepsilon_k^0 - \varepsilon)\, S_k(\varepsilon) + \frac{1}{V}\sum_{\mathbf{q}} v(q)\, \frac{1}{2\pi i} \int\limits_{C+C_1} S_{k+q}(\varepsilon')\, d\varepsilon'\, S_k(\varepsilon) = 1 \quad (22)$$

(see Fig. 3 for the integration contour).

One can easily verify that the solution of this non-linear integral equation has the simple form

$$S_k(\varepsilon) = \frac{1}{\varepsilon_k^0 - \varepsilon - \Sigma_k^{(1)}} = \frac{1}{\varepsilon_k - \varepsilon}, \quad (23)$$

where the quantity $\Sigma_{\mathrm{k}}^{(1)}$ is according to (18) equal to

$$\Sigma_k^{(1)} = \frac{e^2}{\pi\hbar} k_F \left\{ 1 + \frac{k_F^2 - k^2}{2kk_F} \ln \left| \frac{k_F + k}{k_F - k} \right| \right\}. \quad (24)$$

One sees from Eq. (20) that the renormalization which we have performed corresponds to taking the exchange effects exactly into account in all orders. It is clear from (23), as $\Sigma_{\mathrm{k}}^{(1)}$ is independent of ϵ, that when the exchange effects are taken into account exactly the Fermi-filling is conserved, i.e., the distribution function $\mathrm{n(k)}$ evaluated by using (23) has the shape of a Fermi step-function; the limiting momentum $\mathrm{k_F}$ is connected with the chemical potential μ by the relation*

$$\varepsilon_{k_F} = \mu, \qquad \mu = \hbar k_F^2/2m - \frac{e^2}{\pi\hbar} k_F,$$
$$k_F = (3\pi^2 n)^{1/3}. \quad (25)$$

It will be shown in the following that taking the non-exchange part of the interaction into account leads to a change in the rectangular form of the distribution function.

We must introduce for the following the energy operator $\mathrm{M(x - x')}$ which is defined through the relation (see, for instance, reference 3)

$$G(x - x') = G^{(0)}(x - x')$$
$$+ \int d^4x_1\, d^4x_2\, G^{(0)}(x - x_1)\, M(x_1 - x_2)\, G^{(0)}(x_2 - x'). \quad (26)$$

That G is of this form is clear from the structure of the graphs for the single-particle Green's function which start or end with a free electron line $\mathrm{G^{(0)}}$ (see Figs. 1, 2, 4).

If we write down the Fourier expansion of the energy operator

$$M(x - x') = \frac{1}{V}\sum_{\mathbf{k}} e^{i\mathbf{k}(\mathbf{x}-\mathbf{x}')}\, \frac{1}{2\pi i} \int\limits_C d\varepsilon\, e^{-\varepsilon(t-t')} M_k(\varepsilon), \quad (27)$$

we get from (26)

$$G_k(\varepsilon) = G_k^{(0)}(\varepsilon) + G_k^{(0)}(\varepsilon)\, M_k(\varepsilon)\, G_k^{(0)}(\varepsilon), \quad (28)$$

where $\mathrm{G_k^{(0)}}(\epsilon) = (\epsilon_{\mathrm{k}}^{(0)} - \epsilon)^{-1}$.

We can now express the distribution function $\mathrm{n(k)}$ in terms of M, using (16), and we get

$$n(k) = n^{(0)}(k) - \frac{1}{2\pi i} \int\limits_C \frac{M_k(\varepsilon)}{(\varepsilon_k^0 - \varepsilon)^2}\, d\varepsilon = n^{(0)}(k) + \nu(k). \quad (29)$$

The integral in Eq. (29) can be evaluated by means of the residue theorem; to do this we first split $\mathrm{M_k}(\epsilon)$:

$$M_k(\varepsilon) = M_k^+(\varepsilon) + M_k^-(\varepsilon), \quad (30)$$

where $\mathrm{M_k^+}(\epsilon)$ is that part of $\mathrm{M_k}(\epsilon)$ which is regular (without poles) in the right hand half-plane $\mathrm{Re}\,\epsilon > \mu$ (Fig. 3) and $\mathrm{M_k^-}(\epsilon)$ is regular in the left-hand half-plane $\mathrm{Re}\,\epsilon < \mu$ [if $\mathrm{M_k}(\epsilon)$ contains a part which is regular for all ϵ, i.e., a constant, it must be contained in $\mathrm{M_k^-}(\epsilon)$]. After this splitting up we get from Eq. (29)

$$\nu(k) = -\frac{1}{2\pi i} \int\limits_{C+C_1} \frac{M_k^-(\varepsilon)}{(\varepsilon_k^0 - \varepsilon)^2}\, d\varepsilon - \frac{1}{2\pi i} \int\limits_{C+C_2} \frac{M_k^+(\varepsilon)}{(\varepsilon_k^0 - \varepsilon)^2}\, d\varepsilon, \quad (31)$$

where $\mathrm{C_1}$ and $\mathrm{C_2}$ are the semi-circles of infinite radius which lie respectively in the left- and the right-hand half-planes (Fig. 3). Applying the residue theorem to (31) we get

$$\nu(k) = \begin{cases} \nu^+(k), & k > k_F \\ \nu^-(k), & k < k_F, \end{cases} \quad (32)$$

$$\nu^{\pm}(k) = \pm\left(\frac{d}{d\varepsilon} M_k^{\pm}(\varepsilon)\right)_{\varepsilon=\varepsilon_k^0}. \quad (33)$$

One can show that the ground state energy $\mathrm{E_0}$ is a sum of the energy of the non-interacting particles with a distribution function $\mathrm{n(k)}$ plus an extra term connected with interparticle correlations:

$$E_0 = 2\sum_{\mathbf{k}} \varepsilon_k^0 n(k) + \sum_{\mathbf{K}} \zeta(k), \quad (34)$$

where by analogy with (33) $\zeta^{\pm}(\mathrm{k}) = \pm \mathrm{M_k^{\pm}}(\epsilon_{\mathrm{k}}^0)$. To evaluate the distribution function it is now necessary to start from renormalized diagrams in which $\mathrm{G^{(0)}}$ is replaced by S. The contributions to G in the lowest approximation are the diagrams of Figs. 2a, b (we retain for the renormalized free particle propagation function S in the diagrams the previous notation of a full-drawn line). One can, however, easily verify that the diagram of Fig. 2a leads to an infinite contribution; this is connected with the divergence of integrals for small momentum transfers q. These divergences can be removed by renormalizing the interaction lines (see also references 5, 6, 9, 10, and others). To do this it is necessary to sum the class of the most strongly divergent diagrams which are given in Fig. 6. Here the same momentum **q** is transferred along each of the interaction lines. These diagrams correspond to virtual creation and annihilation processes of electron-hole pairs ($k > k_F$ and $k < k_F$), as each upward line in the diagram corresponds to a factor $1 - n^{(0)}(k)$ in the k-representation while a downward line correspond to a factor $n^{(0)}(k)$. Gell-Mann and Brueckner[8] were the first to perform such a summation for an electron gas (in a different technique).

---

*We note that Eq. (23) is not a trivial consequence of the introduction of the principal part of the energy operator Σ (see reference 4). A similar equation would occur if we summed only the diagrams of Fig. 1a, Fig. 2c, Fig. 4a, and so on. The difference lies in the meaning of the quantities μ and $\mathrm{k_F}$.

To sum the diagrams given in Fig. 6 we introduce an effective interaction potential $V(x - x')$ which we define by the graphic equation of Fig. 7

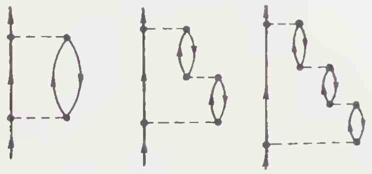

FIG. 6

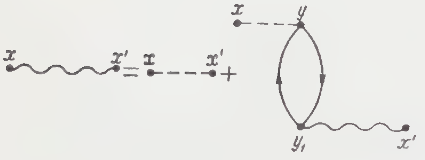

FIG. 7

(the wavy line corresponds to V). We have thus

$$V(x - x') = v(\mathbf{x} - \mathbf{x}')\,\delta(t - t') + \int d\mathbf{y}\, d\mathbf{y}_1\, v(\mathbf{x} - \mathbf{y})\, F(y - y_1)\, V(y_1 - x'), \qquad (35)$$

$$F(x - x') = 2S(x - x')\, S(x' - x). \qquad (36)$$

For the Fourier component of the function $F(x - x')$ we get*

$$F_q(t) = -\frac{2}{V} \sum_{\mathbf{k}} n^{(0)}(k)\,(1 - n^{(0)}(k + q)) \times \exp\{-(\varepsilon^0_{k+q} - \varepsilon^0_k)\, t\}. \qquad (37)$$

The function F determined by Eq. (37) is the same as the electron-hole pair propagation function introduced by Gell-Mann and Brueckner.[8]†

If we write

$$F_q(t) = \frac{1}{2\pi} \int F_q(\omega)\, e^{i\omega t}\, d\omega,$$

we get from (37)*

$$F_q(\omega) = -(mk_F/\pi^2\hbar)\, R_q(u), \qquad u = \omega/q;$$

$$R_q(u) = \frac{1}{2}\left\{1 - u\left(\operatorname{arctg}\frac{2+q}{2u} - \operatorname{arctg}\frac{2-q}{2u}\right) + \frac{1}{2q}\left(1 + u^2 - \frac{q^2}{4}\right)\ln\frac{4u^2 + (2+q)^2}{4u^2 + (2-q)^2}\right\} \qquad (38)$$

(in the last equation we have gone over to dimensionless variables q/k_F, ϵ/ϵ_F, u/u_F, where $u_F = \hbar k_F/m$ is the velocity at the Fermi surface).

One can easily solve Eq. (35) if one goes over to the Fourier representation. The result is

$$V_q(\omega) = v(q)/[1 - v(q)\, F_q(\omega)], \qquad (39)$$

or in dimensionless variables

$$V_q(u) = 4\pi/[q^2 + \alpha r_s R_q(u)], \qquad (40)$$

$\alpha = (4/\pi)(4/9\pi)^{1/3} = 0.663$. Here r_s is the usual parameter occurring in the theory of a free electron gas (see, for instance, reference 12) which is defined as $r_s = r_0/a_0$, where $4\pi r_0^3/3 = V/N = 1/n$; $a_0 = \hbar^2/me^2$ is the Bohr radius; $r_s \sim e^2$. At $T = 0$ the quantity r_s turns out to be in the case of the electron gas the only dimensionless parameter in the theory, and the approximation $r_s \to 0$ (i.e., $n \to \infty$) the only reasonable physical approximation in which there is a small parameter.

As the function $R_q(u)$ does not tend to zero as $q \to 0$, but according to (38) is equal to

$$R_0(u) = 1 - u \operatorname{arctg} u^{-1}, \qquad (41)$$

the result of the summation is to replace the Coulomb potential $v(q) = 4\pi/q^2$ which leads to a divergence as $q \to 0$ by the screened potential $V_q(u) \approx 4\pi/(q^2 + \alpha r_s R_0(u))$ which no longer diverges for small momenta.

We now shall compute $n(k)$ directly. It is necessary in the first non-vanishing approximation in V to sum the diagrams of Fig. 6. We have in that approximation (the summation is over **q**)

$$M^+_k(\varepsilon) = \frac{1}{V} \sum_{|\mathbf{k}+\mathbf{q}| < k_F} v(q)\, \frac{1}{2\pi} \int_{-\infty}^{\infty} d\omega\, \frac{F_q(\omega)\, V_q(\omega)}{-\varepsilon + \varepsilon^0_{k+q} + i\omega},$$

$$M^-_k(\varepsilon) = -\frac{1}{V} \sum_{|\mathbf{k}+\mathbf{q}| > k_F} v(q)\, \frac{1}{2\pi} \int_{-\infty}^{\infty} d\omega\, \frac{F_q(\omega)\, V_q(\omega)}{\varepsilon - \varepsilon^0_{k+q} + i\omega}, \qquad (42)$$

whence we get, using Eq. (33) (the summation is over **q**)

---

*We can replace S here by the renormalized function $G^{(0)}$ obtained from Eq. (8).

†F is that part of the polarization operator which takes the virtual pair creation processes into account. Similarly, V is in the present approximation the propagation function of the Bose branch of the excitations in the system of interacting fermions (i. e., the plasmon propagation function).

*arctg = tan⁻¹.

$$\nu^+(k) = \frac{1}{V} \sum_{|\mathbf{k}+\mathbf{q}|<k_F} v^2(q) \frac{1}{2\pi}$$

$$\times \int_{-\infty}^{\infty} \frac{F_q(\omega)}{(\varepsilon_k^0 - \varepsilon_{k+q}^0 + i\omega)^2} d\omega, \quad k > k_F,$$

$$\nu^-(k) = \frac{1}{V} \sum_{|\mathbf{k}+\mathbf{q}|>k_F} v^2(q) \frac{1}{2\pi}$$

$$\times \int_{-\infty}^{\infty} \frac{F_q(\omega)}{(\varepsilon_{k+q}^0 - \varepsilon_k^0 + i\omega)^2} d\omega, \quad k < k_F. \tag{43}$$

It is clear, first of all, that the relation

$$\sum_{k<k_F} \nu^-(k) + \sum_{k>k_F} \nu^+(k) = 0,$$

which expresses the conservation of particle number, is satisfied. This relation is also valid in the higher approximations.

Changing in Eq. (43) to dimensionless variables, we get

$$\nu^+(k) = \beta r_s^2 \int_{-\infty}^{\infty} du \int \frac{dq}{q} \int_{|\mathbf{k}+\mathbf{q}|<1} \frac{dx}{(-kx + q/2 + iu)^2}$$

$$\times \frac{R_q(u)}{q^2 + \alpha r_s R_q(u)}, \qquad k > 1.$$

$$\nu^-(k) = -\beta r_s^2 \int_{-\infty}^{\infty} du \int \frac{dq}{q} \int_{|\mathbf{k}+\mathbf{q}|>1} \frac{dx}{(-kx + q/2 + iu)^2}$$

$$\times \frac{R_q(u)}{q^2 + \alpha r_s R_q(u)}, \qquad k < 1. \tag{44}$$

where

$$\beta = (2/\pi^3)(4/9\pi)^{2/3} = 0.0175, \qquad x = \cos(\mathbf{k}, \mathbf{q}).$$

One can immediately easily evaluate the magnitude of the discontinuity $\Delta = \nu^+(1) - \nu^-(1)$ from (44):

$$\Delta = -\beta r_s^2 \int_{-\infty}^{\infty} du \int_0^{\infty} q\, dq \int_{-1}^{1} \frac{dx}{u + i(x + q/2)} \frac{R_q'(u)}{(q^2 + \alpha r_s R_q(u))^2}. \tag{45}$$

Integrating over x and replacing $R_q(u)$ by $R_0(u)$ we get the main term of the expansion of Δ as $r_s \to 0$ in the form

$$\Delta \approx 2Ar_s,$$

where the numerical constant A is equal to

$$A = -\frac{\beta}{\alpha} \int_0^{\infty} \frac{R_0'(u)}{R_0(u)} \operatorname{arctg} \frac{1}{u}\, du$$

$$= -\frac{\beta}{\alpha} \int_0^{\infty} \frac{\ln R_0(u)}{1 + u^2} du \qquad (A > 0). \tag{46}$$

One can also obtain from (44) the asymptotic behavior of $\nu^{\pm}(k)$ near $k = 1$. It is of the form

$$\nu^{\pm}(k) \approx \pm A r_s g(|k - 1|/\sqrt{\alpha r_s}), \qquad |k - 1| \ll 1, \tag{47}$$

where the function $g(\xi)$ is equal to

$$g(\xi) = \frac{f(\xi)}{f(0)},$$

$$f(\xi) = -\int_0^{\infty} \frac{R_0'(u)}{R_0(u) - \xi^2/u^2}$$

$$\times \left\{\operatorname{arctg} \frac{1}{u} - \frac{\xi}{uR_0^{1/2}(u)} \operatorname{arctg} \frac{R_0^{1/2}(u)}{\xi}\right\} du. \tag{48}$$

One can find the asymptotic behavior of $g(\xi)$ as $\xi \ll 1$:

$$g(\xi) \approx 1 + \gamma\xi \ln \xi, \qquad \gamma = (\beta/\alpha A)(\pi/2)^2 (1 + 4\sqrt{3}/\pi) \tag{49}$$

(in practice, this asymptotic behavior is, however, insufficient as one needs to know $g(\xi)$ as $\xi \sim 1$).

It is clear from (47) that the particle distribution function $\nu^+(k)$ and the hole distribution function $\nu^-(k)$ near the Fermi surface will be symmetrical (Fig. 8). The magnitude of the discontinuity of the total distribution function $n(k) = n^{(0)}(k) + \nu(k)$ at $k = 1$ is equal to $Z = 1 - \Delta \approx 1 - 2Ar_s$ ($r_s \to 0$).

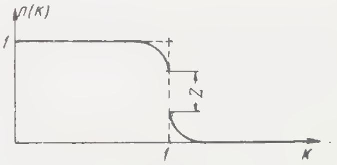

FIG. 8

In conclusion we determine the total number of particles outside the Fermi sphere (which is also equal to the number of holes inside the Fermi sphere) $N' = 2\Sigma\nu^+(k)$, $k > k_F$; this can be done conveniently by starting directly from (44). The main term in the expansion as $r_s \to 0$ is of the form

$$\bar{n} = N'/N \approx Br_s^{3/2}, \tag{50}$$

$$B = -\frac{3\pi\beta}{4\sqrt{\alpha}} \int_0^{\infty} \ln\left(1 + \frac{1}{u^2}\right) \frac{R_0'(u)}{\sqrt{R_0(u)}} u\, du. \tag{51}$$

A numerical integration of Eqs. (46) and (51) leads to the following values of the constants A, B, and γ:

$$A = 0.089, \qquad B = 0.051, \qquad \gamma = 1.61.$$

The dimensionless quantity $\epsilon = Br_s^{3/2}$ characterizes the degree of deviation from the perfect degenerate Fermi gas. r_s changes for different metals between the limits $r_s = 1.8$ to 5.6, whence $\epsilon = 0.12$ to 0.67. One may thus expect that for metals with the highest electron density the approximation considered here is sufficiently good (there remains, of course, the additional circumstance that we replaced the metal lattice by a uniform positive background).

In conclusion I express my sincere gratitude to I. M. Lifshitz and G. E. Zil'berman for a discussion of a number of problems and also to I. E. Dzyaloshinskii for his interest in this paper.

---

[1] Abrikosov, Gor'kov, and Dzyaloshinskii, JETP **36**, 900 (1959), Soviet Phys. JETP **9**, 636 (1959).

[2] T. Matsubara, Prog. Theoret. Phys. (Kyoto) **14**, 351 (1955).

[3] A. Klein and R. Prange, Phys. Rev. **112**, 994 (1958).

[4] V. M. Galitskii and A. B. Migdal, JETP **34**, 139 (1958), Soviet Phys. JETP **7**, 96 (1958).

[5] D. F. Du Bois, Ann. Phys. **7**, 174 (1959); **8**, 24 (1959).

[6] J. Hubbard, Proc. Roy. Soc. (London) **A240**, 539 (1957); **A243**, 336 (1958).

[7] A. B. Migdal, JETP **32**, 399 (1957); Soviet Phys. JETP **5**, 333 (1957).

[8] M. Gell-Mann and K. Brueckner, Phys. Rev. **106**, 364 (1957).

[9] A. A. Vedenov and A. I. Larkin, JETP **36**, 1133 (1959), Soviet Phys. JETP **9**, 806 (1959).

[10] I. A. Akhiezer and S. V. Peletminskii, JETP **38**, 1829 (1960), Soviet Phys. **11**, 1316 (1960).

[11] H. Lehmann, Nuovo cimento **11**, 342 (1954).

[12] D. Pines, Revs. Modern Phys. **28**, 184 (1956).

Translated by D. ter Haar
230

SOVIET PHYSICS JETP VOLUME 13, NUMBER 5 NOVEMBER, 1961

QUANTUM THEORY OF ACOUSTIC OSCILLATIONS OF AN ELECTRON-ION PLASMA IN A MAGNETIC FIELD

P. S. ZYRYANOV

Ural Polytechnic Institute

Submitted to JETP editor November 15, 1960

J. Exptl. Theoret. Phys. (U.S.S.R.) **40**, 1353-1359 (May, 1961)

Conditions for the existence of acoustic excitations are studied on the basis of the quantum dispersion equations for electron-ion plasma oscillations. It is shown that in strong magnetic fields longitudinal ultrasonic vibrations with a wave vector perpendicular to the magnetic field degenerate into ionic vibrations, inasmuch as the screening radius becomes infinite in this case. The decay frequency of ultrasonic waves moving along the magnetic field, as well as across it, is calculated. The decay frequency thus determined is found to oscillate, depending on the magnetic field strength.

1. Classical theory of longitudinal low-frequency oscillations of an electron-ion plasma in a magnetic field with a Maxwellian energy particle distribution in the ground state was considered in the work of Stepanov.[1] An attempt at the construction of a quantum theory was made in the research of Yakovlev and Kalyush;[2] however, since they did not take into account the quantum energy of the orbital motion of the particles in the magnetic field in the ground state, their results did not differ essentially from the results of the work of Stepanov. Moreover, the limits of applicability of the resultant formulas were not given in reference 2, and the damping was not calculated. The final results, with the exception of quite insignificant temperature-dependent corrections, are, in point of fact, the consequence of the hydrodynamic approximation in the description of the motion of ions interacting according to a screening law. Finally, it should be remarked that the assumptions made therein for the calculation of the acoustic branch at low wave numbers, for waves propagating across the magnetic field, contradict the result obtained.

The purpose of the present research was to construct a theory of low-frequency oscillations of the electron-ion plasma which would take into account the quantization of the energy of the orbital motion of charged particles in the magnetic field, and also to explain the dependence of the ultrasonic attenuation coefficient on the direction of the magnetic field.

2. We pause briefly to consider the specific case of absorption of ultrasound in a metal, which we shall approximate in what follows by an electron-ion plasma. We shall represent schematically three mutually interacting subsystems: the ultrasonic wave, the electrons, and the lattice (ions). The energy of the regular motion of the ultrasonic wave can dissipate via the channels shown in Fig. 1. For metals, the relaxation time τ_3 is always large in comparison with τ_1 and τ_2; therefore, in what follows, we shall not take it into account.

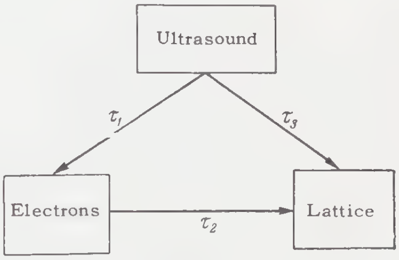

FIG. 1

Two limiting cases can be separated, depending on the ratio of the ultrasonic wavelength λ and the mean free path of the electron l, which is determined by the collisions with the lattice. The first case occurs when $\tau_2 \gg \tau_1$. Here, the slowest process is the transfer of energy obtained by the electrons from the ultrasonic wave to the lattice. This case corresponds to a wavelength $\lambda \gg l$. The electrical conductivity of the metal plays the principal role in such a case. In the second case, $\tau_2 \ll \tau_1$. This situation is realized when $\lambda \ll l$. Here, the slowest process is the process of energy transfer from the ultrasonic wave to the electron; therefore, collisions of electrons with the lattice do not play any role and can be neglected.

In the second case, we can consider the electron-ion system in the plasma approximation. The mechanism of energy transfer from the regular collective motion of the plasma to the individual, random motion of the electrons was first established by Landau[3] in the case of damping of plasma waves. Further investigation of this mechanism in the study of ultrasonic damping was undertaken in the researches of Silin[4] and Kittel.[5] The effect of the magnetic field on the damping was not studied in these researches. An attempt is made below to study the effect of the magnetic field on the ultrasonic absorption coefficient within the framework of the plasma model of the metal.

3. The quantum dispersion relation was found earlier for longitudinal oscillations in a system of particles of one kind.[6] The result is trivially generalized to the case of several kinds of particles interacting with one another by Coulomb's law. For the case of an electron-ion plasma, the dispersion equation has the form

$$1 = \lim_{\gamma\to 0}\frac{G(q)}{2\pi^2\hbar^2\alpha^2}\sum_{nn'}F^2_{nn'}(q_x)\left\{\int dk_z\,\frac{f_{01}(E^{(1)}_{k_z+q_z,n'})-f_{01}(E^{(1)}_{k_z,n})}{E^{(1)}_{k_z+q_z,n'}-E^{(1)}_{k_z,n}-\hbar\omega+i\hbar\gamma}\right.$$
$$\left.+\frac{z^2}{2}\int dk_z\,\frac{f_{02}(E^{(2)}_{k_z+q_z,n'})-f_{02}(E^{(2)}_{k_z,n})}{E^{(2)}_{n_z+q_z,n'}-E^{(2)}_{k_z,n}-\hbar\omega+i\hbar\gamma}\right\}, \qquad (1)$$

where

$$G(q)=4\pi e^2/q^2, \qquad \alpha^2=c\hbar/eH, \qquad \omega_{jc}=e_jH/m_jc,$$
$$E^{(j)}_{k_z,n}=\hbar^2k_z^2/2m_j+\hbar\omega_{jc}(n+{}^1/_2)$$

(j = 1, 2; 1 refers to electrons and 2 refers to ions), $e_1 = -e$, $e_2 = Ze$;

$$F_{nn'}(q_x)$$
$$=(n!/n'!)^{1/2}\exp\{-\alpha^2q_x^2/4\}(-\alpha q_x/\sqrt{2})^{n'-n}L_n^{n'-n}(\alpha^2q_x^2/2),$$
$$L_n^{n'-n}(x)=(1/n!)\,e^{-x}x^{n'-n}\frac{d^n}{dx^n}(e^xx^{n'}), \qquad n'\geqslant n,$$

f_{01} is the degenerate Fermi function, f_{02} is the Maxwellian distribution function of the ions.

For simplicity, we shall neglect the chaotic motion of the ions, although consideration of this motion does not present any difficulties. In the description of the ions, this approximation is equivalent to the hydrodynamic approximation. In such an approximation, we have

$$1=\lim_{\gamma\to 0}\frac{G(q)}{2\pi^2\hbar^2\alpha^2}\sum_{nn'}F^2_{nn'}(q_x)\int dk_z\,\frac{f_{01}(E^{(1)}_{k_z+q_z,n'})-f_{01}(E^{(1)}_{k_z,n})}{E^{(1)}_{k_z+q_z,n'}-E^{(1)}_{k_z,n}-\hbar\omega+i\hbar\gamma}$$
$$+\frac{\omega_{02}^2}{\omega^2-\omega_{2c}^2}\sin^2\vartheta+\frac{\omega_{02}^2}{\omega^2}\cos^2\vartheta,$$
$$\omega_{02}^2=4\pi e_2^2N_{02}/m_2, \qquad \cos\vartheta=\cos(\mathbf{q}\,\mathbf{H}), \qquad (2)^*$$

where N_{02} is the mean number density of the ions.

From Eq. (2), under the condition

$$\omega^2\gg\omega_{2c}^2 \qquad (3)$$

it follows that

$$1=-k_0^2(q_x,\omega,q_z)/q^2+\omega_{02}^2/\omega^2+i\varepsilon''(q_x,\omega,q_z), \qquad (4)$$

where

$$\varepsilon''=\frac{G(q)}{2\pi\hbar^2\alpha^2}\sum_{nn'}F^2_{nn'}(q_x)\int f_{01}(F^{(1)}_{k_z,n})$$
$$\times\{\delta(E^{(1)}_{k_z-q_z,n'}-E^{(1)}_{k_z,n}+\hbar\omega)-\delta(E^{(1)}_{k_z+q_z,n'}$$
$$-E^{(1)}_{k_z,n}-\hbar\omega)\}\,dk_z,$$
$$-k_0^2=\frac{2e^2}{\pi\hbar^2\alpha^2}\,\mathrm{P}\sum_{nn'}F^2_{nn'}(q_x)\int dk_z\,\frac{f_{01}(E^{(1)}_{k_z+q_z,n'})-f_{01}(E^{(1)}_{k_z,n})}{E^{(1)}_{k_z+q_z,n'}-E^{(1)}_{k_z,n}-\hbar\omega}. \qquad (4a)$$

The symbol P means that the integral is taken in the sense of the principal value.

Neglecting damping entirely, we find from (4) that

$$\omega^2=\omega_{02}^2q^2/[q^2+k_0^2(q_x,\omega,q_z)], \qquad (5)$$

ω_{02} is the Langmuir frequency of the ions, while ω_{01} is the Langmuir frequency of the electrons; the quantity k_0^{-1} can be interpreted as the screening radius. Introducing the longitudinal complex dielectric constant of the electrons in the magnetic field

$$\varepsilon=\varepsilon'+i\varepsilon''=1+k_0^2(q_x,\omega,q_z)/q^2+i\varepsilon''(q_x,\omega,q_z), \qquad (6)$$

we can interpret Eq. (4) by a clear cut elementary model.

Actually, let us consider the oscillations of the ions, which are described in the Fourier representation by the equation of motion

$$\omega\mathbf{v}_q=(Ze/m_2)\mathbf{q}\varphi, \qquad (7)$$

by the equation for the potential φ

$$q^2\varphi(\mathbf{q},\omega)=(4\pi Ze/\varepsilon(q_x,\omega,q_z))\,\rho(\mathbf{q},\omega) \qquad (8)$$

(ρ is the number density of the ions), and by the equation of continuity

$$N_{02}\mathbf{q}\cdot\mathbf{v}_q+\omega\rho=0. \qquad (9)$$

From Eqs. (7) — (9) we find the frequency:

$$\omega^2=\omega_{02}^2/\varepsilon(q_x,\omega,q_z). \qquad (10)$$

If we assume that $\epsilon'\gg\epsilon''$, we immediately obtain Eq. (4) from (10) with the aid of (6).

For the existence of an acoustic branch of the vibrations, we must find such a solution for ϵ which has the following asymptotic behavior:

$$\lim_{q\to 0}\varepsilon'\sim\mathrm{const}/q^2.$$

Thus the role of the electronic system reduces to screening the Coulomb field of the point ions and to damping of the acoustic oscillations. In the absence of a magnetic field, the plasma is isotropic; if the ion velocities are small in comparison with

---

$^*(\mathbf{qH})=\mathbf{q}\cdot\mathbf{H}$

the electron velocities, then the screening is spherically symmetric. The screening is anisotropic in the presence of a magnetic field. As is seen from the definition, k_0 depends upon the angle ϑ between the vectors $\mathbf{q}$ and $\mathbf{H}$, and on the frequency ω. Inasmuch as the sound velocity is determined from k_0, it is clear from (5) that the magnetic field leads to space-time dispersion of the acoustic oscillations and to anisotropy in the sound velocity.

We shall consider below the dependence of k_0 on the parameters of the system in different limiting cases, since the general formula for k_0 is too complicated for investigation.

4. We shall consider first the conditions under which we can neglect both the space and the time dispersions of the sound velocity and its anisotropies. In the case of a completely degenerate Fermi function, the expression for k_0^2 can be written in the form

$$-k_0^2 = \frac{2m_1e^2}{\pi\hbar^2\alpha}\sum_{nn'} F_{nn'}^2(q_1)\frac{1}{q_2}\left\{\ln\frac{\Omega+\sqrt{2}\,q_2(n_0-n')^{1/2}+q_2^2/2-(n'-n)}{\Omega-\sqrt{2}\,q_2(n_0-n')^{1/2}+q_2^2/2-(n'-n)}-\ln\frac{\Omega+\sqrt{2}\,q_2(n_0-n)^{1/2}-q_2^2/2-(n'-n)}{\Omega-\sqrt{2}\,q_2(n_0-n)^{1/2}-q_2^2/2-(n'-n)}\right\}, \tag{11}$$

where the dimensionless quantities

$$\Omega = \omega/\omega_{1c}, \qquad q_1 = \alpha q_x,$$

$$q_2 = \alpha q_z, \qquad n_0 = \mu_0/\hbar\omega_{1c} - 1/2$$

have been introduced (μ_0 is the chemical potential of a degenerate Fermi gas in a magnetic field).

For q_1 and q_2, and $\Omega \ll |n'-n|$, and also $n \gg 1$ (large quantum numbers), it follows from (11) that

$$k_0^2 = 3\omega_{01}^2/v_0^2, \tag{12}$$

where v_0 is the Fermi velocity.

It is easy to see that these conditions correspond to the case in which the Larmor radius of the orbit is small in comparison with the sound wavelength. Only in this case can the dispersion of the sound velocity and its anisotropies be neglected for $q^2 \ll k_0^2$.

We now return to a consideration of the dependence of k_0 on the magnetic field and on the angle ϑ between the field and the wave vector of the sound wave. It is shown that k_0 vanishes for $\vartheta = \pi/2$ in the case of very strong magnetic fields. Actually, it follows from (11), for the case $q_z = 0$, that

$$-k_0^2 = \frac{4\sqrt{2}\,m_1e^2}{\pi\hbar^2\alpha}\sum_{nn'} F_{nn'}^2(q_1)\,\frac{(n_0-n)^{1/2}-(n_0-n')^{1/2}}{\Omega-(n'-n)}. \tag{13}$$

The quantity k_0 vanishes for $n_0 < 1$. This means that the screening radius becomes infinite in a direction perpendicular to $\mathbf{H}$. This was also to be expected, since the frequency of plasma oscillations vanishes for $n_0 < 1$ in the direction $\vartheta = \pi/2$ (see reference 6).

The vanishing of the frequency of plasma oscillations for $\vartheta = \pi/2$ can be illustrated by analogy with the oscillations of plasma in a periodic field. In the case $n_0 < 1$, all the electrons are found in the level with $n = 0$, and the nearest level $n = 1$ is separated by an energy $\hbar\omega_{1c} > E_0$ (for metals, $E_0 \sim \hbar\omega_{01}$). In the band model, this is analogous to the situation in which the completely filled band is separated by an energy gap ΔE from an empty band, and plasma oscillations are impossible if $\Delta E > \hbar\omega_{01}$. We note that the screening radius in the direction of the magnetic field does not depend on the field, since $\lim_{q\to 0} F_{nn'} = \delta_{nn'}$, and the magnetic field falls out of the expression for k_0^2.

Thus it is shown that the screening radius, which has a constant value (independent of the magnetic field) along the field, can become infinite for $\vartheta = \pi/2$ in strong fields. It follows from what has been shown that the acoustic vibrations degenerate into ion vibrations with a frequency

$$\omega^2 = \omega_{02}^2 + \omega_{2c}^2 \tag{14}$$

in the case $n_0 < 1$ and $\vartheta = \pi/2$.

The development of acoustic oscillations for $\vartheta = \pi/2$ comes about abruptly when n_0 reaches a value equal to unity. Upon further decrease in H, the dispersion of the sound changes abruptly every time n_0 increases by unity, since new components appear in (13).

5. We now proceed to our fundamental problem — the investigation of the attenuation of ultrasonic vibrations. The damping frequency γ is expressed in accord with (14) by the following formula

$$\gamma = \frac{m_1\omega^3G(q)}{4\pi\hbar^2\alpha\omega_{02}^2}\sum_{nn'}F_{nn'}^2(q_1)\int d\zeta f_{01}(E_{\zeta,n}) \times\{\delta(E_{\zeta-q_2,n'}-E_{\zeta,n}+\Omega)-\delta(E_{\zeta+q_2,n'}-E_{\zeta,n}-\Omega)\} \tag{15}$$

for $\omega \gg \gamma$ (which is confirmed by the result). For $q_1 = 0$ and $\hbar\omega \ll E_0$, it follows from (15) that

$$\gamma_{\vartheta=0} = \gamma_0 = \frac{3\pi}{4}\,\frac{\omega_{01}^3}{\omega_{02}^2}\,\frac{\omega}{v_0^3q^3}. \tag{16}$$

If we neglect the dispersion of the sound velocity in (16), then (16) goes over into the following formula

$$\gamma_0 = \frac{\pi}{12}\,\frac{m_1}{m_2}\,v_0q, \tag{16a}$$

which was first obtained by Silin,[4] and later by Steinberg.[7] It also follows from (16) that γ does not depend on the magnetic field for a longitudinal ultrasonic wave with $\mathbf{q} \parallel \mathbf{H}$.

The greatest interest attaches to the ultrasonic wave with $\mathbf{q} \perp \mathbf{H}$, since the properties of the electron plasma in a direction perpendicular to $\mathbf{H}$ change appreciably in a magnetic field (in contrast with its properties in a direction parallel to the field). It follows from (15) that in this case γ has the form

$$\gamma|_{\vartheta=\pi/2} = \gamma_{\perp} = \frac{m_1\omega^3 G(q)}{\sqrt{2}\,\pi\hbar^2\alpha\omega_{02}^2} \sum_{n=0}^{n_0-\Omega} F^2_{n,\,n+\Omega}(q)\,\{(n_0-n)^{1/2} - (n_0-n-\Omega)^{1/2}\}. \qquad (17)$$

This expression is very complicated in the general case.

For small values of the quantum number $(n \sim 1)$, the value of $\gamma_{\perp}$ undergoes a discontinuous change upon change in the magnetic field strength, since the number of components in (17) changes abruptly upon an increase or decrease of n_0 by unity. For large quantum numbers $n \gg 1$, the asymptotic expansion

$$F^2_{n,\,n+\Omega}(q) \approx J^2_{\Omega}[q(2n+\Omega+1)^{1/2}], \qquad (18)$$

can be used where $J_{\Omega}(x)$ is a Bessel function of the first kind of order Ω. If we take into account the inequalities $n \gg 1$ and $n_0 \gg \Omega$, we can convert in (17) from summation over n to integration and, expanding the term in curly brackets in a series in Ω, we obtain

$$\gamma_{\perp} = \frac{m_1\omega^4 G(q)\sqrt{n_0}}{\sqrt{2}\,\hbar^2\alpha\omega_{02}^2\omega_{1c}} \int_0^{\pi/2} J^2_{\Omega}(r_c q\sin\varphi)\sin\varphi\,d\varphi, \qquad (19)$$

where $r_c = v_0/\omega_{1c}$. The last expression can be rewritten in the form

$$\frac{\gamma_{\perp}}{\gamma_0} = 2r_c q \int_0^{\pi/2} J^2_{\Omega}(r_c q\sin\varphi)\sin\varphi\,d\varphi, \qquad (20)$$

where γ_0 is determined by Eq. (16).

Upon removal of the magnetic field, Eq. (20) changes to the equality

$$\gamma_{\perp} = \gamma_0, \qquad (21)$$

since the anisotropy disappears.

For large values of the argument, or, more precisely, for $r_c q \gg \Omega$, the Bessel function can be replaced by its asymptotic expansion:

$$J_{\Omega}(x) = \sqrt{2/\pi x}\cos(x - \pi\Omega/2 - \pi/4); \qquad (22)$$

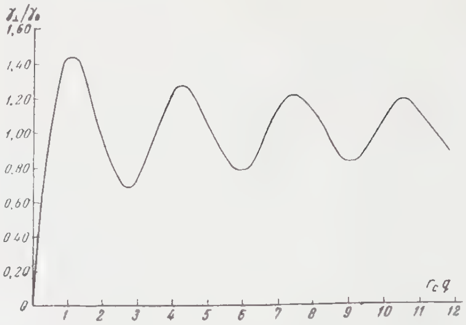

FIG. 2. Dependence of $\gamma_{\perp}/\gamma_0$ on $r_c q$ for $\Omega \ll 1$, according to Eq. (20).

We then get in place of (20)

$$\frac{\gamma_{\perp}}{\gamma_0} = \frac{4}{\pi}\int_0^{\pi/2} \cos^2\left(r_c q\sin\varphi - \frac{\pi}{2}\Omega - \frac{\pi}{4}\right)d\varphi. \qquad (23)$$

The latter integral is equal to

$$\gamma_{\perp}/\gamma_0 = 1 + \sin\pi\Omega J_0(2r_c q) + \cos\pi\Omega\,[2\Omega_0(2r_c q) - S_0(2r_c q)], \qquad (24)$$

where Ω_0 and S_0 are respectively the Lommel-Weber and Struve functions.

For $H \to 0$ or $r \to \infty$, the ratio $\gamma_{\perp}/\gamma_0 = 1$. This is seen immediately from (23), since $\cos^2(x)$ can be replaced by its average value (equal to ½) for $r_c \to \infty$.

The dependence of $\gamma_{\perp}/\gamma_0$ on $r_c q$, which follows from (20), is shown in Fig. 2.

In conclusion, we note that Eq. (20) is valid under the assumptions $\lambda \ll l$, $E_0 \gg \hbar\omega_{1c}$ and $E_0 \gg \hbar\omega(q)$.

---

[1] K. N. Stepanov, JETP **35**, 1155 (1958), Soviet Phys. JETP **8**, 808 (1959).

[2] V. A. Yakovlev and A. V. Kalyush, JETP **39**, 308 (1960), Soviet Phys. JETP **12**, 219 (1961).

[3] L. D. Landau, JETP **16**, 574 (1946).

[4] V. P. Silin, JETP **23**, 649 (1952); **38**, 977 (1960), Soviet Phys. JETP **11**, 703 (1960).

[5] C. Kittel, Acta. Metal. **3**, 295 (1955).

[6] P. S. Zyryanov, JETP **40**, 1065 (1961), Soviet Phys. JETP **13**, 751 (1961).

[7] M. S. Steinberg, Phys. Rev. **111**, 425 (1958).

Translated by R. T. Beyer
231

SOVIET PHYSICS JETP VOLUME 13, NUMBER 5 NOVEMBER, 1961

ON NONLINEAR QUANTIZATION OF A SPINOR EQUATION

D. S. CHERNAVSKII

P. N. Lebedev Physics Institute, Academy of Sciences, U.S.S.R.

Submitted to JETP editor November 17, 1960

J. Exptl. Theoret. Phys. (U.S.S.R.) **40**, 1360-1365 (May, 1961)

A nonlinear spinor equation of the Heisenberg type[1] is considered. A procedure for the determination of the "mass" values of the eigenstates of the spinor field is proposed which is based on the following assumptions: a) the number of "incoming" and "outgoing" lines in the diagrams describing the eigenstates of the field are sufficiently large, and b) only irreducible diagrams are taken into account. The procedure is carried out by means of the self-consistent field method.

1. INTRODUCTION

ONE of the fundamental problems of present-day elementary particle theory is the determination of the eigenmasses of the particles.

Recently, Heisenberg[1] proposed to describe all elementary particles as eigenstates of a single spinor field ψ. In the general case, this problem consists in the determination of a functional Φ_{p_μ} which satisfies the equation

$$\hat{P}_\mu \Phi_{p_\mu} = p_\mu \Phi_{p_\mu}, \qquad (1)$$

where $\hat{P}_\mu$ is the operator of the four-momentum which is related to the energy-momentum tensor T_{ik} and the Lagrangian in the usual way. The eigenvalues p_μ, or more precisely, the quantities $\sqrt{-p_\mu^2} = \mathfrak{M}$ represent the eigenmasses of the stationary states. The lowest states with the lowest values of the eigenmass and spin will correspond to the "elementary" particles. However, in calculating the mass values $\mathfrak{M}$ Heisenberg was confronted with the usual difficulty in this type of problem: the appearance of divergent expressions.*

We note that, in solving the problem of the eigenmass of the particle, one usually (and in the paper of Heisenberg, too) makes the additional assumption that the interaction is adiabatically switched on and off at $t = \pm\infty$. That is, the functional Φ_{p_μ} is written in the form

$$\Phi_{p_\mu} = \Phi_{in} = \psi^+ (p_\mu)\, \Phi_0 \quad \text{for } t = -\infty,$$
$$\overset{*}{\Phi}_{p_\mu} \overset{*}{\Phi}_{out} = \overset{*}{\Phi}_0 \psi^- (p_\mu) \quad \text{for } t = +\infty$$

(here Φ_0 is the functional of the vacuum). In the language of diagrams, this means that one considers a diagram of the type shown in Fig. 1, in which there is only a single thin line on the left $(t = -\infty)$, depicting a single "undressed" particle. It is well known that attempts to calculate the eigenvalue of the energy lead to infinities in this case.

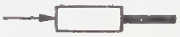

FIG. 1. Diagram of the energy for an interaction which is switched on adiabatically.

It is of interest to try to consider this problem without the assumption of the adiabatic switching-on of the interaction. It is, of course, impossible to solve this problem without any additional assumptions whatsoever. However, one can make different assumptions. Thus let us assume that the occupation numbers characterizing the functional Φ_{p_μ} are always (i.e., also for $t = -\infty$) large.* In the language of diagrams this means that the number of incoming lines (on the left) as well as the number of outgoing lines (on the right) is sufficiently large, i.e., the diagram is "many-tailed."

We note that the "many-tailed" diagrams can also be divided into the class of completely irreducible diagrams (Fig. 2a) and the class of reducible diagrams (Fig. 2b). In the latter, one of the lines contains a self-energy part of lower order (Fig. 2c). It is therefore of interest to consider the problem of the eigenvalue of the energy by taking only the completely irreducible many-tailed diagrams into account. This will be the subject of the present paper.

It is impossible at present to justify convincingly the procedure of separating out the irreducible many-tailed diagrams. However, arguments can be advanced which make it more or less likely that this procedure is sound. First of all, it is

---

*To circumvent this difficulty, Heisenberg proposed to use a Hilbert space for the functionals Φ_{p_μ} with an indefinite metric.[2]

*This assumption is, in a certain sense, the opposite of the assertion that the functional $\Phi_{p_\mu} = \psi^+\Phi_0$ for $t = -\infty$.

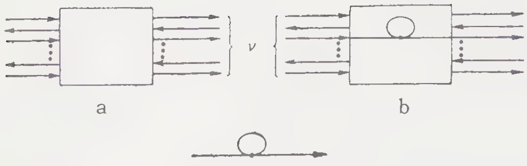

FIG. 2. a – "many-tailed" irreducible diagram for the energy, b – many-tailed reducible diagram, c – self-energy diagram of the lowest order.

relativistically invariant. Second, it can easily be shown that the number of reducible many-tailed diagrams is only a small fraction ($\sim 1/\nu$, where ν is the number of external lines) of the number of completely irreducible diagrams (it is true, however, that this does not necessarily imply that their contribution will also be small). Third, in renormalizable theories (to which, unfortunately, the Heisenberg theory does not belong) the reducible diagrams are automatically excluded after renormalization.* In order to carry out this program, it is convenient to use the method of the self-consistent field (Hartree-Fock method): first, this method has proved its usefulness in the investigation of nonrelativistic systems consisting of many particles and second, it is comparatively simple to exclude the reducible diagrams within the framework of this method.†

It should be noted that what we propose is basically only a program of action. The aim of this program, so far, is only to determine the functionals which correspond to the lowest states. We do not pretend to be able to describe the scattering and the interaction among "real" particles. In our formulation, the scattering problem will be analogous to the problem of the interaction of composite particles. It can be said beforehand that the phenomenological operator for the interaction of real particles (if it can be written down at all) will be complicated and nonlocal, and will differ greatly from the Lagrangian describing the interaction between quanta of the field ψ.

2. METHOD

Let us consider a Lagrangian density of the form ($\hbar = c = 1$)

$$L(x) = \bar{\psi}(x)\gamma_\mu\partial_\mu\psi(x) + m\bar{\psi}(x)\psi(x) + \lambda^2(\bar{\psi}(x)\hat{O}\psi(x))(\bar{\psi}(x)\hat{O}\psi(x)), \tag{2}$$

where $\bar{\psi}(x)$ and $\psi(x)$ are operators of a spinor field; m is a constant with the dimensions of a mass; λ is a coupling constant (with the dimension of a length); and $\hat{O}$ is a spinor operator which depends on the form of the interaction: in the case of scalar coupling, $\hat{O} = 1$, for vector coupling, $\hat{O} = \gamma_\mu$, etc. We note that the expression (2) is a generalization of the Lagrangian of Heisenberg and reduces to it for $m = 0$.

Our discussion will be in the "rest" system, where

$$p_i = 0, \qquad p_0 = E = \mathfrak{M}, \qquad \Phi_{p_\mu} = \Phi'_E. \tag{3}$$

It is entirely possible that one can develop a covariant method of solving the problem under the assumptions made. For the moment, however, it is more convenient to work in the Schrödinger representation in the "rest" system. We note that the time and the space coordinates are not treated in the same way in the "rest" system. This should not worry us, however, since the four space-time coordinates are in general not completely equivalent in our problem, which is characterized by the constant vector p_μ. Indeed, in an arbitrary system of coordinates we can choose as the four independent variables the quantity $\tau = -p_\mu x_\mu/\mathfrak{M}$ and the three quantities $\xi_\mu = x_\mu + x_\nu p_\nu p_\mu/\mathfrak{M}^2$. It is easily seen that the variables ξ_μ represent the projection of the vector x_μ on the plane perpendicular to p_μ, so that only three of them are independent. It is natural that the variables τ and ξ_μ do not necessarily enter in the solution in the same way in an arbitrary system of coordinates. In our "rest" system, $\tau \equiv t$, $\xi_4 = 0$, and $\xi_i \equiv x_i$.*

Let us formulate the problem in the Schrödinger representation, where

$$\Phi'_E = e^{iEt}\Phi_E, \qquad \psi(x) = e^{i\hat{H}t}\psi(\mathbf{x})e^{-i\hat{H}t}. \tag{4}$$

Here $\hat{H}$ is the Hamiltonian, which is equal to

$$\hat{H} = \int d^3x\,\bar{\psi}(\mathbf{x})\gamma_i\partial_i\psi(\mathbf{x}) + m\int d^3x\,\bar{\psi}(\mathbf{x})\psi(\mathbf{x}) - \frac{1}{2}\lambda^2\int d^3x\,(\bar{\psi}(\mathbf{x})\hat{O}\psi(\mathbf{x}))(\bar{\psi}(\mathbf{x})\hat{O}\psi(\mathbf{x})) \qquad (i = 1, 2, 3).$$

The equation which determines the functional Φ_E is†

---

*We note that the meaning of the renormalization of the bare constants (e.g., the mass m_0 and the charge g_0) is in our case different from the usual one. For even after renormalization, the quantities m and g do not represent the observed values, but have the meaning of "bare" constants as before. The observed "mass" is in this case given only by the quantity $\mathfrak{M}$.

†Strictly speaking, the large number of particles in the system is a necessary condition for the applicability of the Hartree-Fock method, not a sufficient one. But at the present moment it is difficult to justify the application of this method more rigorously. It is possible that this can be done more easily later on.

*We note, incidentally, that the possibility of choosing such variables was ignored in the solution of the "classical" equation (i.e., assuming that $\bar{\psi}$ and ψ commute) in the papers of Heisenberg et al.[2] and Kurdgelaidze.[3] These authors, therefore, left a whole class of solutions out of consideration.

†It is, in general, necessary that the functional Φ_E satisfy the condition $\hat{P}_i\Phi_E = 0$ besides the equation (5) ($\hat{P}_i$ is the operator of the space components of the momentum). However, if the number of "external" lines is large, $\nu \gg 1$, this condition is not important and does not affect the final result. This can be seen by considering the problem in momentum space.

$$\hat{H}\Phi_E = E\Phi_E. \tag{5}$$

We shall assume that the commutation relations have the usual form

$$\{\overline{\psi}(\mathbf{x}),\ \psi(\mathbf{x}')\} = \delta(\mathbf{x} - \mathbf{x}'). \tag{6}$$

In this connection, the question of the value of the anticommutator for different times comes up. We shall not discuss this point, since these commutators do not appear either in the final expression or in the course of the investigation (see below).

The solution of Eq. (5) is conveniently found by the variational method. Let us write down the average value of the energy

$$E = \Phi_E^{*}\hat{H}\Phi_E = \int d^3x\ {}_E\langle\overline{\psi}(\mathbf{x})\ (m + \gamma_i\partial_i)\ \psi(\mathbf{x})\rangle_E$$

$$-\ \tfrac{1}{2}\lambda^2\int d^3x\ {}_E\langle(\overline{\psi}(\mathbf{x})\,\hat{O}\,\psi(\mathbf{x}))\ (\overline{\psi}(\mathbf{x})\,\hat{O}\,\psi(\mathbf{x}))\rangle_E, \tag{7}$$

where $\rangle_E \equiv \Phi_E$ and ${}_E\langle \equiv \Phi_E^{*}$. It is seen that minimizing this expression with respect to the functional Φ_E^{*} (with account of the normalization) is equivalent to solving Eq. (5).

For the following it is convenient to expand the functions $\psi(\mathbf{x})$ in terms of some complete orthonormal system of spinors $\Psi_n(\mathbf{x})$:

$$\psi(\mathbf{x}) = \sum_n [a_n^{-}\Psi_n^{(+)}(\mathbf{x}) + b_n^{+}\Psi_n^{(-)}(\mathbf{x})],$$

$$\overline{\psi}(\mathbf{x}) = \sum_n [a_n^{+}\overline{\Psi}_n^{(+)}(\mathbf{x}) + b_n^{-}\overline{\Psi}_n^{(-)}(\mathbf{x})].$$

(Here $\Psi_n^{(+)}$ and $\Psi_n^{(-)}$ are the positive and negative frequency parts of the system of functions Ψ_n.) The operators a_n and b_n satisfy the usual commutation relations

$$\{a_n^{+}, a_m^{-}\} = \{b_n^{+}, b_m^{-}\} = \delta_{mn}, \qquad \{a^{\pm}, a^{\pm}\} = \{b^{\pm}, b^{\pm}\} = 0.$$

We shall not specify the form of the functions $\Psi_n(\mathbf{x})$ any further, since it will be determined by (5).

Up to this point the discussion has been rigorous. In accordance with what has been said above, let us now apply the method of the self-consistent field (Hartree-Fock method) and choose the functional Φ_E of the form*

$$\Phi_E = \sum_\nu C_\nu \prod_i^{\nu'} a_i^{+} \prod_j^{\nu''} b_j^{+}\,\Phi_0, \tag{8}$$

where Φ_0 is the functional of the vacuum. The factors a_i^{+} and b_j^{+} are distributed such that the indices i and j are in natural order; ν' and ν'' are occupation numbers such that $\nu' + \nu'' = \nu$. They are connected with one another in the following way: if the functional Φ_E describes a state with integer spin and zero "charge," $\nu' = \nu'' = \nu/2$; if it describes a state with half-integer spin and "charge" ±1, then $\nu' = \nu'' \pm 1$.

The functions C_ν must satisfy the condition $\Sigma|C_\nu|^2 = 1$ and must, according to the assumption made above, be different from zero only in the region $\nu \sim \nu_0 \gg 1$. In view of this circumstance, we shall in the following neglect terms of order $1/\nu$ as compared to unity. Moreover, we shall not take into account terms which correspond to reducible diagrams.

Substituting the functional (8) in (7), we obtain (we omit the intermediary calculations in view of their complexity)

$$E = \sum_\nu |C_\nu|^2 \Big\{\Big[\int d^3x \sum_k^{\nu'} \overline{\Psi}_k^{(+)}(\mathbf{x})\,(m + \gamma_i\partial_i)\,\Psi_k^{(+)}(\mathbf{x})$$

$$-\int d^3x \sum_l^{\nu''} \overline{\Psi}_l^{(-)}(\mathbf{x})(m + \gamma_i\partial_i)\,\Psi_l^{(-)}(\mathbf{x})$$

$$+\ \tfrac{1}{2}\lambda^2\int d^3x\Big[\sum_{k,l}^{\nu'}[(\overline{\Psi}_k^{(+)}\,\hat{O}\,\Psi_k^{+})(\overline{\Psi}_l^{(+)}\,\hat{O}\,\Psi_l^{+})$$

$$-(\overline{\Psi}_k^{+}\,\hat{O}\,\Psi_l^{+})(\overline{\Psi}_l^{(+)}\,\hat{O}\,\Psi_k^{+})]$$

$$+\sum_{k,l}^{\nu''}[(\overline{\Psi}_k^{(-)}\,\hat{O}\,\Psi_k^{(-)})(\overline{\Psi}_l^{(-)}\,\hat{O}\,\Psi_l^{(-)})$$

$$-(\overline{\Psi}_k^{(-)}\,\hat{O}\,\Psi_l^{(-)})(\overline{\Psi}_l^{(-)}\,\hat{O}\,\Psi_k^{(-)})]$$

$$-2\sum_k^{\nu'}\sum_l^{\nu''}[(\overline{\Psi}_l^{(-)}\,\hat{O}\,\Psi_k^{(+)})(\overline{\Psi}_k^{(+)}\,\hat{O}\,\Psi_l^{(-)})$$

$$-(\overline{\Psi}_k^{(+)}\,\hat{O}\,\Psi_l^{(-)})(\overline{\Psi}_l^{(-)}\,\hat{O}\,\Psi_k^{(-)})]\Big]\Big\}. \tag{9}$$

We note that we have omitted terms of the type $\langle a_k^{+}a_l^{+}\rangle$, $\langle a_k^{+}a_l^{+}a_{k'}^{+}a_{l'}^{+}\rangle$, etc.,* in deriving this expression, since their contribution turned out to be small ($\sim 1/\nu$) in comparison with the contribution from the remaining terms. Another important step in the derivation of the expression above is the omission of terms of the type $\langle a_l^{+}a_k^{-}a_k^{+}a_l^{-}\rangle$. These terms are related to the reducible diagrams of the form shown in Fig. 2b. The number of such terms is small ($\sim 1/\nu$) in comparison with the number of the remaining terms, but the contribution from each of these terms may be infinite. These terms have been discarded on the basis of the considerations above. The terms remaining in (9) do not any more contain the self-interaction (i.e., reducible diagrams of the type shown in Fig. 2c); for

---

*It is easily shown that this form of the functional is equivalent to the usual form of an antisymmetrized product, employing the usual method of quantization in momentum space.

*Terms of this type describe the change of the energy if there is additional creation (or absorption) of particle pairs. The circumstance that their contribution is small is, apparently, connected with the fact that the chemical potential of a pair is equal to zero.

$k = l$, the interaction terms reduce to zero by virtue of the antisymmetrization.

Expression (9) must be varied with respect to two physically distinct groups of parameters: expression (9) must be minimized 1) with respect to the occupation numbers (i.e., with respect to the parameters of the function C_ν), and 2) with respect to the parameters which determine the system of functions $\Psi_n(\mathbf{x})$. As a result of these variations we determine the specific form of the functions $\Psi_n(x)$ and the function C_ν. For example, in the crudest approximation we may write $C_\nu = \delta_{\nu\nu_0}$ (where ν_0 is the variational parameter) and take for the complete system of functions $\Psi_n(x)$ the system of spinor functions for a particle with mass m_0 in a potential well with depth U_0 and width r_0 (m_0, U_0, and r_0 are the variational parameters).

CONCLUSION

We have seen that the problem of the eigenmass of an elementary particle reduces in our case to the problem of the formation of a bound state of a system of many "virtual" particles. Analogous problems concerning the formation of a bound state through the interaction of several particles with one another have been discussed many times. They usually lead to a finite expression for the energy of the system. We therefore hope that the minimization of expression (9) leads in our case also to a finite result.

We hope to carry out this program in the future and also to discuss other problems related to it (for example, the problem of the properties of the physical vacuum).

We also note that an analogous program can also be applied to the "usual" theory which starts with two interacting fields (fermions and bosons) with the "usual" linear coupling between them.

In conclusion, I take this opportunity to express my gratitude to E. L. Feĭnberg, D. A. Kirzhnits, V. Ya. Faĭnberg, and G. A. Milekhin for valuable advice and fruitful discussions.

---

[1] W. Heisenberg, Z. Naturforsch. **9a**, 292 (1954).

[2] Heisenberg, Kortel, and Mitter, Z. Naturforsch. **10a**, 425 (1955); W. Heisenberg, Z. Physik **144**, 1 (1956).

[3] D. F. Kurdgelaidze, JETP **32**, 1156 (1957), Soviet Phys. JETP **5**, 941 (1957); JETP **34**, 1587 (1958), Soviet Phys. JETP **7**, 1093 (1958); JETP **36**, 842 (1959), Soviet Phys. JETP **9**, 594 (1959).

Translated by R. Lipperheide
232

SOVIET PHYSICS JETP VOLUME 13, NUMBER 5 NOVEMBER, 1961

ASYMPTOTIC FORM OF THE VERTEX PART IN ELECTRODYNAMICS

V. G. VAKS

Submitted to JETP editor November 22, 1960; resubmitted February 8, 1961

J. Exptl. Theoret. Phys. (U.S.S.R.) **40**, 1366-1368 (May, 1961)

The vertex part in electrodynamics is found for a certain range of momentum values.

THE vertex part in electrodynamics $\Gamma_\sigma(p, q, l)$ was obtained by Sudakov[1] in the region $l^2 \gg p^2$, $q^2 \gg m^2$, $e^2 \ln(l^2/m^2) \ll 1$. By using the renormalization group method Blank and Shirkov[2] generalized this result to the region in which vacuum polarization plays a role. They considered in addition to the terms of order $\sim e^2 \ln(l^2/p^2) \ln(l^2/q^2)$ treated by Sudakov also terms of order $e^2 \ln(l^2/m^2)$, $e^2 \ln(p^2/m^2)$, and $e^2 \ln(q^2/m^2)$, however assumed, as is customary, that

$$e^2 d_t(l^2) = e^2\left[1 - \frac{e^2}{3\pi}\ln(-l^2/m^2)\right]^{-1} \ll 1,$$

as well as that $e^2 \ln(l^2/p^2) \ll 1$ and $e^2 \ln(l^2/q^2) \ll 1$. As a result of an insufficiently correct application of the method the result obtained by Blank and Shirkov,[2] also cited by Bogolyubov and Shirkov,[3] turned out to be erroneous. Since the problem may be of some interest as far as the method is concerned we present in this note a correct version of the Blank and Shirkov result. We make use of the method and notation of Sudakov.[1]

At first we set the longitudinal part of the photon Green's function $d_l(k^2)$ equal to zero. Then the skeleton diagram of lowest order in $\Gamma_\sigma(p, q, l)$ has the form

$$\Gamma_\sigma^{(2)} = \frac{e^2}{\pi i}\int \gamma_\mu \frac{1}{\hat{p} - \hat{k}} \gamma_\sigma \frac{1}{\hat{q} - \hat{k}} \gamma_\nu \frac{dk}{k^2}\left(\delta_{\mu\nu} - \frac{k_\mu k_\nu}{k^2}\right) \times \left(1 - \frac{e^2}{3\pi}\ln\frac{-k^2}{m^2}\right)^{-1}. \tag{1}$$

It was shown by Abrikosov[4] that the longitudinal term $\sim k_\mu k_\nu$ in Eq. (1) gives, after integration in the region $|k^2| < |l^2|$, only singly logarithmic terms $\sim e^2 \ln(l^2/p^2)$, $e^2 \ln(l^2/q^2)$; whereas the region $|k^2| > |l^2|$ gives no logarithms at all. One may therefore drop this term in Eq. (1) and restrict the integration to the region $|k^2| < |l^2|$.

For the sake of definiteness let $l^2 < 0$; the opposite case will be obtained by analytic continuation. Following Sudakov we introduce the variables u, v, x:

$$k = pu + qv + k_\perp, \qquad k_\perp^2 / l^2 = x,$$

and transform $\Gamma_\sigma^{(2)}$ to the form

$$\Gamma_\sigma^{(2)} = \frac{3i}{4\pi}\gamma_\sigma \int \frac{du}{u}\frac{dv}{v}\frac{dx}{x - uv - i\delta}\left[\beta_l^{-1} - \ln(x - uv)\right]^{-1}. \tag{2}$$

Here

$$\delta \to +0, \qquad \beta_l = \beta\left[1 - \beta\ln(-l^2/m^2)\right]^{-1}, \qquad \beta = e^2/3\pi,$$

and the relevant region of integration is given by

$$\alpha_1 = |q^2/l^2| \ll |u| \ll 1, \qquad \alpha_2 = |p^2/l^2| \ll |v| \ll 1,$$

$$0 < x < \min\{|u|, |v|\}.$$

We integrate first over x. For $uv < 0$ the singular point $x = uv$ lies outside the contour of integration, for $uv > 0$ we deform the contour of integration into the complex x-plane so as to pass the point $x = uv$ from below along a semicircle of radius uv. Taking into account that $\beta_l \ll 1$ we find

$$\Gamma_\sigma^{(2)} = \frac{3i}{4\pi}\gamma_\sigma \int \frac{du}{u}\int \frac{dv}{v}\left[\frac{\theta(uv)\, i\pi}{\beta_l^{-1} - \ln uv} + f(|uv|)\right] = -\frac{3}{2}\gamma_\sigma \int_{\alpha_1}^{1}\frac{du}{u}\int_{\alpha_2}^{1}\frac{dv}{v}\left(\beta_l^{-1} - \ln uv\right)^{-1}, \tag{3}$$

where $\theta(x) = 0$ for $x < 0$, $\theta(x) = 1$ for $x > 0$, and where $f(x)$ is a certain function which drops out of the answer after integration over an even interval of u or v. According to Sudakov,[2] in the 2n-th order relevant contributions to Γ_σ come from those diagrams in which all virtual photon lines surround the point at which the real photon l is emitted. Each such term, in a manner analogous to that described above, is reduced to the form

$$\gamma_\sigma\left(-\frac{3}{2}\right)^n \int \frac{du_1}{u_1}\frac{du_2}{u_2}\cdots\frac{du_n}{u_n}\frac{dv_{i_1}}{v_{i_1}}\frac{dv_{i_2}}{v_{i_2}}\cdots\frac{dv_{i_n}}{v_{i_n}} \times \left(\beta_l^{-1} - \ln u_1 v_1\right)^{-1}\left(\beta_l^{-1} - \ln u_2 v_2\right)^{-1}\cdots\left(\beta_l^{-1} - \ln u_n v_n\right)^{-1}, \tag{4}$$

where the integration is over the region

$$\alpha_1 \ll u_1 \ll u_2 \ldots \ll u_n \ll 1,$$

$$\alpha_2 \ll v_{i_1} \ll v_{i_2} \ldots \ll v_{i_n} \ll 1.$$

If diagrams with all possible distributions of photon lines are combined, then the inequality for the v_{i_k} of Eq. (4) is supplemented by all other possible inequalities among the v_i; consequently one may integrate over all v_i from α_2 to unity independently. If one further symmetrizes over u_i one arrives at the result

$$\Gamma_\sigma^{(2n)} = \frac{\gamma_\sigma}{n!}\left[-\frac{3}{2}\int\limits_{\alpha_1}^{1}\frac{du}{u}\int\limits_{\sigma_2}^{1}\frac{dv}{v}(\beta_l^{-1}-\ln uv)^{-1}\right]^n \equiv \gamma_\sigma\frac{(-J)^n}{n!}. \tag{5}$$

The physical reason which makes the above simplifications possible is connected with the identity and "infrared" smallness of the momenta of the relevant quanta. From Eq. (5) we obtain

$$\Gamma_\sigma = \gamma_\sigma \exp(-J),$$

$$J = \frac{3}{2}\Big[\Big(\beta^{-1}-\ln\frac{xy}{z}\Big)\ln\Big(\beta^{-1}-\ln\frac{xy}{z}\Big) + (\beta^{-1}-\ln z)\ln(\beta^{-1}-\ln z) - (\beta^{-1}-\ln x)\ln(\beta^{-1}-\ln x) - (\beta^{-1}-\ln y)\ln(\beta^{-1}-\ln y)\Big]. \tag{6}$$

Here $z = -l^2/m^2$, $x = -p^2/m^2$, $y = -q^2/m^2$; $xy/z \gg 1$ in accordance with the assumed approximation

$$\beta\ln\frac{z}{x},\quad \beta\ln\frac{z}{y} \ll 1, \qquad \beta\ln z,\ \beta\ln x,\ \beta\ln y \lesssim 1.$$

The result (6) is easily generalized to an arbitrary $d_l(k^2) \neq 0$. At that one should use for the functions G and Γ_μ in internal parts of the diagrams their asymptotic expressions

$$G(p) = \frac{1}{\hat{p}}\alpha^{-1}(-p^2/m^2), \qquad \Gamma_\mu(p_1, p_2, k) = \gamma_\mu\alpha(-f^2/m^2),$$

$$|f^2| = \max\{|p_1^2|, |p_2^2|, |k^2|\},$$

$$\alpha(x) = \exp\Big(\frac{e^2}{4\pi}\int\limits_{\ln x}^{\infty} d_l(\xi)\,d\xi\Big). \tag{7}$$

It is easy to see that the change in Γ_μ according to Eq. (7) is compensated by a corresponding change in the function G at all vertices except for the point at which the external photon l is emitted. Therefore each term in Eq. (5) gets multiplied by $\alpha(-l^2/m^2)$ so that the answer is given by

$$\Gamma_\sigma = \gamma_\sigma\exp\Big(-J + \frac{e^2}{4\pi}\int\limits_{\ln z}^{\infty} d_l(\xi)\,d\xi\Big). \tag{8}$$

The connection between Eqs. (8) and (6) corresponds to a usual gauge transformation of Γ_σ as a result of a change in the gauge of $d_l(k^2)$.[6]

The renormalization invariance of expressions (6) and (8) is easily verified directly from the equations of the renormalization group [Eq. (3) of Blank and Shirkov[2] or Eq. (42.33) of Bogolyubov and Shirkov[3]]. For $e^2 \ln z \ll 1$ we obtain from Eqs. (6) and (8) Sudakov's result

$$\Gamma_\sigma = \gamma_\sigma\exp\Big(-\frac{e^2}{2\pi}\ln\frac{z}{x}\ln\frac{z}{y}\Big). \tag{9}$$

We note in conclusion that the exponential form of the expressions (6) and (8) indicates that it must be possible also to obtain the answer by the renormalization group method. The correct prescription is as follows: making use of a renormalization invariant expression for

$$\frac{e^2}{3\pi}d_l(k^2) = \beta\Big(1-\beta\ln\frac{-k^2}{m^2}\Big)^{-1},$$

one must calculate the correction to Γ_σ in lowest order, and then go over in the usual manner[3] from this "perturbation theory" formula to the exponential expressions (6) and (8). A proof of this prescription in the general case would make it possible to solve in a simple manner certain other problems, such as for example the taking into account in the vertex part $\Gamma_\sigma(p, q, l)$ under discussion of "singly logarithmic" terms of order $e^2\ln(l^2/p^2)$ and $e^2\ln(l^2/q^2)$.

The author is grateful to D. V. Shirkov for a discussion of the results.

---

[1] V. V. Sudakov, JETP **30**, 87 (1956), Soviet Phys. JETP **3**, 65 (1956).

[2] V. Z. Blank and D. V. Shirkov, Doklady Akad. Nauk SSSR **111**, 1201 (1956), Soviet Phys.-Doklady **1**, 752 (1957).

[3] N. I. Bogolyubov and D. V. Shirkov, Введение в теорию квантованных полей Introduction to Quantum Field Theory, Interscience, 1959, Sec. 44.

[4] A. A. Abrikosov, JETP **30**, 96 (1956), Soviet Phys. JETP **3**, 71 (1956).

[5] Abrikosov, Landau, and Khalatnikov, Doklady Akad. Nauk SSSR **95**, 497, 773 (1954).

[6] L. D. Landau and I. M. Khalatnikov, JETP **29**, 89 (1955), Soviet Phys. JETP **2**, 69 (1956).

Translated by A. M. Bincer
233

SOVIET PHYSICS JETP VOLUME 13, NUMBER 5 NOVEMBER, 1961

THE RACAH METHOD IN THE THEORY OF RELATIVISTIC EQUATIONS

L. A. SHELEPIN

Lebedev Physics Institute, Academy of Sciences, U.S.S.R.

Submitted to JETP editor, November 25, 1960

J. Exptl. Theoret. Phys. (U.S.S.R.) **40**, 1369-1383 (May, 1961)

By using the Racah technique we investigate the group properties of relativistically invariant equations of the type $\alpha_\sigma\partial_\sigma\psi + \kappa\psi = 0$. The treatment presented is a further development of the work of the author.[2] A consistent procedure is given for finding the commutation relations which completely determine the algebra of the α matrices, by using the technique of j symbols and transformation matrices. As simple examples we give the complete commutation relations for the Duffin-Kemmer equation with spin 1 and for the generalized Pauli-Fierz equation. A classification is given of covariants which form a U(α)-algebra with respect to reflection and charge conjugation. We obtain relations by means of which the infinitesimal matrix I_{ij} is expressed in terms of the α matrices. We discuss the structure of the complete interaction Lagrangian.

1. INTRODUCTION

DURING the past few years the methods of the theory of angular momentum which were first treated by Racah[1] have been developed further in the form of the theory of j symbols, transformation matrices, and irreducible tensor operators. At the same time, these methods are finding a wider and wider range of application. In particular, they are the basis for the theory of atomic and nuclear spectra, for the scattering of particles, and the theory of parentage coefficients. In the present paper these methods are applied to the theory of relativistically invariant equations of the type

$$\alpha_\sigma\partial_\sigma\psi + \varkappa\psi = 0. \qquad (1.1)$$

In a definite sense the proposed approach is a further extension of previous work of the author.[2] The algebraic method of investigation[2] in which the matrix α_i is treated as a unit symbol has a definite advantage with respect to the writing of the matrices in explicit form[3] or in the form of an expansion in terms of some known matrices.[4]

From the products of the matrices α_i one constructs[2] covariant quantities (called symmetrizers) which transform according to irreducible representations of the Lorentz group. The matrix α_i transforms with respect to the index i like a vector $D(\frac{1}{2}\frac{1}{2})$. For example, from the products of two matrices $\alpha_i\alpha_k$ one can select three symmetrizers corresponding to the expansion

$$D(\tfrac{1}{2}\tfrac{1}{2}) \times D(\tfrac{1}{2}\tfrac{1}{2}) = D(11) + D(1001) + D(00). \qquad (1.2)$$

In reference 2 we gave a procedure for constructing symmetrizers (in tensor and canonical bases) corresponding to the expansion (1.2), and analogous expansions for the products of three or more matrices.

In the U(α)-algebra there are contained basis vectors which transform according to the representation

$$L = \widetilde{S} \times S, \qquad (1.3)$$

where S is the representation according to which ψ transforms in equation (1.1). Equating to zero the basis of the representations contained in the products of the type (1.2) and not contained in (1.3), we obtain a series of commutation relations. However, there is a difficulty in separating identical representations since, even when one includes supplementary symmetry conditions, not all the representations are sorted out.

In Sec. 2 of the present paper we treat a technique based on the theory of angular momentum which enables one, from the representation S and the values of the independent constants in the matrix α_i, to obtain the complete commutation relations and to find all independent covariants of the U(α)-algebra. In Sec. 3 we consider the classification of representations with respect to reflection and charge conjugation, and also formulate various physical requirements in the language of the Racah method. In Sec. 4 we give a table of representations which enables one relatively easily to obtain the commutation relations for equations with spins not exceeding $\frac{3}{2}$. As an example we treat the complete commutation relations for the generalized Pauli-Fierz equation. Finally, in the last section we discuss some specific simplications which arise when the method is applied to equations with interaction.

2. RACAH'S METHOD AS APPLIED TO RELATIVISTIC EQUATIONS

The application of the methods of the theory of angular momentum to relativistically invariant equations is based on the specific structure of the matrices α_i. Since ψ transforms according to a finite dimensional representation S, ∂_i according to the representation $D(\frac{1}{2}\frac{1}{2})$, and $\alpha_\sigma \partial_\sigma \psi$ as does ψ, transforms according to the representation S, the matrix α_i is an aggregate of Clebsch-Gordan coefficients (with certain arbitrary constant factors) which project the space $S \times D(\frac{1}{2}\frac{1}{2})$ on S.[5]

Equation (1.1) can be rewritten in the form

$$\sum_{P'Q's'p'q'mn} a^{ss'}_{PQ;\,P'Q'} (P'{}^1\!/_2 p'm \,|\, Pp)(Q'{}^1\!/_2 q'n \,|\, Qq)\, \partial_{mn} \psi^{P'Q'}_{p'q'} + \varkappa \psi^{PQ}_{pq} = 0. \tag{2.1}$$

Here PQ and P′ Q′ are the weights of the representations, pqp′q′mn are indices of the corresponding basis vectors, and the index s numbers the identical representations.

According to (2.1) the matrix $\alpha^{1/2\ 1/2}_{mn}$ is broken up into individual blocks $\alpha_{PQ;\,P'Q'}$, which are Clebsch-Gordan matrices multiplied by a certain constant coefficient $a^{ss'}_{PQ;\,P'Q'}$:

$$\alpha_{PQ;\,P'Q'} = a_{PQ;\,P'Q'} (P'{}^1\!/_2 p'm \,|\, Pp)(Q'{}^1\!/_2 q'n \,|\, Qq). \tag{2.2}$$

In the process of investigation of the equations — in finding the commutation relations, considering various physical requirements, and computations — we deal with products of the α matrices, i.e., with combinations of Clebsch-Gordan coefficients. In the general case any such combinations can be represented as a complicated expansion in generalized Wigner coefficients; the coefficients of this expansion are the j-symbols.[6] For the theory of relativistic equations the corresponding formulas which are considered below are not very complicated.

If we multiply two matrices with matrix elements of general type

$$\alpha^{M_1N_1} = a_{P_iQ_i;\,P_kQ_k} (P_kM_1p_km_1 \,|\, P_ip_i)(Q_kN_1q_kn_1 \,|\, Q_iq_i), \tag{2.3}$$

$$\alpha^{M_2N_2} = a_{P_kQ_k;\,P_lQ_l} (P_lM_2p_lm_2 \,|\, P_kp_k)(Q_lN_2q_ln_2 \,|\, Q_kq_k) \tag{2.4}$$

[for $M_1 = N_1 = M_2 = N_2 = \frac{1}{2}$, we have the special case of (2.2)] the matrix element of their product has the form

$$\alpha^{M_1N_1}\alpha^{M_2N_2} = \sum_{P_kQ_kp_kq_k} a_{P_iQ_i;\,P_kQ_k} a_{P_kQ_k;\,P_lQ_l} (P_kM_1p_km_1 \,|\, P_ip_i) \times (P_lM_2P_lm_2 \,|\, P_kp_k)(Q_kN_1q_kn_1 \,|\, Q_iq_i)(Q_lN_2q_ln_2 \,|\, Q_kq_k). \tag{2.5}$$

From the product (2.5), according to reference 2 [cf. formula (1.2)], we can separate out a symmetrizer characterized by the indices MN. To do this we can make use of the well-known formula[6]

$$\sum_{m_2} (P_kM_1p_km_1 \,|\, P_ip_i)(P_lM_2p_lm_2 \,|\, P_kp_k)(M_2M_1m_2m_1 \,|\, M_{12}m_{12}) = W_1(P_lM_2P_iM_1;\ P_kM_{12})(P_lM_{12}p_lm_{12} \,|\, P_ip_i). \tag{2.6}$$

The coefficient W_1, which has been treated by Jahn,[7] is related to the Racah coefficient by the equation

$$W_1(P_lM_2P_iM_1;\ P_kM_{12}) = \sqrt{(2P_k+1)(2M_{12}+1)}\, W(P_lM_2P_iM_1;\ P_kM_{12}). \tag{2.7}$$

Thus the matrix element of the irreducible symmetrizer MN, obtained from the product of the two matrices (2.3) and (2.4) has the form

$$\sum_{P_kQ_k} a_{P_iQ_i;\,P_kQ_k} a_{P_kQ_k;\,P_lQ_l} W_1(P_lM_2P_iM_1;\ P_kM_{12}) \times W_1(Q_lN_2Q_iN_1;\ Q_kN_{12}) \times (P_lM_{12}p_lm_{12} \,|\, P_ip_i)(Q_lN_{12}q_ln_{12} \,|\, Q_iq_i). \tag{2.8}$$

If we consider the product of three matrices α, then for the symmetrizer with indices MN we obtain the formula

$$\sum_{P_kQ_kP_lQ_l} a_{P_iQ_i;\,P_kQ_k} a_{P_kQ_k;\,P_lQ_l} a_{P_lQ_l;\,P_mQ_m} \times W_1(P_lM_2P_iM_1;\ P_kM_{12})\, W_1(P_mM_3P_iM_{12};\ P_lM) \times W_1(Q_lN_2Q_iN_1;\ Q_kN_{12})\, W_1(Q_mN_3Q_iN_{12};\ Q_lN) \times (P_mMp_mm \,|\, P_ip_i)(Q_mNq_mn \,|\, Q_iq_i). \tag{2.9}$$

In the most general case the symmetrizer formed from products of α matrices is made up of Clebsch-Gordan coefficients with constant factors $a_{PQ,\,P'Q'}$ not depending on the projection. The factors $a_{PQ,\,P'Q'}$ depend on constant factors in the matrix α_i and on the specific set of j-symbols. Thus, the quantities D(1 1) formed from products of two α matrices and from products, for example, of twelve α matrices differ only in the particular values of the coefficients $a_{PQ,\,P'Q'}$. Any matrix element can be immediately written if we give the number of matrices in the product, the representation, and the method of combining the angular momenta.

To each matrix element there corresponds a simple graphical rule. Thus, for the successive products of two matrices (2.8) and three matrices (2.9), we have Figs. 1a and b. The process of

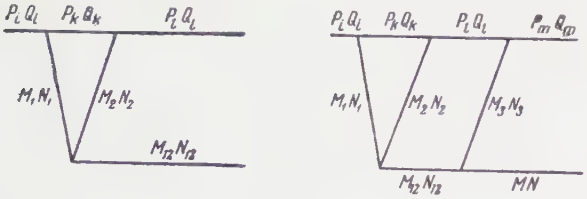

a b

FIG. 1.

writing symmetrizers by using graphs is standard and does not present any difficulties.

If the separating out of irreducible symmetrizers is not done in sequence, any j-symbols can occur. Thus $\alpha_\sigma \alpha_k \alpha_\sigma$ in canonical form corresponds to Fig. 2.

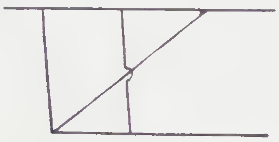

FIG. 2.

The 9j-symbols appear explicitly in the matrix element. However, for the investigation of relativistic equations it is sufficient to consider expressions corresponding to successive addition of angular momenta, in terms of which all others are expanded corresponding to any other law of addition; i.e., it is sufficient to know the coefficients W_1. Moreover, for this investigation one needs only a very restricted set of the W_1 coefficients. In considering these coefficients we must remember the symmetry rules for the Racah coefficients:

$$W(ab\,cd;\,ef) = W(ba\,dc;\,ef) = W(cd\,ab;\,ef) = W(ac\,bd;\,fe)$$
$$= (-1)^{e+f-a-d}\,W(eb\,cf;\,ad) = (-1)^{e+f-b-c}\,W(ae\,fd;\,bc). \tag{2.10}$$

In addition, if e and f are defined uniquely by the assignment of a, b, c, d, the corresponding W_1 is equal to unity. For example,

$$W_1({}^1/_2\,{}^1/_2\,1\,2;\ 1\,{}^3/_2) = W_1({}^1/_2\,{}^1/_2\,{}^3/_2\,{}^1/_2;\ 1\,1) = 1.$$

Then in investigating the products up to six matrices and equations with a maximum spin of $^3/_2$, we need to know altogether 25 W_1 coefficients.

The symmetrizers which can be formed from a specific number of α matrices transforming according to a single representation differ from one another in the coupling scheme. Thus from three matrices one can in general form four linearly independent symmetrizers transforming according to $D(\frac{1}{2}\frac{1}{2})$. In their coupling methods we distinguish coupling schemes which are determined by how the angular momenta add (the graph) and the order of coupling, which is determined by the arrangement of signs on the added angular momenta (cf. reference 6). The transition from one coupling scheme to another is accomplished by means of transformation matrices. To investigate equations (1.1) it is sufficient to choose one coupling method

$$(((j_1j_2)\,j_{12}j_3)\,j_{123}j_4)j_{1234}\ \ldots, \tag{2.11}$$

i.e., one method of successive addition of angular momenta. Since the matrix transforms according to the representation $D(\frac{1}{2}\frac{1}{2})$, each of the successively added angular momenta is equal to $\frac{1}{2}$. Therefore, the symmetrizers differ only in the quantities j_{12}, j_{123}, j_{1234}. Their assignment completely determines the symmetrizer for which we introduce the notation

$$F\,(j_{12}j_{123}j_{1234}\ldots;\ j'_{12}j'_{123}j'_{1234}\ldots). \tag{2.12}$$

In the notation (2.12) we write a complete set of basic symmetrizers for the products of two, three, and four matrices:
two matrices:

$$F(1;\ 1),\qquad F(1;\ 0),\qquad F(0;\ 0); \tag{2.13a}$$

three matrices:

$$F(1\,{}^3/_2;\ 1\,{}^3/_2),\ F(1\,{}^3/_2;\ 1\,{}^1/_2),\ F(1\,{}^3/_2;\ 0\,{}^1/_2),\ F(1\,{}^1/_2;\ 1\,{}^1/_2),$$
$$F(1\,{}^1/_2;\ 0\,{}^1/_2),\ F(0\,{}^1/_2;\ 1\,{}^1/_2),\ F(0\,{}^1/_2;\ 0\,{}^1/_2); \tag{2.13b}$$

four matrices:

$$F(1\,{}^3/_2 2;\ 1\,{}^3/_2 2),\ F(1\,{}^3/_2 2;\ 1\,{}^3/_2 1),\ F(1\,{}^3/_2 2;\ 1\,{}^1/_2 1),$$
$$F(1\,{}^3/_2 2;\ 0\,{}^1/_2 1),\ F(1\,{}^3/_2 2;\ 1\,{}^1/_2 0),\ F(1\,{}^3/_2 2;\ 0\,{}^1/_2 0),$$
$$F(1\,{}^3/_2 1;\ 1\,{}^3/_2 1),\ F(1\,{}^3/_2 1;\ 1\,{}^1/_2 1),\ F(1\,{}^3/_2 1;\ 0\,{}^1/_2 1),$$
$$F(1\,{}^1/_2 1;\ 1\,{}^3/_2 1),\ F(1\,{}^1/_2 1;\ 1\,{}^1/_2 1),\ F(1\,{}^1/_2 1;\ 0\,{}^1/_2 1),$$
$$F(0\,{}^1/_2 1;\ 1\,{}^3/_2 1),\ F(0\,{}^1/_2 1;\ 1\,{}^1/_2 1),\ F(0\,{}^1/_2 1;\ 0\,{}^1/_2 1),$$
$$F(1\,{}^3/_2 1;\ 1\,{}^1/_2 0),\ F(1\,{}^1/_2 1;\ 1\,{}^1/_2 0),\ F(0\,{}^1/_2 1;\ 1\,{}^1/_2 0),$$
$$F(1\,{}^3/_2 1;\ 0\,{}^1/_2 0),\ F(1\,{}^1/_2 1;\ 0\,{}^1/_2 0),\ F(0\,{}^1/_2 1;\ 0\,{}^1/_2 0),$$
$$F(1\,{}^1/_2 0;\ 1\,{}^1/_2 0),\ F(1\,{}^1/_2 0;\ 0\,{}^1/_2 0),$$
$$F(0\,{}^1/_2 0;\ 1\,{}^1/_2 0),\ F(0\,{}^1/_2 0;\ 0\,{}^1/_2 0). \tag{2.13c}$$

For the representation $D(mnnm)$ we have here written only $D(mn)$. The symmetrizer F for $D(nm)$ is obtained by an obvious permutation of the arguments.

The $U(\alpha)$-algebra is determined by the relations between the matrices F. According to Ref. 2, that part of the matrix F is equal to zero which refers to representations not contained in $\tilde{S} \times S$. Thus for $S = D(1001) + D(\frac{1}{2}\frac{1}{2})$ we have $F(1\frac{3}{2};\ 1\frac{3}{2}) = 0$. To find the remaining commutation relations by use of the graphs, we write the corresponding coefficients in the matrix elements of the symmetrizers, which transform according to the same representations, and compare them to one another and thus find the required relations. Thus, for $D(^3/_2\,^1/_2\,^1/_2\,^3/_2)$, if the constant coefficients in the matrix α are equal to unity (Duffin-Kemmer equation), we have $F(1^3/_2;\ 1^1/_2) = \sqrt{3}F(1^3/_2;\ 0^1/_2)$ etc. for all products of three matrices.

In order to find the complete set of commutation relations we must see how the relations between symmetrizers with a larger number of matrices are consequences of the corresponding formulas for symmetrizers with a smaller number of matrices. Thus, when

$$F(1^3/_2;\ 1^3/_2) = 0 \tag{2.14}$$

the symmetrizers

$$F(1^3/_2 2;\ 1^3/_2 2) = F(1^3/_2 2;\ 1^3/_2 1) = F(1^3/_2 1;\ 1^3/_2 2) = F(1^3/_2 1;\ 1^3/_2 1) = 0 \tag{2.15}$$

correspond to the multiplication of $F(1^3/_2;\ 1^3/_2)$ by α from the right; the result of multiplication from the left is also equal to zero. In this case we have in place of

$$F(((j_1j_2)j_{12}j_3)j_{123}j_4j;\ ((j'_1j'_2)j'_{12}j'_3)j'_{123}j'_4j') \tag{2.16}$$

a different order of coupling:

$$F(j_1((j_2j_3)j_{23}j_4)j_{234}j;\ j'_1((j'_2j'_3)j'_{23}j'_4)j'_{234}j'). \tag{2.17}$$

By the use of the transformation matrix, which has been discussed in detail by Yutsis, Levinson, and Vanagas[6], quantities of the type (2.17) can be expanded in the basis vectors (2.16). Using the properties of the transformation matrix[6] we obtain for functions of the type

$$\Phi^\times(j_{12}j_{123}j) \equiv \Phi(j_4((j_1j_2)j_{12}j_3)j_{123}j),$$

the relations

$$\Phi^\times(j_{23}j) = \sum_{j_{12}} W_1(j_1j_2jj_3;\ j_{12}j_{23})\,\Phi(j_{12}j), \tag{2.18}$$

$$\Phi^\times(j_{23}j_{234}j) = \sum_{j_{12}j_{123}} W_1(j_1j_{23}jj_4;\ j_{123}j_{234})\,W_1(j_1j_2j_{123}j_3;\ j_{12}j_{23})\,\Phi(j_{12}j_{123}j), \tag{2.19}$$

$$\begin{aligned}\Phi^\times(j_{23}j_{234}j_{2345}j) = \sum_{j_{12}j_{123}j_{1234}} & W_1(j_1j_{234}jj_5;\ j_{1234}j_{2345}) \\ & \times W_1(j_1j_{23}j_{1234}j_4;\ j_{123}j_{234}) \\ & \times W_1(j_1j_2j_{123}j_3;\ j_{12}j_{23})\,\Phi(j_{12}j_{123}j_{1234}j).\end{aligned} \tag{2.20}$$

The quantities F^X are then obtained in an obvious way:

$$\begin{aligned}F^\times(j_{23}j;\ j'_{23}j') = \sum_{j_{12}j'_{12}} & W_1(j_1j_2jj_3;\ j_{12}j_{23})\,W_1(j'_1j'_2j'j'_3;\ j'_{12}j'_{23}) \\ & \times F(j_{12}j;\ j'_{12}j').\end{aligned} \tag{2.21}$$

Using these formulas we find from (2.14) the relations

$$\begin{aligned}F_{00} &= \frac{1}{3}F_{01} + \frac{\sqrt{2}}{3}F_{02} + \sqrt{\frac{2}{3}}F_{03} = \frac{1}{3}F_{10} + \frac{\sqrt{2}}{3}F_{20} \\ &+ \sqrt{\frac{2}{3}}F_{30} = \frac{\sqrt{2}}{9}(F_{12} + F_{21}) + \frac{\sqrt{6}}{9}(F_{13} + F_{31}) \\ &+ \frac{2\sqrt{3}}{9}(F_{23} + F_{32}) + \frac{1}{9}F_{11} + \frac{2}{9}F_{22} + \frac{2}{3}F_{33} = 0,\end{aligned} \tag{2.22}$$

where the subscripts 0, 1, 2, 3 replace $1\,^3/_2\,2$; $1\,^3/_2\,1$; $1\,^1/_2\,1$; $0\,^1/_2\,1$.

After having determined the consequences of the commutation relations between symmetrizers with a smaller number of matrices, comparing the symmetrizers which remain independent we find additional commutation relations between them (cf., for example, formula (4.4) later on).

Later, in Sec. 3, in the classification of representations with respect to charge conjugation, it is important to know symmetrizers when the order is changed to the reverse order; i.e., it is necessary to know the expansion in basis vectors of quantities of the type

$$\Phi^*(j_{45}j_{345}j_{2345}j) \equiv \Phi((((j_5j_4)j_{45}j_3)j_{345}j_2)j_{2345}j_1j).$$

The appropriate formulas are obtained by using the transformation matrices:

$$\Phi^*((j_2j_1)j) = (-1)^{1-j}\,\Phi(j), \tag{2.23}$$

$$\Phi^*(j_{23}j) = \sum_{j_{12}} (-1)^{^3/_2-j}\,W_1(j_3j_2jj_1;\ j_{23}j_{12})\,\Phi(j_{12}j), \tag{2.24}$$

$$\begin{aligned}\Phi^*(j_{34}j_{234}j) = \sum_{j_{12}j_{123}} & (-1)^{2-j}\,W_1(j_{34}j_2jj_1;\ j_{234}j_{12}) \\ & \times W_1(j_4j_3jj_{12};\ j_{34}j_{123})\,\Phi(j_{12}j_{123}j).\end{aligned} \tag{2.25}$$

The quantities F^* are found in a manner similar to (2.21).

The method developed above makes it possible to obtain the complete system of commutation relations. In various cases, their determination is considerably simplified by considering various symmetry conditions and physical requirements on the equations.

3. SYMMETRY LAWS AND PHYSICAL REQUIREMENTS

In the theory of relativistic equations, in addition to the requirement of relativistic invariance, various symmetry laws and physical requirements play an important role, among them invariance with respect to reflection, charge conjugation, time reversal, Lagrangian symmetry (the existence of a bilinear nondegenerate Lagrangian function), definiteness of the charge density or energy, presence of various spins and mass states. Various questions are related to these requirements; for example, concerning supplementary conditions, concerning the infinitesimal group ring, and equivalent representations. Various physical requirements impose particular additional restrictions on the coefficients $a_{PQ,\,P'Q'}$ in the matrix α. In addition, each symmetry permits one to introduce a distinction between identical representations and thus to give an additional classification of the symmetrizers constituting the $U(\alpha)$-algebra. In the following we consider symmetry with respect to reflection, charge conjugation, and Lagrangian symmetry.

The reflection operation corresponds to the transformation

$$D(PQ) \rightarrow D(QP). \tag{3.1}$$

For equations which are invariant with respect to reflection we have

$$a_{PQ;\,P'Q'} = \pm a_{QP;\,Q'P'}. \tag{3.2}$$

We note that, for quantities F corresponding to (3.1), there must be one and the same type of coupling. If P and Q are different, the representation of the full Lorentz group consists of two representations of the proper group:

$$F(j_1 j_2 \ldots j;\, j'_1 j'_2 \ldots j'), \qquad F(j'_1 j'_2 \ldots j';\, j_1 j_2 \ldots j). \tag{3.3}$$

If P and Q are identical, we can have two types of representations: tensor or pseudo-tensor. For example, among the four symmetrizers $D(\tfrac{1}{2}\tfrac{1}{2})$, consisting of three matrices, we have three vector symmetrizers

$$F(1{}^1/_2;\, 1{}^1/_2), \qquad F(0{}^1/_2;\, 0{}^1/_2),$$
$$F(1{}^1/_2;\, 0{}^1/_2) + F(0{}^1/_2;\, 1{}^1/_2) = F^+(1{}^1/_2;\, 0{}^1/_2)$$

and one pseudo-vector

$$F(1{}^1/_2;\, 0{}^1/_2) - F(0{}^1/_2;\, 1{}^1/_2) = F^-(1{}^1/_2;\, 0{}^1/_2).$$

We denote even representations by $D^+(P;\,P)$, and odd representations by $D^-(P;\,P)$. Then it is not difficult to carry out a classification of the symmetrizers of the $U(\alpha)$-algebra if we remember that products of two even or two odd representations give only even representations, while products of even by odd representations give odd representations; products of two representations of the type (3.3) give equal numbers of even and odd representations. Thus, for $S = D(1\,\tfrac{1}{2}\tfrac{1}{2}\,1) + D(\tfrac{1}{2}\,00\,\tfrac{1}{2})$ we have

$$\begin{aligned} L = {} & D(2112) + D(2002) + D^+({}^3/_2\,{}^3/_2) + D^-({}^3/_2\,{}^3/_2) \\ & + 4D({}^3/_2\,{}^1/_2\,{}^1/_2\,{}^3/_2) + 3D^+(11) + 3D^-(11) + 5D(1001) \\ & + 4D^+({}^1/_2\,{}^1/_2) + 4D^-({}^1/_2\,{}^1/_2) + 2D^+(00) + 2D^-(00). \end{aligned} \tag{3.4}$$

The operation of charge conjugation is associated with a transformation of the matrices. For equations which are invariant with respect to this operation,

$$\alpha_{PQ;\,P'Q'} = \pm \alpha_{P'Q';\,PQ}. \tag{3.5}$$

Using a function F^* with the reverse order of addition of angular momenta, we can write the charge-even function $D(jj')_+$ as

$$F(j_1 j_2 \ldots j,\, j'_1 j'_2 \ldots j') + F^*(j_1 j_2 \ldots j;\, j'_1 j'_2 \ldots j'), \tag{3.6}$$

and the charge-odd function $D(jj')_-$ as

$$F(j_1 j_2 \ldots j;\, j'_1 j'_2 \ldots j') - F^*(j_1 j_2 \ldots j;\, j'_1 j'_2 \ldots j'). \tag{3.7}$$

Using the notation we have introduced and the formulas of Sec. 2, we give the four independent symmetrizers $D(\tfrac{1}{2}\tfrac{1}{2})$, consisting of three matrices;

$$F^+(1{}^1/_2;\, 1{}^1/_2)_+, \qquad F^+(0{}^1/_2;\, 0{}^1/_2)_+,$$
$$F^+(1{}^1/_2;\, 1{}^1/_2)_-, \qquad F^-(1\,{}^1/_2;\, 0{}^1/_2)_-.$$

The relations

$$F^+(0{}^1/_2;\, 0{}^1/_2)_- = \tfrac{1}{2} F^+(1{}^1/_2;\, 0{}^1/_2)_- = - F^+(1{}^1/_2;\, 1{}^1/_2)_-,$$
$$F^+(1{}^1/_2;\, 0{}^1/_2)_+ = 2\sqrt{3}\,[F^+(1{}^1/_2;\, 1{}^1/_2)_+ - F^+(0{}^1/_2;\, 0{}^1/_2)_+]$$

are valid.

For the classification of the symmetrizers of the $U(\alpha)$-algebra with respect to charge conjugation, we consider the matrix elements $\alpha_{PQ;\,P'Q'}$. The non-diagonal elements $\alpha_{PQ;\,P'Q'}$, $\alpha_{P'Q';\,PQ}$ correspond to twice as many equal representations. Half of them are even. To the diagonal element $\alpha_{PQ;\,PQ}$, since under charge conjugation there is a change in the order of addition of the angular momenta to the reverse order, there corresponds a factor $(-1)^{2P_1-P}\,(-1)^{2Q_1-Q}A$, where P_1Q_1 are the angular momenta characterizing S in $\tilde{S} \times S$. The factor A is equal to $+1$ for tensor representations and -1 for spinor representations.

According to the above rules, we give the $U(\alpha)$-algebra with a classification according to reflection and charge conjugation for the following equations:

1. Dirac equation, $S = D(\tfrac{1}{2}\,00\,\tfrac{1}{2})$:

$$\begin{aligned} L = {} & D(1001)_- + D^+({}^1/_2\,{}^1/_2)_+ + D^-({}^1/_2\,{}^1/_2)_- \\ & + D^+(00)_+ + D^-(00)_+. \end{aligned} \tag{3.8}$$

2. Duffin-Kemmer equation (spin 0), $S = D(\tfrac{1}{2}\tfrac{1}{2}) + D(00)$:

$$\begin{aligned} L = {} & D^+(11)_+ + D(1001)_- + 2D^+(00)_+ \\ & + D^+({}^1/_2\,{}^1/_2)_+ + D^+({}^1/_2\,{}^1/_2)_-. \end{aligned} \tag{3.9}$$

3. Ginzburg equation (spin $\tfrac{1}{2}$, $\tfrac{3}{2}$), $S = D(1\,\tfrac{1}{2}\tfrac{1}{2}\,1) + 2D(\tfrac{1}{2}\,00\,\tfrac{1}{2})$:

$$L = D(2112)_- + D(2002)_+ + D^+(^3/_2\,{}^3/_2)_+ + D^-(^3/_2\,{}^3/_2)_- \\ + 3D^+(11)_+ + 2D^+(11)_- + 2D^-(11)_+ + 3D^-(11)_- \\ + 3D(^3/_2\,{}^1/_2\,{}^1/_2\,{}^3/_2)_+ + 3D(^3/_2\,{}^1/_2\,{}^1/_2\,{}^3/_2)_- + 2D(1001)_+ \\ + 8D(1001)_- + 7D^+(^1/_2\,{}^1/_2)_+ + 2D^+(^1/_2\,{}^1/_2)_- \\ + 2D^-(^1/_2\,{}^1/_2)_+ + 7D^-(^1/_2\,{}^1/_2)_- + 5D^+(00)_+ + 5D^-(00)_+ \tag{3.10}$$

For equations which are invariant under Lagrangian symmetry,

$$a_{PQ;\,P'Q'} = \pm a_{Q'P';\,QP}. \tag{3.11}$$

According to (3.2), (3.5), and (3.11) Lagrangian symmetry is a consequence of symmetry with respect to reflection and charge conjugation.

The metric matrix η, by means of which we form an invariant from the product $\psi^*\eta\psi$, can be expressed in terms of the basic covariants, if we consider that its matrix elements have the form

$$a_p\,(PPp - p\,|\,00). \tag{3.12}$$

In treating the spin properties of relativistic systems, the investigation of the infinitesimal group ring constructed from the infinitesimal rotation matrices I_{ij} plays an important part.

The infinitesimal matrix I_{ij} satisfies the well-known relations

$$[I_{ik},\ I_{jl}] = -g_{ij}I_{kl} + g_{il}I_{kj} + g_{kj}I_{il} - g_{kl}I_{ij}, \tag{3.13}$$

$$[\alpha_i,\ I_{jk}] = g_{ij}\alpha_k - g_{ik}\alpha_j. \tag{3.14}$$

These relations can be written in covariant form in the tensor basis. For example, (3.13) has the form

$$I_{i\sigma}I_{\sigma m} - I_{m\sigma}I_{\sigma i} = 2I_{im},$$

$$I_{ik}I_{lm} - I_{lm}I_{ik} = 0, \qquad I_{ik}I_{li} - I_{li}I_{ik} = I_{mk}I_{lm} - I_{lm}I_{mk}. \tag{3.15}$$

In the canonical basis the matrix I_{ij} can be written as I^{10}_{p0}, I^{01}_{0q}. The symmetrizers from I and I, α are made up in a manner analogous to the symmetrizers from α (Sec. 2). We denote the corresponding quantities by F_I, $F_{I\alpha}$. Then the conditions (3.13) and (3.14) take the form

$$F_I(1;1)_- = 0, \qquad F_I(1;0) = I^{10}, \quad F_I(0;1) = I^{01}, \tag{3.16}$$

$$F_{I\alpha}(^3/_2\,{}^1/_2\,{}^1/_2\,{}^3/_2)_+ = 0, \quad F^-_{I\alpha}(^1/_2\,{}^1/_2)_+ = 0, \\ F^+_{I\alpha}(^1/_2\,{}^1/_2)_+ = \alpha^{^1/_2\,{}^1/_2}. \tag{3.17}$$

The relations (3.16) and (3.17) enable us to determine the explicit form of the infinitesimal matrix for $a\psi$ transforming according to a given representation S. The numerical values of the coefficients in the matrix elements of the matrix I^{10} (I^{01})

$$b_{P_iQ_i;\,P_kQ_k}\,(P_k1p_kl\,|\,P_ip_i)(Q_k0q_k0\,|\,Q_kq_k) \tag{3.18}$$

are determined from the relation

$$b_{P_iQ_i;\,P_kQ_k}b_{P_kQ_k;\,P_lQ_l}W_1(P_l1P_i1;\ P_k1)\,W_1(Q_l0Q_i0;\ Q_k0) \\ = b_{P_iQ_i;P_lQ_l}. \tag{3.19}$$

For the Duffin-Kemmer equation (spin 1) we have

$$b_{^1/_2\,{}^1/_2;\ {}^1/_2\,{}^1/_2} = \sqrt{6}/2, \qquad b_{10;\,10} = 2. \tag{3.20}$$

For the Pauli-Fierz equation

$$b_{^1/_2\,0;\ {}^1/_2\,0} = \sqrt{3}/2, \quad b_{^1/_2\,1;\ {}^1/_2\,1} = \sqrt{3/2}, \\ b_{1^1/_2;\ 1^1/_2} = 1, \quad b_{0^1/_2;\ 1^1/_2} = b_{1^1/_2;\ 0^1/_2} = 0. \tag{3.21}$$

Using formulas of the type (3.20) and (3.21) and also the basic symmetrizers of the U(α)-algebra, it is not difficult to find the expression for the infinitesimal matrix I_{ij} in terms of the matrices α (cf. Sec. 4). Knowing it, we can find the supplementary restrictions which are imposed by the presence of definite spin and mass states. Using the spin operator $Z = -(I^2_{12} + I^2_{13} + I^2_{23})$,[4] we separate out the parts of the wave function with definite spin $(Z - \xi(\xi + 1))\psi$, and by using α_0 the part with a definite mass state. The general appearance of the formulas which describe the spin-mass states of the system is the following:

$$[Z - \xi_1(\xi_1 + 1)] \ldots [Z - \xi_r(\xi_r + 1)]\,(\alpha_0^2 - m_1^2) \\ \ldots (\alpha_0^2 - m_s^2) = 0. \tag{3.22}$$

The minimal equations for spin and for mass states are special cases of (3.22):

$$[Z - \xi_1(\xi_1 + 1)]\,[Z - \xi_2(\xi_2 + 1)] \ldots = 0, \tag{3.23}$$

$$(\alpha_0^2 - m_1^2)\,(\alpha_0^2 - m_2^2) \ldots = 0. \tag{3.24}$$

By virtue of relativistic invariance all these formulas can be represented as a definite sum of covariants. Writing formula (3.22) in covariant form and expanding the left side into basic symmetrizers, and equating each of them to zero, we obtain all the relations caused by the presence of specific spin and mass states. Thus, from the relation $\alpha_0^3 - \alpha_0 = 0$ it follows that $F(1\,{}^3/_2;\,1\,{}^3/_2) = 0$ and $\alpha^2_\sigma\alpha_i + \alpha_\sigma\alpha_i\alpha_\sigma + \alpha_i\alpha^2_\sigma = 9\alpha_i$

If we write (3.22) in canonical form, the corresponding expansion can be obtained by means of the usual Clebsch-Gordan coefficients. The treatment of other physical requirements also is simplified considerably in the present formalism.

4. EXAMPLES

As simple examples of the application of the method described, we find the commutation relations and write the basis vectors for equations of which the Pauli-Fierz equation is a special case, and for the Duffin-Kemmer equation (spin 1) (cf. also reference 4). In finding the commutation relations it is very important to have a table of symmetrizers with an additional classification with respect to reflection and charge conjugation. Such a table, formed from the products of two, three, four, and five matrices, enables one immediately to find the commutation relations for particles with maximum spin $^1/_2$, 1, and $^3/_2$. For the investigation of higher spins the table must be extended further.

In order to write down immediately the commutation relations for equations with spin $^1/_2$, 1, and the generalized Pauli-Fierz equation, it is sufficient to give the classification for products of no more than four matrices. In the table, to save space, for the products of three matrices the functions F are written in the form F_{ik}, for four matrices in the form E_{ik}. For three matrices the indices 0, 1, 2 replace the pairs $1^3/_2$, $1^1/_2$, $0^1/_2$; for four matrices the indices 0, 1, 2, 3, replace $1\,{}^3/_2\,2$, $1^3/_2\,1$, $1\,{}^1/_2\,1$, $0\,{}^1/_2\,1$. Below we give the classification, where we have written the independent basis vectors and given their order numbers in square brackets. In the curly brackets, we give the origin of the symmetrizer (to within a factor).

Two matrices:

$$
\begin{array}{llll}
D\,(11): & D^+(11)_+, & F\,(1;\ 1), & [1];\\
D\,(1001): & D\,(10)_-, & F\,(1;\ 0), & [2];\\
D\,(00): & D^+(00)_+, & F\,(0;\ 0), & [3].
\end{array}
$$

Three matrices:

$$
D\,({}^3/_2\,{}^2/_2):\quad D^+({}^3/_2\,{}^3/_3)_+,\quad F_{00},\quad [1];
$$

$$
D\,({}^3/_2\,{}^1/_2\,{}^1/_2\,{}^3/_2):\ \begin{cases}
D\,({}^3/_2\,{}^1/_2)_+, & F_{01}-\sqrt{3}\,F_{02},\ \{F\,(1^3/_2;\ 0^1/_2)_+\},\quad [2];\\
D\,({}^3/_2\,{}^1/_2)_-, & \sqrt{3}\,F_{01}+F_{02},\ \{F\,(1^3/_2;\ 0^1/_2)_-\},\quad [3];
\end{cases}
$$

$$
D\,({}^1/_2\,{}^1/_2):\ \begin{cases}
D^+({}^1/_2\,{}^1/_2)_+, & 5F_{11}+\sqrt{3}\,F^{\mathrm{s}}_{12}+3F_{22},\ \{F\,(1^1/_2;\ 1^1/_2)_+\},\quad [4];\\
D^+({}^1/_2\,{}^1/_2)_+, & 3F_{11}-\sqrt{3}\,F^{\mathrm{s}}_{12}+5F_{22},\ \{F\,(0^1/_2;\ 0^1/_2)_+\},\quad [5];\\
D^+({}^1/_2\,{}^1/_2)_-, & 3F_{11}-\sqrt{3}\,F^{\mathrm{s}}_{12}-3F_{22},\ \{F\,(1^1/_2;\ 1^1/_2)_-\};\quad [6];\\
D^-({}^1/_2\,{}^1/_2)_-, & F^{\mathrm{a}}_{12},\qquad \{F\,(1^1/_2;\ 0^1/_2)_-\},\quad [7].
\end{cases}
$$

Four matrices:

$$
D\,(22):\quad D^+(22)_+,\quad E_{00},\quad \{F\,(1^3/_2 2;\ 1^3/_2 2)_+\},\quad [1];
$$

$$
D\,(2112):\ \begin{cases}
D\,(21)_+, & -2E_{01}+\sqrt{2}\,E_{02}+\sqrt{6}\,E_{03},\quad \{F\,(1^3/_2 2;\ 1^3/_2 1)_+\},\quad [2];\\
D\,(21)_-, & \sqrt{2}\,E_{01}+5E_{02}-\sqrt{3}\,E_{03},\quad \{F\,(1^3/_2 2;\ 1^1/_2 1)_-\},\quad [3];\\
D\,(21)_-, & \sqrt{2}\,E_{01}-E_{02}+\sqrt{3}\,E_{03},\quad \{F\,(1^3/_2 2;\ 0^1/_2 1)_-\},\quad [4];
\end{cases}
$$

$$
D\,(2002):\ \begin{cases}
D\,(20)_+, & E_{04},\quad \{F\,(1^3/_2 2;\ 1^1/_2 0)_+\},\quad [5];\\
D\,(20)_+, & E_{05},\quad \{F\,(1^3/_2 2;\ 0^1/_2 0)_+\},\quad [6];
\end{cases}
$$

$$
D\,(11):\ \begin{cases}
D^+(11)_+, & 2E_{11}+E_{22}+3E_{33}-\sqrt{2}\,E^{\mathrm{s}}_{12},\ \{F\,(0^1/_2 1;\ 0^1/_2 1)_+\},\ [7];\\
D^+(11)_+, & 4E_{11}+8E_{22}-12E_{33}+13\sqrt{2}\,E^{\mathrm{s}}_{12}+\sqrt{6}\,E^{\mathrm{s}}_{13}+2\sqrt{3}\,E^{\mathrm{s}}_{23},\ \{F\,(1^3/_2 1;\,1^1/_2 1)_+\},\\
& \hfill [8];\\
D^+(11)_+, & 4E_{11}-4E_{22}+\sqrt{2}\,E^{\mathrm{s}}_{12}-\sqrt{6}\,E^{\mathrm{s}}_{13}+4\sqrt{3}\,E^{\mathrm{s}}_{23},\quad \{F\,(1^1/_2 1;\ 0^1/_2 1)_+\},\ [9];\\
D^+(11)_+, & \sqrt{6}\,E^{\mathrm{s}}_{13}-\sqrt{3}\,E^{\mathrm{s}}_{23},\quad \{F\,(1^3/_2 1;\ 0^1/_2 1)_+-F\,(1^1/_2 1;\ 0^1/_2 1)_+\},\quad [10];\\
D^+(11)_-, & -2E_{11}+5E_{22}-3E_{33}-2\sqrt{2}\,E^{\mathrm{s}}_{12}+\sqrt{6}\,E^{\mathrm{s}}_{13}+2\sqrt{3}\,E^{\mathrm{s}}_{23},\\
& \hfill \{F\,(1^1/_2 1;\ 1^1/_2 1)_-\},\quad [11];\\
D^+(11)_-, & -2E_{11}-E_{22}+3E_{33}+\sqrt{2}\,E^{\mathrm{s}}_{02},\quad \{F\,(0^1/_2 1;\ 0^1/_2 1)_-\},\quad [12];\\
D^-(11)_+, & -2E^{\mathrm{a}}_{23}+\sqrt{2}\,E^{\mathrm{a}}_{31}+\sqrt{6}\,E^{\mathrm{a}}_{12},\quad \{F\,(1^1/_2 1;\ 0^1/_2 1)_+\},\quad [13];\\
D^-(11)_-, & \sqrt{2}\,E^{\mathrm{a}}_{23}+5E^{\mathrm{a}}_{31}-\sqrt{3}\,E^{\mathrm{a}}_{12},\quad \{F\,(0^1/_2 1;\ 1^3/_2 1)_-\},\quad [14];\\
D^-(11)_-, & \sqrt{2}\,E^{\mathrm{a}}_{23}-E^{\mathrm{a}}_{31}+\sqrt{3}\,E^{\mathrm{a}}_{12},\quad \{F\,(1^3/_2 1;\ 1^1/_2 1)_-\},\quad [15];
\end{cases}
$$

$$
D\,(1001):\ \begin{cases}
D\,(10)_+, & -2E_{14}+\sqrt{2}\,E_{24}+\sqrt{6}\,E_{34},\quad \{F\,(1^3/_2 1;\ 1^1/_2 0)_+\},\quad [16];\\
D\,(10)_+, & -2E_{15}+\sqrt{2}\,E_{25}+\sqrt{6}\,E_{35},\quad \{F\,(1^3/_2 1;\ 0^1/_2 0)_+\},\quad [17];\\
D\,(10)_-, & \sqrt{2}\,E_{14}+5E_{24}-\sqrt{3}\,E_{34},\quad \{F\,(1^1/_2 1;\ 1^1/_2 0)_-\},\quad [18];\\
D\,(10)_-, & \sqrt{2}\,E_{15}+5E_{25}-\sqrt{3}\,E_{35},\quad \{F\,(1^1/_2 1,\ 0^1/_2 0)_-\},\quad [19];\\
D\,(10)_-, & \sqrt{2}\,E_{14}-E_{24}+\sqrt{3}\,E_{34},\quad \{F\,(0^1/_2 1;\ 1^1/_2 0)_-\},\quad [20];\\
D\,(10)_-, & \sqrt{2}\,E_{15}-E_{25}+\sqrt{3}\,E_{35},\quad \{F\,(0^1/_2 1;\ 0^1/_2 0)_-\},\quad [21];
\end{cases}
$$

$$
D\,(00):\ \begin{cases}
D^+(00)_+, & E_{44},\quad \{F\,(1^1/_2 0;\ 1^1/_2 0)_+\},\quad [22];\\
D^+(00)_+, & E_{55},\quad \{F\,(0^1/_2 0;\ 0^1/_2 0)_+\},\quad [23];\\
D^+(00)_+, & E^{\mathrm{c}}_{45},\quad \{F\,(1^1/_2 0;\ 0^1/_2 0)_+\},\quad [24];\\
D^-(00)_+, & E^{\mathrm{a}}_{45},\quad \{F\,(1^1/_2 0;\ 0^1/_2 0)_-\},\quad [25].
\end{cases}
$$

Here $E^s_{ik} = E_{ik} + E_{ki}$, $E^a_{ik} = E_{ik} - E_{ki}$.

For the representations D(mnnm) we give the formulas only for D(mn), since in the case of the reverse order of indices the formulas are identical. In the following the symmetrizer is denoted by the symbol $z^{(i)}_k$, where i is the number of α matrices in the product and k is the number in square brackets.

Using this table we enumerate the commutation relations in canonical form for the Duffin-Kemmer algebra $S = D(\frac{1}{2}\frac{1}{2}) + D(1\,00\,1)$. The symmetrizers appearing in the $U(\alpha)$-algebra transform according to the representation

$$\begin{aligned} L = {} & D\,(2002)_+ + D\,({}^3/_2\,{}^1/_2\,{}^1/_2\,{}^3/_2)_+ + D\,({}^3/_2\,{}^1/_2\;{}^1/_2\,{}^3/_2)_- \\ & + 2D\,(1001)_- + 2D^+(11)_+ + D^-(11)_- + D^+({}^1/_2\,{}^1/_2)_+ \\ & + D^+({}^1/_2\,{}^1/_2)_- + D^-({}^1/_2\,{}^1/_2)_+ \\ & + D^-({}^1/_2\,{}^1/_2)_- + 2D^+(00)_+ + D^-(00)_+. \end{aligned} \tag{4.1}$$

We set the coefficients in the matrix α equal to

$$a_{10;\,{}^1/_2\,{}^1/_2} = a_{01;\,{}^1/_2\,{}^1/_2} = b, \qquad a_{{}^1/_2\,{}^1/_2;\,10} = a_{{}^1/_2\,{}^1/_2;\,01} = c.$$

Then by the method described in section 2 we obtain the commutation relations between the three matrices:

$$z^{(3)}_1 = 0, \quad z^{(3)}_2 = 0, \quad z^{(3)}_4 = -2\sqrt{3}\,bcz^{(1)},$$
$$z^{(3)}_5 = -\frac{10\sqrt{3}}{3}\,bcz^{(1)}. \tag{4.2}$$

Using (2.18) — (2.21) we find basis vectors for four matrices which do not go over into one another by use of (4.2) or to the basis vectors for fewer matrices:

$$z^{(4)}_5, \quad z^{(4)}_{15}, \quad z^{(4)}_{20}, \quad z^{(4)}_{23}, \quad z^{(4)}_{25}. \tag{4.3}$$

Applying the same method to them we find just one more independent commutation relation for four matrices:

$$z^{(4)}_{23} = -\frac{5\sqrt{3}}{6}\,bcz^{(2)}_3 - \frac{1}{2}\,b^2c^2z^{(0)}. \tag{4.4}$$

Formulas (4.2) and (4.4) constitute the complete set of commutation relations. Using formulas (3.20) we obtain an expression for the infinitesimal matrix in terms of the matrices α:

$$I^{10} = \sqrt{6}F\,(1;\,0). \tag{4.5}$$

For the Pauli-Fierz equation the representation is $S = D(1\,\frac{1}{2}\frac{1}{2}\,1) + D(\frac{1}{2}\,00\,\frac{1}{2})$. Then

$$\begin{aligned} L = {} & D\,(2112)_- + D\,(2002)_+ + 2D^+(11)_+ + D^+(11)_- \\ & + D^-(11)_+ + 2D^-(11)_- + 4D\,(1001)_- + D\,(1001)_+ \\ & + D^+({}^3/_2\,{}^3/_2)_+ + D^-({}^3/_2\,{}^3/_2)_- + 2D\,({}^3/_2\,{}^1/_2\,{}^1/_2\,{}^3/_2)_+ \\ & + 2D\,({}^3/_2\,{}^1/_2\,{}^1/_2\,{}^3/_2)_- + 3D^+({}^1/_2\,{}^1/_2)_+ + D^+({}^1/_2\,{}^1/_2)_- \\ & + D^-({}^1/_2\,{}^1/_2)_+ + 3D^-({}^1/_2\,{}^1/_2)_- + 2D^+(00)_+ + 2D^-(00)_+. \end{aligned} \tag{4.6}$$

We set the coefficients in the matrix α equal to

$$a_{{}^1/_2 1;\,1{}^1/_2} = -a_{1{}^1/_2;\,{}^1/_2 1} = \delta, \qquad a_{1{}^1/_2;\,{}^1/_2 0} = a_{{}^1/_2 1;\,0{}^1/_2} = \gamma,$$
$$-a_{{}^1/_2 0;\,1{}^1/_2} = -a_{0{}^1/_2;\,{}^1/_2 1} = \beta, - a_{0{}^1/_2;\,{}^1/_2 0} = a_{{}^1/_2 0;\,0{}^1/_2} = \alpha. \tag{4.7}$$

For the Pauli-Fierz equation

$$\alpha = \sqrt{3}\,\delta = 1/2, \quad \gamma\beta = \sqrt{3}/4. \tag{4.8}$$

The commutation relations between the four matrices for (4.7) are obtained in the usual fashion. We have

$$z^{(4)}_1 = 0, \quad z^{(4)}_2 = 0, \quad b_5 z^{(4)}_k = a_k z^{(2)}_1 + c_k\,(z^{(4)}_7 - z^{(4)}_{10}),$$
$$k = 8, 9, 10; \qquad a_l z^{(4)}_l = a_m z^{(4)}_m,$$
$$l, m = 3, 4; 5, 6; 11, 12; 14, 15; 16, 17;$$
$$\sum_n g_n z^{(4)}_n = z^{(2)}_2, \quad n = 18, 19, 20, 21;$$
$$z^{(4)}_i = d_i z^{(2)}_3 + d'_i z^{(0)}, \quad i = 22, 23, 24. \tag{4.9}$$

The constants appearing here are

Table I.

	δ^4	$\delta^2\gamma\beta$	$\delta\alpha\gamma\beta$	$\gamma^2\beta^2$	$\alpha^2\gamma\beta$
a_3	$\frac{\sqrt{3}}{6}$	$\frac{5}{6}$	$-\frac{\sqrt{3}}{3}$	$-\frac{\sqrt{3}}{6}$	$-\frac{1}{2}$
a_4	$\frac{\sqrt{3}}{18}$	$-\frac{1}{6}$	$\frac{\sqrt{3}}{3}$	$-\frac{\sqrt{3}}{2}$	$-\frac{3}{2}$
a_5	$\frac{\sqrt{3}}{2}$	$\frac{1}{2}$	$\sqrt{3}$	$\frac{\sqrt{3}}{6}$	$\frac{1}{2}$
a_6	$\frac{1}{6}$	$\frac{\sqrt{3}}{2}$	-1	$\frac{1}{2}$	$\frac{\sqrt{3}}{2}$
a_{22}	$\frac{1}{18}$	$\frac{\sqrt{3}}{12}$	$\frac{1}{6}$	$\frac{1}{6}$	$-\frac{\sqrt{3}}{12}$
a_{23}	$\frac{1}{4}$	$-\frac{\sqrt{3}}{6}$	0	$\frac{1}{12}$	0
a_{24}	$-\frac{7\sqrt{3}}{36}$	$\frac{5}{12}$	$\frac{\sqrt{3}}{6}$	$-\frac{5\sqrt{3}}{36}$	$\frac{1}{12}$
e_{11}	$\frac{\sqrt{3}}{9}$	$-\frac{5}{6}$	$-\frac{\sqrt{3}}{3}$	$-\sqrt{3}$	$\frac{3}{2}$
e_{12}	0	0	$-\frac{\sqrt{3}}{3}$	$\frac{\sqrt{3}}{2}$	$-\frac{1}{2}$
e_{13}	$-\frac{17}{18}$	$\frac{\sqrt{3}}{3}$	0	$\frac{3}{2}$	0
e_{14}	$\frac{7}{4}$	$\frac{\sqrt{3}}{3}$	0	0	0
e_{31}	$-\frac{\sqrt{2}}{3}$	$-\frac{\sqrt{6}}{2}$	$-\sqrt{2}$	$-\sqrt{2}$	$\frac{\sqrt{6}}{2}$
e_{32}	$\frac{\sqrt{2}}{6}$	$\frac{\sqrt{6}}{3}$	0	$\frac{\sqrt{2}}{4}$	0
e_{33}	$\sqrt{6}$	$-\frac{3\sqrt{2}}{2}$	$-\sqrt{6}$	$\frac{\sqrt{6}}{6}$	$-\frac{\sqrt{2}}{2}$
e_{34}	$-\frac{\sqrt{6}}{2}$	$2\sqrt{2}$	0	0	0
a_7	$\frac{1}{2}$	-1	0	$\frac{1}{2}$	0
a_8	$\frac{17}{6}$	$\frac{7}{2}$	5	$-\frac{3}{2}$	$-\frac{9}{2}$
a_9	$\frac{7}{6}$	$-\frac{1}{2}$	1	$-\frac{5}{2}$	$\frac{3}{2}$
a_{10}	$\frac{1}{2}$	-1	0	$\frac{1}{2}$	0

Table II.

	$\delta^2\gamma\beta$	$\beta^2\gamma^2$	$\delta\alpha\gamma\beta$	$\alpha^2\gamma\beta$	α^4
a'_{22}	$-\frac{\sqrt{3}}{12}$	0	$\frac{1}{2}$	$-\frac{\sqrt{3}}{4}$	0
a'_{23}	0	$\frac{3}{4}$	0	0	$\frac{1}{4}$
a'_{24}	$\frac{3}{4}$	$-\frac{\sqrt{3}}{12}$	$\frac{\sqrt{3}}{2}$	$-\frac{1}{4}$	$-\frac{\sqrt{3}}{4}$
e_{21}	$-\frac{1}{2}$	0	$-\sqrt{3}$	$\frac{9}{2}$	0
e_{22}	$\frac{3}{2}$	0	$-\sqrt{3}$	0	0
e_{23}	0	$\frac{1}{4}$	0	$\sqrt{3}$	$\frac{9}{2}$
e_{24}	0	$\frac{3}{2}$	0	$\frac{\sqrt{3}}{2}$	$-\frac{3}{2}$

$$d_i = \frac{a_i}{b_6} + \frac{a'_i}{b'_6}, \qquad d'_i = \frac{a_i b'_6}{b_6} + \frac{a'_i b_6}{b'_6}, \qquad c_k = \frac{a'_k b_5 - a_k b'_5}{a'_7 - a'_{10}},$$

$$g_n = \frac{\Delta_n}{\Delta}, \quad b_5 = \frac{\sqrt{6}}{6}\delta^2 + \frac{\sqrt{2}}{2}\gamma\beta, \quad b'_5 = \frac{1}{2}\delta\gamma + \frac{\sqrt{3}}{2}\alpha\gamma,$$

$$b_6 = -\frac{1}{2}\delta^2 + \frac{\sqrt{3}}{6}\gamma\beta. \quad b'_6 = \frac{\sqrt{3}}{2}\beta\gamma - \frac{1}{2}\alpha^2; \tag{4.10}$$

Δ is the determinant formed from the quantities e_{ik} $(i, k = 1, 2, 3, 4)$; Δ_n corresponds to Δ with one row replaced by the quantities b_i $(i = 1, 2, 3, 4)$. Then in Δ_{18} the first row consists of the b_i, in Δ_{19} the second row consists of the b_i, etc; the constants are

$$b_1 = -\frac{\sqrt{3}}{6}\delta^2 - \frac{1}{2}\gamma\beta, \qquad b_2 = \frac{1}{2}\gamma\beta + \frac{\sqrt{3}}{2}\alpha^2,$$

$$b_3 = \frac{\sqrt{2}}{2}\delta^2 - \frac{\sqrt{6}}{6}\gamma\beta, \quad b_4 = \frac{\sqrt{3}}{2}\delta\gamma - \frac{1}{2}\gamma\alpha.$$

The remaining constants are equal to the sum of products of quantities from the first row of tables 1 — 3 by the appropriate coefficients, for example, $a_3 = (\sqrt{3}/6)\,\delta^4 + {}^5\!/_6\,\delta^2\gamma\beta - \ldots$ etc.

These formulas give a complete set of commutation relations. Using the expressions for the symmetrizers of five matrices, one can show that no additional commutation relations arise from them.

Using formulas (3.21) we obtain the expression for the infinitesimal matrix in terms of α:

$$I^{10} = \frac{\Delta'_1}{\Delta'} z_3^{(2)} + \frac{\Delta'_2}{\Delta'} z_{18}^{(4)} + \frac{\Delta'_3}{\Delta'} z_{19}^{(4)} + \frac{\Delta'_4}{\Delta'} z_{20}^{(4)};$$

$$\Delta' = \begin{vmatrix} b_1 & e_{12} & e_{13} & e_{14} \\ b_2 & e_{22} & e_{23} & e_{24} \\ b_3 & e_{32} & e_{33} & e_{34} \\ b_4 & e_{42} & e_{43} & e_{44} \end{vmatrix}, \qquad \Delta'_1 = \begin{vmatrix} \frac{\sqrt{3}}{2} & e_{12} & e_{13} & e_{14} \\ \frac{\sqrt{3}}{2} & e_{22} & e_{23} & e_{24} \\ 1 & e_{32} & e_{33} & e_{34} \\ 0 & e_{42} & e_{43} & e_{44} \end{vmatrix} \text{ etc.} \tag{4.11}$$

Table III.

	$\delta^3\gamma$	$\delta\gamma^2\beta$	$\delta^2\alpha\gamma$	$\delta\alpha^2\gamma$	$\alpha\gamma^2\beta$	$\alpha^3\gamma$
a_{14}	$\frac{\sqrt{3}}{6}$	-1	$-\frac{5}{2}$	$\frac{\sqrt{3}}{2}$	$-\sqrt{3}$	$-\frac{3}{2}$
a_{15}	$\frac{7\sqrt{3}}{6}$	5	$-\frac{3}{2}$	$\frac{7\sqrt{3}}{2}$	$\sqrt{3}$	$\frac{3}{2}$
a_{11}	$\frac{3}{2}$	$\sqrt{3}$	$-\frac{3\sqrt{3}}{2}$	$-\frac{3}{2}$	-3	$-\frac{3\sqrt{3}}{2}$
a_{12}	$\frac{1}{2}$	$-5\sqrt{3}$	$-\frac{9\sqrt{3}}{2}$	$-\frac{9}{2}$	3	$\frac{9\sqrt{3}}{2}$
a_{16}	$\frac{3}{2}$	$\sqrt{3}$	$\frac{\sqrt{3}}{2}$	$-\frac{3}{2}$	1	$-\frac{\sqrt{3}}{2}$
a_{17}	$\frac{\sqrt{3}}{6}$	1	$-\frac{1}{2}$	$\frac{\sqrt{3}}{2}$	$-\sqrt{3}$	$-\frac{3}{2}$
a'_7	$\frac{3}{4}$	-1	$-\frac{3}{4}$	$\frac{3}{4}$	3	$-\frac{3}{4}$
a'_8	$-\frac{19}{2}$	-1	$\frac{15}{2}$	$-\frac{9}{2}$	-3	$\frac{9}{2}$
a'_9	-4	-1	0	3	-3	3
a'_{10}	$\frac{3}{4}$	0	$\frac{1}{4}$	$-\frac{9}{4}$	0	$-\frac{3}{4}$
e_{41}	$\frac{5\sqrt{3}}{12}$	1	$-\frac{5}{4}$	$-\frac{\sqrt{3}}{4}$	$-\sqrt{3}$	$\frac{3}{4}$
e_{42}	$-\frac{\sqrt{3}}{12}$	0	$\frac{1}{4}$	$\frac{\sqrt{3}}{4}$	0	$-\frac{3}{4}$
e_{43}	$-\frac{3}{4}$	$2\sqrt{3}$	$-\frac{5\sqrt{3}}{4}$	$-\frac{3}{4}$	2	$-\frac{\sqrt{3}}{4}$
e_{44}	$-\frac{3}{4}$	$-\sqrt{3}$	$\frac{\sqrt{3}}{4}$	$\frac{3}{4}$	-1	$\frac{\sqrt{3}}{4}$

5. EQUATIONS WITH INTERACTION. CONCLUSION

The method proposed permits one to make simplifications also in the treatment of equations with interaction and, in particular, to write immediately any covariant quantity for a system of interacting fields. As an example, we treat the description of the most general Lagrangian. The Lagrangian of a four fermion interaction (without derivates) $(\overline{\psi}O\psi)(\overline{\varphi}O\varphi)$ contains the invariants which appear in the product

$$D(^1\!/_2\,0\,0\,^1\!/_2) \times D(^1\!/_2\,0\,0\,^1\!/_2) \times D(^1\!/_2\,0\,0\,^1\!/_2) \times D(^1\!/_2\,0\,0\,^1\!/_2), \tag{5.1}$$

i.e., 10 invariants: five of the type $D^+(00)$, and five of the type $D^-(00)$.

To include interactions with derivates one must remember that, because of the commutation of components ∇_i with one another, all antisymmetric combinations of the ∇_i are equal to zero. Covariants can be formed only from the quantities $D^+(mm)_+$. To include first order derivatives we must, in place of (5.1), consider the product

$$[D(00) + D(^1\!/_2\,^1\!/_2)]^2\,[D(^1\!/_2\,0\,0\,^1\!/_2)]^4. \tag{5.2}$$

Usually one imposes the requirement that the coupling shall not exceed the order of the equation. In the Lagrangian $(\bar{\psi} O \nabla \psi)(\bar{\varphi} O \nabla \varphi)$ the derivatives occur in front of different fields, but they may give a second derivative in the equation. Varying with respect to φ, we have

$$\nabla(\bar{\psi} O \nabla \psi)\bar{\varphi} O = (\nabla \bar{\psi} O \nabla \psi)\bar{\varphi} O + (\bar{\psi} O \nabla\nabla \psi)\bar{\varphi} O + (\bar{\psi} O \nabla \psi)\nabla \bar{\varphi} O. \tag{5.3}$$

It is necessary that there be no terms of the second type. They are equal to zero if the quantity $\nabla\nabla$ is an antisymmetric combination. Therefore we must, in the first factor of (5.2),

$$D_1(00) + 2D(^1/_2\,^1/_2) + D(11) + D(1001) + D_2(00) \tag{5.4}$$

drop the covariants $D(1\,1)$, $D_2(00)$ as quantities which exceed the order of the equation.

Thus for a four fermion interaction with derivatives we can write 51 invariants. They are not difficult to write, taking account of the different symmetries. Such a treatment can be generalized to any interaction. It should be noted that Racah's method is entirely applicable to equations which are invariant with respect to three-dimensional rotations.[8]

As we have seen, Racah's methods permit a significant simplification in the theory of relativistically invariant equations, both in the obtaining of the commutation relations, as well as in the investigation of different physical requirements. Undoubtedly, in a future development of the application of Racah's method to relativistic equations, one will find further simplications. Possibly one will succeed in finding a general form of the commutation relations for a given ψ function which completely classifies all symmetrizers according to some group of maximal symmetry, in terms of the ψ and the quantities $a_{PQ,\,P'Q'}$, and to write immediately all the necessary traces of matrices and to find a solution of a whole series of other questions.

In conclusion, I express my deep gratitude to Professors V. L. Ginzburg, V. Ya. Faĭnberg and E. S. Fradkin for continued interest and discussion of the results.

---

[1] G. Racah, Phys. Rev. **62**, 438 (1942); **63**, 367 (1943).

[2] L. A. Shelepin, JETP **37**, 1626 (1959), Soviet Phys. JETP **10**, 1153 (1960).

[3] I. M. Gel'fand and A. M. Yaglom, JETP **18**, 703 (1948).

[4] L. A. Shelepin, JETP **34**, 1574 (1948), Soviet Phys. JETP **7**, 1085 (1958).

[5] G. Ya. Lyubarskii, Теория групп и ее применения в физике (Group Theory and Its Applications to Physics) Pergamon Press, 1961.

[6] Yutsis, Levinson, and Vanagas, Математический аппарат теории момента количества движения (Mathematical Apparatus of the Theory of Angular Momentum). GIPNL Lithuanian S.S.R. 1960.

[7] H. A. Jahn, Proc. Roy. Soc. (London) **A205**, 192 (1951).

[8] L. A. Shelepin, Reports at the XIIIth All-Union Conference on Spectroscopy, 1960, Leningrad (in press).

Translated by M. Hamermesh
234

QUANTUM COUNTERS

A. M. PROKHOROV

P. N. Lebedev Physics Institute, Academy of Sciences, U.S.S.R.

Submitted to JETP editor December 1, 1960

J. Exptl. Theoret. Phys. (U.S.S.R.) **40**, 1384-1386 (May, 1961)

Noise and characteristic transient times in quantum counters are considered.

THE sensitivity of detectors of long-wave radiation can be increased by converting the photons to high-frequency photons in the visible or ultraviolet.[1] It is of interest to analyze the operation of devices of this kind in some detail.

Consider the system shown in the figure. If this system is at a very low temperature, only the lower level (1) is populated. When radiation at a frequency $\nu_{21} = (E_2 - E_1)/h$ is applied to the system level 2 is populated. Suppose there is auxiliary radiation at a frequency $\nu_{32} = (E_3 - E_2)/h$. This radiation causes the transfer of population from level 2 to level 3; because of spontaneous emission, there is then a transfer to the lower level 1, with the emission of photons of frequency ν_{31}. In this way, photons characterized by $h\nu_{21}$ are converted to photons characterized by $h\nu_{31}$.

Let n_i be the population in the i-th level while n is the total population in the system; w_{ik} and w_{ki} are the probabilities for transitions from the i-th level to the k-th level and vice versa, $W_{ik} = W_{ki}$ is the probability for a transition from the i-th level to the k-th level under the effect of the external radiation. We assume that the probabilities w_{13} and w_{23} are so small that they can be set equal to zero, while w_{31} is simply the probability for spontaneous emission; it is assumed that this last process predominates in the present case.

The population equations for levels 1 and 3 are written in the form

$$\begin{aligned} dn_1/dt &= a_{11}n_1 + a_{12}n_3 - (a_{11} + w_{12} + W_{12})\, n, \\ dn_3/dt &= a_{21}n_1 + a_{22}n_3 - a_{21}n, \end{aligned} \tag{1}$$

where

$$a_{11} = -2W_{12} - w_{12} - w_{21}, \qquad a_{12} = w_{31} - w_{21} - W_{12},$$
$$a_{22} = -2W_{32} - w_{31} - w_{32}, \qquad a_{21} = -W_{32}.$$

The solution of the system in (1) is

$$n_1 = Ae^{\alpha_1 t} + Be^{\alpha_2 t} + n_1^0,$$
$$n_3 = A\frac{\alpha_1 - a_{11}}{a_{12}}e^{\alpha_1 t} + B\frac{\alpha_2 - a_{11}}{a_{12}}e^{\alpha_2 t} + n_3^0, \tag{2}$$

where A and B are constants which are determined from the initial conditions while α_1, α_2, n_1^0 and n_3^0 have the following meaning:

$$\alpha_{1,2} = \tfrac{1}{2}(a_{11} + a_{22}) \pm \left[\tfrac{1}{4}(a_{11} - a_{22})^2 + a_{12}a_{21}\right]^{1/2},$$
$$n_1^0 = [1 + a_{22}(w_{12} + W_{12})/(a_{11}a_{22} - a_{12}a_{21})]\, n,$$
$$n_3^0 = -a_{21}(w_{12} + W_{12})\, n\, /\, (a_{11}a_{22} - a_{12}a_{21}). \tag{3}$$

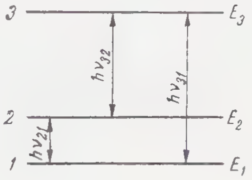

We consider stationary states of the system. Let w_{12}, w_{21}, $W_{12} \ll w_{31} \ll W_{32}$; $w_{32} \ll W_{32}$ so that the population in level 3 is

$$n_3^0 = (w_{12} + W_{12})\, n/w_{31}.$$

The number of photons emitted spontaneously from level 3 to level 1 is

$$N = n_3^0 w_{31} = (w_{12} + W_{12})\, n. \tag{4}$$

It follows from Eq. (4) that when $W_{12} = 0$ there is a "dark" radiation background; in this case the number of emitted photons is

$$N_\mathrm{d} = nw_{12}. \tag{5}$$

If the minimum number of photons of frequency ν_{31} recorded by the detection device is $N_{\min}$, the sensitivity of the quantum counter is a maximum when the condition $N_{\max} \ll N_{\min}$ is satisfied; in accordance with Eq. (5), this means when

$$nw_{12} \ll N_{min}. \tag{6}$$

The population required in the system n is determined from the condition that every photon $h\nu_{21}$ be absorbed. If the absorption coefficient is α, this condition can be written in the form

$$\alpha l = 1, \tag{7}$$

where l is the path length traversed by the photon.

From Eq. (7) we find the number of particles

$$n = Shc\Delta\nu / 8\pi^2\nu_{21}|\mu_{12}|^2, \tag{8}$$

where $\Delta\nu$ is the line width, μ_{12} is the matrix element for the transition between levels 1 and 2 and S is the area of the sample.

The expression in (8) is obtained under the assumption that the radiation passes through the system only once. If the system is a resonator with plane-parallel walls and a quality factor Q, we may say that the photon traverses an effective path length

$$l^* = Q\lambda / 2\pi. \tag{9}$$

The quality factor Q is given by the formula[2]

$$Q = 2\pi l / \lambda (1 - k), \tag{10}$$

where k is the reflection coefficient. From Eqs. (9) and (10) we have

$$l^* = l / (1 - k).$$

Consequently, the population found from Eq. (8) must be multiplied by the factor $(1 - k)$. It is obvious that the smaller the value we obtain for n the larger the value we can take for w_{12} to satisfy the condition in (6).

We now consider the quantity w_{12} in greater detail. If $W_{23} = 0$, the relaxation processes between levels 1 and 2 take place without the participation of level 3. In a two-level system of this kind the relaxation time T_1 is given by the expression

$$T_1 = 1 / (w_{12} + w_{21}).$$

Since $w_{12} = w_{21} \exp\{-h\nu_{21}/kT\}$ then $T_1 \approx 1/w_{21}$ and the quantity w_{12} can be written in the form

$$w_{12} = T_1^{-1} \exp\{-h\nu_{21}/kT\}. \tag{11}$$

If the temperature T is given, in order to reduce w_{12} we must choose a system with a long relaxation time between levels 1 and 2. We may note that it may be possible to achieve the required value of w_{12} by lowering the temperature.

According to Eq. (4), the number of radiated photons is proportional to the signal power if $W_{12} \gg w_{12}$.

We now consider transient processes in the system. As we have shown above, for good sensitivity the quantities w_{12} and w_{21} must be small. If we neglect W_{12}, w_{21}, and w_{12}, in accordance with Eq. (3) the quantities $\alpha_{1,2}$ assume the following values:

$$\alpha_{1,2} = -\tfrac{1}{2}(2W_{32} + w_{32} + w_{31}) \pm \left[W_{32}^2 + w_{32}W_{32} + \tfrac{1}{4}(w_{32} + w_{31})^2\right]^{1/2}.$$

We consider two particular cases:

1) If $W_{32} \ll w_{31}$, w_{32} then

$$\alpha_1 = -w_{31}W_{32}/(w_{31} + w_{32}), \qquad \alpha_2 = -(w_{31} + w_{32}). \tag{12}$$

2) If $W_{32} \gg w_{31}$, w_{32} then

$$\alpha_1 = -w_{31}/2, \qquad \alpha_2 = -2W_{32}. \tag{13}$$

Thus, under the most favorable conditions, where $W_{32} \gg w_{31}$, w_{32}, the rate at which the steady state is established is determined by the slowest exponential factor, i.e., the quantity $\alpha_1 = -w_{31}/2$; in this case, the relaxation time for the transient processes is $\tau = 2/w_{31}$. Consequently the relaxation time for the transient processes is always greater than the lifetime of the system in the excited state.

---

[1] N. Bloembergen, Phys. Rev. Letters **2**, 84 (1959).

[2] A. M. Prokhorov, JETP **34**, 1658 (1958), Soviet Phys. JETP **7**, 1140 (1958).

Translated by H. Lashinsky
235

SOVIET PHYSICS JETP VOLUME 13, NUMBER 5 NOVEMBER, 1961

RELATIVISTIC GENERAL THEORY OF REACTIONS OF THE a + b → c + d + e + . . . *TYPE*

M. I. SHIROKOV

Joint Institute for Nuclear Research

Submitted to JETP editor December 3, 1960

J. Exptl. Theoret. Phys. (U.S.S.R.) **40**, 1387-1391 (May, 1961)

A relativistic theory is constructed for reactions in which there are three or more product particles. This is an extension of the theory of reactions of the type a + b → c + d in the form given by Jacob and Wick and by Chou Kuang-Chao. In this case it has been found necessary to use other variables instead of the Jacobi variables for the relative momenta of the particles. The selection rules for such reactions that follow from parity-conservation are written out.

1. There is a well known form of relativistic general theory of reactions of the type a + b → c + d (that is, there are general expressions for the angular distribution and the polarization in terms of phase shifts), which uses the description of the spin state in terms of projections along the momenta of the particles.[1-3] Besides being relativistic, this form of the theory has the great advantage that its formulas are less cumbersome as compared with the widely used formulas of phase-shift analysis (which are used, for example, in the phase-shift analysis of p-p scattering).

In the present paper the method of Chou Kuang-Chao, Jacob, and Wick, and also that of a previous paper by the writer,[1-3] are applied to construct the theory of reactions of the type a + b → c + d + e + . . . (and also a → c + d + e + . . .). The spins and rest masses of the particles are arbitrary. It is shown that in the relativistic theory it is necessary to use instead of the variables of Jacobi (cf. e.g., Fabri[4]) different momentum variables, which were first used by Dalitz for the description of τ decay.[5]

2. Let us begin with the case of three particles a + b → 1 + 2 + 3. The main propositions of the theory of reactions are presented, for example, in the papers by Jacob and Wick[2] and by the writer.[6]

First of all we must introduce instead of the momenta $\mathbf{p}_1$, $\mathbf{p}_2$, $\mathbf{p}_3$ of the three particles the total momentum $\mathbf{P} = \mathbf{p}_1 + \mathbf{p}_2 + \mathbf{p}_3$ and two relative momenta $\mathbf{p}$ and $\mathbf{p}'$ (whose exact definition is given later). The conservation of $\mathbf{P}$ allows us to eliminate this variable from the description of the reaction.[6] Hereafter we shall suppose that $\mathbf{p}_1 + \mathbf{p}_2 + \mathbf{p}_3 = 0$.

Our main problem is to find the transformation functions $\langle \mathbf{p}\mathbf{p}' m_1 m_2 m_3 | \ldots JM \rangle$ which enable us to go from the description in terms of experimentally measured quantities (the momenta of the particles) to a description in a representation that involves the conserved total angular momentum J and its projection M. The analogous function for two particles is of the form[1-3]

$$\langle \mathbf{p} m_1 m_2 | m_1' m_2' \tilde{p} j m \rangle = \sqrt{\frac{2j+1}{4\pi}} D^j_{m_1+m_2,\, m}(-\pi,\, \vartheta,\, \pi-\varphi)$$
$$\times \delta_{p,\,\tilde{p}}\, \delta_{m_1,\, m_1'}\, \delta_{m_2,\, m_2'}\, q(m_1,\, m_2,\, p). \quad (1)$$

The total angular momentum j of the two particles and its projection m are referred to the center-of-mass system (c.m.s.) of the two particles, with arbitrarily chosen axes z′, y′, x′. ϑ and φ are the spherical angles of the relative momentum $\mathbf{p}$ of the two particles in this system of axes; m_1 and m_2 are the spin projections of particles 1 and 2, referred to the system of axes $z_c \parallel \mathbf{p}$ and $y_c \parallel [\mathbf{z}' \times \mathbf{p}]$ (referred to Lorentz frames which are the rest systems of the particles), and m_1' and m_2' are quantized relative to the same axes z_c, y_c, x_c, but are referred to the c.m.s. of the two particles. The factor q appears as a result of the transformation of the spin variables from the rest systems of the particles to the c.m.s.[3]

To solve the problem with three particles we can in principle go from the variables $(\mathbf{p} m_1 m_2)$ to the variables $(m_1' m_2' j m)$ and then from $(\mathbf{p}' m m_3)$ to $(m m_3 JM)$, regarding the system of particles 1 and 2 as if it were a single particle with the spin variable j. If, however, we use the Jacobi variables (for example, $\mathbf{p}_1 = \mathbf{p}'/2 + \mathbf{p}$, $\mathbf{p}_2 = \mathbf{p}'/2 - \mathbf{p}$, and $\mathbf{p}_3 = -\mathbf{p}'$), the spin projections along $\mathbf{p}$ will not be projections along the momenta of the particles (helicities). And in the formula (1) m_1 and m_2 must be such projections.

Let $\mathbf{p}$ be the momentum of particle 1 in the Lorentz system $K_{1,2}$ in which the total momentum of particles 1 and 2 is zero.[5] Then $-\mathbf{p}$ is the momentum of particle 2. For the total momentum of the system (1, 2, 3) to be zero, the total momentum of the system (1, 2) (relative to the c.m.s. $K_{1,2,3}$ of the three particles) must be equal to $-\mathbf{p}_3$ or $+\mathbf{p}'$. The velocity β of the system $K_{1,2}$ relative to $K_{1,2,3}$ is $\mathbf{p}'/E_{1,2}$, where $E_{1,2} = (p'^2 + \kappa_{1,2}^2)^{1/2}$, where $\kappa_{1,2}$ is the "mass" of the system (1, 2) ($\kappa_{1,2}$ is defined in the usual way as the total energy of (1, 2) in the Lorentz system in which (1, 2) is at rest:

$$\varkappa_{1,2} = \sqrt{p^2 + \varkappa_1^2} + \sqrt{p^2 + \varkappa_2^2};$$

the speed of light is taken to be unity). The momenta of particles 1 and 2 in $K_{1,2,3}$ are obtained by Lorentz transformation (cf. Sec. 18 in the book by Møller[7]):

$$\mathbf{p}_1 = \mathbf{p} - \mathbf{p}'\left[\frac{\mathbf{p}'\mathbf{p}}{p'^2}\left(\frac{E_{1,2}}{\varkappa_{1,2}} - 1\right) - \frac{\sqrt{p^2 + \varkappa_1^2}}{\varkappa_{1,2}}\right],$$

$$\mathbf{p}_2 = -\mathbf{p} - \mathbf{p}'\left[-\frac{\mathbf{p}'\mathbf{p}}{p'^2}\left(\frac{E_{1,2}}{\varkappa_{1,2}} - 1\right) - \frac{\sqrt{p^2 + \varkappa_1^2}}{\varkappa_{1,2}}\right]. \quad (2)$$

To find $\mathbf{p}$, knowing the momenta $\mathbf{p}_1$ and $\mathbf{p}_2$, we must make the inverse transformation

$$\mathbf{p} = \mathbf{p}_1 + (\mathbf{p}_1 + \mathbf{p}_2)\left[\frac{(\mathbf{p}_1 + \mathbf{p}_2, \mathbf{p}_1)}{(\mathbf{p}_1 + \mathbf{p}_2)^2}\left(\frac{E_{1,2}}{\varkappa_{1,2}} - 1\right) - \frac{\sqrt{p_1^2 + \varkappa_1^2}}{\varkappa_{1,2}}\right],$$

$$E_{1,2} = \sqrt{p_1^2 + \varkappa_1^2} + \sqrt{p_2^2 + \varkappa_2^2},$$

$$\varkappa_{1,2} = \sqrt{E_{1,2}^2 - (\mathbf{p}_1 + \mathbf{p}_2)^2}. \quad (3)$$

Thus if Eq. (1) is written for particles 1 and 2, then $\mathbf{p}$ must be the Dalitz variable, and m'_1, m'_2, j, and m must refer to the Lorentz system $K_{1,2}$. The transformation function from $(\mathbf{p}'mm_3)$ to $(m'm'_3JM)$ is also of the form of Eq. (1), and the required function is given by

$$\sum_m \langle \mathbf{p}m_1m_2 | m'_1m'_2\tilde{p}jm\rangle \langle \mathbf{p}'mm_3 | m'm'_3\tilde{p}'JM\rangle$$
$$= \sqrt{\frac{2j+1}{4\pi}} D^j_{m_1+m_2\, m'}(-\pi, \vartheta, \pi - \varphi)$$
$$\times \delta_{p,\tilde{p}}\,\delta_{m_1, m'_1}\,\delta_{m_2, m'_2}\, q(m_1, m_2, p)$$
$$\times \sqrt{\frac{2J+1}{4\pi}} D^J_{m'+m_3,\, M}(-\pi, \vartheta', \pi - \varphi')$$
$$\times \delta_{p',\tilde{p}'}\,\delta_{m_3, m'_3}\, q(m', m_3, p') \quad .$$
$$\equiv \langle \mathbf{p}\mathbf{p}'m_1m_2m_3 | m'_1m'_2m'_3jm'JM\tilde{p}\tilde{p}'\rangle. \quad (4)$$

In this formula J, M, j, m', and m'_3 refer to the system $K_{1,2,3}$, M is quantized relative to some axis system z, y, x, and ϑ' and φ' are the spherical angles of $\mathbf{p}'$ relative to z, y, x. The projections m_3 and m, and also m'_3 and m', are quantized relative to a system of axes with $z' \parallel \mathbf{p}'$ and $y' \parallel [\mathbf{z} \times \mathbf{p}']$; ϑ and φ are the spherical angles of $\mathbf{p}$ in this same system of axes, i.e., ϑ is the angle between $\mathbf{p}$ and $\mathbf{p}'$. Finally, m_1, m_2, m_3 relate to the rest systems of the respective particles.

An important further virtue of the Dalitz variables is the possibility of expressing the total energy of the system of three particles as a function of $|\mathbf{p}|$ and $|\mathbf{p}'|$ only:

$$E = E_{1,2} + \sqrt{p'^2 + \varkappa_3^2} = [p'^2 + (\sqrt{p^2 + \varkappa_2^2}$$
$$+ \sqrt{p^2 + \varkappa_1^2})^2]^{1/2} + \sqrt{p'^2 + \varkappa_3^2}. \quad (5)$$

In the case of Jacobi variables E would also depend on the angle between the relative momenta, and the law of conservation of energy could not be written in the representation containing the absolute values of the momenta and J, M.

We can now write the following expression for an element of the S matrix (or of the matrix $R = S - 1$) of the reaction $a + b \rightarrow 1 + 2 + 3$:

$$\langle \mathbf{p}\mathbf{p}'m_1m_2m_3 | S | \mathbf{p}_am_am_b\rangle = \frac{1}{4\pi\sqrt{4\pi}} \sum_{j,m,J,M} (2J+1)\sqrt{2j+1}$$
$$\times D^j_{m_1+m_2,m}(-\pi, \vartheta, \pi - \varphi)\, D^J_{m+m_3,M}(-\pi, \vartheta', \pi - \varphi')$$
$$\times \langle m_1m_2m_3jmp | S^{JE} | m_am_b\rangle\, D^{*J}_{m_a+m_b,M}(-\pi, \vartheta_a, \pi - \varphi_a). \quad (6)$$

The functions q are included in the notation $\langle | S^{JE} |\rangle$. More exactly, after going over to a representation containing J and M, by their aid we can return from the representation in the projections m'_1, m'_2, m'_3, and m' [see the explanation of Eq. (4)] to the representation in m_1, m_2, m_3, and m (cf. reference 3).

We can perform[6] the summation over M and get

$$\sum_M D^J_{m+m_3,M}(-\pi, \vartheta', \pi - \varphi')\, D^{*J}_{m_a+m_b,M}(-\pi, \vartheta_a, \pi - \varphi_a)$$
$$= D^J_{m+m_3,m_a+m_b}(-\pi, \tilde{\vartheta}', \pi - \tilde{\varphi}'), \quad (7)$$

where $\tilde{\vartheta}'$ and $\tilde{\varphi}'$ are the spherical angles of $\mathbf{p}'$ in the axis system z_a, y_a, x_a relative to which m_a and m_b are quantized (in particular, $z_a \parallel \mathbf{p}_a$). Therefore we can write element (6) in the form

$$\langle m_1m_2m_3pp' | S(\vartheta, \varphi, \vartheta', \varphi') | m_am_bp_a\rangle$$

(here and in what follows we omit the signs ~ over ϑ' and φ').

The formula for $a \rightarrow 1 + 2 + 3$ has the analogous form

$$\langle \mathbf{p}\mathbf{p}'m_1m_2m_3 | S | JM\rangle = \frac{1}{4\pi} \sum_{j,m} \sqrt{(2j+1)(2J+1)}\, D^j_{m_1+m_2,m}$$
$$\times (-\pi, \vartheta, \pi - \varphi)$$
$$\times D^J_{m+m_3,M}(-\pi, \vartheta', \pi - \varphi')\, \langle m_1m_2m_3jmp | S^{J\varkappa} |\rangle. \quad (8)$$

Here J denotes the spin of the decaying particle, M its projection with respect to some axis system, and κ the rest mass of the decaying particle.

3. With the usual method of compounding angular momenta by means of Clebsch-Gordan coefficients we get for a + b → 1 + 2 + 3 the following formula (if the rest masses of all particles are different from zero):

$$\begin{aligned}\langle \mathbf{p}\mathbf{p}'n_1n_2n_3 | S | \mathbf{p}_a n_a n_b\rangle &= \sum Y_{l\mu}(\vartheta,\varphi)\, Y_{l'\mu'}(\vartheta',\varphi')\langle i_1 i_2 n_1 n_2 | i\sigma\rangle\\ &\times\langle il\sigma\mu | jn_j\rangle\langle ji_3n_jn_3 | s'n'\rangle\langle s'l'n'\mu' | JM\rangle\\ &\times\langle iljs'l'p | S^{JE} | sl_ap_a\rangle\langle sl_an\mu_a | JM\rangle\\ &\times\langle i_ai_bn_an_b | sn\rangle Y^*_{l_a\mu_a}(\vartheta_a,\varphi_a). \end{aligned}\tag{9}$$

In Eq. (9) all of the spin projections n are quantized relative to a single system of axes z, y, x, to which all spherical angles also refer; i_1, i_2, i_3 are the spins of particles 1, 2, 3; the summation is over repeated indices. The formula (9) is also relativistic, if we understand **p** and **p′** to be the Dalitz variables and use for the description of the relativistic spin the representation of Foldy and Yu. Shirokov.[8] The formula (6) can be obtained from Eq. (9). To do so we must go over to spin projections along the directions of the momenta of the particles (m-projections) by means of the relation

$$|m\rangle = \sum_{n=-i}^{+i} |n\rangle\, D^i_{n,m}(g),\tag{10}$$

where g is the rotation that brings the axes z, y, x to coincidence with the corresponding system of axes for the m projection. On carrying out some rather cumbersome transformations (cf. e.g., Sec. 2 of reference 6), we get the formula (6), if we use the notation (cf. reference 1 and Appendix B of reference 2)

$$\begin{aligned}\langle m_1m_2m_3jmp | S^{JE} | m_am_b\rangle &= \sum\left\{\sqrt{\frac{2l+1}{2j+1}}\langle i_1i_2m_1m_2 | im_1+m_2\rangle\right.\\ &\left.\times\langle ilm_1+m_20 | jm_1+m_2\rangle\right\}\left\{\sqrt{\frac{2l'+1}{2J+1}}\langle ji_3mm_3 | s'm\right.\\ &\left.+m_3\rangle\langle s'l'm+m_30 | Jm+m_3\rangle\right\}\langle iljs'l'p | S^{JE} | sl_a\rangle\\ &\times\left\{\sqrt{\frac{2l_a+1}{2J+1}}\langle i_ai_bm_am_b | sm_a+m_b\rangle\right.\\ &\left.\times\langle slm_a+m_b0 | Jm_a+m_b\rangle\right\}.\end{aligned}\tag{11}$$

It is clear how much more cumbersome the formula (9) is in comparison with Eq. (6). In particular, in Eq. (6) there is not a single Clebsch-Gordan coefficient. Of course they will appear if for the description of the spin state of the ensemble of particles we use the polarization tensors (cf., e.g., references 1 and 6):

$$\rho(q\tau) = \sqrt{2i+1}\sum_{m,m'}(-1)^{i-m'}\langle iim-m' | q\tau\rangle\,\rho_{m,m'}.$$

Here i is the spin of the particle, and $\rho_{m,m'}$ is the density matrix that describes the spin state of the ensemble of particles. The extension of the expressions for the angular distribution and the polarization tensors of the products of the reaction (cf. references 6 and 9, Sec. 1) to the case of three particles presents no difficulties.

4. No important new difficulties appear in the extension of the formulas (6) and (8) to the case of more than three product particles. Instead of $\mathbf{p}_1$, $\mathbf{p}_2$, $\mathbf{p}_3$, . . . one introduces Dalitz variables; the spherical angles ϑ_i are the angles between the Dalitz momenta. When the number of particles is increased by one an additional transformation function of the type of Eq. (1) appears.

5. In conclusion we write out the selection rules that follow from the invariance of the transition matrix with respect to space reflection and the existence of definite parities for all the particles. These rules are obtained in exactly the same way as in references 1, 2, and 9.

We have

$$\begin{aligned}&\langle m_1m_2\ldots | R(\vartheta,\varphi,\vartheta',\varphi'\ldots) | m_am_b\rangle\\ &= \pi_1^*\pi_2^*\ldots\pi_b\pi_a(-1)^{i_1+i_2+\ldots+i_a+i_b}(-1)^{m_1+m_2+\ldots+m_a+m_b}\\ &\times\langle -m_1,-m_2,\ldots | R(\vartheta,-\varphi;\vartheta',-\varphi',\ldots)\\ &\times | -m_a,-m_b\rangle.\end{aligned}\tag{12}$$

In terms of the coefficients W introduced by the writer,[9] this selection rule has the form

$$\begin{aligned}\langle q_1\tau_1\ldots | W(\vartheta,\varphi,\vartheta',\varphi'\ldots) | q_a\tau_aq_b\tau_b\rangle &= (-1)^{q_1+\ldots+q_a+q_b}\\ &\times(-1)^{\tau_1+\ldots+\tau_a+\tau_b}\langle q_1,-\tau_1\ldots | W(\vartheta,-\varphi;\vartheta',\\ &-\varphi',\ldots) | q_a,-\tau_a;q_b-\tau_b\rangle,\end{aligned}\tag{13}$$

which in particular means for the angular distributions

$$\sigma(\vartheta,\varphi,\vartheta') = \sigma(\vartheta,-\varphi,\vartheta')\tag{14}$$

in the case of three particles,

$$\sigma(\vartheta,\varphi,\vartheta',\varphi',\vartheta'') = \sigma(\vartheta,-\varphi,\vartheta',-\varphi',\vartheta'')\tag{15}$$

in the case of four, and so on. We recall that the angle φ' is measured from the axis $x'' \parallel [\mathbf{p}_a\times\mathbf{p}'']\times\mathbf{p}_a$, and the angle φ from $x' \parallel [\mathbf{p}''\times\mathbf{p}']\times\mathbf{p}''$. The rule (13) (in other formulations) has been repeatedly mentioned in the literature (cf., e.g., a paper by Sona[10]).

Those azimuthal symmetries in cascade reactions involving reactions of the type a + b → 1 + 2 + 3 + . . . that follow from parity conservation are obtained by an obvious extension of the symmetries enumerated by the writer[9] (for cascades of binary reactions, i.e., of reactions of the type a + b → 1 + 2).

[1] Chou Kuang-Chao, JETP **36**, 909 (1959), Soviet Phys. JETP **9**, 642 (1959).

[2] M. Jacob and G. C. Wick, Ann. Phys. **7**, 404 (1959).

[3] M. I. Shirokov, JETP **39**, 633 (1960), Soviet Phys. JETP **12**, 445 (1961).

[4] E. Fabri, Nuovo cimento **11**, 479 (1954).

[5] R. H. Dalitz, Phys. Rev. **94**, 1046 (1954).

[6] M. I. Shirokov, JETP **32**, 1022 (1957), Soviet Phys. JETP **5**, 835 (1957).

[7] C. Møller, The Theory of Relativity, Oxford 1952.

[8] Chou Kuang-Chao and M. I. Shirokov, JETP **34**, 1230 (1958), Soviet Phys. JETP **7**, 851 (1958). Yu. M. Shirokov, JETP **35**, 1005 (1958), Soviet Phys. JETP **8**, 703 (1959).

[9] M. I. Shirokov, JETP **36**, 1524 (1959), Soviet Phys. JETP **9**, 1081 (1959).

[10] P. G. Sona, Nuovo cimento **9**, 334 (1958).

Translated by W. H. Furry
236

SOVIET PHYSICS JETP VOLUME 13, NUMBER 5 NOVEMBER, 1961

THE PARTICLE MASS IN THE ONE-DIMENSIONAL MODEL WITH FOUR-FERMION COUPLING

V. G. VAKS and A. I. LARKIN

Submitted to JETP editor December 3, 1960

J. Exptl. Theoret. Phys. (U.S.S.R.) **40**, 1392-1398 (May, 1961)

The methods of the theory of superconductivity are used to find the mass of a particle in renormalizable theories with vanishing bare mass and involving a weak coupling constant. Only the zero solution for the mass is possible in electrodynamics and in the one-dimensional Thirring model; for the one-dimensional model of two interacting fields a nonvanishing solution is obtained. A finite expression for the charge has been obtained for this model.

1. INTRODUCTION

IT has been proposed by Nambu[1] and the authors[2] that the mass of particles has the same origin as the gap in the energy spectrum of the excitations in a superconductor. The mass is not introduced into the original Lagrangian but arises as a result of "pairing" of particles, which leads to a rearrangement of the vacuum state. As in the theory of superconductivity the mass is equal to zero in any order of perturbation theory but appears in the exact solution. However, the four-fermion interaction considered in the above-mentioned papers leads to strong divergences, which makes quantitative discussion impossible. It is therefore of interest to verify the indicated conjectures on the example of renormalizable theories, where the calculations are possible for small coupling constants.

It turns out that in electrodynamics and in the one-dimensional Thirring model[3] the resultant homogeneous equation for the mass has only the zero solution. However in the one-dimensional model of two interacting fields proposed by Ansel'm[4] there exists in addition to the trivial zero solution also a nonzero solution for the mass. The massless solution turns out to be unstable in this case.

2. ELECTRODYNAMICS AND THE THIRRING MODEL

Abrikosov, Landau, and Khalatnikov[5] have considered the question of the particle mass in electrodynamics in the approximation $e_1^2 < 1$. If $d_l(k^2) = 0$ then the electron Green's function has the form $G(p) = (\hat{p} - m(p^2))^{-1}$. In the case of a vanishing bare mass the quantity $m(p^2)$ obeys the homogeneous equation

$$m(\xi) = \frac{3e_1^2}{4\pi}\int_{\xi}^{L} \frac{m(z)\,dz}{1 + (e_1^2/3\pi)(L - z)}, \tag{1}$$

where $\xi = \ln(p^2/m^2)$, $L = \ln(\Lambda^2/m^2)$, Λ is the cut-off momentum and e_1 is the bare charge.

Equation (1) has only the zero solution. Indeed, the general solution of the differential equation corresponding to Eq. (1) has the form

$$m(\xi) = m(L)\,[1 + (e_1^2/3\pi)(L - \xi)]^{-9/4}. \tag{2}$$

Substituting Eq. (2) into Eq. (1) we obtain $m(\xi) = 0$. The same result is obtained in meson theory for a coupling constant $g_0^2 \ll 1$.

Let us consider the one-dimensional Thirring model. The Lagrangian has the form

$$\mathcal{L}(x) = -u^+\sigma p u - \lambda(u^+\sigma^r u)(u^+\sigma^r u). \tag{3}$$

Here u is a two-component spinor, $\sigma^r = (\boldsymbol{\sigma}, 1)$, the $\boldsymbol{\sigma}$ are the Pauli matrices, and $\sigma p = \sigma_z p_z - p_0$. This model has an exact solution.[3,6] We shall restrict ourselves to the case of small λ and will take into account only terms of order $[\lambda \ln(\Lambda^2/p^2)]^n$, throwing away terms of the form $\lambda[\lambda \ln(\Lambda^2/p^2)]^n$. The totality of diagrams with two incident and two outgoing lines will be referred to as the vertex part $\Gamma_{\alpha\beta\gamma\delta}(p_1, p_2; p_3, p_4)$. As was shown by Ansel'm[7] and Maĭer and Shirkov[8] in the case when the momenta p_i are of the same order Γ does not get renormalized, but simply equals the zero-order expression $4\lambda\sigma^r_{\alpha\gamma}\sigma^r_{\beta\delta}$.

We shall look for the mass of the particle by using the method used in the theory of superconductivity for finding the energy spectrum.[9] We introduce the functions $G(x-y) = \langle T u(x) u^+(y)\rangle$ and $F^+(x-y) = \langle T u^+(x) u^+(y)\rangle$. The Dyson equations for G and F^+ are of the form

$$\begin{aligned} G(p) &= G_0(p)\,[1 + \Sigma_{11}(p)\,G(p) + \Sigma_{20}(p)\,F^+(p)], \\ F^+(p) &= \widetilde{G}_0(-p)\,[\Sigma_{11}(p)\,F^+(p) + \Sigma_{02}(p)\,G(p)]. \end{aligned} \tag{4}$$

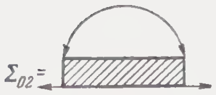

Here $\Sigma_{11}(p)$ represents, as usual, the totality of compact diagrams with one incident and one outgoing line, Σ_{20} and Σ_{02} representing similar totalities with two incident and two outgoing lines respectively. In our approximation the quantity $\Sigma_{11}(p)$ is equal to zero.[7] The matrix $\Sigma_{20}(p) = \Sigma^{+}_{02}(-p)$ is of the form

$$\Sigma^{20}_{\alpha\beta}(p) = \sigma^{y}_{\alpha\beta}\Delta^{*}(p^2).$$

From Eq. (4) we obtain

$$G(p) = -i\sigma' p/(p^2 + |\Delta|^2 - i\delta),$$
$$F^{+}(p) = -\sigma_y \Delta/(p^2 + |\Delta|^2 - i\delta), \tag{5}$$

where

$$\sigma' p = \sigma_z p_z + p_0, \qquad \delta \to +0.$$

In each of the diagrams forming Σ_{02} should enter an odd number of lines representing F or F^{+}; in the asymptotic region $p^2 \gg \Delta^2$ it is sufficient to limit oneself to a single line with F^{+}. The equation for Σ_{02} is shown graphically in the figure. It is of the form

$$\Sigma^{02}_{\alpha\beta}(p) = \int K_{\alpha\beta\gamma\delta}(p, -p;\ p', -p')\, F^{+}_{\gamma\delta}(p')\, \frac{dp'}{(2\pi)^2}, \tag{6}$$

where $K_{\alpha\beta\gamma\delta}(p_1, p_2; p_3, p_4)$ is a four-pole term irreducible with respect to the separation of the lines p_1, p_2 from p_3, p_4.[10] The matrix $K_{\alpha\beta\gamma\delta}$ is of the form $K_{\alpha\beta\gamma\delta} = -4i\lambda\sigma^{r}_{\alpha\gamma}\sigma^{r}_{\beta\delta} K(p_1, p_2; p_3, p_4)$. Substituting this expression into Eq. (6) we obtain

$$\Delta(p) = \int K(p, -p;\ p', -p')\, \frac{\Delta(p')}{p'^2 + |\Delta|^2}\, \frac{dp'}{(2\pi)^2}. \tag{7}$$

Nambu[1] and the authors[2] used for K the zeroth order approximation $K = 1$. In this case the following equation is obtained for Δ:

$$\Delta\left(1 - \frac{\lambda}{4\pi}\ln\frac{\Lambda^2}{|\Delta|^2}\right) = 0. \tag{8}$$

This equation has for arbitrary λ the nonzero solution $|\Delta| = \Lambda\exp(-2\pi/\lambda)$. However in this model such an approximation leads to a qualitatively false result. In the expression for K one must take into account all terms of the order $[\lambda\ln(\Lambda^2/p^2)]^n$. The quantity K was found to within this accuracy by Ansel'm:[7]

$$K(p, -p;\ p', -p') = 1 - (\lambda/4\pi)\ln(\Lambda^2/p_1^2), \tag{9}$$

where $p_1^2 = \max\{p^2, p'^2\}$.

After substitution of Eq. (9) into Eq. (7) and the introduction of the logarithmic variables

$$\xi = \ln\frac{p^2}{m^2}, \qquad z = \ln\frac{p'^2}{m^2}, \qquad L = \ln\frac{\Lambda^2}{m^2}, \qquad m^2 = |\Delta|^2,$$

we obtain the equation

$$\Delta(\xi) = \frac{\lambda}{4\pi}\int_0^L \Delta(z)\,dz - \left(\frac{\lambda}{4\pi}\right)^2\left[(L-\xi)\int_0^{\xi}\Delta(z)\,dz + \int_{\xi}^{L}(L-z)\,\Delta(z)\,dz\right]. \tag{10}$$

Differentiating Eq. (10) with respect to ξ we get

$$\Delta'(\xi) = (\lambda/4\pi)^2\int_0^{\xi}\Delta(z)\,dz. \tag{11}$$

The solution of Eq. (11) is of the form $\Delta(\xi) = \Delta_0 \times \cosh(\lambda\xi/4\pi)$. After substitution of $\Delta(\xi)$ into Eq. (10) we arrive at the following equations for Δ_0:

$$\Delta_0 \exp\left(-\frac{\lambda}{4\pi}\ln\frac{\Lambda^2}{|\Delta_0|^2}\right) = 0, \tag{12}$$

which has only the zero solution.

In the model under discussion this result is quite natural. In order for a mass to appear it is necessary for two massless particles to form a bound state. But in this model there is no physical scattering of two particles — in the exact solution of the two-particle problem there is no reflected wave, only the phase changes.[3] It is therefore natural that in this case the interaction does not lead to the formation of a bound state. Formally this finds its reflection in the fact that in the Thirring model the exact vertex part is momentum independent, whereas a bound state should have a corresponding pole in Γ. Analogous considerations apply in electrodynamics — in the photon Green's function $d_t = [1 + (e_1^2/3\pi)(L - \xi)]^{-1}$ there appears no pole corresponding to a bound state.

3. THE VERTEX PART IN THE ANSEL'M MODEL

Let us consider the one-dimensional four-fermion model with two two-component fields u and v:[4]

$$\mathscr{L}(x) = -u^{+}\sigma p u - v^{+}\sigma p v + \lambda_1(u^{+}\sigma_r u)^2 + \lambda_2(v^{+}\sigma_r v)^2 + \lambda_3(u^{+}\sigma_r u)(v^{+}\sigma_r v) + \lambda_4(u^{+}\sigma_\mu u)(v^{+}\sigma_\mu v). \tag{13}$$

Here the summation over μ is of the form $\sigma_\mu \times \sigma_\mu = \sigma_z \times \sigma_z - 1 \times 1$, the remaining notation being the same as in Eq. (3). One could take in the original Lagrangian $\lambda_1 = \lambda_2 = \lambda_4 = 0$, however, this would not result in a simplification since terms of this form appear in Γ in subsequent approximations.

We introduce the two-row "isotopic" matrices τ_1, τ_2, determined by the relations $\tau_1 u = u$, $\tau_2 v = v$, $\tau_1 v = \tau_2 u = 0$. Then the vertex part is of the following form:

$$\Gamma = i\{\sigma^r\times\sigma^r[(\tau_1\times\tau_1)\,4\alpha_1 + (\tau_2\times\tau_2)\,4\alpha_2 + (\tau_1\times\tau_2)\,\alpha_3] + (\sigma^\mu\times\sigma^\mu)(\tau_1\times\tau_2)\,\alpha_4\}. \tag{14}$$

We shall solve the problem in the same approximation as was used above. When the fact that the Green's function G is given in the asymptotic region by its lowest order approximation is taken into account, one gets by the methods outlined by Ansel'm[4] and Dyatlov, Sudakov and Ter-Martirosyan[10] the following equations* for the α_i:

$$\alpha_1(\xi) = \lambda_1 + \frac{1}{8\pi}\int_\xi^L \alpha_3^2(z)\,dz,$$

$$\alpha_2(\xi) = \lambda_2 + \frac{1}{8\pi}\int_\xi^L \alpha_3^2(z)\,dz,$$

$$\alpha_3(\xi) = \lambda_3 - \frac{1}{\pi}\int_\xi^L \alpha_3(z)\,[\alpha_3(z) + \alpha_4(z) - 2\alpha_1(z) - 2\alpha_2(z)]\,dz,$$

$$\alpha_4(\xi) = \lambda_4 + \frac{1}{\pi}\int_\xi^L \alpha_3(z)\left[\frac{\alpha_3(z)}{2} + \alpha_4(z) - 2\alpha_1(z) - 2\alpha_2(z)\right]dz. \tag{15}$$

Here $\xi = \ln(p^2/m^2)$ and all momenta entering or leaving the vertex part are of order p. Introducing $\lambda = \lambda_1 + \lambda_2$, $\alpha = \alpha_1 + \alpha_2$ and differentiating Eq. (15) we arrive at the following equations:

$$\frac{d\alpha}{d\xi} = -\frac{\alpha_3^2}{4\pi}, \qquad \frac{d\alpha_3}{d\xi} = \frac{\alpha_3}{\pi}(\alpha_3 + \alpha_4 - 2\alpha),$$

$$\frac{d\alpha_4}{d\xi} = -\frac{\alpha_3}{\pi}\left(\frac{\alpha_3}{2} + \alpha_4 - 2\alpha\right). \tag{16}$$

Dividing the second and third of Eqs. (16) by the first and adding the resultant equations we get, after Eq. (15) is taken into account,

$$d(\alpha_3 + \alpha_4)/d\alpha = -2,$$

$$\alpha_3 + \alpha_4 + 2\alpha = \lambda_3 + \lambda_4 + 2\lambda \equiv 4C_1. \tag{17}$$

Further, by quadrature we obtain

$$\alpha_3^2 - 16\alpha^2 + 32\,C_1\alpha = \lambda_3^2 + 8\lambda\,(\lambda_3 + \lambda_4) \equiv 16\,C_2. \tag{18}$$

Substituting Eq. (18) into Eq. (16) we get

$$\int \frac{d\alpha}{\alpha^2 - 2C_1\alpha + C_2} = -\frac{4\xi}{\pi}. \tag{19}$$

Let $D^2 = |C_2 - C_1^2|$. Then for $C_2 - C_1^2 = {}^1\!/_{16}(2\lambda_3 + \lambda_4 - 2\lambda)(2\lambda - \lambda_4) > 0$ we have

$$\alpha = D\,\mathrm{tg}\,\varphi + C_1, \quad \alpha_3 = \pm 4D/\cos\varphi, \quad \alpha_4 = 4C_1 - 2\alpha - \alpha_3;$$

$$\varphi = 4D\pi^{-1}(L - \xi) + \varphi_0, \qquad D\,\mathrm{tg}\,\varphi_0 = \tfrac{1}{4}(2\lambda - \lambda_3 - \lambda_4). \tag{20a†}$$

For $C_2 - C_1^2 < 0$ we have

$$\alpha = D\,\mathrm{th}\,\varphi + C_1, \qquad \alpha_3 = \pm 4D/\mathrm{ch}\,\varphi,$$

$$\alpha_4 = 4C_1 - 2\alpha - \alpha_3; \qquad \varphi = 4D\pi^{-1}(L - \xi) + \varphi_0,$$

$$D\,\mathrm{th}\varphi_0 = \tfrac{1}{4}(2\lambda - \lambda_3 - \lambda_4). \tag{20b}$$

Finally, for $C_2 - C_1^2 = 0$ we have

$$\alpha_3 = \lambda_3[1 \pm \lambda_3\pi^{-1}(L - \xi)]^{-1}, \quad \alpha = \lambda \pm \tfrac{1}{4}(\alpha_3 - \lambda_3),$$

$$\alpha_4 = 4\lambda \pm \lambda_3 - 2\alpha - \alpha_3. \tag{20c}$$

The upper sign in the last formula corresponds to the case $2\lambda - \lambda_4 = 0$, the lower to $2\lambda_3 + \lambda_4 - 2\lambda = 0$. We note that for $\lambda_3 = 0$ the quantities α, α_4 and α_3 are equal to their zeroth order values λ, λ_4 and 0, and, as in the Thirring model, no mass is produced. This case is obtained when the four-fermion interaction is considered to be due to a heavy vector boson with an interaction Lagrangian $(e_1u^+\sigma_\mu u + e_2v^+\sigma_\mu v)A_\mu$.

When the mass m is equal to zero the expressions (20) for Γ are valid for arbitrary momenta p. Then in the case (20a) Γ has poles at the points $\varphi + \varphi_0 = \pi/2 + n\pi$. This is an indication of the appearance of bound states and, consequently, of instability of the massless solution. Let us note that in these same cases there is no "zero charge," the renormalized charge remaining finite also in the limit $L \to \infty$. The behavior of Γ in the case (20c) is determined by the sign of λ_3. In what follows we limit ourselves for the sake of simplicity to the case $\lambda_4 = 2\lambda$, $\lambda_3 = -4\lambda$. Then

$$\alpha = \alpha_4/2 = -\alpha_3/4 = \lambda\,[1 - 4\lambda\pi^{-1}(L - \xi)]^{-1}, \tag{21}$$

and for $\lambda > 0$ the massless solution is unstable.

4. MASS OF THE PARTICLE IN THE ANSEL'M MODEL

We shall seek the particle mass by the same method as was used in Sec. 2. We introduce the functions $G = \langle Tu(x)u^+(y)\rangle$, $F^+ = \langle Tv^+(x)u^+(y)\rangle$ and write out the Dyson equations for these functions:

$$G(p) = G_0(p)\,[1 + \Sigma_{20}(p)\,F^+(p)],$$

$$F^+(p) = \tilde{G}_0(-p)\,\Sigma_{02}(p)\,G(p). \tag{22}$$

We look for $\Sigma_{20}(p) = \Sigma_{02}^+(-p)$ in the form $\Sigma_{20} = \sigma_y\Delta(p^2)$; then G and F^+ are given by Eqs. (5), and the equation for Σ is of the form of Eq. (6). The irreducible four-pole term K has in this case the form

$$K_{\alpha\beta\gamma\delta}(p,-p;\,p',-p') = i\sigma^\mu_{\alpha\gamma}\sigma^\mu_{\beta\delta}K_1 + i\sigma^r_{\alpha\gamma}\sigma^r_{\beta\delta}K_2;$$

$$K_1(\eta) = \lambda_4 + \frac{1}{2\pi}\int_\eta^L [(\alpha_3(z) + \alpha_4(z))^2 - 4\alpha(z)\,\alpha_3(z)]\,dz,$$

$$K_2(\eta) = \lambda_3 + \frac{2}{\pi}\int_\eta^L \alpha_3(z)\,\alpha(z)\,dz, \tag{23}$$

---

*Equations (15) differ from the analogous equations of Ansel'm[4] in which a calculational error was commited. The error, however, did not affect the qualitative results.

†tg = tan, ch = cosh, th = tanh.

where $\eta = \ln(p_1^2/m^2)$, $p_1^2 = \max\{p^2, p'^2\}$. The equation for Δ, analogous to Eq. (7), is written as follows:

$$\Delta(p^2) = 2i\int \frac{\Delta(q^2)dq}{q^2 + m^2(q^2)}[K_1(p, -p; q, -q) + 2K_2(p, -p; q, -q)]. \tag{24}$$

Equation (24) becomes in the special case (21)

$$\Delta(\xi) = \frac{9\lambda}{4\pi}\int_0^L \Delta(z)\,dz + \frac{3}{4\pi}\left(\alpha(\xi)\int_0^\xi \Delta(z)\,dz + \int_\xi^L \alpha(z)\,\Delta(z)\,dz\right). \tag{25}$$

The general solution of the differential equation corresponding to Eq. (25) may be written as follows:

$$\Delta(\xi) = C_1[1 - 4\lambda\pi^{-1}(L - \xi)]^{-1/4} + C_2[1 - 4\lambda\pi^{-1}(L - \xi)]^{-3/4}. \tag{26}$$

Substituting Eq. (26) into Eq. (25) we obtain

$$C_2 = -\tfrac{1}{3}(1 - 4\lambda\pi^{-1}L)^{1/2}C_1, \qquad C_2 = 0. \tag{27}$$

The condition for the existence of a nonzero solution has the form

$$1 - 4\lambda\pi^{-1}L = 0. \tag{28}$$

From Eq. (28) we get

$$m = \Lambda \exp(-\pi/8\lambda). \tag{29}$$

Since terms of order λ were neglected in Eq. (28) in comparison with unity, the expression for m is accurate only to within a numerical factor multiplying the exponential. Correspondingly in the asymptotic region $p^2 \gg m^2$ the quantity $\Delta(p^2)$ is proportional to $[\ln(p^2/m^2)]^{-1/4}$. We note that in this case the approximation of Nambu and the authors,[1,2] i.e., the taking into account of only the first terms in expression (23) for K, results in a numerical inaccuracy only: the factor $\pi/8$ in Eq. (29) is replaced by $\pi/6$.

In the original Lagrangian (13) one may introduce a mass term $m_0(u^+\sigma_y v^+ + v\sigma_y u)$. Then on the right side of Eq. (25) the additional term m_0 will appear. By solving the resultant inhomogeneous equation we obtain the connection between the physical mass m and the bare mass m_0:

$$m\left(1 - \frac{4\lambda}{\pi}\ln\frac{\Lambda^2}{m^2}\right)^{3/4} = m_0. \tag{30}$$

In the limit as m_0 tends to zero the mass m tends to a finite value, determined by Eq. (29). Although the value $m = 0$ is a solution of the homogeneous equation (25), this value is not reached by this limiting procedure.

In the case under consideration the mass appeared as a result of the pairing of particles described by the different fields u and v. Let us consider another possibility, namely when particles of the same type are paired: u with u or v with v. The resultant massive particle would then be identical to its antiparticle, i.e., these would be Majorana particles. In that case one must consider in addition to the function G the functions $F_1^+ = \langle Tu^+(x)u^+(y)\rangle$ and $F_2^+ = \langle Tv^+(x)v^+(y)\rangle$. The calculations are analogous to those described above. Instead of Eq. (27) for Δ we obtain the general expression

$$\Delta(\xi) = C_1[1 - 4\lambda\pi^{-1}[L - \xi)]^{1/4} + C_2[1 - 4\lambda\pi^{-1}(L - \xi)]^{-5/4}. \tag{31}$$

Substituting Eq. (31) into the appropriate integral equation we get

$$C_2 = \tfrac{1}{5}(1 - 4\lambda\pi^{-1}L)^{3/2}C_1, \qquad C_1 = 0. \tag{32}$$

Equation (32) possesses only the zero solution $C_1 = C_2 = 0$, i.e., the mass is equal to zero and no Majorana-type pairing occurs.

In the one-dimensional model under consideration it is possible to form out of the spinors u, u^+, v, v^+ in addition to $u\sigma_y v$ and $u\sigma_y u$ a number of other scalars, which would in the three-dimensional case transform like components of a vector or tensor (for example $u\sigma_x v$ and $u^+\sigma_y v$). This leads to the possibility of pairing of a type different from that considered above. It turns out that all these pairings are absent if the constants are so related as to result in Eq. (21); for different relations among the constants some of these pairings do appear.

When the relation (29) is taken into account the expression (21) for the vertex part becomes

$$\alpha(p^2) = \pi/4\ln(p^2/m^2). \tag{33}$$

Consequently, in the asymptotic region $p^2 \gg m^2$ the effective interaction (33) depends only on the observable mass m and does not contain the bare constant λ or the cut-off parameter Λ.

---

[1] Y. Nambu, preprint (1960).

[2] V. G. Vaks and A. I. Larkin, JETP **40**, 282 (1961), Soviet Phys. JETP **13**, 192 (1961).

[3] W. Thirring, Ann. of Phys. **3**, 91 (1958).

[4] A. A. Ansel'm, JETP **36**, 863 (1959), Soviet Phys. JETP **9**, 608 (1959).

[5] Abrikosov, Landau, and Khalatnikov, Doklady Akad. Nauk SSSR **96**, 261 (1954).

[6] V. Glaser, Nuovo cimento **9**, 990 (1958).

[7] A. A. Ansel'm, JETP **35**, 1522 (1958), Soviet Phys. JETP **8**, 1065 (1959).

[8] M. É. Maĭer and D. V. Shirkov, Doklady Akad. Nauk SSSR **122**, 45 (1958), Soviet Physics-Doklady **3**, 931 (1958).

[9] L. P. Gor'kov, JETP **34**, 735 (1958), Soviet Phys. JETP **7**, 505 (1958).

[10] Dyatlov, Sudakov, and Ter-Martirosyan, JETP **32**, 767 (1957), Soviet Phys. JETP **5**, 631 (1957).

Translated by A. M. Bincer
237

SOVIET PHYSICS JETP VOLUME 13, NUMBER 5 NOVEMBER, 1961

ANGULAR CORRELATIONS IN INELASTIC SCATTERING OF HIGH-ENERGY NUCLEONS

G. L. VYSOTSKII

Physico-Technical Institute, Academy of Sciences, Ukrainian S.S.R.

Submitted to JETP editor December 3, 1960

J. Exptl. Theoret. Phys. (U.S.S.R.) **40**, 1399-1403 (May, 1961)

Angular correlations for the inelastic scattering of high-energy nucleons by nuclei with zero spin and zero isotopic spin are examined. The calculation is carried out in the impulse approximation at small angles. It is shown that the correlation function and its dependence on the nucleon scattering angle are mainly determined by the parity and isotopic spin of the excited level.

A great amount of data has accumulated in recent years on the polarization of high-energy protons in the inelastic scattering by nuclei with excitation of the low-lying levels.[1] Some of the features of these experimental results have been successfully explained by Kerman, McManus, and Thaler[2] with the help of the impulse approximation. The experiments show that in a number of cases the angular distribution of the polarization of the inelastic group of protons is the same or almost the same as for the elastic group. This fact has been regarded as a confirmation of the assumption of the rotational nature of the excited levels, since the Born approximation calculations with a nonspherical optical model potential yield the same polarization for the elastic and inelastic scattering.[3] However, it was shown in reference 2 that the observed regularities have a more general character. In the impulse approximation, which is valid for high energies, the amplitude for the inelastic scattering of the nucleons by nuclei is expressed in terms of the amplitude for nucleon-nucleon scattering and the reduced nuclear matrix elements, which play the role of phenomenological parameters.

In the impulse approximation, the observed similarity between the polarization of the groups of elastically and inelastically scattered nucleons for even-even nuclei connected with the excitation of a level with $\pi = (-)^J$ (J is the spin of the level) is explained in a natural way by the smallness of the ratio of the reduced matrix element with spin flip over the matrix element without spin flip, independently of the nature of the excited level. One can also explain the small polarization connected with the excitation of levels of even-even nuclei with the parity $\pi = (-)^{J+1}$ and a number of other features. It is, therefore, of interest to consider the predictions of the theory of inelastic scattering in the impulse approximation with regard to the p-γ correlations. The investigation of the p-γ correlations in the inelastic scattering of high-energy nucleons is of interest not only as a test of the theory of inelastic scattering, but also from the point of view of using this process for the determination of the spectroscopic properties of the levels. This refers, in particular, to the isotopic spin, which does not play an important role in low energy scattering experiments.

In the first nonvanishing approximation, the inelastic scattering amplitude T is related to the nucleon-nucleon scattering amplitude M in the following way (we consider small angle scattering):

$$T = -\frac{\hbar^2}{2\pi^2 m} N\overline{M}, \qquad \overline{M} = \langle f | M e^{-i\mathbf{QR}} | i \rangle, \tag{1}$$

$$M = A + B(\boldsymbol{\sigma}_0\mathbf{n})(\boldsymbol{\sigma}_1\mathbf{n}) + C(\boldsymbol{\sigma}_0\mathbf{n} + \boldsymbol{\sigma}_1\mathbf{n})$$
$$+ E(\boldsymbol{\sigma}_0\mathbf{q})(\boldsymbol{\sigma}_1\mathbf{q}) + F(\boldsymbol{\sigma}_0\mathbf{p})(\boldsymbol{\sigma}_1\mathbf{p}). \qquad (2)^*$$

Here N is the number of particles in the nucleus, f and i are the labels of the excited and ground states of the nucleus,*

$$\mathbf{q} = \mathbf{Q}/Q = (\mathbf{k}_0' - \mathbf{k}_0)/|\mathbf{k}_0' - \mathbf{k}_0|,$$

$$\mathbf{n} \quad [\mathbf{k}_0\mathbf{k}_0']/|[\mathbf{k}_0\mathbf{k}_0']|, \qquad \mathbf{p} \quad [\mathbf{qn}],$$

and $\mathbf{k}_0$ and $\mathbf{k}_0'$ are the wave vectors of the incident and scattered nucleons. We have omitted the index for the total isotopic spin t = 0, 1 in the system of the two nucleons in the quantities A, B, C, etc. in (2). In place of the quantities A_0 and A_1, B_0 and B_1, etc. it is convenient to introduce the following linear combinations: $A(0) \equiv \frac{1}{4}(3A_1 + A_0)$, $A(1) \equiv \frac{1}{4}(A_1 - A_0)$ and analogously for B, C, etc. The quantities A, B, etc., also depend on Q^2. The lower indices 0 and 1 of the spin operators σ denote the nucleons.

---

*$(\boldsymbol{\sigma}_0\mathbf{p}) = \boldsymbol{\sigma}\cdot\mathbf{p}$; $[\mathbf{qn}] = \mathbf{q}\times\mathbf{n}$.

We shall use a coordinate system with the z axis along **q** and the x and y axes along the vectors **n** and **p**, respectively. It is convenient to separate out the components of M which transform according to an irreducible representation of the rotation group:

$$M = M^{(0)} + \sum_{\mu} (-)^{\mu} M^{(1)}_{-\mu}\sigma^{(1)}_{1\mu}, \qquad \sigma^{(1)}_{10} = \sigma_{1z},$$

$$\sigma^{(1)}_{1,\pm 1} = \mp (\sigma_{1x} \pm i\sigma_{1y}) / \sqrt{2}.$$

In our system of coordinates, we have

$$M^{(0)} = A + C\sigma_0\mathbf{n}, \qquad M^{(1)}_1 = -(C + B\sigma_0\mathbf{n} + iF\sigma_0\mathbf{p})/\sqrt{2},$$

$$M^{(1)}_0 = E\sigma_0\mathbf{q}, \qquad M^{(1)}_{-1} = (C + B\sigma_0\mathbf{n} - iF\sigma_0\mathbf{p})/\sqrt{2}.$$

We then obtain the following expression for M in terms of the reduced matrix elements:

$$M = \sum_{\alpha=0,1} M^{(0)}_{(\alpha)} \sum_{l} \frac{(J_0M_0l0 \mid JM)}{(2J+1)^{1/2}} N_{l\alpha}$$

$$+ \sum_{\mu} (-)^{\mu} M^{(1)}_{-\mu}(\alpha) \sum_{l,k} \frac{(1\mu l0 \mid k\mu)(J_0M_0k\mu \mid JM)}{(2J+1)^{1/2}} Q_{kl\alpha}. \tag{3}$$

Here the quantities M(α) are expressed in terms of A(α), B(α), etc., and

$$N_{l0} = \langle JT \| \rho_l Y \| J_0T_0\rangle, \quad N_{l1} = f(TT_0)\langle JT \| \rho_l Y_l \tau^{(1)} \| J_0T_0\rangle, \tag{4}$$

$$Q_{kl0} = \langle JT \| \rho_l T_k(l) \| J_0T_0\rangle,$$

$$Q_{kl1} = f(TT_0)\langle JT \| \rho_l T_k(l)\, \tau^{(1)} \| J_0T_0\rangle;$$

$$e^{-i\mathbf{QR}} = \sum_{l} \rho_l Y_{l0}, \quad e^{-i\mathbf{QR}}\sigma^{(1)}_{1\mu} = \sum_{lk} (1\mu l0 \mid k\mu)\, \rho_l T_{k\mu}(l), \tag{5}$$

$$f(TT_0) = \pm (T_0T_310 \mid TT_3)/(2T+1)^{-1/2}$$

(the plus sign corresponds to protons, the minus sign, to neutrons); J_0, M_0, and T_0 are the spin, its projection, and the isotopic spin of the initial state of the nucleus; J, M, and T are the corresponding quantities for the final state of the nucleus. Processes involving charge exchange are excluded in the expression for $f(TT_0)$.

As is known, the angular distribution of the γ quanta emitted by a system of oriented nuclei is connected with the spin tensors defining the polarization of the nuclei in the following way:

$$w(\vartheta, \varphi) = \sum_{LL'Fq} (2F+1)^{-1/2} G_F(LL'J_fJ)\, C_LC_{L'}\rho_{Fq}Y_{Fq}(\vartheta, \varphi),$$

$$G_F(LL'J_fJ) = (-)^{J_f-J-1}(2J+1)^{1/2}(2L+1)^{1/2}(2L'+1)^{1/2}$$

$$\times (L1L'-1 \mid F0)\, W(JJLL';\ FJ_F), \tag{6}$$

where the W are the Racah coefficients. The multipole transitions L(L′) with amplitude $C_L(C_{L'})$ go from a level with spin J to a level with spin J_f. Here ρ_{Fq} are spin tensors which define the polarization of the nuclei.

The problem therefore reduces to the calculation of the spin tensors ρ_{Fq}, for which we have the expression

$$\rho_{Fq}I_0 = \sum_{M_0MM'} (-)^{J-M'}(JMJ-M' \mid Fq)\ \mathrm{Sp}\ \overline{M}_{M_0M}\overline{M}^{+}_{M_0M'},$$

where

$$I_0 = \sum_{M_0M} \mathrm{Sp}\ \overline{M}_{M_0M}\overline{M}^{+}_{M_0M}$$

agrees with the cross section for the process except for a factor.

Let us consider the angular correlations for a nucleus with vanishing spin and isotopic spin, $J_0 = T_0 = 0$. In this case the angular correlations are essentially determined by the parity and isotopic spin of the excited level. The selection rules permit the values T = 0, 1 for the isotopic spin of the level. For T = 0 only the terms with κ = 0 are different from zero, and for T = 1 the only nonvanishing terms are those with α = 1. Furthermore, if the parity of the level is "normal," $\pi = (-)^J$, we have the selection rule $l = J$ for the reduced matrix elements without spin flip and $l = k = J$ for the matrix elements with spin flip. On the other hand, if the parity of the level is "anomalous," $\pi = (-)^{J+1}$, the matrix elements without spin flip vanish, and the matrix elements with spin flip are subject to the selection rule $k = J$, $l = J-1, J+1$. As a result we obtain the following expressions for the spin tensors defining the polarization of nuclei with an excited level with parity $\pi = (-)^J$:

$$\rho_{F0} = (-)^J (J0J0 \mid F0)\,[|A|^2 + |C|^2 - \tfrac{1}{2}(|B|^2 + |C|^2$$

$$+ |F|^2)\,\lambda\,(J1J-1 \mid F0)/(J0J0 \mid F0)]\,K^{-1},$$

$$\lambda = |Q_{JJ\alpha}|^2/|N_{J\alpha}|^2,$$

$$K = |A|^2 + |C|^2 + \tfrac{1}{2}(|B|^2 + |C|^2 + |F|^2)\,\lambda; \tag{7}$$

$$\rho_{F1} = i(-)^J\sqrt{2}\,(11J0 \mid J1)(J0J1 \mid F1)\,|AC^*$$

$$+ CB^*|\sqrt{\lambda}\,K^{-1}\sin(\Phi - \Phi_0), \tag{8}$$

$$\Phi = \arg(AC^* + CB^*), \qquad \Phi_0 = \arg N_{J\alpha} - \arg Q_{JJ\alpha};$$

$$\rho_{F2} = \frac{(-)^{J+1}}{2}(J1J1 \mid F2)(11J0 \mid J1)^2(|B|^2$$

$$+ |C|^2 - |F|^2)\,\lambda K^{-1}. \tag{9}$$

F takes the value 2 for dipole transitions (electric and magnetic) and the values 2, 4 for electric quadrupole transitions. The value $\rho_{00} = (2J+1)^{-1/2}$ follows from the normalization of the density matrix. The quantities ρ_{F0} and ρ_{F2}, which are measured directly in experiment, are real and depend, just like the polarization of the elastically scattered nucleons, on the single parameter λ, the ratio of the reduced matrix element with spin flip over the

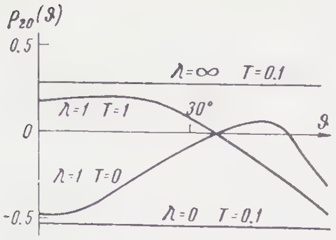

ρ_{20} as a function of the scattering angle of the nucleon at the energy 156 Mev. The 2^+ level is excited. The curves refer to the isotopic spin values $T = 0$ and $T = 1$ and three values of λ: 0, 1, and ∞. For $\lambda = 1$, the curves corresponding to different values of the isotopic spin are very different from each other.

reduced matrix element without spin flip. The quantity ρ_{F1} depends, owing to the interference of the last two processes, also on the additional parameter Φ_0, which, however, like λ, is independent of the scattering angle of the nucleon. The angular dependence is contained in the quantities A, B, etc., which have been derived by Kerman, McManus, and Thaler[2] as functions of the scattering angle in the center of mass system of the two nucleons.

Thus the measurement of the polarization of the inelastically scattered nucleons allows us to determine the spin tensors, i.e., the form of the correlation function.

The investigation of the polarization of the protons in the inelastic scattering from the levels 4.43 Mev of the nucleus C^{12} and 6.14 Mev of the nucleus O^{16} indicates that the parameter λ is small.[2] The spin tensors ρ_{F1} and ρ_{F2} must in this case be small to explain the angular correlations, and ρ_{F0} $(F = 2, 4)$ is close to the value $(-)^J(J0J0 \mid F0)$ and depends weakly on the scattering angle of the proton.

In the case when the reduced matrix elements with spin flip are of the same order as those without spin flip, the spin tensors depend strongly on the isotopic spin of the excited level, more strongly than the polarization of the nucleons. This situation is illustrated by the figure, where we show the dependence of the 2^+ level on the scattering angle of the nucleon for $T = 0$ and 1 (the nucleus is regarded as infinitely heavy). If $\lambda = 1$, the values of ρ_{20} for $T = 0$ and $T = 1$ are radically different. In the two opposite limits $\lambda = 0$ and $\lambda = \infty$, the dependence on T disappears.

For transition with "anomalous" change of parity, the spin tensors have the form

$$\rho_{F0} = (-)^{J+1}(J1J-1 \mid F0)(|B|^2 + |C|^2 + |F|^2)(1-\mu)K'^{-1}, \tag{10}$$

$$\rho_{F1} = 0,$$

$$\rho_{F2} = \frac{(-)^J}{2}(J1J1 \mid F2)(|B|^2 + |C|^2 - |F|^2)(1-\mu)K^{-1};$$

$$K' = (|B|^2 + |C|^2 + |F|^2)(1-\mu) + 2|E|^2\mu;$$

$$\mu = \left(\sum_l \frac{|Q_{Jl\alpha}|^2}{2l+1}\right)^{-1} \sum_{ll'} \frac{(10l0 \mid J0)(10l'0 \mid J0)}{2J+1} Q_{Jl\alpha} Q^*_{Jl'\alpha}. \tag{11}$$

In the case of transitions with anomalous change of parity, the spin tensors also depend only on the single parameter μ. ρ_{F1} is in this case identically equal to zero, and the term with $\sin\varphi$ in the correlation function is absent.

The formulas above are, of course, also applicable to those cases where the levels are de-excited by the emission of an α particle or a β particle instead of a γ ray. Only formula (6) will have to be modified.

Our discussion has shown that the measurement of the correlation function in the inelastic scattering of high-energy nucleons yields information on the parity of the excited states. That is, if we observe a term of the form $P_{21}(\cos\vartheta)\sin\varphi$ in the correlation function (this implies that $\rho_{F1} \neq 0$), we know that the parity changes in the normal way $[\pi = (-)^J]$. If instead we observe a term of the form $P_{22}(\cos\vartheta)\cos 2\varphi$, the parity changes in an anomalous manner $[\pi = (-)^{J+1}]$. Moreover, the investigation of the dependence of the coefficients of the correlation function on the scattering angle of the proton permits us in certain appropriate cases (λ sufficiently large) to determine the isotopic spin of the level.

---

[1] Chesnut, Hafner, and Roberts, Phys. Rev. **104**, 449 (1956). Hillman, Johansson, and Tyrén, Nucl. Phys. **4**, 648 (1957). Alphonce, Johansson, and Tibell, Nucl. Phys. **4**, 672 (1957). Tyrén, Hillman, and Johansson, Nucl. Phys. **3**, 336 (1957). J. M. Dickson and D. C. Salter, Nuovo cimento **6**, 235 (1957).

[2] Kerman, McManus, and Thaler, Ann. of Physics **8**, 551 (1959).

[3] M. Ruderman, Phys. Rev. **98**, 267 (1955). K. Nishimura and M. Ruderman, Phys. Rev. **106**, 558 (1957). Th. A. J. Maris and H. Tyrén, Nucl. Phys. **3**, 35 (1957).

Translated by R. Lipperheide
238

SOVIET PHYSICS JETP VOLUME 13, NUMBER 5 NOVEMBER, 1961

DISPERSION EQUATION FOR AN ORDINARY WAVE MOVING IN A PLASMA PERPENDICULAR TO AN EXTERNAL MAGNETIC FIELD

Yu. N. DNESTROVSKII and D. P. KOSTOMAROV

Moscow State University

Submitted to JETP editor December 3, 1960

J. Exptl. Theoret. Phys. (U.S.S.R.) **40**, 1404-1410 (May, 1961)

A general qualitative investigation is carried out on the dispersion equation for an ordinary wave moving in a plasma perpendicular to an external magnetic field. The regularities found are illustrated by some results of a numerical solution of the dispersion equation.

INTRODUCTION

IT is known that two types of waves can exist in a homogeneous, unbounded plasma located in a homogeneous external magnetic field $\mathbf{H}_0$. The direction of propagation of these waves is perpendicular to the field $\mathbf{H}_0$. The first of these types is a purely transverse wave with an electric vector polarized along the field $\mathbf{H}_0$ (ordinary wave), and the second consists of waves in which the electric vector is polarized perpendicular to $\mathbf{H}_0$ (extraordinary and plasma waves). The frequency ω and the propagation constant k of these waves are related by the dispersion equations, which are obtained with the aid of Maxwell's equations and a linearized kinetic equation for the electrons (without consideration of collisions). Depending on the character of the problem of the dispersion equation considered, one can determine the propagation constant as a function of the frequency or, conversely, the frequency as a function of the propagation constant.

In the present work, we shall be interested in the dispersion equation for the ordinary wave:[1-6]

$$D(k, \omega) = k^2 - \frac{\omega^2}{c^2} + \frac{\omega_0^2 \omega}{2c^2 \omega_H \sin(\pi\omega/\omega_H)} \times \int_0^{2\pi} \exp\left\{-\frac{Tk^2}{m\omega_H^2}(1 - \cos\tau)\right\} \cos\frac{\omega}{\omega_H}(\tau - \pi)\, d\tau = 0. \quad (1)$$

Here $\omega_H = eH_0/mc$ is the Larmor frequency, $\omega_0 = \sqrt{4\pi Ne^2/m}$ is the plasma frequency, T is the temperature of the electrons in energy units. By means of transformations similar to those used by Gross,[7] Eq. (1) can be written in the form

$$D(k, \omega) = k^2 - \frac{\omega^2}{c^2} + \frac{\omega_0^2 \omega}{c^2 \omega_H} \sum_{n=-\infty}^{\infty} \frac{\zeta_n(Tk^2/m\omega_H^2)}{\omega/\omega_H - n} = 0, \quad (1')$$

where $\zeta_n(x) = e^{-x} I_n(x)$, $I_n(x)$ is the Bessel function of imaginary argument. In some cases, the second form of writing is the more convenient.

Equation (1) was studied in a number of researches.[2-4,6] The characteristic feature of the methods of investigation employed has been the preliminary expansion of the equation in some small parameter; usually, it is assumed that $Tk^2/m\omega_H^2 \ll 1$. However, the behavior of the roots of Eq. (1) and of the simplified equations have a number of essential differences. Equation (1) loses meaning for $\omega = n\omega_H$. In this case, the motion of the electrons over the Larmor curves falls into resonance with the vibrations in the field of the wave. The simplified equations, in the first place, do not take into account resonances of higher orders, and in the second place lead to formulas which are inapplicable even in the vicinity of the first resonance, since k^2 increases without limit in this region. Finally, because of the non-uniformity of the expansion in the small parameter, it is not possible to study the problem of the total number of roots and their distribution over the complex plane. Therefore, analysis of Eq. (1) in the works mentioned is incomplete, and is clearly incorrect in a number of cases. We have, therefore, set up the problem in the present work of giving a sufficiently detailed and mathematically rigorous study of the dispersion equation (1). At the same time we shall give the results of a numerical solution of Eq. (1) which illustrates the regularities that have been established.

1. PRELIMINARY INVESTIGATION OF THE DISPERSION EQUATION

We shall begin our investigation of the dispersion equation (1) with a case in which it is required to find the propagation constant for a given frequency. We introduce the dimensionless variables:

$$s = k^2c^2 / \omega^2 = N^2, \qquad \alpha = \omega / \omega_H,$$
$$\beta = \omega_0 / \omega_H, \qquad \gamma = T / mc^2,$$

(N^2 is the square of the index of refraction). Then we have, in place of (1) and (1′),

$$\mathscr{D}(s, \alpha, \beta, \gamma) = s - 1 + \frac{\beta^2}{2\alpha \sin \alpha\pi} \int_0^{2\pi} \exp\{- s\alpha^2\gamma(1 - \cos \tau)\} \cos \alpha(\tau - \pi)\, d\tau = 0, \tag{2}$$

$$\mathscr{D}(s, \alpha, \beta, \gamma) = s - 1 + \frac{\beta^2}{\alpha} \sum_{n=-\infty}^{\infty} \frac{\zeta_n(s\alpha^2\gamma)}{\alpha - n} = 0. \tag{2′}$$

We shall seek the roots of Eq. (2) $s = s(\alpha, \beta, \gamma)$ for all possible positive values of α ($\alpha \neq n$). Real roots are considered in Secs. 2 and 3, and complex roots in Sec. 4. Every positive root s of Eq. (2) determines a pair of real roots of Eq. (1), $k = \pm\sqrt{s}\ \omega/c$, and every negative root determines a pair of purely imaginary roots $k = \pm i\sqrt{-s}\ \omega/c$; finally, every complex root of Eq. (2), together with its corresponding complex conjugate root, determines four complex roots of Eq. (1) which can be written in the form $k = p \pm iq$, $k = -p \pm iq$.

A comparison of the signs of the functions $\mathscr{D}(s, \alpha, \beta, \gamma)$ at $s = 0$ and $s = \pm\infty$ plays an important role in the investigation of the real roots of Eq. (2). By direct calculation, we find that

$$\mathscr{D}(0, \alpha, \beta, \gamma) = \beta^2 / \alpha^2 - 1. \tag{3}$$

On the other hand, the behavior of the function $\mathscr{D}$ as $|s| \to \infty$ is characterized by the following asymptotic formula:

$$\mathscr{D}(s, \alpha, \beta, \gamma) \approx s + \sqrt{\pi / 8}\, \beta^2 e^{-2s\alpha^2\gamma} / \alpha \sin \alpha\pi \sqrt{-s\alpha^2\gamma}. \tag{4}$$

Thus

$$\lim_{s\to+\infty} \mathscr{D}(s, \alpha, \beta, \gamma) = +\infty, \tag{5}$$

$$\lim_{s\to-\infty} \mathscr{D}(s, \alpha, \beta, \gamma) = +\infty\ \mathrm{sign}(\sin \alpha\pi). \tag{6}$$

In the study of the behavior of the roots in the vicinity of cyclotron resonances, it is convenient to make use of the equation in the form (2′). It should be noted that only two terms of the series play an important role for small γ and $\alpha \sim n$: the zero term and the n-th term. The first of these is the only nonvanishing term of the series for $s\gamma \to 0$, the second approaches infinity for $\alpha \to n$. Therefore, one can make use of a simplified equation of the form

$$\zeta_n(sn^2\gamma) = (\alpha - n)\, n\beta^{-2}\, [1 - s - \beta^2 n^{-2} \zeta_0(sn^2\gamma)] \tag{7}$$

for the qualitative investigation of the behavior of the roots $\alpha \sim n$.

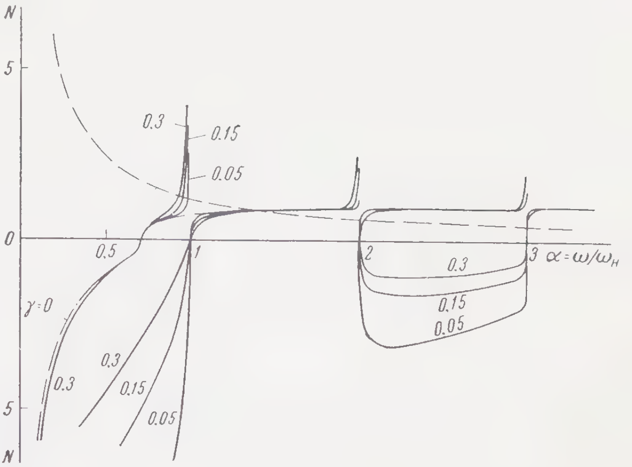

FIG. 1. Frequency dependence of the index of refraction for $\beta = \sqrt{0.5}$ and for various values of γ.

Equation (1) is obtained by means of the nonrelativistic kinetic equation; therefore, it is reasonable to consider only small values of the parameter γ. We compare Eq. (2) with the degenerate equation which is obtained from (2) for $\gamma = 0$ ($T = 0$):

$$\mathscr{D}(s, \alpha, \beta, 0) = s - 1 + \beta^2 / \alpha^2 = 0. \tag{8}$$

According to this equation, there exist traveling waves in the plasma at zero temperature for $\alpha > \beta$ ($\omega > \omega_0$); for $\alpha < \beta$ ($\omega < \omega_0$), propagation of an ordinary wave is impossible (in the first case, the root of Eq. (8) is positive, in the second, it is negative). This conclusion does not carry over completely to Eq. (2); however, a number of peculiarities of the solutions of this equation also depend significantly on the relation between α and β. Therefore, proceeding to the investigation of Eq. (2), we consider separately the cases $\alpha > \beta$ and $\alpha < \beta$.

2. INVESTIGATION OF THE REAL ROOTS OF EQUATION (2) FOR $\alpha > \beta$ ($\omega > \omega_0$)

In the region of change of the parameter α under consideration, we have

$$\mathscr{D}(0, \alpha, \beta, \gamma) < 0. \tag{9}$$

Taking into account (5) and (9), we find that Eq. (2) necessarily has a positive root for $\alpha > \beta$. As $\gamma \to 0$, this root approaches the solution of Eq. (8). We therefore compare the signs of the function $\mathscr{D}$ for $s = -\infty$ [Eq. (6)] and $s = 0$ [the inequality (9)]. If $\sin \alpha\pi > 0$, then the signs are opposite. For such α, Eq. (2) also has a negative root which approaches $-\infty$ as $\gamma \to 0$. If now $\sin \alpha\pi < 0$, then the signs of the function $\mathscr{D}$ are identical for $s = -\infty$ and $s = 0$. In this case, Eq. (2) has no negative roots for sufficiently small values of γ. By considering the equation in the form (2′), we can

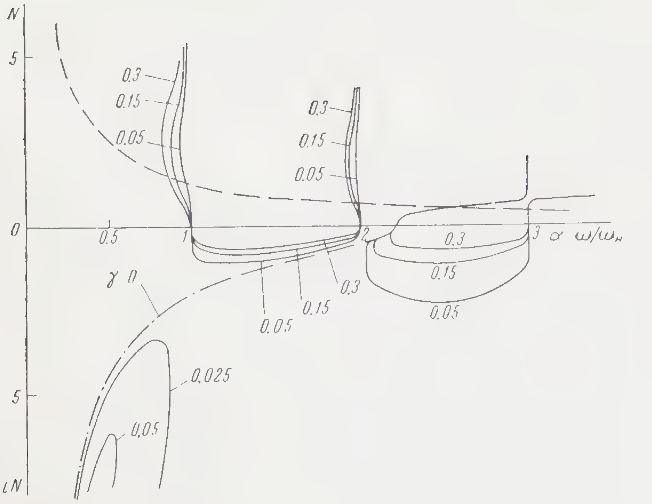

FIG. 2. Frequency dependence of the index of refraction for $\beta = \sqrt{5}$ and for various values of γ.

investigate the behavior of the roots in the vicinity of the resonances $\alpha \sim n$. As $\alpha \to n - 0$, the negative root approaches $+\infty$; as $\alpha \to n + 0$, it approaches zero. The negative root approaches zero as $\alpha \to n$.

Results of a numerical solution of Eq. (2) are shown in Figs. 1 and 2. The index of refraction $N = \sqrt{s}$ is plotted along the positive ordinate, corresponding to the positive root; the quantity $iN = \sqrt{-s}$, corresponding to the negative root, is plotted along the negative ordinate. We see that the positive root is almost everywhere close to the root of the degenerate equation (8) for $\alpha > \beta$. The drawings give a graphic picture of the behavior of the roots in the vicinity of the resonance points. Finally, the peculiarities of the dependence of the roots on the parameter γ are very well seen from the drawings.

3. INVESTIGATION OF THE REAL ROOTS OF EQUATION (2) FOR $\alpha < \beta$ ($\omega < \omega_0$)

By comparing the signs of the expressions $\mathscr{D}(\pm\infty, \alpha, \beta, \gamma)$ and $\mathscr{D}(0, \alpha, \beta, \gamma)$ for $\alpha < \beta$, we arrive at the following conclusions:

1. If $\sin \alpha\pi > 0$, then Eq. (2) has an even number of positive and negative roots.

2. If $\sin \alpha\pi < 0$, then Eq. (2) has an even number of positive and an odd number of negative roots.

Comparison of Eq. (2) with Eq. (8) shows that Eq. (2) generally does not have positive roots for small values of γ, and for frequencies far from the resonance. So far as the negative roots are concerned, such a root will be unique if $\sin \alpha\pi < 0$. As $\gamma \to 0$, this root approaches the solution of Eq. (8). In the case in which $\sin \alpha\pi > 0$, Eq. (2) has two negative roots; as $\gamma \to 0$, one of these approaches the solution of Eq. (8), the other approaches $-\infty$.

By considering the equation in the form (2′), we can investigate the behavior of the roots in the vicinity of the resonances. The picture in the given case is seen to be more complicated than for $\alpha > \beta$. It is most important to note the following.

1. In the vicinity of each resonance $\alpha \sim n$, there is a region $\bar{\alpha}_n(\beta, \gamma) < \alpha < n$ in which Eq. (2) has two positive roots. As $\alpha \to n - 0$, one of these approaches 0, and the other approaches $+\infty$.

2. In the vicinity of each resonance $\alpha \sim n$, there is a region in which Eq. (2) no longer has real roots. For resonances of odd order, this region is located to the left of the point $\alpha = n$: $\tilde{\alpha}_n(\beta, \gamma) < \alpha < \bar{\alpha}_n(\beta, \gamma)$; for resonances of even order, it is located to the right of the point $\alpha = n$: $n < \alpha < \tilde{\alpha}_n(\beta, \gamma)$.

We shall not describe the remaining peculiarities of behavior of roots in the vicinity of the cyclotron resonances in any detail; the general picture can be seen from Fig. 2. We only note that the number of real roots of Eq. (2) in the region $\alpha > \beta$ does not exceed 2, and in the region $\alpha < \beta$, it does not exceed 3.

4. COMPLEX ROOTS OF EQUATION (2)

In the investigation of complex roots of Eq. (2), we make use in principle of an argument which goes as follows; if the function $F(s)$ is analytic everywhere in the region G except for a finite number of singular points of the type of poles, and does not vanish on the boundary of the region Γ, then the change of $\arg F(s)$ in passing about the contour in a positive direction, divided by 2π, is equal to the difference between the number of zeros and poles of the function $F(s)$ in the region G:

$$N - P = \frac{1}{2\pi} \operatorname{var}(\arg F(s)) \tag{10}$$

(each zero and pole is considered as many times as its multiplicity).

The function $\mathscr{D}(s, \alpha, \beta, \gamma)$ has no finite singularities in the plane of the complex variable s; therefore, for it there will only be the number of zeros on the left side of Eq. (10).

Let us consider a circle of sufficiently large radius R in the complex plane of the variable s; the center of the circle is at the origin of the coordinates. If Eq. (2) has roots on the bounding circle, then one can either go around these roots by means of a local deformation of the curve, or decrease the radius R slightly. For the calculation of the change of $\arg \mathscr{D}$ along the boundary of the region, we make use of the asymptotic formula

(4) for the function $\mathscr{D}$ as $|s| \to \infty$, which is valid for both real and complex values of s in the interval $-3\pi/2 < \arg s < 3\pi/2$. It is evident from this formula that, in crossing the right semicircle, $\arg \mathscr{D}$ changes by a quantity of the order of π, and in crossing the semicircle on the left, by a quantity of the order of $4\alpha^2\gamma R$. The total variation of $\arg \mathscr{D}$ on the contour would be a quantity of the order of $4\alpha^2\gamma R$ which increases without limit as $R \to \infty$. This means that Eq. (2) has an infinite (denumerable) set of roots.

Since the number of real roots is finite (not larger than 3), the number of complex roots must be infinitely great. It is evident from the asymptotic formula (4) that for $s \to \infty$ the roots are grouped beside the imaginary axis in the second and third quadrants. If the parameters α and β are fixed, while γ approches 0, then all complex roots will tend to infinity.

5. DETERMINATION OF THE FREQUENCY AS A FUNCTION OF THE PROPAGATION CONSTANT FROM THE DISPERSION EQUATION (1)

We now consider Eq. (1) from another point of view, in which it is required to find the frequency $\omega = \omega(k)$ from this equation for a given real propagation constant k. Such a problem can easily be investigated with the help of the results obtained above.

To find the real roots of Eq. (1), it is necessary to find in the plane α, N the points of intersection of the line $N = kc/\omega_H\alpha$ (the dashed curve in the drawings) with the curve of the function $N = \sqrt{s(\alpha, \beta, \gamma)}$. To each such point α^*, N^* there corresponds a pair of roots of Eq. (1): $\omega = \pm\omega_H\alpha^*$. The analysis carried out in Secs. 2 and 3 shows that the number of points of intersection will be infinitely large. If we enumerate the abcissas of these points in increasing order ($\alpha_1 < \alpha_2 < \alpha_3 < \ldots$), then their distribution along the α axis will possess the following features (see Figs. 1 and 2):

1. The values of α_n lie within the limits $n-1 < \alpha_n < n$ $(n = 1, 2, 3, \ldots)$.
2. One of the abcissas α_{n_0} is close to the abcissa of the point of intersection of the lines $N = kc/\omega_H\alpha$ и $N = \sqrt{1-\beta^2/\alpha^2}$, i.e. $\alpha_{n_0} \approx \sqrt{\beta^2 + (kc/\omega_H)^2}$.
3. For $1 \le n < n_0$, the quantity $\alpha_n \approx n$.
4. For $n_0 < n < \infty$, the value of $\alpha_n \approx n-1$.

Thus to each real value of k there corresponds an infinite number of real roots of Eq. (1): $\pm\omega(k) = \pm\omega_H\alpha_n$, and $\omega_n \approx \sqrt{\omega_0^2 + k^2c^2}$, and $\omega_n \approx n\omega_H$ for $1 \le n < n_0$; $\omega_n \approx (n-1)\omega_H$ for $n_0 < n < \infty$.

We shall now show that Eq. (1) does not possess any complex roots $\omega = \omega(k)$. For this purpose, we consider circles C_m of radius $R_m = \omega_H(m + 1/2)$ in the plane of the complex variable ω; here m is a sufficiently large integer. On circles of such a type we have

$$\left| \sum_{n=-\infty}^{\infty} \frac{\zeta_n(Tk^2/m\omega_H^2)}{\omega/\omega_H - n} \right| < A,$$

where A is some constant independent of the number m. Consequently, for sufficiently large values of m,

$$\frac{1}{2\pi}\operatorname{var}(\arg D)\Big|_{C_m} = \frac{1}{2\pi}\operatorname{var}\left(\arg\left[-\frac{\omega^2}{c^2}\right]\right)\Big|_{C_m} = 2.$$

On the other hand, inside the circle C_m, the function $D(k, \omega)$ has $2m + 2$ real roots and 2m poles of first order at the points $\omega = \pm n\omega_H$ $(n = 1, 2, \ldots, m)$. Since, in accord with (10), the total number of zeros of the function D inside the circle C_m must be equal to $2m + 2$, this means that the complex roots $\omega = \omega(k)$ are absent from Eq. (1).

CONCLUSIONS

The investigation that has been carried out makes it possible to draw the following conclusions on the peculiarities of the solutions of the dispersion equation (1):

1. For $\omega > \omega_0$, $\omega \ne \omega_H n$ Eq. (1) always has a pair of real roots $\pm k(\omega)$.
2. For all $\omega < \omega_0$, regions exist in the neighborhood of the resonance frequencies $\omega \sim n\omega_H$ in which Eq. (1) has two pairs of real roots. Outside these regions Eq. (1) has no real roots for $\omega < \omega_0$.
3. For $\omega < \omega_0$, regions exist in the vicinity of the resonance frequencies in which Eq. (1) has neither real nor purely imaginary roots [the real roots are lacking in Eq. (2)].
4. For each value $\omega \ne n\omega_H$, Eq. (1) has an infinite set of quartets of complex roots:

$$k = p_n(\omega) \pm iq_n(\omega), \qquad k = -p_n \pm iq_n.$$

5. For any real value of k, Eq. (1) has an infinite set of pairs of real roots $\pm\omega_n(k)$. It has no complex roots $\omega = \omega(k)$.

The authors express their gratitude to A. A. Chechina for her help in carrying out the calculations.

[1] G. V. Gordeev, JETP **24**, 445 (1953).

[2] M. E. Gershman, JETP **24**, 659 (1953).

[3] M. E. Gershman, JETP **37**, 695 (1959), Soviet Phys. JETP **10**, 497 (1960).

[4] M. E. Gershman, JETP **38**, 912 (1960); Soviet Phys. JETP **11**, 657 (1960).

[5] A. G. Sitenko and K. N. Stepanov, JETP **31**, 642 (1956), Soviet Phys. JETP **4**, 512 (1957).

[6] J. E. Drummond, Phys. Rev. **110**, 293 (1958).

[7] E. D. Gross, Phys. Rev. **82**, 232 (1951).

Translated by R. T. Beyer
239

SOVIET PHYSICS JETP VOLUME 13, NUMBER 5 NOVEMBER, 1961

RELATIVE PROBABILITIES OF ALPHA DECAY TO ROTATIONAL LEVELS OF NONAXIAL EVEN-EVEN NUCLEI

V. S. ROSTOVSKII

Moscow State University

Submitted to JETP editor December 6, 1960

J. Exptl. Theoret. Phys. (U.S.S.R.) **40**, 1411-1417 (May, 1961)

The wave function for a system consisting of a nucleus and α particle is derived under the assumption that it is constant on the surface of a nonaxial nucleus. The relative probabilities for α decay to the levels of the ground and "anomalous" rotational bands of the daughter nucleus are also determined. The results are compared with the experiments.

THE effect of nonsphericity of nuclei on the relative probabilities of α decay of even-even nuclei to the rotational levels of the daughter nucleus has been considered in several papers,[1-5] where it has been assumed, however, that the nucleus is axially symmetrical. In view of the success of the theory of nonaxial nuclei, proposed by Davydov and Filippov[6] and developed in many subsequent papers, it is interesting to consider the effect of nonaxiality on the α decay, a topic to which the present paper is devoted. We use the analytic solution method proposed by Nosov.[2]

We consider a system consisting of an α particle in the electric field of the daughter nucleus. The nucleus is assumed nonaxial with unchanging internal state, i.e., the rotation is considered adiabatic with respect to the β and γ oscillations of the surface and the single-particle motions inside the nucleus. Outside the effective range of the nuclear forces, the system satisfies the equation

$$\left[-\frac{\hbar^2}{2\mu}\Delta + \frac{\hbar^2}{2}\sum_{\nu=1}^{3} A_\nu \hat{J}_\nu^2 + V(\mathbf{r}, \theta_i) - E\right]\Psi = 0,$$
$$A_\nu = [4B\beta^2 \sin^2(\gamma - 2\pi\nu/3)]^{-1}, \qquad (1)$$

where μ is the reduced mass of the system, $\hat{\mathbf{J}}$ the momentum operator of the daughter nucleus, A_ν the reciprocals of the nuclear moments of inertia, $\mathbf{l}$ the momentum operator of the α particle, $V(\mathbf{r}, \theta_i)$ the potential energy of the electrostatic interaction between the nucleus and the α particle, and E to the total energy of α decay to the ground state.

In the case of even-even nuclei, the total momentum of the system, equal to the spin of the parent nucleus, is zero. The solution should therefore satisfy the condition

$$(\hat{\mathbf{J}} + \hat{\mathbf{l}})\Psi = 0. \qquad (2)$$

We seek the solution Ψ of Eq. (1) in the form of a superposition of particular solutions $\psi_{l\tau}$, representing at infinity the daughter nucleus in some rotational state $\Phi^r_{JM\tau}(\theta_i)$, and an α particle with momentum l removed from this nucleus. The expansion coefficients are determined from the values of the wave function on the surface of the nucleus.

The rotational wave functions of the nucleus

$$\Phi^r_{JM\tau} = \left(\frac{2J+1}{16\pi^2}\right)^{1/2}\sum_K a_K(1+\delta_{K0})^{-1/2}[D^J_{MK}(\theta_i) + (-1)^J D^J_{M,-K}(\theta_i)]$$

($K \gg 0$ and even only) satisfy the equation

$$\frac{\hbar^2}{2}\sum_{\nu=1}^{3} A_\nu \hat{J}_\nu^2 \Phi^r_{JM\tau} = E^r_{J\tau}\Phi^r_{JM\tau}; \qquad (3)$$

the quantities $a_K(J, \tau; \gamma)$ and $E^r_{J,\tau}$ are given in the papers by Davydov and co-workers.[6,7] From the vanishing of the total momentum of the system it follows that $J = l$ and as $r \to \infty$ the angular part of the sought particular solution has the form

$$\Phi_{l\tau} = \sum_m (l, l, m, -m \mid 0, 0)\, Y_{lm}(\vartheta, \varphi)\, \Phi^r_{l,-m,\tau}(\theta_i).$$

We change to a coordinate system r, ϑ', φ', which rotates with the nucleus. In this system $\Phi_{l\tau}$ assumes the form

$$\Phi_{l\tau}(\vartheta', \varphi') = \frac{1}{4\pi}\sum_{K \geqslant 0} a_K(1+\delta_{K0})^{-1/2}[Y_{lK}(\vartheta', \varphi') + (-1)^l Y_{l,-K}(\vartheta', \varphi')], \qquad (4)$$

and the potential energy is independent of the Euler angles, which characterize the orientation of the nucleus in the space $V = V(r, \vartheta', \varphi')$. For the case of nonspherical nuclei with radius

$$R = R_0\left[1 + \sum_{n=2}^{\infty}\sum_m \alpha_{nm} Y_{nm}(\vartheta', \varphi')\right] \equiv R_0(1+\xi)$$

the latter can be expanded in powers of the nuclear deformations α_{nm}. Accurate to linear terms of the expansion, we have in the region outside the nucleus

$$V(r, \vartheta', \varphi') = \frac{2Ze^2}{r}\left[1 + \sum_{n,m} \frac{3\alpha_{nm}}{2n+1}\left(\frac{R_0}{r}\right)^n Y_{nm}(\vartheta', \varphi')\right].$$

We seek a particular solution $\psi_{l\tau}$ in the form

$$\psi_{l\tau} = \Phi_{l\tau} \exp\,[\sigma(r, \vartheta', \varphi'; l, \tau)]; \qquad (5)$$

here σ is bounded by the condition that as $r \to \infty$ it contain only the diverging wave and be independent of the angle variables ϑ' and φ'. Substituting (5) in (1) and taking (2), (3), and (4) into account, we obtain an equation for σ:

$$\left[\left(\frac{\partial\sigma}{\partial r}\right)^2 + \frac{\partial^2\sigma}{\partial r^2} + \frac{2}{r}\frac{\partial\sigma}{\partial r}\right]\Phi_{l\tau} + \frac{2\mu}{\hbar^2}\left[E - E^r_{l\tau} - \frac{\hbar^2 l(l+1)}{2\mu r^2} - V\right]$$
$$- \sum_{\nu=1}^{3}\left(\frac{1}{r^2} + \mu A_\nu\right)\{[(\hat{l}_\nu\sigma)^2 + (\hat{l}^2_\nu\sigma)]\,\Phi_{l\tau}$$
$$+ 2\,(\hat{l}_\nu\sigma)\,(\hat{l}_\nu\Phi_{l\tau})\} = 0. \qquad (6)$$

To solve this equation we use the method, proposed by Nosov,[2] of expanding σ in a double series in powers of ħ (quasiclassical approximation, lower index) and in powers of the nuclear deformation ξ (upper index):

$$\sigma = \sigma^{(0)}_{-1} + \sigma^{(1)}_{-1} + \sigma^{(0)}_{0} + \ldots \qquad (7)$$

Substituting (7) in (6) and collecting terms of equal orders in ħ and ξ, we obtain a system of equations for $\sigma^{(q)}_p$:

$$\left[\frac{\partial\sigma^{(0)}_{-1}}{\partial r}\right]^2 - \sum_{\nu=1}^{3}\left(\frac{1}{r^2} + \mu A_\nu\right)[\hat{l}_\nu\sigma^{(0)}_{-1}]^2$$
$$+ \frac{2\mu}{\hbar^2}\left[E - E^r_{l\tau} - \frac{\hbar^2 l(l+1)}{2\mu r^2} - \frac{2Ze^2}{r}\right] = 0,$$
$$\frac{\partial\sigma^{(1)}_{-1}}{\partial r}\frac{\partial\sigma^{(0)}_{-1}}{\partial r} - \sum_{\nu=1}^{3}\left(\frac{1}{r^2} + \mu A_\nu\right)[\hat{l}_\nu\sigma^{(0)}_{-1}]\,[\hat{l}_\nu\sigma^{(1)}_{-1}]$$
$$- \frac{6\mu Ze^2}{\hbar^2 R_0}\sum_{n,m}\frac{\alpha_{nm}}{2n+1}\left(\frac{R_0}{r}\right)^{n+1} Y_{nm} = 0, \qquad (6a)$$
$$\left\{\frac{\partial\sigma^{(0)}_{0}}{\partial r}\frac{\partial\sigma^{(0)}_{-1}}{\partial r} + \frac{1}{2}\frac{\partial^2\sigma^{(0)}_{-1}}{\partial r^2} + \frac{1}{r}\frac{\partial\sigma^{(0)}_{-1}}{\partial r}\right\}\Phi_{l\tau} - \sum_{\nu=1}^{3}\left(\frac{1}{r^2} + \mu A_\nu\right)$$
$$\times\left\{\Phi_{l\tau}\,[\hat{l}_\nu\sigma^{(0)}_{+1}]\,[\hat{l}_\nu\sigma^{(0)}_{0}] + \frac{1}{2}\,\Phi_{l\tau}\hat{l}^2_\nu\sigma^{(0)}_{-1} + (\hat{l}_\nu\Phi_{l\tau})\,[\hat{l}_\nu\sigma^{(0)}_{-1}]\right\} = 0.$$

This system is solved by successive approximations. If we confine ourselves to the first three terms of the expansion of σ in the double series (7), $\sigma = \sigma^{(0)}_{-1} + \sigma^{(1)}_{-1} + \sigma^{(0)}_{0}$, then the solution has the form

$$\sigma = i\int_{r_{l\tau}}^{r} k_{l\tau}(r)\,dr + i\,\frac{6\mu Ze^2}{\hbar^2 R_0}\sum_{n,m}\frac{\alpha_{nm}}{2n+1}\,Y_{nm}\int_{r}^{\infty}\left(\frac{R_0}{r}\right)^{n+1}\frac{dr}{k_{l\tau}(r)}$$
$$- \ln\,[r\sqrt{k_{l\tau}(r)}],$$
$$k_{l\tau}(r) = \frac{\sqrt{2\mu}}{\hbar}\left[E - E^r_{l\tau} - \frac{\hbar^2 l(l+1)}{2\mu r^2} - \frac{2Ze^2}{r}\right]^{1/2}, \qquad (8)$$

where $r_{l\tau}$ is the turning point, determined from the condition $k_{l\tau}(r_{l\tau}) = 0$.

As already noted, the complete solution of Eq. (1) is sought in the form of a superposition of particular solutions $\psi_{l\tau}$:

$$\Psi = \sum_{l,\tau} b_{l\tau}\psi_{l\tau}.$$

The expansion coefficients $b_{l\tau}$ are expressed in terms of the values of the wave function on the surface of the nucleus, Ψ_S, which is assumed known. We first write down the expression for the particular solution on the surface of the nucleus S, equal to $\Phi_{l\tau}\exp\{\sigma[R(\vartheta', \varphi'), \vartheta', \varphi'; l, \tau]\}$. Since we have considered in the solution of the system (6a) only the terms linear in ξ, and since $\hbar^2 l(l+1)/2\mu r^2 \ll E$ and $E^r_{l,\tau} \ll E$ when l is small, we can expand (8), at $r = R(\vartheta', \varphi')$, in powers of ξ, $l(l+1)$, and $E^r_{l,\tau}$ and confine ourselves to the linear terms of the expansion. Then, introducing the notation*

$$k^2 = 2\mu E/\hbar^2, \qquad \varkappa^2_b = 4\mu Ze^2/\hbar^2 R_0,$$
$$\varkappa = \sqrt{\varkappa^2_b - k^2}, \qquad \gamma_\alpha = 2\varkappa/\varkappa^2_b R_0,$$
$$\gamma_n = E^{-1}\,[\varkappa R_0 + (\varkappa^2_b R_0/k)\operatorname{arctg}(\varkappa/k)],$$
$$\chi(\vartheta', \varphi') = \frac{3}{2}\varkappa^2_b\sum_{n,m}\frac{\alpha_{nm}}{2n+1}R_0^{n+1}Y_{nm}(\vartheta', \varphi')\int_{R_0}^{\infty}\frac{dr}{r^{n+1}\sqrt{\varkappa^2_b R_0/r - k^2}}$$

and taking (5) into account, we obtain, apart from a constant factor independent of l or τ,

$$\psi_{l\tau}|_S = \Phi_{l\tau}\exp\left[\tfrac{1}{2}\gamma_\alpha l(l+1) + \tfrac{1}{2}\gamma_n E^r_{l\tau} - \varkappa R_0\xi + \chi\right].$$

We now readily obtain the expansion coefficients

$$b_{l\tau} = c_{l\tau}\exp\left[-\tfrac{1}{2}\gamma_\alpha l(l+1) - \tfrac{1}{2}\gamma_n E^r_{l\tau}\right],$$

where we put

$$c_{l\tau} = \int \Psi_S\Phi^*_{l\tau}\exp(\varkappa R_0\xi - \chi)\,d\theta_i\sin\vartheta'\,d\vartheta'\,d\varphi'. \qquad (9)$$

Let us calculate the flux through a sphere of infinite radius. Substituting $\psi_{l\tau}$ into the expression for the flux density and integrating over the angles θ_i, ϑ', and φ' we find that at large r the flux through this sphere is the same for all l and τ. The relative probability of emission of an α particle with momentum l and excitation of the daughter nucleus in the state l, τ is thus proportional to $|b_{l\tau}|^2$, i.e.,

$$w_{l\tau} = \exp\,[-\gamma_\alpha l(l+1) - \gamma_n E^r_{l\tau}]\,|c_{l\tau}|^2.$$

Let us examine the result obtained under two additional assumptions: 1) the wave function is

---

*arctg = tan⁻¹.

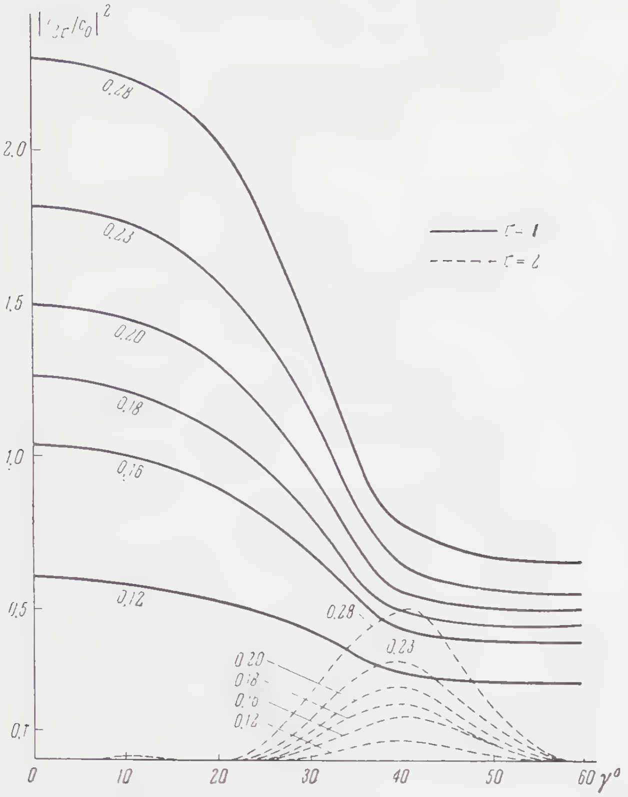

FIG. 1. Dependence of $|c_{2\tau}/c_0|^2$ on the nonaxiality parameter γ. Solid curves—for $\tau = 1$; dotted curves – for $\tau = 2$. The numbers on the curves indicate the value of the parameter $\beta\sqrt{5/4\pi}$ for $\varkappa R_0(1 - k^2/2\varkappa_b^2) = 16.2$.

constant on the surface of the nucleus, $\Psi_S = \text{const}$; 2) the nucleus has only quadrupole deformation (in the frame fixed to the nucleus):

$$\alpha_{20} = \beta\cos\gamma, \qquad \alpha_{22} = \alpha_{2,-2} = \beta\sin\gamma/\sqrt{2},$$

$$\alpha_{21} = \alpha_{2,-1} = 0, \qquad \alpha_{nm} = 0 \quad \text{for} \quad n \neq 2.$$

Then

$$\xi = \beta\left(Y_{20}\cos\gamma + \frac{Y_{22} + Y_{2,-2}}{\sqrt{2}}\sin\gamma\right),$$

$$\chi = \frac{1}{5}\xi R_0 \frac{\varkappa(\varkappa_b^2 + 2k^2) + 2ik^3}{\varkappa_b^2}.$$

Let us substitute in (9) the resultant expressions for ξ and χ, formula (4) for $\Phi_{l\tau}$, $\Psi_S = \text{const}$, and integrate over the angle variables. Accurate to a constant factor (independent of l and τ and therefore of no effect on the calculation of the relative probabilities) we obtain

$$c_{l\tau} = \sum_K a_K(1 + \delta_{K0})^{-1/2} f_{lK},$$

where $K \geqslant 0$ and even only, and

$$f_{lK} = \frac{1}{2}{}' \int [Y_{lK} + (-1)^l Y_{l,-K}] \exp\left\{\left[\frac{4}{5}\varkappa\left(1 - \frac{k^2}{2\varkappa_b^2}\right) - i\,\frac{2k^3}{5\varkappa_b^2}\right]\right.$$
$$\left.\times R_0\beta\left[\cos\gamma Y_{20} + \frac{\sin\gamma}{\sqrt{2}}(Y_{22} + Y_{2,-2})\right]\right\} d\Omega$$

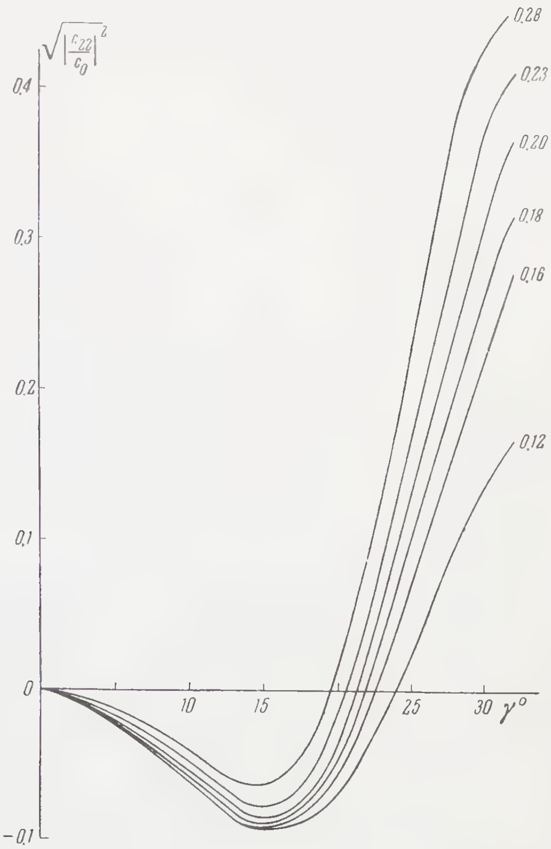

FIG. 2. Dependence of $\sqrt{|c_{22}/c_0|^2}$ on the nonaxiality parameter γ. The numbers on the curves have the same meaning as in Fig. 1.

For odd l, all the f_{lK} vanish, i.e., under the foregoing assumptions the α decay to levels with odd l is forbidden, in agreement with the experimental data. For even l, the integrals f_{lK} were evaluated numerically [with $\kappa R_0 (1 - k^2/2\kappa_b^2) = 16.2$], and the coefficients $a_K(l, \tau; \gamma)$ were taken from Davydov et al.[6,7] The values of $|c_{l\tau}/c_0|^2$ as functions of β and γ were obtained for $l = 2, 4, 6$ and $\tau = 1, 2$. It was found that $\text{Re}\, c_{l\tau} \gg \text{Im}\, c_{l\tau}$. For $l = 2$ the results are shown on the curves; it is more convenient to plot for the anomalous rotational band ($\tau = 2$) the quantities $\sqrt{|c_{22}/c_0|^2}$, using in front of the square root the same sign as for $\text{Re}(c_{22}/c_0)$.

The table lists the theoretical values of the relative α-decay probabilities, calculated for several nuclei, and the corresponding experimental values. The probability of decay to the ground level is assumed to be unity. The radius of the nucleus is calculated from the formula $R_0 = 1.2 \times 10^{-13} A^{1/3}$ cm. The nonaxiality parameter γ is determined from the energy ratio E_{22}/E_{21} of the first two levels with spin 2^+ (from E_{41}/E_{21} for Ra^{224}, Ra^{226}, and U^{234}). Where no experimental values were known for the E_{41} and E_{61} levels, the

Relative probabilities of α decay to rotational levels of even-even nuclei

Daughter nucleus	γ, deg	w_{21}/w_0, % exp.	$\sqrt{\frac{5}{4\pi}}\beta$	w_{22}/w_0, % theor.	w_{22}/w_0, % exp.	w_{41}/w_0, % theor.	w_{41}/w_0, % exp.	w_{61}/w_0, % theor.	w_{61}/w_0, % exp.	Reference
Rn^{218}	30	4.4	0,36	0.04	0.01	0,003	0,002	$5\cdot10^{-8}$*	—	[8]
Rn^{220}	26	5,0	0.27	0.014	0.01	0.003*	—	$5\cdot10^{-8}$*	—	[8]
Rn^{222}	25	6.1	0.32	0.006	0.013	0.003*	—	$4\cdot10^{-8}$*	—	[8]
Ra^{224}	22	39.5	0.31		—	0.43	0.3	$4\cdot10^{-4}$	weak	[9]
Ra^{226}	20	31.6	0.24		—	0.24	0.26	$1\cdot10^{-4}$	10^{-5}	[1,9]
Th^{228}	10	47.1	0.24	$2\cdot10^{-7}$	—	0.67	0.47	$6\cdot10^{-4}$*	—	[9]
Th^{230}	9	39	0.20	$4\cdot10^{-8}$	—	0.42	0.4	$3\cdot10^{-4}$*	—	[9]
U^{232}	9	44.8	0.20	$3\cdot10^{-6}$	—	0.70	0.26	0.001	0.003	[9]
U^{234}	13	38.8	0.18		—	0.53	0.13	0.001	0.006	[9]
Pu^{238}	8	35.7	0.16	$1\cdot10^{-6}$	$5\cdot10^{-6}$	0.48	0.05	$7\cdot10^{-4}$	0.008	[9]
Pu^{240}	8	30.3	0.15	$1\cdot10^{-6}$	—	0.35	0.02	$4\cdot10^{-4}$	0.005	[9,10]
Cf^{250}	8	20	0.11	$1\cdot10^{-5}$	—	0.18	0,3	$3\cdot10^{-4}$*	—	[9,11]

theoretical level positions determined from γ and E_{21} were used;[6,7] the probabilities of decay to these levels are designated by an asterisk. The nuclear deformation β was determined from the condition that the theoretical and experimental values of the α-decay probability be equal at the lower level with spin 2^+:

$$w_{21}^{\text{theor}} = w_{21}^{\text{exp}}. \tag{10}$$

We note that the ratio E_{22}/E_{21} does not determine γ uniquely, for the same result is obtained under the transformation $\gamma \rightarrow 60° - \gamma$. The course of the curve $|c_{21}/c_0|^2$ makes it possible to resolve this ambiguity. It is found that γ ranges from 0 to 30° for all the α-radioactive nuclei considered here. This follows from the fact that when $30° < \gamma \leq 60°$ the fulfillment of condition (10) necessitates impossibly high values of the deformation β.

For the main rotational band $(\tau = 1)$ the curves of $|c_{l1}/c_0|^2$ differ little in form. The curves of $|c_{41}/c_0|^2$ and $|c_{61}/c_0|^2$ fall off somewhat more rapidly than $|c_{21}/c_0|^2$ with increasing γ (for fixed β), but at the same time they increase more rapidly with increasing β (for fixed γ). This causes the theoretical probabilities of α decay to the levels of the main rotational band to depend little on the nonaxiality of the nucleus γ if β is determined from condition (10), and to make these values close to the probabilities obtained by Nosov[2] under the assumption of axial symmetry for the nucleus $(\gamma \rightarrow 0)$; for nonaxial nuclei, the deformations β must be assumed to be somewhat larger than for axial ones.

The theory of nonaxial nuclei makes it possible to calculate the probabilities of decay to the levels of the "anomalous" rotational band $(\tau = 2)$, particularly to the second level with spin 2^+. These probabilities are found to be strongly dependent on the nonaxiality of the nucleus γ. As can be seen from the table, agreement with experiment is found to be good for nuclei for which experimental data are available on the probabilities of α decay to the second level with spin 2^+.

In conclusion, I consider it my duty to thank Prof. A. S. Davydov for formulating the problem and for valuable remarks.

---

[1] J. O. Rasmussen and B. Segall, Phys. Rev. **103**, 1298 (1956).

[2] V. G. Nosov, Doklady Akad. Nauk SSSR **112**, 414 (1957), Soviet Phys.-Doklady **2**, 48 (1957); Izv. Akad. Nauk SSSR, Ser. Fiz. **21**, 1551 (1957), Columbia Tech. Transl. p. 1541.

[3] V. M. Strutinskii, JETP **32**, 1412 (1957), Soviet Phys.-JETP **5**, 1150 (1957).

[4] I. Perlman and J. O. Rasmussen, Alpha Radioactivity, Handbuch der Physik, **42**, 109 (1957).

[5] Gol'din, Adel'son-Vel'skii, Birzgal, Piliya, and Ter-Martirosyan, JETP **35**, 184 (1958), Soviet Phys. JETP **8**, 127 (1959).

[6] A. S. Davydov, and G. F. Filippov, JETP **35**, 440 (1958), Soviet Phys. JETP **8**, 303 (1959).

[7] A. S. Davydov and V. S. Rostovskii, JETP **36**, 1788 (1959), Soviet Phys. JETP **9**, 1275 (1959).

[8] Stephens, Asaro, and Perlman, Phys. Rev. **119**, 796 (1960).

[9] B. S. Dzhelepov and L. K. Peker, Схемы распада радиоактивных ядер (Decay Schemes of Radioactive Nuclei), Acad. Sci. U.S.S.R. (1958).

[10] Bunker, Dropesky, Knight, Starner, and Warlen, Phys. Rev. **116**, 143 (1960).

[11] Wandenbosch, Diamond, Sjoblom, and Fields, Phys. Rev. **115**, 115 (1959).

Translated by J. G. Adashko
240

SOVIET PHYSICS JETP VOLUME 13, NUMBER 5 NOVEMBER, 1961

DEPOLARIZATION OF μ^+ MESONS AND POLARIZATION OF Σ^+ PARTICLES IN A MAGNETIZED PARAMAGNETIC GAS

A. M. PERELOMOV

Submitted to JETP editor December 13, 1960

J. Exptl. Theoret. Phys. (U.S.S.R.) **40**, 1418-1422 (May, 1961)

A formula is derived for the degree of depolarization of polarized μ^+ mesons in a paramagnetic gas situated in a magnetic field. Exchange of electrons between the gas atoms and a μ^+e^- atom is taken into account. The degree of depolarization depends on the fraction of μ^+-mesons capturing an electron, on the probability of electron exchange, and on the magnetic field strength. The degree of polarization in a paramagnetic gas of initially unpolarized Σ^+ particles is also computed.

1. INTRODUCTION

In connection with the discovery of nonconservation of parity, the problem has arisen of the degree of depolarization of μ^+ mesons in a medium. In $\pi^+ \to \mu^+ + \nu$ decay the μ^+ mesons* are produced completely polarized. Such mesons are brought to rest in a time which is short compared to their lifetime. After slowing down† they capture electrons giving rise to muonium atoms‡ (μ^+e^-), and are partially depolarized as a result of the hyperfine interaction, i.e., the interaction between the magnetic moments of the meson and the electron. After the formation of muonium the meson polarization will be equal to ½, since in the $\mu^+_\uparrow e^-_\uparrow$ system the meson is not depolarized, while in the $\mu^+_\uparrow e^-_\downarrow$ system it is completely depolarized.

When unpolarized positively charged fermions, for example Σ^+ particles, are introduced into a magnetized paramagnetic gas the formation of atoms and the hyperfine splitting will lead to polarization of the particles, and the degree of polarization will be of the order of magnitude of the electron polarization and will be much greater than the polarization of Σ^+ corresponding to the magnetic field. Such a mechanism for the polarization of protons has been proposed by Zavoĭskii.[3]

Further depolarization depends on the electron exchange between an atom of μ^+e^- and the atoms of the surrounding medium and occurs only in a paramagnetic gas. At first sight it would seem that the greater the number of exchanges the more complete will be the depolarization. In actual fact the depolarization will be small if the probability of exchange is large. The non-occurrence of depolarization in the case of a large number of exchanges can be explained in the following manner: suppose that in a time corresponding to the hyperfine splitting, $\tau = \hbar/\epsilon$ (ϵ is half the hyperfine splitting energy), there occur n exchanges and $n > 1$. Then the depolarization during the time $\Delta t = \tau/n$ is equal to $(\Delta t/\tau)^2 = n^{-2}$, since transitions between states of the discrete spectrum occur in accordance with $1 - \cos(t/\tau)$. The depolarization during the time τ is equal to $1/n$. It can be seen that it tends to zero for a large number of exchanges. In other words, if the electrons are exchanged rapidly their magnetic field is averaged out and does not lead to a reversal of the meson spin. Such a possibility can be realized in a metal where the density of free electrons is great. However, if the probability of exchange is neither too great nor too small, then, since the meson lifetime is much greater than the time corresponding to the hyperfine splitting, there exists a broad range within which the mesons must be completely depolarized.

By placing a muonium atom in a magnetic field we decrease the average depolarization during a decay time. The effect of the magnetic field in the absence of exchange has been taken into account by Ferrell and Chaos.[4] In the work of Sens et al.[5] exchange has been taken into account. However, this has been taken into account only roughly: it was assumed that exchange occurs after exactly defined time intervals. Section 2 of the present paper gives exact formulas for the degree of depolarization taking exchange into account. Solutions of the equations are discussed in Sec. 3. A formula is given for the degree of polarization of initially unpolarized Σ^+ hyperons or of other positively charged fermions in a magnetized paramagnetic gas with exchange taken into account.*

---

*The word "mesons" will henceforth refer to μ^+ mesons.

†The depolarization of μ^+ mesons in the course of slowing down has been investigated by Ferrell, Lee, and Pal.[1]

‡The results of Hughes et al.[2] show that at least in some gases 100% production of muonium occurs.

It is not clear whether similar formulas can be used to explain the depolarization of μ^+ mesons in a solid, for example in an emulsion. From the formulas obtained it follows that the polarization must decrease with time exponentially. Swanson's experiments[6] show that in the majority of substances this does not occur. However, the formulas for polarization averaged over the meson decay time agreed well with the experimental data.[7]

2. DERIVATION OF EQUATIONS

We consider the mechanism of depolarization. We take the μ^+e^- atom to be situated in a magnetic field parallel to the z axis. Such a system obeys the following Schrödinger equation:

$$\mathcal{H}\psi = E\psi,$$

$$\mathcal{H} = \mathcal{H}_0 + \tfrac{16}{3}\pi g_1 g_2 \left(\tfrac{1}{4} + \mathbf{s}_1\mathbf{s}_2\right)\delta(\mathbf{r}) - g s_z H - G S_z H. \quad (1)$$

Here $\mathbf{r}_i$, m_i, $\mathbf{s}_i$, g_i are respectively the position vector, the mass, the spin and the gyromagnetic ratio in units of $e\hbar/2m_ic$ for the electron (subscript 1) and for the μ meson (subscript 2):

$$g = \tfrac{1}{2}(g_1 - g_2); \quad G = \tfrac{1}{2}(g_1 + g_2); \qquad \mathbf{s} = \mathbf{s}_1 - \mathbf{s}_2;$$
$$\mathbf{S} = \mathbf{s}_1 + \mathbf{s}_2; \qquad \mathbf{r} = \mathbf{r}_1 - \mathbf{r}_2.$$

If the energy is measured in units of $\epsilon = 8\pi g_1 g_2 |\psi(0)|^2/3 = 1.84 \times 10^{-5}$ ev, and the magnetic field is measured in units of $H_0 = \epsilon/g = 1580$ gauss, $x = H/H_0$, then the Hamiltonian assumes the following form

$$\mathcal{H} = \mathcal{H}_0 + \tfrac{1}{2}(1 + 4\mathbf{s}_1\mathbf{s}_2) - x s_z - G g^{-1} x S_z. \quad (2)$$

The eigenfunctions of this Hamiltonian $\mathcal{H}$ and its energy levels have the following form

$$\Psi_{11} = \varphi(r)\alpha(1)\alpha(2), \qquad E_{11} = E_0 - Gg^{-1}x;$$
$$\Psi_{1-1} = \varphi(r)\beta(1)\beta(2), \qquad E_{1-1} = E_0 + Gg^{-1}x;$$
$$\Psi_+ = \varphi(r)\,[(f+g)\alpha(1)\,\beta(2) + (f-g)\beta(1)\,\alpha(2)]/\sqrt{2},$$
$$E_+ = E_0 + \Delta;$$
$$\Psi_- = \varphi(r)\,[(f-g)\alpha(1)\,\beta(2) - (f+g)\beta(1)\,\alpha(2)]/\sqrt{2},$$
$$E_- = E_0 - \Delta, \quad (3)$$

where $\alpha(\beta)$ means that the particle spin is directed up (down),

$$f = \sqrt{{}^1/_2(1 + 1/\Delta)}; \qquad g = \sqrt{{}^1/_2(1 - 1/\Delta)},$$
$$\Delta = \sqrt{1 + x^2}. \quad (4)$$

The spin state of the system μ^+e^- is described by the density matrix $\rho(t)$ which has for its system of basis vectors

$$\chi_1 = \alpha_\mu\alpha_e, \quad \chi_2 = \alpha_\mu\beta_e, \quad \chi_3 = \beta_\mu\alpha_e, \quad \chi_4 = \beta_\mu\beta_e$$

and of all the off-diagonal elements only ρ_{23} and ρ_{32} differ from zero, while all the other off diagonal ρ_{ik} are equal to zero, since as the system develops freely in time states with different components of the spin along the z axis do not mix. The collisions in which the component of the spin of the system along the z axis are altered are incoherent ones and, therefore, the wave functions which after the collision correspond to different spin components are not related by definite phase relations.

The density matrix is found in the usual manner. If the system has the probability w^γ of being in the state $\Psi^\gamma = \sum_i c_i^\gamma \Psi_i$ where all the states Ψ^γ are incoherent with respect to each other, i.e., are not related by definite phase relations, then we have

$$\rho_{ik} = \sum_\gamma w^\gamma c_i^\gamma c_k^{\gamma *}.$$

For the average value of any physical quantity O specified by a matrix with respect to the same set of basis vectors we have $\langle O \rangle = \mathrm{Tr}(\rho O)$.

We write down the equation for the density matrix, taking into account the fact that the change of the density matrix per unit time is equal to the change of the density matrix as a result of its free development in time without collisions, $(d\tilde{\rho}/dt)$ plus its change as a result of collisions:

$$d\rho/dt = d\tilde{\rho}/dt + w(\rho' - \rho). \quad (5)$$

The first term may be obtained if we know the energy levels of the system in the magnetic field. By considering collisions of the μ^+e^- atom with the atoms of the surrounding medium under the condition that the medium contains equal numbers of atoms with any arbitrary spin component parallel to the direction of the magnetic field $(\mu H/kT \ll 1)$ we shall obtain ρ' (ρ' is the density matrix after the collision). Since Coulomb forces play the principal role in collisions, we need not take into account the spin of the μ meson and the interaction of the magnetic moment of the electron with the gas atom. Moreover, the equations involve the amplitudes a_+ and a_- for the exchange of an electron with a gas atom in states of total angular momentum respectively given by $j + \frac{1}{2}$ and $j - \frac{1}{2}$ (j is the spin of the gas atom). It turns out that the equations contain only the quantity w which is the probability that during the time τ the process $\mu^+e^-_\uparrow + A \rightarrow \mu^+e^-_\downarrow + A'$ will occur. It can be shown that w is proportional to $|a_+ - a_-|^2$, and this is natural, since it is specifically this quantity that is associated with the reversal of spin.

---

*We note that although the formation of the Σ^+e^- atom increases the effect of polarization of Σ^+, nevertheless, because of the short lifetime of Σ^+ this effect is small and, apparently, cannot be observed experimentally.

As a result of this we obtain the following system of equations (we have taken $\tau = \hbar/\epsilon$ for the unit of time):

$$d\rho_{11}/dt = -w(\rho_{11} - \rho_{22}), \qquad d\rho_{44}/dt = -w(\rho_{44} - \rho_{33}),$$
$$d\rho_{22}/dt = -w(\rho_{22} - \rho_{11}) + i(\rho_{23} - \rho_{32}),$$
$$d\rho_{33}/dt = -w(\rho_{33} - \rho_{44}) - i(\rho_{23} - \rho_{32}),$$
$$d\rho_{23}/dt = -2(w + i|x|)\rho_{23} + i(\rho_{22} - \rho_{33}),$$
$$d\rho_{32}/dt = -2(w - i|x|)\rho_{32} + i(\rho_{33} - \rho_{22}). \qquad (6)$$

In the formation of the μ^+e^- atom the meson is totally polarized, so that the initial conditions will be the following:

$$\rho_{11}(0) = {}^1/_2, \qquad \rho_{22}(0) = {}^1/_2, \qquad \text{all other } \rho_{ik}(0) = 0. \quad (7)$$

In the case when the particles capturing the electrons are unpolarized, but the gas is magnetized, the initial conditions will be

$$\rho_{11}(0) = n_\uparrow/2(n_\uparrow + n_\downarrow), \qquad \rho_{22}(0) = n_\downarrow/2(n_\uparrow + n_\downarrow),$$
$$\rho_{33}(0) = n_\uparrow/2(n_\uparrow + n_\downarrow), \qquad \rho_{44}(0) = n_\downarrow/2(n_\uparrow + n_\downarrow),$$
$$\text{all other } \rho_{ik} = 0. \qquad (8)$$

Here $n_\uparrow$ and $n_\downarrow$ are the numbers of electrons with the spins respectively up and down.

The polarization of the μ^+ mesons at time t is equal to

$$P(t) = \rho_{11}(t) + \rho_{22}(t) - \rho_{33}(t) - \rho_{44}(t). \qquad (9)$$

On averaging over the μ^+ meson lifetime we obtain

$$\overline{P} = \lambda \int_0^\infty P(t)e^{-\lambda t}dt, \qquad (10)$$

where λ is the probability of decay in the time τ, $\lambda \approx 10^{-5}$ for a μ meson.

3. DISCUSSION OF THE SOLUTIONS

On solving Eqs. (6) subject to the initial conditions (7) we obtain

$$\overline{P} = a\lambda\left[\frac{1}{\lambda + \alpha} - \frac{\alpha(\lambda + \alpha)}{\alpha\lambda^2 + (4w - \alpha)\alpha\lambda + 4w}\right]$$
$$- \frac{\alpha\lambda^2}{\alpha\lambda^2 + (4w - \alpha)\alpha\lambda + 4w},$$
$$a = (2w - \alpha)/[2w - \alpha^2(2w - \alpha)], \qquad (11)$$

where α is the real root of the equation

$$\mu^3 - 4w\mu^2 + 4(w^2 + \Delta^2)\mu - 4w = 0, \qquad (12)$$

Δ is defined by (4).

It follows from equation (12) that

$$w/(w^2 + \Delta^2) \leqslant \alpha \leqslant 4w/(w^2 + 4\Delta^2)$$

and that there are no other real roots. By neglecting terms of order λ^2 and λ we obtain

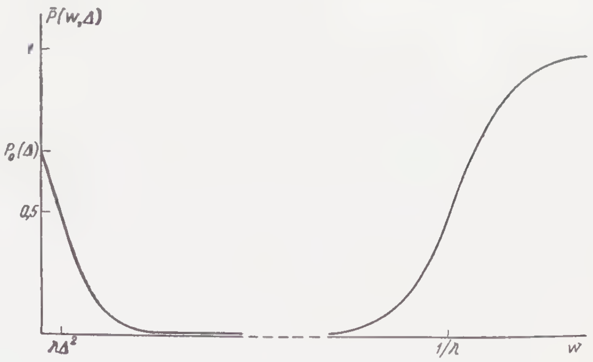

Graph of the function $\overline{P}(w, \Delta)$ for $\lambda \ll 1$, $\Delta \ll 1/\lambda$; $P_0(\Delta) = 1 - 1/2\Delta^2$.

$$P(t) = ae^{-\alpha t}, \qquad \overline{P} = \frac{2w - \alpha}{2w - \alpha^2(2w - \alpha)}\,\frac{\lambda}{\lambda + \alpha}. \qquad (13)$$

We see that $\overline{P}$ is not small only when $\alpha \lesssim \lambda$, i.e., for $w \ll \Delta$ and $w \gg \Delta$ (cf. diagram). In the case $w \ll \Delta$ we have

$$\overline{P} = \left(1 - \frac{1}{2\Delta^2}\right)\frac{1}{1 + w/\lambda\Delta^2}. \qquad (14)$$

If $w \ll \lambda\Delta^2$, then the usual formula is obtained (cf. reference 4)

$$\overline{P} = (1 - 1/2\Delta^2). \qquad (15)$$

For $w \gg \Delta$

$$\overline{P} = (1 + 1/\lambda w)^{-1}. \qquad (16)$$

If $w \gg 1/\lambda$, then $\overline{P} = 1$. When $\alpha \gg \lambda$ we have $\overline{P} \approx 0$.

If we take into account the fact that not all the μ mesons capture electrons we obtain

$$P = (1 - f) + f\overline{P}, \qquad (17)$$

where f is the fraction of mesons capturing electrons.

On solving (6) subject to the initial conditions (8) we obtain

$$\overline{P} = pb\left[\frac{\lambda}{\lambda + \alpha} - \frac{\lambda\alpha(\alpha + \lambda)}{\alpha\lambda^2 + (4w - \alpha)\alpha\lambda + 4w}\right],$$
$$b = \frac{\alpha}{2w + \alpha^2(\alpha - 2w)}, \qquad p = \frac{n_\uparrow - n_\downarrow}{n_\uparrow + n_\downarrow}. \qquad (18)$$

In the case $w \ll \Delta \ll \lambda$

$$\overline{P} = p\left[\frac{2}{\lambda^2} + \frac{w(4 - 3/\Delta^2)}{2\Delta^2\lambda}\right]. \qquad (19)$$

In the case $w \ll \lambda \ll \Delta$

$$\overline{P} = \frac{p}{2\Delta^2}\left[1 + \left(1 - \frac{1}{2\Delta^2} - \frac{1}{\lambda^2}\right)\frac{w\lambda}{\Delta^2}\right]. \qquad (20)$$

In conclusion, I express my gratitude to A. O. Vaĭsenberg on whose initiative this work has been carried out, and also to Academician Ya. B. Zel'dovich for directing this work.

---

[1] Ferrell, Lee, and Pal, Phys. Rev. **118**, 317 (1960).

[2] Hughes, McColm, Ziock, and Present, Phys. Rev. Letters **5**, 63 (1960).

[3] E. K. Zavoĭskii, JETP **32**, 408 (1957), Soviet Phys. JETP **5**, 338 (1957).

[4] R. A. Ferrell and F. Chaos, Phys. Rev. **107**, 1322 (1957).

[5] Sens, Swanson, Telegdi, and Yovanovich, Phys. Rev. **107**, 1465 (1957).

[6] R. A. Swanson, Phys. Rev. **112**, 580 (1958).

[7] A. O. Vaĭsenberg and V. A. Smirnit-skii, JETP **39**, 242 (1960), Soviet Phys. JETP **12**, 175 (1961).

Translated by G. Volkoff
241

SOVIET PHYSICS JETP VOLUME 13, NUMBER 5 NOVEMBER, 1961

QUASICLASSICAL PARTICLES IN A ONE-DIMENSIONAL PERIODIC POTENTIAL

A. M. DYKHNE

Institute for Radiophysics and Electronics, Siberian Section, Academy of Sciences, U.S.S.R.

Submitted to JETP editor, December 13, 1960

J. Exptl. Theoret. Phys. (U.S.S.R.) **40**, 1423-1426 (May, 1961)

The widths of the energy gaps in the spectrum of a quasiclassical particle in a one-dimensional periodic potential are calculated. The widths are found to be exponentially small. The factor in front of the exponential and the energy spectrum near the edge of the band are determined.

THE energy spectrum of a particle in a periodic field cannot be determined in the general case. Any specific computation can be carried out using perturbation theory only when the period potential is much smaller than the particle energy. The purpose of the present paper is to find the spectrum in the quasiclassical approximation.

We shall treat the one-dimensional case. The potential U is a periodic function of x with period L. The condition for quasiclassical behavior, $kL \gg 1$, where k is the quasimomentum of the particle, is assumed to be satisfied. If the energy of the particle E is less than the maximum value $U_{\max}$ of the potential, the dispersion can be determined by the usual WKB method.

However, if $E > U_{\max}$, the usual WKB method leads to an incorrect result. In fact, the quasiclassical wave function ($\hbar = 1$)

$$\psi(x) = p^{-1/2} \exp\left(i \int^{x} p\, dx\right) \tag{1}$$

has the form of a Bloch wave, and the dependence of the energy on quasimomentum is given by the equation

$$kL = \int_0^L p\, dx. \tag{2}$$

The spectrum thus obtained is continuous. However, we know very well that in the spectrum there actually are energy gaps which cannot be found by using the ordinary WKB method. In fact, as we shall see from the following, the width of the energy gaps is an exponentially small quantity and cannot be found by expansion in powers of a small parameter.

The method developed below is analogous to one proposed by Pokrovskii and Khalatnikov[1] for finding the amplitude for reflection at a barrier. The method enables one to determine the energy gaps with a relative accuracy 1/kL. We choose as our two linearly independent solutions of the Schrödinger equation two complex conjugate functions. When they are displaced by an amount equal to the period, these functions are transformed as follows:

$$f(x+L) = Df(x) + Rf^*(x),$$
$$f^*(x+L) = D^*f^*(x) + R^*f(x), \tag{3}$$

where R, D are certain constants.

From the condition of constancy of the Wronskian for f and f*, we have

$$|D|^2 = 1 + |R|^2. \tag{4}$$

Forming the general solution $\psi(x)$ from the functions (3), and writing the condition $\psi(x+L) = \lambda\psi(x)$, we get the dispersion equation in the usual way. It has the form

$$\lambda^2 - 2\lambda \operatorname{Re} D + 1 = 0. \tag{5}$$

So far we have not used the quasiclassical approximation. We now use it for calculating the quantity D. For this purpose we consider the behavior of the functions f(x) and f*(x) in the complex x plane. [U(x) is assumed to be an analytic function on the real axis.] Let us assume that the quantity $E - U(x)$ has simple zeros in the upper half plane at the points $x_n = x_0 + nL$ (where n is integral). We consider the behavior of the solutions f(x) and f*(x) on the line (l) along which $\operatorname{Im} \int_{x_0}^{x} p\, dx = 0$ and the line conjugate to it in the lower half plane. The approximate appearance of these curves is shown in the figure. At the points x_n these curves make an angle equal to $2\pi/3$.

As the function f(x) we choose a solution which behaves like $p^{-1/2} \exp[i(\tau - \tau_0)]$ on the segment l_1 ($\tau = \int^{x} p\, dx$, $\tau(x_0) \equiv \tau_0$). Since the point x_0 is the "turning point," to find the solution in the region l_2 we must join the quasiclassical solution with the solution of the Airy equation. Using the well-known formulas for joining at the turning point (cf., for example, reference 2), we find the solution over the region l_2 in the form

$$f(x+L) = p^{-1/2}\{\exp[i(\tau(x+L)-\tau_0)] \\ -i\exp[-i(\tau(x+L)-\tau_0)]\}. \tag{6}$$

This expression can be written as

$$f(x+L) = p^{-1/2}\{e^{i\varphi}\exp[i(\tau(x)-\tau_0)] \\ -ie^{-i\varphi}\exp[-i(\tau(x)-\tau_0)]\},$$

$$\varphi = \int_0^L p\,dx. \tag{7}$$

On the level line $\mathrm{Im}(\tau-\tau_0) = 0$ both exponents in (7) are of the same order, so that this form is correct. Furthermore we note that the function $f^*(x)$ on the curve l^* behaves like $p^{-1/2} \times \exp[-i(\tau-\tau_0^*)]$. In extending it from the line l^* to l it increases. Therefore on the line l the function $f^*(x)$ will behave like

$$f^*(x) = p^{-1/2}\{\exp[-i(\tau-\tau_0^*)] + A\exp[i(\tau-\tau_0)]\}. \tag{8}$$

The coefficient A in the decreasing exponential remains undetermined in this continuation, but the coefficient in the increasing exponential is not changed.

Comparing (7) and (8) we can find the coefficient R which enters in (3). It is equal to

$$R = i\exp[i(\tau_0-\tau_0^*)](1+O(1/kL)). \tag{9}$$

The modulus of the quantity D is determined from (4) and (8). As we see from (7),

$$\arg D = \varphi(1+O(1/kL)). \tag{10}$$

The forbidden energy bands are determined from the condition of reality of λ in equations (5). Thus we have

$$|\cos\varphi| \geqslant 1-|R|^2/2. \tag{11}$$

For the center of the n-th energy gap E_n, we find from (11) and (7) the well-known expression

$$\int_0^L \sqrt{2m(E_n-U)}\,dx = \pi n(1+O(1/kL)).$$

For the width of the gap we get

$$\Delta_n = \frac{2}{T_n}\exp\left[i\int_{x_0^*}^{x_0}\sqrt{2m(E-U)}\,dx\right](1+O(1/kL)). \tag{12}$$

Here T_n is the time of passage of a classical particle with energy E_n through one period of the potential.

As we see from (12), the widths of the energy gaps are actually exponentially small. As for the positions of the energy gaps, they are determined only to within the accuracy of a power.

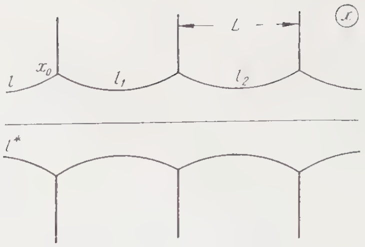

The expressions obtained above correspond to the case

$$U_{max}kL/E \gg 1, \qquad (1-U_{max}/E)kL \gg 1. \tag{13}$$

In similar fashion we can also treat other cases

$$\frac{U_{max}}{E}kL \lesssim 1, \qquad \left(1-\frac{U_{max}}{E}\right)kL \lesssim 1.$$

In the first of these cases the zeros of the function $p^2(x)$ are located near the poles of the function $U(x)$. Then for the determination of the quantities R, D one must use the hypergeometric equation in place of the Airy equation.

In the second case, the zeros x_0 and x_0^* of the function $p^2(x)$ are close to one another. Then for the joining of the quasiclassical wave functions one must use parabolic cylinder functions. However, as it is easy to show, the value arg D in both cases can be taken from equation (10), while the value of R formally coincides with the amplitude for reflection of the particle from the potential field, vanishing as $x \to \pm\infty$.

Using the results of references 3 and 4, where the calculation of R was done respectively for the first and second cases, we obtain the following expressions for the widths of the energy gaps. In the first case

$$\Delta_n = \frac{2}{T_n}|F(\mu_n)|\exp\left[i\int_{x_0^*}^{x_0}\sqrt{2m(E-U)}\,dx\right],$$

$$\left(1-\frac{U_{max}}{E}\right)kL \gg 1. \tag{14}$$

Here $\mu_n = \sqrt{2m/E_n}\,U_0$, U_0 is the residue of the function $U(x)$ at the pole which is nearest to the zero of x_0,

$$F(\mu) = \frac{2\pi\exp[i\mu\ln(i\mu/2e)]}{\Gamma(i\mu/2)\Gamma(1+i\mu/2)}. \tag{15}$$

In the second case we have

$$\Delta_n = \frac{2}{T_n}\left[2\,\mathrm{ch}\left(2i\int_{x_0^*}^{x_0}\sqrt{2m(E-U)}\,dx\right)\right]^{-1/2}, \qquad \frac{U_{max}}{E}kL \gg 1. \tag{16}$$

It is not difficult to see that formula (12) is obtained from (14) and (16) for the case when both inequalities (13) are satisfied.

In all the cases treated, the energy spectrum near the edges of the zones differs markedly from (2). Relatively simple computations lead to the rule

$$E = E_n \pm \sqrt{(\Delta_n/2)^2 + v_n^2(\Delta k_n)^2}, \qquad L\Delta k_n \ll 1, \quad (17)$$

where v_n is the velocity of a classical particle with energy E_n; $\Delta k_n = k - \pi n/L$; and the quantity Δ_n is taken from (12), (14), or (16).

The author is grateful to V. L. Pokrovskii for valuable comments.

[1] V. L. Pokrovskii and I. M. Khalatnikov, JETP **40**, 1713 (1961), Soviet Phys. JETP, in press.

[2] L. D. Landau and E. M. Lifshitz, Quantum Mechanics, Pergamon Press, 1958.

[3] Pokrovskii, Ulinich, and Savvinykh, JETP **34**, 1629 (1958), Soviet Phys. JETP **7**, 1119 (1958).

[4] V. A. Fock, Радиотехника и электроника (Radio Engineering and Electronics) **1**, 560 (1956).

Translated by M. Hamermesh
242

SOVIET PHYSICS JETP VOLUME 13, NUMBER 5 NOVEMBER, 1961

NORMALIZATION OF THE WAVE FUNCTIONS OF QUASISTATIONARY STATES

A. M. DYKHNE and A. V. CHAPLIK

Institute of Radiophysics and Electronics, Siberian Branch, Academy of Sciences, U.S.S.R.

Submitted to JETP editor December 13, 1960

J. Exptl. Theoret. Phys. (U.S.S.R.) **40**, 1427-1428 (May, 1961)

A method is given for determining the norm of quasistationary states. This method does not depend on any assumption about the spherical symmetry of the potential and is much simpler than that proposed by Zel'dovich.[1]

As is well known, quasistationary states can be described approximately by means of a stationary Schrödinger equation with complex energy values. If we attempt to use perturbation theory for these states, then a difficulty is brought about by the divergence of the normalization integral. A method of determining the norm in this case was pointed out by Zel'dovich,[1] and involved a number of rather subtle analyses.

We wish to turn attention to a simpler method of determining the normalization integral. Its use is not limited to a spherically symmetric potential, which was the case considered by Zel'dovich.

Our assertion amounts to the following. The wave functions of the quasistationary states must be so normalized that

$$\int_{\tilde{V}} \psi_E^2 \, d\tau = 1. \tag{1}$$

Integration over $\tilde{V}$ means that in integration in spherical coordinates the integral over r is computed along some contour C which lies in the upper half-plane.

The contour C must satisfy two requirements: 1) the integral (1) must converge; 2) there must be no singularities in the potential $V(r, \theta, \varphi)$, between the contour C and the real axis r for any θ and φ considered as parameters.

If the potential is a piecewise analytic function for real r, then the contour C runs along the real axis up to some point R lying to the right of all points of discontinuity of the analyticity. In this case, analytic continuation of the potential can be performed in the complex plane from the last region of analyticity $(r > R)$.

The proof of the assertion made above lies in the fact that the transition to the contour C can be carried out even for a non-stationary Schrödinger equation, that is, for an exact formulation of the problem. Because of the requirements on the contour C mentioned above, such a transition cannot cause any objection.

In accomplishing such a transition, we must solve the Schrödinger equation in the space $\tilde{V}$. In this case, a solution, which behaves asymptotically (for large r) as $f(\theta, \varphi) e^{ikr}/r$, falls off exponentially in $\tilde{V}$, as a consequence of which all the integrals containing the wave functions converge.

We note that, in spite of the fact that the wave functions vanish at infinity, the energy values are complex because of the non-Hermitian character of the Hamiltonian in $\tilde{V}$. It is obvious that for complex values of the energy $E = E_0 + i\gamma$ the contour C must (as $r \to \infty$) make an angle $\alpha > \gamma/E_0$ with the real axis in order that the normalization integral converge.

If the wave functions are normalized by means of (1), then perturbation theory, and also an expansion in the quasistationary states, can be carried out exactly the same as was done in the case of stationary states. It is not difficult to prove that, for the cases considered by Zel'dovich,[1] our definition (1) leads to his results. For example, for the spherically symmetric potential $V(r)$, which vanishes for $r > R$, we get in the s state:

$$\frac{1}{4\pi}\int_{\tilde{V}} \psi^2 \, d\tau = \int_{V} \left(\psi^2(r) - \frac{C^2 e^{2ikr}}{r^2} \right) r^2 \, dr + \int_{\tilde{V}} \frac{C^2 e^{2ikr}}{r^2} r^2 \, dr,$$

$$\psi(r) \sim C e^{ikr}/r \text{ for } r \to \infty. \tag{2}$$

The first integral on the right hand side of (2) converges, and it can be taken along the real axis. Thus,

$$\frac{1}{4\pi}\int_{\tilde{V}} \psi^2 \, d\tau = \int_0^\infty \left(\psi^2(r) - r^{-2} C^2 e^{2ikr} \right) r^2 \, dr - C^2/2ik,$$

which is identical with the result of Zel'dovich.

---

[1] Ya. B. Zel'dovich, JETP **39**, 776 (1960), Soviet Phys. JETP **12**, 542 (1961).

Translated by R. T. Beyer
243

SOVIET PHYSICS JETP VOLUME 13, NUMBER 5 NOVEMBER, 1961

ROTATIONAL STATES OF ODD NUCLEI WITH SMALL NONAXIALITY

A. S. DAVYDOV and R. A. SARDARYAN

Moscow State University

Submitted to JETP editor December 15, 1960

J. Exptl. Theoret. Phys. (U.S.S.R.) **40**, 1429-1433 (May, 1961)

We compute the dependence of the energy spectrum of the excited states of odd nuclei with spin $^5/_2$ in the ground state on the ratio of the rotational energy to the coupling energy between the external nucleon and nonspherical part of the core potential.

INTRODUCTION

THE presence of an "energy gap" in the spectrum of single-nucleon states of even-even nuclei facilitates the separation of collective excitations that correspond to the rotation of the nucleus and to the change in the form of its surface. In odd nuclei the energy of single-nucleon excitations differs little from the energy of collective excitations, and they can therefore be separated only in some particular cases. The interaction between rotation of the nucleus and the motion of an external nucleon changes the structure of the rotational spectrum corresponding to the adiabatic approximation.

To investigate low excited states of odd atomic nuclei we consider a nucleon model consisting of a core and one outer nucleon. We assume that the form of the nucleus differs little from an ellipsoid of revolution (low nonaxiality).

Nuclei with ground-state spins $^1/_2$ or $^3/_2$ call for a special analysis (see, for example, references 1 and 2). We shall therefore investigate in the present article the case of nuclei whose ground-state spin is $^5/_2$. The same method can be extended to include nuclei with larger spins. It will be shown that the sequence of spins of the first excited states and the ratio of their energies are determined by a single parameter, corresponding to the ratio of the rotational energy to the energy of interaction between the external nucleon and the nonspherical part of the potential of the nuclear core.

1. ENERGY STATES

The Hamiltonian operator of a system consisting of a nuclear core and one nucleon can be written in the form

$$H = H_p + H_r + H_{int}. \qquad (1.1)$$

Here H_p is the Hamiltonian operator of the internal state of the nuclear core and the external nucleon in a centrally-symmetrical field;

$$H_r = \sum_i a_i (\hat{I}_i - \hat{j}_i)^2 \qquad (1.2)$$

is the rotational-energy operator, where $\hat{I}_i$ and $\hat{j}_i$ are respectively the projections of the total angular momentum and of the momentum of the outer nucleon on the coordinate axes fixed in the nucleus, and a_i are quantities determined by the moments of inertia of the nucleus;

$$H_{int} = -T\beta \{\cos\gamma (3\hat{j}_3^2 - \hat{j}^2) + \sqrt{3}\sin\gamma (\hat{j}_1^2 - \hat{j}_2^2)\}. \qquad (1.3)$$

The Schrödinger equation with the Hamiltonian operator (1.1) reduces to systems of algebraic equations for each value of the total momentum I, if we seek the solution in the form

$$\Psi_\tau (I) = \sum_{K,\Omega>0} A^{I\tau}_{K\Omega} \sqrt{\frac{2I+1}{16\pi^2}} \{D^I_{mK}\varphi^j_\Omega + (-1)^{I-j} D^J_{m,-K}\varphi^j_{-\Omega}\}, \qquad (1.4)$$

where D^I_{mK} are generalized spherical functions determining the orientation of the nucleus in space; φ^j_Ω are the wave functions of the external nucleon in the coordinate system fixed in the nucleus.

In the case of small nonaxiality $\gamma \approx 0$ and we can retain in the operator (1.3) only the first term, putting $\cos\gamma \approx 1$. We can then put in (1.2) $a_1 = a_2$, and finally it is necessary to put in (1.4) $K = \Omega$, so that the double summation reduces to summation over K only. If we use the matrix elements of operators (1.2) and (1.3) with wave functions (1.4) as given by O. Bohr,[1] the problem of determining the energy of the excited states of the nucleus reduces to a solution of secular equations of the type

$$|\langle l | H_r + H_{int} | K \rangle - E(I)\delta_{lK}| = 0 \qquad (1.5)$$

for each value of the total angular momentum I.

Equation (1.5) will contain only two parameters: $D = a_1 + a_2$ and $T\beta$. Thus, the excitation energies, measured in $T\beta$ units, depend only on one parameter $\xi = D/\beta T$. The figure shows the results of the calculations for the case of nuclei with $j = {}^5/_2$.

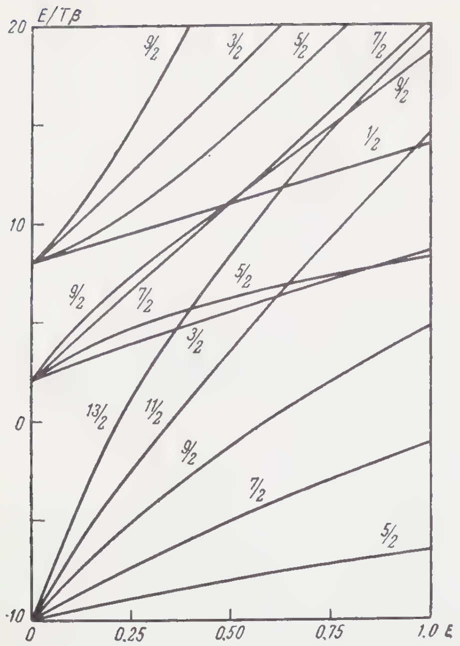

In using the figure, it is necessary to reckon the energy from the first line corresponding to a nuclear ground-state spin $5/2$. When $\xi < 0.25$, the spectrum of the excited states breaks up into three bands. The first band with spin sequence $5/2$, $7/2$, $9/2$, $11/2$, and $13/2$ can be called the "main rotational band." However, the rules governing the spacing of these levels differ from the rules derived from the adiabatic theory of rotational states for axially-symmetrical nuclei:

$$E_J = A\{I(I+1) - I_0(I_0+1)\}. \tag{1.6}$$

In particular, when $I = 5/2$ the interval rule following from (1.6) is

$$E_{7/2} : E_{9/2} : E_{11/2} : E_{13/2} : \ldots = 1 : 2.29 : 3.86 : 5.76 : \ldots .$$

Table I. Spins and energies (kev) of the levels of U^{233}

Theory (ξ=0.25)	Experiment[3]	Theory (ξ=0.25)	Experiment[3]
$5/2$ 0	$5/2$ 0	$5/2$ 342	$5/2$ 341
$7/2$ 40	$7/2$ 40	$7/2$ 387	$1/2$ 400
$9/2$ 92.5	$9/2$ 92	$9/2$ 405	$3/2$ 417
$3/2$ 318	$3/2$ 313		

As can be seen from the figure, the relative distances between levels of the "main rotational band" depend on the value of ξ. When $\xi = 0.25$, the interval rule for these levels reduces to 1 : 2.3 : 4.0 : 6.3, and when $\xi = 1$, the interval rule has the form 1 : 2.1 : 3.9 : 4.8.

Tables I, II, and III list the theoretical and experimental values of spins and energies of the levels of the odd nuclei U^{233}, Np^{237}, and Th^{229}. The parameter ξ is determined from the first two experimental values of the energies of the levels with the same parity.

2. PROBABILITIES OF ELECTROMAGNETIC TRANSITIONS BETWEEN EXCITED STATES

To each value of the total momentum $I = 1/2, 3/2, \ldots$ there will correspond, generally speaking several energy levels which can be distinguished by the index $\tau = 1, 2, \ldots$ Consequently, the excited states will be characterized by two numbers, I and τ. Knowing the energies $E_{I\tau}$, we can readily calculate the coefficients $A_K^{I\tau} = A_{KK}^{I\tau}$, which determine with the aid of (1.4) the wave functions of the excited states of the nucleus, and then calculate the probabilities of electromagnetic transitions between these states.

In the case of nuclei with small nonaxiality, the operator of electric quadrupole transitions has the form

$$Q_{2\mu} = eQ_0 D^2_{\mu 0}, \tag{2.1}$$

where e is the unit electric charge and Q_0 is the internal quadrupole moment. The reduced probability of the electric quadrupole transitions is expressed in terms of the coefficients $A_K^{I\tau}$ with the aid of the formula

$$B(E2;\ I\tau \to I'\tau') = \frac{5e^2Q_0^2}{16\pi}\left|\sum_K A_K^{I'\tau'} A_K^{I\tau}(2I0K \mid I'K)\right|^2. \tag{2.2}$$

The operator of magnetic dipole transition is

$$\mathfrak{M}(1\nu) = (-1)^\nu \sqrt{\frac{3}{4\pi}}\,\mu_0 (g_j - g_R) \sum_{\mu=-1}^{1} D^1_{\nu\mu} \hat{j}_\mu, \tag{2.3}$$

Table II. Spins and energies (kev) of levels of Np^{237}

Levels with positive parity		Levels with negative parity	
Theory (ξ=0.30)	Experiment[4]	Theory (ξ=0.45)	Experiment[4]
$5/2$ 0	$5/2$ 0	$5/2$ 0	$5/2$ 0+59.6
$7/2$ 33.2	$7/2$ 33,2	$7/2$ 43.4	$7/2$ 43.4+59.6
$9/2$ 76.7	$9/2$ 76,4	$9/2$ 99.5	$9/2$ 98.9+59.6
$1/2$ 324	$1/2$ 332.3	$11/2$ 173	$11/2$ 165.4+59.6
$5/2$ 352	$5/2$ 368.5	$3/2$ 213	$3/2$ 207,9+59.6
$3/2$ 390	$3/2$ 371	$5/2$ 226	— —
		$13/2$ 245	$13/2$ 345.4+59.6

Table III. Spins and energies (kev) of levels of Th^{229}

Levels of positive parity		Levels with negative parity	
Theory ($\xi = 0.25$)	Experiment[5]	Theory ($\xi = 0.50$)	Experiment[5]
$^5/_2$ 0	$^5/_2$ 0	$^5/_2$ 0	$^5/_2$ 0+29
$^7/_2$ 42.3	$^7/_2$ 42.3	$^7/_2$ 43	$^7/_2$ 43+29
$^9/_2$ 97.7	$^9/_2$ 97	$^9/_2$ 96.5	$^9/_2$ 97+29
$^{11}/_2$ 169	$^{11}/_2$ 163	$^{11}/_2$ 166	$^{11}/_2$ 166+29
$^{13}/_2$ 267	$^{13}/_2$ 237		
$^3/_2$ 335	$^3/_2$ 316		
$^5/_2$ 359	$^5/_2$ 364		

Table IV. Reduced probabilities of E2 and M1 transitions for nuclei with $\xi = 0.25$ between the states $I\tau \to I'\tau'$

Transition $I\,\tau \to I'\tau'$	$\frac{B(E2)}{e^2Q_0^2}$	$\frac{B(M1)}{\mu_0^2(g_j - g_R)^2}$	Transition $I\tau \to I'\tau'$	$\frac{B(E2)}{e^2Q_0^2}$	$\frac{B(M1)}{\mu_0^2(g_j - g_R)^2}$
$^9/_2 1 \to {}^5/_2 1$	1.0	—	$^5/_2 2 \to {}^3/_2 1$	3.0	0.22
$^9/_2 1 \to {}^7/_2 1$	3.0	0.37	$^5/_2 2 \to {}^7/_2 1$	0.002	0.27
$^7/_2 1 \to {}^5/_2 1$	3.5	0.27	$^5/_2 2 \to {}^5/_2 1$	0.005	0.12
$^3/_2 1 \to {}^5/_2 1$	0.041	0.41	$^5/_2 2 \to {}^9{}_{12} 1$	0.03	
$^3/_2 1 \to {}^7/_2 1$	0.067	—			

where μ_0 is the nuclear magneton, g_j and g_R are respectively the gyromagnetic ratios for the single-nucleon and collective motions, and $\hat{j}_\mu$ are the spherical projections of the operator of angular momentum of the nucleon and the coordinate system fixed in the nuclear core. The action of the operator $\hat{j}_\mu$ on the wave function of the nucleon is determined by the equation

$$\hat{j}_\mu \varphi_K^j = (-1)^\mu \sqrt{j(j+1)}\,(j1K+\mu, -\mu \mid jK)\,\varphi_{\mu+K}.$$

With the aid of the functions (1.4) and the operator (2.3) we determine the reduced probability of magnetic dipole transition

$$B(M1;\ I\tau \to I'\tau') = (3/4\pi)\mu_0^2(g_j - g_R)^2$$
$$\times \Big| \sum_{\mu,K} (-1)^\mu A_{K+\mu}^{I'\tau'} A_K^{I\tau} (j1K+\mu,$$
$$-\mu \mid jK)(1I\mu K \mid I', K+\mu)$$
$$- (-1)^{I'-j} A_{1/2}^{I'\tau'} A_{1/2}^{I\tau} (j1 - {}^1/_2 1 \mid j\,{}^1/_2)(1I - 1\,{}^1/_2 \mid I', -{}^1/_2) \Big|^2. \tag{2.4}$$

When summing over μ and K in (2.4), it is necessary to sum over all positive values of K when $\mu = 0$ and 1, and to sum only over the values $K \geq {}^3/_2$ when $\mu = -1$.

Table IV lists the values of the reduced probabilities of quadrupole electric and dipole magnetic transitions between the first collective excited states of nuclei with ground-spin state $^5/_2$ and $\xi = 0.25$, as calculated from formulas (2.2) and (2.4).

---

[1] A. Bohr, Dan. Math. Fys. Medd. **26**, 14 (1952).

[2] A. S. Davydov, Nucl. Phys. **16**, 597 (1960).

[3] Bisgard, Dahl, and Ofesen, Nucl. Phys. **12**, 612 (1959).

[4] B. S. Dzhelepov and L. P. Peker, Схемы распада радиоактивных ядер (Decay Schemes of Radioactive Nuclei) Academy of Sciences U.S.S.R., (1958).

[5] Dzhelepov, Ivanov, Nedovesov, and Puzynovich, Izv. Akad. Nauk SSSR, Ser. Fiz. **24**, 258 (1960), Columbia Technical Translations, p. 247.

Translated by J. G. Adashko
244

SOVIET PHYSICS JETP VOLUME 13, NUMBER 5 NOVEMBER, 1961

STABILITY OF MAGNETIC TANGENTIAL DISCONTINUITIES IN RELATIVISTIC HYDRODYNAMICS

M. T. ZHUMARTBAEV

Institute of Nuclear Physics, Academy of Sciences, Kazakh S.S.R.

Submitted to JETP editor December 15, 1960

J. Exptl. Theoret. Phys. (U.S.S.R.) **40**, 1434-1439 (May, 1961)

Small perturbations of the discontinuity surface in relativistic magnetohydrodynamics are examined. It is shown that in the case of small perturbations the magnetic tangential discontinuity is conserved as such. Stability of magnetic tangential discontinuities is investigated. In particular, their instability region is determined in the ultrarelativistic case.

1. INTRODUCTION

THE stability of magnetic tangential discontinuities in nonrelativistic hydrodynamics was investigated by Syrovat-skii.[1,2] He came to the important conclusion that the magnetic field stabilizes the flow. In this connection, great interest is attached to investigations of the stability of a magnetic tangential discontinuity in relativistic hydrodynamics. In the first part of the present article we derive the boundary conditions for a perturbed discontinuity on the basis of the general Lorentz transformation.* It follows from these conditions that the magnetic tangential discontinuity is conserved as such under small perturbations.

In the second part we investigate the stability of a magnetic tangential discontinuity. Conditions are derived for the stability in two particular cases, of large and small angles between the wave vector $\mathbf{k}_0$ and the direction common to the parallel vectors **v** and **H**. All the calculations were made for a medium with infinite conductivity, and in the nonrelativistic approximation the final formulas go into those obtained by Syrovat-skii.[1,2]

2. PERTURBATION OF DISCONTINUITY SURFACE

In the coordinate system tied to the unperturbed discontinuity, the following conservation laws apply on the normal to the discontinuity surface:

$$\{Wu_f^2 + p + (H^2 - 2H_f^2 + E^2 - 2E_f^2)/8\pi\} = 0, \quad (2.1)$$

$$\{Wu_f u_\tau - (H_f H_\tau + E_f E_\tau)/4\pi\} = 0, \quad (2.2)$$

$$\{Wu_f u_4 + i([\mathbf{EH}]\mathbf{f})/4\pi\} = 0, \quad (2.3)\dagger$$

$$\{nu_f\} = 0, \quad (2.4)$$

$$\{H_f\} = 0, \quad (2.5)$$

$$\{\mathbf{E}\tau\} = 0 \quad (2.6)$$

where **f** is a unit vector normal to the discontinuity surface, τ the direction of the tangent, and W the heat function per unit volume; the braces denote the difference between the corresponding values on the two sides of the discontinuity.

We now change to a coordinate system in which the normal velocity of the perturbed discontinuity is zero. We make the change with the aid of the general Lorentz formula for the velocity and the field. The normal **f** and the two independent directions τ_1 and τ_2 tangent to the perturbed discontinuity surface have the following components

$$\mathbf{f}(1, -\partial\xi/\partial y, -\partial\xi/\partial z), \qquad \tau_1(\partial\xi/\partial y, 1, 0),$$
$$\tau_2(\partial\xi/\partial z, 0, 1).$$

We can then readily obtain in the new system of coordinates, the boundary conditions on the perturbed discontinuity accurate to terms up to second order of smallness relative to the perturbations of the velocity $\delta\mathbf{v}$ and of the field **h** (in the case of infinite conductivity), using Eqs. (2.1) – (2.6) for the parameters of the unperturbed discontinuity.

After simple transformations, introducing the notation

$$h_\mathrm{f} = h_x - H_y\partial\xi/\partial y - H_z\partial\xi/\partial z, \qquad \gamma = \sqrt{1 - v^2/c^2},$$
$$v_f + \delta v_f = \delta v_x - \partial\xi/\partial t - v_y\partial\xi/\partial y - v_z\partial\xi/\partial z, \quad (2.7)$$

we obtain the following boundary conditions for the tangential discontinuity ($v_x = 0$, $H_x = 0$):

$$\left\{\delta p + \frac{1}{4\pi}\left[(\mathbf{Hh}) + \frac{1}{c^2}[\mathbf{vH}]_x([\mathbf{H}\delta\mathbf{v}]_x - [\mathbf{vh}]_x)\right]\right\} = 0, \quad (2.8)*$$

---

*The need for using the general Lorentz transformation in the solution of three-dimensional problem is mentioned by Stanyukovich.[3] The same reference considers several general transformations for a medium with variable μ and ε.

†$[\mathbf{E\,H}] = \mathbf{E} \times \mathbf{H}$.

*$(\mathbf{H\,h}) = \mathbf{H} \cdot \mathbf{h}$.

$$\left\{\frac{w}{\gamma}+\frac{H^2}{4\pi n}\gamma\right\}\frac{n\,(v_f+\delta v_f)}{\gamma}=\frac{1}{4\pi}\left\{(\mathbf{vH})\right\}h_f, \qquad (2.9)$$

$$\frac{1}{4\pi}\left\{H_y+\frac{v_z}{c^2}[\mathbf{vH}]_x\right\}h_f=\left\{\frac{wv_y}{c^2\gamma}+\frac{[\mathbf{vH}]_x}{4\pi nc^2}\gamma\right\}\frac{n\,(v_f+\delta v_f)}{\gamma}, \qquad (2.10)$$

$$\frac{1}{4\pi}\left\{H_z-\frac{v_y}{c^2}[\mathbf{vH}]_x\right\}h_f=\left\{\frac{wv_z}{c^2\gamma}-\frac{[\mathbf{vH}]_x}{4\pi nc^2}\gamma\right\}\frac{n\,(v_f+\delta v_f)}{\gamma}, \qquad (2.11)$$

$$\{v\ \}\,h_f=\left\{\frac{1}{n}H_y\gamma\right\}\frac{n\,(v_f+\delta v_f)}{\gamma}, \qquad (2.12)$$

$$\{v_z\}\,h_f=\left\{\frac{1}{n}H_z\gamma\right\}\frac{n\,(v_f+\delta v_f)}{\gamma}, \qquad (2.13)$$

where w is the heat function per particle.

The system of five equations (2.9) — (2.13) for the two unknowns h_f and $n\,(v_f+\delta v_f)/\gamma$ admits of only one vanishing trivial solution

$$h_f=h_x-H_y\partial\xi/\partial y-H_z\partial\xi/\partial z=0,$$
$$v_f+\delta v_f=\delta v_x-\partial\xi/\partial t-v_y\partial\xi/\partial y-v_z\partial\xi/\partial z=0. \qquad (2.14)$$

Thus, the magnetic tangential discontinuity is conserved as such under small perturbations.

3. STABILITY OF MAGNETIC TANGENTIAL DISCONTINUITY

For perturbations of the form $\exp i\,(\mathbf{k}\cdot\mathbf{r}-\omega t)$, we can readily reduce the system $\partial T_i^k/\partial x^k=0$, using Maxwell's and the continuity equations, to a system of equations in three unknowns δv_x, δv_y, and δv_z. The required existence of a nontrivial solution of such a system leads to a dispersion equation of the form

$$a_1\omega_0^6+a_2\omega_0^5+a_3\omega_0^4+a_4\omega_0^3+a_5\omega_0^2+a_6\omega_0+a_7=0, \qquad (3.1)$$

where $\omega_0=\mathbf{k}\cdot\mathbf{v}-\omega$, and the coefficients are algebraic functions of W, the velocity of sound c_0, k^2, $(\mathbf{k}\cdot\mathbf{v})$, etc.

We can separate from (3.1) the factor

$$F=\left[1+\gamma^2\frac{H^2}{4\pi W}\right]\frac{\omega_0^2}{\gamma^2}-\frac{(\mathbf{vH})\,(\mathbf{kH})}{2\pi W}\omega_0-\frac{c^2\,(\mathbf{kH})^2}{4\pi W}\gamma^2. \qquad (3.2)$$

The equation $F=0$ yields a solution, known to be stable, with real ω, and can be discarded.

Separation of the second factor yields

$$\begin{aligned}&\frac{1}{\gamma^4}\left\{\left[1+\gamma^2\frac{H^2}{4\pi W}\right]+\frac{(1-c_0^2/c^2)}{c^2\gamma^2}\left[v^2+\gamma^2\frac{(\mathbf{vH})^2}{4\pi W}\right]\right\}\omega_0^4\\&-\frac{1}{\gamma^4}\left\{2\frac{c_0^2}{c^2}\left[\mathbf{kv}+\gamma^2\frac{(\mathbf{vH})\,(\mathbf{kH})}{4\pi W}\right]+\frac{\mathbf{kv}}{2\pi W}\left[\gamma^2H^2\right.\right.\\&\left.\left.+\left(1-\frac{c_0^2}{c^2}\right)\frac{(\mathbf{vH})^2}{c^2}\right]\right\}\omega_0^3-\frac{1}{\gamma^2}\left\{\left\langle\frac{c^2}{4\pi W}\left[H^2+\frac{(1-c_0^2/c^2)}{c^2\gamma^2}(\mathbf{vH})^2\right]\right.\right.\\&\left.+\frac{c_0^2}{\gamma^2}\right\rangle\left[k^2-\frac{1}{c^2}(\mathbf{kv})^2\right]+\left.\frac{c_0^2\mathbf{kH}}{4\pi W}\left[\gamma^2\mathbf{kH}-4\frac{(\mathbf{kv})\,(\mathbf{vH})}{c^2}\right]\right\}\omega_0^2\\&+\frac{c_0^2\mathbf{kH}}{2\pi W\gamma^2}\left\{\gamma^2(\mathbf{kH})(\mathbf{kv})+\mathbf{vH}\left[k^2-\frac{1}{c^2}(\mathbf{kv})^2\right]\right\}\omega_0\\&+\frac{c_0^2c^2}{4\pi W}(\mathbf{kH})^2\left[k^2-\frac{1}{c^2}(\mathbf{kv})^2\right]=0. \qquad (3.3)\end{aligned}$$

Instability corresponds to values of k_x whose imaginary part differs from zero. We put $k_x=-i$ and then the perturbation will be bounded away from the discontinuity, provided the conditions

$$\operatorname{Re}\lambda_1>0, \qquad \operatorname{Re}\lambda_2<0, \qquad (3.4)$$

are satisfied, where λ_1 and λ_2 pertain to the regions $x<0$ and $x>0$ respectively. By means of Eq. (3.3) we can express the dependence of λ on k:

$$\lambda=k_0\sqrt{1-k^2/k_0^2}. \qquad (3.5)$$

As shown in the preceding section, the boundary conditions (2.14) should hold on the perturbed surface of the tangential discontinuity:

$$\delta v_x-i\omega_0\xi=0, \qquad h_x-i\mathbf{k}\mathbf{H}\xi=0. \qquad (3.6)$$

We must also add to these conditions the boundary equation (2.8). Eliminating ξ from (3.6), we obtain the independent boundary condition

$$h_{x_1}/\mathbf{kH}_1=h_{x_2}/\mathbf{kH}_2. \qquad (3.7)$$

From the system of equations of relativistic magnetohydrodynamics we can readily derive the following expression for small velocity and magnetic-field perturbations:

$$\delta\mathbf{v}=-c_0^2\frac{\delta n}{\omega_0 n\Delta_0}(A\mathbf{k}+B\mathbf{v}+C\mathbf{H}), \qquad (3.8)$$

$$\mathbf{h}=-c_0^2\frac{\delta n}{\omega_0^2 n\Delta_0}\{\mathbf{kH}\,(A\mathbf{k}+B\mathbf{v})-(Ak^2+B\mathbf{kv})\,\mathbf{H}\}, \qquad (3.9)$$

where $A=\omega_0^2/\gamma^4$; $B=\omega_0^2(\omega_0-\mathbf{k}\cdot\mathbf{v})/c^2\gamma^4$, C and Δ_0 are functions of ω_0, H, W, k, and v.

Eliminating with the aid of (3.7) — (3.9) the components $\delta\mathbf{v}$ and $\mathbf{h}$ from the boundary equation (2.8), and using (3.3), we obtain after several transformations an equation that determines the possible values of ω:

$$\lambda_1/W_1F_1=\lambda_2/W_2F_2, \qquad (3.10)$$

where λ is expressed in terms of k^2 by means of (3.5), and F is defined in (3.2).

An investigation of the stability of a magnetic tangential discontinuity in relativistic hydrodynamics reduces to an investigation of the roots of (3.10). If for certain values of the parameters contained in (3.10) the equation has no root ω with positive imaginary parts (for all values of k_0), then this magnetic tangential discontinuity is stable against the small perturbations considered here. In the opposite case, it is unstable.

If there is no magnetic field (i.e., $H_1=0$, $H_2=0$), we arrive at the less interesting hydrodynamic problem, that of stability of a tangential discontinuity. It is known that such a discontinuity is absolutely unstable. To investigate the roots of (3.2) we confine ourselves, following Syrovat-skii,[2] to the particular case of discontinuities, in which the flow of the medium is along the magnetic field, i.e., when the vectors $\mathbf{H}_1$, $\mathbf{H}_2$, $\mathbf{v}_1$, and $\mathbf{v}_2$ are parallel in some system of coordinates.

We denote the cosine of the angle between the direction of the wave vector $\mathbf{k}_0$ and the general direction of the vectors $\mathbf{v}$ and $\mathbf{H}$ by ν. We first investigate the roots of (3.10) as $\nu \to 0$. The equation (3.10) is of the same order in ω as the corresponding equation in Syrovat-skii's paper,[2] because it has one multiple root $\omega = 0$ when $\nu = 0$, and two simple real roots. But since the transition from the real root to the imaginary one (to the pair of complex conjugate roots) is possible only through a multiple root, the imaginary roots of (3.10) should tend to zero together with ν. This enables us to neglect the ratio k^2/k_0^2 under the radical sign as much smaller than unity, and then ω is given by

$$W_1\left\{\frac{1}{\gamma_1^2}\left[1+\gamma_1^2\frac{H_1^2}{4\pi W_1}\right]\left(\frac{\omega}{k_0}-v_1\nu\right)^2+\frac{v_1H_1^2\nu}{2\pi W_1}\left(\frac{\omega}{k_0}-v_1\nu\right)-\frac{c^2H_1^2\nu^2}{4\pi W_1}\gamma_1^2\right\}=-W_2\left\{\frac{1}{\gamma_2^2}\left[1+\gamma_2^2\frac{H_2^2}{4\pi W_2}\right]\left(\frac{\omega}{k_0}-v_2\nu\right)^2+\frac{v_2H_2^2\nu}{2\pi W_2}\left(\frac{\omega}{k_0}-v_2\nu\right)-\frac{c^2H_2^2\nu^2}{4\pi W_2}\gamma_2^2\right\}. \tag{3.11}$$

The roots of (3.11) are real if the following condition is satisfied

$$\left(\frac{H_1^2}{4\pi}+\frac{H_2^2}{4\pi}\right)+\frac{(H_1^2/4\pi+H_2^2/4\pi)^2}{W_1+W_2}-\frac{W_1W_2}{c^2(W_1+W_2)}\frac{(v_2-v_1)^2}{\gamma_1^2\gamma_2^2}\geqslant 0. \tag{3.12}$$

The second term of this condition tends to zero in the non-relativistic limit, but at relativistic energy density it can make a considerable contribution to the stabilization of the flow.

An investigation of the roots of (3.10) for the case of arbitrary ν is best carried out for a narrower class of discontinuities, namely when the heat function, the velocity of sound, and the field intensity have the same values on both sides of the discontinuity:

$$W_1=W_2\equiv W,\qquad c_{01}=c_{02}\equiv c_0,\qquad H_1=H_2\equiv H. \tag{3.13}$$

If $v_0=(v_2-v_1)/(1-v_1v_2/c^2)$ ($\mathbf{v}_1$ and $\mathbf{v}_2$ are parallel) is the value of the jump on the discontinuity, then in the "symmetrical" system of coordinates we have

$$v_1=-\frac{v_0}{2}\left(1-\frac{v_1v_2}{c^2}\right),\qquad v_2=\frac{v_0}{2}\left(1-\frac{v_1v_2}{c^2}\right).$$

Solving these equations for v_1 and v_2, we find

$$v_1=-\frac{c^2}{v_0}\left(1-\sqrt{1-\frac{v_0^2}{c^2}}\right)=-V_0,$$
$$v_2=\frac{c^2}{v_0}\left(1-\sqrt{1-\frac{v_0^2}{c^2}}\right)=V_0. \tag{3.14}$$

Introducing the notation

$$\Omega=\omega/c_0k_0,\qquad \alpha=H/\sqrt{4\pi W},$$
$$\beta_0=V_0/c_0,\qquad \beta=v_0/c_0, \tag{3.15}$$

squaring both halves of (3.10), and discarding the root $\Omega = 0$, we obtain an algebraic equation of the eighth degree for Ω, in the form

$$b_1\Omega^8+b_2\Omega^6+b_3\Omega^4+b_4\Omega^2+b_5=0, \tag{3.16}$$

where the coefficients are functions of the parameters α, β_0, $y = c_0/c$, and ν. Ω should vanish on the boundary of the instability region.

At certain values of the parameters, the free term b_5 may vanish, and then (3.16) has a multiple root $\Omega^2 = 0$. If b_5 reverses sign as it goes through zero, Ω^2 also reverses sign, and this effects a transition from a pair of real roots to a pair of complex-conjugate roots (pure imaginary). Then the equation $b_5 = 0$ specifies, for a given ν, a curve in the plane (α, β_0), which is the region of the boundary of the instability region.

The equation $b_5 = 0$ yields two curves:

$$\alpha^2=y^2\beta_0^2/(1-y^2\beta_0^2), \tag{3.17}$$

$$(\alpha/y)^4\{2(1-\beta_0^2)^2+\nu^2\beta_0^2(1-y^2)(2-y^2\beta_0^2-\beta_0^2)\}-(\alpha/y)^2\beta_0^2\{4(1-\beta_0^2)^2+\nu^2\beta_0^2(1-y^2)(1-2y^2\beta_0^2+\beta_0^2)/(1-y^2\beta_0^2)\}+2\beta_0^4-\nu^2\beta_0^6(1-y^2)/(1-y^2\beta_0^2)=0. \tag{3.18}$$

Equation (3.18) defines a real curve only when

$$\nu^2\geqslant\frac{8[1-y^2(1-y^2\beta_0^2+\beta_0^2)]}{8+(1-\beta_0^2)^2-8y^2\beta_0^2(2-y^2\beta_0^2)}\,\frac{1-y^2\beta_0^2}{1-y^2}. \tag{3.19}$$

The condition (3.19) yields two intervals of values of β_0 for each value of ν:

$$\beta_0^2\leqslant\frac{\nu^2+8y^2(\nu^2-1)-2\nu^2(1-y^2)\sqrt{2(\nu^{-2}-1)}}{\nu^2+8y^4(\nu^2-1)}, \tag{3.20}$$

$$\beta_0^2\geqslant\frac{\nu^2+8y^2(\nu^2-1)+2\nu^2(1-y^2)\sqrt{2(\nu^{-2}-1)}}{\nu^2+8y^4(\nu^2-1)}. \tag{3.21}$$

The intervals (3.20) and (3.21) are meaningful only when ν varies within the limits

$$0\leqslant\nu\leqslant 1.$$

We shall henceforth consider the ultrarelativistic case, i.e., $y = 1/\sqrt{3}$. In this case, according to (3.15), β and β_0 change in the same interval of values from 0 to $\sqrt{3}$. When $\nu^2 = 1$, (3.20) and (3.21) imply $\beta_0^2 \leq 1$ and $\beta_0^2 \geq 1$, respectively.

As $\nu \to 0$ we obtain $\beta_0 \to \sqrt{3}$, and curve (3.17) is the boundary of the stability region. Equation (3.17) coincides with one of the real roots of (3.12). In fact, in a "symmetrical" system of coordinates, the equation of the curve that serves as the boundary of the stability region at low values of ν, assumes the form

$$\alpha^4 + \alpha^2 - y^2\beta_0^2/(1 - y^2\beta_0^2)^2 = 0. \tag{3.22}$$

This equation has two roots:

$$\alpha_1^2 = y^2\beta_0^2/(1 - y^2\beta_0^2), \qquad \alpha_2^2 = -1/(1 - y^2\beta_0^2). \tag{3.23}$$

The second root of (3.23) has no physical meaning and should be discarded. Thus, as $\nu \to 0$ we arrive at the previous boundary (3.17) of the instability region. On the other hand, in the region $0 \le \beta_0 \le 1$ $(\nu = 1)$ the limit is the curve (3.18). In fact, when $\nu = 1$, the equation $b_5 = 0$ assumes the form

$$\left\{\alpha^2 - \frac{y^2\beta_0^2}{1 - y^2\beta_0^2}\right\}^2 \left\{\beta_0^4 (1 - y^2)\left[1 + \frac{(1 - y^2)}{y^2}\alpha^2\right]\right.$$
$$\left. - 2(1 - y^2\beta_0^2)\left[(\beta_0^2 - 1)\frac{\alpha^2}{y^2} + \beta_0^2\right]\right\} = 0. \tag{3.24}$$

It follows therefore that the vanishing of Ω^2 on the curve (3.17) occurs without a reversal in the sign, and the limit of the stability region when $\nu = 1$ is the curve

$$\alpha = \beta_0 \left[(3 - 2\beta_0^2)/(9 - 12\beta_0^2 + 5\beta_0^4)\right]^{1/2} \tag{3.25}$$

(we have put here $y = 1/\sqrt{3}$).

Thus, the region of instability of magnetic tangential discontinuities (in the ultrarelativistic case) is bounded on the left by the curve (3.25) when $\beta_0 \le 1$ and by the curve (3.17) when $\beta_0 \ge 1$. The curves (3.17) and (3.25) are shown in the figure and the plane (α, β_0). The instability region is shaded. The discontinuities whose parameters lie outside the region will be stable against small perturbations.

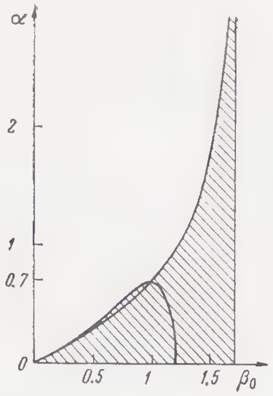

We note that the stability criterion for a magnetic tangential discontinuity can be represented in the form

$$\frac{H^2}{8\pi} \geqslant \frac{1}{4}\left(\frac{1}{\sqrt{1 - v_0^2/c^2}} - 1\right) W, \tag{3.26}$$

where the expression in the right half (without the ¼) is the analog of the kinetic energy of a particle in relativistic hydrodynamics.

In conclusion, I thank K. P. Stanyukovich for discussions and valuable advice, and also F. I. Frankel' for interest in the work. I also take this opportunity to thank Zh. S. Takibaev for support.

---

[1] S. I. Syrovat-skii, JETP **24**, 632 (1953).

[2] S. I. Syrovat-skii, Trudy, Physics Institute, Academy of Sciences, 8, 14 (1956).

[3] K. P. Stanyukovich, Тр. Конференции по магнитной гидродинамике (Transactions of Conference on Magnetohydrodynamics), Riga, (1960).

Translated by J. G. Adashko
245

SOVIET PHYSICS JETP VOLUME 13, NUMBER 5 NOVEMBER, 1961

ON NEUTRON TRANSFER IN NUCLEAR COLLISIONS

T. L. ABELISHVILI

Institute of Electronics, Automation, and Telemechanics, Academy of Sciences, Georgian S.S.R.

Submitted to JETP editor December 16, 1960

J. Exptl. Theoret. Phys. (U.S.S.R.) **40**, 1440-1445 (May, 1961)

Neutron transfer in nuclear collisions is investigated in the case when the effect of the Coulomb field is significant. At energies above the Coulomb barrier the possibility of formation of a compound nucleus is taken into account. The differential cross section attains a maximum which shifts towards smaller angles as the energy is increased. The angular dependence of the cross section depends weakly on the angular momentum of the state into which the neutron is captured. The calculation is restricted to the case when the Q of the reaction is small compared to the energy of the colliding nuclei.

NEUTRON transfer occurring in the bombardment of atomic nuclei by nitrogen ions has been studied in recent years in a number of experimental papers (cf. references 1 — 4). A study was made of the energy dependence of the neutron transfer cross section[5-7] and of the angular distribution in the reaction $N^{14}(N^{14}N^{13})N^{15}$ at energies of 23.3, 21.1, 19.2, and 16.3 Mev.[1] At an energy of 23.3 Mev, Reynolds and Zucker[1] have observed a maximum at 50° in the center of mass system (c.m.s.). The angle corresponding to the maximum number of scattered particles was found to increase as the energy was decreased.

At energies below the Coulomb barrier the transfer of a nucleon can be due to the penetration through the Coulomb barrier. At high energies when the distance of closest approach of the colliding nuclei becomes equal to or less than the sum of the nuclear radii the formation of a compound nucleus becomes possible. In this case the angular distribution of the inelastic scattering of nuclei accompanied by nucleon transfer is characterized by a sharp falling off at large angles corresponding to small nuclear impact parameters.

Good agreement with experimental data on the elastic scattering of charged particles was obtained by means of the semiclassical theory based on the assumption according to which the l-th partial wave is completely absorbed if the impact parameter associated with it is less than or equal to the sum of the radii of the colliding nuclei, while the wave whose impact parameter is greater than the sum of the nuclear radii remains unperturbed and has the phase corresponding to Coulomb scattering.[8,9] Such a semiclassical theory was first proposed by Akhiezer and Pomeranchuk[10] in the study of diffraction scattering of fast charged particles.

We can assume that the hypothesis just quoted holds also in the case of inelastic scattering. We shall investigate in the c.m.s. collisions of nuclei of mass numbers A_1 and A_2 as a result of which a neutron is transferred from the nucleus A_1 to the nucleus A_2 ($A_1 \gg 1$, $A_2 \gg 1$). The problem is considerably simplified in the limiting case $\eta_i = Z_1Z_2e^2/\hbar v_i > 1$, $\eta_f = Z_1Z_2e^2/\hbar v_f > 1$, when the quasiclassical approximation is applicable.

The amplitude for neutron transfer, similarly to the amplitude for stripping,[11] can be written in the form

$$f = -\frac{\mu}{4\pi\hbar^2}\int \Phi^*_{l'}(\rho')\,\psi^{(-)*}_{\mathbf{k}_f}(\mathbf{r}')\,V(\rho)\,\psi^{(+)}_{\mathbf{k}_i}(\mathbf{r})\,\varphi_l(\rho)\,d\mathbf{r}\,d\rho. \quad (1)$$

Here ρ is the position vector of the neutron with respect to the core $A_1 - 1$ in the nucleus A_1, ρ' is the position vector of the neutron with respect to the core A_2 in the nucleus $A_2 + 1$, $\mathbf{r}$ and $\mathbf{r}'$ are respectively the position vectors of the center of mass of the nucleus A_1 and of the core $A_1 - 1$ with respect to the center of mass of the nucleus A_2, μ is the reduced mass of the colliding nuclei, $V(\rho)$ is the potential for the nuclear interaction between the neutron and the core $A_1 - 1$, $\varphi_l(\rho)$ is the wave function for the neutron of angular momentum l in the nucleus A_1, $\Phi_{l'}(\rho')$ is the wave function for the neutron of angular momentum l' in the nucleus $A_2 + 1$. $\psi^{(+)}_{\mathbf{k}_i}(\mathbf{r})$ denotes the Coulomb wave function for the relative motion of the nuclei A_1 and A_2 which at infinity consists of a plane wave with the propagation vector $\mathbf{k}_i$ and a spherical diverging wave; $\psi^{(-)}_{\mathbf{k}_f}(\mathbf{r}')$ is the Coulomb wave function for the relative motion of the nuclei $A_1 - 1$ and $A_2 + 1$, which at infinity contains a wave with propagation vector $\mathbf{k}_f$ and a converging spherical wave

$$\psi_{\mathbf{k}_i}^{(+)}(\mathbf{r}) = \exp\left(-\tfrac{1}{2}\pi\eta_i + i\mathbf{k}_i\mathbf{r}\right)\Gamma(1 + i\eta_i)\, F(-i\eta_i,\ 1;\ i(k_i r - \mathbf{k}_i\mathbf{r})),$$

$$\psi_{\mathbf{k}_f}^{(-)}(\mathbf{r}') = \exp\left(-\tfrac{1}{2}\pi\eta_f + i\mathbf{k}_f\mathbf{r}'\right)\Gamma(1 - i\eta_f)\, F(i\eta_f,\ 1;\ -i(k_f r' + \mathbf{k}_f\mathbf{r}')). \tag{2}$$

If we take the neutron mass M to be much smaller than the mass of the core $A_1 - 1$, we can set $\mathbf{r}' \approx \mathbf{r}$ and $\boldsymbol{\rho}' \approx \mathbf{r} + \boldsymbol{\rho}$. Further, on noting that if the energy of the relative motion of the colliding nuclei is not great (lower than the Coulomb barrier), then in the evaluation of (1) the region inside the nucleus $A_2 + 1$ is not important, we see that, therefore, the function $\Phi_{l'}(\mathbf{r} + \boldsymbol{\rho})$ in (1) can be replaced by its value in the exterior region

$$\Phi_{l'}(\mathbf{r} + \boldsymbol{\rho}) = N_{l'} Y_{l'm'}(\theta', \Phi')\, k_{l'}(\alpha\,|\mathbf{r} + \boldsymbol{\rho}|), \qquad |\mathbf{r} + \boldsymbol{\rho}| > R', \tag{3}$$

where $k_{l'}(x) = \sqrt{\pi/2x}\, K_{l'+\frac{1}{2}}(x)$ is Macdonald's spherical harmonic, $\alpha = \sqrt{2M\epsilon'}/\hbar$ (ϵ' is the binding energy of the captured neutron in the nucleus $A_2 + 1$), $Y_{l'm'}(\theta', \Phi')$ is the spherical harmonic corresponding to the state of angular momentum l'; θ', Φ' are the angles specifying the orientation of the vector $\mathbf{r} + \boldsymbol{\rho}$, $N_{l'}$ is a normalization constant, R' is the radius of the nucleus $A_2 + 1$.

If $\alpha R'$ exceeds $l'(l' + 1)/2$, then the function in (3) can be replaced by its asymptotic expression

$$k_{l'}(x) = \pi e^{-x}/2x. \tag{4}$$

For example, in the case of neutron transfer from a N^{14} nucleus to another N^{14} nucleus $\alpha R' = 2.8$, $l' = 1$, and, therefore, formula (4) is a good approximation.

By choosing for the potential $V(\rho)$ the rectangular well model

$$V(\rho) = \begin{cases} -V_0, & \rho < R \\ 0, & \rho > R \end{cases}$$

(R is the radius of the nucleus A_1), the function $\varphi_l(\boldsymbol{\rho})$ can be written in the form

$$\varphi_l(\boldsymbol{\rho}) = N_l j_l(\chi\rho)\, Y_{lm}(\vartheta_\rho, \varphi_\rho), \qquad \rho \leqslant R,$$

$$\chi = \sqrt{2M(V_0 - \varepsilon)/\hbar^2}, \tag{5}$$

where $j_l(\chi\rho)$ is the spherical Bessel function of order l, (ϵ is the neutron binding energy in the nucleus A_1) and N_l is a normalization constant.

By utilizing the well known expansion

$$\frac{\exp(-\alpha|\mathbf{r} + \boldsymbol{\rho}|)}{|\mathbf{r} + \boldsymbol{\rho}|} = \frac{4\pi}{\sqrt{r\rho}} \sum_{\lambda,\nu} (-1)^\lambda I_{\lambda+1/2}(\alpha\rho)\, K_{\lambda+1/2}(\alpha r)\, Y_{\lambda\nu}^{*}(\vartheta, \varphi) \times Y_{\lambda\nu}(\vartheta_\rho, \varphi_\rho), \qquad \rho < r, \tag{6}$$

where $I_{\lambda+\frac{1}{2}}(x)$ is a Bessel function of imaginary argument, ϑ, φ are the angles specifying the orientation of the vector $\mathbf{r}$ and ϑ_ρ, φ_ρ are the angles specifying the orientation of the vector $\boldsymbol{\rho}$, we rewrite the amplitude f in the following form:

$$f = N_l N^{*} \frac{\pi\mu V_0}{2\hbar^2\sqrt{\alpha\chi}} \sum_{\lambda,\nu} (-1)^\lambda \int_0^R \frac{1}{\rho} I_{\lambda+1/2}(\alpha\rho)\, J_{l+1/2}(\chi\rho) \times Y_{lm}(\vartheta_\rho, \varphi_\rho)\, Y_{\lambda\nu}^{*}(\vartheta_\rho, \varphi_\rho)\, d\boldsymbol{\rho} \int \psi_{\mathbf{k}_f}^{(-)*}(\mathbf{r})\, k_\lambda(\alpha r)\, \psi_{\mathbf{k}_i}^{(+)}(\mathbf{r}) \times Y_{l'm'}^{*}(\theta', \Phi')\, Y_{\lambda\nu}(\vartheta, \varphi)\, d\mathbf{r}. \tag{7}$$

It should be noted that the angles θ', Φ' are functions of ϑ, φ, ϑ_ρ, φ_ρ, ρ, $\mathbf{r}$. However, approximately we can set $\theta' \approx \vartheta$ and $\Phi' \approx \varphi$. Such a replacement is valid if the effective value of $\boldsymbol{\rho}$ is small in comparison with the effective value of $\mathbf{r}$. We can make an estimate of the error made as the result of such replacement in the case of the example $l = l' = 0$. In this case the exactly calculated amplitude can be compared with the amplitude obtained if we neglect in the function $\Phi_0^*(\mathbf{r}+\boldsymbol{\rho})$ of formula (1) the quantity $\boldsymbol{\rho}$ compared to $\mathbf{r}$. It can be easily seen that the replacement of $\Phi_0^*(\mathbf{r}+\boldsymbol{\rho})$ by $\Phi_0(\mathbf{r})$ does not affect the nature of the angular distribution for $l' = 0$. We should, therefore, expect that the replacement $\theta' \to \vartheta$ and $\Phi' \to \varphi$ in the general case $l' \neq 0$ will also not lead to any significant change in the angular distribution.

Thus, for the amplitude of the reaction we obtain the following expression:

$$f = N_l N_{l'}^{*} \frac{\pi\mu V_0 B_l}{2\hbar^2\sqrt{\alpha\chi}} (-1)^l \int \psi_{\mathbf{k}_f}^{(-)*}(\mathbf{r})\, k_l(\alpha r)\, \psi_{\mathbf{k}_i}^{(+)}(\mathbf{r})\, Y_{l'm'}(\vartheta, \varphi) \times Y_{lm}(\vartheta, \varphi)\, d\mathbf{r},$$

$$B_l = \frac{R}{\chi^2 + \alpha^2}\left\{J_{l+1/2}(\chi R)\frac{d}{dR} I_{l+1/2}(\alpha R) - I_{l+1/2}(\alpha R)\frac{d}{dR} J_{l+1/2}(\chi R)\right\}. \tag{8}$$

In evaluating the integral remaining in (8) we can again make use of the asymptotic expression (4) for $k_l(\alpha r)$ if the condition $\alpha r_{\text{eff}} > l(l + 1)/2$ is satisfied. If in making the estimate we make use of the value

$$r_{\text{eff}} = Z_1 Z_2 e^2/E + [\varepsilon'(A - 1) - \varepsilon A]^2/4\varepsilon' A,$$

$$A = A_1 A_2/(A_1 + A_2),$$

obtained in evaluating the integral in (8) by the saddle point method, it can be easily seen that at energies of the order of the Coulomb barrier

$$\alpha r_{\text{eff}} \approx \tfrac{2}{3}(\sqrt[3]{A_1} + \sqrt[3]{A_2}).$$

In the case of the reaction $N^{14}(N^{14}N^{13})N^{15}$ at $E \approx 9$ Mev, $\epsilon' = 10.8$ Mev, $\epsilon = 10.6$ Mev (cf. reference 11) we have $\alpha r_{\text{eff}} \approx 5$.

When this condition is satisfied the integral (8) can be written in the form[11]

$$\int \psi_{\mathbf{k}_f}^{(-)*}(\mathbf{r})\, k_l(\alpha r)\, \psi_{\mathbf{k}_i}^{(+)}(\mathbf{r})\, Y_{l'm'}(\vartheta, \varphi)\, Y_{lm}(\vartheta, \varphi)\, d\mathbf{r}$$
$$= \frac{\pi}{2\alpha} Y_{lm}(\vartheta_0, \varphi_0)\, Y_{l'm'}(\vartheta_0, \varphi_0) \int \frac{e^{-\alpha r}}{r} \psi_{\mathbf{k}_f}^{(-)*}(\mathbf{r})\, \psi_{\mathbf{k}_i}(\mathbf{r})\, d\mathbf{r}. \tag{9}$$

Here $\mathbf{r}_0(r_0, \vartheta_0, \varphi_0)$ is the saddle point, where the function $F(\mathbf{r}) = -\alpha r + \ln(\psi_{\mathbf{k}_f}^{(-)*}(\mathbf{r})\,\psi_{\mathbf{k}_i}^{(+)}(\mathbf{r}))$ has an extremum.

We expand the Coulomb wave functions $\psi_{\mathbf{k}_i}^{(+)}(\mathbf{r})$ and $\psi_{\mathbf{k}_f}^{(-)}(\mathbf{r})$ into partial waves:[13]

$$\psi_{\mathbf{k}}^{(\pm)}(\mathbf{r}) = 4\pi \sum_{lm} i^l \exp[\pm i\delta_l(\eta)]\,(kr)^{-1} Y_{lm}^{*}(\mathbf{k})\, Y_{lm}$$
$$\times (\vartheta, \varphi)\, F_l(kr), \tag{10}$$

where $\delta_l(\eta) = \arg\Gamma(l + 1 + i\eta)$ is the Coulomb phase shift, and $F_l(kr)$ is the regular solution of the radial wave equation for angular momentum l:

$$F_l(kr) = e^{-\pi\eta/2} \frac{|\Gamma(l+1+i\eta)|}{2\Gamma(2l+2)} (2kr)^{l+1} e^{-ikr} F(l+1$$
$$- i\eta, 2l+2, 2ikr). \tag{11}$$

On substituting (10) into the integral (9) and on carrying out the integration over the angles we obtain

$$\int \frac{e^{-\alpha r}}{r} \psi_{\mathbf{k}_f}^{(-)*}(\mathbf{r})\, \psi_{\mathbf{k}_i}^{(+)}(\mathbf{r})\, d\mathbf{r} = 4\pi \sum_l (2l+1)$$
$$\times \exp[i\delta_l(\eta_i) + i\delta_l(\eta_f)]\, P_l(\cos\theta) \frac{1}{k_i k_f}$$
$$\times \int_0^\infty F_l(k_i r) \frac{e^{-\alpha r}}{r} F_l(k_f r)\, dr \tag{12}$$

($P_l(\cos\theta)$ is a Legendre polynomial, θ is the angle between the vectors $\mathbf{k}_i$ and $\mathbf{k}_f$).

In the quasiclassical case $(\eta_i, \eta_f > 1)$ we can utilize the following approximate expression for the radial functions:[14]

$$F_l(kr) = \left[\frac{f(r)}{k^2}\right]^{-1/4} \sin\varphi, \qquad \varphi = \frac{\pi}{4} + \int_{\tilde{r}}^{r} [f(r)]^{1/2}\, dr,$$
$$f(r) = k^2 - \frac{2k\eta}{r} - \frac{l(l+1)}{r^2}, \tag{13}$$

where $\tilde{r}$ is the classical turning point determined by the condition $f(\tilde{r}) = 0$. If we restrict ourselves to the consideration of the case when the Q of the reaction $Q = E_{A_1-1} - E_{A_1} = \epsilon' - \epsilon$ is much smaller than the kinetic energy of the colliding nuclei we have

$$\frac{1}{k_i k_f} \int_0^\infty F_l(k_i r) \frac{e^{-\alpha r}}{r} F_l(k_f r)\, dr$$
$$= \frac{1}{2k^2} \exp\left(-\frac{\alpha\eta}{k} + \xi \operatorname{arctg} \frac{\xi k}{\alpha\eta}\right) K_{i\xi}(\varepsilon c),$$
$$\xi = \eta_f - \eta_i, \qquad k = (k_i + k_f)/2, \qquad \eta = (\eta_i + \eta_f)/2,$$
$$\varepsilon = \sin^{-1}(\theta/2), \qquad c = \sqrt{(\alpha\eta/k)^2 + \xi^2} \approx \alpha\eta/k. \tag{14}^*$$

For $\xi \ll 1$ and $\eta \gg 1$ we have

$$\exp[\xi \operatorname{arctg}(\xi k/\alpha\eta)] \approx 1, \qquad K_{i\xi}(\varepsilon c) \approx (\pi/2\varepsilon c)^{1/2} e^{-\varepsilon c}$$

(cf. reference 15).

Therefore

$$\frac{1}{k_i k_f} \int_0^\infty F_l(k_i r) \frac{e^{-\alpha r}}{r} F_l(k_f r)\, dr$$
$$= \frac{1}{2k^2} \left(\frac{\pi}{2\alpha a\varepsilon}\right)^{1/2} \exp[-\alpha a(1 + \sin^{-1}(\theta/2))], \tag{15}$$

where $a = \eta/k = Z_1Z_2e^2/\mu v^2$. Thus, on substituting (15) into (12) we obtain the following expression for the amplitude for neutron transfer in nuclear collisions:

$$f(\theta) = i\sqrt{\frac{\pi^7}{2\chi a}} \frac{N_l N_{l'}^{*} V_0 \mu}{k\hbar^2\alpha^2} B_l (-1)^l Y_{lm}(\vartheta_0, \varphi_0)$$
$$\times Y_{l'm'}^{*}(\vartheta_0, \varphi_0) \sqrt{\sin\frac{\theta}{2}}\, f_0'(\theta) \exp\{-\alpha a(1 + \sin^{-1}(\theta/2)\}, \tag{16}$$

$$f_0(\theta) = \sum_l \frac{1}{2ik}(2l+1) \exp[2i\delta_l(\eta)]\, P_l(\cos\theta). \tag{17}$$

At energies much lower than the Coulomb barrier $f_0(\theta)$ is the ordinary amplitude for Coulomb scattering. As can be seen from (16) the angular dependence of the cross section is given by the expression $\sin^{-3}(\theta/2)\exp(-2\alpha a/\sin(\theta/2))$ (cf. also reference 7). This expression increases with increasing angle θ reaching a maximum,* after which a falling off begins determined by the factor $\sin^{-3}(\theta/2)$. As the energy increases the maximum of the angular distribution shifts towards smaller angles.

At energies greater than the Coulomb barrier it is necessary to take into account the possibility of formation of a compound system in nuclear collisions. In the quasiclassical case the formation of the system is possible if the orbital angular momentum l is less than $l_{\max}$ determined by the condition

$$l_{max}(l_{max} + 1)$$
$$= 2\mu\hbar^{-2}(R_{A_1} + R_{A_2})(E - Z_1Z_2e^2/(R_{A_1} + R_{A_2})). \tag{18}$$

In this case in formula (17) which determines the elastic scattering amplitude we must restrict our summation to values of $l \geq l_{\max}$.

Owing to the possibility of formation of a compound system, the angular distribution of nuclei in the case of neutron transfer will fall off sharply at angles greater than $\theta = \theta_0$, where θ_0 can be roughly estimated by means of the following formula:

$$R_{A_1} + R_{A_2} = \frac{Z_1Z_2e^2}{2E}\left(1 + \sin^{-1}\frac{\theta_0}{2}\right). \tag{19}$$

---

*arctg = $\tan^{-1}$.

*The angle $\theta_{\max}$ is determined by the condition $\sin(\theta_{\max}/2) = 2\alpha a/3$.

In a similar manner Reynolds and Zucker[9] have succeeded in explaining the angular distribution of the elastically scattered particles in the reaction $N^{14}(N^{14}N^{14})N^{14}$ at an energy in the laboratory system (l.s.) of 21.5 Mev, by setting $l_{max} = 6$ and $R = 4 \times 10^{-13}$ cm.

Thus, at energies above the Coulomb barrier the angular dependence of the neutron transfer cross section will be given by the expression

$$\frac{d\sigma}{d\Omega}(\theta) \sim \left| \sin^{-3/2}\frac{\theta}{2} \exp\left(-i\eta \ln \sin^2\frac{\theta}{2} + 2i\delta_0 - \alpha a/\sin\frac{\theta}{2}\right) + \frac{1}{i\eta}\sin^{1/2}\frac{\theta}{2}\exp\left(-\alpha a/\sin\frac{\theta}{2}\right) \sum_{l=0}^{l=l_{max}} (2l+1) \times \exp(2i\delta_l) P_l(\cos\theta)\right|^2. \tag{20}$$

In collisions of identical nuclei it is necessary to take recoil into account. In this case the angular distribution can be roughly obtained in the following manner:

$$d\sigma/d\Omega = |f(\theta)|^2 + |f(\pi - \theta)|^2. \tag{21}$$

Evidently there will be observed two maxima, symmetric with respect to $\theta = \pi/2$, the separation between which increases with increasing energy.

A more exact result can be obtained by treating the identical nuclei quantum mechanically. In the case of the reaction $N^{14}(N^{14}N^{13})N^{15}$ the angular distribution is given by the following expression[7]

$$d\sigma/d\Omega = \tfrac{2}{3}(2d\sigma_a/d\Omega + d\sigma_s/d\Omega), \tag{22}$$

where $d\sigma_a/d\Omega$ and $d\sigma_s/d\Omega$ are the cross sections for the antisymmetric and the symmetric states:

$$d\sigma_{a,s}/d\Omega = |f(0) \mp f(\pi - \theta)|^2. \tag{23}$$

On substituting (16) into (23), on noting that $l = l' = 1$, and on taking into account the weak dependence of ϑ_0 on the scattering angle θ we obtain

$$\frac{d\sigma_{s,a}}{d\Omega} = \frac{1}{\sqrt{2}}\frac{63}{2048}\pi^5 |N_1|^2 |N_1'|^2 \left(\frac{Ze}{E}\right)^2 V_0^2 \hbar^3 M^{-3/2} \varepsilon'^{-2}(V_0 - \varepsilon)^{-1/2} \times B_1^2 e^{-2\alpha a} \left| \sin^{-3/2}\frac{\theta}{2}\exp\left(-i\eta \ln \sin^2\frac{\theta}{2} + 2i\delta_0 - \alpha a/\sin\frac{\theta}{2}\right) \pm \cos^{-3/2}\frac{\theta}{2}\exp\left(-i\eta \ln \cos^2\frac{\theta}{2} + 2i\delta_0 - \alpha a/\cos\frac{\theta}{2}\right) + \frac{1}{i\eta}\sin^{1/2}\frac{\theta}{2}\exp\left(-\alpha a/\sin\frac{\theta}{2}\right) \times \sum_{l=0}^{l=l_{max}} (2l+1)\exp(2i\delta_l) P_l(\cos\theta) \pm \frac{1}{i\eta}\cos^{1/2}\frac{\theta}{2}\exp\left(-\alpha a/\cos\frac{\theta}{2}\right) \sum_{l=0}^{l=l_{max}} (2l+1) \times \exp(2i\delta_l) P_l(-\cos\theta)\right|^2. \tag{24}$$

The energy dependence of the neutron transfer cross section can be roughly estimated by integrating $|f(\theta)|^2$ from $\theta = 0$ to $\theta = \theta_0$. We obtain the result

$$\sigma(E) \sim \frac{1}{E}\exp\left[-\frac{\alpha Z_1 Z_2 e^2}{E}\left(1 - \sin^{-1}\frac{\theta_0}{2}\right)\right]. \tag{25}$$

In order to improve the results given by formula (25) we can utilize the experimentally observed dependence of θ_0 on energy.

It should be noted that at energies below the Coulomb barrier formula (25) leads to too rapid a falling off of the cross section with decreasing energy (cf., reference 7).

In conclusion the author wishes to take this opportunity of expressing his sincere gratitude to A. G. Sitenko for his assistance in this work.

---

[1] H. L. Reynolds and A. Zucker, Phys. Rev. **101**, 166 (1956).

[2] Reynolds, Scott, and Zucker, Phys. Rev. **102**, 237 (1956).

[3] Webb, Reynolds, and Zucker, Phys. Rev. **102**, 749 (1956).

[4] Halbert, Handley, Pinajian, Webb, and Zucker, Phys. Rev. **106**, 251 (1957).

[5] V. I. Gol'danskii, JETP **36**, 526 (1959), Soviet Phys. JETP **9**, 366 (1959).

[6] E. M. Lifshitz, JETP **8**, 930 (1938).

[7] G. Breit and M. Ebel, Phys. Rev. **103**, 679 (1956).

[8] J. Blair, Phys. Rev. **95**, 1218 (1954).

[9] H. L. Reynolds and A. Zucker, Phys. Rev. **102**, 1378 (1956).

[10] A. I. Akhiezer and I. Ya. Pomeranchuk, J. Phys. (U.S.S.R.) **9**, 471 (1945).

[11] K. A. Ter-Martirosyan, JETP **29**, 713 (1955), Soviet Phys. JETP **2**, 620 (1956).

[12] H. Bethe and P. Morrison, Elementary Nuclear Theory (Russ. Transl.) IIL, 1958.

[13] A. Sommerfeld, Atombau und Spektrallinien, Vieweg, Brunswick, 1951.

[14] Alder, Bohr, Huus, Mottelson, and Winter, Revs. Modern Phys. **28**, 432 (1956).

[15] G. N. Watson, Treatise on the Theory of Bessel Functions, Cambridge, 1944.

Translated by G. Volkoff
246

SOVIET PHYSICS JETP VOLUME 13, NUMBER 5 NOVEMBER, 1961

QUANTUM THEORY OF SOUND ABSORPTION BY METALS IN A MAGNETIC FIELD

V. G. SKOBOV

Leningrad Physico-Technical Institute, Academy of Sciences, U.S.S.R.

Submitted to JETP editor December 19, 1960

J. Exptl. Theoret. Phys. (U.S.S.R.) **40**, 1446-1451 (May, 1961)

We have studied the influence of electron scattering on the absorption of sound by metals in strong magnetic fields for the case of large spatial dispersion. We considered the case where the electron scattering is caused by their interaction with neutral impurities.

GUREVICH, Firsov, and the present author[1] studied the deformation absorption of sound in metals for the case of a strong magnetic field $\Omega \gg kT$ and a long mean free path of the conduction electrons (Ω is the electron Larmor frequency, T the temperature, and k Boltzmann's constant).* We showed that the theory under those conditions should essentially be a quantum-theoretical one and that when the magnetic field changes the sound absorption may show gigantic oscillations.

The cause of these oscillations is the following one. In the case $\Omega \gg kT$ in the region of the tail of the Fermi distribution, which is responsible for the transport properties, only narrow ranges of k_z-values (the component of the quasi-momentum in the direction of the magnetic field **H**) turn out to be allowed, while for $\Omega \ll kT$ all values of k_z are allowed. The position of these ranges on the Fermi surface is determined by the value of H and when H is changed other values of k_z become allowed. On the other hand, when the electron mean free path is sufficiently large those electrons which move in phase with the sound wave will play the main role in the absorption of sound. Other electrons can absorb sound only during collisions with scatterers, and their contribution to the absorption is proportional to the small quantity $1/\varkappa l$ (reference 2) ($\varkappa$ is the sound wave vector and l the average mean free path of the conduction electrons). When the magnetic field is changed the position of the allowed k_z-intervals changes, and if the angle between the directions of $\varkappa$ and **H** is considerably different from a right angle the electrons moving in phase with the sound wave turn out to be sometimes in the region of the tail of the Fermi distribution and sometimes outside it. This leads to the gigantic oscillations in the absorption coefficient.

Assuming existence of an electron relaxation time, we showed that collisions are not important and that the oscillations remain gigantic for $\omega < \nu$, provided the inequality

$$(\varkappa l)^2 \gg \zeta / \Omega,$$

where ζ is the chemical potential of the metal, ω the sound frequency, and ν the collision frequency of the electrons with the scatterers, is satisfied.

The present paper is devoted to a study of the influence of scattering of the electrons on the absorption of sound by metals for the case of a strong magnetic field $\Omega \gg kT$ and a strong spatial dispersion $\varkappa l \gg 1$ ($l = v_F/\nu$; v_F is the Fermi velocity). We consider the case where the transverse electrical fields which occur when the crystal is deformed do not play an important role, so that we can neglect them. We assume that the electron scattering is caused by their interaction with randomly distributed fixed centers, the radius of action of which is small compared with their average mutual distance and with the electron wave length. For the sake of simplicity we restrict our consideration to that of an isotropic quadratic electron spectrum and do not take the electron spin into account.

Let the electron Hamiltonian when there is no sound be $\mathcal{H} = \mathcal{H}_0 + V$, where

$$\mathcal{H}_0 = (\mathbf{p} - e\mathbf{A})^2/2m, \qquad V = \sum_j V_j \equiv \sum_j V(\mathbf{r} - \mathbf{r}_j); \quad (1)$$

here **A** is the vector potential of the magnetic field **H**, **p** the electron quasi-momentum operator, m the effective mass, and V_j the potential of the interaction between an electron and a scattering center at $\mathbf{r}_j$.

The perturbation caused by the interaction of an electron with the sound wave is taken to be of the form

$$\mathcal{H}'(t) = \tfrac{1}{2}(Ue^{-i\omega t} + U^{+}e^{i\omega t}), \qquad U = U_0 e^{i\varkappa\mathbf{r}}, \quad (2)$$

---

*We use a system of units where $\hbar = c = 1$.

U_0 is a Hermitian operator which, generally speaking, is a function of the electron quasi-momentum operator. In the case of inductive sound absorption the perturbation has, for instance, the form $A_\mu(t) J_\mu$ where J_μ is the operator of the μ-th component of the current density, $\mathbf{A}(t) = [\mathbf{H} \times \mathbf{u}(t)]$, where $\mathbf{u}(t)$ is the displacement vector in the sound wave.

In the case of deformation absorption

$$\mathcal{H}'(t) = \Lambda_{ik} u_{ik}(t), \tag{3}$$

where $u_{ik} = \frac{1}{2}(\partial u_i/\partial x_k + \partial u_k/\partial x_i)$ is the deformation tensor of the crystal, and where the tensor Λ_{ik} in general depends on the quasi-momentum $\mathbf{p}$. In the present paper we shall consider the deformation absorption of sound by metals with a low carrier concentration (such as bismuth) for which $\Lambda_{ik} = \text{const}$.

The energy absorbed by the electrons per unit time is given in the first Born approximation in $\mathcal{H}'$ by the formula[2,4]

$$Q = \frac{\pi\omega}{2} \sum_{ab} \langle |U_{ba}|^2 \delta(\omega_{ab} + \omega) [f_a(1 - f_b) - f_b(1 - f_a)] \rangle. \tag{4}$$

Here a and b characterize the stationary states of the Hamiltonian $\mathcal{H}$, $\omega_{ab} = E_a - E_b$ is the energy difference, and f_a is the probability of finding an electron in the state a. Since the scattering of electrons by fixed centers is elastic and temperature-independent, f_a is simply the Fermi function of the argument $(E_a - \zeta)/kT$. The pointed brackets $\langle \ldots \rangle$ indicate here and henceforth an average over the positions of the scattering centers $\mathbf{r}_j$.

One easily writes Eq. (4) in the form

$$Q = \frac{\pi\omega}{2} \int_{\Omega/2}^{+\infty} dE\, [f(E) - f(E + \omega)]\, I(E), \tag{5}$$

$$I(E) = \sum_{ab} \langle |U_{ba}|^2 \delta(E - E_b + \omega) \delta(E - E_a) \rangle. \tag{6}$$

Using the identity

$$\delta(x) = \frac{1}{2\pi i} \lim_{\varepsilon \to +0} \left(\frac{1}{x - i\varepsilon} - \frac{1}{x + i\varepsilon} \right)$$

and writing (6) in operator form we find that $I(E)$ is a linear combination of four terms

$$\frac{1}{(2\pi)^2} \operatorname{Sp} \left\langle \left\{ \frac{1}{E - \mathcal{H} \pm i\varepsilon} U^+ \frac{1}{E + \omega - \mathcal{H} \pm i\varepsilon} U \right\} \right\rangle, \tag{7}$$

which can conveniently be evaluated in the $\mathcal{H}_0$ representation. The eigenfunctions of the Hamiltonian $\mathcal{H}_0$ are characterized by the magnetic quantum number n, the component of the wave vector along the direction of the magnetic field k_z, and X, the coordinate center of rotation of the electron.[5] The totality of these quantum numbers will be denoted by indices $\alpha, \beta, \ldots$

To evaluate (7) we need the exact Green's function

$$G_{\beta\alpha}(u) = \left\langle \left(\beta \left| \frac{1}{u - \mathcal{H}} \right| \alpha \right) \right\rangle, \tag{8}$$

averaged over the positions of the scatterers $(u = E + i\epsilon)$. We have shown[6,7] that $G(u)$ can be written as a series

$$G(u) = \frac{1}{u - \mathcal{H}_0} + \sum_j \frac{1}{u - \mathcal{H}_0} \langle T^j(u) \rangle \frac{1}{u - \mathcal{H}_0} + \sum_{j \neq k} \frac{1}{u - \mathcal{H}_0} \left\langle T^j(u) \frac{1}{u - \mathcal{H}_0} T^k(u) \right\rangle \frac{1}{u - \mathcal{H}_0} + \ldots, \tag{9}$$

$$T^j_{\beta\alpha}(E + i\varepsilon) = \Psi^*_\beta(\mathbf{r}_j) \Psi_\alpha(\mathbf{r}_j) \frac{2\pi f/m}{1 + iK(E) f}. \tag{10}$$

Here $\Psi_\alpha(r)$ is an eigenfunction of $\mathcal{H}_0$ and f is the amplitude for the scattering of a zero-energy free electron by the potential V_j,

$$K(E) = \sum_{n=0}^{N} \frac{m\Omega}{[2m[E - \Omega(n + 1/2)]]^{1/2}}, \tag{11}$$

where N is that integer which leads to one imaginary term in the sum (11). $T^j_{\beta\alpha}(E_\alpha + i\epsilon)$ is the amplitude for the transition from the state α to β when an electron is scattered by the j-th center.

In the series (9) each term of the expansion in powers of T is a sum over all possible scatterer numbers $j, k, l, \ldots$ except for terms where any two adjacent numbers are the same. One can show that cross terms of the kind

$$\frac{1}{u - \mathcal{H}_0} T^j(u) \frac{1}{u - \mathcal{H}_0} T^k(u) \frac{1}{u - \mathcal{H}_0} T^j(u) \frac{1}{u - \mathcal{H}_0} \times T^k(u) \frac{1}{u - \mathcal{H}_0}$$

correspond to the simultaneous scattering of an electron by two centers j and k, and give a small contribution to $G(u)$ if $f \ll \lambda$; $f \ll a$, and $\Omega \ll E$, where λ is the electron wavelength and a the mean distance between the scatterers. We shall therefore drop such terms.

We introduce the operator for the scattering by the j-th center, averaged over the positions of all the other centers:

$$\tau^j(u) = T^j(u) + T^j(u) \left[\left\langle \frac{1}{u - \mathcal{H}} \right\rangle - \frac{1}{u - \mathcal{H}_0} \right] T^j(u) + T^j(u) \left[\left\langle \frac{1}{u - \mathcal{H}} \right\rangle - \frac{1}{u - \mathcal{H}_0} \right] T^j(u) \left[\left\langle \frac{1}{u - \mathcal{H}} \right\rangle - \frac{1}{u - \mathcal{H}_0} \right] T^j(u) + \ldots. \tag{12}$$

To evaluate the matrix element $\tau^j_{\beta\alpha}(u)$ we must know the asymptotic expression of the function

$$q(\mathbf{r}, \mathbf{r}'; u) = \frac{2\pi i}{m} \sum_{\alpha\beta} \Psi^*_\beta(\mathbf{r}') \left(\beta \left| \left\langle \frac{1}{u - \mathcal{H}} \right\rangle - \frac{1}{u - \mathcal{H}_0} \right| \alpha \right) \Psi_\alpha(\mathbf{r}) \tag{13}$$

as $|\mathbf{r}'-\mathbf{r}|\sim r_0$, where r_0 is the action radius of a scattering center. It is fairly obvious that at such small distances this quantity is independent of the coordinates (one can choose the gauge of the vector potential **A** in such a way). If we denote it by $q(E)$ and sum the geometric series obtained from (12) we find

$$\tau^j_{\beta\alpha}(E+i\varepsilon)=\Psi^*_\beta(\mathbf{r}_j)\,\Psi_\alpha(\mathbf{r}_j)2\pi f/m[1+i\,[K(E)+q(E)]f]. \tag{14}$$

One can easily express the Green's function $G_{\alpha\beta}(u)$ in terms of $\tau^j(u)$:

$$G_{\beta\alpha}(u)=\frac{\delta_{\alpha\beta}}{u-E_\alpha}+\sum_j\frac{1}{u-E_\beta}\langle\tau^j_{\beta\alpha}(u)\rangle\frac{1}{u-E_\alpha}+\sum_{j\neq k}\sum_\delta\frac{1}{u-E_\beta}\left\langle\tau^j_{\beta\delta}(u)\frac{1}{u-E_\delta}\tau^k_{\delta\alpha}(u)\right\rangle\frac{1}{u-E_\alpha}+\ldots \tag{15}$$

There are now no longer any two numbers of scattering centers j, k, *l*, ... equal in any term of the expansion in powers of $\tau(u)$. The average over $\mathbf{r}_j$ of the product of several different $\tau^j(u)$ is thus equal to the product of the averages. Taking into consideration that

$$\sum_j\langle\Psi^*_\beta(\mathbf{r}_j)\,\Psi_\alpha(\mathbf{r}_j)\rangle=n_s\delta_{\alpha\beta},$$

where n_s is the number of scatterers per unit volume, and that according to the sum rule the quantity

$$-2\,\mathrm{Im}\sum_j\langle\tau^j_{\alpha\alpha}(E+i\varepsilon)\rangle=-(4\pi f n_s/m)\,\mathrm{Im}\,[1+i\,(K+q)f]^{-1}=\nu(E) \tag{16}$$

is the total probability that an electron of energy E is scattered per unit time, we get

$$G_{\beta\alpha}(E+i\varepsilon)=\delta_{\alpha\beta}\,[E-E_\alpha+i\nu(E)/2]^{-1}. \tag{17}$$

We have dropped $\mathrm{Re}\,\Sigma_j\langle\tau^j_{\alpha\alpha}\rangle$ which leads to a renormalization of the energy.

We can now use (17) to verify that the asymptotic expression of $q(\mathbf{r},\mathbf{r}':u)$ at small distances is indeed independent of the coordinates. A direct evaluation leads to the equation

$$q(E)=K\,[E+i\nu(E)/2]-K(E), \tag{18}$$

the form of the function $K(E)$ was given in the foregoing by (11). Substituting this expression for $q(E)$ into (16) we get the following equation for $\nu(E)$:*

$$\nu(E)=\nu_0(E)(2mE)^{-1/2}\,\mathrm{Re}K\,[E+i\nu(E)/2], \tag{19}$$

where

$$\nu_0(E)=4\pi f^2(2E/m)^{1/2}n_s$$

is the scattering probability when there is no magnetic field. In the denominator of (19) we neglected the quantity Kf as compared to unity.

The equation we have obtained gives us immediately the value of $\nu(E)$ provided the condition

$$\Omega\ll(E\nu_0)^{1/2} \tag{20}$$

is satisfied. Indeed, in that case

$$K(E+i\nu/2)\approx(2mE)^{1/2}$$

and (19) leads to the equation $\nu(E)=\nu_0(E)$. If, however, condition (20) is not satisfied, $\nu(E)$ increases when $E\to\Omega(n+\frac{1}{2})$.

In the following we shall be interested in the case $\nu_0\ll kT$. Condition (20) is then replaced by the less restrictive one:

$$\Omega\ll(\zeta kT)^{1/2}, \tag{21}$$

which is easily satisfied in metals. We shall thus assume that $\nu(E)\approx\nu_0$; the increase of $\nu(E)$ in energy ranges which are small compared to kT will not show up in the final results because of the averaging over the Fermi distribution.

We shall not consider the matrix elements $U_{\alpha'\alpha}$. If $\boldsymbol{\kappa}\parallel\mathbf{H}$,

$$(n'X'k'_z\,|\,U\,|\,nXk_z)\qquad U_0\delta_{n'n}\,\delta_{X'X}\,\delta_{k'_z,\,k_z+\varkappa}.$$

If $\boldsymbol{\kappa}$ makes an angle with **H** the matrix elements of U which are nondiagonal in n will be different from zero. One sees, however, easily that if

$$\varkappa_\perp R\ll 1, \tag{22}$$

where $\kappa_\perp$ is the component of $\boldsymbol{\kappa}$ perpendicular to **H**, and R the Larmor radius of the electron, these matrix elements are smaller than the diagonal ones in the ratio $(\kappa_\perp R)^{|n'-n|}$. The same occurs in the semi-classical approximation $\Omega\ll\zeta$ under condition (22) for an arbitrary electron spectrum and an arbitrary dependence $\Lambda_{ik}=\Lambda_{ik}(\mathbf{p})$. For the sake of simplicity we consider the case $\boldsymbol{\kappa}\parallel\mathbf{H}$.

If we use the Green's function (17) and the transition amplitude (14) we can write each of the terms of (7) as a power series

$$\mathrm{Sp}\left\{\frac{1}{E-H+i\varepsilon}U^+\frac{1}{E+\omega-H-i\varepsilon}U\right\}=\sum_{\alpha\alpha'}\frac{1}{E-E_\alpha+i\nu/2}U^+_{\alpha\alpha'}\frac{1}{E+\omega-E_{\alpha'}-i\nu/2}\times\left\{U_{\alpha'\alpha}+\sum_j\sum_{\beta\beta'}\left\langle\tau^j_{\alpha'\beta'}\frac{1}{E+\omega-E_{\beta'}-i\nu/2}\times U_{\beta'\beta}\frac{1}{E-E_\beta+i\nu/2}\tau^j_{\beta\alpha}\right\rangle+\ldots\right\}. \tag{23}$$

An estimate of the second term within the braces for the case $\kappa l\gg 1$ shows that except for a small neighborhood around $E=\Omega(n+\frac{1}{2})$ it is of the order $U_0/\kappa l$, i.e., the series (23) is an expansion in the small parameter $1/\kappa l$.* We have thus

---

*This equation is similar to the one obtained by Bychkov[8] for $\mathrm{Im}\,\Sigma_\alpha G_{\alpha\alpha}(u)$.

$$I(E) = \frac{1}{(2\pi)^2} \sum_{\alpha\alpha'} |U_{\alpha'\alpha}|^2 \frac{\nu(E)}{(E-E_\alpha)^2+\nu^2/4} \, \frac{\nu(E)}{(E-E_{\alpha'}+\omega)^2+\nu^2/4}, \tag{24}$$

and summing over X and k_z and neglecting ω we get

$$I(E) \approx \frac{V_0}{(2\pi)^3} |U_0|^2 (8m)^{1/2} m\Omega \sum_{n=0}^{N-1} \frac{\nu(E)\,[E-\Omega(n+1/2)]^{-1/2}}{2\varkappa^2 m^{-1}[E-\Omega(n+1/2)]+\nu^2}, \tag{25}$$

where V_0 is the volume of the crystal. It is clear that in the case

$$(\varkappa l)^2 \gg \zeta/\Omega \tag{26}$$

it is sufficient to restrict oneself in (25) to the one term for which $[E - \Omega(n + 1/2)]$ is a minimum. When H changes, this quantity and with it the energy Q absorbed by the electrons, oscillates strongly and this causes the gigantic oscillations in the absorption of sound.[1]

In the opposite case when

$$(\zeta/\Omega) \gg (\varkappa l)^2 \gg 1, \tag{27}$$

many values of n are important in Eq. (25) and to evaluate I(E) we can use the Poisson summation formula

$$\sum_{n=0}^{\infty} \varphi(n) = \frac{1}{2}\varphi(0) + \sum_{k=-\infty}^{+\infty} \int_0^{\infty} dn\varphi(n) \exp(2\pi ikn).$$

If we use this formula we get easily the final expression for the sound absorption coefficient

$$\Gamma(H) = \Gamma_0 \left\{1 + \varkappa l \left(\frac{\Omega}{\zeta}\right)^{1/2} \sum_{n=1}^{\infty} (-1)^n A_n \frac{\cos[2\pi n\zeta/\Omega - \pi/4]}{\pi\sqrt{n}}\right\},$$

$$A_n = \frac{2\pi^2 nkT/\Omega}{\mathrm{sh}(2\pi^2 nkT/\Omega)}, \qquad \Gamma_0 = \frac{m^2 |\Lambda_{ik} u_{ik}|^2}{2\pi\rho |\mathbf{u}|^2 s\varkappa}, \tag{28}^\dagger$$

where ρ is the crystal density, s the sound velocity, and Γ_0 the sound absorption coefficient when there is no magnetic field.

In all cases those electrons from the region of the tail of the Fermi distribution which satisfy the condition

$$\varkappa l_z \lesssim 1, \tag{29}$$

play the main role in the absorption of sound; in Eq. (29) $l_z = v_z/\nu$, v_z is the z component of the velocity. In the case (26) there are, depending on the magnitude of the magnetic field either a group of electrons satisfying condition (29) or there are no such electrons on the Fermi surface. This also causes the gigantic oscillations of the absorption coefficient. In the case (27) there is always a number of electron groups satisfying condition (29). The relative amplitude of the oscillations is in that case thus small and is, as is usual in such cases, proportional to the square root of the number of these groups.

In conclusion I express my gratitude to Yu. A. Bychkov and L. D. Landau for valuable discussions.

[1] Gurevich, Skobov, and Firsov, JETP **40**, 786 (1961), Soviet Phys. JETP **13**, 552 (1961).

[2] Akhiezer, Kaganov, and Lyubarskii, JETP **32**, 837 (1957), Soviet Phys. JETP **5**, 685 (1957).

[3] V. L. Gurevich, JETP **37**, 1680 (1959), Soviet Phys. JETP **10**, 1190 (1960).

[4] L. D. Landau and E. M. Lifshitz, Эдектродинамика сплошных сред (Electrodynamics of Continuous Media), Gostekhizdat, 1957, p. 454.

[5] L. D. Landau and E. M. Lifshitz, Квантовая механика (Quantum Mechanics) Gostekhizdat 1948, p. 534.

[6] V. G. Skobov, JETP **37**, 1467 (1959), Soviet Phys. JETP **10**, 1039 (1960).

[7] V. G. Skobov, JETP **38**, 1304 (1960), Soviet Phys. JETP **11**, 941 (1960).

[8] Yu. A. Bychkov, JETP **39**, 1401 (1960), Soviet Phys. JETP **12**, 971 (1961).

Translated by D. ter Haar
247

---

*In the case $\varkappa \perp \mathbf{H}$, the second and later terms in (23) are not small compared to the first one and one must solve the integral equation obtained from (23) to evaluate I(E).

†sh = sinh.

SOVIET PHYSICS JETP VOLUME 13, NUMBER 5 NOVEMBER, 1961

CONTRIBUTION TO THE THEORY OF SUPERFLUIDITY IN AN IMPERFECT FERMI GAS

L. P. GOR'KOV and T. K. MELIK-BARKHUDAROV

Institute of Physics Problems, Academy of Sciences, U.S.S.R.

Submitted to JETP editor December 21, 1960

J. Exptl. Theoret. Phys. (U.S.S.R.) **40**, 1452-1458 (May, 1961)

The Cooper effect in a low-density Fermi gas is studied. The magnitude of the transition temperature into the superfluid state is determined.

It is well known that the basis of superconductivity is the so-called Cooper effect[1] which consists in that the existence of an effective attraction between the electrons in a metal leads to the formation of electron pairs in a singlet state. The exchange of phonons between the electrons is the mechanism that causes the presence of such an attraction. We consider in the present paper the phenomenon of superfluidity in a low-density Fermi gas. The main methodological difference in this case consists in that in the theory of superconductivity the transition temperature is expressed in terms of a quantity of the order of the Debye temperature $\tilde{\omega} \ll \mu$, which is used as the natural parameter for a cutoff, while in a low-density Fermi-gas the only small parameter is its density, or more accurately, the quantity $f_0 p_0^2/v$, where f_0 is the s-wave scattering amplitude for interparticle scattering, and p_0 and v are respectively the limiting momentum and the velocity on the Fermi surface.

For our investigation it is convenient to use quantum field-theoretical methods. We shall assume, starting from Cooper's idea, that the attraction between the particles leads to the formation of bound pairs. Such a pair is a Bose formation. The temperature-dependent Green's function of a free boson $\mathfrak{G}(\mathbf{p}\omega)$ is of the form[2,3]

$$(i\omega_n - \varepsilon(\mathbf{p}) + \mu)^{-1}, \qquad \omega_n = 2\pi n T$$

and for $\omega_n = 0$ becomes infinite as soon as the so-called Bose condensation takes place $[\mu(T_c) = 0]$.

The two-particle Green's function plays the same role for a bound pair as the Green's function of a boson. If one studies the dependence of the two-particle Green's function on the total energy and momentum of the two particles (i.e., on the energy and momentum of the bound pair as a whole) one can find the temperature of the transition of the system into the superfluid state from the condition that this quantity should become infinite when the transition takes place. At lower temperatures bound pairs begin to form and to "condense." The normal ground state of attractive Fermi-particles is thus unstable. The tendency to form bound pairs will at absolute zero cause a change in the ground state of non-interacting fermions under the influence of their mutual attraction. We shall determine the temperature at which the transition to the superfluid state takes place and we shall also study the characteristic singularities of the vertex part of a Fermi system of weakly mutually attracting particles at T = 0 which appear because of the above-mentioned instability of the usual ground state. For the sake of convenience we shall start with the study of the vertex part at absolute zero.

The vertex function $\Gamma_{\alpha\beta\gamma\delta}(p_1, p_2, p_3, p_4)$ is defined through the Fourier component of the two-particle Green's function

$$G_{\alpha\beta\gamma\delta}(x_1, x_2, x_3, x_4) = \langle T(\psi_{1\alpha}\psi_{2\beta}\overset{+}{\psi}_{3\gamma}\overset{+}{\psi}_{4\delta})\rangle \qquad (1)$$

by the following relation

$$\begin{aligned} G_{\alpha\beta\gamma\delta}&(p_1, p_2, p_3, p_4) \\ &= (2\pi)^8 G(p_1) G(p_2) [\delta(p_1 - p_3)\delta(p_2 - p_4)\delta_{\alpha\gamma}\delta_{\beta\delta} \\ &- \delta(p_1 - p_4)\delta(p_2 - p_3)\delta_{\alpha\delta}\delta_{\beta\gamma}] \\ &+ i(2\pi)^4 G(p_1)G(p_2)G(p_3)G(p_4)\Gamma_{\alpha\beta\gamma\delta}(p_1, p_2, p_3, p_4)\delta(p_1 \\ &+ p_2 - p_3 - p_4). \qquad (2) \end{aligned}$$

The Hamiltonian of the interparticle interaction is of the form

$$H_{int} = \frac{1}{2}\int V(x - y)\,\psi_1^+(x)\,\psi_2^+(y)\,\psi_2(y)\,\psi_1(x)\,d^4x\,d^3y,$$
$$V(x - y) = V(\mathbf{x} - \mathbf{y})\delta(x_0 - y_0). \qquad (2a)$$

It was shown by Landau[4] that the singularities of Γ for small values of the momentum transfer ($q = p_3 - p_1$ or $p_4 - p_1$) are connected with the existence of so-called "zero sound." We shall study the singularities of the vertex function* as far as the vari-

---

*A study of these singularities in general form in the theory of a Fermi liquid was made in an unpublished paper by A. A. Abrikosov, L. P. Gor'kov, L. D. Landau, and I. M. Khalatnikov. In the model considered the same approach allowed us to obtain more detailed results.

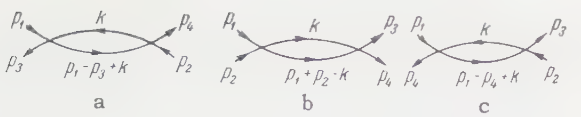

FIG. 1

able $q = p_1 + p_2$ is concerned. To do this we consider the diagrams of the first orders in perturbation theory (Fig. 1).

Singularities of the "zero-sound" type are connected with the diagrams of Fig. 1a, c. As far as the diagram of Fig. 1b is concerned, it contains an integral of two Green's functions of the form $f_0^2 \int G(k)\, G(q-k)\, d^4k$. Substituting here for $G(k)$ the Green's function of a perfect Fermi gas

$$G(k) = [\omega + \mu - \varepsilon(\mathbf{k}) + i\delta \operatorname{sign}(\varepsilon(\mathbf{k}) - \mu)]^{-1},$$

we get after integrating over the frequency

$$-2\pi i f_0^2 \int \frac{d^3k}{\varepsilon + 2\mu - \varepsilon(\mathbf{k}) - \varepsilon(\mathbf{q}-\mathbf{k}) + i\delta},$$

$$\varepsilon(\mathbf{k}) > \mu, \quad \varepsilon(\mathbf{q}-\mathbf{k}) > \mu,$$

$$2\pi i f_0^2 \int \frac{d^3k}{\varepsilon + 2\mu - \varepsilon(\mathbf{k}) - \varepsilon(\mathbf{q}-\mathbf{k}) - i\delta},$$

$$\varepsilon(\mathbf{k}) < \mu, \quad \varepsilon(\mathbf{q}-\mathbf{k}) < \mu. \tag{3}$$

This integral diverges at large k; this is connected with the fact that in that range it is the same as the Born correction to the scattering amplitude of two particles in vacuo. One can thus remove the divergence for large k by renormalizing the scattering amplitude. However, at small $q \ll p_0$ and $\epsilon \ll \mu$ the result obtained diverges logarithmically also near the Fermi surface for $k \sim p_0$. The integration in (3) leads thus when q and ϵ are small to a logarithmic term of the order $(p_0^2 f_0^2/v) \times \ln\{qv/\mu, \epsilon/\mu\}$. The large magnitude of the logarithm can be compensated by the small parameter $p_0^2 f_0/v \ll 1$.

To evaluate the vertex part in that range of $\{qv, \epsilon\}$ values perturbation theory turns out to be insufficient and we must sum a whole "ladder" of diagrams shown in Fig. 1b. We write down the equation for the vertex part in such a way that we explicitly separate off special integrations of the type (3):

$$\Gamma_{\alpha\beta\gamma\delta}(p_1, p_2, p_3, p_4) = \widetilde{\Gamma}_{\alpha\beta\gamma\delta}(p_1, p_2, p_3, p_4)$$
$$+ \frac{i}{2(2\pi)^4} \int \widetilde{\Gamma}_{\alpha\beta\xi\eta}(p_1, p_2, k, q-k)\, G(k)\, G(q-k)\, \Gamma_{\xi\eta\gamma\delta}(k, q$$
$$-k, p_3, p_4)\, d^4k, \tag{4}$$

where $\widetilde{\Gamma}_{\alpha\beta\gamma\delta}(p_1, p_2, p_3, p_4)$ is the totality of those diagrams which are irreducible in the sense that they cannot be divided by a vertical line into two parts which are joint by two fermion lines directed to one side.

The above-mentioned divergence in the large momentum region can be removed as follows. We define a vertex function for particles, interacting in vacuo, using the equation (Belyaev[5] and Galitskii[6] introduced this quantity)

$$\Gamma^{(0)}_{\alpha\beta\gamma\delta}(p_1, p_2, p_3, p_4) = \Gamma^{(1)}_{\alpha\beta\gamma\delta}(p_1, p_2, p_3, p_4)$$
$$+ \frac{i}{2(2\pi)^4} \int \Gamma^{(1)}_{\alpha\beta\xi\eta}(p_1, p_2, k, q-k)\, G^{(0)}(k)\, G^{(0)}(q-k)\, \Gamma^{(0)}_{\xi\eta\gamma\delta}$$
$$\times (k, q-k, p_3, p_4)\, d^4k, \tag{5}$$

where $\Gamma^{(1)}_{\alpha\beta\gamma\delta}(p_1, p_2, p_3, p_4)$ is the term of first order in the interaction, which is equal to $V(p_3 - p_1)\, \delta_{\alpha\gamma}\delta_{\beta\delta} - V(p_3 - p_2)\, \delta_{\alpha\delta}\delta_{\beta\gamma}$ while $G^{(0)}(k)$ is the vacuum particle Green function:

$$G^{(0)}(k) = (\omega - \varepsilon(\mathbf{k}) + i\delta)^{-1}.$$

If we write (5) in the form

$$\Gamma^{(1)}_{\alpha\beta\gamma\delta}(p_1, p_2, p_3, p_4) = L\Gamma_{\alpha\beta\gamma\delta}(p_1, p_2, p_3, p_4)$$
$$\equiv \Gamma^{(0)}_{\alpha\beta\gamma\delta}(p_1, p_2, p_3, p_4) - \frac{i}{2(2\pi)^4} \int \Gamma^{(1)}_{\alpha\beta\xi\eta}(p_1, p_2, k, q-k)$$
$$\times G^{(0)}(k)\, G^{(0)}(q-k)\, \Gamma^{(0)}_{\xi\eta\gamma\delta}(k, q-k, p_3, p_4,)\, d^4k$$

and then subtract from both sides of Eq. (4) the integral

$$\frac{i}{2(2\pi)^4} \int \Gamma^{(1)}_{\alpha\beta\xi\eta}(p_1, p_2, k, q-k)\, G^{(0)}(k)\, G^{(0)}(q-k)\, \Gamma_{\xi\eta\gamma\delta}(k, q$$
$$-k, p_3, p_4)\, d^4k,$$

we get

$$L\Gamma_{\alpha\beta\gamma\delta}(p_1, p_2, p_3, p_4) = L\Gamma^{(0)}_{\alpha\beta\gamma\delta}(p_1, p_2, p_3, p_4)$$
$$+ \widetilde{\Gamma}^*_{\alpha\beta\gamma\delta}(p_1, p_2, p_3, p_4)$$
$$\frac{i}{2(2\pi)^4} \int L\Gamma^{(0)}_{\alpha\beta\xi\eta}(p_1, p_2, k, q-k)\, [G(k)\, G(q-k)$$
$$- G^{(0)}(k)\, G^{(0)}(q-k)]\, \Gamma_{\xi\eta\gamma\delta}(k, q-k, p_3, p_4)\, d^4k$$
$$+ \frac{i}{2(2\pi)^4} \int \widetilde{\Gamma}^*_{\alpha\beta\xi\eta}(p_1, p_2, p_3, p_4)\, G(k)\, G(q-k)$$
$$\times \Gamma_{\xi\eta\gamma\delta}(k, q-k, p_3, p_4)\, d^4k, \tag{6}$$

where $\widetilde{\Gamma}^*_{\alpha\beta\gamma\delta}(p_1, p_2, p_3, p_4)$ stands for all irreducible diagrams from the second order in the interaction onwards.

We get the vertex part $\Gamma_{\alpha\beta\gamma\delta}(p_1, p_2, p_3, p_4)$ up to terms of order $p_0^2 f_0^2/v$ inclusive. It is clear that as the diagrams for $\widetilde{\Gamma}$ do not contain logarithmic integrations we can restrict ourselves in this order in the expression for $\widetilde{\Gamma}^*$ to terms of second order in f_0 (Fig. 2)

Applying to both sides of Eq. (6) the operator L^{-1} we are led to the following equation

$$\Gamma_{\alpha\beta\gamma\delta}(p_1, p_2, p_3, p_4) = \Gamma^{(0)}_{\alpha\beta\gamma\delta}(p_1, p_2, p_3, p_4) + \frac{i}{2(2\pi)^4} \int \Gamma^{(0)}_{\alpha\beta\xi\eta}$$
$$\times (p_1, p_2, k, q-k)\, [G(k)\, G(q-k) - G^{(0)}(k)\, G^{(0)}(q-k)]$$
$$\times \Gamma_{\xi\eta\gamma\delta}(k, q-k, p_3, p_4)\, d^4k + \frac{i}{2(2\pi)^4} \int \widetilde{\Gamma}^*_{\alpha\beta\zeta\eta}(p_1, p_2, k, q$$
$$-k)\, G(k)\, G(q-k)\, \Gamma_{\xi\eta\gamma\delta}(k, q-k, p_3, p_4)\, d^4k. \tag{7}$$

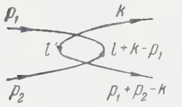

FIG. 2

Within the accuracy which we have adopted $L\widetilde{\Gamma}^* = \widetilde{\Gamma}^*$ and we have neglected in the terms which do not contain logarithmic integrations quantities of second order in f_0. As far as $\Gamma^{(0)}$ is concerned in the integral on the right hand side of (7), we must evaluate it up to terms in second order in f_0:

$$\Gamma^{(0)}_{\alpha\beta\xi\eta}(p_1, p_2, k, q-k) = V(\mathbf{k}-\mathbf{p}_1)\,\delta_{\alpha\xi}\delta_{\beta\eta} - V(\mathbf{k}-\mathbf{p}_2)\,\delta_{\alpha\eta}\delta_{\beta\xi}$$
$$\frac{i}{2(2\pi)^4}\int [V(\mathbf{l}-\mathbf{p}_1)\,V(\mathbf{k}-\mathbf{l})$$
$$V(\mathbf{l}-\mathbf{p}_2)\,V(\mathbf{l}-\mathbf{q}+\mathbf{k})]\,G^{(0)}(l)\,G^{(0)}(q-l)\,\delta_{\alpha\xi}\delta_{\beta\eta}\,d^4l$$
$$-\frac{i}{2(2\pi)^4}\int [V(\mathbf{l}-\mathbf{p}_1)\,V(\mathbf{k}-\mathbf{q}+\mathbf{l})$$
$$V(\mathbf{l}-\mathbf{p}_2)\,V(\mathbf{k}-\mathbf{l})]\,G^{(0)}(l)\,G^{(0)}(q-l)\,\delta_{\alpha\eta}\delta_{\beta\xi}\,d^4l. \qquad (8)$$

If we use the relation between the scattering amplitude for two particles in vacuo and the interaction potential

$$V(\mathbf{k}_1-\mathbf{k}_2) = f(\mathbf{k}_1, \mathbf{k}_2) + \frac{m}{(2\pi)^3}\int \frac{f(\mathbf{k}_1, \mathbf{l})\,f^*(\mathbf{k}_2, \mathbf{l})\,d^3\mathbf{l}}{l^2-k_2^2-i\delta} \qquad (9)$$

and the well-known relation between the imaginary part of the scattering amplitude and the effective scattering cross section

$$\operatorname{Im} f(\mathbf{k}_1, \mathbf{k}_2) = -\frac{mk_1}{16\pi^2}\int d\mathbf{n}\, f(\mathbf{k}_1, k_1\mathbf{n})\,f^*(\mathbf{k}_2, k_1\mathbf{n}), \qquad (10)$$

we get after substituting (9) and (10) into Eq. (8) an expression for $\Gamma^{(0)}_{\alpha\beta\xi\eta}(p_1, p_2, k, q-k)$:

$$\Gamma^{(0)}_{\alpha\beta\xi\eta}(p_1, p_2, k, q-k) = f_0\,(1 - if_0p_0^2/4\pi v)\,(\delta_{\alpha\xi}\delta_{\beta\eta} - \delta_{\alpha\eta}\delta_{\beta\xi}). \qquad (11)$$

When one uses a Green's function in $G(p)$ one should, strictly speaking, evaluate its value up to terms of second order in f_0. Galitskii[6] has, however, shown that the correction of second order in f_0 to the perfect Fermi-gas Green's function leads merely to a renormalization of the Fermi energy. We shall thus in the following use the perfect Fermi-gas Green's functions assuming μ to be the renormalized Fermi energy.

The contribution to $\Gamma^*_{\alpha\beta\xi\eta}(p_1, p_2, k, q-k)$ in the intervals $\epsilon \ll \mu$ and $q \ll p_0$ which are of interest to us is equal to

$$\frac{if_0^2}{(2\pi)^4}\int G(l)\,G(p_1-k+l)\,d^4l\,(\delta_{\alpha\xi}\delta_{\beta\eta} - \delta_{\alpha\eta}\delta_{\beta\xi}).$$

Substituting $\Gamma^{(0)}_{\alpha\beta\xi\eta}(p_1, p_2, k, q-k)$ and $\widetilde{\Gamma}^*_{\alpha\beta\xi\eta}(p_1, p_2, k, q-k)$ into Eq. (7) and taking into account that of the terms of second order in f_0 we need only the logarithmic ones, we get the following expression for the vertex function:

$$\Gamma_{\alpha\beta\gamma\delta}(p_1, p_2, p_3, p_4) = \Gamma^{(0)}_{\alpha\beta\gamma\delta}(p_1, p_2, p_3, p_4)$$
$$\left\{1 - \frac{if_0}{(2\pi)^4}\left(1 - \frac{if_0p_0^2}{4\pi v}\right)\int [G(k)\,G(q-k)\right.$$
$$-G^{(0)}(k)\,G^{(0)}(q-k)]\,d^4k$$
$$\left.+\frac{f_0^2}{(2\pi)^8}\int G(l)\,G(p_1-k+l)\,G(k)\,G(q-k)\,d^4l\,d^4k\right\}^{-1}. \qquad (12)$$

The first of these integrals gives in the denominator of (12) a term

$$-\frac{p_0^2f_0}{(2\pi)^2 v}\left(1 - \frac{if_0p_0^2}{4\pi v}\right)\left(2 + \ln\frac{\varepsilon^2 - q^2v^2 + i\delta}{64\mu^2} + \frac{\varepsilon}{qv}\ln\frac{\varepsilon + vq - i\delta}{\varepsilon - vq + i\delta}\right).$$

As we need only take into account the logarithmic term we must, when evaluating the second integral, put $p_1 = k = p_0$, $\epsilon_1 = \omega = \mu$ after integrating over l and we must average over the direction of the vector $\mathbf{k}$. We get

$$\frac{2f_0^2p_0^4}{3(2\pi)^4v^2}\,(1 + 2\ln 2)\ln\frac{\varepsilon^2 - q^2v^2}{64\mu^2}.$$

Substituting the results of these calculations into (12) we get

$$\Gamma_{\alpha\beta\gamma\delta}(p_1, p_2, p_3, p_4) = -(2\pi)^2 vp_0^{-2}\,(\delta_{\alpha\gamma}\delta_{\beta\delta}$$
$$-\delta_{\alpha\delta}\delta_{\beta\gamma})\,\{(2\pi)^2 v/p_0^2|f_0| - i\pi + \frac{8}{3} - \frac{14}{3}\ln 2$$
$$+\ln\frac{\varepsilon^2 - q^2v^2 + i\delta}{\mu^2} + \frac{\varepsilon}{qv}\ln\frac{\varepsilon + qv - i\delta}{\varepsilon - qv + i\delta}\}^{-1}. \qquad (13)$$

We shall consider (13) to be the analytical continuation of $\Gamma_{\alpha\beta\gamma\delta}(p_1, p_2, p_3, p_4)$ in the upper half-plane of the variable ϵ. Let $q = 0$ to begin with. We see that $\Gamma_{\alpha\beta\gamma\delta}(p_1, p_2, p_3, p_4)$ has a pole at $\epsilon_0 = i\Delta$, where $\Delta = \mu\,(2/e)^{7/3}\exp\{-2\pi^2 v/|f_0|p_0^2\}$. If we express the vertex part $\Gamma_{\alpha\beta\gamma\delta}(p_1, p_2, p_3, p_4)$ in terms of ϵ_0 it has the form

$$\Gamma_{\alpha\beta\gamma\delta}(p_1, p_2, p_3, p_4) = -(2\pi)^2 vp_0^{-2}\,(\delta_{\alpha\gamma}\delta_{\beta\delta} - \delta_{\alpha\delta}\delta_{\beta\gamma})$$
$$\times\left\{-2 + \ln\frac{\varepsilon^2 - q^2v^2 + i\delta}{\varepsilon_0^2} + \frac{\varepsilon}{qv}\ln\frac{\varepsilon + vq - i\delta}{\varepsilon - vq + i\delta}\right\}^{-1}.$$

For small $qv \ll \Delta$ the position of the pole $\epsilon(\mathbf{q})$ approaches the real axis: $\epsilon(\mathbf{q}) = i\Delta(1 - q^2v^2/6\Delta^2)$. When q increases further $|\epsilon(\mathbf{q})|$ decreases and it tends to zero when $vq_{max} = e\Delta$ as

$$\varepsilon = (2e\Delta i/\pi)\ln(e\Delta/vq) \approx 2e\Delta i\,(q_{max} - q)/\pi q_{max}.$$

The Cooper phenomenon, i.e., the instability of a fermion system when there are attractions between the particles, leads thus to the occurrence in the vertex part of poles in the upper half-plane of the complex variable $\epsilon = \omega_1 + \omega_2$. Only those particles for which the total momentum is relatively small ($q \ll p_0$) will here display a tendency to form bound pairs. The quantity Δ has clearly the meaning of the reciprocal of the relaxation time of the system.

We turn now to the problem of determining the temperature at which the system makes the transition to the superfluid state. Because we cannot apply the usual technique at finite temperatures we must use the Matsubara quantities.[2,3] In the Matsubara method we have instead of (2) the following connection between the two-particle Green's function and the vertex part

$$\begin{aligned}&\mathfrak{G}_{\alpha\beta\gamma\delta}(\omega_1\mathbf{p}_1, \omega_2\mathbf{p}_2, \omega_3\mathbf{p}_3, \omega_4\mathbf{p}_4)\\ &\quad = (2\pi)^3T^{-1}\{(2\pi)^3T^{-1}[\mathfrak{G}(\omega_1\mathbf{p}_1)\mathfrak{G}(\omega_2\mathbf{p}_2)\\ &\quad \times \delta_{\omega_1\omega_4}\delta(\mathbf{p}_1-\mathbf{p}_4)\delta_{\alpha\delta}\delta_{\beta\gamma}-\mathfrak{G}(\omega_1\mathbf{p}_1)\mathfrak{G}(\omega_2\mathbf{p}_2)\delta_{\omega_1\omega_3}\delta(\mathbf{p}_1\\ &\quad -\mathbf{p}_3)\delta_{\alpha\gamma}\delta_{\beta\delta}]-\tfrac{1}{2}\mathfrak{G}(\omega_1\mathbf{p}_1)\mathfrak{G}(\omega_2\mathbf{p}_2)\mathfrak{G}(\omega_3\mathbf{p}_3)\mathfrak{G}(\omega_4\mathbf{p}_4)\\ &\quad \times \mathfrak{T}_{\alpha\beta\gamma\delta}(\omega_1\mathbf{p}_1, \omega_2\mathbf{p}_2, \omega_3\mathbf{p}_3, \omega_4\mathbf{p}_4)\}\\ &\quad \times \delta_{\omega_1+\omega_2-\omega_3-\omega_4}\delta(\mathbf{p}_1+\mathbf{p}_2-\mathbf{p}_3-\mathbf{p}_4). \qquad (14)\end{aligned}$$

At the beginning of this paper we have already remarked that one can define the critical temperature as the temperature at which the Bose "condensation" of bound pairs sets in. At that point the two-particle Green's function. or what amounts to the same, according to (14), the vertex part, tends to infinity for the first time. We note that the dependence of the temperature dependent quantity $\mathfrak{T}_{\alpha\beta\gamma\delta}(\omega_1\mathbf{p}_1, \omega_2\mathbf{p}_2, \omega_3\mathbf{p}_3, \omega_4\mathbf{p}_4)$ on the variable $\epsilon = \omega_1 + \omega_2$ is defined only in the discrete points $\epsilon_n = 2\pi nTi$, $n = 0, \pm 1, \pm 2, \ldots$ At the critical temperature the position of the pole is $\epsilon = 0$. Moreover, it is clear from similarity considerations that the Fourier component of the Matsubara quantity $\mathfrak{T}_{\alpha\beta\gamma\delta}(\omega_1 + \omega_2 = 0,\ \mathbf{p}_1 + \mathbf{p}_2 = 0)$ becomes infinite at the transition.

The remainder of our discussion will refer to the case $\epsilon = \omega_1 + \omega_2 = 0$, $\mathbf{q} = \mathbf{p}_1 + \mathbf{p}_2 = 0$.

The diagram of Fig. 1b contains in second order in f_0 an integral over the product of two Matsubara Green's functions $\mathfrak{G}(\omega\mathbf{k})$ for the perfect Fermi gas of the form

$$2\pi i f_0^2 T\sum_{\omega_n}\int \mathfrak{G}(\omega_n\mathbf{k})\,\mathfrak{G}(-\omega_n, -\mathbf{k})\,d^3\mathbf{k},$$

which after summation over ω_n becomes

$$\pi i f_0^2\int\frac{d^3\mathbf{k}}{\mu-\varepsilon(\mathbf{k})}\,\mathrm{th}\,\frac{\mu-\varepsilon(\mathbf{k})}{2T}. \qquad (15)^*$$

The integral (15) diverges for large k. The divergence of this integral can be removed in the same way as at absolute zero by renormalizing the scattering amplitude. The integral diverges, however, also near the Fermi surface where its magnitude is $\sim(f_0p_0^2/v)\ln(T/\mu)$ which is compensated by the smallness of the parameter $f_0p_0^2/v \ll 1$. To evaluate $\mathfrak{T}_{\alpha\beta\gamma\delta}(\omega_1\mathbf{p}_1, \omega_2\mathbf{p}_2, \omega_3\mathbf{p}_3, \omega_4\mathbf{p}_4)$ we must therefore again sum a "ladder" of diagrams such as Fig. 1b. We write down an equation for $\mathfrak{T}_{\alpha\beta\gamma\delta}(\omega_1\mathbf{p}_1, \omega_2\mathbf{p}_2, \omega_3\mathbf{p}_3, \omega_4\mathbf{p}_4)$ which is similar to Eq. (5):

$$\begin{aligned}&\mathfrak{T}_{\alpha\beta\gamma\delta}(\omega_1\mathbf{p}_1,\ \omega_2\mathbf{p}_2,\ \omega_3\mathbf{p}_3,\ \omega_4\mathbf{p}_4)\\ &\qquad \widetilde{\mathfrak{T}}_{\alpha\beta\gamma\delta}(\omega_1\mathbf{p}_1,\ \omega_2\mathbf{p}_2,\ \omega_3\mathbf{p}_3,\ \omega_4\mathbf{p}_4)\\ &\quad -\frac{T}{2(2\pi)^3}\sum_{\omega_n}\int\widetilde{\mathfrak{T}}_{\alpha\beta\xi\eta}(\omega_1\mathbf{p}_1,\ \omega_2\mathbf{p}_2,\ \omega_n\mathbf{k},\ \varepsilon-\omega_n,\ \mathbf{q}-\mathbf{k})\\ &\quad \times\mathfrak{G}(\omega_n\mathbf{k})\,\mathfrak{G}(\varepsilon-\omega_n,\ \mathbf{q}-\mathbf{k})\\ &\quad \times\mathfrak{T}_{\xi\eta\gamma\delta}(\omega_n\mathbf{k},\ \ \varepsilon-\omega_n,\ \ \mathbf{q}-\mathbf{k},\ \ \omega_3\mathbf{p}_3,\ \ \omega_4\mathbf{p}_4)\,d^3\mathbf{k}. \qquad (16)\end{aligned}$$

We obtain an equation to determine the temperature at which the transition into the superfluid state takes place from (16) if we take into account that $\widetilde{\mathfrak{T}}$ has no singularities of the kind (15) and that we need only to know of the terms in $\widetilde{\mathfrak{T}}^{(2)}$ that one which gives a contribution $\sim(f_0^2p_0^4/v^2)\times\ln(T/\mu)$. Near the point where $\mathfrak{T}_{\alpha\beta\gamma\delta}(\epsilon, \mathbf{q})$ becomes infinite Eq. (16) becomes of the form

$$\begin{aligned}1 = &-\frac{T_c}{(2\pi)^3}\sum_{\omega_n}\int V(\mathbf{p}_1-\mathbf{k})\,\mathfrak{G}(\omega_n\mathbf{k})\,\mathfrak{G}(-\omega_n, -\mathbf{k})\,d^3\mathbf{k}\\ &-\frac{T_c}{(2\pi)^3}\sum_{\omega_n}\int\widetilde{\mathfrak{T}}^{(2)}(\omega_1\mathbf{p}_1, \omega_2\mathbf{p}_2, \omega_n\mathbf{k}, -\omega_n, -\mathbf{k})\,\mathfrak{G}(\omega_n\mathbf{k})\\ &\times\mathfrak{G}(-\omega_n, -\mathbf{k})\,d^3\mathbf{k}. \qquad (17)\end{aligned}$$

We have here taken into account that $\mathfrak{T}^{(1)}_{\alpha\beta\gamma\delta}(\omega_1\mathbf{p}_1, \omega_2\mathbf{p}_2, \omega_n\mathbf{k}, -\omega_n, -\mathbf{k})$ is independent of the fourth components of the momenta and is thus the same as the quantity $\Gamma^{(1)}_{\alpha\beta\gamma\delta}(\mathbf{p}_1, \mathbf{p}_2, \mathbf{k}, -\mathbf{k})$.

As at $T = 0$, the divergence in the first integral in (17) far from the Fermi surface can be removed by renormalizing the scattering amplitude; after that Eq. (17) is reduced to the form

$$\begin{aligned}1 = &-\frac{2f_0}{(2\pi)^3}\left(1-\frac{if_0p_0^2}{4\pi v}\right)\int\left[\frac{\mathrm{th}\,(\mu-\varepsilon(\mathbf{k}))/2T_c)}{\mu-\varepsilon(\mathbf{k})}\right.\\ &\left.+\frac{1}{\mu-\varepsilon(\mathbf{k})+i\delta}\right]d^3\mathbf{k}-\frac{T_c}{(2\pi)^3}\sum_{\omega_n}\int\widetilde{\mathfrak{T}}^{(2)}(\omega_1\mathbf{p}_1, \omega_2\mathbf{p}_2, \omega_n\mathbf{k},\\ &-\omega_n, -\mathbf{k})\,\mathfrak{G}(\omega_n\mathbf{k})\,\mathfrak{G}(-\omega_n, -\mathbf{k})\,d^3\mathbf{k}. \qquad (18)\end{aligned}$$

The contribution to $\mathfrak{T}^{(2)}$ which contains all irreducible diagrams of second order in the interaction is given by the expression

$$-\frac{f_0^2T_c}{(2\pi)^3}\sum_{\varepsilon_n}\int\mathfrak{G}(\varepsilon_n, \mathbf{l})\,\mathfrak{G}(\varepsilon_n+\omega_1-\omega_n, \mathbf{l}+\mathbf{p}_1-\mathbf{k})\,d^3\mathbf{l}.$$

The first integral in (18) gives the contribution

$$-\frac{p_0^2f_0}{2\pi^2v}\left(1-\frac{if_0p_0^2}{4\pi v}\right)\left(\ln\frac{8\gamma\mu}{T_c\pi}-2-\frac{i\pi}{2}\right), \qquad (19)$$

where $\ln\gamma$ is Euler's constant.

---

*th = tanh.

The evaluation of the second integral in (18) proceeds taking the same considerations into account as at the absolute zero. The result of these calculations is

$$-\frac{p_0^4 f_0^2}{12\pi^4 v^2}(1+2\ln 2)\ln\frac{8\gamma\mu}{T_c\pi}. \tag{20}$$

Substituting (19) and (20) into (18) we get

$$-\frac{2\pi^2 v}{|f_0|\, p_0^2} = \ln\left[\frac{T_c\pi}{\gamma\mu}\left(\frac{e}{2}\right)^{7/3}\right].$$

The temperature of the transition into the superfluid state is thus determined by the relation

$$T_c = (\gamma\mu/\pi)(2/e)^{7/3}\exp\{-2\pi^2 v/p_0^2|f_0|\}$$

or, $T_c = \gamma\Delta/\pi$, where Δ is the previously determined quantity which has the meaning of the reciprocal of the relaxation time of the system.

It is of interest to note that as in the model considered the integration practically is performed near the Fermi surface the relation between the "gap" width and the transition temperature must be the same as in the theory of superconductivity, and it follows thus that the gap width at $T = 0$ is equal to the reciprocal of the relaxation time of the system.

In conclusion we express our gratitude to Academician L. D. Landau for valuable discussions of the results of this paper.

---

[1] L. Cooper, Phys. Rev. **104**, 1189 (1956).

[2] Abrikosov, Gor'kov, and Dzyaloshinskii, JETP **36**, 900 (1959), Soviet Phys. JETP **9**, 636 (1959).

[3] E. S. Fradkin, JETP **36**, 1286 (1959), Soviet Phys. JETP **9**, 912 (1959).

[4] L. D. Landau, JETP **35**, 97 (1958), Soviet Phys. JETP **8**, 70 (1959).

[5] S. T. Belyaev, JETP **34**, 417 (1958), Soviet Phys. JETP **7**, 328 (1958).

[6] V. M. Galitskii, JETP **34**, 151 (1958), Soviet Phys. JETP **7**, 104 (1958).

Translated by D. ter Haar
248

SOVIET PHYSICS JETP VOLUME 13, NUMBER 5 NOVEMBER, 1961

BIPOLAR STATES OF CURRENT CARRIERS IN IONIC CRYSTALS

V. L. VINETSKII

Physics Institute, Academy of Sciences, Ukrainian S.S.R.

Submitted to JETP editor December 22, 1960

J. Exptl. Theoret. Phys. (U.S.S.R.) **40**, 1459-1468 (May, 1961)

The system consisting of two conduction electrons in an ionic crystal interacting with the polarization and elastic deformation of the crystal is considered. It is shown that the previous[1] conclusion about the possibility of bipolaron formation does not depend essentially on the approximations applied in reference 1 (variational method, classical treatment of ionic motion) and remains valid in a more rigorous solution.

The effect of elastic deformation, which was not taken into account in reference 1, leads to an improvement in the criterion for the existence of bipolarons and an increase in their binding energy. The motion of bipolarons is considered and the energy of the ground state, effective mass, and moment of inertia are calculated. It is concluded that bipolaron states of the current carriers can exist in ionic crystals at sufficiently low temperatures.

ONE of the approximations usually applied in polaron theory consists in neglecting the exchange degeneracy of the "outer" electrons. In the adiabatic approximation[2,3] or in the intermediate binding approximation,[4,5] such a treatment corresponds to choosing a multiplicative form

$$\psi(\mathbf{r}_1 \ldots \mathbf{r}_i \ldots \mathbf{r}_N) = \prod_{i=1}^{N} \psi_i(\mathbf{r}_i), \qquad (1)$$

for the electron part of the wave function of the system; here N is the number of conduction electrons in the crystal.

It is more consistent, however, to choose the corresponding antisymmetrized product as the wave function of the many-electron system under consideration. If the overlap of the single-electron wave functions in the Fock determinant is small, then the multiplicative approximation is a good one. Small overlap of the single-electron functions occurs, obviously, when the Coulomb repulsion of the electrons (proportional to n^{-2}, where n is the index of refraction of the crystal) exceeds the attractive force due to the interaction of each electron with the polarization produced by the remaining electrons (this force is proportional to $c = n^{-2} - \varepsilon^{-1}$, where ε is the dielectric constant), i.e., for sufficiently small values of the parameters n^2 and c. Then the average distance between conduction electrons is large (in semiconductors, for reasonable values of the concentration of conduction electrons), and the exchange interaction can be neglected.

The exchange forces become essential in the case of significant overlap of the single-electron wave functions. This circumstance can lead to the formation of polaronic quasimolecules in the ionic crystals that have sufficiently high values of n^2 and c. The semiclassical theory constructed by the author and Giterman for two conduction electrons showed that the formation of bipolarons is energetically favorable in crystals with parameters satisfying the condition $n^2 c \geq 0.95$. A bipolaron is a quasiparticle consisting of a self-consistent state of two conduction electrons and the axially symmetric polarization potential well which is produced by them and which binds them.

The treatment in reference 1, like that used in polaron theory,[2] relies on a straight variational method for calculating the electron part of the wave function of the system. Because of the small value of the calculated energy for bipolaron formation, it might be suspected that this value is due to an insufficiently good choice of the approximate wave function in polaron theory.

Below it will be shown that the previous[1] conclusion about the possible existence of the bipolaron is not based essentially on the variational method. The treatment carried out here differs from that in the previous work in being consistently quantum mechanical. Besides the interaction of the conduction electrons with the polarization deformation, the interaction with the elastic deformation of the crystal is also taken into account. Translation and rotation of bipolarons are also considered.

1. GROUND STATE OF BIPOLARON AT REST

The Hamiltonian of the system consisting of an ionic crystal and two "outer" electrons can be written in the form[2,3,6,7]

$$\hat{H} = -\frac{\hbar^2}{2\mu}\sum_{i=1}^{2}\Delta_i + \sum_{\mathbf{k},\,\alpha,\,i} c^{i}_{\mathbf{k}\alpha}\chi_{\mathbf{k}\alpha}(\mathbf{r}_i)\,q_{\mathbf{k}\alpha} + \sum_{\mathbf{k},\,\alpha}\frac{\hbar\omega_{\mathbf{k}\alpha}}{2}\left(q^2_{\mathbf{k}\alpha} - \frac{\partial^2}{\partial q^2_{\mathbf{k}\alpha}}\right) + \frac{e^2}{n^2\,|\mathbf{r}_1 - \mathbf{r}_2|}, \qquad (2)$$

where the first term is the kinetic energy of the conduction electrons, the second term is their interaction with the polarization and elastic deformations of the crystal, the third is the energy of the ionic oscillations, and the fourth is the energy of electrostatic repulsion of the electrons under consideration; μ is the effective mass of the band electron, $\mathbf{k} = (k_1, k_2, k_3)$ is the index of the normal mode, α is the number of the branch of the mode, $\chi_{\mathbf{k}\alpha}(\mathbf{r}) = (2/V)^{1/2}\sin(\mathbf{k}_\alpha\cdot\mathbf{r} + \pi/4)$ are the functions used as a basis for the expansion of the inertial polarization $\mathbf{P}(\mathbf{r})$ and displacement $\mathbf{u}(\mathbf{r})$, $\omega_{\mathbf{k}\alpha}$ and $q_{\mathbf{k}\alpha}$ are the frequency and normal coordinate of the mode.

Below, the case of an isotropic crystal is considered:

$c_{\mathbf{k}\alpha} = -e\sqrt{4\pi\hbar\omega_{\mathbf{k}\alpha}c}\,/\,|\mathbf{k}|$ — for longitudinal optical modes,
$c_{\mathbf{k}\alpha} = a\sqrt{\hbar\omega_{\mathbf{k}\alpha}/E}$ — for longitudinal acoustic modes,
$c_{\mathbf{k}\alpha} = 0$ — for transverse optical and acoustic modes.

Here $E = K + (4/3)\mu_0$, where K and μ_0 are the bulk and shear moduli, respectively; a is the constant of the deformation potential.

We seek a solution of the Schrödinger equation with the Hamiltonian (2) in the adiabatic approximation. The main criterion for this approximation is the inequality[2]

$$\hbar\omega_{\mathbf{k}\alpha} \ll \mu c^2/m. \qquad (3)$$

Thus, large values of c, for which bipolaron states occur (according to reference 1 and the results of the present work), also favor fulfillment of the inequality (3).

According to Pekar,[3] solution of the Schrödinger equation in the adiabatic approximation is equivalent to finding the minimum of the corresponding functional with an approximate wave function of the form

$$\Psi(\ldots\mathbf{r}_i\ldots q_{\mathbf{k}\alpha}\ldots) = \psi(\ldots\mathbf{r}_i\ldots)\,\Phi(\ldots q_{\mathbf{k}\alpha}\ldots).$$

Minimization with respect to $\Phi(\ldots q_{\mathbf{k}\alpha}\ldots)$ leads to the following value for the energy of the system:

$$\overline{H} = \sum_{\mathbf{k}\alpha}\frac{\hbar\omega_{\mathbf{k}\alpha}}{2}(2n_{\mathbf{k}\alpha} + 1) + \min_\psi J[\psi], \qquad n_{\mathbf{k}\alpha} = 0, 1, 2, \ldots;$$

$$J[\psi] = \frac{\hbar^2}{\mu}\int|\nabla_1\psi(\mathbf{r}_1, \mathbf{r}_2)|^2\,d\tau_{12} + \frac{e^2}{n^2}\int\frac{\psi^2(\mathbf{r}_1, \mathbf{r}_2)}{|\mathbf{r}_1 - \mathbf{r}_2|}\,d\tau_{12} - 2\sum_{\mathbf{k}\alpha}\frac{c^2_{\mathbf{k}\alpha}K^2_{-\mathbf{k}\alpha}}{\hbar\omega_{\mathbf{k}\alpha}},$$

$$K_{-\mathbf{k}\alpha} = -\int|\psi(\mathbf{r}_1, \mathbf{r}_2)|^2\,\chi_{-\mathbf{k}}(\mathbf{r}_1)\,d\tau_{12}. \qquad (4)$$

As indicated by the remarks above, the electron wave function of the system is sought in the form

$$\psi(\mathbf{r}_1, \mathbf{r}_2) = \mathrm{const}\cdot[\psi_a(\mathbf{r}_1)\psi_b(\mathbf{r}_2) + \psi_a(\mathbf{r}_2)\psi_b(\mathbf{r}_1)].$$

The single-electron wave functions $\psi_a(\mathbf{r}_i)$ and $\psi_b(\mathbf{r}_i)$ will be determined later.

Substitution of $\psi(\mathbf{r}_1, \mathbf{r}_2)$ into the functional $J[\psi]$ leads to the expression

$$J_{\mathrm{bp}}[\psi] = \frac{\hbar^2}{\mu}\,\frac{R_1 + SR_2}{1 + S^2} + \frac{e^2}{n^2}\,\frac{u_2 + u_4}{1 + S^2} - ce^2\,\frac{u_1 + u_2 + 4Su_3 + 2S^2u_4}{(1 + S^2)^2} - \frac{a^2}{E}\,\frac{v_1 + (1 + 2S^2)v_2 + 4Sv_3}{(1 + S^2)^2}. \qquad (5)$$

where

$$S = \int\psi_a\psi_b\,d\tau, \qquad R_1 = \int(\nabla\psi_a)^2\,d\tau, \qquad R_2 = \int\nabla\psi_a\nabla\psi_b\,d\tau,$$

$$u_1 = \int\frac{\psi^2_a(1)\,\psi^2_a(2)}{r_{12}}\,d\tau_{12}, \qquad u_2 = \int\frac{\psi^2_a(1)\,\psi^2_b(2)}{r_{12}}\,d\tau_{12},$$

$$u_3 = \int\frac{\psi^2_a(1)\psi_a(2)\psi_b(2)}{r_{12}}\,d\tau_{12}, \qquad u_4 = \int\frac{\psi_a(1)\psi_b(1)\psi_a(2)\psi_b(2)}{r_{12}}\,d\tau_{12},$$

$$v_1 = \int\psi^4_a\,d\tau, \qquad v_2 = \int\psi^2_a\psi^2_b\,d\tau, \qquad v_3 = \int\psi^3_a\psi_b\,d\tau. \qquad (6)$$

We consider first the case of a crystal in which the ineraction between the conduction electrons and the elastic vibrations can be neglected $(a^2/E \to 0)$. We seek $\psi_a(\mathbf{r}_i)$ and $\psi_b(\mathbf{r}_i)$ by a variational method. As a result of this, the calculated bipolaron energy will be raised somewhat. We will represent the approximating functions in the variational method in the form

$$\psi_a(\mathbf{r}_i) = k^{3/2}\psi^0_a(k\mathbf{r}_i), \qquad \psi_b(\mathbf{r}_i) = k^{3/2}\psi_b(k\mathbf{r}_i), \qquad (7)$$

where $\psi^0_a(\mathbf{r}_i)$ and $\psi^0_b(\mathbf{r}_i)$ are the exact electron wave functions of a polaron and **k** is the varied parameter. The functions (7) are normalized to unity for all values of k.

Substitution of (7) into the functional (5), variation with respect to k, and use of the expression obtained by Pekar[2] for the polaron functional J_p lead to

$$Q = \frac{J_{\mathrm{bp}}}{2J_{\mathrm{p}}} = \frac{1}{(n^2c)^2}\,\frac{R_1}{(1 + S^2)^3(R_1 + SR_2)\,u_1^2}\,[(u_2 + u_4)(1 + S^2) - n^2c\,(u_1 + u_2 + 4Su_3 + 2S^2u_4)]^2. \qquad (8)$$

The functions $\psi(\mathbf{r})$ in the integrands of S, R_i, and u_i are the exact electron wave functions $\psi^0_a(\mathbf{r})$ and $\psi^0_b(\mathbf{r})$ of the polaron.

The value of the ratio $Q = J_{bp}/2J_p$ depends on R, the distance between the points a and b chosen for the approximate $\psi(\mathbf{r}_1, \mathbf{r}_2)$. To determine the bipolaron energy, Q must be minimized with respect to R. Without solving this problem exactly, we will show that, at least for $n^2c = 1$, there is always a value of R for which $Q > 1$. For this purpose, we expand Q(R) in powers of R. Taking R along the z axis for convenience, it is not difficult to show that

$$Q = 1 + \frac{1}{2}\left(\frac{1}{2}R_1 + \frac{R_3}{6R_1} + \frac{2\pi v_1}{3u_1} + \frac{2u_5}{u_1}\right)R^2 + \ldots, \qquad (9)$$

where

$$R_3 = \int (\Delta\psi_a)^2\, d\tau, \qquad u_5 = \int \frac{1}{r_{12}}\psi_a^2(1)\,\psi_a(2)\frac{\partial^2}{\partial z^2}\psi_a(2)\, d\tau_{12}.$$

To go further, it is necessary to compute the coefficient of R^2 in the expansion (9). This can be done by choosing the best polaron function found by the variational technique

$$\psi(\mathbf{r}) = 0{,}1229\,\alpha^{3/2}(1 + \alpha r + 0.4516\,\alpha^2 r^2)\, e^{-\alpha r},$$
$$\alpha = 0.6585\mu e^2 c/\hbar^2 \qquad (10)$$

in place of the "exact" wave function. The error in the polaron energy calculated with the function (10) is only a fraction of a per cent.[2] Calculating the integrals R_i, u_i, and v_i we find

$$(\partial^2 Q/\partial R^2)_{R=0} = \alpha^2(0.4105 - 0.2062) > 0. \qquad (11)$$

If, instead of (10), we use the wave function

$$\psi = \frac{\alpha^{3/2}}{\sqrt{7\pi}}(1 + \alpha r)\, e^{-\alpha r}, \qquad \alpha = \frac{\mu e^2 c}{2\hbar^2}, \qquad (12)$$

which gives the polaron energy to 1 – 2 per cent, a value of $\partial^2 Q/\partial R^2$ nearly equal to that in (11) is found. Other approximations used in the polaron theory lead to similar results. Obviously, a small variation of $\psi(\mathbf{r})$ about the exact value $\psi_0(\mathbf{r})$ cannot affect substantially the fulfillment of the criterion (11); the derivative $(\partial^2 Q/\partial R^2)_{R=0}$ is essentially positive.

Thus, if $n^2c = 1$, Q(R) has its minimum at $R = 0$ and is equal to unity at this point. For $R > 0$, this ratio, which is underestimated because of the use of a variational method with just the one approximation parameter k, becomes greater than unity; this assures the energetic stability of the bipolaron.

If n^2c decreases from unity, the ratio Q(R) decreases, as is clear from Eq. (8); obviously, however, if n^2c is large enough it can stay greater than unity.

Substitution of (12) into Eq. (8) for Q(R) and maximization with respect to R allow the values of Q and R at the maximum of Q(R) to be determined for arbitrary n^2c. The results obtained coincide with the results of the semiclassical treatment.[1] Bipolaron formation is energetically favored for

$$n^2c \gtrsim 0.95 \qquad (13)$$

($Q_{max} = 1.08$ for $n^2c = 1$). More exact results can be obtained if the following are taken into account:

a) correlation in the motion of the electrons, which introduces into the expression for the approximate function a factor that depends on the separation $|\mathbf{r}_1 - \mathbf{r}_2|$ of the electrons;

b) polar states which correspond to an approximating function of the form

$$\psi(\mathbf{r}_1, \mathbf{r}_2) = N\{\psi_a(1)\psi_b(2) + \psi_a(2)\psi_b(1) + \gamma_a\psi_a(1)\psi_a(2) + \gamma_b\psi_b(1)\psi_b(2)\},$$

where γ_a and γ_b are variational parameters and N is the normalization factor;

c) mutual deformation of the ψ-clouds of the electrons, as a result of which the polaron function which is originally spherically symmetric becomes axially symmetric.

We have estimated ΔJ, the reduction in the bipolaron energy, due to these causes,* using the numerical results obtained in solving the analogous problem in the theory of F-centers.[7-10] The radius of the electron ψ-cloud is larger in the bipolaron than in color centers, and therefore the values for the additional binding energy of the bipolaron are underestimated. Even this underestimate is rather significant and amounts to 3 – 5 per cent of the total bipolaron energy.

We turn now to the consideration of the interaction with elastic deformation. In order to find the minimum of $J_{bp}(R)$ and decide whether or not the bipolaron occurs, it is necessary to repeat with the functional (5) the calculation performed in reference 1. Owing to computational difficulties the calculation has not been accomplished for arbitrary values of n^2, c, a, and E; it can be performed for a particular crystal with given values of these parameters. To obtain an estimate of the role of the interaction between the conduction electrons and the elastic deformation of the crystal, we will again consider the special case $n^2c = 1$, $R = 0$. Using (5) and the results of references 6 and 11, we obtain

$$J_{bp}/2J_p > Q(0) = 1 + B,$$

where B, which has been calculated by the author,[11] is the ratio of the interaction energy of the polaron with the elastic deformation of the lattice to the total polaron energy:

---

*The results of this calculation will be published separately.

$$B = \frac{(1-\sqrt{1-\gamma})^3}{\gamma - 2(1-\gamma)(1-\sqrt{1-\gamma})}, \qquad \gamma = \frac{437}{2^8 \cdot 7\pi} \frac{e^2\mu^2a^2c}{\hbar^4 E}.$$

According to the estimate made by the author,[11] in a real crystal B can have values up to several tenths. B increases with increasing γ. Thus, the elastic interaction can play a significant role in bipolaron formation if, besides a large value of c, the crystal also has large values of the parameters a and μ and small elastic moduli.

2. BIPOLARON MOTION

Up to this point in our treatment, we have not considered the possibility of bipolaron motion, which can occur because of the translational and rotational symmetry of the isotropic crystal. In the solution of this problem, the mathematical apparatus developed by Pekar[12,13] for treating a nucleon moving in a meson field and generalized to the case where the normal modes have branches with different dispersion laws can be used.

The minimum value of the potential energy, $J[\psi(\mathbf{r}_1, \mathbf{r}_2)]$, of the system will be realized in every case when the function

$$\tilde{\psi} = Y_{\vartheta,\varphi} T_{\xi} \psi(\mathbf{r}_1, \mathbf{r}_2)$$

with arbitrary values of $\boldsymbol{\xi}$, ϑ, and φ is used for $\psi(\mathbf{r}_1, \mathbf{r}_2)$; here T_ξ is the bipolaron translation operator for displacement $\boldsymbol{\xi}$, $Y_{\vartheta,\varphi}$ is the bipolaron rotation operator, and the angles ϑ and φ give the position of the bipolaron symmetry axis in an arbitrarily chosen Cartesian coordinate system. The order of operation of $Y_{\vartheta,\varphi}$ and T_ξ on $\psi(\mathbf{r}_1, \mathbf{r}_2)$ is not essential, but since these operators do not commute, we specifically consider translation first and then rotation. Under these conditions, the coordinate transformation is

$$x'_\mu = \sum_{\nu=1}^{3} a_{\mu\nu}(x_\nu - \xi_\nu), \tag{14}$$

where the matrix $\|a\|$ has the form:

$$\|a\| = \begin{Vmatrix} \cos\vartheta\cos\varphi & \sin\varphi & -\sin\vartheta\cos\varphi \\ -\cos\vartheta\sin\varphi & \cos\varphi & \sin\vartheta\sin\varphi \\ \sin\vartheta & 0 & \cos\vartheta \end{Vmatrix}. \tag{15}$$

We consider the states of the system in which the potential energy differs little from its minimum value. The polarization $\mathbf{P}(\mathbf{r})$ and the elastic displacement $\mathbf{u}(\mathbf{r})$ can be written in the form:

$$\mathbf{P}(\mathbf{r}) = \mathbf{P}_0(\mathbf{r}, \boldsymbol{\xi}, \vartheta, \varphi) + \mathbf{P}'(\mathbf{r}),$$

$$\mathbf{u}(\mathbf{r}) = \mathbf{u}_0(\mathbf{r}, \boldsymbol{\xi}, \vartheta, \varphi) + \mathbf{u}'(\mathbf{r}), \tag{16}$$

where $\mathbf{P}_0$ and $\mathbf{U}_0$ belong to the family of solutions corresponding to the equilibrium state of the system and are chosen such that $\mathbf{P}'$ and $\mathbf{u}'$ can be considered as small perturbations in the region of space where the wave function of the electrons differs from zero.

In accordance with the above, the parameters $\boldsymbol{\xi}$, ϑ, and φ which appear in $\mathbf{P}_0$ and $\mathbf{u}_0$ are determined by minimizing the energy of the system, H_1, as calculated by perturbation theory, for states near the equilibrium state. This energy is

$$H_1 = J[\psi_0] + \frac{1}{2}\sum_{\alpha,\mathbf{k}} \hbar\omega_{\mathbf{k}\alpha} [(q_{\mathbf{k}\alpha} - q^0_{\mathbf{k}\alpha})^2 - \partial^2/\partial q^2_{\mathbf{k}\alpha}], \tag{17}$$

where $q^0_{\mathbf{k}\alpha}$ are the new equilibrium positions of the harmonically oscillating ions; they depend on the parameters $\boldsymbol{\xi}$, ϑ, φ:

$$q^0_{\mathbf{k}\alpha} = \frac{2c_{\mathbf{k}\alpha}}{\hbar\omega_{\mathbf{k}\alpha}} \int \tilde{\psi}^2 \chi_{-\mathbf{k}}(\mathbf{r}_1)\, d\tau_{12}.$$

In place of the condition for finding the values of $\boldsymbol{\xi}$, ϑ, and φ which lead to the best description of the states of the system in which the configuration is nearly the equilibrium configuration with the approximation (16), one can use, according to Pekar,[12] the relation

$$\sum_{\alpha} \int \frac{\partial \varphi^0_\alpha}{\partial v_i} \hat{\omega}_\alpha \varphi_\alpha d\tau = 0; \tag{18}$$

where $v_i = \xi_i\ (i = 1, 2, 3)$, $v_4 = \varphi$, $v_5 = \vartheta$;

$$\varphi_\alpha(\mathbf{r}) = \sum_{\mathbf{k}} \varphi_{\mathbf{k}\alpha} \chi_{\mathbf{k}}(\mathbf{r}), \qquad \varphi_{\mathbf{k}\alpha} = \sqrt{\frac{\hbar}{2\omega_{\mathbf{k}\alpha}}}\, q_{\mathbf{k}\alpha},$$

$$\varphi^0{}_{\mathbf{k}\alpha} = \sqrt{\frac{\hbar}{2\omega_{\mathbf{k}\alpha}}}\, q^0_{\mathbf{k}\alpha};$$

The operator $\hat{\omega}_\alpha$ is equal to ω_0 for the optical modes ($\alpha = 1$); for the acoustic modes ($\alpha = 2$), it acts according to $\hat{\omega}_{\mathbf{k}_2}\chi_{\mathbf{k}}(\mathbf{r}) = (E/\rho)^{1/2}\, \mathbf{k}\chi_{\mathbf{k}}(\mathbf{r})$.

In terms of the coordinates $q_{\mathbf{k}}$ and $q^0_{\mathbf{k}}$, (18) takes the form

$$\sum_{\mathbf{k},\alpha} q_{\mathbf{k}\alpha} \partial q^0_{\mathbf{k}\alpha}(\ldots v_i \ldots)/\partial v_i = 0. \tag{19}$$

We seek the solution of the Schrödinger equation with the Hamiltonian (17) (with the supplementary condition (19)) in the form

$$\psi = \psi(\mathbf{r}_1, \mathbf{r}_2)\, \Phi(\ldots q_{\mathbf{k}\alpha} \ldots),$$

$$\Phi(\ldots q_{\mathbf{k}\alpha} \ldots) = V(\ldots v_i \ldots) \exp\left\{-\frac{1}{2}\sum_{\alpha,\mathbf{k}} (q_{\mathbf{k}\alpha} - q^0_{\mathbf{k}\alpha})^2\right\}. \tag{20}$$

The variables $q_{\mathbf{k}\alpha}$ enter Φ directly and are also contained in the $v_i(\ldots q_{\mathbf{k}\alpha} \ldots)$. We will use $\partial/\partial^* q_{\mathbf{k}\alpha}$ to designate differentiation with respect to only the $q_{\mathbf{k}\alpha}$ which do not occur as variables in the v_i. Then

$$\frac{\partial^2}{\partial q^2_{\mathbf{k}\alpha}} = \frac{\partial^2}{\partial^* q^2{}_{\mathbf{k}\alpha}} + \sum_{i,j} \frac{\partial v_i}{\partial q_{\mathbf{k}\alpha}} \frac{\partial v_j}{\partial q_{\mathbf{k}\alpha}} \frac{\partial^2}{\partial v_i \partial v_j} + \sum_{i,j} \frac{\partial v_j}{\partial q_{\mathbf{k}\alpha}} \left(\frac{\partial}{\partial v_j} \frac{\partial v_i}{\partial q_{\mathbf{k}\alpha}}\right) \frac{\partial}{\partial v_i}$$
$$+ \sum_i \frac{\partial v_i}{\partial q_{\mathbf{k}\alpha}} \left(\frac{\partial^2}{\partial v_i \partial^* q_{\mathbf{k}\alpha}} + \frac{\partial^2}{\partial^* q_{\mathbf{k}\alpha} \partial v_i}\right). \tag{21}$$

The derivatives $\partial v_i/\partial q_{\mathbf{k}\alpha}$ occurring in (21) can be calculated from the conditions (18) and (19). By varying $q_{\mathbf{k}\alpha}$ arbitrarily, i.e., by arbitrary variation of $\varphi_\alpha(\mathbf{r})$, we obtain

$$-\sum_j dv_j \sum_\alpha \int \frac{\partial^2 \varphi_\alpha^0}{\partial v_i \partial v_j} \hat{\omega} \varphi_\alpha d\tau = \sum_\alpha \int \frac{\partial \omega_\alpha^0}{\partial v_i} \hat{\omega} \delta \varphi_\alpha d\tau = \frac{\hbar}{2} \sum_{\alpha, \mathbf{k}} \frac{\partial q_{\mathbf{k}\alpha}}{\partial v_i} dq_{\mathbf{k}\alpha}. \tag{22}$$

By using the fact that, due to the choice of ξ, ϑ, and φ, φ_α differs little from φ_α^0, replacing φ_α by φ_α^0 in (22), and introducing the notation

$$R_{ij}^{(n)} = \sum_\alpha \int \frac{\partial \varphi_\alpha^0}{\partial v_i} \frac{\partial \hat{\omega}_\alpha^n \varphi_\alpha^0}{\partial v_j} d\tau,$$

we represent Eq. (22) in the form

$$\sum_i R_{ij}^{(1)} \partial v_j / \partial q_{\mathbf{k}\alpha} = \tfrac{1}{2} \hbar \partial q_{\mathbf{k}\alpha}^0 / \partial v_i.$$

The solution of this system of linear equations gives the desired values of the derivatives $\partial v_i / \partial q_{\mathbf{k}\alpha}$.

Substitution of the above relations into the Hamiltonian (17) leads to

$$H_1 \Phi = \Big\{ J[\psi_0] + \sum_{\alpha, \mathbf{k}} \frac{1}{2} \hbar \omega_{\alpha\mathbf{k}} - \frac{\hbar}{2} \frac{O^{(2)} + P^{(2)}}{O^{(1)} + P^{(1)}}$$

$$- \hbar \frac{O^{(2)}}{O^{(1)}} - \hbar \frac{R^{(2)}}{R^{(1)}} + \mathscr{H}(\vartheta, \varphi) \Big\} \Phi.$$

$$\mathscr{H}(\vartheta, \varphi) = -\frac{1}{2} \Big\{ A \Delta_\xi + \sum_{i, j=1}^{3} A_{ij} \frac{\partial^2}{\partial \xi_i \partial \xi_j}$$

$$+ A_5 \Big(\frac{\partial^2}{\partial \vartheta^2} + \operatorname{ctg} \vartheta \frac{\partial}{\partial \vartheta} + \frac{1}{\sin^2 \vartheta} \frac{\partial^2}{\partial \varphi^2} \Big) \Big\}, \tag{23}^*$$

where

$$A = \frac{\hbar^2}{2} \frac{O^{(2)}}{O^{(1)2}}, \qquad A_{ij} = \frac{\hbar^2}{2} \left[\frac{O^{(2)} + P^{(2)}}{(O^{(1)} + P^{(1)})^2} - \frac{O^{(2)}}{O^{(1)2}} \right] a_{i3} a_{j3},$$

a_{i3}, a_{j3} are components of the matrix (15)

$$O^{(n)} = -\sum_\alpha \int \frac{\partial^2 \varphi_\alpha^0(\mathbf{r})}{\partial x^2} \hat{\omega}_\alpha^n \varphi_\alpha^0(\mathbf{r})\, d\tau,$$

$$O^{(n)} + P^{(n)} = -\sum_\alpha \int \frac{\partial^2 \varphi_\alpha^0(\mathbf{r})}{\partial z^2} \hat{\omega}_\alpha^n \varphi_\alpha^0(\mathbf{r})\, d\tau,$$

$$R^{(n)} = R_{55}^{(n)}, \qquad A_5 = \hbar^2 R^{(2)} / 2R^{(1)2}$$

By setting $V(\ldots v_i \ldots) = \exp(i\mathbf{f} \cdot \boldsymbol{\xi}) F(\vartheta, \varphi)$, we obtain the equation for F:

$$\Big\{ -\frac{1}{2} A_5 \Big[\frac{\partial^2}{\partial \vartheta^2} + \operatorname{ctg} \vartheta \frac{\partial}{\partial \vartheta} + \frac{1}{\sin^2 \vartheta} \frac{\partial^2}{\partial \varphi^2} \Big]$$

$$+ \frac{1}{2} A f^2 + \frac{1}{2} \sum_{i, j=1}^{3} A_{ij} f_i f_j \Big\} F = WF. \tag{24}$$

For sufficiently small $\mathbf{f}$, the last term in (24) can be treated as a perturbation. Then, in the zeroth approximation

$$F(\vartheta, \varphi) = e^{im\varphi} P_l^{|m|}(\cos \vartheta), \qquad W^0 = \frac{1}{2} A_5 l(l+1) + \frac{1}{2} A f^2,$$
$$m = 0, \pm 1, \pm 2 \ldots; \qquad l = 0, 1, 2, \ldots, \tag{25}$$

$P_l^{|m|}$ is the associated Legendre function. The matrix element of the perturbation is

$$W' = \frac{1}{2} B f^2 \langle \cos^2 \delta \rangle, \qquad B = \frac{\hbar^2}{2} \left\{ \frac{O^{(2)} + P^{(2)}}{[O^{(1)} + P^{(1)}]^2} - \frac{O^{(2)}}{O^{(1)2}} \right\},$$

$$\langle \cos^2 \delta \rangle = \int \cos^2 \delta \, | F(\vartheta, \varphi) |^2 \, d\tau_{\vartheta, \varphi}; \tag{26}$$

where δ is the angle between the direction of the translational motion of the bipolaron and its symmetry axis.

The quantity $W_1 = \frac{1}{2}(A + B \langle \cos^2 \delta \rangle) f^2$ is the translational kinetic energy of the bipolaron, and $M = \hbar^2/(A + B \langle \cos^2 \delta \rangle)$ is its effective phonon-field mass; the latter, as is evident from formulas (25) and (26), depends on the rotational quantum numbers, l and m. For example, for a non-rotating bipolaron (l, m = 0) we have $M_{0,0} = \hbar^2/(A + \frac{1}{3}B)$; for $l = 1$, $m = 0$, we have $M_{1,0} = \hbar^2/(A + \frac{3}{5}B)$, etc.

The quantity $W_2 = \frac{1}{2} A_5 l(l+1)$ is the rotational energy of the bipolaron; $I = \hbar^2/A_5$ is the phonon-field moment of inertia. The total energy of the moving (translating and rotating) bipolaron is

$$H_1 = J[\psi_0] - \frac{\hbar}{2} \frac{O^{(2)} + P^{(2)}}{O^{(1)} + P^{(1)}} - \hbar \frac{O^{(2)}}{O^{(1)}} - \hbar \frac{R^{(2)}}{R^{(1)}}$$

$$+ \frac{\hbar^2 f^2}{2M_{l,m}} + \frac{\hbar^2 l(l+1)}{2\mathscr{J}}.$$

The criterion for the existence of bipolarons takes the form

$$Q = H_1(\mathbf{f}, l, m = 0)/2H_{\mathrm{p}}$$
$$= \frac{J_{min}[\psi(\mathbf{r}_1, \mathbf{r}_2)] - \hbar O^{(2)}/O^{(1)} - \hbar(O^{(2)} + P^{(2)})/2(O^{(1)} + P^{(1)}) - \hbar R^{(2)}/R^{(1)}}{2\{(J_{min}[\psi])_{\mathrm{p}} - 3\hbar O_{\mathrm{p}}^{(2)}/2O_{\mathrm{p}}^{(1)}\}} > 1. \tag{27}$$

The subscript "p" indicates that the corresponding quantity refers to polarons, not bipolarons.

The remainder of the calculation amounts to just the computation of the integrals $O^{(n)}$, $P^{(n)}$, and $R^{(n)}$ which appear in the expressions for the bipolaron energy, effective mass, and moment of inertia.

This problem does not involve any difficulties of principle, but in many cases involves cumbersome computations. If only the optical modes ($\alpha = 1$) are considered and the frequency dispersion is neglected, then the criterion for bipolaron existence (27) can be written

$$Q = \frac{J_{min}[\psi(\mathbf{r}_1, \mathbf{r}_2)] - 5\hbar\omega_0/2}{2(J_{min}[\psi(\mathbf{r})])_{\mathrm{p}} - 6\hbar\omega_0} > 1,$$

where ω_0 is the limiting frequency.

This criterion is somewhat stricter than that given above in Eq. (13). The reason for the difference is that the equivalence mentioned in Sec. 1 of this paper between the adiabatic approximation and the variational method with multiplicative wave functions holds for systems which do not have translational symmetry. If the latter is present, then the treatment of the present section is more rigorous and does not give complete equivalence.

---

*ctg = cot.

However, for the values of the frequency ω_0 usually encountered in ionic crystals, the difference of $\frac{1}{2}\hbar\omega_0$ between the bipolaron energies of this section and of Sec. 1 is not very significant. The bipolaron energy decrement, ΔJ, mentioned in the remarks following Eq. (13), is related to $\frac{1}{2}\hbar\omega_0$ by (according to the estimate)

$$|\Delta J| \gtrsim 1/2\, \hbar\omega_0.$$

Such a quantitative change in the bipolaron existence criterion does not change in principle the conclusion that bipolarons can exist.

The values of the bipolaron effective mass and moment of inertia can be calculated in the same approximation with the aid of the integrals

$$O^{(n)} = -2e^2c\omega_0^{n-2}\int \frac{1}{r_{13}}\psi^2(\mathbf{r}_1, \mathbf{r}_2)\frac{\partial^2}{\partial x_3^2}\psi^2(\mathbf{r}_3, \mathbf{r}_4)\, d\tau_{1234}$$

$$= -e^2c\omega_0^{n-2}(1+S^2)^{-2}[\langle aaaa\rangle + \langle aabb\rangle$$

$$+2S(\langle aaab\rangle + \langle abaa\rangle) + 2S^2\langle abab\rangle],$$

$$3O^{(n)} + P^{(n)} = 8\pi ce^2\omega_0^{n-2}\int \psi^2(\mathbf{r}_1, \mathbf{r}_2)\,\psi^2(\mathbf{r}_1, \mathbf{r}_3)\, d\tau_{123}$$

$$= 4\pi ce^2\omega_0^{n-2}(1+S^2)^{-2}[v_1 + (1+2S^2)\,v_2 + 4Sv_3],$$

where

$$\langle klmn\rangle = \int \psi_k(\mathbf{r}_1)\,\psi_l(\mathbf{r}_1)\,\frac{1}{r_{12}}\frac{\partial^2}{\partial x_2^2}\psi_m(\mathbf{r}_2)\,\psi_n(\mathbf{r}_2)\, d\tau_{12}.$$

The two-point integrals $\langle klmn\rangle$, v_2, v_3 and S can be reduced to linear combinations of the overlap integrals tabulated by Kopineck.[15]

By using the limiting values of the integrals $O^{(n)}$ and $P^{(n)}$, it is easy to find, in particular, the limiting value of the ratio of the effective masses of the bipolaron and polaron:

$$M_{0,0}/M_p \to 4 \quad (R \to 0), \qquad M_{0,0}/M_p \to 2 \quad (R \to \infty).$$

3. CONCLUSION

The results obtained above show that the current carriers can be bipolarons in ionic crystals with sufficiently high values of the parameters n^2, c, μ, a, E^{-1}, and $(\hbar\omega_0)^{-1}$.

The conclusion does not contradict the assertion that bipolarons cannot exist which is contained in Pekar's monograph,[2] since only the special case $R = 0$, $a = 0$ is considered there.

The case $c = 0$, $a = 0$ corresponds to the "doublon" state considered by Vol'kenshteĭn and Bonch-Bruevich.[14] The doublon energy level, however, is located above the bottom of the conduction band. Due to the presence of lattice polarization and elastic deformation, the paired states of the current carriers are appropriate to the ground state of the system. This circumstance can lead to a large number of experimentally verifiable effects, for example, superconductivity, and also sharp changes in magnetic, optical, and other properties of the crystal around the temperature at which the ratio of the equilibrium concentrations of bipolarons and polarons — which are excited states of the current carriers — goes through unity.

It is possible that taking into account exchange forces due to interaction of the quasiparticles with the phonon field could lead to the appearance of quasimolecules in other cases (for example, biexcitons). This problem may also be of interest in many-body theory other than that used in solid state problems, for example, in the treatment of nucleons interacting with the meson field.

The author expresses his profound gratitude to M. F. Deĭgen for many valuable discussions which occurred while this work was being done, and also to M. I. Kaganov, S. I. Pekar, and the other participants in the Fourth All-Union Conference on Semiconductor Theory who took part in evaluating this work.

---

[1] V. L. Vinetskii and M. Sh. Giterman, JETP **33**, 730 (1957), Soviet Phys. JETP **6**, 560 (1958).

[2] S. I. Pekar, Исследования по электронной теории кристаллов (Investigations in the Electron Theory of Crystals), Gostekhizdat 1951.

[3] S. I. Pekar, JETP **22**, 641 (1952).

[4] V. M. Buĭmistrov and S. I. Pekar, JETP **32**, 1193 (1957), Soviet Phys. JETP **5**, 970 (1957).

[5] V. M. Buĭmistrov and S. I. Pekar, JETP **33**, 1271 (1957), Soviet Phys. JETP **6**, 977 (1958).

[6] M. F. Deĭgen and V. L. Vinetskii, JETP **32**, 1382 (1957), Soviet Phys. JETP **5**, 1125 (1957).

[7] O. F. Tomasevich, Dissertation, Kiev University, 1953.

[8] M. F. Deĭgen, JETP **21**, 992 (1951).

[9] M. F. Deĭgen and V. L. Vinetskii, JETP **32**, 289 (1957), Soviet Phys. JETP **5**, 226 (1957).

[10] V. L. Vinetskii, JETP **33**, 780 (1957), Soviet Phys. JETP **6**, 600 (1958).

[11] V. L. Vinetskii, Физика твердого тела **2**, 2544 (1960), Soviet Phys. Solid State **2**, 2267 (1961).

[12] S. I. Pekar, JETP **27**, 398 (1954).

[13] S. I. Pekar, JETP **27**, 411 (1954).

[14] F. F. Vol'kenshtein and V. L. Bonch-Bruevich, JETP **20**, 624 (1950).

[15] H. J. Kopineck, Z. Naturforsch. **5a**, 420 (1950); **6a**, 177 (1951); **7a**, 785 (1952).

Translated by M. Bolsterli
249

SOVIET PHYSICS JETP VOLUME 13, NUMBER 5 NOVEMBER, 1961

TWISTED SPACE AND NONLINEAR FIELD EQUATIONS

V. I. RODICHEV

Moscow Regional Pedagogical Institute

Submitted to JETP editor December 22, 1960

J. Exptl. Theoret. Phys. (U.S.S.R.) **40**, 1469-1472 (May, 1961)

It is shown that in a twisted space the nonlinear spinor equations considered in the field theory of elementary particles follow from a variational principle in which the Dirac Lagrangian is supplemented by the scalar torsion of the space.

1. One of the simplest generalizations of Euclidean space is a twisted Riemann space, in which the metric is Galilean and the geodesics are straight lines. Such a space (see Appendix) is characterized by a completely antisymmetric torsion tensor $\Phi_{\alpha\beta\epsilon}$. We note that unlike the graviational field components $\Gamma_{\alpha\beta,\epsilon}$, which, like the field $\Phi_{\alpha\beta\epsilon}$, have a definite geometrical meaning, the latter quantities are a tensor field, and therefore cannot be locally reduced to zero by any change of coordinates. The field $\Phi_{\alpha\beta\epsilon}$ can be given a simple physical interpretation; it can be regarded as the proper field of a particle, since its presence does not affect the motion of the particle (the geodesic line is still straight).

In a twisted space covariant differentiation can be defined (see Appendix) for tensor and spinor quantities, though since the metric is Galilean there is no difference between covariant and contravariant components. Then

$$^{*}(A_\mu)_{,\sigma} = \partial A_\mu/\partial x^\sigma + \Phi_{\sigma\lambda\mu}\mathbf{A}_\lambda, \tag{1}$$

$$D_\sigma\Psi = \partial\Psi/\partial x^\sigma - \left(\tfrac{1}{4}\Phi_{\sigma\alpha\beta}\gamma_\alpha\gamma_\beta + i/\varphi_\sigma\right)\Psi, \tag{2}$$

where φ_σ is interpreted as the vector potential of the electromagnetic field.

We get the field equations by starting with the Einstein variational principle

$$S = \int (L - b{}^{*}R)\, d^4x, \tag{3}$$

where b is a dimensional constant and *R is the scalar curvature of the space, which in our case is

$$^{*}R = \Phi_{\alpha\beta\varepsilon}\Phi_{\alpha\varepsilon\beta}. \tag{4}$$

Let us consider in particular the equations of a spinor field for which the invariant Lagrangian L is written in the following way:

$$\begin{aligned} L &= \frac{1}{2i}\{\Psi^{+}\gamma_\alpha(D_\alpha\Psi) - (D_\alpha\Psi)^{+}\gamma_\alpha\Psi\} \\ &= \frac{1}{2i}\{\Psi^{+}\gamma_\alpha\Psi_{,\alpha} - \Psi^{+}_{,\alpha}\gamma_\alpha\Psi\} - \frac{1}{4i}\Phi_{\alpha\beta\varepsilon}(\Psi^{+}\gamma_\alpha\gamma_\beta\gamma_\varepsilon\Psi) \\ &\quad - (\Psi^{+}\gamma_\alpha\Psi)\varphi_\alpha, \qquad \Psi_{,\alpha} = \partial\Psi/\partial x^\alpha. \end{aligned} \tag{5}$$

The summation is taken with $\alpha \neq \beta \neq \epsilon$.

Let us examine the case in which $\varphi_\alpha = 0$. Since the derivatives of the field $\Phi_{\alpha\beta\epsilon}$ do not occur in the action integral (3), variation with respect to this field at once gives

$$\Phi_{\alpha\beta\varepsilon} = (1/8ib)(\Psi^{+}\gamma_\alpha\gamma_\beta\gamma_\varepsilon\Psi). \tag{6}$$

Varying the expression (5) with respect to Ψ^{+} and using Eq. (6), we get

$$\gamma_\alpha\Psi_{,\alpha} + (i/32b)(\Psi^{+}\gamma_\alpha\gamma_\beta\gamma_\varepsilon\Psi)\gamma_\alpha\gamma_\beta\gamma_\varepsilon\Psi = 0. \tag{7}$$

Equation (6) shows that the field $\Phi_{\alpha\beta\epsilon}$ is produced by the spin, and therefore it is quite natural to interpret it as the proper field of the particle.

Going over from the tensor $\Psi^{+}\gamma_\alpha\gamma_\beta\gamma_\epsilon\Psi$ to the corresponding dual axial vector $\Psi^{+}\gamma_\alpha\gamma_5\Psi$, we get

$$(\Psi^{+}\gamma_\alpha\gamma_\beta\gamma_\varepsilon\Psi)^2 = 6(\Psi^{+}\gamma_\alpha\gamma_5\Psi)^2. \tag{8}$$

We can then write Eq. (7) in the form

$$\gamma_\alpha\Psi_{,\alpha} + i\lambda_0^2(\Psi^{+}\gamma_\alpha\gamma_5\Psi)\gamma_\alpha\gamma_5\Psi = 0, \tag{9}$$

where we have introduced the notation $\lambda_0^2 = (3/16)\,b$. Thus we have obtained the nonlinear spinor equation with axial-vector nonlinear term.[4]

2. The interpretation of the Lagrangian (5) and the action integral (3) considered in the preceding section is not the only one possible. We shall consider another aspect of the theory, in which the equation (9) appears as an approximation.

If in the Lagrangian (5) we go over from the tensors $\Phi_{\alpha\beta\epsilon}$ and $\Psi^{+}\gamma_\alpha\gamma_\beta\gamma_\epsilon\Psi$ to the corresponding dual axial vectors, Eq. (5) takes the form

$$L = \frac{1}{2i}\{\Psi^+\gamma_\lambda\Psi_{,\lambda} - \Psi^+_{,\lambda}\gamma_\lambda\Psi\} - (\Psi^+\gamma_\lambda\Psi)\,\varphi_\lambda - (\Psi^+\gamma_\lambda\gamma_5\Psi)\,\widetilde{\varphi}_\lambda, \tag{10}$$

where φ_λ and $\widetilde{\varphi}_\lambda$ are vector (electromagnetic) and axial-vector (quasi-electromagnetic) potentials produced by the corresponding vector and axial-vector currents. Introducing a new constant, we can write the second term of the action integral (3) in the form

$$-b^*R = b\Phi_{\alpha\beta\varepsilon}\Phi_{\alpha\beta\varepsilon} = (k_0^2/8\pi\alpha_1)\,\widetilde{\varphi}_\lambda\widetilde{\varphi}_\lambda. \tag{11}$$

In addition to the electromagnetic field tensor $H_{\mu\nu}$ we must now introduce the pseudotensor $\widetilde{H}_{\mu\nu}$ of the quasi-electromagnetic field; the total Lagrangian can then be written in the form

$$L_{\text{gen}} = L + \frac{1}{16\pi\alpha}H^2_{\lambda\sigma} + \frac{1}{16\pi\alpha_1}\{\widetilde{H}^2_{\lambda\sigma} + 2k_0^2\widetilde{\varphi}^2_\lambda\}. \tag{12}$$

Varying this with respect to Ψ^+, φ_λ, $\widetilde{\varphi}_\lambda$ leads to the following field equations:

$$\gamma_\alpha\left\{\frac{\partial}{\partial x_\alpha} - i\varphi_\alpha - i\gamma_5\widetilde{\varphi}_\alpha\right\}\Psi = 0,$$

$$\frac{\partial^2}{\partial x_\lambda^2}\varphi_\mu = -4\pi\alpha\,(\Psi^+\gamma_\mu\Psi),$$

$$\frac{\partial^2}{\partial x_\lambda^2}\widetilde{\varphi}_\mu - k_0^2\widetilde{\varphi}_\mu = -4\pi\alpha_1\,(\Psi^+\gamma_\mu\gamma_5\Psi). \tag{13}$$

For the fields $H_{\mu\nu}$ and $\widetilde{H}_{\mu\nu}$ we obviously get the Maxwell equations and the Proca-Yukawa equations, respectively. In cases in which second derivatives can be neglected in the latter equations, we find

$$\widetilde{\varphi}_\mu \approx 4\pi\alpha_1 k_0^{-2}\,(\Psi^+\gamma_\mu\gamma_5\Psi). \tag{14}$$

Substituting this in the first equation of the system (13) and neglecting φ_α, we get Eq. (9) as an approximate equation. Thus inclusion of a torsion of space leads to a new axial-vector field, to which, as is well known, there correspond axial vector mesons when second quantization is used.

APPENDIX

1. As is well known, in the general case the change of the components of a vector on parallel displacement can be written

$$dA^\mu = -{}^*\Gamma^\mu_{\sigma\lambda}A^\lambda dx^\sigma, \tag{15}$$

where ${}^*\Gamma^\mu_{\sigma\lambda}$ are the affine connection coefficients, which are asymmetrical in the lower indices and can be written as the sum of a symmetric part and an antisymmetric part:

$${}^*\Gamma^\mu_{\sigma\lambda} = \widetilde{\Gamma}^\mu_{\sigma\lambda} + C^\mu_{\sigma\lambda}. \tag{16}$$

The quantities $C^\mu_{\sigma\lambda}$, called the components of the torsion, form a tensor and violate the parallelogram law.[1]

On introducing a metric and requiring conservation of the length of a vector on parallel displacement, we can divide ${}^*\Gamma^\mu_{\sigma\lambda}$ into metric and nonmetric parts:

$${}^*\Gamma_{\mu\nu,\sigma} = \Gamma_{\mu\nu,\sigma} + \Pi_{\mu,\nu\sigma}; \tag{17}$$

here $\Gamma_{\mu\nu,\sigma}$ are the ordinary Christoffel symbols, and

$$\Pi_{\mu,\nu\sigma} = -\Pi_{\mu,\sigma\nu} = C_{\sigma\mu,\nu} + C_{\sigma\nu,\mu} + C_{\mu\nu,\sigma}. \tag{18}$$

The equation of the geodesic lines in such a space can be written in the following way:

$$\frac{d^2x^\mu}{d\tau^2} + \widetilde{\Gamma}^\mu_{\sigma\lambda}\frac{dx^\sigma}{d\tau}\frac{dx^\lambda}{d\tau} = 0, \tag{19}$$

where by Eqs. (16) – (18) the $\widetilde{\Gamma}^\mu_{\sigma\lambda}$ are given by

$$\widetilde{\Gamma}^\mu_{\sigma\lambda} = \Gamma^\mu_{\sigma\lambda} + C^\mu_{\cdot\sigma,\lambda} + C^\mu_{\cdot\lambda,\sigma}. \tag{20}$$

In our special case of a space with Galilean metric, in which the geodesic lines are straight, we have

$$\Gamma^\mu_{\sigma\lambda} = 0, \qquad \widetilde{\Gamma}^\mu_{\sigma\lambda} = 0. \tag{21}$$

It then follows from Eq. (20) that the torsion must be a completely antisymmetric tensor. In this case let us introduce the notation

$$C_{\sigma\mu,\nu} = \Phi_{\sigma\mu\nu}. \tag{22}$$

The scalar curvature of the space, which in this case depends only on the torsion components, can be written

$${}^*R = \Phi_{\alpha\beta\varepsilon}\Phi_{\alpha\varepsilon\beta}. \tag{23}$$

2. In order to write the equations of an unquantized spinor field in an affinely connected space, we can use a method developed by Rumer.[2] Let $\Omega_\mu(\alpha)$, $\Omega^\mu(\alpha)$ denote the components of the metric tensor of Lamé. Here μ is the index of the ordinary covariant or contravariant component, and the index in parentheses (α) indicates the number of the invariant orthogonal component, so that

$$g_{\mu\nu} = \Omega_\mu(\alpha)\,\Omega_\nu(\alpha), \qquad g^{\mu\nu} = \Omega^\mu(\alpha)\,\Omega^\nu(\alpha), \;\ldots$$

Then in the parallel displacement of a vector the change of the orthogonal components of the vector that corresponds to Eq. (15) is

$$dA(\alpha) = {}^*\Delta_\sigma(\alpha\beta)\,A(\beta)\,dx^\sigma, \tag{24}$$

where ${}^*\Delta_\sigma(\alpha\beta)$ are the generalized Ricci rotation coefficients. Since by hypothesis A^2 remains unchanged in parallel displacement,

$${}^*\Delta_\sigma(\alpha\beta) = -{}^*\Delta_\sigma(\beta\alpha), \qquad {}^*(\Omega_\mu(\alpha))_{,\sigma} = 0, \tag{25}$$

where the brackets ${}^*(\;)_{,\sigma}$ denote the covariant derivative relative to ${}^*\Gamma^\mu_{\sigma\lambda}$ and ${}^*\Delta_\sigma(\alpha\beta)$. The last of the conditions (25) and Eq. (17) give

$$^*\Gamma_{\sigma\mu,\,\nu} = \Gamma_{\sigma\mu,\,\nu} + \Pi_{\sigma,\,\mu\nu} = \Omega_\nu(\alpha)\frac{\partial\Omega_\mu(\alpha)}{\partial x^\sigma} + {}^*\Delta_{\sigma,\,\mu\nu}, \qquad (26)$$

In Riemann space (without torsion) we have

$$\Gamma_{\sigma\mu,\,\nu} = \Omega_\nu(\alpha)\frac{\partial\Omega_\mu(\alpha)}{\partial x^\sigma} + \Delta_{\sigma,\,\mu\nu}, \qquad (27)$$

where $\Delta_{\sigma,\mu\nu}$ are the ordinary Ricci rotation coefficients, which depend on $\Omega_\mu(\alpha)$, $\Omega^\nu(\alpha)$ and their derivatives.

Comparing Eqs. (26) and (27), we find

$$^*\Delta_{\sigma,\,\mu\nu} = \Delta_{\sigma,\,\mu\nu} + \Pi_{\sigma,\,\mu\nu}, \qquad (28)$$

i.e., the same tensor $\Pi_{\sigma,\mu\nu}$ gives the nonmetric parts of both $^*\Gamma_{\sigma\mu,\nu}$ and $^*\Delta_{\sigma,\mu\nu}$.

The change of a spinor on parallel displacement is written

$$d\Psi = {}^*B_\sigma\Psi dx^\sigma, \qquad d\Psi^+ = -\Psi^{+*}B_\sigma dx^\sigma, \qquad (29)$$

where

$$^*B_\sigma = \tfrac{1}{4}\,{}^*\Delta_\sigma(\alpha\beta)\,\gamma(\alpha)\,\gamma(\beta) + iI\varphi_\sigma \qquad (30)$$

are the generalized displacement matrices,[2,3] and $\gamma(\alpha)$ and I are Dirac matrices. Then the covariant derivative of a spinor is written in the following way;

$$D_\sigma\Psi = \partial\Psi/\partial x^\sigma - {}^*B_\sigma\Psi, \qquad (31)$$

and the Lagrangian of the spinor field can be put in the form (the mass term is omitted here)

$$L = (1/2i)\ \{\Psi^+\gamma(\alpha)\,(D_\sigma\Psi) - (D_\sigma\Psi)^+\gamma(\alpha)\,\Psi\}\ \Omega^\sigma(\alpha). \qquad (32)$$

In the case of interest to us here, that of a space with the Galilean metric, we obviously have

$$\begin{aligned} &g_{\mu\nu} = \delta_{\mu\nu}, \qquad \Omega_\mu(\alpha) = \delta_{\mu\alpha}, \\ &\Delta_{\sigma,\,\mu\nu} = 0, \qquad \overset{*}{\Delta}_{\sigma,\,\mu\nu} = \Phi_{\sigma\mu\nu}, \end{aligned} \qquad (33)$$

and Eqs. (31) and (32) go over into the formulas (2) and (5) used earlier.

---

[1] P. K. Rashevskii, Риманова геометрия и тензорный анализ (Riemannian Geometry and Tensor Analysis), Gostekhizdat 1953, page 413.

[2] Yu. B. Rumer, Исследования по 5-оптике (Studies in Five-dimensional Optics), Gostekhizdat, 1956, page 110.

[3] V. Fock and D. Ivanenko, Compt. rend. **188**, 1470 (1929).

[4] Nonlinear Quantum Field Theory (Russian Translations), Collection of articles, edited by D. D. Ivanenko, IIL, 1959, pp. 19, 351.

Translated by W. H. Furry
250

SOVIET PHYSCIS JETP VOLUME 13, NUMBER 5 NOVEMBER, 1961

NATURE OF THE AMPLITUDE SINGULARITIES IN QUANTUM FIELD THEORY

A. P. RUDIK

Submitted to JETP editor December 24, 1960

J. Exptl. Theoret. Phys. (U.S.S.R.) **40**, 1473-1475 (May, 1961)

Restrictions on the nature of the singularities of quantum field theory amplitudes are derived within the framework of perturbation theory.

LET us consider the amplitude describing the process of mutual transformation of n particles. Suppose that the masses of the particles are given. Then the amplitude is a function of 3n – 10 invariants. Generally speaking this function will have singularities for certain relations among these invariants. We limit ourselves to the consideration of just those singularities that correspond to a single relation among the invariants.

We shall study the amplitude within the framework of perturbation theory and for real values of the invariants. Let us consider some arbitrary perturbation-theory diagram. Then the location and nature of the singularities of this diagram for a single relation among the invariants may be obtained by Landau's method.[1] According to this method the location of the singularity is determined by the following system of equations:

$$\sum_{(C)} \alpha_i q_i = 0, \tag{1}$$

$$\sum_{i=1}^{l} \alpha_i = 1, \tag{2}$$

$$\sum_{i_r} q_{i_r} = p_r, \tag{3}$$

$$q_i^2 = m_i^2. \tag{4}$$

Here the q_i stand for the four-momentum of the virtual particle corresponding to the i-th line in the diagram, the m_i stand for its mass, the p_r stand for the four-momentum of the real particle which enters the r-th vertex in the diagram, and α_i is the Feynman parameter corresponding to the i-th line. The summation in Eq. (1) is over all independent contours (C) of the diagram. The summation over i_r in Eq. (3) is over all virtual particles that enter the r-th vertex.

The nature of the singularities is determined as follows: Let us fix the values of 3n – 11 invariants. Then the value of the (3n – 10)-th invariant R is determined at the singular point by the system of equations (1) — (4) and is equal to R_0, where R_0 is a function of the first 3n – 11 invariants. The singularity is of the form

$$(R/R_0 - 1)^{\varkappa} \tag{5}$$

or

$$(R/R_0 - 1)^{\varkappa} \ln (R/R_0 - 1). \tag{5'}$$

Equation (5′) holds for positive integer values of κ; for all other values of κ Eq. (5) is valid. The quantity κ is related to the number of lines l and the number of vertices v in the diagram by

$$\varkappa = (3l - 4v + 3)/2. \tag{6}$$

It is the aim of this paper to clarify the question of what restrictions are imposed on the values of the quantity κ by the condition that the system of equations (1) — (4) give at the singular point just one relation among the invariants. We begin the considerations with processes for which $n \geq 5$. Under these circumstances all four-vectors of the real and virtual particles lie in the four-dimensional space.

As is well known,[2] only Eqs. (1) and (2) can be used for the determination of α_i at the singular point. The number of unknown α_i entering these equations is equal to l — the number of lines in the diagram. The number of equations in (1) and (2) is equal to $4(l - v + 1) + 1$, where $l - v + 1$ is the number of independent contours in the diagram. Consequently, the number of α_i left undetermined by Eqs. (1) and (2) is equal to

$$\Delta = -3l + 4v - 5. \tag{7}$$

Let us consider now Eqs. (3) and (4). The number of unknown components of the four-vectors q_i and invariants entering these equations is equal to $4l + 3n - 10$. The number of equations in (3) and (4) is equal to $l + 4(v - 1)$, since one of the vector equations (3) gives the overall four-momentum conservation law for the real particles. The number of components of the four-vectors q_i and the invariants left undetermined by Eqs. (3) and (4) is equal to

$$S = 3l - 4v + 3n - 6. \tag{8}$$

Altogether the number of unknown quantities left undetermined by Eqs. (1) — (4) is equal to

$$\Delta + S = 3n - 11, \tag{9}$$

i.e., one fewer than the number of invariants. The relevant question however is: are these undetermined quantities the invariants or the α_i. The following cases are possible:

1) $\Delta = 0$. Then all the α_i are determined at the singular point and there exists just one relation among the invariants and the masses of the virtual particles.

2) $\Delta = -\lambda < 0$. Then all the α_i are determined at the singular point and in addition λ of the equations (1) may be used along with Eqs. (3) and (4) so that only one relation arises among the invariants and the virtual particle masses at the singular point.

3) $\Delta = \lambda > 0$. In this case λ of the α_i are left undetermined at the singular point. Then $\lambda + 1$ relations are imposed on the components of the four-vectors q_i and the invariants.

Consequently, in order that there be just one relation among the invariants it is necessary for $n \geq 5$ that the condition $\Delta \leq 0$ be satisfied. It then follows from Eqs. (7) and (6) that $\kappa \geq -1$. In an analogous fashion it can be shown that for $n = 4$, when all four-vectors lie in a three-dimensional space, $\kappa \geq -1/2$ for just one relation among the invariants; and for $n = 3$, when all four-vectors lie in a two-dimensional space, $\kappa \geq 0$. It therefore follows that the amplitude for an arbitrary process will, within the framework of perturbation theory for one relation among the invariants at the singular point, have a singularity no stronger than a simple pole.

The author expresses his deep indebtedness to Academician L. D. Landau, V. N. Gribov, and B. L. Ioffe for useful remarks.

---

[1] L. D. Landau, JETP **37**, 62 (1959), Soviet Phys. JETP **10**, 45 (1960).

[2] L. B. Okun' and A. P. Rudik, Nucl. Phys. **14**, 261 (1960) [sic!].

Translated by A. M. Bincer
251

CHANGE IN THE MOMENTA OF CHARGES COLLIDING IN A MAGNETIC FIELD

Yu. N. BARABANENKOV

Moscow State University

Submitted to JETP editor December 26, 1960

J. Exptl. Theoret. Phys. (U.S.S.R.) **40**, 1476-1480 (May, 1961)

Scattering of two charged particles in a homogeneous and time-independent magnetic field is examined under the assumption of weak Coulomb interaction. The change in the particle momenta in scattering of the particles is calculated. It is shown that for two like charges the momentum change decreases exponentially with increase of the impact parameter. Because of Larmor resonance, the momentum change of oppositely charged particles decreases with increase in the impact parameter according to a power law. The magnetic field screens the interaction of the charged particles during the scattering. Equivalent spherically symmetric potentials constitute a graphic interpretation of this type of effect of the magnetic field. In the case of like charges, these potentials would be of the Debye type; in the case of opposite charges, they would be of the power type.

THE changes in momenta (and coordinates) of charged particles colliding in a magnetic field were reduced to quadratures in the work of E. M. Lifshitz[1] under the assumption of a weak Coulomb interaction. However, the author limited himself to a certain qualitative analysis of these integrals. The present research is a further development of the work of E. M. Lifshitz and contains a detailed analysis of the change of momenta of charges colliding in a magnetic field.

We shall therefore consider the collision of two charged particles e_k, m_k $(k = 1, 2)$ in a homogeneous and time-independent magnetic field **H**. Initially, we shall assume that the particles approach each other along the magnetic field without a Coulomb interaction. At some instant of time $(t = 0)$ they lie in the x, y plane, which is perpendicular to the magnetic field. We shall represent the radius vector of the particles at this instant of time in the following fashion: $\mathbf{r}_k = \mathbf{Q}_k + \boldsymbol{\rho}_k$. The quantity $\boldsymbol{\rho}_k = \mathbf{h} \times \mathbf{p}_k^{\perp}/m_k\omega_k$ is the Larmor radius vector of the particle, $\mathbf{p}_k$ is the component of momentum perpendicular to the magnetic field, $\omega_k = e_kH/m_kc$ is the Larmor frequency, $\mathbf{h}$ is the unit vector along the magnetic field. The vector $\mathbf{Q}_{\perp} = \mathbf{Q}_1 - \mathbf{Q}_2$ is known as the impact parameter of the collision.

We now take the Coulomb interaction of the particles into consideration. In accordance with the work of E. M. Lifshitz just cited, the increase in the momenta of the particles in the collision can be written in the form

$$\Delta(p_{kx}^{\perp} + ip_{ky}^{\perp}) = -\int_{-\infty}^{\infty} dt\left(\frac{\partial}{\partial x} + i\frac{\partial}{\partial y}\right)\Phi_t e^{-i\omega_k t},$$

$$\Delta p_k^{\parallel} = -\int_{-\infty}^{\infty} dt\,\frac{\partial \Phi_t}{\partial z}. \qquad (1)$$

The formulas given here were obtained by perturbation theory with respect to the Coulomb interaction potential Φ. We use the notation $\Phi_t = S_{-t}\Phi(|\mathbf{r}_1 - \mathbf{r}_2|)$, where S_t is the operator of motion of the charges in the magnetic field without interaction,[2] $p_k^{\parallel}$ is the component of the momentum of the particles along the magnetic field.

We proceed to the calculation of the integrals (1). First, we consider the special case in which $\rho_1 = \rho_2 = 0$ or $\omega_1 = \omega_2$ and $\boldsymbol{\rho}_1 = \boldsymbol{\rho}_2$. In this case, the quadratures are calculated in finite form. The following formulas are obtained for the increases in the momenta of the particles:

$$\Delta\mathbf{p}_k = \pm\frac{2e_1e_2\mathbf{R}}{|U|R^2}\frac{R}{|\rho_k^{\parallel}|}K_1\left(\frac{R}{|\rho_k^{\parallel}|}\right). \qquad (2)$$

Here,

$$U = p_1^{\parallel}/m_1 - p_2^{\parallel}/m_2, \qquad \rho_k^{\parallel} = U/\omega_k, \qquad \mathbf{R} = \mathbf{r}_1 - \mathbf{r}_2,$$

K_1 is a MacDonald function;[3] the plus sign holds for $k = 1$, the minus sign for $k = 2$.

In accord with (2), the increases in the momenta for $R \gg |\rho_k^{\parallel}|$ are exponentially small quantities:

$$\Delta\mathbf{p}_k = \pm\frac{2e_1e_2\mathbf{R}}{|U|R^2}\left(\frac{\pi R}{2|\rho_k^{\parallel}|}\right)^{1/2}\exp\left(-\frac{R}{|\rho_k^{\parallel}|}\right). \qquad (3)$$

We return to the calculation of the integrals (1) in the general case. The increases in the momenta of the particles are conveniently written in the form

$$\Delta \mathbf{p}_k = \Delta p_k^{\parallel} \mathbf{h} + \Delta p_k^{\perp} (\mathbf{p}_k^{\perp}/p_k^{\perp}) + \Delta' p_k^{\perp} [\mathbf{h}\mathbf{p}_k^{\perp}]/p_k, \qquad (4)^*$$

where $\Delta p_k^{\perp}$ is the increase in the absolute value of the perpendicular component of the momentum, $\Delta' p_k^{\perp}$ is the corresponding change in the direction. We now introduce the phases α_k of the vectors $\mathbf{p}_k^{\perp}$ at the time $t = 0$, and expand the quadratures (1) in a double Fourier series in these phases. The Fourier expansion leads to the following formulas:

$$\Delta p_1^{\parallel} = \frac{2e_1e_2}{|U|} \sum_{n_1,\, n_2=-\infty}^{\infty} \widetilde{k}_{n_1n_2} A_{n_1n_2} \sin (n_1\bar{\alpha}_1 + n_2\bar{\alpha}_2),$$

$$\Delta p_2^{\parallel} = -\Delta p_1^{\parallel},$$

$$\Delta p_k^{\perp} = -\frac{2e_1e_2}{|U|\rho_k} \sum_{n_1,\, n_2=-\infty}^{\infty} n_k A_{n_1n_2} \sin (n_1\bar{\alpha}_1 + n_2\bar{\alpha}_2). \qquad (5)$$

We used the notation

$$\bar{\alpha}_1 = \alpha_1 - (\pi/2), \qquad \bar{\alpha}_2 = (\alpha_1 \pm \pi) - (\pi/2),$$

$$\widetilde{k}_{n_1n_2} = (n_1\omega_1 + n_2\omega_2)/U.$$

The phases α_k are measured from the x axis, along which the vector $Q_\perp$ is directed. The amplitudes $A_{n_1n_2}$ are equal to

$$A_{n_1n_2} = \int_0^\infty \frac{k_\perp dk_\perp}{k_\perp^2 + \widetilde{k}_{n_1n_2}^2} J_{n_1}(k_\perp \rho_1) J_{n_2}(k_\perp \rho_2) J_{n_1+n_2}(k_\perp Q_\perp), \qquad (6)$$

where J_n is a Bessel function.

We shall limit ourselves below to a consideration of the case in which the distance between the centers of the Larmor circles of the colliding particles at the time $t = 0$ is larger than the sum of their Larmor radii; $Q_\perp > |\rho_1| + |\rho_2|$. In this case (see Watson[3])

$$A_{n_1n_2} = I_{n_1}(|\widetilde{k}_{n_1n_2}|\rho_1) I_{n_2}(|\widetilde{k}_{n_1n_2}|\rho_2) K_{n_1+n_2}(|\widetilde{k}_{n_1n_2}| Q_\perp), \qquad (7)$$

where I_n is a Bessel function of purely imaginary argument, K_n is a MacDonald function.

We now return to analysis of the amplitude $A_{n_1n_2}$, which is represented by Eq. (7). Taking into account the behavior of the MacDonald functions at large and small values of the argument, we can conclude that the amplitudes are maxima in order of magnitude when $n_1\omega_1 + n_2\omega_2 = 0$ (we assume the ratio ω_1/ω_2 to be rational). The corresponding harmonics in the expansions (5) will be called resonant.† The amplitudes of the resonant harmonics are equal to

$$A_{n_1n_2} = \frac{(|n_1| + |n_2| - 1)!}{2\,|n_1|!\,|n_2|!} \left(\frac{\rho_1}{Q_\perp}\right)^{|n_1|} \left(\frac{\rho_2}{Q_\perp}\right)^{|n_2|}, \qquad (8)$$

if the signs of the charges of the corresponding particles are different, and are equal to 0 if the signs of the particles are the same.

We now go on to the amplitudes of the non-resonant harmonics. For their estimate, it is advantageous to make use of the asymptotic function $K_n(nx)$ for large values of the index n:

$$K_n(nx) \sim (\pi/2n)^{1/2} (x^2 + 1)^{-1/4} [x^{-1} + (x^{-2} + 1)^{1/2}]^n$$
$$\times \exp [-n (x^2 + 1)^{1/2}] [1 + a(x)/n + \ldots],$$
$$|a(x)| \leqslant \tfrac{1}{12}. \qquad (9)$$

This formula can be obtained by the application of the Laplace method for the asymptotic estimate of integrals[4] to the integral representation of the MacDonald function:[3]

$$K_n(nx) = \frac{1}{2} \int_{-\infty}^{\infty} \exp \{-n (x \operatorname{ch} t - t)\}\, dt. \qquad (10)^*$$

Without going into details, we write down the result of the investigation: if $Q_\perp \gg |\rho_1| + |\rho_2|$ and $Q_\perp \gg |\rho_k^{\parallel}|$, then the amplitudes of the non-resonant harmonics are exponentially small [see Eq. (14) below]. We note that, in accord with (5), the resonant harmonics do not make a contribution to the increase in the components of the momenta of the particles parallel to the magnetic field.

We now sum up. We come to the conclusion that the increases in the components of the momenta of particles perpendicular to the magnetic field, for large values of the impact collision parameter $Q_\perp$, are exponentially small if the signs of the charges are identical, and fall off with increase in the impact parameter according to a power law if the signs of the charges are different. Changes in the components of momenta parallel to the magnetic field are exponentially small.

It was noted above that the amplitudes of the resonant harmonics differ from 0 only in the case of differently charged particles. The latter circumstance has the following physical meaning: if a time periodic force with frequency ν acts on a charge which is rotating in a magnetic field with its own Larmor frequency ω, then resonance takes place for $\nu + \omega = 0$ (and not for $|\nu| = |\omega|$). It is of interest to consider in particular the case in which the specific charges of the colliding particles are identical: $e_1/m_1 = e_2/m_2$. In this case, the law of conservation of momentum is satisfied, which can be written in the form $\Delta \mathbf{p}_1 = \Delta \mathbf{p}$, $\Delta \mathbf{p}_2 = -\Delta \mathbf{p}$, where $\mathbf{p} = (m_2\mathbf{p}_1 - m_1\mathbf{p}_2)/(m_1 + m_2)$ = momentum of the relative motion of the particles. For the latter, a formula is valid which is analogous to (4) in which

---

*$[\mathbf{h}\mathbf{p}_k^{\perp}] = \mathbf{h} \times \mathbf{p}_k^{\perp}$.

†The idea of the possibility of resonance in the scattering of charges in a magnetic field belongs to A. I. Morozov.

*ch = cosh.

$$\Delta p^{\parallel} = \frac{4e_1e_2}{|U|\rho^{\parallel}} \sum_{n_1, n_2 = -\infty}^{\infty} \left(\frac{\rho}{|\rho|}\right)^n a_n(\xi, \eta) \sin n\bar{\alpha},$$

$$\Delta p^{\perp} = -\rho^{\parallel} \Delta p^{\parallel}/\rho,$$

$$\Delta' p^{\perp} = -\frac{2e_1e_2}{|U||\rho^{\parallel}|}\left[-\frac{\rho}{|\rho|}\frac{\theta(\xi < \eta)}{\eta} + \sum_{n=1}^{\infty}\left(\frac{\rho}{|\rho|}\right)^{n-1} c_n(\xi, \eta) \cos n\bar{\alpha}\right]. \tag{11}$$

Here

$$\rho^{\parallel} = \rho_k^{\parallel}, \qquad \rho = |(\mathbf{p}_1^{\perp}/m_1) - (\mathbf{p}_2^{\perp}/m_2)|/\omega_k,$$
$$\xi = Q_{\perp}/|\rho^{\parallel}|, \qquad \eta = |\rho|/|\rho^{\parallel}|, \qquad \bar{\alpha} = \alpha - (\pi/2),$$

where α is the phase of the vector $\mathbf{p}^{\perp}$. The function $\theta(\xi < \eta) = 1$ for $\xi < \eta$, and equal to 0 for $\xi > \eta$. The amplitudes a_n and ξ_n are equal to the following:

$$a_n(\xi, \eta) = nI_n(n\eta)K_n(n\xi), \qquad \xi > \eta,$$
$$c_n(\xi, \eta) = 2nI'_n(n\eta)K_n(n\xi), \qquad \xi > \eta. \tag{12}$$

As investigation shows, for $\xi \gg \eta$ and $\xi \gg 1$, the series of amplitudes a_n and ξ_n tend to zero as $n \to \infty$ no more slowly than the geometric progression with base $\eta e^{-\xi}$. Therefore, limiting ourselves in (11) to the first harmonics, we get

$$\Delta p_k^{\parallel} \sim \pm P^{\parallel}\xi^{-1/2}e^{-\xi}, \qquad \Delta p_k^{\perp} \sim P_k^{\perp}\xi^{-1/2}e^{-\xi}, \tag{14}$$

where $P^{\parallel}$, $P_k^{\perp}$ are certain functions of α, $\alpha_k\eta$. Estimates analogous to (14) are given also in the cited paper by E. M. Lifshitz,[1] and in the work of Belyaev.[2]

Up to this point we have considered changes of momenta of particles in collisions. However, no less interest attaches to the consideration of the scattering angles of the particles. By the angle of the scattering of a particle χ_k we shall mean the change of angle between the direction of its momentum and the direction of its magnetic field. We shall regard as equivalent the spherically symmetric potential $\Pi_k(r)$ $(k = 1, 2)$ which, without participation of magnetic field with impact parameter $Q_{\perp}$, scatters the k-th particle through an angle χ_k. The equivalent potential for the given angle of scattering χ_k satisfies an integral equation of the form (see reference 5)

$$\chi_k = -\frac{2m_kQ_{\perp}}{p_k^2}\int_{Q_{\perp}}^{\infty} \Pi'_k(r)\frac{dr}{(r^2 - Q_{\perp}^2)^{1/2}}. \tag{15}$$

If we consider the solution of this equation[6] for large values of r, we find that

$$\Pi_k(r) \sim (p_k^2|\rho^{\parallel}|/2m_kr)\exp(-r/|\rho^{\parallel}|) \tag{16}$$

for particles with equal specific charges (a similar formula holds for identically charged particles),

$$\Pi_k(r) \sim (p_k^2/2m_k)(\rho_1/r)^{M_1}(\rho_2/r)^{M_2} \tag{17}$$

for differently charged particles. In the latter formula, M_1 and M_2 are relatively prime natural numbers in which $|\omega_1|/|\omega_2| = M_2/M_1$. The appearance of the Debye potential (16) as an equivalent potential is a graphic physical interpretation of the screening action of the magnetic field[2] in the scattering of two charged particles. However, as follows from (17), the equivalent potential in the scattering of differently charged particles has the form of a power potential.

In conclusion, I take this opportunity to express my deep gratitude to A. I. Morozov for his numerous discussions and valuable observations in the completion of the present work.

---

[1] E. M. Lifshitz, JETP **7**, 390 (1937).

[2] S. T. Belyaev, Физика плазмы (Collection, Plasma Physics) Academy of Sciences Press **3**, 66 (1958).

[3] G. N. Watson, A Treatise on the Theory of Bessel Functions (Russian translation) IIL, 1949, pp. 91, 92, 470.

[4] M. A. Evgrafov, Асимптотические оценки и целые функции (Asymptotic Estimates and Entire Functions) Gostekhizdat, 1957.

[5] L. D. Landau and E. M. Lifshitz, Механика (Mechanics) Fizmatgiz, 1958.

[6] H. Bateman, Phil. Mag. **19**, 582 (1910).

Translated by R. T. Beyer
252

SOVIET PHYSICS JETP VOLUME 13, NUMBER 5 NOVEMBER, 1961

ON RELATIVISTIC PERTURBATION THEORY FOR A COULOMB FIELD

V. G. GORSHKOV

Leningrad Physico-Technical Institute, Academy of Sciences, U.S.S.R.

Submitted to JETP editor December 26, 1960

J. Exptl. Theoret. Phys. (U.S.S.R.) **40**, 1481-1490 (May, 1961)

The relativistic perturbation series for a Coulomb field is summed. The relativistic perturbation series is represented in the form of a new series each term of which can be expressed linearly through an infinite nonrelativistic series. An integral equation defining the terms of this series is determined. All infrared divergences are collected together in a phase factor.

1. INTRODUCTION

THE absence of an analytical formula for the "incoming" ("outgoing")[1] wave function of a charged relativistic particle in the Coulomb field necessitates the use of various approximate expressions for this function whenever calculations are made. The first type of approximation consists in using only a finite number of terms in the expansion of the wave function in terms of states with given angular momentum and parity. Calculations of this type are called "exact" (see, for example, reference 1). If the series converges, this method allows us, in principle, to achieve any degree of accuracy if a sufficient number of terms is included. However, such calculations involve an enormous amount of numerical work and have, therefore, been carried out only for very few particular cases.

A second method makes use of the Born approximation, i.e., it is based on perturbation theory.[2,3] Since the convergence properties of the Born series are not known and, furthermore, each term of the series contains infrared divergences connected with the long range of the Coulomb field, there is notoriously little trust in the perturbation-theoretical approach. As a consequence, the limit of applicability of perturbation theory is extremely low ($\alpha ZE/p \ll 1$), which restricts the use of this method to the uninteresting region of small Z.

The third method makes use of the Furry-Sommerfeld-Maue (FSM) function, which has a convenient analytic form.[4] However, this function must in general be regarded as containing only the first two terms (the zeroth and the first) of the expansion of the exact function in powers of αZ.

It is shown in the present paper that the summation of the nonrelativistic perturbation series leads to the known expression for the nonrelativistic wave function. All infrared divergences are collected together in a phase factor and, therefore, do not affect the physical processes. Furthermore, it turns out that the relativistic perturbation series can be represented in the form of a series in powers of αZ, each term of which is expressed linearly through the infinite nonrelativistic series, and hence through a known function (see the remarks above). No further infrared divergences appear aside from those collected together in a phase factor in the nonrelativistic series. Thus all infrared divergences are separated out in the form of this phase factor also in the case of the complete relativistic wave function. The resulting expansion remains valid for small momenta, in contrast to the Born expansion.

2. SUMMATION OF THE PERTURBATION SERIES IN THE NONRELATIVISTIC CASE

In order to cope with the infrared divergences, one usually considers first a potential of the form $eZe^{-\lambda r}/r$ and then lets λ go to zero.[2] The Schrödinger equation for the "outgoing" wave function of a charged particle in this potential field has the following form in momentum space ($\hbar = c = 1$):

$$\varphi_0(\mathbf{p}, \mathbf{f}) = \delta(\mathbf{q}_{fp}) + 2E\beta \frac{1}{\mathbf{f}^2 - \mathbf{p}^2 - i\varepsilon} \int \frac{1}{\mathbf{q}_{fs}^2 + \lambda^2} \varphi_0(\mathbf{p}, \mathbf{s})\, d^3s;$$

$$\beta = \alpha Z/2\pi^2, \qquad \alpha = e^2 = 1/137, \qquad \mathbf{q}_{fs} = \mathbf{f} - \mathbf{s}, \quad (1)$$

where Z is the charge of the nucleus ($Z > 0$ for attraction), and E and **p** are the energy and momentum of the particle.[2]

---

[1] We shall use the term "outgoing" ("incoming") for functions which have the asymptotic form of the sum of a plane wave and a diverging (converging) wave.

[2] This equation cooresponds to the ordinary Schrödinger equation for $E = m$; however, in the following we shall regard E as the relativistic energy of the particle: $E^2 = p^2 + m^2$. We note that **p** is the momentum of the particle in the usual sense only in the asymptotic region, where the field vanishes, because E is the total energy of the particle.

Using the method of successive approximations, we can write (1) in the form of a series in powers of $2E\beta$:

$$\varphi_0(\mathbf{p}, \mathbf{f}) = \delta(\mathbf{q}_{fp}) + \sum_{n=1}^{\infty} (2E\beta)^n \varphi_0^n(\mathbf{p}, \mathbf{f}), \tag{2}$$

$$\varphi_0^n(\mathbf{p}, \mathbf{f}) = \int \frac{d^3s_1}{(\mathbf{q}_{ps_1}^2 + \lambda^2)(\mathbf{s}^2 - \mathbf{p}^2 - i\varepsilon)(\mathbf{q}_{s_1s_2}^2 + \lambda^2)} \cdot \int \frac{d^3s_2}{(\mathbf{s}_2^2 - \mathbf{p}^2 - i\varepsilon)(\mathbf{q}_{s_2s_3}^2 + \lambda^2)} \cdots \int \frac{d^3s_{n-1}}{(\mathbf{s}_{n-1}^2 - \mathbf{p}^2 - i\varepsilon)(\mathbf{q}_{s_{n-1}f}^2 + \lambda^2)} \frac{1}{\mathbf{f}^2 - \mathbf{p}^2 - i\varepsilon}. \tag{2a}$$

Starting with the first term, we apply successively the following relation to (2a) (see reference 5, Appendix A):

$$\int \frac{d^3s}{(\mathbf{q}_{sr}^2 - a^2)(\mathbf{s}^2 - \mathbf{p}^2 - i\varepsilon)(\mathbf{q}_{sk}^2 + \lambda^2)} = \int_0^1 \frac{dx}{\Lambda} \int \frac{1}{2} \frac{\partial}{\partial\Lambda} \frac{1}{\mathbf{q}_{fr_x}^2 - \Lambda^2} \frac{d^3s}{\mathbf{q}_{sk}^2 + \lambda^2} = \pi^2 i \int_0^1 \frac{dx}{\Lambda} \frac{1}{\mathbf{q}_{kr_x}^2 - (\Lambda + i\lambda)^2},$$

$$\Lambda^2 = (p^2 - r^2x)(1 - x) + a^2x + i\varepsilon(1 - x), \quad \mathbf{r}_x = \mathbf{r}x, \tag{3}$$

Then (2a) can be written in the form

$$\varphi_0^n(\mathbf{p}, \mathbf{f}) = \left(\frac{\pi^2 i}{p}\right)^n \int_0^1 \frac{dy_1}{\Lambda_1} \int_0^1 \frac{dy_2}{\Lambda_2} \cdots \int_0^1 \frac{dy_n}{\Lambda_n} \frac{1}{2\pi^2 i} \frac{\partial}{\partial(p\Lambda_n)} \frac{1}{\mathbf{q}_{fp_n}^2 - (p\Lambda_n)^2}, \tag{4}$$

where

$$p^2\Lambda_k^2 = (p^2 - p_{k-1}^2 y_k)(1 - y_k) + (\Lambda_{k-1} + i\lambda)^2 y_k + i\varepsilon(1 - y_k),$$

$$\mathbf{p}_k = \mathbf{p} y_1 y_2 \ldots y_k,$$

or

$$\Lambda_k^2 = (1 - y_1y_2\ldots y_k)^2 - \eta^2 y_1y_2\ldots y_k + (2i\eta\Lambda_1 - \eta^2) y_2y_3\ldots y_k + (2i\eta\Lambda_{k-1} - \eta^2) y_k + i\varepsilon(1 - y_k),$$

$$\eta = \lambda/p.$$

Introducing the new variables

$$x_k = 1 - y_1y_2\ldots y_k, \quad dy_k = -dx_k/(1 - x_{k-1}),$$

we obtain

$$\varphi_0^n(\mathbf{p}, \mathbf{f}) = \left(\frac{\pi^2 i}{p}\right)^n \int_0^1 \frac{dx_1}{(1 - x_1)\Lambda_1} \int_{x_1}^1 \frac{dx_2}{(1 - x_2)\Lambda_2} \cdots \int_{x_{n-1}}^1 \frac{dx_n}{(1 - x_n)\Lambda_n} F(\mathbf{f}, \mathbf{p}; x_n),$$

$$F(\mathbf{f}, \mathbf{p}; x_n) = \frac{1}{2\pi^2 i}(1 - x_n) \frac{\partial}{\partial(p\Lambda_n)} \frac{1}{\mathbf{q}_{fp_n}^2 - (p\Lambda_n)^2},$$

$$\Lambda_k^2 = x_k^2 - \eta^2 x_k + (2i\eta\Lambda_1 - \eta^2)\frac{1 - x_n}{1 - x_1} + \ldots + (2i\eta\Lambda_{n-1} - \eta^2)\frac{1 - x_n}{1 - x_{n-1}} + i\varepsilon\frac{x_n - x_{n-1}}{1 - x_{n-1}}. \tag{5}$$

The following relation will be important for the subsequent discussion:

$$\Lambda_n|_{x_n = x_{n-1}} = \Lambda_{n-1} + i\eta. \tag{6}$$

Let us now introduce a quantity a such that

$$\eta \ll a \ll 1. \tag{7}$$

We split up all integrals in (5) into a part with $x_k < a$ and a part with $x_k > a$ and neglect a as compared to unity and η as compared to a, according to (7). We then obtain

$$\varphi_0^n(\mathbf{p}, \mathbf{f}) = \left(\frac{\pi^2 i}{p}\right)^n \{A_0B_n + A_1B_{n-1} + \ldots + A_kB_{n-k} + \ldots + A_nB_0\}, \tag{8}$$

$$B_k = B_k(a) = \int_a^1 \frac{dx_1}{(1 - x_1)x_1} \cdots \int_{x_{k-1}}^1 \frac{dx_k}{(1 - x_k)x_k} F(x_k) = \int_a^1 \frac{dx_1}{(1 - x_1)x_1} B_{k-1}(x_1), \tag{8a}$$

$$B_0(x) = F(x) = -\frac{1}{2\pi^2}\frac{\partial}{\partial\varepsilon}\frac{1 - x}{(\mathbf{q}_{fp} + \mathbf{p}x)^2 - (|\mathbf{p}|x + i\varepsilon)^2}, \tag{8b}$$

$$A_k = \int_0^a \frac{dx_1}{\Lambda_1} \int_{x_1}^a \frac{dx_2}{\Lambda_2} \cdots \int_{x_{k-1}}^a \frac{dx_k}{\Lambda_k}, \qquad A_0 = 1, \tag{8c}$$

$$\Lambda_k^2 = x_k^2 + 2i\eta(\Lambda_1 + \Lambda_2 + \ldots + \Lambda_{k-1}) - k\eta^2. \tag{8d}$$

The function $B_0(x)$ goes over into $\delta(\mathbf{q}_{fp})$ for $x, \epsilon \to 0$.

In (8b) we have replaced $(px)^2 + i\epsilon$ by $(px + i\epsilon)^2$, which allowed us to include the zero order term (2) [corresponding to the case when x is exactly zero in (8b)] in (8) without changing the rules for bypassing the poles.

Expression (8) agrees with the n-th term of the product of two series. We can therefore write (2) in the form

$$\varphi_0(\mathbf{p}, \mathbf{f}) = \sum_{k=0}^{\infty} \alpha^k B_k \sum_{m=0}^{\infty} \alpha^m A_m = B(\alpha, \mathbf{p}, \mathbf{f}, a) A(\alpha, \eta, a), \tag{9}$$

$$B(\alpha, \mathbf{p}, \mathbf{f}, a) = \sum_{k=0}^{\infty} \alpha^k B_k, \tag{9a}$$

$$A(\alpha, \eta, a) = \sum_{m=0}^{\infty} \alpha^m A_m. \tag{9b}$$

Here $\alpha = \pi^2 i 2E\beta/p = ie^2ZE/p = i\xi$.

It is easy to find an analytic expression for the function (9a). By integrating (8a) by parts, starting with the last term, and using $F(1) = 0$, we find

$$B_k = -\frac{1}{k!}\int_a^1 \left(\ln\frac{x}{1-x} - \ln a\right)^k dF(x), \qquad k = 0, 1, \ldots \tag{10}$$

Thus we obtain for (9a)

$$B(\alpha, \mathbf{p}, \mathfrak{f}, a) = -\int_a^1 \exp\left[\alpha\left(\ln\frac{x}{1-x} - \ln a\right)\right] dF(x)$$

$$= -a^{-\alpha}\int_a^1 x^{\alpha}(1-x)^{-\alpha}\, dF(x). \tag{11}$$

Integrating (11) by parts and using the fact that

$$\alpha\int_0^a x^{\alpha-1}(1-x)^{-\alpha-1}F(x)dx = F(0)a^{\alpha},$$

with an accuracy up to terms of order a, we find

$$B(\alpha, \mathbf{p}, \mathfrak{f}, a) = a^{-\alpha}\alpha\int_0^1 x^{\alpha-1}(1-x)^{-\alpha-1}F(x)\,dx \tag{12}$$

Let us now consider (9b). We change the variables in (8c) to $z_k = x_k + \Lambda_k$, taking into account (8d). Considering the fact that (6) implies

$$z_k\big|_{x_k=x_{k-1}} = z_{k-1} + i\eta,$$

we obtain ($\gamma = i\eta$)

$$A_k = A_k(\gamma) = \int_{\gamma}^{2a}\frac{dz_1}{z_1}\int_{z_1+\gamma}^{2a}\frac{dz_2}{z_2}\ldots\int_{z_{k-1}+\gamma}^{2a}\frac{dz_k}{z_k} = \int_{\gamma}^{2a}\frac{dz}{z}A_{k-1}(z+\gamma). \tag{13}$$

As in the case of expression (8a), we integrate by parts, starting with the last term, and use the relation $|z_k| \geq |\gamma|$. We then obtain for (13) (see Appendix A)[3]

$$A_k = b_0\frac{1}{k!}\ln^k\frac{2a}{\gamma} + b_2\frac{1}{(k-2)!}\ln^{k-2}\frac{2a}{\gamma}$$

$$+ \ldots + b_n\frac{1}{(k-n)!}\ln^{k-n}\frac{2a}{\gamma} + \ldots + b_k, \tag{14a}$$

$$b_k = b_k(x=1)$$

$$= \int_0^{x=1}\frac{dy}{y}\left\{\sum_{n=0}^{k-1}\frac{(-1)^n}{n!}[\ln^n(1+y)]b_{k-n-1}\left(\frac{y}{1+y}\right) - b_{k-1}(y)\right\}, \tag{14b}$$

$$b_0 = 1, \qquad b_1 = 0, \qquad b_2 = -\frac{\pi^2}{12}. \tag{14c}$$

We note that (14a) represents the general term of the product of two series, in analogy to (8). We therefore find for (9b)

$$A(\alpha, \eta, a) = \sum_{k=0}^{\infty}\frac{\alpha^k}{k!}\left(\ln^k\frac{2a}{\gamma}\right)\sum_{m=0}^{\infty}\alpha^m b_m = a^{\alpha}\exp\left(\alpha\ln\frac{2p}{i\lambda}\right)b(\alpha), \tag{15}$$

$$b(\alpha) = \sum_{m=0}^{\infty}\alpha^m b_m. \tag{15a}$$

In Appendix A we shall make an estimate of the radius of convergence of (15a) and show that it is at least larger than unity. Substituting (15) and (12) in (9), we obtain finally

$$\varphi_0(\mathbf{p}, \mathfrak{f}) = e^{\pi\xi/2}\, i\xi b(i\xi)$$

$$\times\int_0^1 x^{i\xi-1}(1-x)^{-i\xi-1}F(x)dx\exp\{i\xi\ln(2p/\lambda)\}. \tag{16}$$

In going over to coordinate space,

$$\psi(\mathbf{p}, \mathbf{r}) = \int e^{i\mathfrak{f}\mathbf{r}}\varphi(\mathbf{p}, \mathfrak{f})d^3f, \tag{17}$$

we have

$$\psi_0(\mathbf{p}, \mathbf{r}) = e^{\pi\xi/2}\, i\xi\, b(i\xi)$$

$$\times\int_0^1 x^{i\xi-1}(1-x)^{-i\xi}e^{i(pr-\mathbf{pr})x}\,dx\, e^{i\mathbf{pr}}\exp(i\xi\ln(2p/\lambda)). \tag{18}$$

The known expression for the "outgoing" nonrelativistic function of a charged particle in the Coulomb field has the form

$$\psi_0(\mathbf{p}, \mathbf{r}) = Ne^{i\mathbf{pr}}{}_1F_1(i\xi, 1; i\rho), \qquad \rho = pr - \mathbf{pr}, \tag{19a}$$

$$N = e^{\pi\xi/2}\Gamma(1-i\xi) \tag{19b}$$

or

$$\psi_0(\mathbf{p}, \mathbf{r}) = e^{\pi\xi/2}\, i\xi\,\frac{1}{\Gamma(1+i\xi)}\int_0^1 x^{i\xi-1}(1-x)^{-i\xi}e^{i(pr-\mathbf{pr})x}\,dxe^{i\mathbf{pr}}. \tag{19c}$$

Since the functions (18) and (19c) satisfy the same equation and boundary conditions and have the same normalization (the incident wave has unit amplitude), it follows that $b(i\xi)$ must differ from $1/\Gamma(1+i\xi)$ only by a phase factor within its radius of convergence. Comparing the first few terms of the expansions of $b(i\xi)$ [formula (14c)] and of $1/\Gamma(1+i\xi)$ (reference 6), we obtain

$$b(i\xi) = e^{-i\xi C}/\Gamma(1+i\xi), \tag{20}$$

where C is the Euler constant. Thus the series (2) differs from the function (19a) by the phase factor

$$M' = \exp\{i\xi\ln(2p/\lambda)\}\exp\{-i\xi C\}.$$

However, if we agree to regard the normalization factor (19b) as defined only by its modulus, we can leave out the phase factor in (20). Then the difference between (18) and (19c) is given by the infrared phase factor

---

[3] We note that, if we set equal to zero all λ in (2a) except the first, the result will be convergent and $A_k = (k!)^{-1}\ln^k(2a/\gamma)$, i.e., this leads to a violation of the normalization of the wave function.

$$M = \exp\{i\xi \ln (2p/\lambda)\}. \tag{21}$$

By analytic continuation of (20) into the region in which convergence is guaranteed, we find that the radius of convergence of b (iξ) is infinite, since the right-hand side of (20) has no poles. For an estimate of the radius of convergence of (9a), we write (12) in coordinate space [see formula (18)] and replace the oscillatory exponent by unity, assuming $\mathbf{r} = 0$. Then we obtain

$$\alpha \int_0^1 x^{\alpha-1} (1-x)^{-\alpha}\, dx = \frac{\alpha\Gamma(\alpha)\,\Gamma(1-\alpha)}{\Gamma(1)} = \frac{\pi\alpha}{\sin \pi\alpha}. \tag{22}$$

The right-hand side of this expression has its first pole at $\alpha = 1$. It follows from this that the radius of convergence of (9a) is equal to unity. Thus the over-all radius of convergence of (2) is also equal to unity.

The perturbation series (2) for the Coulomb field is a majorant for potentials with shorter range than the Coulomb potential. For example, it is easily seen that the modulus of the general term (2a) decreases as λ increases. Since the series (9a), (9b), and hence (2) are absolutely convergent for small but finite λ, it can be asserted that the perturbation series for the Yukawa potential has a radius of convergence which is not smaller than unity.

It is easy to verify that the replacement of iϵ by $-$iϵ converts the "outgoing" function into the "incoming" one. Indeed, since the series is convergent, it follows from (2a) that

$$\varphi_0(\mathbf{p}, \mathbf{f}) = \varphi_0(-\mathbf{p}, -\mathbf{f}); \qquad \varphi_0^*(\mathbf{p}, \mathbf{f}; i\varepsilon) = \varphi_0(\mathbf{p}, \mathbf{f}; -i\varepsilon). \tag{23}$$

Taking the complex conjugate of both sides of (17) and using (23), we easily obtain the well-known relation

$$\psi_0^{in}(\mathbf{p}, \mathbf{r}) = \{\psi_0^{out}(-\mathbf{p}, \mathbf{r})\}^*. \tag{23a}$$

In this way we have obtained the result that the perturbation series for the "incoming" and "outgoing" wave functions of a nonrelativistic charged particle in the Coulomb field converges for $\xi = \alpha ZE/p \leq 1$ and diverges for $\xi > 1$. It follows, in particular, that the series diverges for arbitrarily small values of Z if p = 0.

The limit of unity for the radius of convergence is due only to a single term in (19c), namely, the function $\Gamma(1 - i\xi)$ in the normalization factor, which has a pole for $i\xi = 1$. All the other factors in (19c) have an infinite radius of convergence. If we use a finite number of terms of the perturbation series (2), but separate out the expansion of the normalization factor (19b) and replace it by its exact value, we can therefore extend the radius of convergence of the remaining expansion to values which are not limited by the condition $\xi \leq 1$.

Furthermore, it is easily seen from (19a) that the expansion in terms of ξ contains only the normalization factor (19b) [in (18) also the phase factor]. The expansion of the confluent hypergeometric function has the form

$$F(i\xi; 1; i\rho) = 1 + i\xi \sum_{k=1}^{\infty} \frac{1}{k \cdot k!} (i\rho)^k + \ldots + (i\xi)^n \sum_{k=n}^{\infty} C_k (i\rho)^k + \ldots,$$

i.e., each ξ^n stands together with a factor ρ^{n+k} $k \geq 0$. Hence the expansion is really in terms of αZ, where each term has a finite value and is proportional to $(\alpha Z)^n$ for arbitrary values of the momentum. It follows that the wave function can be obtained with an accuracy up to terms of order $(\alpha Z)^n$, independently of the momentum, in the following way: take n successive Born approximations, leave out the expansion of the phase and normalization factors and multiply by the exact value of the normalization factor (19b).

3. DISCUSSION OF THE RELATIVISTIC PERTURBATION THEORY

This section is a direct continuation and generalization of the discussion presented in an earlier paper of the author.[5] We write the Dirac equation for the "outgoing" wave in momentum space:

$$\varphi(\mathbf{p}, \mathbf{f}) = \delta(\mathbf{q}_{fp})\, u(\mathbf{p}) + \beta \frac{m - i\hat{f}}{\mathbf{f}^2 - \mathbf{p}^2 - i\varepsilon} \int \frac{\gamma_n}{\mathbf{q}_{fs}^2 + \lambda^2} \varphi(\mathbf{p}, \mathbf{s}), \tag{24}$$

$$(i\hat{p} + m)\, u(\hat{\mathbf{p}}) = 0, \qquad \hat{f} = \boldsymbol{\gamma}\cdot\mathbf{f} + \gamma_4 f_4,$$

$$f_0 = E, \qquad \beta = \alpha Z/2\pi^2. \tag{24a}$$

Let us set

$$\varphi(\mathbf{p}, \mathbf{f}) = \{\varphi_0(\mathbf{p}, \mathbf{f}) + \Phi(\mathbf{p}, \mathbf{f})\}\, u(\mathbf{p}). \tag{25}$$

Using (1), (24a) and the identity ($\tilde{q} = \boldsymbol{\alpha}\cdot\mathbf{q}$)

$$(m + i\hat{f})\gamma_4 = 2E + \tilde{q}_{fp} + \gamma_4(m + i\hat{p}),$$

$$\beta \frac{\tilde{q}_{fp}}{\mathbf{f}^2 - \mathbf{p}^2 - i\varepsilon} \int \frac{1}{\mathbf{q}_{fs}^2 + \lambda^2} \varphi_0(\mathbf{p}, \mathbf{s})\, d^3s = \frac{1}{2E} \tilde{q}_{fp} \varphi_0(\mathbf{p}, \mathbf{f}) \equiv \varphi_{\mathrm{I}}(\mathbf{p}, \mathbf{f}), \tag{26}$$

we substitute (25) in (24) and obtain the following equation[4] for $\Phi(\mathbf{p}, \mathbf{f})$:

---

[4] In obtaining (26) we have used $\mathbf{q}, \delta(\mathbf{q}) = 0$; thus the expansion of φ_{I} in powers of ξ begins with ξ. We note that our discussion is valid for any static potential, where the function $\varphi_0 + \varphi_{\mathrm{I}}$ will be the analogue of the FSM function.

$$\Phi(\mathbf{p}, \mathbf{f}) = \varphi_I(\mathbf{p}, \mathbf{f}) + \beta \frac{m - i\hat{f}}{\mathbf{f}^2 - \mathbf{p}^2 - i\varepsilon} \int \frac{\gamma_4}{\mathbf{q}_{fs}^2 + \lambda^2} \Phi(\mathbf{p}, \mathbf{s})\, d^3s. \tag{27}$$

Writing (27) in the form of a series in powers of αZ, we have

$$\varphi(\mathbf{p}, \mathbf{f}) = \{\varphi_0(\mathbf{p}, \mathbf{f}) + \alpha Z \varphi_1(\mathbf{p}, \mathbf{f}) + (\alpha Z)^2 \varphi_2(\mathbf{p}, \mathbf{f}) + \ldots\} u(\mathbf{p}), \tag{28}$$

where $\varphi_0(\mathbf{p}, \mathbf{f})$ is defined by (1) and

$$\varphi_1(\mathbf{p}, \mathbf{f}) = \frac{1}{2p\xi} \tilde{q}_{fp} \varphi_0(\mathbf{p}, \mathbf{f}), \qquad \xi = \frac{\alpha Z E}{p}; \tag{28a}$$

$$\varphi_2(\mathbf{p}, \mathbf{f}) = \frac{1}{2\pi^2} \frac{(m - i\hat{f})\gamma_4}{\mathbf{f}^2 - \mathbf{p}^2 - i\varepsilon} \int \frac{\varphi_1(\mathbf{p}, \mathbf{s})}{\mathbf{q}_{fs}^2 + \lambda^2} d^3s, \tag{28b}$$

$$\varphi_n(\mathbf{p}, \mathbf{f}) = \frac{1}{2\pi^2} \frac{(m - i\hat{f})\gamma_4}{\mathbf{f}^2 - \mathbf{p}^2 - i\varepsilon} \int \frac{\varphi_{n-1}(\mathbf{p}, \mathbf{s})}{\mathbf{q}_{fs}^2 + \lambda^2} d^3s. \tag{28c}$$

The series (28) can also be obtained directly from the expansion of (24) in powers of ξ. For this purpose we must expand the numerators in each term of the resulting series, using the identity

$$\prod_{n=1}^{k} (m - i\hat{s}_n)\gamma_4 = (2E)^k + \sum_{n=1}^{k} (2E)^{k-n} (m - i\hat{s}_1)\gamma_4 \ldots (m - i\hat{s}_{n-1})\gamma_4 \tilde{q}_{s_n p}.$$

We must then collect all terms with the same matrix structure of the numerator and different powers of 2E. Then (24) appears in the form of the series (28), where $\varphi_0(\mathbf{p}, \mathbf{f})$ is given by the series (2). The first three terms of (28) were obtained by this method in reference 5. According to the discussion of the paper just mentioned (see footnote 3), the terms of the series (28), where φ_0 is replaced by the series (2), will not contain any additional infrared divergences besides those contained in φ_0 [this also follows directly from the convergence of the integrals (28c) for $\lambda \to 0$]. Since all terms in (28) are linearly expressed in terms of φ_0, all infrared divergences can be separated out of the complete function (25) in the form of the phase factor (21). It can also easily be shown that φ_0 and φ_1 give a finite contribution for $p \to 0$. Let us assume that the same holds also for φ_{n-1}. Replacing $\mathbf{f}$ by $p\mathbf{f}_1$ and $\mathbf{s}$ by $p\mathbf{s}_1$ ($\lambda, \epsilon \to 0$) in (28c), we see that $\varphi_n \sim 1/p^3$ and hence $\varphi_n d^3f = \varphi_n p^3 d^3f_1$ is finite. Thus the expansion (28) is valid even for $p \to 0$.

The integrals appearing in (28b, c) can be transformed to a simpler form. Let us consider, for example, the function (28b), the first correction to the FSM function. Following reference 5, we can write (28b) in the form

$$\varphi_2(\mathbf{p}, \mathbf{f}) = \frac{1}{\mathbf{f}^2 - \mathbf{p}^2 - i\varepsilon} \{2\mathbf{p} \cdot \mathbf{J} + \tilde{q}_{fp} \tilde{J}\}, \tag{29}$$

$$\mathbf{J}(\mathbf{p}, \mathbf{f}) = \frac{1}{2p\xi} \frac{1}{2\pi^2} \int \frac{\mathbf{q}_{sp} \varphi_0(\mathbf{p}, \mathbf{s})}{\mathbf{q}_{fs}^2 + \lambda^2} d^3s, \qquad \tilde{J} = \alpha \cdot \mathbf{J}, \tag{29a}$$

The vector (29a) lies in the plane $(\mathbf{p}, \mathbf{f})$, because of the relation $\mathbf{J}(\mathbf{p}, \mathbf{f}) = -\mathbf{J}(-\mathbf{p}, -\mathbf{f})$ [see formula (23)]. Hence we can write

$$\mathbf{J}(\mathbf{p}, \mathbf{f}) = a\mathbf{q}_{fp} + b\mathbf{p}. \tag{29b}$$

Substituting (29b) in (29), we obtain

$$\varphi_2(\mathbf{p}, \mathbf{f}) = a + b \frac{\mathbf{p}^2 + \tilde{f}\tilde{p}}{\mathbf{f}^2 - \mathbf{p}^2 - i\varepsilon}. \tag{30}$$

A representation for the functions a and b is given in Appendix B. It has the form

$$\begin{Bmatrix} a \\ b \end{Bmatrix} = -\frac{N}{4p\xi\pi^3} \oint^{(0^+1^+)} \left(\frac{-x}{1-x}\right)^{i\xi} \times \left[\int_0^\infty \begin{Bmatrix} p \\ -i\lambda \end{Bmatrix} \frac{d\lambda'}{[(\mathbf{q}_{fp} + \mathbf{p}x)^2 - (px + i\lambda')^2]^2}\right] dx, \tag{31}$$

where N is given by (19b). Formula (31) can be reduced to a single quadrature; however, the expression quoted above is more convenient for the calculation of matrix elements.

Both integrals (31) can be evaluated by retaining only the zeroth order term in the expansion in powers of αZ. However, in this case it is simpler to use (29a) directly. Indeed, the zeroth order term of (31) is obtained by substituting the series (2) in (29a) and discarding all terms except the first nonvanishing term. In this way we find

$$\mathbf{J}_0(\mathbf{p}, \mathbf{f}) = \int \frac{\mathbf{q}_{sp} d^3s}{(\mathbf{q}_{fs}^2 + \lambda^2)(\mathbf{s}^2 - \mathbf{p}^2 - i\varepsilon)(\mathbf{q}_{sp}^2 + \lambda^2)}. \tag{29'}$$

The integral (29′) has been computed in a number of papers. Using the results of Gavrila,[3] we obtain[5]

$$a_0 = \frac{\pi^2 p}{2\Delta} \left\{\pi \frac{\mathbf{pq}}{pq} + \frac{\mathbf{fp}}{fp} i \ln \frac{f + p + i\lambda}{-f + p + i\lambda} + i \ln \frac{q^2}{f^2 - (p + i\lambda)^2}\right\},$$

$$b_0 = \frac{\pi^2 q}{2\Delta} \left\{\pi + \frac{\mathbf{fq}}{fq} i \ln \frac{f + p + i\lambda}{-f + p + i\lambda} + \frac{\mathbf{pq}}{pq} i \ln \frac{q^2}{f^2 - (p + i\lambda)^2}\right\},$$

$$\Delta = f^2 p^2 - (\mathbf{fp})^2, \qquad \mathbf{q} = \mathbf{f} - \mathbf{p}. \tag{31'}$$

Expression (29a′) represents the zeroth order term in the expansion of (29a) in powers of αZ. In accordance with what has been said in Sec. 1, we must simply multiply (29′) by the normalization factor (19b) in order to take account of all terms of the expansion of (29′) in terms of the parameter $\xi = \alpha ZE/p$. We note that in reference 5 an expression for (29) is given which is equivalent to (30) and (31), but which is more convenient for the calculations.

---

[5] The expressions (30), (31′) were obtained in a somewhat different manner by Johnson and Mullin.[7]

Analogous expressions can also be obtained for the higher-order terms in the expansion (28). These involve a correspondingly larger number of quadratures. They are more compact than the corresponding terms in the Born approximation, do not contain infrared divergences, and remain valid for small energies.

The functions (28), with φ_0 given by its exact value (16), can be combined with the higher Born approximations in carrying out calculations. One must only see to it that the phase factors (or their expansions) are identical for all terms.

In order to exclude the infrared divergences in calculations employing a Born series for the wave function, we must reorder this series into the series (28) and then multiply each term of the resulting series (28) by the complex conjugate of the phase factor (21) up to the power to which the expansion in the corresponding term is carried out. When both expansions are multiplied out, the divergences must cancel out. This recipe can easily be tested on the example of formulas (10) and (12) in reference 5.

The author expresses his gratitude to L. A. Sliv and B. A. Volchok for useful comments.

APPENDIX A

Let

$$A_k(x) = \sum_{m=0}^{k} \frac{1}{m!} b_{k-m}(x) \ln^m \frac{2a}{x}, \qquad A_0 = 1; \qquad \text{(A.1)}$$

$$b_{n+1}(x) = \int_x^{2a} \frac{dz}{z} \left\{ \sum_{l=0} \frac{(-1)^l}{l!} \ln^l \left(1 + \frac{\gamma}{z}\right) b_{n-l}(z+\gamma) - b_n(z) \right\},$$

$$b_0 = 1. \qquad \text{(A.2)}$$

We show that (13) leads to the same expressions for A_{k+1} and b_{k+1}. We have

$$A_{k+1}(x) = \int_x^{2a} \frac{dz}{z} A_k(z+\gamma); \qquad |z| \geqslant |x| \gg |\gamma|. \qquad \text{(A.3)}$$

With the help of the identity

$$\ln[2a/(z+\gamma)] = \ln(2a/z) - \ln(1+\gamma/z),$$

we obtain

$$A_{k+1}(x) = \int_x^{2a} \frac{dz}{z} \sum_{m=0}^{k} \sum_{n=0}^{m} \frac{1}{n!}$$

$$\times \ln^n \frac{2a}{z} \cdot \left[\frac{(-1)^{m-n}}{(m-n)!} \ln^{m-n} \left(1 + \frac{\gamma}{z}\right) \right] b_{k-m}(z+\gamma).$$

Changing the order of summation and replacing $m - n$ by l, we find

$$A_{k+1}(x) = \int_x^{2a} \sum_{n=0}^{k} \frac{1}{n!} \ln^n \frac{2a}{z}$$

$$\times \sum_{l=0}^{k-n} \frac{(-1)^l}{l!} \ln^l \left(1 + \frac{\gamma}{z}\right) b_{k-n-l}(z+\gamma) \frac{dz}{z}. \qquad \text{(A.4)}$$

Noting that

$$db_{n+1}(z)$$

$$= -\frac{dz}{z} \left\{ \sum_{l=0}^{n} \frac{(-1)^l}{l!} \left[\ln^l \left(1 + \frac{\gamma}{z}\right) \right] b_{n-l}(z+\gamma) - b_n(z) \right\}, \qquad \text{(A.5)}$$

we can write (A.4) in the form

$$A_{k+1}(x) = -\int_x^{2a} \sum_{n=0}^{k} \frac{1}{n!} \ln^n \frac{2a}{z} \cdot db_{k-n+1}(z)$$

$$- \int_x^{2a} \sum_{n=0}^{k} b_{k-n}(z) \cdot \frac{1}{n!} \ln^n \frac{2a}{z} \frac{dz}{z}. \qquad \text{(A.6)}$$

Integrating the first term in (A.6) by parts, we obtain expressions which coincide with (A.1) and (A.2) for k → k + 1. Making the transformation of variables $\gamma/z = y$ in (A.2), we obtain (14b).

We show now that $|b_{k+1}(x)| < x^k$ and $b_k < 1$, i.e., that the radius of convergence of (15a) is larger than unity. These inequalities are satisfied by b_1 and b_2. Assume that they are fulfilled for b_k. Using the inequality

$$(n!)^{-1} \ln^n (1+y) < \ln^n (1+y) \leqslant y^n,$$

we obtain from (14b)

$$|b_{k+1}(x)| < \int_0^x \frac{dy}{y} \sum_{n=0}^{k} y^n y^{k-n} = \int_0^x dy\, k y^{k-1} = x^k.$$

Thus the inequality is fulfilled for all k.

APPENDIX B

Using the representation of the hypergeometric function in the form of a contour integral,[4] we obtain

$$\varphi_0(\mathbf{p}, \mathbf{s}) = \frac{N}{2\pi i} \oint^{(0^+, 1^+)} \frac{dx}{x} \left(\frac{-x}{1-x}\right)^{i\xi} \frac{1}{2\pi^2 i} \frac{\partial}{\partial B} \frac{1}{(\mathbf{q}_{sp} + \mathbf{p}x)^2 - (B + i\varepsilon)^2}, \qquad \text{(B.1)}$$

where $\mathbf{B} = \mathbf{p}x$. Substituting (B.1) in (29a) and noting that

$$\frac{1}{2\pi^2 i} \frac{\partial}{\partial B} \int \frac{\mathbf{q}_{sp}\, d^3 s}{(q_{fs}^2 + \lambda^2)\,[(\mathbf{q}_{sp} + \mathbf{p}x)^2 - (B + i\varepsilon)^2]}$$

$$= \nabla_B \frac{-p}{2\pi^2 i} \int \frac{d^3 s}{(q_{fs}^2 + \lambda^2)\,[(\mathbf{q}_{sp} + \mathbf{B})^2 - (B + i\varepsilon)^2]}$$

$$= \nabla_B \frac{-p}{2} \frac{1}{P} \ln \frac{P + B + i\lambda}{-P + B + i\lambda} = p \nabla_B \int_\lambda^\infty \frac{d\lambda'}{P^2 - (B + i\lambda')^2}, \qquad \text{(B.2)}$$

where $\mathbf{P} = \mathbf{q}_{\mathrm{fp}} + \mathbf{B}$, we find

$$\mathbf{J} = \frac{N}{4\pi^2\xi} \frac{1}{2\pi} \oint^{(0^+,\,1^+)} dx \left(\frac{-x}{1-x}\right)^{i\xi} \nabla_B \int_{\lambda}^{\infty} \frac{d\lambda'}{P^2-(B+i\lambda')^2} . \qquad \text{(B.3)}$$

By evaluating the gradient, we obtain the expressions (30) and (31).

---

[1] J. C. Jager and H. R. Hulm, Proc. Roy. Soc. **148**, 708 (1935).

[2] R. H. Dalitz, Proc. Roy. Soc. **A206**, 509 (1951).

[3] M. Gavrila, Phys. Rev. **113**, 514 (1959).

[4] H. A. Bethe and L. C. Maximon, Phys. Rev. **93**, 768 (1954); A. Nordsieck, Phys. Rev. **93**, 785 (1954).

[5] V. G. Gorshkov, JETP **39**, 1411 (1960), Soviet Phys. JETP **12**, 983 (1960).

[6] I. M. Ryzhik, Таблицы интегралов, сумм, рядов и произведений (Tables of Integrals, Sums, Series, and Products) Gostekhizdat (1948).

[7] W. R. Johnson and C. J. Mullin, Phys. Rev. **119**, 1270 (1960).

Translated by R. Lipperheide
253

SOVIET PHYSICS JETP VOLUME 13, NUMBER 5 NOVEMBER, 1961

ELECTRON TERMS IN THE FIELD OF TWO DIFFERENT COULOMB CENTERS

S. S. GERSHTEĬN and V. D. KRIVCHENKOV*

Joint Institute for Nuclear Research

Submitted to JETP editor December 26, 1960

J. Exptl. Theoret. Phys. (U.S.S.R.) **40**, 1491-1502 (May, 1961)

It is demonstrated that the Neumann-Wigner theorem on the impossibility of intersection of terms of the same symmetry is not valid for electrons in the field of two Coulomb centers. Terms for large and small distances between the nuclei are compared for the case when the nuclear charges are different. It is indicated that term intersections exist which are important for charge-exchange processes during collisions between hydrogen atoms and nuclei.

INTRODUCTION

We consider a negatively charged particle located in the field of two stationary Coulomb centers with charges Z_1 and Z_2. In the case when $Z_1 = Z_2$, this system represents essentially a molecular hydrogen ion, whose wave functions and energy terms have been thoroughly investigated.[1-4] It is interesting to examine the case $Z_1 \neq Z_2$. Systems of this kind arise, for example, when the hydrogen mesic atom ($Z_1 = 1$) approaches nuclei of other elements ($Z_2 > 1$)† or when multiply-charged ions such as He^{++}, Li^{+++} etc. pass through hydrogen.

Schrödinger's equation for the problem of two Coulomb centers (in atomic units $e = 1$, $\hbar = 1$, $m = 1$) has the form

$$-\frac{1}{2}\Delta\Psi + \left(-\frac{Z_1}{r_1} - \frac{Z_2}{r_2} + \frac{Z_1Z_2}{R}\right)\Psi = E\Psi, \qquad (1)$$

where R is the distance between nuclei, and r_1 and r_2 are the distances from the electron to the first and second nuclei, respectively. Introducing the elliptic coordinates

$$\xi = (r_1 + r_2)/R, \qquad \eta = (r_1 - r_2)/R, \qquad \varphi = \operatorname{arctg}(y/x), \qquad (2)‡$$

we can separate the variables in Eq. (1). Putting

$$\Psi = X(\xi)Y(\eta)e^{im\varphi}, \qquad (3)$$

we obtain the following equations for the functions $X(\xi)$ and $Y(\eta)$:

$$\frac{d}{d\xi}\left[(\xi^2 - 1)\frac{dX}{d\xi}\right] + \left(-\frac{m^2}{\xi^2 - 1} + R(Z_1 + Z_2)\xi - p^2\xi^2 + A\right)X = 0, \qquad (4a)$$

$$\frac{d}{d\eta}\left[(1 - \eta^2)\frac{dY}{d\eta}\right] + \left(-\frac{m^2}{1 - \eta^2} + R(Z_2 - Z_1)\eta + p^2\eta^2 - A\right)Y = 0, \qquad (4b)$$

$$p^2 = -R^2W/2, \qquad W = E - Z_1Z_2/R. \qquad (5)$$

The quantity A is the separation constant.

To determine the eigenvalues of (1) it is customary to find the separation constant A from Eqs. (4a) and (4b) respectively as a function of the parameters p and R. Let $A = A_{n\xi}(R, p, m)$ and $A = A_{n\eta}(R, p, m)$ be the eigenvalues of the separation constant, determined from (4a) and (4b) subject to the condition that $X(\xi)$ be finite at $\xi = 1$ and $\xi = \infty$, and $Y(\eta)$ be finite at $\eta = \pm 1$ (n_ξ and n_η are the numbers of the eigenvalues). Then the equality

$$A_{n_\xi}(R, p, m) = A_{n_\eta}(R, p, m) \qquad (6)$$

enables us to determine the function $p = p_{n_\xi, n_\eta, m}(R)$ and, consequently, the molecular terms

$$E = E_{n_\xi, n_\eta, m}(R).$$

It is obvious that as $R \rightarrow \infty$ the energy of the terms should be expressed through the quantum numbers of the hydrogen-like atoms with charge Z_1 and Z_2, whereas the molecular terms should go, as $R \rightarrow 0$, into the energy levels of the compound atom with nuclear charge $Z_1 + Z_2$.

The purpose of the present work is a comparison of the molecular terms at large and small distances between nuclei, i.e., the determination of the level of the combined atom into which the level of the individual atom (with charge Z_1 or Z_2) goes as the distance between nuclei decreases from $R = \infty$ to $R = 0$. At first glance it may appear that such a comparison is easy to obtain from the well-known Neumann-Wigner theorem on the impossibility of intersection of terms of the same symmetry.[5] However, as will be shown in the next section, the single-electron molecule under consideration is an exceptional case, for which the Neumann-Wigner theorem is not satisfied. The terms will therefore be compared by calculating the number of zeros of the functions $X(\xi)$ and $Y(\eta)$ at large and small distances between nuclei respectively, as is done for H_2^+ in Bethe's book.[6] We have established at the same time that intersections of molecular terms do exist, a very important factor in charge-exchange processes in atomic collisions.

---

*Staff member of the Moscow State University.

†Being electrically neutral, hydrogen mesic atoms pass practically freely through the electron shells of the atoms. Interaction processes between hydrogen mesic atoms and other nuclei (particularly charge exchange) are due to the smallness of the mesic-atomic orbits at the distances where the effect of the electron shell of the atom on the interaction can be neglected.

‡arctg = $\tan^{-1}$.

POSSIBILITY OF INTERSECTION OF TERMS OF THE SAME SYMMETRY

The well known statement of Neumann and Wigner, that terms of the same symmetry cannot intersect in the case of diatomic molecules, is based on the following considerations (see, for example, reference 7). Assume that at a certain distance R_0 between the nuclei the Hamiltonian $\hat{H}(R_0)$ has nearly equal eigenvalues E_1^0 and E_2^0, corresponding to eigenfunctions ψ_1^0 and ψ_2^0. Writing for the Hamiltonian $\hat{H}(R)$ at R close to R_0

$$\hat{H}(R) = \hat{H}(R_0) + (\delta\hat{H} / \delta R_0 \delta R = \hat{H}(R_0) + \hat{V}, \tag{7}$$

we can readily show that the difference between the eigenvalues of the energy at the point R is

$$\{[(E_1^0 + V_{11}) - (E_2^0 + V_{22})]^2 + 4V_{12}^2\}^{1/2}, \tag{8}$$

where V_{ik} are the matrix elements of the operator $\hat{V} = (\delta\hat{H}/\delta R)_0 \delta R$, taken over the wave functions ψ_1^0 and ψ_2^0.

For the terms to intersect it is necessary that both members under the square root in Eq. (8) vanish simultaneously. It is usually assumed that this condition can be satisfied only for terms of different symmetry, when $V_{12} \equiv 0$. On the other hand, in the case of terms of the same symmetry we have $V_{12} \not\equiv 0$ and simultaneous vanishing of both members of the equation is generally impossible, since they are functions of only one parameter δR.

We shall show later on that a diatomic molecule with one electron is an exceptional case, when simultaneous vanishing of both members in expression (8) for terms of the same symmetry, and hence intersection of terms of the same symmetry is possible. Writing down the Hamiltonian of the system in elliptical coordinates

$$\hat{H} = -\frac{2}{R^2(\xi^2-\eta^2)}\left\{\frac{\partial}{\partial\xi}(\xi^2-1)\frac{\partial}{\partial\xi} + \frac{\partial}{\partial\eta}(1-\eta^2)\frac{\partial}{\partial\eta} + \frac{\xi^2-\eta^2}{(\xi^2-1)(1-\eta^2)}\frac{\partial^2}{\partial\varphi^2}\right\} - \frac{2Z_1}{R(\xi-\eta)} - \frac{2Z_2}{R(\xi+\eta)} + \frac{Z_1Z_2}{R}, \tag{9}$$

we obtain from the operator $\hat{V}$ an expression which can be represented as

$$\hat{V} = \frac{\delta\hat{H}}{\delta R}\delta R = \left\{-\frac{2}{R}\hat{H} + \frac{Z_1Z_2}{R^2} - \frac{1}{R}\left(\frac{Z_1}{r_1} + \frac{Z_2}{r_2}\right)\right\}\delta R. \tag{10}$$

Calculation of the matrix element V_{12} shows that the integrals of the first two constituents vanish because of the orthogonality of the functions ψ_1^0 and ψ_2^0, and we therefore obtain

$$V_{12} = -\frac{\delta R}{R}\int\left(\frac{Z_1}{r_1} + \frac{Z_2}{r_2}\right)d\tau. \tag{11}$$

Let us examine the matrix element of $1/r_1$ for functions of the same symmetry (the same m). Substituting ψ_1^0 and ψ_2^0 as given by (3) we obtain

$$\left\langle\frac{1}{r_1}\right\rangle_{12} = \frac{\pi R^2}{2}\left\{\int_1^\infty X_1\xi X_2\,d\xi \int_{-1}^{+1} Y_1Y_2\,d\eta - \int_1^\infty X_1X_2\,d\xi \int_{-1}^{+1} Y_1\eta Y_2\,d\eta\right\}. \tag{12}$$

On the other hand, it follows from Eqs. (4a) and (4b) for the functions X_1, X_2, and Y_1, Y_2, that

$$(A_1 - A_2)\int_1^\infty X_1X_2\,d\xi = (p_1^2 - p_2^2)\int_1^\infty X_1\xi^2X_2\,d\xi,$$

$$(A_1 - A_2)\int_{-1}^{+1} Y_1Y_2\,d\eta = (p_1^2 - p_2^2)\int_{-1}^{+1} Y_1\eta^2Y_2\,d\eta. \tag{13}$$

The separation constant A can be regarded as the eigenvalue of the corresponding operators in (4a) and (4b) for given p and R. Inasmuch as the eigenvalue spectrum is nondegenerate for the one-dimensional equation, we have $A_1 \neq A_2$ (if $\psi_1^0 \neq \psi_2^0$ and $R \neq 0$) and consequently, taking (5) and (13) into account, we can represent $\langle r_1^{-1}\rangle_{12}$ in the form

$$\left\langle\frac{1}{r}\right\rangle_{12} = \frac{\pi R^4}{4}\frac{(E_1^0 - E_2^0)}{(A_1 - A_2)}\{\langle\xi^2\rangle_{12}\langle\eta\rangle_{12} - \langle\xi\rangle_{12}\langle\eta^2\rangle_{12}\}. \tag{14}$$

An analogous argument for $\langle r_2^{-1}\rangle_{12}$ yields

$$V_{12} = \mathrm{const}\cdot(E_1^0 - E_2^0)\delta R. \tag{15}$$

Thus, in the approximation considered here V_{12} vanishes simultaneously with $E_1^0 - E_2^0$, and consequently terms of the same symmetry can intersect.

That in the H_2^+ molecule the terms of the same symmetry actually intersect has been known for a long time (see, for example, reference 6, Fig. 52), but the connection between this result and the general Neumann-Wigner theorem has never been discussed (as far as the authors know). The foregoing analysis shows that the intersection of terms of the same symmetry in the two-center problem is in some sense "accidental." The intersection takes place only for an exact Coulomb interaction which leads to the separation of variables in (4); any perturbation that disturbs the possibility of separation of variables (for example, allowance for the finite dimensions of the nuclei) causes the terms to move appart.

COMPARISON OF TERMS FOR LARGE AND SMALL DISTANCES

The number of roots of the functions $X(\xi)$ and $Y(\eta)$ in the intervals $1 < \xi < \infty$ and $-1 < \eta < 1$ cannot vary with the parameter R.* This fact can be used to compare terms for large and small distances between nuclei. Let n_ξ be the number of zeros of the function $X(\xi)$ $(1 < \xi < \infty)$, and let n_η be the number of zeros $Y(\eta)$ $(-1 < \eta < +1)$. Then, recognizing that as $R \to 0$ Eq. (4a) changes into the equation for the radial function of a hydrogen-like atom with nucleus $Z_1 + Z_2$, and Eq. (4b) changes into the equation for the associated Legendre polynomials, it is easy to express the quantum numbers of the compound atom through n_ξ and n_η.

As $R \to 0$

$$n_r = n_\xi, \qquad l - |m| = n_\eta, \tag{16}$$

where l is the orbital momentum and n_r is the radial quantum number of the combined atom. The principle quantum number of the compound atom N is expressed through n_ξ, n_η, and m with the aid of the equation

$$N = n_r + l + 1 = n_\xi + n_\eta + |m| + 1. \tag{17}$$

As $R \to \infty$, the elliptical coordinates go into parabolic coordinates, and the equations in (4) go into equations for the hydrogen-like atom Z_1 (or Z_2) in parabolic coordinates. In order to compare terms at larger and smaller distances, it is necessary to express n_ξ and n_η through the parabolic quantum numbers of the separated atoms. Such an expression is quite easy to derive for n_ξ. Introducing the variable

$$\nu = (\xi - 1)R, \qquad 0 \leqslant \nu < \infty, \tag{18}$$

we obtain from (4a) an equation which has the following form when $\nu \ll R$ $(R \gg 1)$

$$\nu X'' + X' + \left[-\frac{m^2}{4\nu} - \frac{p^2}{R^2}\nu + \frac{A - p^2 + R(Z_1 + Z_2)}{2R}\right] X = 0. \tag{19}$$

A solution of (19), finite at $\nu = 0$, is the function

$$X = \nu^{|m|/2} e^{-p\nu/R} F \times \left(\frac{|m| + 1}{2} - \frac{A - p^2 + R(Z_1 + Z_2)}{4p};\ |m| + 1;\ \frac{2p}{R}\nu\right) \tag{20}$$

[$F(\alpha; \gamma; x)$ is the confluent hypergeometric function].

In order for the solution (20) to remain bounded with increasing ν, it is necessary that the first argument of the confluent hypergeometric function be equal to a negative integer $(-n_1)$. The separation constant is consequently

$$A = A_\xi = p^2 - R(Z_1 + Z_2) + 2p(2n_1 + |m| + 1), \tag{21}$$

and the number of positive roots of the function (20) is n_1. Thus

$$n_\xi = n_1, \tag{22}$$

where n_1 is the parabolic quantum number. (We note that for large R $\nu \approx r_1 - z_1$ near the first nucleus and $\nu = r_2 + z_2$ near the second one; the z axis is assumed to join the first nucleus to the second.)

Let us find now an expression for n_η. To be specific, we assume that the electron remains at the nucleus Z_1 after the nuclei have separated. Introducing a new variable μ:

$$\mu = R(1 + \eta), \qquad 0 \leqslant \mu \leqslant 2R, \tag{23}$$

we obtain in the region $\mu \ll R$ $(R \gg 1)$ the following equations for $Y(\mu)$:

$$\mu Y'' + Y' + \left\{-\frac{m^2}{4\mu} - \frac{p^2}{R^2}\mu + \frac{-A + p^2 - R(Z_2 - Z_1)}{2R}\right\} Y = 0. \tag{24}$$

A solution of (24), finite when $\mu = 0$ and exponentially decreasing when $\mu \gg 1$ (the electron is assumed to be at the nucleus Z_1!), is the function

$$Y(\mu) = \mu^{|m|/2} e^{-p\mu/R} F(-n_2;\ |m| + 1;\ 2p\mu/R), \tag{25}$$

where n_2 is a positive integer. The separation constant now has the form

$$A = A_\eta = p^2 - 2p(2n_2 + |m| + 1) - R(Z_2 - Z_1). \tag{26}$$

---

*Actually, were the number of roots inside the indicated intervals to increase or decrease with changing R, this would mean that a multiple root ξ_0 (or η_0) exists for some $R = R_0$, i.e., $X(\xi_0) = X'(\xi_0) = 0$ [or $Y(\eta_0) = Y'(\eta_0) = 0$]. By virtue of (4), this should lead to $X(\xi) \equiv 0$ [or $Y(\eta) \equiv 0$].

Equating (21) and (26) we obtain for the electron energy

$$W = -2p^2/R^2 = -Z_1^2/2n^2, \qquad n = n_1 + n_2 + |m| + 1, \tag{27}$$

i.e., the energy of an isolated atom with nucleus Z_1. The wave function (3), in which $X(\xi)$ and $Y(\eta)$ are specified by (20) and (25) respectively, is the wave function of the isolated atom Z_1 in parabolic coordinates.

The members of higher order in $1/R$ can be obtained by expanding the solutions (4a) and (4b) in Laguerre polynomials. Inclusion of the next two terms in the series gives for the separation constant

$$\begin{aligned} A = A_\xi = p^2 &+ \{2p(2n_1+|m|+1) - R(Z_1+Z_2)\} \\ &+ \{(2n_1+1)(n_1+|m|+1) \\ &- n_1 - (Z_1+Z_2)(2n_1+|m|+1)R/2p\} \\ &- (R^2/16p^3)\{(Z_1+Z_2)^2(2n_1+|m|+1) \\ &- (Z_1+Z_2)(2p/R)[(2n_1+|m|+1)(2n_1+|m|+2) \\ &+ 2n_1(n_1+|m|)] \\ &+ (4p^2/R^2)(2n_1+|m|+1)[(n_1+1)(n_1+|m|+1) \\ &+ n_1(n_1+|m|)]\}; \end{aligned} \tag{28}$$

$$\begin{aligned} A = A_\eta = p^2 &- \{2p(2n_2+|m|+1) + R(Z_2-Z_1)\} \\ &+ \{(2n_2+1)(n_2+|m|+1) - n_2 \\ &+ (Z_2-Z_1)(2n_2+|m|+1)R/2p\} \\ &+ (R^2/16p^3)\{(Z_2-Z_1)^2(2n_2+|m|+1) \\ &+ (Z_2-Z_1)(2p/R)[(2n_2 \\ &+|m|+1)(2n_2+|m|+2) + 2n_2(n_2+|m|)] \\ &+ (4p^2/R^2)(2n_2+|m|+1)[(n_2+1)(n_2+|m|+1) \\ &+ n_2(n_2+|m|)]\}. \end{aligned} \tag{29}$$

Equating (28) and (29) we obtain, as expected, for the atom Z_1 in the field of the nucleus Z_2,

$$W = -Z_1^2/2n^2 - Z_2/R + \tfrac{3}{2}(n_1 - n_2)nZ_2/Z_1R^2. \tag{30}$$

The function (25) has n_2 roots located at a finite distance from the nucleus Z_1. In the case when $Z_1 = Z_2$, owing to the symmetry of the Hamiltonian with respect to reflection at the center of the molecule [invariance of (4b) under a substitution of $-\eta$ for η], the solution of (4b) should have near Z_2 a form analogous to (25) (with the sign of η reversed). It is therefore possible to express n_η directly in terms of n_2: $n_\eta = 2n_2$ for symmetrical terms and $n_\eta = 2n_2 + 1$ for antisymmetrical ones (see reference 6).

When $Z_1 \neq Z_2$ the determination of the number of zeros n_η is a more complicated matter and calls for an investigation of the behavior of the function $Y(\eta)$ near the second nucleus $\eta \approx 1$). Introducing the variable

$$\mu_1 = R(1-\eta), \qquad 0 \leqslant \mu_1 \leqslant 2R, \tag{31}$$

we can write (4b) near $\mu_1 \ll R$ in the form

$$\mu_1 Y'' + Y' + \left\{-\frac{m^2}{2\mu_1} - \frac{p^2}{R^2}\mu_1 + \frac{-A + p^2 + R(Z_2 - Z_1)}{2R}\right\} Y = 0, \tag{32}$$

where the constants A and p/R are determined by the conditions (21) and (26).

A solution of (32), finite when $\mu_1 = 0$ (apart from a constant factor), is

$$Y = \mu_1^{|m|/2} e^{-p\mu_1/R} F(\alpha; |m|+1; 2p\mu_1/R), \tag{33}$$

where

$$\alpha = -n_2 - n(Z_2 - Z_1)/Z_1. \tag{34}$$

Depending on the magnitude and the sign of α, three different possibilities may occur: (1) $\alpha > 0$, (2) $\alpha < 0$ and Z_2n/Z_1 not an integer, (3) $\alpha < 0$ and $Z_2n/Z_1 = n'$ an integer. Let us consider each of these cases.

(1) The condition $\alpha > 0$ is possible only when $Z_1 > Z_2$ and n_2 are sufficiently small

$$0 \leqslant n_2 < n(Z_1 - Z_2)/Z_1. \tag{35}$$

In this case the solution (33) increases exponentially with increasing μ_1 $(1 \ll \mu_1 \ll R)$. Thus the wave function of the electron near the nucleus Z_2 cannot be represented in the form of the wave function of a hydrogen-like atom with nucleus Z_2, and is merely the function of a hydrogen atom with nucleus Z_1, but distorted in the vicinity of the nucleus Z_2. Inasmuch as the confluent hypergeometric function $F(\alpha;\ |m|+1;\ 2p\mu_1/R)$ has no positive roots when $\alpha > 0$, it is clear that the zeros of the function $Y(\eta)$ are all located near the nucleus Z_1 and according to (25)

$$n_\eta = n_2. \tag{36}$$

(2) If $\alpha < 0$ and Z_2n/Z_1 is not an integer, then the investigated level (as $R \to \infty$) of the atom Z_1 [see (27)] coincides with none of the levels of the atom Z_2. Therefore, as in case (1), the wave function of the electron near Z_2 is essentially the wave function of an atom with nucleus Z_1, distorted by the field of Z_2. At large distances between the nuclei, the Coulomb field of Z_2 hardly changes the wave function of the electron near Z_1 [see (25)], whereas its influence in the vicinity of Z_2 itself is large. When $\alpha < 0$ oscillations of the wave function occur near Z_2 (see Fig. 1). Considering that for non-integral α $(\alpha < 0)$ the number of zeros of the confluent hypergeometric function $F(\alpha;\ |m|+1;\ 2p\mu_1/R)$ is equal to $\{\mathrm{Ent}(-\alpha)+1\}$ (where $\mathrm{Ent}(x)$ is the integral part of x), we can determine n_η from (25), (33), and (34);

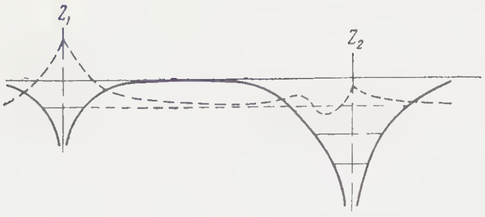

FIG. 1

$$n_\eta = n_2 + 1 + \mathrm{Ent}\,[n_2 + n\,(Z_2 - Z_1)\,/\,Z_1]. \tag{37}$$

(3) If $\alpha < 0$ and $Z_2n/Z_1 = n'$, where n' is an integer, then the level of the atom Z_1 (27) coincides with that level of the atom Z_2, whose principal quantum number is n'. From (20), (33), and (34) we see that the wave function of the electron near Z_2 is the wave function of a hydrogen-like atom with parabolic quantum numbers $n_1' = n_1$ and $n_2' = n' - n_1 - |m| - 1$. In this case therefore, as $R \to \infty$, degeneracy takes place and the regular wave functions have the form (3), where $X(\xi)$ is given by (20) and $Y(\eta)$ is a linear combination of (25) and (33). Taking into account the fact that an additional root appears for one of the linear combinations of (25) and (33) in the interval $-1 < \eta < 1$, we obtain

$$n_\eta = n_2 + n_2' \tag{38a}$$

or

$$n_\eta = n_2 + n_2' + 1. \tag{38b}$$

It will be shown in the appendix that (38a) and (38b) hold when the electron is at the nucleus with the smaller or larger charge, respectively, as $R \to \infty$.

Using (16), (17), and (35) — (38), let us summarize the results obtained. Assume, specifically, that $Z_1 < Z_2$ and that (n_1, n_2, m) and (n_1', n_2', m) are the parabolic quantum numbers of the atoms Z_1 and Z_2 as $R \to \infty$. We then have:

A. If the electron is located (when $R = \infty$) at the nucleus $Z_1(Z_1 < Z_2)$, then

$$l = \begin{cases} n_2 + |m| + 1 + \mathrm{Ent}\left(n_2 + n\dfrac{Z_2 - Z_1}{Z_1}\right), & \text{when } \dfrac{Z_2}{Z_1}n \neq \text{interger} \\ 2n_2 + |m| + n\,\dfrac{Z_2 - Z_1}{Z_1}, & \text{when } \dfrac{Z_2}{Z_1}n = \text{interger} \end{cases}, \tag{39}$$

$$N = \begin{cases} n + 1 + \mathrm{Ent}\left(n_2 + n\dfrac{Z_2 - Z_1}{Z_1}\right), & \text{when } \dfrac{Z_2}{Z_1}n \neq \text{interger} \\ n_2 + n\dfrac{Z_2}{Z_1}, & \text{when } \dfrac{Z_2}{Z_1}n = \text{interger} \end{cases} \tag{40}$$

B. If the electron is located (when $R = \infty$) at the nucleus $Z_2(Z_2 > Z_1)$, then

$$l = \begin{cases} n_2' + |m|, & \text{when } n_2' \geqslant n'\,\dfrac{Z_2 - Z_1}{Z_2} \\ n_2' + |m| + 1 \\ \quad + \mathrm{Ent}\left(n_2' - n'\,\dfrac{Z_2 - Z_1}{Z_2}\right), & \text{when } n_2' < n'\dfrac{Z_2 - Z_1}{Z_2} \end{cases}, \tag{41}$$

$$N = \begin{cases} n', & \text{when } n_2' < n'\dfrac{Z_2 - Z_1}{Z_2} \\ n' + 1 + \mathrm{Ent}\left(n_2' - n'\dfrac{Z_2 - Z_1}{Z_2}\right), & \text{when } n_2' \geqslant n'\dfrac{Z_2 - Z_1}{Z_2} \end{cases} \tag{42}$$

Formulas (39) — (42) establish the connection between the terms of the isolated atoms (at $R = \infty$) and the terms of the combined atom ($R = 0$).

BEHAVIOR OF TERMS AT SMALL DISTANCES BETWEEN NUCLEI

The behavior of the terms when the distances between the nuclei are small can be explained by using as the zeroth approximation the states of a combined atom with charge $Z_1 + Z_2$, located in the center of charge of the nuclei Z_1 and Z_2. Regarding

$$U = -\left(\frac{Z_1}{r_1} + \frac{Z_2}{r_2}\right) + \frac{Z_1 + Z_2}{r} \tag{43}$$

as a perturbation, we can show (as is done for the case $Z_1 = Z_2$, see reference 5) that the regular functions of the zeroth approximation, with allowance for degeneracy, are the wave functions of the combined atom $Z_1 + Z_2$:*

$$\psi^0 = v_{N,l}(r)\,Y_{lm}(\vartheta, \varphi), \tag{44}$$

and that the energy of the terms is given (accurate to R^2) by the expression

$$W = -\frac{(Z_1 + Z_2)^2}{2N^2} - 2Z_1Z_2(Z_1 - Z_2)^2\,\frac{[l\,(l+1) - 3m^2]\,R^2}{N^3 l\,(l+1)\,(2l-1)\,(2l+1)\,(2l+3)}. \tag{45}$$

The sequence of the terms is the same as given by Bethe[6] for the case $Z_1 = Z_2$. (The energy of the s terms is obtained formally from (4b) by putting in it $m = 0$, canceling by l, and setting $l = 0$.)

TERM INTERSECTIONS CORRESPONDING TO CHARGE EXCHANGE

The behavior of the terms when the distances between nuclei are large is determined from the formulas

$$W_1 \approx -\frac{Z_1^2}{2n^2} - \frac{Z_2}{R} + \frac{3}{2}\,\frac{(n_1 - n_2)\,n\,Z_2}{Z_1}\,\frac{}{R^2},$$

$$W_2 \approx -\frac{Z_2^2}{2n'^2} - \frac{Z_1}{R} + \frac{3}{2}\,\frac{\left(n_1' - n_2'\right)\,n'}{Z_2}\,\frac{Z_1}{R^2}, \tag{46}$$

where W_1 and W_2 correspond to the states in which the electron is located at the nucleus Z_1 or Z_2, respectively, as $R \to \infty$. The dependence

---

*To prove this statement it is essential that the radial Coulomb functions satisfy the relation

$$\int_0^\infty v_{N,l}(r)\,v_{N,l+2}(r)\,\frac{dr}{r} = 0.$$

This relation can be derived from an analysis of the integrals of the generating function of the Laguerre polynomials.

on m appears in terms of order R^{-4}, corresponding to the second approximation for the Stark effect.

Knowing the arrangement of the terms at large and small distances [see (46) and (45)] and using formulas (39) — (42), which establish the connection between the terms, we can schematically represent the course of the terms at medium distances between nuclei. Figure 2 shows the course of the σ terms for the case $Z_1 = 2$ and $Z_2 = 3$, from which we can infer the presence of a large number of intersections. Particular interest attaches to intersections of terms corresponding, as $R \to \infty$, to states in which the electron is at different nuclei, for example 3pσ and 3dσ, 4fσ and 3sσ, etc. The presence of such intersections influences appreciably the probability of charge exchange in atomic collisions.

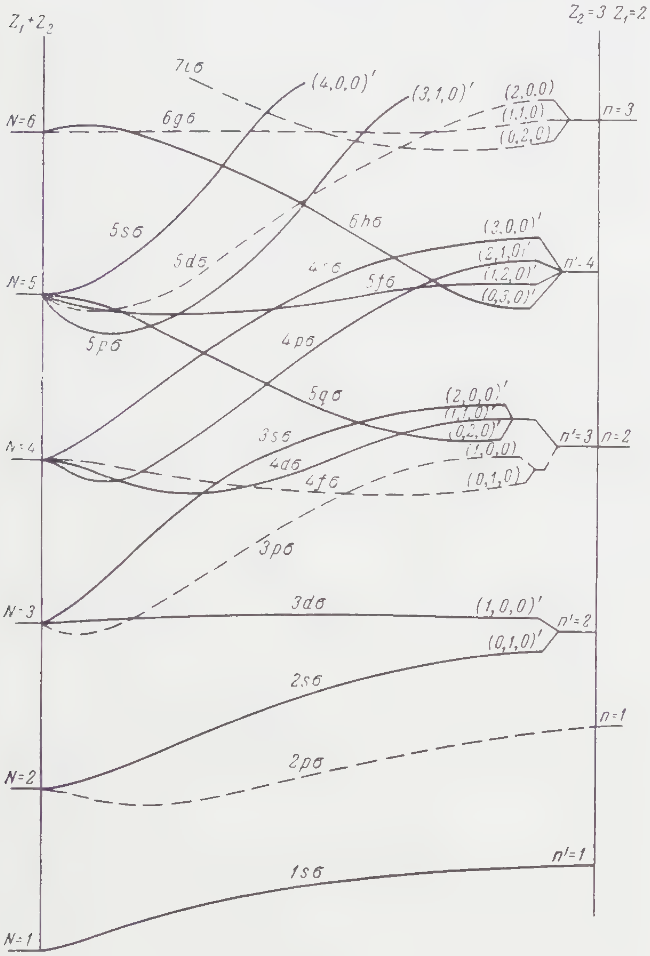

FIG. 2. σ terms for the case $Z_1=2$, $Z_2=3$. The parentheses contain the parabolic quantum numbers (n_1, n_2, m). The quantum numbers pertaining to the nucleus Z_2 are primed.

Let us consider especially the case $Z_1 = 1$, $Z_2 = Z > 1$, which is of practical interest in many of the problems mentioned in the introduction. Assume that the electron is on the hydrogen K orbit at infinity. The corresponding term (including the nuclear interaction Z_1Z_2/R) behaves as $(-\frac{1}{2} - 9Z^2/2R^4)$ at large distances, and yields Coulomb repulsion of the nuclei at small distances. On the other hand, the terms corresponding at infinity to the states of the electron at the Z nucleus, increase at large distances as $-Z^2/2n^2 + (Z-1)/R$ with decreasing R. Therefore, at sufficiently large Z, some terms of the nucleus Z, lying at infinity below the K level of the hydrogen atom, should intersect the corresponding hydrogen term. [From formulas (39) — (42) it follows that when R = 0 the term corresponding to the K orbit of the hydrogen atom lies above those terms of the nucleus Z, which were located below this term at R = ∞, i.e., the terms should intersect twice (see Fig. 3).]

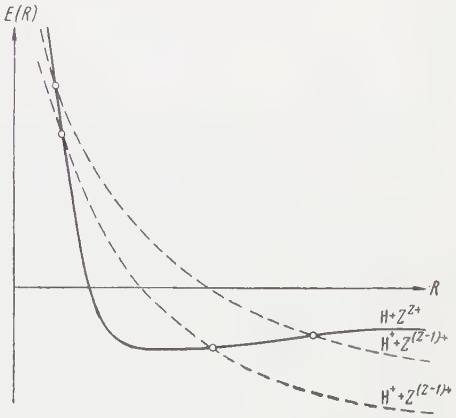

FIG. 3

This intersection occurs apparently even for $Z \geq 3$ [it is known to be missing in the case of the molecule HeH^{++}, see reference (8)] and should assure a greater charge-exchange probability in collisions between the hydrogen atom and the nucleus Z.

For terms corresponding to excited levels of the hydrogen atom, cases of intersection are encountered more frequently. The rapid transfer of negative mesons from hydrogen by the nuclei Z > 1 (see reference 9) is apparently due to precisely this circumstance.

In conclusion, the authors express their deep gratitude to L. D. Landau, L. I. Lapidus, A. A. Logunov, and Ya. A. Smorodinskii for valuable discussions and to N. S. Isaeva for preparation of the manuscript.

APPENDIX

WAVE FUNCTIONS FOR THE DEGENERATE CASE

In the case when the parabolic quantum numbers of the atoms Z_1 and Z_2 are equal, $n_1 = n_1'$ and $m = m'$, and the principal quantum numbers satisfy the relation $Z_1/n = Z_2/n'$ (i.e., the energy levels of the isolated atoms coincide), the wave function in the two-center problem can be approximately written in the form of a linear combination of the corresponding atomic functions ψ_1 and ψ_2:

$$\Psi = a\psi_1 + b\psi_2, \tag{A.1}$$

where

$$\psi_1 = C_1(r_1 + z_1)^{|m|/2} e^{-Z_1(r_1+z_1)/2n} F(-n_2;\ |m| + 1;\ Z_1(r_1+z_1)/n) \times (r_1 - z_1)^{|m|/2} e^{-Z_1(r_1-z_1)/2n} F(-n_1;\ |m| + 1;\ Z_1(r_1 - z_1)/n) e^{im\varphi}, \tag{A.2}$$

$$C_1 = \left(\frac{Z_1}{n}\right)^{|m|+3/2} \frac{1}{(m!)^2} \left[\frac{(n_1 + |m|)!\,(n_2 + |m|)!}{\pi n\,(n_1)!\,(n_2)!}\right]^{1/2}, \tag{A.3}$$

the z axis is directed from the first nucleus to the second; analogous formulas hold for ψ_2 ($n_1 = n'$; $Z_1/n = Z_2/n'$).

Noting that near the first nucleus (as $R \to \infty$) we have

$$r_1 - z_1 \approx R(\xi - 1), \qquad r_1 + z_1 \approx R(1 + \eta),$$

and near the second nucleus

$$r_2 + z_2 \approx R(\xi - 1), \qquad r_2 - z_2 \approx R(1 - \eta),$$

we can represent the function (A.1) in the form (3):

$$\Psi = e^{-Z_1R\xi/n}(\xi - 1)^{|m|/2} F(-n_1;\ |m| + 1;\ Z_1R(\xi - 1)/n)\, Y(\eta), \tag{A.4}$$

$$Y(\eta) = aC_1e^{-Z_1R\eta/n}(1 + \eta)^{|m|/2} F(-n_2;\ |m| + 1;\ Z_1R(1 + \eta)/n) + bC_2e^{Z_1R\eta/n}(1 - \eta)^{|m|/2} F(-n_2';\ |m| + 1;\ Z_1R(1 - \eta)/n). \tag{A.5}$$

Depending on the sign of the ratio a/b, the function $Y(\eta)$ can have either $n_2 + n_2'$ or $n_2 + n_2' + 1$ roots in the interval $-1 < \eta < 1$.

Substituting (A.1) in the Schrödinger equation (1), we obtain the secular equation for the energy

$$(Z_2K_2 + \varepsilon)a + (Z_1A_1 + \varepsilon S)b = 0, \tag{A.6}$$

$$(Z_2A_2 + \varepsilon S)a + (Z_1K_1 + \varepsilon)b = 0. \tag{A.7}$$

Here

$$E = -\frac{Z_1}{2n^2} + \frac{Z_1Z_2}{R} + \varepsilon, \qquad K_1 = \int |\psi_2|^2 \frac{1}{r_1}\, d\tau,$$
$$K_2 = \int |\psi_1|^2 \frac{1}{r_2}\, d\tau, \qquad S = \int \psi_1^*\psi_2\, d\tau, \qquad A_1 = \int \psi_1^*\psi_2 \frac{1}{r_1}\, d\tau,$$
$$A_2 = \int \psi_2^*\psi_1 \frac{1}{r_2}\, d\tau. \tag{A.8}$$

Noting that the quantities A_1, A_2, and S are exponentially small compared with K_1 and K_2 (accurate to terms of order R^{-2}; $K_1 \approx K_2 \approx 1/R$), we can represent the solutions (A.6) in the form

$$\varepsilon_{\mathrm{I}} = -Z_2K_2 + \frac{Z_2(A_2 - SK_2)(Z_1A_1 - Z_2SK_2)}{Z_1K_1 - Z_2K_2}, \tag{A.9}$$

$$\left(\frac{b}{a}\right)_{\mathrm{I}} = -\frac{Z_2(A_2 - SK_2)}{Z_1K_1 - Z_2K_2} \approx \frac{Z_2R}{Z_2 - Z_1}(A_2 - SK_2); \tag{A.10}$$

$$\varepsilon_{\mathrm{II}} = -Z_1K_1 - \frac{Z_1(A_1 - SK_1)(Z_2A_2 - Z_1SK_1)}{Z_1K_1 - Z_2K_2}, \tag{A.11}$$

$$\left(\frac{a}{b}\right)_{\mathrm{II}} = \frac{Z_1(A_1 - SK_1)}{Z_2K_1 - Z_2K_2} \approx -\frac{Z_1R}{Z_2 - Z_1}(A_1 - SK_1). \tag{A.12}$$

It is seen from the foregoing expressions that the solution marked by the subscript I corresponds as $R \to \infty$ to the state for which the electron is at the nucleus Z_1 ($b/a \to 0$), while solution II corresponds to the state with the electron at the nucleus Z_2 ($a/b \to 0$). In this lies the essential difference between the case $Z_1 \neq Z_2$ and the case $Z_1 = Z_2$, for which the function (A.1) remains, as $R \to \infty$, a symmetrical or antisymmetrical combination of ψ_1 and ψ_2.

Confining ourselves in the calculation of the quantities in (A.8) to the members of highest order in R ($R \gg 1$), we obtain according to (A.10) and (A.12)

$$\left(\frac{b}{a}\right)_{\mathrm{I}} \approx (-1)^{n_2+n_2'} \frac{Z_2}{Z_2 - Z_1}\left(\frac{2Z_1}{n}\right)^{n_2+n_2'+1/2} \times \frac{2^{|m|+1/2}}{[nn'(n_2)!\,(n_2')!\,(n_2 + |m|)!\,(n_2' + |m|)!]^{1/2}} \times \frac{\Gamma(n_2 + |m|/2 + 3)\,\Gamma(n_2' + |m|/2 + 1)}{(n_2 + n_2' + |m| + 3)!} R^{n_2+n_2'+|m|+2} e^{-Z_1R/n}, \tag{A.13}$$

$$\left(\frac{a}{b}\right)_{\mathrm{II}} \approx (-1)^{n_2+n_2'+1} \frac{Z_1}{Z_2 - Z_1}\left(\frac{2Z_1}{n}\right)^{n_2+n_2'+1/2} \times \frac{2^{|m|+1/2}}{[nn'(n_2)!\,(n_2')!\,(n_2 + |m|)!\,(n_2' + |m|)!]^{1/2}} \times \frac{\Gamma(n_2 + |m|/2 + 1)\,\Gamma(n_2' + |m|/2 + 3)}{(n_2 + n_2' + |m| + 3)!} R^{n_2+n_2'+|m|+2} e^{-Z_1R/n} \tag{A.14}$$

The functions $F(-n_2;\ |m| + 1;\ Z_1R(1 + \eta)/n)$ and $F(-n_2';\ |m| + 1;\ Z_1R(1 - \eta)/n)$ in (A.5) have respectively n_2 and n_2' roots lying near the nuclei Z_1 and Z_2. If the addition of these functions does not give rise to an additional root in $Y(\eta)$, the sign of the ratio a/b should be $(-1)^{n_2+n_2'}$. Taking this remark into consideration, we can readily deduce from formulas (A.13) and (A.14) that the additional root arises when the electron is at the nucleus with the greater charge.

We note that this conclusion agrees with the oscillator theorem, since, as can be seen from (A.9) and (A.11), the term corresponding at large R to an electron at the nucleus with the greater charge lies $|Z_1 - Z_2|/R$ higher than the corresponding term for the electron at the nucleus with the smaller charge.

---

[1] M. Morse, E. and C. G. Stuekelberg, Phys. Rev. **33**, 932 (1929). J. E. Lennard-Jones, Trans. Farad. Soc. **24**, 668 (1929).

[2] E. Teller, Z. Physik **61**, 458 (1930). E. A. Hylleraas, Z. Physik **71**, 739 (1931).

[3] G. Jaffe, Z. Physik **87**, 535 (1934).

[4] Bates, Ledsham, and Stewart, Phil. Trans. Roy. Soc. **246**, 911 (1953).

[5] J. v. Neumann and E. Wigner, Phys. Z. **30**, 467 (1929).

[6] H. Bethe, Quantum Mechanics of Simplest Systems (Russian translation) ONTI, M-L, 1934.

[7] L. D. Landau and E. M. Lifshitz, Quantum Mechanics, Pergamon, 1958.

[8] B. R. Bates and T. R. Carson, Proc. Roy. Soc. **A234**, 207 (1956).

[9] Panofsky, Aamont, and Handley, Phys. Rev. **81**, 565 (1951).

Translated by J. G. Adashko
254

SOVIET PHYSICS JETP VOLUME 13, NUMBER 5 NOVEMBER, 1961

THE PROPERTIES OF SOME STRONGLY DEFORMED NUCLEI

LIU YÜAN, N. I. PYATOV, V. G. SOLOV'EV, I. N. SILIN, and V. I. FURMAN

Joint Institute for Nuclear Research

Submitted to JETP editor December 26, 1960

J. Exptl. Theoret. Phys. (U.S.S.R.) **40**, 1503-1510 (May, 1961)

An improved scheme of single-particle levels of a self-consistent field is employed to investigate some properties of strongly deformed nuclei in the range $150 < A < 190$, on the basis of the superfluid model of the nucleus. The mean values of the pair coupling constants are evaluated by comparing the calculated pair energies with the experimental data. The density of the low-energy single-particle energy levels of odd nuclei is calculated and found to agree with the experimental data and to be approximately double the level density predicted by the Nilsson scheme. Some regularities in the behavior of weakly excited states in even-even nuclei are noted. On the average, the calculation error due to conservation of the number of particles does not exceed 6 percent.

THE superfluid model of the nucleus, proposed by one of the authors[1] and based on the unified or the shell model, takes account of the residual short-range interactions of the nucleons in the nucleus by the Bogolyubov variational principle.[2] To describe such interactions, we use a Hamiltonian in the form

$$H = \sum_{s\sigma} [E_s - \lambda]\, a^+_{s\sigma} a_{s\sigma} - G \sum_{ss'} a^+_{s+} a^+_{s-} a_{s'-} a_{s'+}, \qquad (1)$$

where E_s are the single-particle levels of the self-consistent field, λ is a parameter that plays the role of the chemical potential, $(s\sigma)$ are the quantum characteristics of the level $(\sigma = \pm 1)$, and G is the short-range pair-coupling constant. We note that the number of particles is conserved in the mean.

The properties of the transuranic elements were investigated earlier (see reference 3, where the principal equations of the problem are given). In the present paper we investigate, on the basis of the superfluid model, the properties of strongly deformed nuclei in the region $150 < A < 190$.

From a comparison of the calculated pair energies with the experimental data we shall determine and compare with experiment the pair-coupling constants G and calculate the spectra of single-particle levels for some odd and even-even nuclei.

MODIFICATION OF THE NILSSON SCHEME

We use the levels of the Nilsson scheme[4] as the single-particle levels E_s in our calculations. An analysis of the scheme, carried out on the basis of known spectroscopic data,[5-7] shows that the proton shell is in general satisfactorily described by the Griffin and Rich scheme.[8] We shall make significant changes only in the neutron level schemes for $82 < N < 126$:

a) All the eigenvalues of neutrons with $N = 6$ will be increased by $0.25\hbar\omega_0^0$ (corresponding to a parameter $\mu = 0.33$) (see Nilsson's paper[4] for notation), with the exception of the states $i\,^{13}\!/_2$, which will be increased by $0.06\hbar\omega_0^0$ $(\mu = 0.42)$.

b) We drop the $h\,^{11}\!/_2$ subshell $0.3\hbar\omega_0^0$ $(\mu = 0.65)$;

c) The $f\,^5\!/_2$ eigenvalues are raised $0.06\hbar\omega_0^0$ $(\mu = 0.42)$.

d) The $p\,^3\!/_2$ eigenvalues are dropped $0.01\hbar\omega_0^0$ to agree with experimental data on nuclei with 109 neutrons.

e) The $^1\!/_2^-[521]$ level is raised $0.04\hbar\omega_0^0$, as in reference 8.

The corrected Nilsson scheme, shown in Fig. 1, gives correct ground states for all nuclei with $93 < N < 109$ and gives for some nuclei the required sequence of first excited levels. It agrees essentially with the corrected scheme given by Nilsson and Prior,[9] with the exception of the $^{11}\!/_2^-[505]$ level.

The ground states given in reference 3 were calculated on a "Strela" computer. The problem was reduced to the least-squares method and solved by linearization. The specified energy levels of the average field and of the coupling constant G were used to calculate the correlation function C, the chemical potential λ, the mean square fluctuation of the number of particles $(\overline{\Delta n^2})^{1/2}$, and the system energy ϵ, accurate to 4 — 6 significant decimal places.

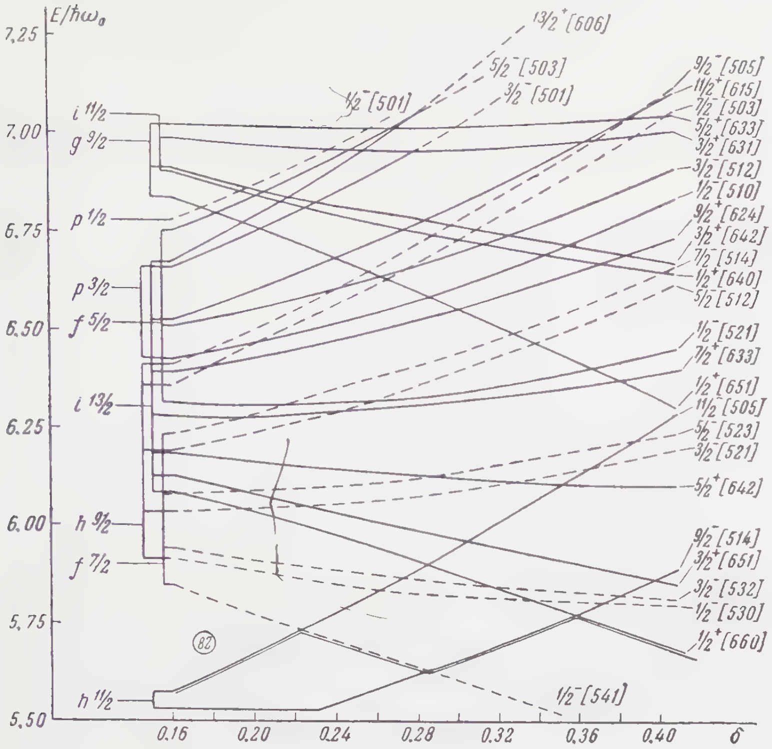

FIG. 1. Nilsson scheme for $82 < N < 126$.

PAIR ENERGIES AND CORRELATION FUNCTIONS

To determine G we calculated the neutron and proton pair energies P_N and P_Z by the formula

$$P_N = 2\varepsilon(Z, N-1) - \varepsilon(Z, N) - \varepsilon(Z, N-2). \qquad (2)$$

The calculated pair energies of the neutron system for $G_N = 0.020$ and $0.024\,\hbar\omega_0^0$ and of the proton system for $G_Z = 0.024$ and $0.028\,\hbar\omega_0^0$, along with the corresponding experimental data,[10,11] are shown in Figs. 2 and 3. From a comparison of the calculated pair energies with the experimental data we have determined the average values of the pair coupling constants

$$G_N = 0.024\,\hbar\omega_0^0, \qquad G_Z = 0{,}026\,\hbar\omega_0^0. \qquad (3)$$

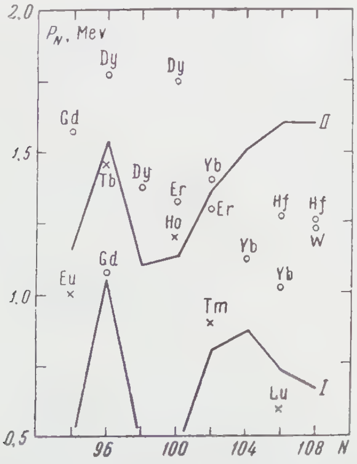

FIG. 2. Calculated (continuous curves) and experimental[10,11] values of the neutron pair energies (○ – even-even nuclei, × – nuclei with odd A); curve I – for $G = 0.020\hbar\omega_0^0$, curve II – for $G = 0.024\hbar\omega_0^0$.

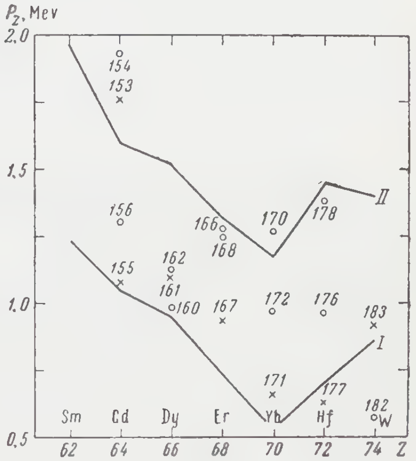

FIG. 3. Calculated (continuous curves) and experimental[10,11] values of proton pair energies (○ – even-even nuclei, × – nuclei with odd A); curve I – for $G = 0.024\hbar\omega_0^0$, curve II – for $G = 0.028\hbar\omega_0^0$.

We note that the pair energy decreases with the increasing deformation, owing to the diminished role of the residual interactions.

By fixing the scheme of single-particle levels on the basis of an analysis of the experimental spectra of odd nuclei, with allowance for superfluidity, and by determining the constants G_N and

G_Z from the pair energies, we eliminate ipso facto all arbitrariness from the subsequent calculations.

Let us investigate the behavior of the correlation function $C = G\Sigma_s u_s v_s$ and of the chemical potential λ corresponding to the ground states of even-even and odd nuclei. The variation of the chemical potential λ with the degree of filling of the shell, for a system with an even number of neutrons, is shown in Fig. 4. The value of λ fluctuates about the Fermi-surface energy, the deviations reaching an order of 1 Mev. The fluctuations in the difference $|\lambda - E_F|$ become even greater for the excited states. The deviation of λ from E_F is particularly great in the excited states of even systems.

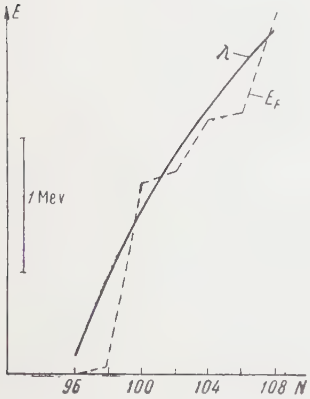

FIG. 4. Variation of Fermi-surface energy E_F and chemical potential λ of the ground states of an even neutron system; $G = 0.024\hbar\omega_0^0$.

The behavior of the functions C for the ground states of even and odd systems are demonstrated in Figs. 5 and 6. We note that the values of C for the ground states of odd systems depend strongly on the course of the single-particle levels that are closest to the Fermi-surface energy. It is seen from the scheme for single-particle neutron levels (Fig. 1) that in the region of deformations $\delta = 0.26 - 0.36$ the energy difference between the levels $N = 97$ and $N = 99$ reaches 1.4 Mev, which leads to a sharp reduction in C for the corresponding odd nuclei. The values of C for the ground states of even systems are less sensitive to the behavior of single-particle levels. The values of C for odd systems $(2n-1)$ are on the average 20 — 30 percent less than the values of C for even systems $(2n)$, in agreement with the estimates of Nilsson and Prior.[9]

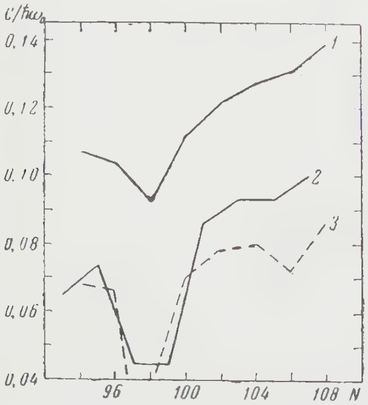

FIG. 5. Behavior of the correlation function C of the neutron system as a function of the number of neutrons N in a nucleus (ground state): 1 – even-even system with $G = 0.024\hbar\omega_0^0$, 2 – odd system with $G = 0.024\hbar\omega_0^0$, 3 – even-even system with $G = 0.020\hbar\omega_0^0$.

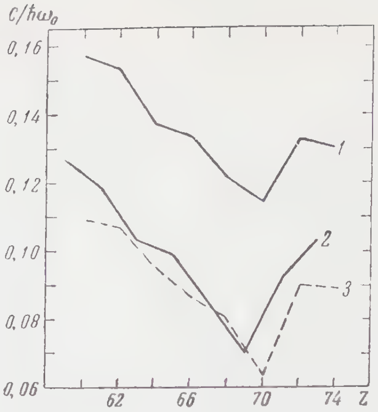

FIG. 6. Behavior of correlation function C of proton system as a function of the number of protons Z in the nucleus (ground state): 1 – even-even system with $G = 0.028\hbar\omega_0^0$, 2 – odd system with $G = 0.028\hbar\omega_0^0$, 3 – even-even system with $G = 0.024\hbar\omega_0^0$.

Thus, the appearance of a single quasi-particle leads to a considerable weakening of superfluidity. It should be noted that the values of C decrease as a rule with increasing deformation, thus demonstrating the diminished role of pair correlations with increasing δ. The function C for single-quasi particle states of odd systems has a minimum for the ground state and increases for the excited states with increasing excitation energy, approaching thereupon the value for the ground state of the corresponding even system, as can be readily seen from Table I. (The symbol $K+1$ denotes the level following the level K, etc.) In the case of an even system, the function C for two quasi-particle excited states diminishes by 30 percent and more, vanishing sometimes. With increasing excitation energy, the magnitude of this correlation function increases.

SINGLE-PARTICLE LEVELS OF ODD NUCLEI

On the basis of the superfluid model of the nucleus let us calculate now, in the region of interest to us, the spectrum of single-particle levels of nuclei with odd N as well as odd Z. In Fig. 7 we show by way of an example the calculated and experimental values of the levels of Dy^{161} and

Table I. Characteristics of ground and excited states of odd nuclei

State of system		$C/\hbar\omega_0^0$	$(\overline{\Delta n^2})^{1/2}$	$\frac{E_F-\lambda}{\hbar\omega_0^0}$
$N=95,\ \delta=0.30,\ G=0.024\,\hbar\omega_0^0$				
$K-3$;	$^{11}/_2{}^-$ [505]	0.091	2.01	−0.018
$K-2$;	$^3/_2{}^+$ [651]	0.090	2.00	−0.017
$K-1$;	$^3/_2{}^-$ [521]	0.077	1.77	−0.004
K;	$^5/_2{}^+$ [642]	0.074	1.71	+0.010
$K+1$;	$^5/_2{}^-$ [523]	0;076	1.75	+0.016
$K+2$;	$^7/_2{}^+$ [633]	0.094	2.08	+0.033
$K+3$;	$^1/_2{}^-$ [521]	0.095	2.09	+0.034
$Z=71,\ \delta=0.28,\ G=0.028\text{-}\hbar\omega_0^0$				
$K+3$;	$^1/_2{}^-$ [541]	0.101	—	+0.123
$K+2$;	$^9/_2{}^-$ [514]	0.089	—	+0.118
$K+1$;	$^5/_2{}^+$ [402]	0.080	—	+0.113
K;	$^7/_2{}^+$ [404]	0.068	—	+0.106
$K-1$;	$^1/_2{}^+$ [411]	0.104	—	+0.067
$K-2$;	$^7/_2{}^-$ [523]	0.106	—	+0.065
$K-3$;	$^3/_2{}^+$ [411]	0.110	—	+0.065

Lu^{175}. We note that the excitation energies which we have calculated agree better with the experimental data than those given by the Nilsson scheme. However, in view of the strong dependence of the determined levels of the odd nuclei on the behavior of the levels of the average field, it is difficult to expect a detailed agreement with the experimental data. We shall therefore investigate the densities of the single-particle levels.

The average density of the calculated neutron levels was found to be 3.3 times the 1-Mev level for $99 \leq N \leq 109$, compared with 3.1 for the similarly averaged experimental levels.[12] The average density of the calculated proton levels for $63 \leq Z \leq 73$ is found to be 3.4 times the 1-Mev level, compared with 3.6 for the experimental levels. The average densities of the calculated (single-particle) proton and neutron levels are 1.7 times the level densities in the corresponding Nilsson scheme. The calculations are in agreement with Bakke's investigations[13] of the density of single-particle levels.

Thus, as in the transuranic region,[3] the density of low-energy levels agrees with experiment and is approximately twice the level density given by the Nilsson scheme. We note that the increase in the level density is connected with the superfluid properties of the ground and excited states. The necessary level density cannot be obtained by any modification of the single-particle levels in the independent-particle model.

SPECTRA OF EVEN-EVEN NUCLEI AND ESTIMATE OF THE CALCULATION ACCURACY

The most interesting and promising is the application of methods based on the superfluid nuclear model to the analysis of spectra of even-even nuclei. It was shown in reference 3 that in the excited state of an even system $|K, K+1\rangle$, where one quasi-particle is at the K level (K denotes the totality of quantum numbers corresponding to the Fermi-surface energy of the given nu-

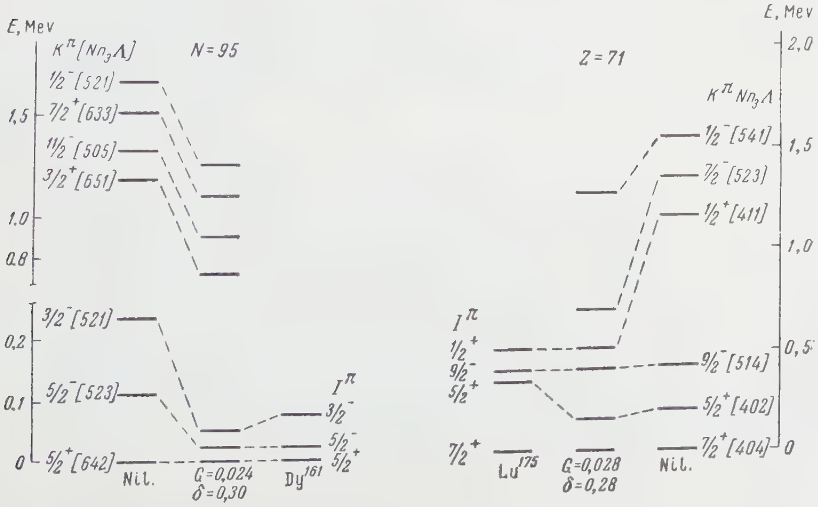

FIG. 7. Spectra of single-particle excitations of nuclei with odd number of particles. The letters "Nil" denote the spectrum after Nilsson, the spectrum in the center has been obtained for the superfluid model of the nucleus, and the spectra of Dy and Lu are experimental without rotational lines). G is given in units of $\hbar\omega_0^0$ ($\hbar\omega_0^0 = 41\ A^{-1/3}$ Mev).

Table II. Spectrum of ${}_{70}\mathrm{Yb}^{172}_{102}$

State	$C/\hbar\omega_0^0$	$(\overline{\Delta n^2})^{1/2}$	$\frac{E_F-\lambda}{\hbar\omega_0^0}$	K^π	E, Mev
		Proton levels $\delta=0.29,\ G_Z=0.028\ \hbar\omega_0^0$			
$0\rangle$	0.109	2.00	—0.084	0^+	0
$K,\ K+1\rangle$	0	0	—0.130	$3^+,\ (4^+)$	1.54
$K,\ K+2\rangle$	0	0	—0.114	$(2^+),\ 3^+$	1.69
$K-1,\ K+1\rangle$	0	0	—0.124	$(0^-),\ 7^-$	1.76
$K-1,\ K+2\rangle$	0 ~	0	—0.102	$1^-,\ (6^-)$	1.91
$K,\ K+3\rangle$	0 ~	0	—0.101	$(4^-),\ 5^-$	1.91
$K,\ K\rangle$	0.084	1.82	—0.165	0^+	2.29
$K+1,\ K+1\rangle$	0.084	1.77	0	0^+	2.40
$K-2,\ K+1\rangle$	0.019	0.40	—0.099	$(2^+),\ 5^+$	2.50
$K-1,\ K\rangle$	0.086	1.84	—0.165	$(3^-),\ 4^-$	2.50
$K+1,\ K+2\rangle$	0.086	1.79	0	$(1^+),\ 6^+$	2.55
$K+2,\ K+2\rangle$	0.087	1.81	0	0^+	2.68
$K-1,\ K-1\rangle$	0.088	1.87	—0.166	0^+	2.70
		Neutron levels $\delta=0.29,\ G_N=0.024\ \hbar\omega_0^0$			
$0\rangle$	0.108	2.33	0	0^+	0
$K,\ K+1\rangle$	0.034	0.87	—0.023	$(2^+),\ 3^+$	0.98
$K+1,\ K+1\rangle$	0.053	1.45	+0.013	0^+	1.08
$K-1,\ K+1\rangle$	0.046	1.20	—0.032	$1^-,\ (6^-)$	1.11
$K,\ K\rangle$	0.057	1.49	—0.050	0^+	1.17
$K,\ K+2\rangle$	0.054	1.41	—0.002	$3^+,\ (4^+)$	1.25
$K-1,\ K\rangle$	0.061	1.59	—0.052	$(3^-),\ 4^-$	1.30
$K-1,\ K+2\rangle$	0.058	1.54	—0.011	$(0^-),\ 7^-$	1.33
$K+1,\ K+2\rangle$	0.061	1.62	+0.019	$(1^+),\ 6^+$	1.38
$K-1,\ K-1\rangle$	0.065	1.67	—0.054	0^+	1.42
$K+2,\ K+2\rangle$	0.067	1.74	+0.025	0^+	1.66
$K,\ K+3\rangle$	0.064	1.61	+0.005	$(4^-),\ 5^-$	2.03
$K+1,\ K+3\rangle$	0.068	1.73	+0.023	$2^-,\ (7^-)$	2.16

cleus with $G = 0$) and the other is at the level $K+1$, the superfluidity of the system is greatly reduced, and in many cases simply vanishes. This is connected with the fact that the levels K and $K+1$ are blocked for correlated pairs, and therefore a large gap appears in the states accessible to pairs. Inasmuch as the number of states below this gap is equal to the number of particles, and the pairs cannot favor, from the energy point of view, the levels $K+2$ and higher, owing to the large loss in kinetic energy, the superfluidity in the state $|K, K+1\rangle$ is very small. In this connection, the energy of the system in the state $|K, K+1\rangle$ is reduced and as a rule the energy difference in this state is essentially less than the gap width $2C_0$, where C_0 is the value of the correlation function in the ground state.

Let us illustrate these arguments with ${}_{70}\mathrm{Yb}^{172}$ as an example, for which the calculated characteristics of the excited states are listed in Table II. There is no superfluidity in the excited states $|K, K+1\rangle$, $|K, K+2\rangle$ and others, i.e., $C = 0$, whereas in the ground state $C_0 = 0.12\,\hbar\omega_0^0 = 0.85$ Mev; in higher energy states the superfluidity increases, approaching the value of the ground state. In the case of a neutron system, the superfluid properties are much weaker in the state $|K, K+1\rangle$, inasmuch as $C = 0.034\,\hbar\omega_0^0$, whereas in the ground state $C_0 = 0.126\,\hbar\omega_0^0 \approx 0.93$ Mev.

Let us compare now the calculated spectrum of Yb^{172} with the experimental data[14] obtained in an investigation of the decay of ${}_{71}\mathrm{Lu}^{172}$ with the configuration $\{$neutrons $\frac{1}{2}^-[521]\downarrow$; protons $\frac{7}{2}^+[404]\uparrow\}$, i.e., $I^\pi = 4^-$, $k = 4$. There is no doubt that the excited state 3^+3 with energy 1.17 Mev in the spectrum of Yb^{172} is a single-particle one, and can be either a proton state of the form $\{\frac{7}{2}^+[404]\downarrow\} - \{\frac{1}{2}^+[411]\downarrow\}$, or a neutron state $\{\frac{1}{2}^-[521]\downarrow + \frac{5}{2}^-[512]\uparrow\}$. The level 3^+3 is an example of the $|K, K+1\rangle$ state, and its energy is less than the energy of the gap, since the neutron gap is $2C_0 = 1.86$ Mev and the proton gap is $2C_0 = 1.7$ Mev. In view of the reduced superfluidity of the system in the $|K, K+1\rangle$ state, the moment of inertia J of the system in this state should increase, as confirmed by experiment, since $\hbar^2/2J = 13$ for the ground state and $\hbar^2/2J = 11$ for the state $|K, K+1\rangle$.

We note that the moment of inertia of a system in an excited state depends on the superfluid properties of both the given state and of the other states. Therefore the sharp reduction in the correlation function C for a given state does not lead to a considerable change in the moment of inertia of the system in the same excited state, compared with the moment of inertia of the system in the ground or other excited states.

We note that those states 0^+ in which both quasi-particles are at the same level have been calculated with lower accuracy than the other states. The conservation of the number of particles in the mean leads to several difficulties which are concentrated at these states. One of the two quasi-particle states is superfluous, and the ground state and the 0^+ state are not orthogonal to each other. Actually, in the case of Er^{166}, with $\delta = 0.31$, $G_N = 0.024\,\hbar\omega_0^0$ and $G_Z = 0.028\,\hbar\omega_0^0$, estimates of the non-orthogonality lead to the following results:

a) proton states

$$\langle K-1,\ K-1\,|\,0\rangle = 0.30,$$
$$\langle K,\ K\,|\,0\rangle = -0.39,$$
$$\langle K+1,\ K+1\,|\,0\rangle = 0.38,$$

$$\langle K+1,\ K+1\,|\,K-1,\ K-1\rangle = -0.10,$$
$$\langle K,\ K\,|\,K-1,\ K-1\rangle = -0.02,$$
$$\langle K+1,\ K+1\,|\,K,\ K\rangle = -0.13;$$

b) neutron states

$$\langle K-1,\ K-1\,|\,0\rangle = 0.08,$$
$$\langle K,\ K\,|\,0\rangle = 0.12,$$
$$\langle K+1,\ K+1\,|\,0\rangle = -0.10,$$

$$\langle K+1,\ K+1\,|\,K-1,\ K-1\rangle = -0.15,$$
$$\langle K,\ K\,|\,K-1,\ K-1\rangle = 0.$$
$$\langle K+1,\ K-1\,|\,K,\ K\rangle = -0.23;$$

here $|\,0\,\rangle$ is the ground state.

Using the formulas of reference 15, let us estimate the error due to conservation of the number of particles in the mean. The calculated rms values $(\overline{\Delta n^2})^{1/2}$ of the fluctuation of the number of particles are given in Tables I and II. The relative magnitude of the fluctuation $(\overline{\Delta n^2})^{1/2}/2\Omega$ (Ω is the number of summed levels) changes appreciably on going from the ground state to the excited ones, but is nowhere more than 6 percent. Thus, the accuracy of our calculations is restricted not by the conservation of number of particles in the mean, but principally by the accuracy to which the single-particle levels of the self-consistent field are known.

In conclusion we consider it our pleasant duty to thank N. N. Bogolyubov, K. L. Gromov, B. S. Dzhelepov, and L. K. Peker for very fruitful discussions of the work.

---

[1] V. G. Solov'ev, Doklady Akad. Nauk SSSR **133**, 325 (1960), Soviet Phys.-Doklady **5**, 778 (1961).

[2] N. N. Bogolyubov, Doklady Akad. Nauk SSSR **119**, 244 (1958), Soviet Phys.-Doklady **3**, 292 (1958); JETP **34**, 73 (1958), Soviet Phys. JETP **7**, 51 (1958).

[3] V. G. Solov'ev, Preprint, Joint Institute for Nuclear Research, D-545, 1960; JETP **40**, 654 (1961), Soviet Phys. JETP **13**, 456 (1961).

[4] S. G. Nilsson, Kgl. Dan. Vid. Selsk. Mat.-Fys. Medd. **29**, No. 16 (1955).

[5] B. R. Mottelson and S. G. Nilsson, Mat.-Fys. Skr. Dan. Vid. Selsk. **1**, No. 8 (1959).

[6] B. S. Dzhelepov and L. K. Peker, Схемы распада радиоактивных ядер (Decay Schemes of Radioactive Nuclei), Academy of Sciences U.S.S.R. (1958).

[7] Материалы совещания по нейтронно-дефицитным изотопам (Materials of Conference on Neutron-Deficient Isotopes), Dubna, (1959).

[8] J. J. Griffin and M. Rich, Phys. Rev. Lett. **3**, 342 (1959).

[9] S. G. Nilsson and O. Prior, Preprint.

[10] W. H. Johnson, Jr. and V. B. Bhanot, Phys. Rev. **107**, 1669 (1957).

[11] V. A. Kravtsov, JETP **36**, 1224 (1959), Soviet Phys. JETP **9**, 871 (1959).

[12] Harmatz, Handley, and Mihelich, Phys. Rev. **119**, 1345 (1960).

[13] F. N. Bakke, Nucl. Phys. **9**, 670 (1958/59).

[14] R. G. Wilson and M. L. Pool, Phys. Rev. **118**, 1067 (1960).

[15] S. T. Belyaev, Mat.-Fys. Medd. Dan. Vid. Selsk. **31**, No. 11 (1959). V. G. Solov'ev, JETP **35**, 823 (1958) and **36**, 1869 (1959), Soviet Phys. JETP **8**, 572 (1959) and **9**, 1331 (1959).

Translated by J. G. Adashko
255

SOVIET PHYSICS JETP VOLUME 13, NUMBER 5 NOVEMBER, 1961

ENERGY DEPENDENCE OF CROSS SECTIONS NEAR THE "THRESHOLD" FOR UNSTABLE PARTICLE PRODUCTION

A. I. BAZ'

Submitted to JETP editor December 28, 1960

J. Exptl. Theoret. Phys. (U.S.S.R.) **40**, 1511-1515 (May, 1961)

The energy dependence of the cross sections for elastic scattering, X(aa)X, and for the reaction X(ab)Y are determined near the "threshold" for production of an unstable particle Y, which decays immediately after it is produced (Y → c + d). The results obtained may be useful in nuclear physics.

1. INTRODUCTION

THE form of the energy dependence of an arbitrary two-particle reaction X(ab)Y near its threshold is well known.[1] It is also known that the cross section for elastic scattering X(aa)X exhibits an anomaly (a peak or cusp) at the threshold point.[2,3] In all the papers cited, however, it is assumed that the particles b and Y are stable, so that both at the beginning and the end of the reaction only two particles are present, namely a + X and b + Y respectively.

If one of the final particles, say Y, is actually unstable (width Γ) and decays after some time

$$Y \to c + d, \tag{1}$$

then formally one is dealing with a three-particle reaction

$$X + a \to \underset{\searrow\, Y+b\, \nearrow}{b + c + d.} \tag{2}$$

As a consequence of the existence of a finite width Γ the threshold will not be sharp in this case, but will be "smeared" out in an energy region $\Delta E \sim \Gamma$ near the energy E_r of the particle Y.

Such a situation arises very often in nuclear reactions, in which one of the reaction products is an excited nucleus, in high energy physics in strange particle production, etc. In this connection it becomes of interest to study the energy dependence of cross sections near the "threshold" for production of an unstable particle Y. This turns out to be possible in a quite general manner. In Sec. 2 we obtain an expression for the cross section for reaction (1), and in Sec. 3 for the elastic scattering process X(aa)X. For simplicity we consider throughout the case of spinless neutral particles.

2. REACTION CROSS SECTION NEAR THRESHOLD

Let us consider reaction (2) in more detail. For energies E of the colliding particles X + a near E_1 (see Fig. 1), the cross section for the reaction X + a → b + c + d, just like the total cross section for any three-particle reaction, is proportional to $\sigma \sim (E - E_1)^2$ and is consequently very small if E is sufficiently close to E_1.

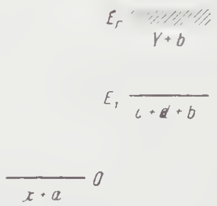

FIG. 1

The distribution of the final particles (b + c + d) in energy (spectrum) near threshold should be statistical (provided there is no zero energy resonance among the particles b, c, and d) as is illustrated by the curve labeled 1 in Fig. 2; the figure shows schematically the differential cross section $\sigma(\epsilon_{cd}, E)$ as a function of the energy of relative motion of particles c + d; $\epsilon_{cd} = E - E_1 - \epsilon_b$, where ϵ_b is the energy carried off by particle b.

The statistical form of the spectrum corresponds to

$$\sigma(\varepsilon_{cd}, E) \approx \text{const} \cdot \sqrt{\varepsilon_{cd}(E - E_1 - \varepsilon_{cd})}. \tag{3}$$

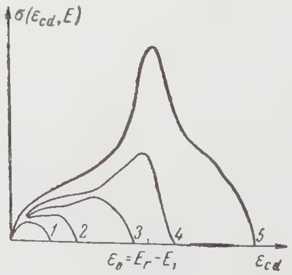

FIG. 2

Let us now increase the energy E, gradually approaching E_r. Simultaneously the form of the spectrum will change in some manner (curve 2 in Fig. 2): the nearer we approach E_r the more pronounced becomes the maximum at the upper end of the spectrum (curve 3). When E exceeds E_r the maximum stabilizes at $\epsilon_{cd} = E_r - E_1 \equiv \epsilon_0$ (curve 4) and as E is increased further remains at the same place (curve 5).

The appearance of the maximum is due to a resonant interaction between particles c and d ($c + d \rightleftarrows Y$) and is simplest understood in the following manner. If the interaction of particle b with c and d is neglected then the differential cross section for the reaction should be of the following form[4] (by analogy with the well known expression for two-particle reactions):

$$\sigma(\varepsilon_{cd}, E) = (\varepsilon_{cd}\varepsilon_b)^{-1/2} |\psi_{\varepsilon_{cd}}\varphi_{\varepsilon_b}|^2 \zeta, \tag{4}$$

where ψ_ϵ is the value of the wave function describing the relative motion of the pair c + d (with the energy ϵ) at the surface of the region within which the reaction takes place, φ_ϵ is the corresponding value of the wave function describing the motion of particle b relative to the pair c + d, and ζ is some function determined by the details of the nuclear interaction.

It follows from the assumption of the existence of the quasistable particle Y that a resonance appears in the elastic scattering $c + d \rightarrow c + d$ at the energy $\epsilon_{cd} = \epsilon_0$ i.e., that ψ_ϵ has as a function of the energy a pole at $\epsilon = \epsilon_0 - i\Gamma$.[5] This means that near $\epsilon_{cd} \sim \epsilon_0$

$$|\psi_{\varepsilon_{cd}}|^2 \sim [(\varepsilon_{cd} - \varepsilon_0)^2 + \Gamma^2]^{-1} \tag{5}$$

and, correspondingly, the spectrum (4) has a maximum near $\epsilon_{cd} \approx \epsilon_0$

$$\sigma(\varepsilon_{cd}, E) \sim (\varepsilon_{cd}\varepsilon_b)^{-1/2} \frac{|\varphi_{\varepsilon_b}|^2}{(\varepsilon_{cd} - \varepsilon_0)^2 + \Gamma^2}, \tag{6}$$

with the form of the spectrum in this region given by the Breit-Wigner curve.

We are now in a position to find the energy dependence of the total cross section near the threshold for production of Y

$$\sigma(E) = \int_0^{E-E_1} \sigma(\varepsilon, E)\, d\varepsilon. \tag{7}$$

To this end we note that the main contribution to (7) in this energy region comes from the resonance maximum (6) at $\epsilon \approx \epsilon_0$, and the lower part of the spectrum ($\epsilon < \epsilon_0$) leads to the appearance in $\sigma(E)$ of a small term, whose energy dependence is weak. We may therefore replace in Eq. (7) the lower limit by $\epsilon_0 - \Delta$ (Δ is some quantity $\gg \Gamma$) and obtain, after discarding all factors that vary slowly with the energy near $\epsilon = \epsilon_0$, (it is assumed that Y + b are produced in an S state, so that $|\varphi_{\epsilon b}|^2 \sim \epsilon_b = E - E_1 - \epsilon$, and that $\Gamma \ll \epsilon_0$)

$$\sigma(E) \sim \int_{\varepsilon_0-\Delta}^{E-E_1} d\varepsilon \frac{\sqrt{E - E_1 - \varepsilon}}{(\varepsilon - \varepsilon_0)^2 + \Gamma^2} \sim \int_{1-\Delta/\varepsilon_0}^{1} dx \frac{(1-x)^{1/2}}{[x - 1 - \alpha]^2 + \gamma^2}$$
$$\int_0^{\Delta/\varepsilon_0} dy \frac{y^{1/2}}{(y-\alpha)^2 + \gamma^2},$$

where $\alpha = (E - E_r)/\epsilon_0$, $\gamma = \Gamma/\epsilon_0$.

In the case of interest to us, when $|\alpha| \ll 1$ and $\gamma \ll 1$, the main contribution to the last integral comes from the region of small values of y so that we may let the upper limit go to infinity; we then obtain immediately

$$\sigma(E) \sim \int_0^\infty dy \frac{y^{1/2}}{(y-\alpha)^2 + \gamma^2} = \frac{\pi}{\gamma} \mathrm{Re}\,(\alpha$$
$$+ i\gamma)^{1/2} = \frac{\pi}{\Gamma} \varepsilon_0^{1/2} \mathrm{Re}\,[E - (E_r - i\Gamma)]^{1/2}. \tag{8}$$

Consequently the cross section for reaction (2) equals near the "threshold"

$$\sigma(E) \approx a\, \mathrm{Re}\,[E - (E_r - i\Gamma)]^{1/2}, \tag{9}$$

where a is some constant. The physical meaning of this result is perfectly obvious.

Were Y a stable particle (with $\Gamma = 0$) then $\sigma(E)$ would be proportional to $(E - E_r)^{1/2}$ above threshold and would be equal to zero for $E < E_r$. Because in our case the threshold is not sharp this picture is smeared out.

The function $\mathrm{Re}\,[E - (E_r - i\Gamma)]^{1/2}$ is plotted in Fig. 3. This function is equal to

$$\frac{1}{\sqrt{2}} [\sqrt{(E-E_r)^2 + \Gamma^2} + (E - E_r)]^{1/2}$$
$$= \begin{cases} (E - E_r)^{1/2} [1 + \frac{1}{4}\Gamma^2/(E - E_r)^2], & E - E_r > \Gamma \\ \Gamma / 2\sqrt{E_r - E}, & E_r - E > \Gamma. \end{cases} \tag{10}$$

By precisely the same method as above one may calculate the cross section for reaction (2) in the case when Y + b are produced in a state with $l \neq 0$. One then finds that, near the threshold,

$$\sigma_l(E) \approx a_l\, \mathrm{Re}\,[E - (E_r - i\Gamma)]^{l+1/2} + m, \tag{11}$$

where the constant term corresponds to that part of the total cross section that arises from the integration over the lower part of the spectrum ($\epsilon_{cd} < \epsilon_0$). Strictly speaking such a term should also be included in Eq. (9), however for the case $l = 0$ it is, apparently, unimportant since the first term in Eq. (11) is then sufficiently large.

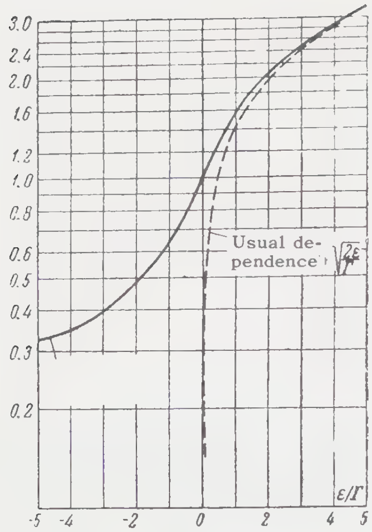

FIG. 3

3. ELASTIC SCATTERING CROSS SECTION

Let us consider now the cross section for elastic scattering X(a, a)X near the "threshold" for the production of Y. If we limit ourselves to S-states, then we have for the elastic and inelastic cross sections the formulas

$$\sigma_{el} = \pi k^{-2} |1 - S|^2, \qquad \sigma_{reac} = \pi k^{-2} (1 - |S|^2), \tag{12}$$

where k is the wave vector of the colliding particles a + X, and S is usually written as $e^{2i\delta}$ [δ is the scattering phase shift for the reaction X(a, a)X]. From here we obtain right away [see Eq. (9)]

$$|S|^2 = 1 - k^2 \sigma_{reac}/\pi = 1 - (k^2 a/\pi) \operatorname{Re} [E - (E_r - i\Gamma)]^{1/2}. \tag{13}$$

It follows from Eq. (10) that, if the width Γ of the paricle Y is small, the inelastic cross section σ(E) is small in the region near threshold and, correspondingly,

$$|S| = 1 - (k^2 a/2\pi) \operatorname{Re} [E - (E_r - i\Gamma)]^{1/2}. \tag{14}$$

Noting now the obvious equality

$$|1 + \alpha| = 1 + \operatorname{Re} \alpha,$$

valid for an arbitrary complex number α for $|\alpha| \ll 1$, and remembering that S should be an analytic function of the energy, we get

$$S = e^{2i\delta_0} [1 - (k^2 a/2\pi) (E - (E_r - i\Gamma))^{1/2}], \tag{15}$$

where δ_0 is a certain real quantity which may be considered to be constant in the vicinity of the "threshold." In the case of a stable Y (Γ = 0) this formula reduces to the usual expression for S (see Baz'[2]).

As was shown by the author,[2] formula (15) when substituted into the expression for σ_{el} (12) leads, in the case Γ = 0, to the appearance of characteristic singularities in the elastic cross section at the threshold point (peaks or cusps). The instability of Y (Γ ≠ 0) leads to a smearing out of these singularities (for a more detailed statement see below). Consequently the singularities in the elastic scattering cross section are smoothed out for sufficiently large Γ. With the exception of this circumstance the case of an unstable Y does not differ in any way from the previously discussed[2] case Γ = 0. In particular, all conclusions about the possibility of deducing important information (scattering phase shifts, etc.) from the study of the singularities in the elastic scattering cross section near the threshold point remain valid (provided, of course, that Γ is not so large as to completely "smear out" these singularities).

4. CONCLUDING REMARKS

The above-obtained formulas (9), (11) and (15) may be summarized as follows: the cross section for the reaction X(ab)Y has an energy dependence of the form $\sim (E - E_r)^{l+1/2}$ in the case of a stable Y, and of the form $\sim \operatorname{Re} [E - (E_r - i\Gamma)]^{l+1/2}$ in the case of production of an unstable particle; otherwise there is no difference between the two cases. For $E - E_r > \Gamma$ these functional dependences are practically the same (see Fig. 3). They differ from each other only in the region near E_r and below threshold.

If the production cross section of the unstable Y is known experimentally then it is easy to deduce from the form of the energy dependence the width Γ of this particle. To this end one only needs to choose the parameters E_r and Γ in Eq. (9) so as to best approximate the experimental curve.

Equation (9) may turn out to be useful in one further respect: to estimate the magnitude of the cross section for the reaction X + a → b + c + d below "threshold" when the production cross section above "threshold" is known. Indeed, above "threshold" the cross section (9) becomes $\sigma_{reac} \approx a(E - E_r)^{1/2}$ and the magnitude of the constant a may be easily determined since in this region, as a rule, the production cross section is sufficiently large. Knowing a, E_r and Γ, we obtain directly from Eqs. (9) and (10) the magnitude of the three-particle production cross section below threshold

$$\sigma_{reac} \gtrsim a\Gamma / 2(E_r - E)^{1/2}.$$

The "width" of particle Y may also be determined from the behavior of the elastic scattering cross section X(aa)X near threshold by studying the degree to which the threshold singularity is "smeared out." As an illustration of this we calculate the cross section for s-wave scattering. By substituting Eq. (15) into Eq. (12) we get

$$\sigma_{\mathrm{el}} = 4\pi k^{-2} \sin^2 \delta_0 - 2a \{\sin^2 \delta_0 \operatorname{Re} [E - (E_r - i\Gamma)]^{1/2} + \sin \delta_0 \cos \delta_0 \operatorname{Im} [E - (E_r - i\Gamma)]^{1/2}\};$$

and the energy dependence of the cross section near threshold, as determined by the second term in this formula, makes it possible to find Γ. As an example we show in Fig. 4 the form of the singularity in σ_{el} for various values of Γ.

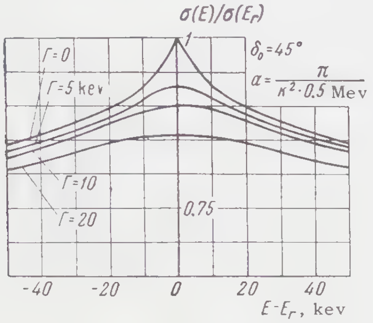

FIG. 4

We have assumed throughout that the unstable particle decays into two stable ones: Y → c + d. Using the same method as above it can be shown that Eqs. (9), (11) and (15) remain valid no matter what the mode of decay of Y (three-particle decay mode, as in the case of the neutron $n \rightarrow p + e^- + \nu$, four-particle mode, etc.).

We take this opportunity to express gratitude to Ya. A. Smorodinskii for interest in this work.

---

[1] E. P. Wigner, Phys. Rev. **73**, 1002 (1948).

[2] A. I. Baz', JETP **33**, 923 (1957), Soviet Phys. JETP **6**, 709 (1958).

[3] G. Breit, Phys. Rev. **107**, 1612 (1957).

[4] A. B. Migdal, JETP **28**, 3 (1955), Soviet Phys. JETP **1**, 2 (1955). K. Watson, Phys. Rev. **88**, 1163 (1952).

[5] L. D. Landau and E. M. Lifshitz, Quantum Mechanics, Pergamon, 1958, Sec. 119.

Translated by A. M. Bincer
256

SOVIET PHYSICS JETP VOLUME 13, NUMBER 5 NOVEMBER, 1961

ON THE SHAPE OF THE CRITICAL ISOTHERM NEAR THE CRITICAL POINT

A. V. VORONEL'

Institute of Physico-Technical and Radiotechnical Measurements

Submitted to JETP editor December 29, 1960

J. Exptl. Theoret. Phys. (U.S.S.R.) **40**, 1516-1518 (May, 1961)

The quantity $B \equiv (\partial^3 p/\partial V^3)_{T_c}$, which characterizes the shape of the critical isotherm near the critical point that terminates the liquid-vapor equilibrium, is calculated for five simple substances and for water. The agreement of the results obtained by four different methods enables us to assert that $B < 0$ for simple liquids and that this quantity can be reliably estimated. It is shown that rough approximate values of B for simple substances can be obtained from known values of the critical parameters p_c and V_c.

THE character of the singularity which occurs in the thermodynamic quantities at the critical point at the end of the curve of phase equilibrium between liquid and vapor for a pure substance has not been elucidated up to the present. If we assume that the thermodynamic quantities at the critical point can be expanded in power series in the small deviation of the density, then we can write for this point the following conditions (cf. reference 1):

$$(\partial p / \partial V)_{T_c} = 0, \tag{1}$$

$$(\partial^2 p / \partial V^2)_{T_c} = 0, \tag{2}$$

$$(\partial^3 p / \partial V^3)_{T_c} < 0. \tag{3}$$

The condition (3) requires experimental verification.[1] The quantity $(\partial^3 p/\partial V^3)_{T_c}$ (which we denote by B for brevity), if it is not zero, determines the shape of the critical isotherm, which is a third-degree parabola in the neighborhood of the critical point if the condition (3) is satisfied.

In the present work our purpose has been to get estimates of the values of B for various substances by different methods. It must be agreed that the least reliable method for obtaining this quantity is direct repeated differentiation of the p-V-T data obtained experimentally. By this method one can at best get the order of magnitude of the quantity desired. Values obtained by this method for several simple substances are given in the second column of the table under the heading p-V-T. For comparison with these values, values for water are included in the table which differ from these values by more than an order of magnitude.

In a paper by Habgood and Schneider[1] graphical differentiation gave for xenon $B = 0$, but a detailed analysis shows that the error in this estimate is not less than 1×10^{-5} atm-mole^3/cm^9.

Values of $(\partial^3 p/\partial V^3)_{T_c}$, atm-mole^3/cm^9

Substance	$p-V-T$	ΔC_v	g	l. c. s.
Xe	0—1	3.5	4	
CO_2	1—6	12	11	10
C_2H_4	3—5	—	3,5	2.5
C_2H_6	—	—	2,3	2
SF_6	0.2—0.5	—	0,7	0.5
H_2O	50—150	140	—	130
N_2	—	—	—	5.5
Ar	—	—	—	13
H_2	—	—	—	5.4
CH_4	—	—	—	5.7

The quantity B can be found more accurately from the data on the specific heat at constant volume near the critical point, as is shown in a paper by the writer.[3]

The third column of the table, headed ΔC_V, gives the results of calculations from the experimental data of references 3 — 9. The possible error of the values in this column is about 50 percent, and is due both to the error in the determination of the discontinuity of the specific heat from the experimental data and to that in the determination (from p-V-T data) of the coefficient $(\partial^2 E/\partial V^2)_{T_c}$, which appears in the formula for calculating B.

Evidently the greatest accuracy for the quantity B can be obtained from measurements of the hydrostatic effect, by a method previously described by the writer.[10] Values so obtained are given in the fourth column of the table under the arbitrary heading g. Experimental data from references 11 — 13 have been used here.

We note that the critical isotherm is precisely the sort of thing that obeys the law of corresponding states, and consequently in reduced coordinates the data for the various substances fit on a single curve. This means that for this class of substances the third derivative in the reduced coordinates will have the same value, i.e.,

$$\frac{V_c^3}{p_c}\left(\frac{\partial^3 p}{\partial V^3}\right)_{T_c} = \alpha, \qquad (4)$$

where α is a constant which does not depend on the substance. Now if we know the third derivative for one substance, we can find its value for all others.

Of course the accuracy of this method is not high, since the substances obey the law of corresponding states only to a very rough approximation. It seems very natural, however, that the values of B, if they are not zero, will be of the order of the combination of the critical parameters that has the same dimensions, p_c/V_c^3.

Taking the data for Xe as the most reliable, we get for this substance $\alpha = 1.2$. The van der Waals equation gives $\alpha = 9$. The difference between these numbers characterizes the degree of applicability of the van der Waals equation at the critical point.

The values of B calculated for the various substances by using Eq. (4) are given in the fifth column of the table, under the heading l.c.s. (law of corresponding states). Evidently the accuracy of these data is of the same order as the accuracy of the data in the second column.

An examination of the table shows that the condition (3) is satisfied for a broad class of substances. In all cases considered the third derivative of the critical isotherm at the critical point is different from zero. Moreover, the rather good agreement of the values obtained by the various methods, and the roughly equal orders of magnitude for the various substances, show that the numerical values of B have evidently been correctly determined.

Thus the equation of the critical isotherm near the critical point can be written in the form $p - p_c = (B/6)(V - V_c)^3$, and the table given here provides a qualitative characterization of the differences of shape of the critical isotherm for the different substances. The numerical values of B determine the radii of curvature of the curve near the critical point.

By means of the relation (4) we can calculate the required quantity and reconstruct the curve for many simple substances.

We can evidently assert that the singularity of the thermodynamic potential at the critical point is such that it does not affect the first four terms of the expansion in powers of the departure of the density from its critical value.

In conclusion the writer thanks M. Sh. Giterman for a discussion of the results of this work.

---

[1] L. D. Landau and E. M. Lifshitz, Статистическая физика (Statistical Physics), Gostekhizdat, 1951.

[2] H. W. Habgood and W. G. Schneider, Canad. J. Chem. **32**, 98 (1954).

[3] A. V. Voronel', J. Phys. Chem. (U.S.S.R.) **33**, 958 (1961).

[4] A. Michels and J. Strijland, Physica **18**, 613 (1952).

[5] Michels, Bijl, and Michels, Proc. Roy. Soc. **A160**, 376 (1937).

[6] H. W. Habgood and W. G. Schneider, Canad. J. Chem. **32**, 164 (1954).

[7] Kh. I. Amirkhanov and A. M. Kerimov, Doklady Akad. Nauk SSSR **113**, 368 (1957).

[8] Kh. I. Amirkhanov and A. M. Kerimov, Теплоэнергетика (Heat Power Engineering) **9**, 68 (1957).

[9] N. B. Vargaftik, Теплофизические свойства вещества (справочник) [The Thermophysical Properties of Matter (Handbook)], State Power Press, 1956.

[10] A. V. Voronel' and M. Sh. Giterman, JETP **39**, 1162 (1960), Soviet Phys. JETP **12**, 809 (1961).

[11] M. A. Weinberger and W. G. Schneider, Canad. J. Chem. **30**, 422 (1952).

[12] S. G. Whiteway and S. G. Mason, Canad. J. Chem. **31**, 569 (1953).

[13] H. L. Lorentzen, Acta Chem. Scand. **7**, 1335 (1953).

Translated by W. H. Furry
257

SOVIET PHYSICS JETP VOLUME 13, NUMBER 5 NOVEMBER, 1961

Letters to the Editor

POSSIBLE OBSERVATION OF He^8 *NUCLEI*

O. V. LOZHKIN and A. A. RIMSKII-KORSAKOV

Radium Institute, Academy of Sciences, U.S.S.R.

Submitted to JETP editor January 24, 1961

J. Exptl. Theoret. Phys. (U.S.S.R.) 40, 1519-1520 (May, 1961)

An investigation of the stability (relative to neutron emission) of the isotopes of light nuclei with an excess of neutrons has led Zel'dovich[1] to infer a large probability for the existence of the He^8 nucleus. The expected binding energy of the neutron is about 1 Mev, and the beta-decay energy is approximately 12 Mev. The transition to the 3.2-Mev level in Li^8 would have a half-life on the order of 0.01 sec.[2,3]

If the He^8 nucleus really exists, it seems possible to observe its formation in the process of fragmentation of heavy nuclei under the action of high-energy particles, leading to the emission of fragments with a wide spectrum of charges and masses. The nuclear emulsion technique permits observation of the He^8 track, for owing to its relatively long lifetime the nucleus will not undergo decay before being stopped in the emulsion (the slowing-down time is about 10^{-11} sec); in a certain number of cases a distinctive (T-shaped) track similar to the tracks of Li^8 and B^8 nuclei will be formed if the beta decay proceeds to the ground state of $Li^8(2^+)$. This is to be expected on the basis of the following chain of transitions for the He^8 nucleus:

$$He^8(0^+)\xrightarrow{\beta}Li^8(2^+)\xrightarrow[0.8\ \mathrm{sec}]{\beta}Be^{*8}\xrightarrow[10^{-21}\ \mathrm{sec}]{}2He^4_2.$$

A difference between the tracks of He^8 and Li^8 nuclei will result from the difference in ionization characteristics of these two nuclei.

Another, considerably more probable decay mode for He^8 is in competition with decay by this chain. Not yielding a T-shaped track and therefore indistinguishable from the case of alpha-particle emission, this decay goes not to the ground state but to an excited state of Li^8:

$$He^8(0^+)\xrightarrow{\beta}Li^{8*}(1^+)\rightarrow Li^7+n.$$

A very approximate estimate showed that such a decay mode is 2 — 3 orders more probable. It is impossible, however, to observe the presence of hundreds or even thousands of He^8 tracks which do not give rise to the T-shaped track in the presence of the very large number of alpha particles and protons formed in these breakups.

Below are described two cases of observation of "strange" T-shaped tracks in an emulsion irradiated by high energy (930 Mev and 9 Bev) protons.

The first track was discovered accidentally when investigating fragmentation at 930 Mev, the second after examining around 170 T-shaped tracks of particles produced by 9-Bev protons. Both tracks were strange in that the density of developed grains per unit path length was uncharacteristically low for Li^8 nuclear tracks.

Owing to the short range of the particles under investigation (23μ and 37μ in first and second cases respectively), it is impossible to determine their charge by one of the well-known methods. We can only compare the ionization characteristics of the given particles with those of He^4 and Li^8 nuclei. The measured density of developed grains in the tracks of the given particles was approximately 25% lower than the density of Li^8 tracks, and was even lower than the average grain density in He^4 tracks (by about 10%). Supposing the given particles to be Li^8 nuclei, such an unusually low density of developed grains forces us to question their nature. If the particles in question actually decay at the stopping point into two alpha particles, which is consistent with their ranges (the total lengths of the alpha-particle tracks are 7.5 and 9.7μ), and at the same time have an ionizing power lower than that of the Li^8 nucleus, we may assume that in these cases we are dealing with He^8 nuclei.

The fact that the density of developed grains in these tracks is even somewhat lower than in alpha-particle tracks is further evidence that the given tracks may be He^8 tracks. Actually, with low residual ranges ($\lesssim 20\mu$), He^8 ions may be expected to possess lower ionizing power than He^4 ions, since at low ion velocities (close to and lower than the velocity of the orbital electrons of the slowing-down material) the specific energy losses of the particles become proportional to the square of particle velocity.[4] Consequently, if the residual ranges of He^8 and He^4 ions are equal, the specific energy losses are lower for the heavier ions.

An examination of various factors which could cause such an interpretation to be rejected (accidental superposition of tracks, reduced sensitivity of emulsion, or local inhomogeneity in development of the investigated tracks) indicates that their probability is low, although it is impossible to exclude the possibility of some such accident completely. Therefore at the present time we can only speak of the possible observation of He^8 nuclei.

If such nuclei are actually formed in the process of fragmentation, further confirmation of their existence can be obtained through investigation of the T-shaped tracks in an emulsion sensitive to particles with minimal ionization, by successfully establishing the emission of two decay electrons at the stopping point.

We take the occasion to express our gratitude to Professor N. A. Perfilov for discussion of the results.

---

[1] Ya. B. Zel'dovich, JETP **38**, 1123 (1960), Soviet Phys. JETP **11**, 812 (1960).

[2] V. I. Gol'danskii, JETP **38**, 1637 (1960), Soviet Phys. JETP **11**, 1179 (1960).

[3] Baz', Gol'danskii, and Zel'dovich, Usp. Fiz. Nauk **72**, 211 (1960), Soviet Phys.-Uspekhi **3**, 729 (1961).

[4] E. Fermi and E. Teller, Phys. Rev. **72**, 399 (1947).

Translated by Mrs. J. D. Ullman
258

A NOTE CONCERNING π-Λ RESONANCE

A. L. LYUBIMOV

Joint Institute for Nuclear Research

Submitted to JETP editor February 7, 1961

J. Exptl. Theoret. Phys. (U.S.S.R.) **40**, 1520-1522 (May, 1961)

It is well known that a connection exists between the possible resonances of the pion-hyperon system and the scattering amplitude. In particular, in the phenomenological analysis of the data on the K^--proton interaction[1] one finds that if one assumes that only the S state is involved and that the real part of the K^--p scattering amplitude is negative, there exists in the nonphysical region a singularity that corresponds to a pion-hyperon resonance.

In the recently published papers by Tuan[2] and by Ross and Shaw[3] the experimentally observed Λ-π resonance was identified with the above resonance. However, the investigations of the interference between Coulomb and nuclear scattering seem to indicate that this interference is constructive.[5] But in that case there should be no resonances in the pion-hyperon system which would correspond to a K^--p interaction in an S state.* Since the K^- meson is supposedly a pseudoscalar particle[6] the orbital angular momenta on both sides of the reaction

$$K^- + p \rightarrow \Lambda + \pi^0 \tag{1}$$

have to be the same.

From this it follows that the observed Λ-π resonance should not be related to an S state. Since the momentum of the particles in the center-of-mass system at resonance is ~ 200 Mev/c, it is natural to assume that it cannot be due to D waves. This way it follows that if the foregoing propositions are true then the observed π-Λ resonance has to be in a P state.†

This conclusion is supported by the circumstance that in the K^--p reaction the yield of Λ hyperons is small compared to that of Σ hyperons for K^- capture at rest, while it increases rapidly at momenta of 300 to 400 Mev/c where P waves become important.‡

A strong resonance of the π-Λ system in a P state indicates an analogy with the $(\frac{3}{2}, \frac{3}{2})$ resonance of the π-N system.

At present there exist published data on the different channels of the K^--p reaction for capture at rest and for the momenta 300, 400 and 1150 Mev/c. The ratio of the Λ to Σ yields at 1150 Mev/c is still larger than at 300 and 400 Mev/c. This can be an indication of either a continuous increase of the yield ratio in the considered energy interval** or of the chance that there is some resonance of the Λ-π system close to 1150 Mev/c. In this connection one can remark that if one would want to extend the analogy between the π-Λ and π-N systems and expect a second π-Λ resonance corresponding to the second $I = \frac{3}{2}$ resonance of the π-N system as well as that c.m.s. momenta are close (which they are for the first resonance), then the second resonance of reaction (1) should lie close to a K^- momentum of 1.1 Bev/c in the laboratory system.

At present there do not exist direct experimental data on the cross section of reaction (1) at 1150 Mev/c. The existing data at this energy for the different hyperon production channels[7,4] are insufficient to perform the necessary analysis in isospin states. However, approximate calculations performed on their basis show that the cross section of reaction (1) at 1150 Mev/c seems to be larger than that of any reaction leading to the production of a Σ hyperon and a π meson.

The author expresses his gratitude to B. N. Valuev, V. I. Ogievetskii and L. B. Okun' for discussions.

---

*We consider here resonances connected with noticeable cross sections, of which the Λ-π resonance is one.

†Evidently, if the K meson were even the resonance would be in an S state.

‡The decay $Y^* \to \Sigma + \pi$ also has to take place. It is however considerably rarer than the $Y^* \to \Lambda + \pi$ decay, firstly, because of the smaller phase space (roughly by a factor 3) and, secondly, because it is not a pure isospin $I = 1$ state. In this connection we remark that $\Sigma\pi$ resonances can exist with $I = 0$ and 2.

**We note that qualitatively such a behavior of the Λ to Σ yield ratio could be expected if the Sakata model were valid: Σ hyperons, being composite particles, should dissociate at high energies to form Λ-hyperons.

---

[1] R. H. Dalitz and S. F. Tuan, Ann. of Phys. **8**, 100 (1959); **10**, 307 (1960).

[2] S. F. Tuan, Nuovo cimento **18**, 1301 (1960).

[3] M. Ross and G. Shaw, Phys. Rev. Letters **5**, 578 (1960).

[4] Alston, Alvarez, Eberhard, Good, Graziano, Ticho, and Wojcicki, Proc. 1960. Annual Int. Conf. High Energy Physics Univ. Rochester (1960), p. 445.

[5] Melkanoff, Prowse, and Stork, Phys. Rev. Letters **4**, 183 (1960).

[6] The Helium Bubble Chamber Collaboration Group, Presented by G. Puppi, Proc. 1960 Annual Int. Conf. High Energy Physics, Univ. Rochester (1960), p. 419.

[7] L. Alvarez, Proc. Int. Conf. High Energy Physics, Kiev (1959).

Translated by M. Danos
259

MAGNETIC PROPERTIES OF POLYCRYSTALLINE ALLOY OF Cu *WITH 22.8 ATOMIC PERCENT* Mn

I. G. FAKIDOV and B. V. ZNAMENSKII

Institute of Metal Physics, Academy of Sciences, U.S.S.R.; Sverdlovsk State Pedagogical Institute

Submitted to JETP editor February 24, 1961

J. Exptl. Theoret. Phys. (U.S.S.R.) **40**, 1522-1523 (May, 1961)

THE magnetic properties of solid solutions of copper and manganese have been studied in a number of investigations.[1-6] Scheil and Wachtel[6] showed that among all the alloys of the copper-manganese system, the alloy with 22.5 atomic percent manganese content has the largest magnetic susceptibility, being antiferromagnetic in the disordered state and ferromagnetic in the ordered.

Because we considered these peculiarities of the magnetic properties of this alloy very significant, we decided to carry out a somewhat more detailed study of its physical properties in the disordered state. For this purpose an alloy containing, according to the results of a chemical analysis, 22.8 atomic % manganese was prepared by high-frequency melting in vacuum. The necessary specimens were cut from the ingot thus obtained and were subjected to a prolonged anneal and to subsequent quenching.

The results of measurement showed that the magnetic susceptibility of the alloy is independent of the field at magnetic fields up to 3000 oe and goes through a maximum at temperature 94° K; furthermore, in the range of fields mentioned the magneto-caloric effect has the negative sign. From this we concluded that the alloy Cu + 22.8 atomic % Mn is antiferromagnetic, with a Néel point near 94° K. However, this antiferromagnet, at temperatures below T_N and at external magnetic fields exceeding a certain critical or threshold value H_t, exhibits properties characteristic of ferromagnets: measurements of the magnetocaloric effect, which is positive, reveal the presence of spontaneous magnetization; and in fields above 10 000 oe the magnetization approaches saturation.

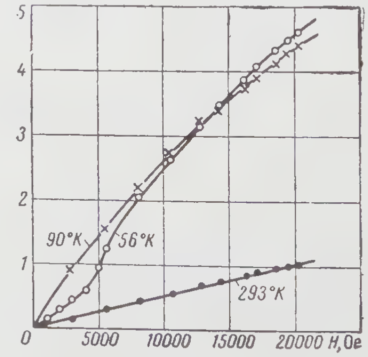

FIG. 1

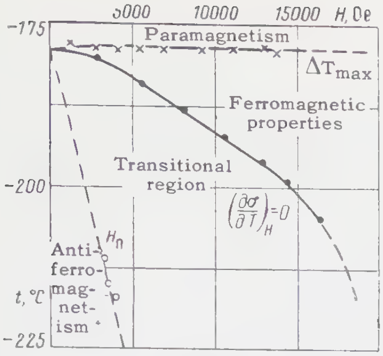

FIG. 2

The magnitude of the threshold field changes with change of temperature and, for example, is equal to 4000 oe at 56° K. Above 94° K, the alloy studied is paramagnetic and obeys the Curie-Weiss law at all values of the external magnetic field.

Figure 1 shows magnetization curves taken at temperatures below, near, and above the magnetic transformation point. Figure 2 gives, by way of graphic representation, an approximate diagram of the magnetic states of the alloy as they depend on the temperature and on the intensity of the external magnetic field. T_{max} corresponds to the temperature at which, in the given magnetic field, the magnetocaloric effect reaches a maximum.

It should be mentioned that the alloy we studied is similar in its magnetic properties to the intermetallic compound $MnAu_2$. It would be very valuable to study the magnetic structure of this alloy by neutron diffraction and to compare it with the magnetic structure of $MnAu_2$, which consists of a complicated spiral distribution of magnetic moments.[6]

The authors are very grateful to V. N. Novogrudskii and É. A. Zavadskii for their share in the discussion of the results of the measurements, and also to L. V. Smirnov, who prepared the alloy.

---

[1] L. Néel, J. phys. radium **3**, 160 (1932).

[2] S. Valentiner and G. Becker, Z. Physik **80**, 735 (1933).

[3] Otter, Flanders, and Klokholm, Phys. Rev. **99**, 599 (1955).

[4] H. P. Myers, Can. J. Phys. **34**, 527 (1956).

[5] Owen, Browne, Arp, and Kip, J. Phys. Chem. Solids **2**, 85 (1957).

[6] E. Scheil and E. Wachtel, Z. Metallk. **48**, 571 (1957).

[7] A. J. P. Meyer and P. Taglang, J. phys. radium **17**, 457 (1956).

[8] L. Néel, Compt. rend. **242**, 1549 (1956).

[9] Herpin, Mériel, and Villain, Compt. rend. **249**, 1334 (1959).

Translated by W. F. Brown, Jr.
260

A SEARCH FOR NEAR-THRESHOLD ANOMALIES IN THE ENERGY DEPENDENCE OF THE TOTAL CROSS SECTION FOR INTERACTION OF PROTONS

I. M. VASILEVSKII, Yu. D. PROKOSHKIN, and V. I. RYKALIN

Joint Institute for Nuclear Research

Submitted to JETP editor February 27, 1961

J. Exptl. Theoret. Phys. (U.S.S.R.) **40**, 1524-1525 (May, 1961)

As has been shown by Wigner and by Baz',[1] the energy dependence of the cross section for the elastic scattering of two particles can have an anomalous character near the threshold for the production of a new particle. The shape of such an anomaly is a narrow "peak" or "step"; the anomaly is associated with a sharp change of the derivative of the cross section at threshold point. Near-threshold anomalies can also occur in the energy dependence of the total cross section for the interaction of two particles (for more details see the review article by Fonda[2]).

We have made a search for these anomalies in the neighborhood of the thresholds for the production of π-meson pairs in proton collisions (580 — 600 Mev). Studies of the energy dependence of the total cross section σ for the interaction of protons were also made in regions above and below the thresholds. Observations of anomalies in such cases could be an indication of the existence of new particles[3] and could make it possible to determine their masses.

A differential ionization chamber was used for the registration of the protons. This made it possible to achieve an accuracy in determining the relative shape of the energy dependence of the cross section which is an order of magnitude better than the accuracy characteristic of earlier experiments,[4] in which particle counters were used to measure σ.

The proton beam brought out from the chamber of the six-meter synchrocyclotron of the Joint In-

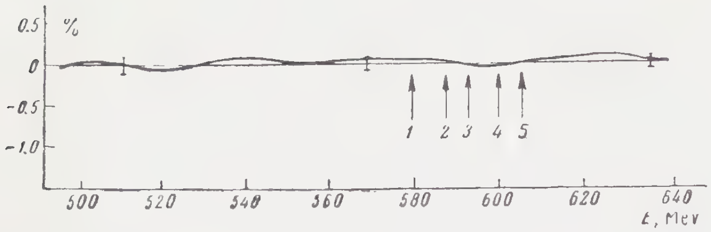

Dependence of the quantity $[\sigma(E)-\overline{\sigma}(E)]/\overline{\sigma}(E)$ on the proton energy E. The thresholds of the reactions $pp \to pp\pi^0\pi^0$(1), $pp \to d\pi^0\pi^+$(2), $pp \to pn\pi^0\pi^+$(3), $pp \to pp\pi^+\pi^-$(4), and $pp \to nn\pi^+\pi^+$(5) are indicated by arrows.

stitute for Nuclear Research was shaped by a system of collimators, and then was sent through three identical thin-walled ionization chambers. The first chamber served as a monitor. The second and third chambers, with the polyethylene target placed between them, formed the differential ionization chamber. The current i_2 from this differential chamber was proportional to the amount of weakening of the beam in passing through the target, i.e., to the product of the total cross section and the beam intensity J. The current i_2 was amplified and recorded on the chart of a recording potentiometer.

As the thickness of the filter by which the proton beam was slowed down was smoothly increased, a curve was traced on the chart of the potentiometer; this curve shows the variation of the quantity $i_2 \sim \sigma J$ as the proton energy E is decreased. Simultaneously another potentiometer registered the change of the current $i_1 \sim J$ from the monitoring chamber. The desired quantity $\sigma(E)$ was obtained by dividing i_2 by i_1. This operation was performed by a continuously acting electronic device, whose output, proportional to i_2/i_1, was recorded on the chart of a third potentiometer. The measurements were repeated many times to eliminate the effects of small fluctuations in the current from the differential chamber.

The energy of the beam was determined to an accuracy better than 1 Mev (cf. reference 5). The energy resolution was ±5 Mev and was due to the dispersion of the beam (±3 Mev)[5] and energy losses in the target (±4 Mev).

The results of the measurements are shown in the diagram. It shows the fractional deviation of the measured cross section $\sigma(E)$ from the smoothed energy dependence $\overline{\sigma}(E)$ found by averaging over a broad range of energies; in the region in question this smoothed dependence is linear.[4] As can be seen from the diagram, in the entire range studied, 490 — 640 Mev, there are no anomalies in the energy dependence of the total cross section for pp interaction that exceed the errors of measurement (0.1 percent).

It follows from this that there is little probability that a bound state "π meson + nucleon" with binding energy close to zero exists.

At the same time control experiments were made with a graphite target. The energy dependence of the total cross section for carbon should not contain any appreciable anomalies, owing to the motions of the nucleons in the carbon nucleus. In agreement with this, the measurements showed that for carbon the deviation of $\sigma(E)$ from $\overline{\sigma}(E)$ does not exceed 0.05 percent.

In conclusion we take the occasion to thank A. I. Baz', L. I. Lapidus, and B. Pontecorvo for a discussion of this work.

---

[1] E. Wigner, Phys. Rev. **73**, 1002 (1948). A. I. Baz', JETP **33**, 923 (1957), Soviet Phys. JETP **6**, 709 (1958).

[2] L. Fonda, Inelastic Collisions and Threshold Effects, Preprint, 1960.

[3] Zinov, Konin, Korenchenko, and Pontecorvo, JETP **36**, 1948 (1959), Soviet Phys. JETP **9**, 1386 (1959). V. I. Gol'danskii and Ya. A. Smorodinskii, JETP **36**, 1950 (1959), Soviet Phys. JETP **9**, 1387 (1959).

[4] Dzhelepov, Moskalev, and Medved', Doklady Akad. Nauk SSSR **104**, 380 (1955). Chen, Leavitt, and Shapiro, Phys. Rev. **103**, 211 (1956).

[5] I. M. Vasilevskii and Yu. D. Prokoshkin, Атомная энергия (Atomic Energy) **7**, 225 (1959).

Translated by W. H. Furry
261

EFFECT OF TEMPERATURE ON HYPERFINE STRUCTURE OF GAMMA RADIATION

V. S. SHPINEL', V. A. BRYUKHANOV, and N. N. DELYAGIN

Institute for Nuclear Physics, Moscow State University

Submitted to JETP editor, March 9, 1961

J. Exptl. Theoret. Phys. (U.S.S.R.) **40**, 1525-1527 (May, 1961)

In investigating the resonance absorption of γ quanta with energy 23.8 kev by Sn^{119} nuclei, it was found[1] that in a white tin crystal (β-Sn) at liquid nitrogen temperature the lines of radiation (or absorption) are split into two components. The existence of such a splitting was later confirmed by other measurements[2] in which we used as the source of γ quanta Sn^{119m} which was contained as a constituent of a polycrystal of β-Sn (at liquid nitrogen temperature), while the absorbers were various compounds containing tin. The observed splitting was interpreted as a hyperfine structure of the γ ray caused by an interaction of the quadrupole moment of the Sn^{119} nucleus in the excited state with the inhomogeneous electric field in the β-Sn crystal.

In the present work we have investigated the effect of temperature of the β-Sn crystal on the magnitude of the quadrupole interaction. When the temperature of the crystal is changed, there is a change in the amplitude of the thermal vibrations of the atoms and a change in the interatomic distances; consequently, one may expect a change in the gradient of the electric field at the Sn^{119} nucleus. As a source of γ quanta, we used Sn^{119m} contained in a polycrystal of SnO_2. It was shown earlier[2] that for SnO_2 there is no splitting of the radiated line, and the radiation of γ quanta without energy loss to recoil occurs with high probability even at room temperature. The source thickness was 6 mg/cm^2. By measurements with SnO_2 absorbers of various thicknesses it was shown that in such a source the effect of broadening of the radiated line because of self-absorption is negligible. For example, with a SnO_2 absorber of thickness 4 mg/cm^2 the line width in the absorption spectrum was 6×10^{-8} ev, which is close to twice the natural width of the 23.8 kev excited state of Sn^{119}.

The measurements of the spectrum of the resonance radiation were carried out in an apparatus which was described briefly earlier.[1] In all the measurements the source (SnO_2) was at room temperature, while the absorbers (natural β-Sn) were at liquid-nitrogen temperature, dry-ice temperature, and room temperature. We used absorbers of various thicknesses in the range from 5 to 50 mg/cm^2, prepared either from rolled tin foil, or by sputtering of metallic tin in vacuum onto an organic backing. Typical resonance absorption spectra are shown in the figure (along the abscissa, we give the quantity $\Delta E = Ev/c$, where $E = 23.8$ kev, v is the velocity of the source with respect to the absorber; along the ordinates, we give the intensity of γ radiation passing through the absorber, proportional to the total number of recorded pulses N). In the upper part of the figure is shown the absorption spectrum for an absorber of β-Sn, 5 mg/cm^2 thick, at liquid nitrogen temperature. One sees two absorption maxima corresponding to the quadrupole splitting of the absorption line. The separation of the maxima is $(1.10 \pm 0.15) \times 10^{-7}$ ev, which agrees with the value obtained by us earlier.[1,2] The middle part of the figure shows the absorption spectrum for a β-Sn absorber 12 mg/cm^2 thick at dry-ice temperature, and the lower part of the figure for an absorber 30 mg/cm^2 thick at room temperature. For such absorber thicknesses and temperatures there is no essential broadening of the absorption line because of absorber thickness. Control measurements with an absorber of $SnNb_3$ (there is no quadrupole interaction[1] in the $SnNb_3$ crystal) showed that in the absence of splitting the line width in the absorption spectrum corresponds to the natural width of the excited state. The lines in the absorption spectrum shown in the figure have considerably greater width (1.4×10^{-7} ev for dry-ice temperature and 1.05×10^{-7} ev for room temperature). In the two last spectra the hyperfine structure components are no longer resolved, but the observed line widths and their dependence on temperature shows the presence of quadrupole splitting in these cases also. For the magnitude of the quadrupole splitting at temperatures 195 and 293° K we obtain the values $(8.0 \pm 1.5) \times 10^{-8}$ and $(4.6 \pm 1.4) \times 10^{-8}$ ev, respectively. Thus we observe a decrease in the magnitude of the quadrupole interaction as the temperature of the crystal increases. This dependence is a consequence of the temperature variation of the average of the components of the tensor of the electric field gradient along the prin-

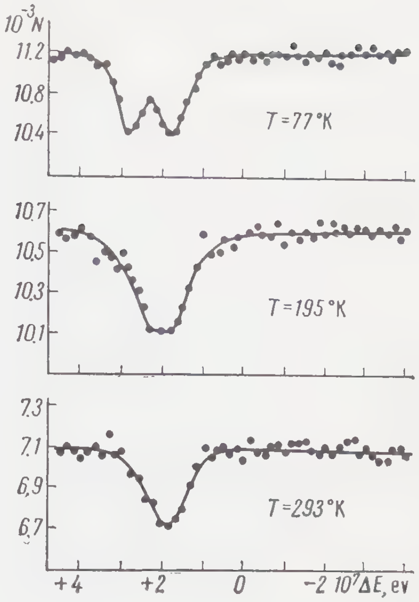

cipal axis $\langle q \rangle = \langle \partial^2 V/\partial z^2 \rangle$, and the angular orientation of this tensor with respect to its static direction. In addition, with temperature there may be some change also in the asymmetry parameter $\eta = |(q_{xx} - q_{yy})/q_{zz}|$. The calculations of Kushida et al.[3] lead to the following dependence of the value of the splitting on the temperature: $\Delta = a(1 + bT + c/T)$. The constants a, b, and c are functions of volume and can be obtained from measurements of the dependence of Δ on pressure for different temperatures. A comparison of the experimental data with theoretical computation should enable one to determine the quadrupole moment of the Sn^{119} nucleus in the excited state.

The dependence found in the present work for the quadrupole splitting as a function of temperature explains the result of Boyle, Bunbury, and Edwards[4] who observed no splitting of the absorption line in the β-Sn crystal. In their work the absorber was at room temperature, in which case the quadrupole splitting does not exceed in magnitude the width of the line in the absorption spectrum even for a thin source. But the width of their source was such that as a result of self-absorption the line width of the radiated line was increased by a factor of two compared to the natural width. Under such conditions of the experiment, the quadrupole splitting could not be observed. (In the work of Picou et al.[5] the quadrupole splitting was also not observed at liquid nitrogen temperature, which is possibly explained by the use in their work of extremely thick source and absorber.)

As we see from the figure, the influence of the temperature shows itself not only in the magnitude of the quadrupole splitting, but also in the location of the centers of the absorption curves in the spectra. The observed line shift with changing temperature exceeds by several factors the value of the so-called "temperature shift"[6] and contradicts the data of the work of Boyle et al.,[7] who found good agreement with the theory. The reason for this discrepancy is difficult to analyze, since these authors do not give all the necessary data; it is possible that in their work there was an influence on the measured effect of the change in line shape with change in temperature, which was not taken into account. One may assume that the change in internal field in the β-Sn crystal with changing temperature not only leads to a change in the value of the quadrupole interaction, but also changes the energy of the γ transition as a whole, which has an effect on the observed shifts in the absorption line.

[1] N. N. Delyagin et al., JETP **39**, 220 (1960), Soviet Phys. JETP **12**, 159 (1961).

[2] V. A. Bryukhanov et al., JETP **40**, 713 (1961), Soviet Phys. JETP **13**, 499 (1961).

[3] Kushida, Benedek, and Bloembergen, Phys. Rev. **104**, 1364 (1956).

[4] Boyle, Bunbury, and Edwards, Preprint, (1960).

[5] J. L. Picou et al., Preprint, (1960). Cf. also E. Cotton, J. Phys. Radium, Paris, **21**, 265 (1960).

[6] R. V. Pound and G. A. Rebka, Phys. Rev. Letters **4**, 274 (1960).

[7] A. J. F. Boyle et al., Proc. Phys. Soc. (London) **76**, 165 (1960).

Translated by M. Hamermesh
262

RATIO OF πN → ππN *REACTION CROSS SECTIONS OF 290 Mev AND* π-π *INTERACTION*

Yu. A. BATUSOV, S. A. BUNYATOV, V. M. SIDOROV, and V. A. YARBA

Joint Institute for Nuclear Research

Submitted to JETP editor March 16, 1961

J. Exptl. Theoret. Phys. (U.S.S.R.) **40**, 1528-1530 (May, 1961)

THE process of the production of the second meson in the reaction πN → ππN at different energies has recently been widely used to obtain information on the π-π interaction. In the collision of a π meson and a proton above the threshold for the production of the second meson (~170 Mev) the following processes are possible:

$$(1)\ \pi^- + p \rightarrow n + \pi^+ + \pi^-, \quad (2)\ \pi^- + p \rightarrow p + \pi^0 + \pi^-,$$
$$(3)\ \pi^- + p \rightarrow n + \pi^0 + \pi^0, \quad (4)\ \pi^+ + p \rightarrow n + \pi^+ + \pi^+,$$
$$(5)\ \pi^+ + p \rightarrow p + \pi^+ + \pi^0.$$

In order to explain certain qualitative features of the π-π interaction, it is of interest to establish relations between the cross sections of the above processes. Of these reactions, (1) and (2) have been investigated in detail at an energy of the primary meson of the order of 1 Bev.[1-3] At lower energies only reaction (1) has been studied in detail.[4-6] The cross section for it at 290 Mev was found to be $\sigma_1 = 0.61 \pm 0.13$ mb.[5] The cross section of reaction (2) has not been measured directly.

Zinov and Korenchenko[7] have measured the combined cross section $2\sigma_1 + 0.7\sigma_2$. Combined with the data of Perkins et al.,[4] who have determined σ_1, one can obtain at 317 Mev the estimate $\sigma_2 = 0.2 \pm 1.2$ mb. At 220 Mev there have been observed[8] three events corresponding to reaction (1) and no event of reaction (2) was found. In the present paper we shall estimate the ratio of the cross sections of reactions (2) and (1) at a meson energy of 290 ± 15 Mev.

A search for the reactions (1) and (2) was undertaken in emulsions irradiated in the Synchrocyclotron Laboratory of the Joint Institute for Nuclear Research. The emulsions were area scanned for stopping of secondary π^- mesons. The tracks then were followed back to the point of production. The events where the production took place on hydrogen were decided by the criteria described in reference 5. A total of 1058 stars associated with π^- mesons were found. Amongst them 12 events of reaction (1) and 5 events of reaction (2) were found. Taking into account geometric corrections concerning the probability of registration of π mesons by the emulsion chamber we obtain for the ratio of the cross sections of reaction (2) to (1) the value $\sigma_2/\sigma_1 = 0.3 \pm 0.2$.* With $\sigma_1 = 0.61 \pm 0.13$ mb this gives for reaction (2) at 290 ± 15 Mev a cross section $\sigma_2 = 0.2 \pm 0.1$ mb (see the footnote, however.) If one extrapolates the results of the calculations Goebel and Schnitzer[9] for the statistical model including π-π interaction to 290 Mev one obtains for this ratio the value $\sigma_2/\sigma_1 \approx 0.2$.

At present there do not exist equivalent data for the reaction (3) in the energy region around 300 Mev. The combined cross section for reactions (4) and (5) at 290 Mev is estimated[10] to be ~ 0.1 mb. This way, according to the available experimental information, the largest of the measured cross sections is that for reaction (1), while those for reactions (2), (4) and (5) are small compared to σ_1.

Utilizing charge independence one can obtain relations between the cross sections for reactions (1) — (5) if one assumes that the π mesons interact only in one of the possible isospin states which have $T_\pi = 2, 1, 0$. If they interact only in the state with $T_\pi = 2$ then reaction (4) will have the largest cross section while the cross sections of reactions (1), (2), (3) and (5) will be $1/18$, $1/4$, $1/9$ and $1/4$ of σ_4 respectively. As remarked above, in reality σ_1 has the largest value and the other cross sections, including σ_4 are small compared to σ_1. If $T_\pi = 1$ then $\sigma_3 = \sigma_4 = 0$ while σ_2 and σ_5 cannot both be small compared to σ_1. However, the obtained results and the results of reference 10 indicate that both σ_2 and σ_5 are small compared to σ_1.

Finally, we assume that the π mesons interact only in the state with $T_\pi = 0$ (indeed, such an assumption has been made by Korenchenko[7]). Then from charge independence immediately follows that $\sigma_3 = \sigma_1/2$, $\sigma_2 = \sigma_4 = \sigma_5 = 0$. Experimental data on σ_3 are as yet not available while the values of σ_2, σ_4 and σ_5 are indeed small compared to σ_1.

This way the presently available information concerning the relations between the cross sections of the reactions $\pi N \rightarrow \pi\pi N$ at an energy of 290 Mev indicates that the π mesons interact with themselves in the considered energy range† predominantly in the state with isospin $T_\pi = 0$. Consequently at energies below 300 Mev the most important contribution is due to transitions from an initial state with $T = 1/2$.

In reference 11 it was indicated that there possibly exists a resonance in the π-π system at a low energy (total energy of the system of two π mesons 310 ± 10 Mev) in an isospin state with $T_\pi = 0$ or $T_\pi = 1$. V. V. Anisovich has pointed out to us that such a resonance would have a strong influence on the ratios between the cross sections of the reactions $\pi N \rightarrow \pi\pi N$ at energies of the order 250 — 290 Mev. In this energy range the meson-nucleon interaction cross sections are still small. On the other hand, the mesons are produced at an energy close to the resonance. The data of the present work contradict the assumption that there exists a resonance in the interaction of two π mesons at a total energy of 310 ± 10 Mev in a state with isospin $T_\pi = 1$. The interaction in a $T_\pi = 0$ state seems to predominate. However, the obtained results do not allow to make definite statements about the existence of a resonance in the considered energy range.

The authors thank Professor V. P. Dzhelepov for his interest in the work and V. V. Anisovich for his useful discussions.

---

*This value represents an upper limit because for reaction (2) a possible background from production off bound nucleons of the nuclei of the emulsion was not subtracted.

†The total energy of the two π mesons in their center of mass system is contained in the interval 280 – 370 Mev.

---

[1] Alles-Borelli, Bergia, Perez Ferreira, and Waloschek, Nuovo cimento **14**, 211 (1959).

[2] I. Derado and N. Schmitz, Phys. Rev. **118**, 309 (1960).

[3] Pickup, Ayer, and Salant, Proc. of the 1960 Int. Conf. High Energy Phys. Rochester, Rochester Univ. Press 1960, p. 69; Pickup, Robinson, and Salant, ibid. p. 72.

[4] Perkins, Caris, Kenney, and Perez-Mendez, Phys. Rev. **118**, 1364 (1960).

[5] Batusov, Bogachev, Bunyatov, Sidorov, and Yarba, Doklady Akad. Nauk SSSR **133**, 52 (1960), Soviet Phys.-Doklady **5**, 731 (1961).

[6] Batusov, Bunyatov, Sidorov, and Yarba, JETP **39**, 1850 (1960) and **40**, 459 (1961); Soviet Phys. JETP **12**, 1290 (1961) and **13**, 320 (1961).

[7] V. G. Zinov and S. M. Korenchenko, JETP **34**, 301 (1958), Soviet Phys. JETP **7**, 210 (1958); S. M. Korenchenko, Thesis, Laboratory of Nuclear Problems, Joint Institute for Nuclear Research.

[8] Deahl, Derrick, Fetkovich, Fields, and Yodh, Proc. of the 1960 Annual Int. Conf. on High Energy Phys. Rochester, Rochester Univ. Press 1960, p. 185.

[9] G. Goebel and H. J. Schitzer, Proc. of the 1960 Annual Int. Conf. on High Energy Phys. Rochester, Rochester Univ. Press 1960, p. 298.

[10] Batusov, Bogachev, Sidorov, and Ciulli, Doklady Akad. Nauk SSSR **128**, 491 (1959), Soviet Phys.-Doklady **4**, 1015 (1960).

[11] Abashian, Booth, and Growe, Phys. Rev. Letters **5**, 258 (1960).

[12] Akimov, Komarov, Marish, Savchenko, and Soroko, JETP 40, 1532 (1961), this issue p. 1073.

Translated by M. Danos
263

SEARCH FOR ANOMALIES IN THE ENERGY DEPENDENCE OF THE CROSS SECTION OF THE REACTION $p + p \rightarrow d + \pi^+$ *NEAR THRESHOLD OF PION PAIR PRODUCTION*

Yu. K. AKIMOV, O. V. SAVCHENKO, and
L. M. SOROKO

Joint Institute for Nuclear Research

Submitted to JETP editor March 22, 1961

J. Exptl. Theoret. Phys. (U.S.S.R.) **40**, 1530-1532 (May, 1961)

RECENTLY in a number of papers (cf., e.g., reference 1) there has been a broad discussion of effects associated with anomalies in the energy dependence of a reaction near thresholds for inelastic processes. No one has as yet succeeded in observing effects of this sort at high energies, and therefore the problem of testing the results of the theory is now of considerable interest. We have made an attempt to detect near-threshold singularities in the reaction

$$p + p \rightarrow d + \pi^+ \tag{1}$$

at proton energies from 574 to 648 Mev, where the following processes of π-meson pair production are possible:

$$p + p \rightarrow \begin{cases} p + p + \pi^0 + \pi^0, & Q = 579.03 \text{ Mev} \\ d + \pi^+ + \pi^0, & Q = 587.48 \text{ Mev} \\ n + p + \pi^0 + \pi^+, & Q = 592.53 \text{ Mev} \\ p + p + \pi^+ + \pi^-, & Q = 600.08 \text{ Mev} \\ n + n + \pi^+ + \pi^+, & Q = 606.06 \text{ Mev} \end{cases} \tag{2}$$

Furthermore, in this energy range one can expect anomalies near the threshold for production of the hypothetical ω particle, which has been discussed in reference 2 as one of the ways of explaining the experimental data. In p-p collisions the ω particle can be produced in the reactions

$$p + p \rightarrow \begin{cases} d + \omega^+ \\ n + p + \omega^+ \end{cases} \tag{3}$$

The range of proton energies from 574 to 648 Mev corresponds to a range of masses for the ω particle from 275 to 305 Mev.

The choice of the reaction (1) for the observation of near-threshold singularities was made for the following reasons. First, the total and differential cross sections of the reaction (1) change only by small amounts in the range of energies of the incident protons from 574 to 648 Mev,[3] and this to some extent facilitates the search for anomalies near the thresholds of other reactions. Second, we may suppose that owing to the small cross section of the reaction (1) possible anomalous effects may be most clearly marked in just this reaction. Finally, the method that we have used to measure the differential cross section of the reaction (1) may give greater sensitivity to near-threshold anomalies than would be obtained in measurements of the total cross section.

We have measured the yield of deuterons in the low-energy branch of the reaction (1) for a single angle in the laboratory coordinate system (l.s.) as a function of the energy of the incident protons over the range 574 — 648 Mev. The proton beam of intensity 10^{11} sec^{-1} was focused with magnetic quadrupole lenses on a polyethylene target 5 mm thick. The secondary particles produced in the target were separated out by a brass collimator placed at an angle of 5.8° with the axis of the beam, were deflected by an electromagnet through an angle of 27°, passed through a steel collimator in the concrete shielding wall, and were registered by a telescope made up of five scintillation counters. The charged particles were identified by their momentum, specific ionization, and range,[4] which

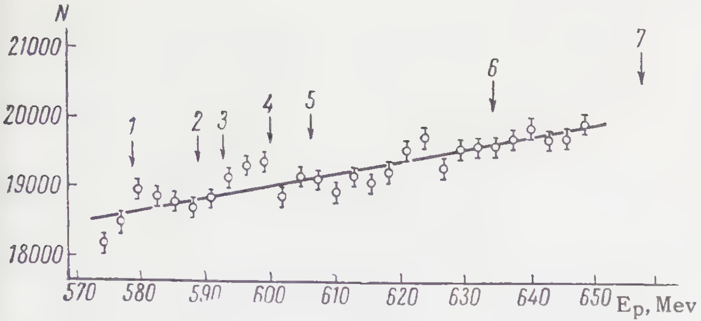

Energy dependence of the differential cross section of the reaction $p + p \rightarrow d + \pi^+$ for the angle 5.8° in the l.s. The straight line drawn in the diagram was obtained by the method of least squares. The arrows 1, 2, 3, 4, 5 show the positions of the thresholds of the reactions (2); the arrows 6 and 7 show the positions of the thresholds of reaction (3) for masses 295 and 305 Mev for the ω particle.

made it possible to distinguish deuterons reliably against the background of photons coming from the target.

The energy of the proton beam was varied by means of polyethylene blocks placed in front of the magnetic quadrupole lenses. The proton energy was determined within an interval of 2.8 Mev, which was approximately the energy dispersion of the proton beam.[5]

The kinematics of the reaction (1) are such that for an angle of 5.8° in the l.s. the momentum of the deuterons of the low-energy branch varies by only 3 percent as the proton energy is decreased from 650 to 570 Mev. This decidedly simplifies the measurements and makes it possible to determine the energy dependence of the differential cross section for the reaction (1) by measuring the deuteron yield at the maximum of the resolution curve, instead of finding the area under the resolution curve at each proton energy. At each proton energy a determination was made of the value of the current in the deflecting magnet that corresponded to the position of the peak of the deuterons from the reaction (1); this was calculated from calibration curves of the resolving power, with half-width about 2 percent, measured at three energies: 574, 607, and 657 Mev. With this procedure the inaccuracy in supplying the required current through the deflecting magnet could not cause an error of more than 0.3 percent in the results.

The averaged results of two series of measurements, without subtraction of the background of deuterons from the carbon target, which was about 15 percent, are shown in the diagram. The data were approximated by a straight line, constructed by the method of least squares. If we take into account only the statistical errors of the measurements, amounting to 0.7 percent, the χ^2 test indicates that the experimental data are not consistent with this straight line. If, however, we suppose that besides the statistical errors there is an additional dispersion in the measurements which amounts to 0.5 percent, the χ^2 test gives a 10-percent probability for the fit of the linear dependence to the experimental data. Since the results of a comparison of the separate series of measurements do not allow us to exclude such an amount of instability of the apparatus, the spread of the experimental points which is seen in the diagram cannot be ascribed to real anomalies in the energy dependence of the differential cross section for the reaction (1).

It follows from the results of this work that if the near-threshold anomalies predicted by the theory do exist in the reaction (1), their magnitude does not exceed 2 percent of the average differential cross section of reaction (1) over the proton-energy range 574 — 648 Mev.

---

[1] R. G. Newton, Phys. Rev. **114**, 1611 (1959).

[2] Abashian, Booth, and Crowe, Phys. Rev. Letters **5**, 258 (1960).

[3] M. G. Meshcheryakov and B. S. Neganov, Doklady Akad. Nauk SSSR **100**, 677 (1955).

[4] Akimov, Komarov, Savchenko, and Soroko, Приборы и техника эксперимента (Instrum. and Exptl. Techniques) **4**, 71 (1960).

[5] I. M. Vasilevskii and Yu. D. Prokoshkin, Атомная энергия (Atomic Energy) **7**, 225 (1959).

Translated by W. H. Furry
264

SEARCH FOR ANOMALIES IN THE SPECTRUM OF THE H^3 *NUCLEI EMITTED IN THE REACTION* $p + d \rightarrow H^3 + \pi^+ + \pi^0$ *AT A PROTON ENERGY OF 670 Mev*

Yu. K. AKIMOV, V. I. KOMAROV, K. S. MARISH, O. V. SAVCHENKO, and L. M. SOROKO

Joint Institute for Nuclear Research

Submitted to JETP editor March 22, 1961

J. Exptl. Theoret. Phys. (U.S.S.R.) **40**, 1532-1535 (May, 1961)

THERE has recently been much discussion of the problem of the resonance interaction of two π mesons with the isotopic spin $T_{\pi\pi} = 1$. The only experimental indication of the possibility of such a resonance are the preliminary results of Abashian, Booth, and Crowe,[1] who studied the momentum spectrum of the He^3 and H^3 nuclei produced in the reactions

$$p + d \to \begin{cases} He^3 + \pi^0, & (1a) \\ He^3 + \pi^0 + \pi^0, & (1b) \\ He^3 + \pi^+ + \pi^-, & (1c) \end{cases}$$

$$p + d \to \begin{cases} H^3 + \pi^+, & (2a) \\ H^3 + \pi^+ + \pi^0, & (2b) \end{cases}$$

and observed peaks in these spectra which can be interpreted as manifestations of a π-π resonance with $T_{\pi\pi} = 1$ or of the formation of a new particle with mass 310 Mev and isotopic spin $T = 1$. The schemes for the formation of the new particle are

$$p + d \to He^3 + \omega^0, \tag{1d}$$

$$p + d \to H^3 + \omega^+. \tag{2c}$$

In view of the large discrepancy between the observed resonance energy and the theoretically predicted value,[2] and also of the importance of the question of the isotopic spin of the π-π resonance, it is of great interest to get more precise momentum spectra of the H^3 nuclei produced in the reactions (2b) and (2c). For this purpose we have measured the region of the momentum spectrum of the H^3 nuclei that belongs to the low-energy branch of reaction (2a), at proton energy 670 Mev. The identification of the charged particles produced in gaseous deuterium and hydrogen targets was made from the momentum, specific ionization, range, and time of flight. The results of the measurements are shown in the diagram, where the abscissa is the current in the deflecting magnet, which is proportional to the momentum of the H^3 nuclei, and the ordinate is the difference between the counts from the gas target filled with deuterium and with hydrogen. Arrow 1 indicates the value of the current that corresponds to the lower limit of the spectrum of H^3 nuclei from the reaction (2b). Arrow 2 indicates the value of the current that corresponds to the total energy of two π mesons in their c.m.s., which is 320 Mev, and a momentum of 875 Mev for the H^3 nucleus.

A statistical treatment of the results of the measurements shows that with probability 90 percent, the yield of H^3 nuclei of momentum 875 Mev at angle 5.8° in the l.s. does not exceed 6 percent of the yield of H^3 nuclei at the same angle in reaction (2a). The cross section for the reaction (2a) was measured by a comparison with the cross section for the reaction $p + p \to d + \pi^+$.[3] The cross section for reaction (2a) calculated in the c.m.s. and referred to the angle of emergence of the π^+ meson was found to be

$$\frac{d\sigma}{d\Omega}(\theta_\pi = 12°) = (9.1 \pm 0.5) \cdot 10^{-30} \text{ cm}^2/\text{sr}$$

The cross section for reactions (2b), (2c), referred to the angle between the velocity vector of the motion of the center of mass of the mesons and the axis of the beam, or to the angle of emergence of the ω particle, has the upper limit, in the c.m.s.,

$$\frac{d\sigma}{d\Omega}(\theta_\omega = 20°) \leqslant 0.2 \cdot 10^{-30} \text{ cm}^2/\text{sr}$$

with probability 90 percent.

The cross section for the high-energy branch of reaction (1a) was also measured. The differential cross section in the c.m.s., referred to the angle of emergence of the π^0 meson, is

$$\frac{d\sigma}{d\Omega}(\theta_{\pi^0} = 154°) = (0.295 \pm 0.032) \cdot 10^{-30} \quad \text{cm}^2/\text{sr}$$

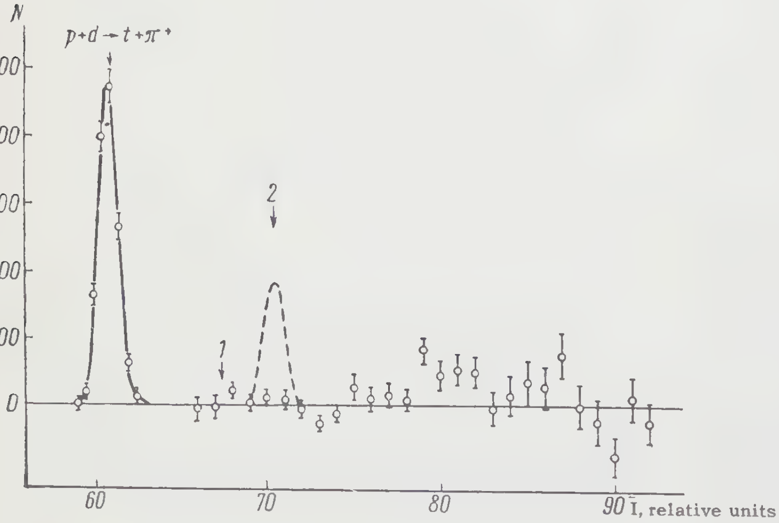

Fig. 1

Besides this, the yield of He^3 nuclei from reactions (1b), (1c), which was measured for three momenta, shows that the cross section for these reactions is comparable with that for (2a).

For a quantitative comparison of the data with the results of reference 1, a calculation of the angular distributions of reactions (2a) and (2c) was made in the impulse approximation.[4,5] The angular distribution found for reaction (2a) agrees qualitatively with a large forward-backward asymmetry.[6,7] The calculation for reactions (2b), (2c) was made on the assumption that first there is production of two π mesons or of an ω particle in the reactions

$$p + p \rightarrow d + \pi^+ + \pi^0, \qquad p + p \rightarrow d + \omega^+, \qquad (3)$$

and then the neutron and deuteron combine into a tritium nucleus. The angular distributions of reactions (2b), (2c) calculated on the two extreme assumptions about the angular distribution of the deuterons in the reactions (3), an isotropic distribution and a $\cos^2\theta$ distribution, differ only slightly at angles close to 0° or 180° in the c.m.s. This fact allows us to compare the data[1] relating to the high-energy branch of the reactions (2b), (2c) with our values of the differential cross sections for the low-energy branch. The yield of H^3 nuclei measured in reference 1 and recalculated in this way is shown in the diagram by a dashed line. It exceeds the upper limit found in this work for the cross section of reactions (2b) and (2c) by about an order of magnitude.

Thus the results obtained here do not confirm the existence of a resonance of two π mesons in a state with isotopic spin $T_{\pi\pi} = 1$ and total energy from 275 to 420 Mev in their c.m.s., and also allow us to exclude the existence of an ω particle with isotopic spin $T = 1$ and mass ~ 310 Mev. Since there are now definite indications of the nonexistence of a vector meson with $T = 0$[8] and mass in the range from 300 to 400 Mev, the explanation of the anomaly found in reference 1 in terms of the existence of such a meson also seems improbable.

We must seek a possible cause of the anomaly in the spectrum of the He^3 nuclei produced in reactions (1b) and (1c) in threshold effects[9,10] associated with the endothermal process $\pi^0 + \pi^0 \rightarrow \pi^+ + \pi^-$.* As is shown by an analysis of the threshold effects made by means of dispersion relations,[11] departures from monotonic energy dependence in reactions with three particles in the final state can spread rather far from the threshold of the corresponding endothermal process.

Another conclusion from this work is that the cross section for production of two π mesons in the state with isotopic spin $T_{\pi\pi} = 0$ is about an order of magnitude larger than the upper limit on the cross section for the production of two π mesons in the state with $T_{\pi\pi} = 1$, right up to a total energy of the two π mesons in their c.m.s. of about 400 Mev. This relation between the cross sections evidently changes at higher energies, as is indicated by the data on processes $\pi N \rightarrow \pi\pi N$ obtained at energies ~ 500 Mev.[12]

The writer thank L. I. Lapidus for his interest in this work and a discussion, and B. M. Pontecorvo for helpful comments.

---

*L. I. Lapidus pointed out the possibility of this interpretation.

---

[1] Abashian, Booth, and Crowe, Phys. Rev. Letters **5**, 258 (1960).

[2] W. R. Frazer and J. R. Fulco, Phys. Rev. Letters **2**, 365 (1959); Phys. Rev. **117**, 1609 (1960).

[3] M. G. Meshcheryakov and B. S. Neganov, Doklady Akad. Nauk SSSR **100**, 677 (1955).

[4] S. Bludman, Phys. Rev. **94**, 1722 (1954).

[5] M. Ruderman, Phys. Rev. **87**, 383 (1952).

[6] Harting, Kluyver, Kusumegi, Rigopoulos, Sachs, Tibell, Vanderhaeghe, and Weber, Phys. Rev. **119**, 1716 (1960).

[7] Akimov, Savchenko, and Soroko, JETP **38**, 643 (1960), Soviet Phys. JETP **11**, 462 (1960).

[8] Gomez, Burkhardt, Daybell, Ruderman, Sands, and Talman, Phys. Rev. Letters **5**, 170 (1960).

[9] L. I. Lapidus and Chou Kuang-Chao, JETP **39**, 364 (1960), Soviet Phys. JETP **12**, 258 (1961).

[10] L. Fonda and R. G. Newton, Phys. Rev. **119**, 1394 (1960).

[11] L. I. Lapidus and Chou Kuang-Chao, JETP **39**, 112 (1960), Soviet Phys. JETP **12**, 82 (1961).

[12] W. J. Willis, Phys. Rev. **116**, 753 (1959).

Translated by W. H. Furry
265

CONTENTS OF COMING ISSUES

SOVIET PHYSICS JETP VOLUME 13, NUMBER 6 DECEMBER, 1961

CONTENTS

Russian Reference

Investigation of the $V^{51}(C^{12}, 2n)Cu^{61}$ Reaction . . . . A. S. Karamyan and A. A. Pleve 40, 1541
Destruction of Superconductivity in Thin Tin Films . . . . A. M. Kolchin, Yu. G. Mikhaĭlov, N. M. Reĭnov, A. V. Rumyantseva, A. P. Smirnov, and V. N. Totubalin 40, 1543
Investigation of Large Ionization Bursts Produced by Cosmic Ray Particles at Sea Level J. Babecki, Z. Buja, N. L. Grigorov, J. Loskiewicz, A. Oles, and V. Ya. Shestoperov 40, 1551
Magnetic and Magnetoelastic Properties of Dysprosium and Gadolinium. . . . . K. P. Belov, R. Z. Levitin, S. A. Nikitin, and A. V. Pedko 40, 1562
Neutron Polarization in the Reaction $C^{12}(d, n)N^{13}$ . . . . I. I. Levintov, I. S. Trostin 40, 1570
Isotope Masses and Binding Energy of Nuclei in the Region From Strontium to Ruthenium . . . . R. A. Demirkhanov, V. V. Dorokhov, and M. I. Dzkuya 40, 1572
Thermal Conductivity and Diffusion of Weak He^3-He^4 Solutions in the Temperature Range from the λ-Point to 0.6°K. . . . . T. P. Ptukha 40, 1583
Electron Paramagnetic Resonance of the Fe^{3+} Ion in Corundum . . . . L. S. Kornienko and A. M. Prokhorov 40, 1594
Energy Spectrum and Total Number of Low Energy Cosmic Ray Photons in the Stratosphere . . . . A. N. Charkhch'yan and T. N. Charakhch'yan 40, 1602
Paramagnetic Resonance of Mn^{2+} in SrS . . . . A. A. Manenkov and A. M. Prokhorov 40, 1606
The $Cl^{35}(n, p)$ Reaction and Neutron Resonance Parameters of Chlorine. . . . . Yu. P. Popov and F. L. Shapiro 40, 1610
Excitation of the He^4 Nucleus by 150-Mev Pions . . . . Yu. A. Budagov, P. F. Yermolov, E. A. Kushnirenko, and V. I. Moskalev 40, 1615
On the Experimental Verification of the $\Delta I = \frac{1}{2}$ Selection Rule for Lepton Decay of K Mesons. . . . . D. V. Neagu, E. O. Okonov, N. I. Petrov, A. M. Rozanova, and V. A. Rusakov 40, 1618
Emulsion Study of the Interaction Between 8.7-Bev Protons and Quasi-Free Nucleons . . . . K. I. Alekseeva, G. B. Zhdanov, E. A. Zamchalova, M. I. Tretyakova, and M. N. Shcherbakova 40, 1625
Specific Heat of Nickel-Zinc System Ferrites in the Low-Temperature Region . . . . M. O. Kostryukova 40, 1638
Variation of the Axial and Radial Dimensions of an Electron Cluster during Synchrotron Acceleration . . . . F. A. Korolev, A. G. Ershov, and O. F. Kulikov 40, 1644
Elastic Scattering of 8.7-Bev Protons by Emulsion Nuclei . . . . B. P. Bannik, V. G. Grishin, and L. V. Silverstrov 40, 1653
Investigation of Electron Packets in a Microtron . . . . V. P. Bykov 40, 1658
On the Nature of Spin-Lattice Interaction in Chromium Corundum. I. . . . . G. M. Zverev 40, 1667
Lepton Decay of the Λ-Hyperon and the Probability for $K_{\mu 2}$ and K_{e3} Processes . . . . G. M. Gandel'man 40, 1672
Conductivity-Electron Interaction Induced by Spin Waves in a Ferromagnetic Substance . . . . S. V. Vonsovskii and M. S. Svirskii 40, 1676
Angular Distribution Function for Particles in a Shower Produced by a Primary Particle of a Given Energy . . . . V. V. Gushavin and I. P. Ivanenko 40, 1682
Light Absorption by Electrons of Nonmetallic Crystals in an Electric Field . . . . V. A. Yakovlev 40, 1695
Electron Polarizability and Diamagnetic Susceptibility of Neutral Atoms in the Thomas-Fermi Model. . . . . T. Tietz 40, 1699
Theory of Absorption of Sound in Dilute He^3 in He II Solutions . . . . A. A. Andreev 40, 1705

Double Dispersion Relations and the Photoproduction of Pions. II . . . N. F. Nelipa and V. A. Tsarev 40, 1710
On Superbarrier Reflection of High Energy Particles . . . V. L. Pokrovskii and I. M. Khalatnikov 40, 1713
Concerning the Theory of Spin-Lattice Relaxation in Radicals in Liquids . . . I. V. Aleksandrov and G. M. Zhidomirov 40, 1720
Branching of Electron and Photon Green's Functions . . . V. G. Vaks 40, 1725
Suppression of Two-Meson Annihilation in Antiproton-Proton Interaction . . . É. O. Okonov 40, 1728
Magnetic Dipole Transitions in Even-Even Nuclei with Quadrupole Collective Excitations . . . D. P. Grechukhin 40, 1732
Electromagnetic Corrections to Weak Interactions . . . I. F. Ginzburg and V. V. Serebryakov 40, 1738
Magnetohydrodynamic Combustion . . . R. V. Polovin and V. P. Demutskii 40, 1746
Singularity in the Schwarzschild Solution of the Gravitation Equation . . . Yu. A. Rylov 40, 1755
Casuality Conditions in Quantum Theory . . . V. Ya. Faĭnberg 40, 1758
Collision Integral for Charged Particles . . . V. P. Silin 40, 1768
Spatial Dispersion in a Relativistic Plasma . . . V. N. Tsytovich 40, 1775
Spectrum of Galactic and Solar Cosmic Rays . . . S. I. Syrovat-skii 40, 1788
Angular Correlations in Statistical Nuclear Reactions . . . V. M. Strutinskii 40, 1794
Electromagnetic Waves in a Medium Possessing a Continuous Energy Spectrum II . . . V. S. Mashkevich 40, 1803
Effect of Diffusion on the Scattering of Neutrons and Photons by Crystal Imperfections and on the Mössbauer Effect . . . M. A. Krivoglaz 40, 1812
Peculiarities of the Behavior of Multicharged Ions in a Plasma . . . A. V. Gurevich 40, 1825
On the Theory of Energy Dissipation Processes of Molecular Oscillations in Liquids . . . K. A. Valiev 40, 1832
Resonance Diffraction of Waves in Lamellar Inhomogeneous Media . . . L. V. Iogansen 40, 1838
Coulomb Excitation of Λ Particles . . . B. N. Valuev 40, 1844
Singularities of Cosmological Solutions of Gravitational Equations. III . . . E. M. Lifshitz, V. V. Sudakov, and I. M. Khalatnikov 40, 1847
Scattering of K Mesons on Nucleons at Large Orbital Momenta . . . Yu. P. Nikitin 40, 1856
Effect of Anisotropy on Threshold Phenomena in Superconductors . . . V. L. Pokrovskii and M. S. Ryvkin 40, 1859
Interaction of Charged Particles Beams with Low Frequency Plasma Oscillations . . . A. I. Akhiezer, A. B. Kitsenko, and K. N. Stepanov 40, 1866

LETTERS TO THE EDITOR

Asymmetry of Beta Radiation from Co^{60} Nuclei Polarized in a Cobalt-Iron Alloy . . . B. N. Samoĭlov, V. V. Sklyarevskii, V. D. Gorobchenko, and E. P. Stepanov 40, 1871
Temperature Dependence of Hyperfine Splitting of Dy^{161} Levels in Paramagnetic Dysprosium Oxide . . . V. V. Sklyarevskii, B. N. Samoĭlov, and E. P. Stepanov 40, 1874
Paramagnetic Resonance in Metallic Aluminum . . . A. A. Galkin and V. P. Naberezhnykh 40, 1876
Small-Angle Scattering of 0.8- and 2.8-Mev Neutrons . . . Yu. A. Aleksandrov, G. V. Anikin, and A. S. Soldatov 40, 1878
Production of Negative-Temperature States in p-n Junction of Degenerate Semiconductors . . . N. G. Basov, O. N. Krokhin, and Yu. M. Popov 40, 1879
Rarefaction Shock Waves in Iron and Steel . . . A. G. Ivanov and S. A. Novikov 40, 1880
Recombination Glow of Indium Antimonide in Avalanche Breakdown . . . N. G. Basov, B. D. Osipov, and A. N. Khvoshchev 40, 1882
Author Index to Volume 40 . . . 40, 1883
Analytical Subject Index to Volume 40 . . . 40, 1898

Russian Reference

Secondary Ion Emission From Metals Induced by 10 — 100 kev Ions . . . B. V. Panin 41, 3

Triple Fission of Uranium Induced by Fast Neutrons . . . N. A. Perfilov, Z. I. Solov'eva, and R. A. Filov 41, 11

Nuclear-Active Particles in Atmospheric Showers . . . J. S. Babecki, Z. A. Buja, N. L. Grigorov, J. S. Loskiewicz, E. I. Massalski, A. A. Oles, V. Ya Shestoperov, and S. Fischer 41, 13

Mean Energy of the Y^{90} Beta Spectrum . . . E. I. Biryukov, B. S. Kuznetsov, and N. S. Shimanskaya 41, 22

Angular Distribution of 14-Mev Neutrons Elastically Scattered on Carbon, Nitrogen and Sulfur . . . V. V. Bobyr', L. Ya. Grona, and V. I. Strizhak 41, 24

Electron Loss and Capture by 200 — 1500 Kev Helium Ions in Various Gases . . . L. I. Pivovar, V. M. Tubaev, and M. T. Novikov 41, 26

Elastic Scattering of 5.45-Mev Protons on Zirconium Nuclei . . . V. Ya. Golovnya, A. P. Klucharev, and B. A. Shilyaev 41, 32

Charge Distribution of Fragments in Nuclear Disintegrations . . . P. A. Gorichev, O. V. Lozhkin, and N. A. Perfilov 41, 35

Total Cross Sections for Interaction of 4.75 and 3.7 Bev/c K^+ and π^+-Mesons with Protons and Nuclei . . . M. F. Lykhachev, V. S. Stavinsky, Hsü Yün-ch'ang, and Chang Nai-sen 41, 38

Spectroscopic Investigation of a Toroidal Discharge . . . V. G. Averin, M. A. Mazing, and A. I. Pisanko 41, 42

Elastic Scattering of 10 — 15 Mev Alpha particles on Gold and Aluminum . . . M. P. Konstantinova, E. V. Myakinin, A. M. Romanov, and T. V. Tsaresa 41, 49

Elastic Back Scattering of 2.8-bev/c π^- Mesons on Neutrons . . . Yu. D. Bayukov, G. A. Leksin, D. A. Suchkov, Ya. Ya. Shalamov, and V. A. Shebanov 41, 52

Scattering of 1 — 5 Bev/c Muons in Lead . . . S. A. Azimov, G. G. Arushanov, Kh. Zaĭnutdinov, R. Karimov, V. S. Masagutov, and M. Kh. Ésterlis 41, 56

Yield of Fast Photoneutrons From C^{12} and Al^{127} . . . V. Presperin and L. A. Kulchitskii 41, 60

Excited Levels of Ne^{22} . . . A. M. Romanov, E. V. Myakinin, and M. P. Konstantinova 41, 64

Excitation of Nuclear Rotational Levels in μ-Mesic-Atom Transitions . . . G. E. Belovitskii 41, 66

Angular Distribution of 6.8-Mev Protons Elastically Scattered on Nickel and Zirconium Isotopes . . . A. K. Val'ter, I. I. Zalyubovskii, A. P. Klyutcharev, V. A. Lutsik, B. F. Orlenko, M. V. Pasechnik, V. S. Prokopenko, and N. N. Pucharev 41, 71

The Cross Section for Production of Hypernuclei in Emulsion by 9-Bev Protons . . . I. B. Berkovich, A. P. Zhdanov, F. G. Lepekhin, and Z. S. Khokhlova 41, 75

Interaction of 78-Mev π^+ Mesons in Propane . . . R. G. Salukvadze and D. Neagu 41, 78

Effect of Unilateral Compression on the Electric Properties of p-Type Germanium at Low Temperatures . . . M. A. Il'ina and I. A. Kurova 41, 81

Correlation Between the Normal Polarization Components in the pp-Scattering at 650 Mev. I . . . B. M. Golovin, V. P. Dzhelepov, and R. Ya. Zul'karneev 41, 83

Capture of Several Electrons by Fast Multicharged Ions . . . V. S. Nikolaev, L. N. Fateeva, I. S. Dmitriev, and Ya. A. Teplova 41, 89

Relaxation Phenomena in the Paramagnetic Resonance of Mn^{2+} Ions in the Cubic Crystal Field of SrS . . . . A. A. Manenkov and V. A. Milyaev 41, 100
Angular Distribution of μ Mesons in $\pi - \mu$ Decay . . . . A. O. Vaĭsenberg, É. D. Kolganova, and Z. V. Minervina 41, 106
μ^--Meson Capture in Carbon Involving the Formation of B^{12*} . . . . A. O. Vaĭsenberg 41, 109
Wave Resonance of Light and Gravitational Waves . . . . M. E. Gertsenshteĭn 41, 113
Anisotropy of Gamma Radiation in the Mössbauer Effect . . . . A. Gel'berg 41, 115
Production of Tritium in Collisions of Fast Protons with Heavy Nuclei . . . . S. V. Izmaĭlov and I. I. P'yanov 41, 118
Calculation of the Spin-Lattice Relaxation Time for Radicals in Molecular Crystals . . . . I. V. Aleksandrov and G. M. Zhidomirov 41, 127
Dispersion in Ferroelectric . . . . D. G. Sannikov 41, 133
Analysis of Cosmic-Ray Showers Produced by High-Energy Primary Particles, Based on the Excited Nucleon Model . . . . L. A. San'ko, Zh. S. Takibaev, and P. A. Usik 41, 139
Limiting Values of the $\pi^{\pm}$ p Scattering Amplitude . . . . V. P. Kanavets, I. I. Levintov, and B. V. Morozov 41, 146
Interaction of Transverse Oscillations in a Plasma . . . . A. P. Kazantsev and I. A. Gilinskiĭ 41, 154
Electromagnetic Properties of a Relativistic Plasma. III . . . . V. P. Silin and E. P. Fetisov 41, 159
The Shell Model and the Shift of Single-Particle Levels in Nuclei of the "Core + Nucleon" Type, Due to Addition of a Pair of Nucleons . . . . V. E. Asribekov 41, 171
Rotation of the Plane of Polarization of Light in the Case of Parity Nonconservation . . . . A. M. Perelomov 41, 183
Diamagnetic Perturbations in Media, Caused by Ionizing Radiation . . . . G. A. Askar'yan 41, 186
Space and Charge Parities of a Proton-Antiproton System and its Multi-Pion Annihilation . . . . M. I. Shirokov 41, 190
Determination of the Pion-Nucleon Coupling Constant From the Differential Cross Cross Sections for Elastic pp scattering . . . . Yu. M. Kazarinov, V. S. Kiselev, I. N. Silin, and S. N. Sokolov 41, 197
Radiative Corrections to Beta Decay . . . . . B. V. Geshkenbeĭn and V. S. Popov 41, 199
A Relativistic Field-Theory Model with an Exact Solution . . . . D. A. Kirzhnits and S. A. Smolyanskii 41, 205
The Farady Effect for Excitons . . . . I. P. Ipatova and R. F. Kazarinov 41, 209
Possibility of Generation and Amplification of Hypersound in Paramagnetic Crystals . . . . U. Kh. Kopvillem and V. D. Korepanov 41, 211
Excitation of Nuclei in Heavy μ-Mesic Atoms . . . . D. F. Zaretskii and V. M. Novikov 41, 214
Nonadiabatic Corrections to the Rotational Spectrum of Atomic Nuclei . . . . Yu. T. Grin' 41, 222
Reflection of Electromagnetic Waves in Gyrotropic Media From a Magnetic Field Wave . . . . G. I. Freĭdman 41, 226
Nucleon Correlations in Photonuclear Reactions I. Photodisintegration of He^4 . . . . G. M. Shklyarevskii 41, 234
The Neutrino and the Density of Matter in the Universe . . . . B. Pontecorvo and Ya. Smorodinskii 41, 239
On the $K^+ \rightarrow \pi^+ + \pi^0 + e^+ + e^-$ Decay . . . . I. G. Ivanter 41, 244
A Gauge-Invariant Formulation of Neutral Vector Field Theory . . . . V. I. Ogievetskii and I. V. Polubarinov 41, 247

Integral Equations for $\pi\pi$ Scattering and Problems Related to Convergence of the Amplitude Expansion . . . . J. Fischer and S. Ciulli 41, 256

Disintegration of Nonevolutional Shock Waves . . . . R. V. Polovin and K. P. Cherkasova 41, 263

High-Frequency Magnetic Susceptibility of a Uniaxial Ferromagnetic Crystal in a Longitudinal Magnetic Field . . . . M. I. Kaganov and V. M. Tsukernik 41, 267

Single Meson Contribution to Photoproduction of π^- Mesons on Protons . . . . L. V. Laperashvili and S. G. Matinyan 41, 276

On the Excitation of Nuclei by Muons in Heavy Mesic Atoms . . . . . V. M. Novikov 41, 276

Contribution to the Theory of Absorption of Supersonic Waves by Metals in a Magnetic Field . . . . G. L. Kotkin 41, 281

Contribution to the Theory of Electromagnetic Fluctuations in a Nonequilibrium Plasma . . . . F. V. Bunkin 41, 288

The Role of the Single-Meson Pole Diagram in Scattering of Gamma Quanta by Protons . . . . L. I. Lapidus and Chou Kuang-chao 41, 294

LETTERS TO THE EDITOR

Beta and Gamma Spectra of Te^{117} . . . . N. A. Vartanov, Yu. A. Ryukhin, I. P. Selinov, V. L. Chikhladze, and D. E. Khulelitze 41, 303

Possibility of Registration of Gravitational Radiation under Laboratory Conditions . . . . V. B. Braginskii and G. I. Rukman 41, 304

Asymmetry in Angular Distribution of Neutrons Emitted in the Capture of Negative Muons in Calcium. . . . . V. S. Evseev, V. I. Komarov, V. Z. Kush, V. S. Roganov, V. A. Chrnogorova, and M. M. Szymczak 41, 306

Correction to the Article ‘Connection between Matrices of Various Transitions and Multiple Processes.’ . . . . B. T. Vavilov 41, 307